

**The Development of an Assimilative Capacity Model  
for the Sustainable Management of Nutrients within  
the Ria Formosa in southern Portugal**

**Ana Cristina Florindo de Brito**

A thesis submitted in partial fulfilment of the requirements of  
Edinburgh Napier University for the degree of Doctor of Philosophy

This research programme was carried out in collaboration with the  
University of the Algarve, Portugal.

**January 2010**

**EDINBURGH NAPIER UNIVERSITY**

**EDINBURGH**

## **Declaration**

I declare that all the work presented in this thesis was undertaken by me. I also declare that this thesis was written by me and that the work contained herein is my own responsibility. Several publications resulted from this project and they were written in collaboration with Prof. Teresa Fernandes, Prof. Paul Tett, Dr. Alice Newton and Dr. John Icely.

Ana Cristina Florindo de Brito

January 2010

The following chapters, or part of them, have been published or submitted to international journals. Note that the content of each paper and the correspondent chapter are different.

### **Chapter 3**

Brito, A., Newton, A., Tett, P., Fernandes, T., 2009. Development of an optimal methodology for the extraction of microphytobenthic chlorophyll. *Journal of International Environmental Application and Science*, **4(1)**, 42-54.

### **Chapter 4**

Brito, A., Newton, A., Tett, P., Fernandes, T., 2009. Temporal and spatial variability of microphytobenthos in a shallow coastal lagoon: Ria Formosa (Portugal). *Estuarine, Coastal and Shelf Science*, **83**, 67-76.

### **Chapter 5**

Brito, A., Newton, A., Tett, P., Fernandes, T., 2009. Understanding the importance of sediments to water quality in coastal shallow lagoons. *Journal of Coastal Research*, **56**, 381-384.

Brito, A., Newton, A., Tett, P., Fernandes, T., 2010. Sediment-water interactions in a coastal shallow lagoon, Ria Formosa (Portugal): Implications within the Water Framework Directive. *Journal of Environmental Monitoring*, *in press*. DOI:10.1039/B909429F.

### **Chapter 6**

Brito, A., Newton, A., Tett, P., Icely, J., Fernandes, T., 2010. The yield of microphytobenthic chlorophyll from nutrients: enriched experiments in microcosms. *Journal of Experimental Marine Biology and Ecology*. DOI:10.1016/j.jembe.2009.11.010.

### **Chapter 7**

Brito, A., Newton, A., Tett, P., Fernandes, T., *submitted*. The role of microphytobenthos on shallow coastal lagoons: A modelling approach. *Biogeochemistry*.

---

# Contents

---

	<b>Acknowledgements</b>	iv
	<b>Summary</b>	vi
<b>1.</b>	<b>Introduction</b>	1
1.1	Primary Production	2
1.2	Coastal Lagoons	10
1.3	Eutrophication	18
1.4	Modelling	25
1.5	Aims and Objectives	33
1.6	Thesis Outline	34
<b>2.</b>	<b>Study Site</b>	36
2.1	Climate	38
2.2	Hydrodynamics	41
2.3	Physico-chemical parameters	44
2.4	Socio-economy	53
2.5	Legal considerations	53
<b>3.</b>	<b>The development of an optimal methodology for the extraction of microphytobenthic chlorophyll</b>	56
	Abstract	57
3.1	Introduction	58
3.2	Material and methods	60
3.3	Results	65

3.4	Discussion	70
3.5	Comments and recommendations	75
3.6	References	76
<b>4.</b>	<b>Seasonal, spatial and vertical variability of microphytobenthos</b>	<b>80</b>
	Abstract	81
4.1	Introduction	82
4.2	Material and methods	88
4.3	Results	95
4.4	Discussion	105
4.5	References	112
<b>5.</b>	<b>Physico-chemical and biological elements in the water column and sediments</b>	<b>115</b>
	Abstract	116
5.1	Introduction	117
5.2	Material and methods	120
5.3	Results	129
5.4	Discussion	147
5.5	Conclusions	160
5.6	References	161
<b>6.</b>	<b>The yield of microphytobenthic chlorophyll from nitrogen: enriched experiments in microcosms</b>	<b>166</b>
	Abstract	167
6.1	Introduction	168
6.2	Material and methods	177
6.3	Results	192

6.4	Discussion	199
6.5	Conclusions	206
6.6	References	207
<b>7.</b>	<b>Biogeochemical model for the sustainable management of nutrients within the Ria Formosa</b>	<b>211</b>
	Abstract	212
7.1	Introduction	213
7.2	Development of the model	220
	<i>Stage 1</i>	221
	<i>Stage 2</i>	234
	<i>Stage 3</i>	250
	<i>Stage 4</i>	259
7.3	Sensitivity Analysis	279
7.4	Estimating the Assimilative Capacity	285
7.5	Exploration of different scenarios	289
7.6	Final considerations	292
7.7	References	293
<b>8.</b>	<b>General Discussion</b>	<b>298</b>
8.1	General considerations	299
8.2	Overview and Future studies	305
<b>9.</b>	<b>References (global list)</b>	<b>307</b>
	<b>Appendixes</b>	<b>325</b>

## **Acknowledgements**

A PhD is first of all an outstanding adventure and experience, both on scientific and social aspects. It leads to unexpected conclusions through cognitive challenges or to an abyss of questions, always with hard work. It allows you to work in international and vibrant environments, absorb different cultures and meet interesting people. But, it also expects you to walk through adversities with grace. This process is full of human lessons and irreplaceable for personal evolution.

I would like to express my deepest admiration and gratitude to all my supervisors, Prof. Teresa Fernandes, Prof. Paul Tett from Napier University and Dr. Alice Newton from the University of Algarve. I have really appreciated all the scientific support provided by them. I also have to thank them for the immense patience during our meetings and the encouragement to overcome problems. These aspects were essential for the success of the project. Finally, I have to say that I feel honoured by all the trust you have placed in me, especially during the difficult field work in Portugal.

Secondly, I really want to thank all the staff at Edinburgh Napier University, who always made me feel very welcome, even when I was arriving and disappearing in a few days period, due to the frequent travels between Portugal and Scotland! Very special thanks to Callum Whyte, Elisa Capuzzo and Fiona Culhane for the great atmosphere in our Office. I am always thinking about that coffee smell and the rich selection of groceries in the table! I cannot forget Sabine Schäffer and Estela Romero, who during their short-stay in Edinburgh, turned normal days into really happy days. Other very special thanks to Dr. John Kinross, who gave me precious help during laboratorial work. He brings hope when everything else seems to fall apart in the lab. He is definitely an inspiration to all students. Finally, but not less important, I want to express my gratitude to Dr. John Icely and Brugo Fragoso for the help during the experimental procedures.

I could not end these acknowledgements without mentioning the importance of the lecturers of my first degree, Environmental Biology in the Faculty of Sciences of the University of Lisbon, especially Dr. Maria Teresa Rebelo and Dr. Henrique Cabral, who enthusiastically support my ideas of doing a PhD.

All in all, it would not have been possible to go through this long process without the support of the most special people in my life: my family, Pedro, all my precious friends and Boris, my cat pal. They managed to keep my emotional and mental health in place. I do have to apologize for all my absences.

This project was funded by a PhD grant from the Portuguese Foundation ‘Fundação para a Ciência e a Tecnologia (FCT)’ – POCI 2010- SFRH/BD/21525/2005 and initial studentship (from October to December 2005) from Edinburgh Napier University. It also received support from the European Framework 6 specific targeted research project ECASA (DG Fish Contract 006540).



## Summary

Mathematical modelling approaches have been widely used to evaluate the capacity of an ecosystem to assimilate anthropogenic wastes. This is essential to develop sustainable management strategies and for the prevention of eutrophication. This project aimed to assess the importance of the benthic-pelagic interactions in Ria Formosa and to develop a simple biogeochemical model for the management of nutrient inputs. This was done by adapting the simple version of the CSTT model, for pelagic eutrophication, to the system and by adding a benthic primary producer, the microphytobenthos (MPB), which was previously indicated as one of the main components of the system.

This research project has three main parts: 1) field work that provided context and data for model testing; 2) experimental work, which aimed at evaluating key parameters of the system to be used in the modelling approach; 3) model development work that was used to test hypotheses and provided a synthesis of ecological achievements.

An initial assessment of the optimal methodology for MPB chlorophyll extraction was carried out to implement a strategy for an accurate chlorophyll measurement. The MPB temporal, spatial and vertical variability was investigated. The complex temporal pattern revealed a small influence of seasonality. However, phytoplankton was found to have a much more important seasonal component. The most important component of the MPB variability was found to be the small and large scale spatial variability, which explains around 61% of the total variance. MPB was also found to be the most important source of chlorophyll to the lagoon system, contributing around 99% of the total chlorophyll.

The experimental approach carried out to investigate the yield of MPB chlorophyll from nutrients, which was previously considered to be one of the most important parameters of the CSTT model for phytoplankton, revealed interesting results. Estimates were found to be larger than the values used for phytoplankton.

The development process of the biogeochemical dCSTT-MPB model allowed the investigation of the importance of several processes. Pore water nutrients were found to be essential to support the large MPB community. Moreover, MPB cells were also found to have a large impact on the pelagic chlorophyll concentrations by re-suspension. The model was able to predict concentrations in the appropriate range of values observed in the lagoon. However, the temporal pattern is still weakly simulated and improvements are still required.

**Keywords:** microphytobenthos, spatio-temporal variability, coastal lagoons, eutrophication, yield, Water Framework Directive, dCSTT model.

# CHAPTER 1

---

General Introduction

---

## 1.1. Primary Production

### 1.1.1 Photosynthesis

The earliest microorganisms (organisms of microscopic size) are called primary heterotrophs (Gr. *Heteros*: another; *trophos*: feeder) because they depended on the environment for nutrition (Hickman *et al.*, 2001). These organisms evolved as the chemical changes on Earth provided larger quantities of nutrients in the prebiotic soup. These earliest organisms were probably similar to bacteria of genus *Clostridium* (Hickman *et al.*, 2001). When nutrients started to decrease, cells that were able to convert precursors to a required nutrient by having enzymatic activity were in a position of selective advantage. Autotrophy (Gr. *autos*: self; *trophos*: feeder) evolved from the capacity of utilizing proteins for catalytic functions in the form of photosynthesis (Hickman *et al.*, 2001).

Photosynthesis is one of the most important processes on Earth. During photosynthesis photoautotrophic organisms, or primary producers, are able to use radiant energy to convert simple molecules (carbon dioxide and water) into complex organic molecules that can be used as sources of energy and molecular building blocks (Raven *et al.*, 1999). Besides this, photosynthesis releases oxygen. This is the most important source of oxygen to our oxidative atmosphere and is crucial to cellular respiration (Williams *et al.*, 2002).

The light energy has to be absorbed first in order to be used by a living system. The substance that does this is called pigment. Most pigments can only absorb light within certain wavelengths following a specific pattern. This is known as the absorption spectrum (Figure 1.1, Raven *et al.*, 1999). The action spectrum of photosynthesis reveals the responsible pigment for the process by the similarity between the action spectrum and the absorption spectrum. In this context, it is clear that chlorophylls are the principal pigments, especially chlorophyll *a* (chl *a*).

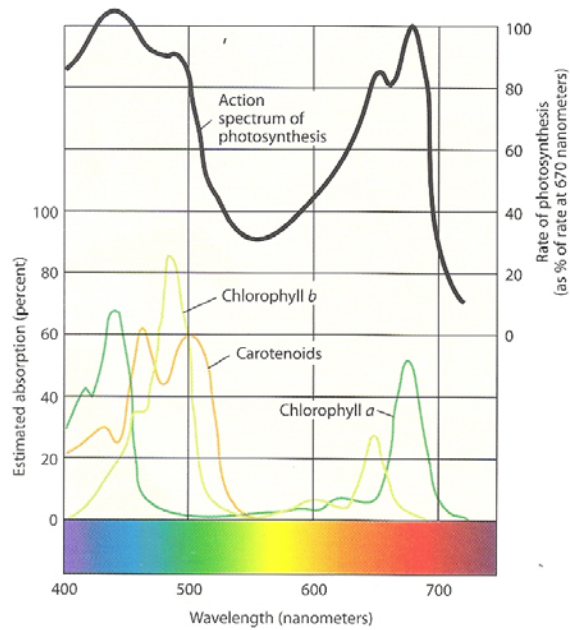


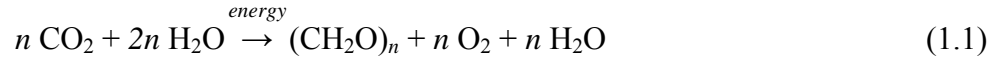
Figure 1.1 - Action spectrum of photosynthesis and the absorbance spectrum of several pigments according to the wavelength in nm (Raven *et al.*, 1999).

The main photosynthetic pigments are the chlorophylls, the carotenoids and the phycobilins and each group has several kinds of molecules (Hall and Rao, 1999). Chlorophyll *a* is essential for the oxygen-generating photosynthesis and occurs in all photosynthetic eukaryotes and cyanobacteria. The other pigments are called accessory pigments and their role in the process is either helping to collect light energy or protecting chlorophyll from damage (Raven *et al.*, 1999). All these pigments can absorb light in the visible band (400 to 700nm). This band can be called photosynthetically available radiation (PAR) and corresponds approximately to 40-50% of the total radiation at sea level (Kirk, 1994). There are other organisms that do not fit with what is described above and these are photosynthetic bacteria, other than cyanobacteria. These organisms do not produce oxygen since they have bacteriochlorophyll (purple bacteria) or chlorobium chlorophyll (green sulfur bacteria) present as their principal pigment (Raven *et al.*, 1999). They are able to absorb light outside the visible band and are associated with extreme conditions like frozen lakes (Karr *et al.*, 2003) and lakes with high concentration of sulphate (Tonolla *et al.*, 2005).

The photosynthetic process includes light and dark reactions. In the light reaction, light energy is used to form ATP (Adenosine Triphosphate) from ADP (Adenosine Diphosphate) and to reduce  $\text{NADP}^+$  (Nicotinamide Adenine Dinucleotide Phosphate) to NADPH (Nicotinamide Adenine Dinucleotide Phosphate-Oxidase) with release of oxygen and hydrogen (from the molecule of water) (Williams *et al.*, 2002).

During the dark reaction the energy of ATP and the reducing power of NADPH is then used to promote the conversion of CO<sub>2</sub> into organic compounds (carbohydrates) in a process called Calvin cycle (Williams *et al.*, 2002).

Thus, the overall reaction of photosynthesis is:



### 1.1.2 Limitations of Photosynthesis

The pelagic domain can be divided vertically in relation to the penetration of light in several zones. The most important for this work is the euphotic (Gr. *eu*: good, well; *photos*: light) zone which is, according to the European Environment Agency, “*the upper, illuminated zone of aquatic ecosystems: it is above the compensation level and therefore the zone of effective photosynthesis*” (EEA, 2006). The compensation point is when the respiration balances photosynthesis (Figure 1.2). Respiration can be seen as the reverse reaction of photosynthesis and involves the breakdown of complex molecules with consumption of oxygen, production of carbon dioxide, water and energy. This is the process from which cells can take the energy they need. It is clear that the community of benthic algae has a geographical restriction, since they can only develop in shallow areas (Nybakken, 1997).

Photosynthesis has a clear variation with illumination as represented in Figure 1.2, by the photosynthesis-irradiance (P-I) curve (Dring, 1992). The amount of respiration at low light intensities overcomes photosynthesis until the light compensation point ( $E_c$ ) and photosynthesis increases until a maximum is reached –  $P_{max}$ . When photosynthesis becomes light saturated ( $P_{max}$ ), the primary producers cannot use any more light because enzymes cannot act fast enough to process light (Parsons *et al.*, 1984). The saturation onset parameter ( $E_k$ ) represents the saturating irradiance, i.e., the point at which the extrapolated initial slope ( $\alpha$ ) intercepts  $P_{max}$ . When organisms are exposed to light intensity above the point at which they are light saturated, the P-I curve may show a decrease in the photosynthetic rate. This is called photoinhibition, which is a state of physiological stress and involves damage of some components of photosystems (especially Photosystem-II) (Adir *et al.*, 2003).

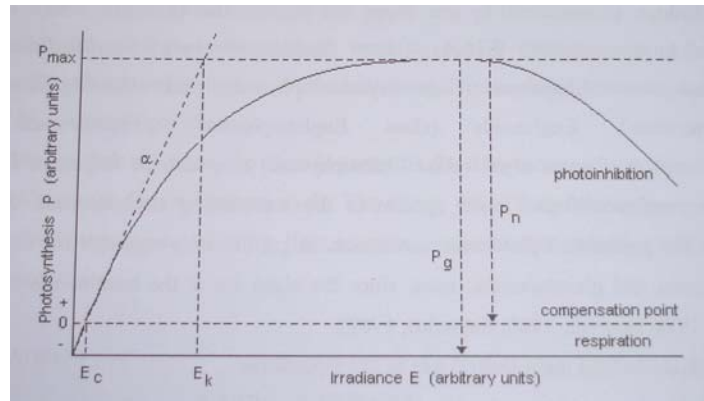


Figure 1.2 – Photosynthesis – Irradiance (P-I) curve.  $P_{max}$  represents the maximum photosynthesis,  $P_g$  the gross photosynthesis (the total production due to photosynthesis) and  $P_n$  the net photosynthesis (deducting the respiration to gross photosynthesis). From Parsons *et al.*, (1984).

The solar radiation that reaches the Earth's surface is different along the planet, decreasing from the equator towards the poles. This will influence the primary production and consequently the biomass of organisms. However, light is not the only factor regulating primary production. There must also be nutrients in a sufficient concentration. If all the conditions required are optimal, a bloom of photosynthetic organisms can occur (Summerhayes and Thorpe, 1996). So, for example, in temperate regions two peaks can be observed: one during spring, when the light intensity increases and there are nutrients that were accumulated during winter and another in autumn, after the breakdown of the thermic stratification (when it occurs given that is not a general occurrence) and induced resuspension of nutrients (Nybakken, 1997).

Primary production in seawater can be limited by low concentrations of some essential elements, such as nitrogen, phosphorus, silicate, iron and manganese (McLusky and Elliott, 2004). Other nutrients are also required but are usually in excess, so they are not limiting. Redfield *et al.* (1963) indicates that photosynthetic organisms from seawater produce biomass with a mean C:N:P ratio of 106:16:1 (the Redfield Ratio by atoms). The proportion of nutrients absorbed by these aquatic organisms and the C:N:P ratio may vary between species (Neill, 2005). The N:P ratio of 16:1 corresponds approximately to the average ratio consistently found in the sea for nitrogen and phosphate. Therefore the uptake of nutrients with a certain ratio influences the chemical structure of organisms (Falkowski and Davis, 2004). A direct connection exists between the sea chemistry and the living process. The residence time of nitrogen and phosphorus is very high and about one order of magnitude larger than the circulation time, so this global average is not surprising (Falkowski and Davis, 2004).

Variation in the stoichiometry of dissolved inorganic nutrients may predict which nutrient is limiting. As stated in the Liebig's Law of the Minimum, the growth is not controlled by the total amount of resources, but by the scarcest one. The plant growth can only be improved by increasing the amount of the limiting nutrient. However, even if the Redfield ratio is achieved, and there is no limiting nutrient, the maximum growth rate may not be achieved because there may be other factors controlling the growth, such as light (Tett *et al.*, 1985), as stated before.

Another factor that can control biomass is grazing (which means consumption of primary producers by herbivores). Generally, there is a strong link, in terms of positive correlation, between the total biomass of the primary producers and the biomass of the grazers. A bloom of phytoplankton, for example, may lead to a high increase in grazers' biomass. However, this is not a simple process. The herbivores have preferences, so they will add some pressure on specific species, allowing others to increase their biomass. Moreover, species evolve and 'anti-grazers strategies' have been developed, in terms of form, size, chemical composition or release of inhibiting exudates (Granéli *et al.*, 1993). These strategies have costs and may result in smaller growth rates. Some important grazer groups of phytoplankton are copepoda and rotifera. Within the benthic community, the grazers may be molluscs like bivalves and gastropods, or may include polychaetas.

Summarizing, there are two kinds of controls of photosynthetic organisms within any aquatic system: bottom-up and top-down controls. Bottom-up control promotes the growth of the organisms (mainly sunlight and nutrients); top-down control regulates biomass by grazing or predation.

### 1.1.3 Primary Producers

The primary producers are widely diverse and some are just now being identified. It is possible to find these organisms almost everywhere, from the bacterial species in a lake to a big tree in a garden. However, in this work attention will be given to 2 groups that exist and are very relevant to coastal dynamics: the phytoplankton and the microphytobenthos (Serpa, 2005; Tett *et al.*, 2003; Newton *et al.*, 2003; Underwood and Kromkamp, 1999).

The **phytoplankton** (Gr.*phytos*: plant; *plankton*: drifting) is responsible for most of the primary production in the oceans. They provide food that support direct or indirectly

the animal population in the open sea (Jeffrey *et al.*, 1997). There are tens of thousands of species, characterized by size, shape and pigmentation (Jeffrey *et al.*, 1997). The phytoplankton consists of microscopic unicellular algae, however some may form colonies. The principal groups are diatoms (Class Bacillariophyceae), dinoflagellates (Class Dinophyceae) and coccolithophores (Class Prymnesiophyceae) (Jeffrey *et al.*, 1997). Euglenophytes (Class Euglenophyta), green algae (Class Chlorophyceae) and cryptomonads (Class Cryptophyceae) may also be important in coastal waters (Loureiro, 2006). Sometimes, when the conditions are favorable, population explosions may occur, an event called bloom. Blooms of dinoflagellates are well known and can produce a change in the colour of the water, producing a red tide. Succession of phytoplanktonic species may be observed in response to changes in environmental conditions (McLusky and Elliott, 2004). During an episode of water column stratification, species that can swim to zones with favorable conditions of light and nutrients will benefit in relation with others (Casas *et al.*, 1999).

**Microphytobenthos** (MPB) are unicellular microalgae and cyanobacteria that live in the bottom of aquatic systems. Some of each may form chains of cells that distinguish from macroalgae because the latter have differentiated tissues and grow from an embryo. Their primary productivity is very high, estimated by Cahoon (1999) as about  $5 \times 10^8$  grams carbon per year. The contribution can be up to 25% of the total annual primary production (Colijn, 1982; Colijn and de Jonge, 1984) or even larger, depending on the intertidal flats characteristics. Therefore, the MPB are a very important component of many marine ecosystems, especially intertidal and shallow systems (Guarini *et al.*, 1998; MacIntyre *et al.*, 1996; Morris, 2005; Underwood and Kromkamp, 1999). There are several factors that may affect the productivity, such as temperature, light availability and emersion period, as well as dynamic factors such as the concentration of nutrients (Bartoli *et al.*, 2003; Blackford, 2002; Migné *et al.*, 2004; Perkins *et al.*, 2003; Serôdio *et al.*, 2005; Sundbäck *et al.*, 2000). MPB live and photosynthesize on the surficial sediment, but under certain conditions (strong winds and currents), can be easily suspended into the water column (De Jonge and Van Beusekom, 1992; Irigoien and Castel, 1997; Koh *et al.*, 2007). They may represent up to 50% of the total microalgal chlorophyll present in the water column (De Jonge and Van Beusekom, 1992). An evidence of this is the presence in the water column of benthic (*Navicula* sp.) and epiphytic diatoms (*Melosira* sp.; Irigoien and Castel, 1997). MPB are an important source of food for grazers (Defew *et al.*, 2002; de Jonge and Van



Beusekom, 1992; Kromkamp *et al.*, 1998) such as sediment (e.g. *Nereis diversicolor*) and surface (e.g. *Hydrobia ulvae*) dwellers. Microphytobenthos have a high surface area in relation to volume, which allow them to have a rapid uptake of nutrients and a fast growth rate (Rosenberg and Ramus, 1984; Hein *et al.*, 1995).

The main groups of microphytobenthos are diatoms, dinoflagellates and cyanobacteria. The classification of these groups is the subject of discussion across the scientific community because of the development of molecular techniques that introduce more information about phylogeny. According to the classification proposed by Throndsen *et al.* (2007), diatoms and dinoflagellates belong to the Eukarya Domain and cyanobacteria to the Bacteria Domain. Diatoms are classified as being part of the Division Heterokontophyta, Class Bacillariophyceae. Dinoflagellates are considered to be part of the Division Dinophyta, Class Dinophyceae and cyanobacteria are classified as part of the Division Cyanophyta, Class Cyanophyceae. Diatoms are strongly dependent on silica, because they have an outer shell made of silica. They are often the dominant group, adding a golden coloration to the sediment (Edmunds *et al.*, 2004).

Diatoms secrete mucopolysaccharides (mucilage), forming a network of extracellular polymeric substances (EPS) in the sediment (Figure 1.3). The biofilm that consists of cells and mucilage is an important source of carbon for the benthic community and also contributes to the protection against desiccation (Tolhurst *et al.*, 2003). These EPS are water soluble (Perkins *et al.*, 2003) and known to stabilize the sediment by trapping new sediment particles and affecting the permeability of the sediment (Hedtkamp, 2005; Lundkvist *et al.*, 2007; Martins-Loução, 2003). EPS are secreted to help in the process of mobility (De Brouwer and Stal, 2001). However they may also result from an overflow of the metabolism due to nutrient limitation during photosynthesis (Blanchard *et al.*, 2000). Underwood and Paterson (2003) indicated that when cells are experiencing nutrient limitation, they channel the excess energy into carbon production. This process allows cells to maintain the electron flow during photosynthesis without damaging the structures. The production of EPS is also larger if cells use  $\text{NH}_4^+$  instead of  $\text{NO}_3^-$ , because the energy used to reduce nitrate is not necessary and it is transferred to carbon production (Underwood and Paterson, 2003). EPS carbohydrates can be extracted from the sediment with several reagents and measured as glucose equivalents (Underwood *et al.*, 2005).

The stability of sediments is influenced by several physical and biological processes. The biological influence includes the existence of EPS, but also bioturbation,

biofiltration or faeces excretion (Tolhurst *et al.*, 2003). Underwood and Paterson (1993) suggested that the elimination of biological activity from the sediment increased its stability due to compaction. This process of stabilization has been described for both intertidal and subtidal systems and for sand and mud (Hedtkamp, 2005; Yallop *et al.*, 1994). The physical influence on the stability of sediments is related to the substrate mineralogy, water content, particle size, shape and density. It is considered that the more important influences are EPS content and water content (Tolhurst *et al.*, 2003). Water content is probably the only one affecting sediment stability in a short time scale, since it changes during a tidal cycle with emersion and immersion.

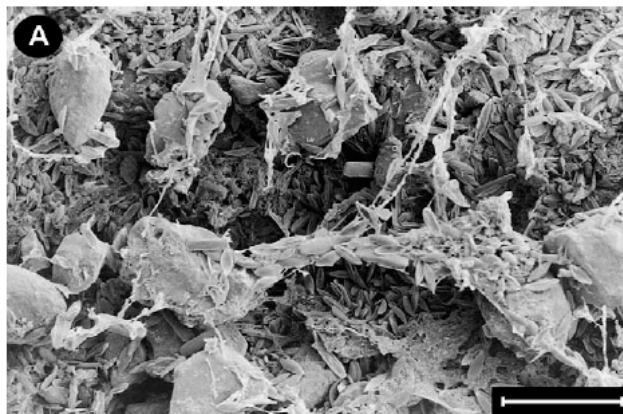


Figure 1.3 – Low-temperature scanning electron micrographs of the surface intertidal sediments, showing high densities of cells embed in a matrix of EPS (From Jesus *et al.*, 2005).

Although EPS and water content are pointed out (Hedtkamp, 2005; Lundkvist *et al.*, 2007) as the relevant factors affecting sediment stability, several recent studies showed that stability is poorly correlated with these parameters, but it is instead linked to chlorophyll *a* (Defew *et al.*, 2002; Paterson *et al.*, 2000). De Brouwer *et al.* (2002) found that the effect of EPS on sediment stability is stronger in the presence of living algae, when compared with only EPS in absence of cells. Tolhurst *et al.* (2003) showed that sediment stability is primarily controlled by diatom migration instead of EPS or water content, which did not appear to be significant in their studies. This subject is still controversial and more research needs to be done in order to clarify these processes.

Microphytobenthos are characterized by their high levels of heterogeneity, both spatial (Brotas and Plante-Cuny, 1998; Jesus *et al.*, 2005; Seuront and Spilmont, 2002) and temporal (Cartaxana *et al.*, 2006; Easley *et al.*, 2005). Therefore it is important to study their distribution at different scales, from centimetres to kilometres and from minutes to years.

## 1.2 Coastal Lagoons

Coastal lagoons are shallow aquatic ecosystems that develop at the interface between coastal terrestrial and marine ecosystems, and are within transitional units which are normally called ecotones (Gönenç and Wolflin, 2005). They are commonly found on coasts with low to moderate tidal ranges. They occupy about thirteen percent of the total world's coastline (Joint Nature Conservation Committee, 2007). They are usually parallelly elongated to the general trend of the coastline and separated from the open sea by barriers (Joint Nature Conservation Committee, 2007). These barriers are frequently sandbanks or shingle. By existing at the interface of the terrestrial and marine environments, these lagoons show a wide range of geographical and ecological variation (Gönenç and Wolflin, 2005; Joint Nature Conservation Committee, 2007). The physical, chemical and biological components of ecotones have a linear development on a large extension that can go to tens of kilometers and usually a short transversal area of a few meters (Gönenç and Wolflin, 2005). One of the characteristics of the coastal lagoons is the lighted bottom and the high effect of winds in the water column, due to the shallowness. The wind affects the entire water column and promotes the resuspension of materials, nutrients and small organisms from the sediment (Figure 1.4; Gönenç and Wolflin, 2005).

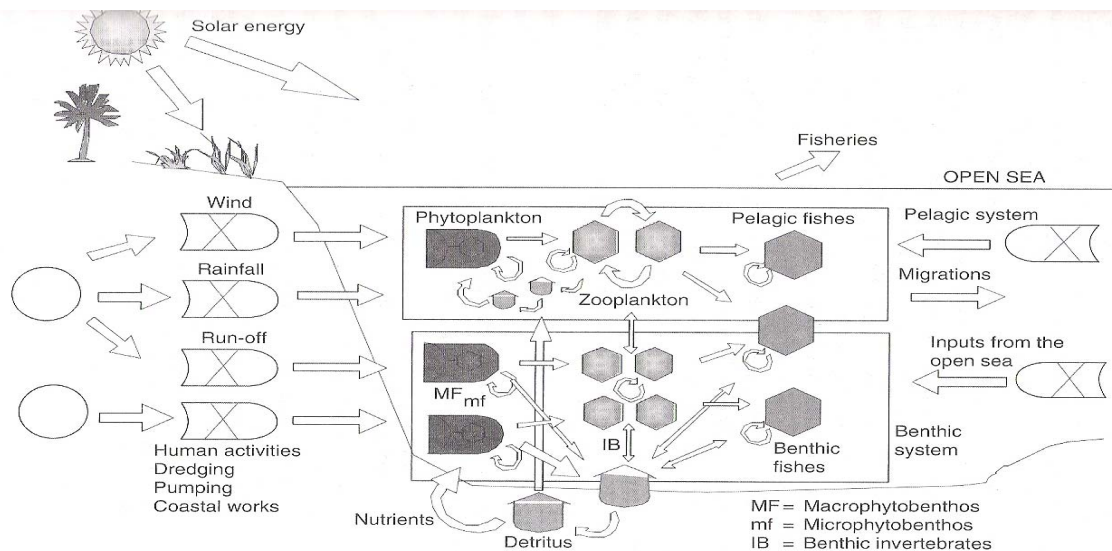


Figure 1.4 – Diagram showing the main components of a coastal lagoon and its relationships (from Gönenç and Wolflin, 2005).

Coastal lagoons are very valuable components of coastal systems. Historically, they have been one of the preferred areas for human settlement and provide excellent

opportunities for tourism, fisheries and other aquatic products. They also have a relevant role on animal ecology. They are important nursery areas for several species.

The concept of sustainable management of lagoons is often either not clearly understood nor applied (Gönenç and Wolflin, 2005). In fact, deterioration of these environments is becoming more evident due to issues such as dissolved oxygen deficits, turbidity, aquatic toxicity, odours, impacts on benthic animals, fish mortality (Gönenç and Wolflin, 2005).

Lagoons are also known by their highly sensitive areas called wetlands, in the exact transition from landscape to waterscape. Wetlands vary greatly because they are present in a wide range of local ecosystems and distributed across continents (inland wetlands) and at the land/sea interface (coastal wetlands). Their variability is caused by regional and local natural differences such as soil composition, topography, climate and others like anthropogenic impacts, which may influence some of the aspects referred to before (EPA, 2007). About one quarter of the global wetlands are in the coast (Gönenç and Wolflin, 2005).

There is an increasing need to manage these environments correctly, in a way that the needs of today are met and the future needs are not compromised. This is called sustainability and it is the only solution to keep the socio-economic and ecological system healthy in the lagoon (Gönenç and Wolflin, 2005). Sustainable management should be achieved for the whole area and for a long-term timeframe using the best available information, knowledge and tools, like models. One of the most common problems encountered in coastal lagoons is the nutrient loading caused by sewage and the run-off of enriched water (from agriculture or golf courses), for example. It is important to determine the problems or threats to the system so that a correct and efficient sustainable management is possible.

### **1.2.1 Nutrient cycles**

In order to develop the appropriate management strategies of coastal lagoons, a good understanding of the nutrient cycles is needed.

#### **1.2.1.1 Nitrogen**

Nitrogen is a very important nutrient because of its key role in the regulation of primary productivity. The most important forms are ammonium/ammonia ( $\text{NH}_4^+ / \text{NH}_3$ ), nitrate ( $\text{NO}_3^-$ ) and nitrite ( $\text{NO}_2^-$ ), altogether constituting DIN (dissolved inorganic nitrogen) which can be used by phytoplankton for growth or bacteria as an electron receptor (Gönenç and Wolflin, 2005). Ammonium is preferentially taken up by phytoplankton, compared with nitrate, since its oxidation state is equivalent to the cellular nitrogen (Gönenç and Wolflin, 2005) and so, less energy is needed for assimilation. In shallow waters, larger organisms than phytoplankton have a large storage capacity for nitrogen and therefore their dissolved concentrations may be smaller.

### *Nitrification*

Nitrification is the process of transformation of ammonium to nitrate in two steps (Figure 1.5), first to nitrite and afterwards to nitrate (under aerobic conditions), by

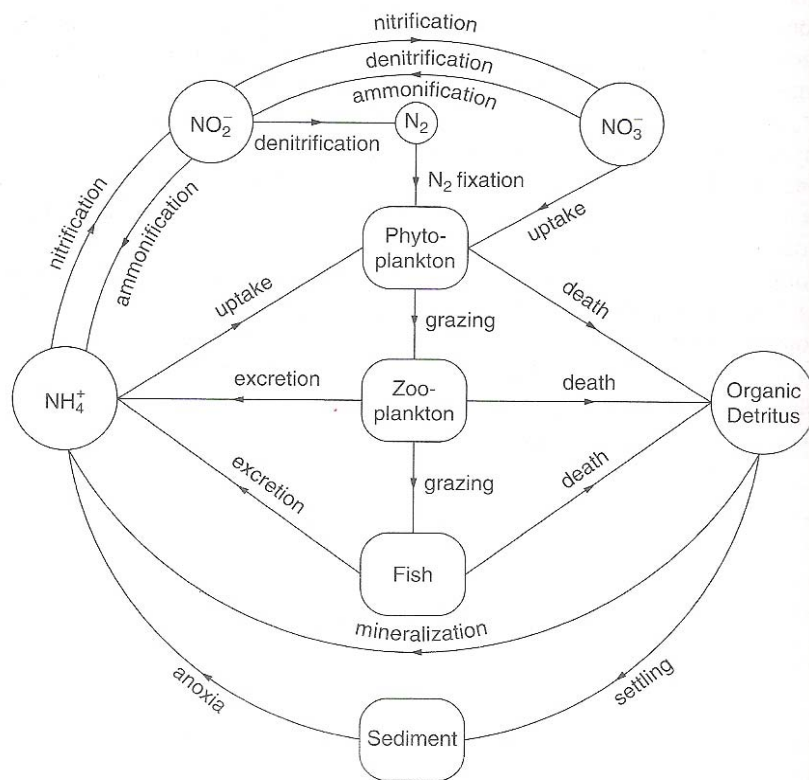


Figure 1.5 – Nitrogen cycle (from Gönenç and Wolflin, 2005)

microorganisms. This process takes place both in the water column and in the sediment. However, it is very limited in the water column. For example, the nitrification rates in coastal waters may vary from  $0.001$  to  $0.1 \mu\text{mol.l}^{-1}.\text{h}^{-1}$  and in the

sediment rates may vary from 30 to 100  $\mu\text{mol.m}^{-2}.\text{h}^{-1}$  (Gönenç and Wolflin, 2005; Fasham, 1984). These rates are influenced by several factors, one of which is the temperature, the nitrification rates are larger for temperatures from 25 to 35 °C.

### *Denitrification*

Denitrification is the process of reduction of nitrate to nitrogen gas under anoxic conditions. This process acts by removing part of the dissolved available nitrogen and may act as a buffer to eutrophication. This process is also temperature dependent and its rate increases as the temperature increases. Recent developments have shown that nitrogen gas can also be directly produced by the anaerobic oxidation of ammonium, a process called anammox ([http\\www.anammox.com](http://www.anammox.com)), according to the following equation:



The nitrate available for denitrification in the sediment comes almost exclusively from the nitrification process. Diffusion of nitrate from the water column is also a possibility. The concentration of this nutrient in the sediment is normally 3 to 4 times larger than in the water column (Gönenç and Wolflin, 2005).

The benthic algae and macrofauna have been shown to influence denitrification rates in the sediment by changing the oxygen and nitrate concentrations (Seitzinger, 1988). Seitzinger (1988) has also given values of denitrification rates in estuarine and coastal sediments from 50 to 250  $\mu\text{mol N. m}^{-2}.\text{h}^{-1}$ .

### *Ammonification*

The most accepted process of reduction of nitrate in shallow marine sediment is denitrification. However, it has also been shown that the reduction of nitrate to ammonium is another possibility (ammonification ; Gönenç and Wolflin, 2005). This process also occurs under anoxic conditions.

### *Mineralisation of Organic Nitrogen*

Mineralisation is the process of transformation of organic compounds into ammonium. It is assumed that excretion is the largest contribution of ammonium to the

water column, while in the sediment is the decomposition of organic matter. This is because in shallow systems, the organic matter is mineralised mainly in the upper layers of the sediment due to the rapid settling rates (Seitzinger, 1988). Mineralisation in the sediment can occur under oxic (0-5mm depth) and anoxic conditions (Gray and Elliott, 2009). This process is also temperature dependent, showing a maximum in the summer.

Most of the primary production is therefore supported by nutrient recycling rather than nutrient inputs alone. In some shallow systems the nutrient recycling may be responsible for 20 to 80 % of the phytoplankton nitrogen requirements (Gönenç and Wolflin, 2005).

#### *Nitrogen release from sediment*

Most of the nitrogen recycled in the water column comes from the sediment by diffusion of ammonium or nitrate (Gönenç and Wolflin, 2005). As stated before, inorganic compound concentrations are seasonal in the sediment, so during the summer it is mostly ammonium that is released, when the mineralisation rate is high and the aerobic zone small, due to the high temperatures. During the winter, nitrification is high and the aerobic zone is larger and therefore mainly nitrate is released (Gönenç and Wolflin, 2005).

Fasham (1984) reported ammonium fluxes of 50 to 800  $\mu\text{mol.m}^{-2}.\text{h}^{-1}$  for estuarine and coastal sediments. Kemp *et al.* (1990) reported fluxes of about 46  $\mu\text{mol.m}^{-2}.\text{h}^{-1}$  in April and 753  $\mu\text{mol.m}^{-2}.\text{h}^{-1}$  in August within temperate areas.

#### 1.2.1.2 Phosphorus

Phosphorus is another important nutrient and can be limiting to growth. However the quantities needed are much smaller than the amounts of nitrogen or silicon. There are several sources of phosphorus in coastal systems. Most of domestic wastewaters are rich in phosphorus because commercial cleaning products contain it. Besides, phosphorus is used as fertilizer in agriculture.

Dissolved phosphorus includes orthophosphate ( $\text{PO}_4^{3-}$ ), polyphosphates, organic colloids and phosphorus combined with adsorptive colloids and low-molecular-weight phosphate esters (Gönenç and Wolflin, 2005). The phosphorus cycle is very complex (Figure 1.6).

### *Uptake of phosphorus*

Dissolved inorganic phosphorus (DIP or orthophosphate) is the only compound assimilated by plants, algae or bacteria (Gönenç and Wolflin, 2005). For this nutrient, algae have an advantage of uptake over bacteria under low concentrations, since they have a larger storage capacity.

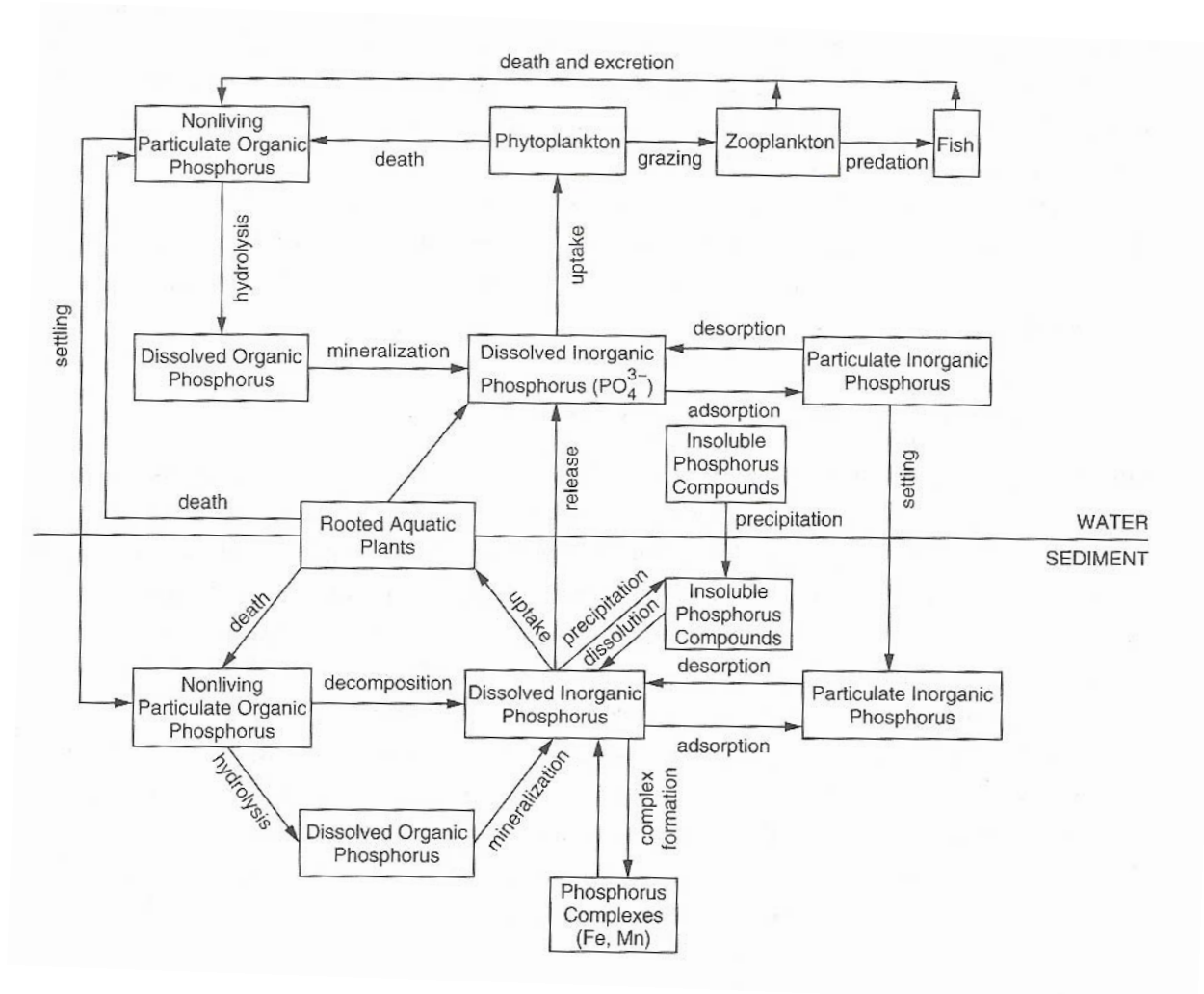


Figure 1.6 – Phosphorus cycle (Gönenç and Wolflin, 2005).

### *Mineralisation*

Part of the phosphorus released during respiration or death of phytoplankton is already in the inorganic form. However, some is in the organic form and has to be mineralised. This process occurs mainly in the sediment of the shallow systems and the settling rate is high. After mineralisation the phosphorus is either released or buried into deeper layers.



### *Phosphorus release from sediment*

Exchange across the water-sediment interface is regulated by mechanisms associated with water-mineral equilibria, microbial activities and enzymatic reactions. Phosphate adsorbs rapidly under aerobic conditions. The release of the adsorbed phosphorus from the sediment is a process that is physico-chemical dependent. It depends on factors such as temperature, pH or redox potential. During the summer the redox potential tends to be low and the pH value is high, which causes the release of the compound. During the winter, the phosphorus may be kept in the sediment because the redox potential is high and the pH should be neutral (Gönenç and Wolflin, 2005). During the summer, Nielson and Cronin (1981) reported releasing rates of  $-15$  to  $50 \mu\text{mol}\cdot\text{m}^{-2}\cdot\text{h}^{-1}$ . The most relevant source of phosphorus to the water column is the surface flows because normally phosphate binds to the sediment.

#### 1.2.1.3 Silicon

Silicon is considered a minor nutrient. However, it is very important because it is part of the external structure of diatoms, one of the most relevant groups of coastal phytoplankton and microphytobenthos. It is needed in large quantities and it can be limiting for algae that need this compound.

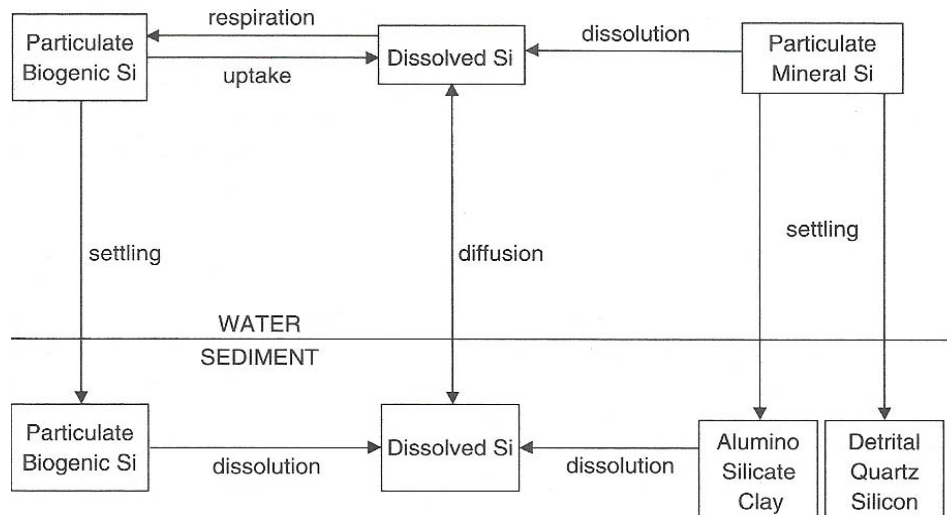


Figure 1.7 - Silicon cycle (Gönenç and Wolflin, 2005).

There are three forms of silicon in coastal waters: detrital quartz, aluminosilicate clays and dissolved silicon (Gönenç and Wolflin, 2005). There is no organic form of silicon and therefore the cycle is much simpler than the phosphorus cycle (Figure 1.7).

The dominant input of dissolved silicate occurs as riverine inputs, as a consequence of weathering reactions. The rate of chemical weathering depends on physical conditions of temperature, rainfall amount and the mineral composition of rocks. Lagoons that have minimal input of freshwater depend mainly on run-off, which may cause a decrease in the silicon concentration during dry seasons.

Species, that do not need silicon to grow may benefit from a low concentration of silicon. However, diatoms are very important in the system dynamics since they grow very rapidly, have short lifetimes, are grazed heavily and are rarely nuisance.

#### *Uptake of silicon*

Silicon is assimilated by diatoms, who need this nutrient to produce their skeletons. Officer and Ryther (1980) suggested half-saturation constants for diatoms of 0.5 to 5  $\mu\text{M}$  and maximum *in situ* growth between 2 to 4  $\text{d}^{-1}$ . Dinoflagellates, microflagellate and eukaryotic nonmotile ultraplankton (0.2 – 5  $\mu\text{m}$ ) species have small values, compared to diatoms, of less than 2.5  $\text{d}^{-1}$  of maximum growth rate. The silicon content of diatoms makes them heavy, therefore they sink. Diatoms are an important source of silicon to the sediment and reflect the productivity of the water column.

#### *Dissolution of Silicon*

The dissolution of diatom skeletons is more important as source of silicon than their decomposition by microorganisms. Moreover, Officer and Ryther (1980) suggested that the dissolution rates (chemical process) are slow compared with regeneration rates of nitrogen and phosphorus (grazers and bacteria biologically mediated regeneration). However, Fasham (1984) measured silica fluxes of 1  $\text{mmol} \cdot \text{m}^{-2} \cdot \text{h}^{-1}$  during summer in USA, which was higher than predicted.

## 1.3 Eutrophication

Eutrophication can be simply defined as the natural or man-induced process by which a body of water becomes enriched in dissolved mineral nutrients (particularly phosphorus and nitrogen) that stimulate the growth of photosynthetic organisms and enhances organic production in the water body.

Nowadays, eutrophication is instantly associated with human actions (Cloern, 2001). Simple activities or processes such as recreation, agriculture, aquaculture, animal production, sewage discharges are just some examples of why the concept of eutrophication has evolved to be linked with anthropogenic sources, since the 1800's when the problem started to be recognised (de Jonge *et al.*, 2002; McLusky and Elliott, 2004). There are coastal areas that show what is called natural eutrophication because of their local natural characteristics, like the geomorphology (e.g. percentage of subtidal and intertidal areas) or the shape of the tidal curve (de Jonge *et al.*, 2002). Some areas with low hydrodynamic energy or with other characteristics that lead to the accumulation of organic matter (such as lagoons, lakes) may be considered naturally enriched (de Jonge *et al.*, 2002). It has been accepted that eutrophication in some freshwaters is a natural consequence of the aging of lake basins (considered to be less deep and more productive along time). Nevertheless, recent studies show that this evolution of a non-impacted lake basin is not inevitable (Smith *et al.*, 2006) although it is extremely rare to find a water system without influence from human activities.

### 1.3.1 Natural Eutrophication – Upwelling

Upwelling is a phenomenon that involves the movement of water masses induced by wind. There are several types of upwelling, however the coastal eutrophication is the best known. Coastal upwelling is driven by the Coriolis Effect that is the deflection of any current of water or air to the right in the Northern Hemisphere or to the left in the Southern Hemisphere caused by the rotation of Earth (Press and Siever, 2001). So, when wind blows in the Northern hemisphere and the Coriolis Effect deflects the wind offshore, the water surface is deflected in the same direction, moving away the warm waters from the coast. Thus, deeper water (at low temperature and rich in nutrients that accumulate in deeper water layers) comes up, creating an upwelling current (Figure

1.8). Photosynthetic organisms can then utilise the new nutrients that were brought to the surface to produce organic compounds.

Areas where this event occurs have high levels of primary productivity. Since primary producers are at the base of the oceanic food chain, the high production will propagate up in the food chain. Every year, these regions are responsible for a large production of fish and influences several migrations of larger inhabitants of the ocean. Areas like the coast of Peru, Chile, Arabian Sea, western South Africa, eastern New Zealand and the California coast are known as upwelling regions (www.noaa.gov).

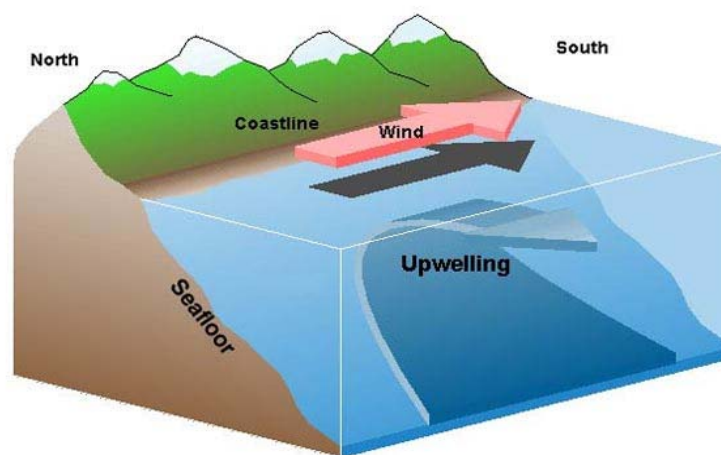


Figure 1.8 –Upwelling phenomenon in the northern hemisphere. Source: National Oceanic and Atmospheric Administration (www.noaa.gov).

### 1.3.2 Anthropogenic eutrophication

Anthropogenic eutrophication of coastal waters has been considered one of the major threats to the health of marine ecosystems for more than 30 years (Bachmann *et al.*, 2006). This phenomenon is being widely discussed and analysed all over the world and new strategies and objectives are being established in order to minimize the problem. There are several definitions for anthropogenic eutrophication. The Helsinki Commission (HELCOM, 2005) defines eutrophication as:

*“a condition in an aquatic ecosystem where high nutrient concentration stimulate the excessive growth of algae, which leads to an inbalanced function of the ecosystem”.*

Nixon (1995) defines eutrophication as:

*“an increase in the rate of supply of organic matter to the ecosystem”.*

The Urban Waste Water Treatment Directive (UWWTD) (C.E.C., 1991) define eutrophic conditions as:

*“enrichment of water by nutrients especially compounds of nitrogen and phosphorus, causing an accelerated growth of algae and higher forms of plant life to produce an undesirable disturbance to the balance of organisms present in the water and the quality of the water concerned”.*

Along several years, the definitions of eutrophication were not clear and were composed by difficult concepts. The UWWTD definition introduces the idea of “undesirable disturbance to the balance of organisms”. This concept is still being discussed and its recognition is essential. Although it is being better understood now, it is still very difficult to assess this. Undesirable Disturbance was defined as (Tett *et al.*, 2007):

*“ a perturbation of a marine ecosystem that appreciably degrades the health or threatens the sustainable human use of that ecosystem”.*

The concept of ecosystem health is not very clear. However, a new approach to assess ecosystems is emerging and can bring light to this. Nevertheless, to progress in this area it would be helpful to give a general idea about what has been recognised as the standard symptoms of anthropogenic eutrophication and where it is most likely to occur.

Some coastal areas have natural conditions that can be favorable to eutrophication, such as: zones with high input of freshwater and vertical stratification that can be nutrient depleted during the summer, with the bottom isolated from air changes; and inshore (enclosed) zones with small rates of exchange with the sea, like fjords and rias.

Regarding the symptoms of eutrophication, a cascade of events can happen (Tett *et al.*, 2007). Everything starts with the increase of dissolved nutrients in the water, which will allow primary producers to grow and to increase their biomass, resulting in a possible algal bloom. An increase in the biomass of pelagic organisms will lead to an increase of the organic matter in the water column (and a decrease of light penetration) and in the sea-bed (which can lead to a change in the balance of benthic organisms) and in deeper waters (which can lead to dangerous situations of depletion of oxygen – hypoxia and anoxia). The algal bloom may be composed by toxic algae which may result in an Harmful Algal Bloom (HAB), which may be responsible for the death of organisms at other levels in the food chain. When the bloom dies, there will be an accumulation of organic matter and a depletion of oxygen in the bottom. Besides this, when the pelagic nutrient concentration increases, a change in the balance of pelagic

species may happen, since it is likely to fuel a rapid growth of opportunistic species, which are able to uptake nutrients at a higher rate and to multiply very quickly.

Recently, Ecological Quality Objectives (EcoQOs) have been developed with the aim of helping in the assessment of eutrophication and management of the ecosystem (McLusky and Elliott, 2004; Painting *et al.*, 2005). An EcoQO is defined as “*the desired level of the Ecological Quality (EcoQ) relative to the reference level*” and EcoQ as “*an overall expression of the structure and function of the aquatic systems*” (Painting *et al.*, 2005). The reference level was defined as the level of the EcoQ where the anthropogenic influence on the ecological system is minimal. A connection between the EcoQOs and the Environmental Quality Standards (EQSs) should be kept, with EQS providing an exact value for an environmental indicator that should be used when assessing eutrophication (Tett, 2003).

A useful tool in the evaluation of eutrophic status in an ecosystem is the knowledge of its carrying capacity and assimilative capacity. These concepts went through an intemporal discussion about their definitions. Although the definitions are not perfectly established yet, there is some consensus.

Verhulst (1838) modified the Malthus model to include the idea of carrying capacity “*being the maximum population level that a given environment can support given finite resources (food, space, water, etc.)*”. This concept had several definitions for population level, ecosystem level or even biosphere level. However, a more general definition was obtained by Monte-Luna *et al.* (2004): “*carrying capacity is the limit of growth or development of each and all hierarchical levels of biological integration, beginning with the population, and shaped by processes and interdependent relationships between finite resources and the consumers of those resources*”.

Assimilative capacity (AC) is the ability of an area to maintain a “healthy” environment and “accommodate” wastes. The assimilative capacity of a system is “*a property of the environment defined as its ability to accommodate a particular activity or rate of activity without unacceptable impacts*” (GESAMP, 1986). Knowledge about the assimilative capacity of an ecosystem is essential to the sustainable management of the water body. This can be applied to mathematical models, which will be able to explore a range of loading scenarios to find which are acceptable in the system and do fit in the EcoQOs (Laurent *et al.*, 2006).

A healthy ecosystem can be defined as a system that can resist and recover from disturbance (Costanza *et al.*, 1992) and this can be assessed looking to the following

components: *vigour*, *organisation*, *resistance* to disturbance and *resilience* (Tett *et al.*, 2007). *Vigour* of an ecosystem was defined as (Tett *et al.*, 2007):

“ *its biologically-mediated fluxes of energy and materials as well as its ability to recover from disturbance by means of recolonization and population growth*”.

The fluxes of energy are illustrated in Figure 1.9 (a). The relation between production and ecosystem health is not linear and there is a need to adapt the concept regarding the coupling between production (new primary production or new organic matter) and consumption (use of the new material). This scheme deals with 3 status categories (Tett *et al.*, 2007):

- Oligotrophy: poor rate of production and it is likely to be smaller than the consumption rate; low rates of both, so any unbalance should not have a disturbing effect;
- Optimal rate of production, likely to be greater than the consumption, but the misbalance should not have an extensive disturbing effect on the ecosystem; however, may be possible to have a decay of blooms of primary producers and local hypoxia;
- Polutrophy: high rate of production, with poor coupling, which leads to disturbances like hypoxia and anoxia in sediment and deep waters.

Only the last state corresponds to undesirable disturbance if it relates to anthropogenic nutrient enrichment. Nevertheless, if a situation of nutrient enrichment is present and the primary production is increasing, there should be concern regarding the evolution of the environment, even if it is in the beginning an oligotrophic state. In addition, the ecohydrodynamics of the site should be taken into account since it characterises the effectiveness of coupling and the point when the system reaches polutrophy (Tett *et al.*, 2007). The *vigour* can be assessed simply by the annual primary production, for example (see Tett *et al.*, 2007).

The *organisation* (or *structure*) of an ecosystem deals with its biodiversity, food web and biophysical structure. This can be assessed by using for example, the Infaunal Trophic Index (ITI), AZTI Marine Biotic Index (AMBI) or Phytoplankton Community Indices (PCIs) which take into account natural, seasonal variability (Tett *et al.*, 2007). Exception is made to the assessment of the food web that is extremely complex. Modelling is one option to assess it, but is not as simple as the calculation of an index.

The concepts of *resistance* and *resilience* are illustrated in Figure 1.9 (b) (Tett *et al.*, 2007). When an ecosystem is in a situation of increasing ecological pressure, it shows a

degree of resistance by reacting up to a certain point, when drastic changes can happen. The ability and the degree to which the system recovers from the disturbance is the resilience. In a drastic case, the system may switch to a new stable state.

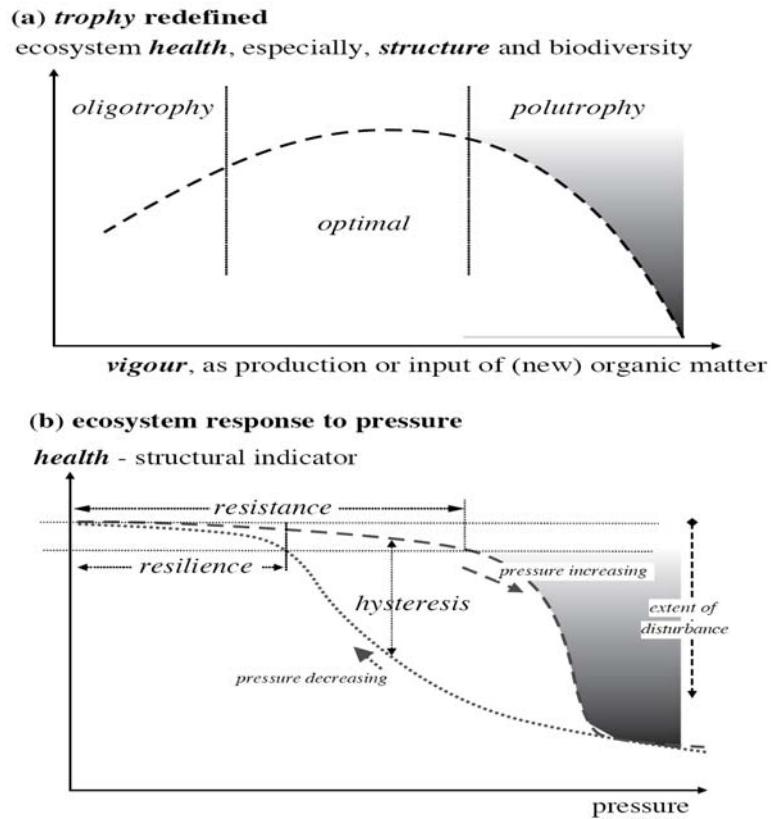


Figure 1.9 - Ecosystem Health and Undesirable Disturbance (Tett *et al.*, 2007). The figure a) relates health with vigour, showing vigour response to nutrient enrichment. Figure b) shows the response of structure to pressure. Both figures should be used together.

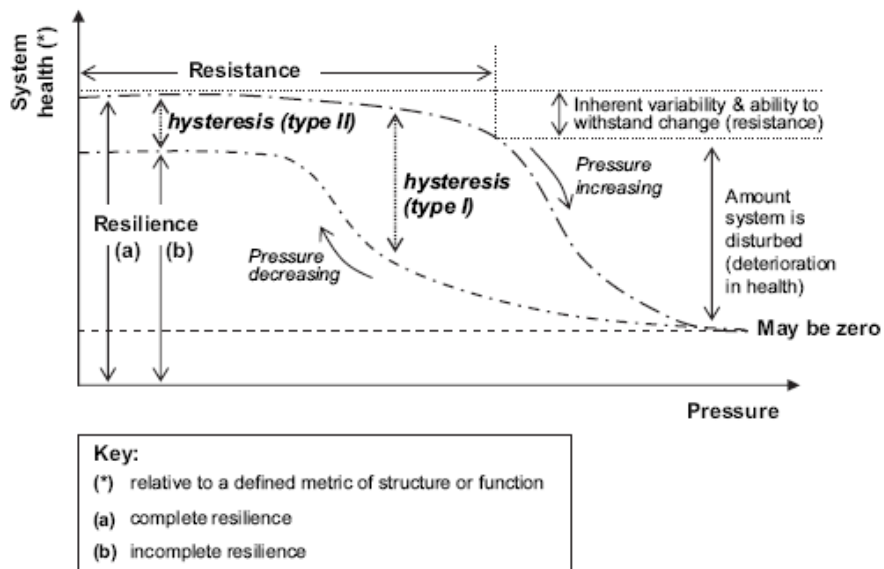


Figure 1.10 – Conceptual model of changes to the state of a system with increasing pressure (from Elliott *et al.*, 2007; revised from Tett *et al.*, 2007).



Elliott *et al.* (2007) revised the concept of resilience based on the Figure 1.9 (b) as the ‘degree of recovery, based upon a given measure, compared to the original status – complete resilience results in a return to the original level, partial resilience is the return to some lower (or higher) level’. Therefore, Elliott *et al.* (2007) consider that recovery may be incomplete and that resilience may be measured by an indicator of system health (Figure 1.10).

Tett *et al.* (2007) also suggested a list of indicators to diagnose undesirable disturbance, such as: bulk indicators, frequency statistics, flux measurements, structural indicators and indicator species. Some were already discussed above (flux measurements and structural indicators), for the others a deeper analysis of the article is recommended. They are not covered here because they are outside the scope of this work.

Applying the concepts described above implies the knowledge of the area’s conditions. The ecohydrodynamic characteristics of the zone should be known. Given this, five water types were defined by Tett *et al.* (2007). Each type will have different requirements for the assessment of eutrophication. The types are:

- Shallow clear waters, in which seabed is included in the euphotic zone; phytoplankton should be an important component of the system here;
- Optically deep mixed waters, where light can be limiting, so phytoplankton are unlikely to be stimulated by nutrient enrichment;
- Offshore stratified waters, which has a layer in the surface that is nutrient depleted; adding nutrients may stimulate phytoplankton growth;
- Regions of Freshwater Influence (ROFIs), which are characterized by high turbidity, tidal influence and a significant freshwater content with a consequent intermittent stratification;
- Regions of Restricted Exchange (RREs), which are inshore and where eutrophication risk depends on the rate of exchange with the sea.

This approach needs to be analysed jointly with the *EcoQOs* proposed by the OSPAR (OSPAR, 2001). Tett *et al.* (2007) proposed new *EcoQOs*, which reflect the *Ecological Quality Standards (EQSs)*. Previously, in the UK an operational definition of eutrophication was proposed with 10 mg.chl.m<sup>-3</sup> given as an Environmental Quality Standard (EQS) for coastal waters (CSTT, 1997).

## 1.4 Modelling

*“Analysis based on a model, expressed by a differential equation, ..., is a useful tool in putting ecological theories to a quantitative test.”*

*Riley (1946)*

Over the years, the main focus of the scientific community regarding eutrophication events was on freshwater systems (Cloern, 2001). Nixon (1995) indicates that a decade or two were necessary to apply this concept to coastal waters, so most of the mathematical modelling approaches used were strongly influenced by limnologists (Cloern, 2001). It is relatively consensual that Gordon Riley was one of the first persons to apply modelling approaches to marine environments (Riley, 1946). He created a simple model which allows predicting the values of one variable - phytoplankton biomass (P).

$$\frac{dP}{dt} = P(\mu - r - G) \quad \text{mmol phytoplankton-C.m}^{-3}.\text{d}^{-1} \quad (1.3)$$

G is the grazing pressure ( $\text{d}^{-1}$ ), r is the relative respiration rate ( $\text{d}^{-1}$ ) and  $\mu$  is the relative growth rate ( $\text{d}^{-1}$ ).

Although this model was an important achievement in model's progress and predicted values similar to observations, the model has some weaknesses. Phytoplankton have an exponential increase in biomass, because there is nothing in the model to decrease the growth rate when the finite carrying capacity is approached (Tett and Wilson, 2000). This has to be achieved using data that force the growth rate to decrease, by increasing the severity of nutrient limitation, for example (Tett and Wilson, 2000).

Recent developments have been made. Nowadays, many scientists are working in the development of several approaches to the problem (mathematical models, indicators, and indices). There is a need for indicators of ecosystem change, and modelling tools to predict these indicators, in order to determine the state of the system and the impacts suffered from phenomena such as nutrient enrichment of waters. An indicator is “*any continuous variable that points to some aspect of the state or health of an ecosystem*” (Tett *et al.*, 2007) and an index (plural *indices*) is used to express the interaction of a group of indicators or a non-dimensional variable formed from a ratio of indicators to a reference value. Some examples of indices developed in the past are the diversity

indices (e.g. Shannon-Wiener and Simpson Indices) and the richness indices (e.g. Margalef Index), as well as others on the community level such as AMBI (Borja *et al.*, 2000), used for benthic fauna.

An important indicator used to analyse the trophic status of coastal waters is phytoplankton biomass (as chlorophyll *a*; Tett *et al.*, 2007). An environmental quality standard was defined by the Comprehensive Studies Task Team (CSTT, 1997), following the precautionary principle, according to which coastal waters would be eutrophic if its summer concentration exceeded 10 mg chl.m<sup>-3</sup>.

Models are representations of the reality, using differential equations, which attempt to capture the major features of processes of a system. According to Fennel and Neumann (2004) models are “*mathematical tools by which we analyse, synthesise and test our understanding of the dynamics of the system through retrospective and predictive calculations.*” They can be used to describe parts of complex systems, such as food webs of marine systems or even ecosystems. The resolution of a model depends on the initial question and objectives. More complex models do not correspond directly to more accurate and realistic results. Complex and dynamic models imply a higher number of variables (changing in time and space) and the understanding and quantification of processes used to describe these variables. Very often the knowledge about these processes is very little. Model development has to be kept within reasonable limits and needs to be focused.

The model structure has four principal components: state variables, mathematical equations to describe processes involved in the model, forcing variables and parameters. State variables represent the elements we want to simulate. Each state variable is represented by one differential equation and described by their own processes, basically outfluxes and influxes. Mathematical equations are used to describe several processes on which the state variables depend. If we consider phytoplankton chlorophyll as a state variable, obvious processes involved would be growth, and grazing, for example. Assuming that a second state variable is a nutrient used by this phytoplankton, then we would have something in the growth mathematical formulation that would interact and affect the values of this second state variable, decreasing it, because it is being consumed by algae. Forcing variables are functions or variables that will affect the system and introduce specific variability in time and space. For example, if growth is influenced by the temperature, with the addition of a set of temperature values throughout a year, a more site-specific output will be obtained,

since, for example, it is different if the site is in the south of Portugal or in England. The same applies to irradiance. So, the mathematical equations will also define the relationship between the forcing variables and the state variables. The parameters are single values that are constant through the simulation. They may be used to introduce the volume of water of a site in the model, if necessary.

Models should be as simple as possible and as complex as necessary. According to the UWWTD definition, eutrophication has three components: nutrient enrichment, increase of plant growth and undesirable disturbances. For the first component, nutrient enrichment, there are a couple of simple models that can easily be used to simulate it. The simplest approach assesses the nutrient concentration when in equilibrium, balancing the inputs against losses from a box (*“Equilibrium Concentration Enhancement”* - ECE model; Gillibrand and Turrell, 1997). This is a screening model, it simulates the value of only one variable and it is very useful to identify sites at risk (Tett and Lee, 2005).

The ECE model is a simplification of the general Equation 1.4 for the rate of change of a variable  $Y$  in the presence of sources. This equation is an example of coupled models, since it deals with physics, biology and chemistry. In eutrophication studies, the variable  $Y$  is generally an important nutrient in plant growth, like *Dissolved Available Inorganic Nitrogen – DAIN*, symbolized by  $S$ .

$$\frac{\partial Y}{\partial t} = -\nabla \phi_Y + \beta_Y + \Gamma_Y \quad (1.4)$$

Where:

- The first term deals with physical transport, being the divergence of the flux vector ( $\phi_Y$ ), including advective and diffusive terms;
- $\beta_Y$  is the sum of the biological and chemical sources and sinks of the variable;
- $\Gamma_Y$  is the input of the variable from a farm or a river, for example.

The term  $\phi_Y$  refers to physical transport and is a conservative part of the model. Physics regulates for example position of organisms, nutrient availability and their turbulent mixing (Fennel and Neumann, 2004). The term  $\beta_Y$  refers to the sum of the non-conservative parts of the model, the biological processes such as growth.

If we consider the case of a well-mixed box of Volume  $V$  ( $m^3$ ), the divergence problem is solved and only the concentration exchanges between the water inside ( $S$ ) and outside ( $S_0$ ) the box have to be considered at a specific rate ( $E, d^{-1}$ ).

$$\nabla \phi_Y = E(S - S_0) \quad (1.5)$$

Considering the simplest case, when there is no active biological or chemical processes ( $\beta_Y = 0$ ). The nutrient input ( $\Gamma_Y$ ) is  $si$  ( $mmol \cdot d^{-1}$ ), which transformed to a concentration in order to be added to the differential equation is  $\frac{si}{V}$  ( $mmol \cdot m^{-3} \cdot d^{-1}$ ).

$$\frac{dS}{dt} = -E(S - S_0) + \frac{si}{V} \quad mmol \cdot m^{-3} \cdot d^{-1} \quad (1.6)$$

In the steady state:

$$S_{eq} = S_0 + \frac{si}{EV} \quad mmol \cdot m^{-3} \cdot d^{-1} \quad (1.7)$$

The term  $\frac{si}{EV}$  is commonly named as equilibrium concentration enhancement (Tett *et al.*, 2007).

The second component, increase of plant growth, deals with the conversion of nutrients into biomass. Gowen *et al.* (1992) proposed the use of a single parameter, the yield of phytoplankton chlorophyll from nutrient for the conversion. This parameter was then investigated by Edwards (2001). CSTT applied this parameter to convert the ECE model into the CSTT model, predicting the worst-case biomass with a very simple model (Tett and Lee, 2005).

The CSTT model (Figure 1.11) treats the study area as a well-mixed box of volume  $V$   $m^3$  exchanging water with sea at a specific rate  $E$  ( $d^{-1}$ ), like the ECE model.

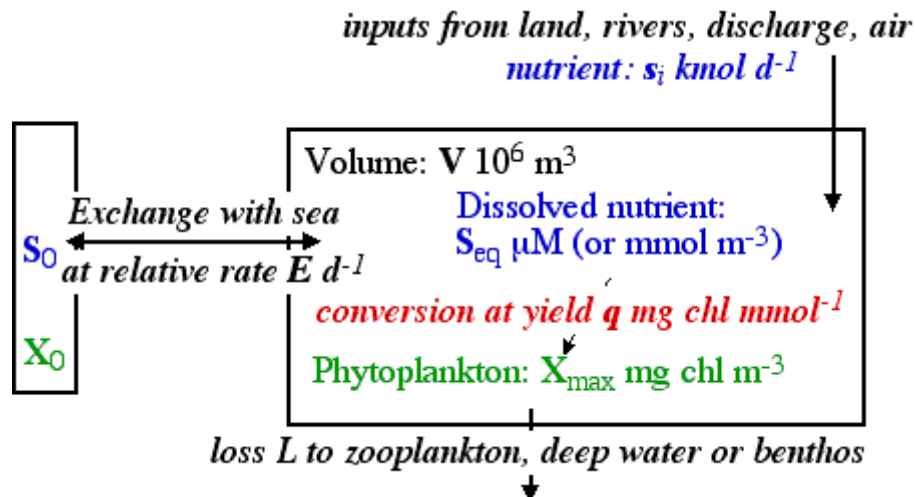


Figure 1.11 – Scheme of the simple CSTT model.

The CSTT model is as ECE model, a steady-state simplification of a dynamic model (Tett *et al.*, 2003). The dynamic model is defined by two differential equations, one for nutrients (S) and another for phytoplankton chlorophyll (X).

$$\frac{dS}{dt} = -\frac{\mu X}{q} + e \frac{LX}{q} - E(S - S_0) + \frac{si}{V} \quad \text{mmol.m}^{-3}.\text{d}^{-1} \quad (1.8)$$

$$\frac{dX}{dt} = (\mu - L)X - E(X - X_0) - \frac{F}{V}X_0 \quad \text{mg chl.m}^{-3}.\text{d}^{-1} \quad (1.9)$$

The subscript 0 refers always to the concentrations in the sea and the subscript i refers to inputs, in this case of nutrients ( $si$ ,  $\text{mmol.d}^{-1}$ ) to the box. L is the phytoplankton loss rate ( $\text{d}^{-1}$ ),  $\mu$  is the phytoplankton growth rate ( $\text{d}^{-1}$ ),  $e$  is the fraction of nutrient element content in the organic material,  $q$  is the yield of chlorophyll from nutrients ( $\text{mg chl.mmol}^{-1}$ ) and F is the volume of freshwater input ( $\text{m}^3.\text{d}^{-1}$ ).

Considering a scenario of total absence of consumption of nutrients by algae, or losses (caused by denitrification, for example), the steady-state equation is just the same as for the ECE model (Equation 1.7). In this case, and considering that the total amount of nutrients is converted to chlorophyll, the maximum chlorophyll concentration obtained is:

$$X_{\max} = X_0 + qS_{eq} \quad \text{mg chl.m}^{-3} \quad (1.10)$$

The lower value of phytoplankton chlorophyll is taken to define the minimum and the nutrient that leads to that result is considered the limiting. The maximum value of chlorophyll obtained is compared with the EQS considered by CSTT,  $10 \text{ mg chl.m}^{-3}$  in summer for eutrophic conditions, as referred previously. When using this model for eutrophication assessment, it is essential to keep in mind that it is very unlikely that a total conversion of nutrients to phytoplankton chlorophyll will occur due to important losses or lack of light for growth.

The steady state model was used for the management of nutrients and assessment of eutrophication in the United Kingdom (CSTT, 1994). The CSTT model was then applied to several sites within Europe during the OAERRE project (Tett *et al.*, 2003).

Inside the scope of the third component of the eutrophication definition, undesirable disturbances, are the consequences of the algae growth, which is the second component. These consequences may include the change in the balance of organisms. Some species or lifefoms may be more stimulated by nutrient enrichment than others and benefit from it (Tett and Lee, 2005). To deal with these questions, more complex models are needed, with 3 to 10 variables (Tett and Lee, 2005). These models are in the domain of the

biogeochemical models, i.e., element conservative (Tett and Wilson, 2000). The Fjord-Env model is an example and has been widely used in Norway for more than fifteen years (Stigebrandt, 2001). It deals with water transparency and oxygen concentration. However, as said before, an important aspect of undesirable disturbance is the balance of organisms. To study this subject it is necessary to use models with food web simulations and these models are in the domain of the ecological models. Tett and Wilson (2000) defined ecological models as “including at least one degree of freedom amongst a set of state variables with common conserved quantity”. These models can describe dynamic interactions between state variables in such a way that variations of the rates can be calculated constantly during the simulation (Fennel and Neumann, 2004). The result may be similar to what would be obtained using Lotka-Volterra equations, periodic oscillations, or even chaotic behaviour (Tett and Lee, 2005). The Lotka-Volterra model is well known as reflecting prey-predator interactions and it deals with two differential equations, one for prey population and the other for predator population (Kremer and Nixon, 1978), as presented below (Equations 1.11 and 1.12).

$$\frac{dN_1}{dt} = N_1(b_1 - d_1N_2) \quad \text{prey} \quad (1.11)$$

$$\frac{dN_2}{dt} = N_2(b_2N_1 - d_2) \quad \text{predator} \quad (1.12)$$

$N_1$  and  $N_2$  correspond to prey and predator population size,  $b$  is a constant birth rate and  $d$  is a constant death rate. The output of this model is represented in Figure 1.12, a periodic oscillation.

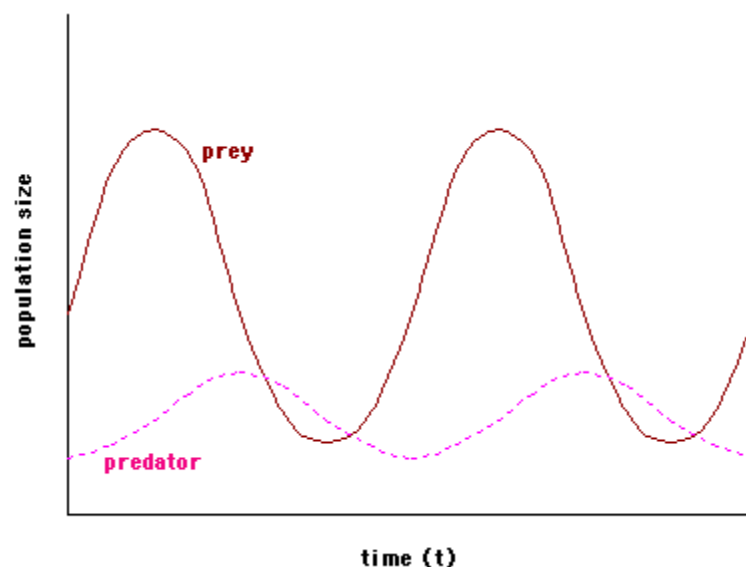


Figure 1.12 – Periodic Oscillation of the prey and predator populations. Source: <http://www.tiem.utk.edu/bioed/bealsmodules/predator-prey.html>.

The European Regional Seas Ecosystem Model (ERSEM) is a very well known example of a complex ecosystem model and an ecological model. ERSEM model was designed for temperate ecosystems and uses site-dependent aspects such as latitude depth, irradiance and transparency to a physical model (Baretta-Bekker *et al.*, 1997). The ERSEM model is now in its version II, slightly different from version I. The model simulates the concentrations of carbon, nitrogen, phosphorus and silicon in the pelagic and benthic systems. It deals with three groups of the microbial food web: primary producers, consumers and decomposers. In this version II, two more functional groups of organisms (picoalgae and dinoflagellates) were added to the list of organisms that includes autotrophic flagellates, diatoms, heterotrophic nanoflagellates, bacteria, microzooplankton and mesozooplankton in a heterogenous mixture. This was done in order to achieve more realistically the concept of Legendre and Rassoulzadegan (1995) of a continuum of food webs, ranging from a dominance of the microbial loop (under oligotrophic conditions) to a herbivorous food web (in upwelling or other nutrient-pulse situations).

More recently, Laurent *et al.* (2006) developed an assimilative capacity model for a shallow fjord in Scotland – Loch Creran. This model is a dynamic version of the simple CSTT model. Loch Creran has two basins separated by a sill. The upper basin, the one near the river is much smaller than the main basin. In this approach the small basin was neglected. It is assumed that all the freshwater input goes to the surface layer of the main basin. This model deals with the system as three boxes as represented in Figure 1.13. The water column was divided in ‘upper’ and ‘lower’ layers.

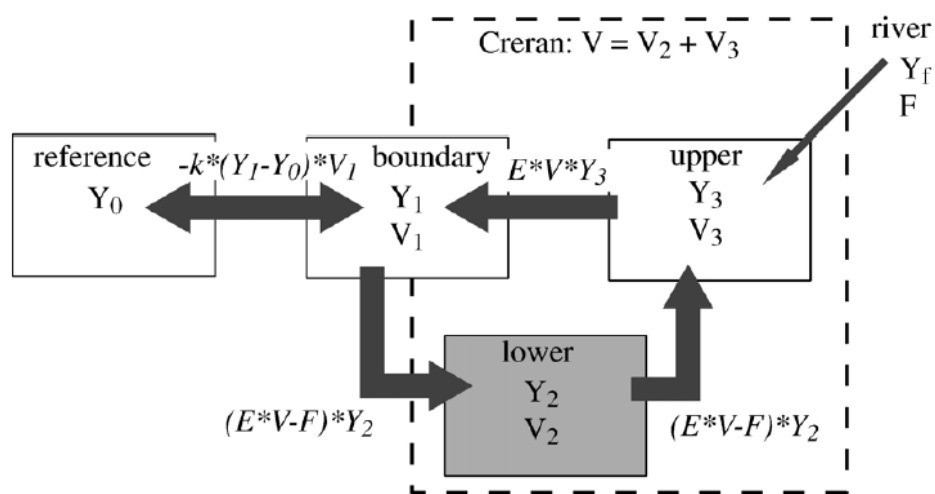


Figure 1.13 – Graphical representation of the three-box model (from Laurent *et al.*, 2006).



The volume of each box is represented by  $V$ ,  $E$  is the exchange rate with the boundary box,  $Y$  is the nutrient concentration, which in this case is dissolved inorganic nitrogen (DIN) or dissolved inorganic phosphorus (DIP), and  $F$  is the volume of water discharged by the rivers.

This model will predicts the chlorophyll  $a$ , DIP and DIN concentrations. However, it is not comprehensive enough yet to work as an assimilative capacity model. A set of useful and representative indicators to assess ecosystem health has to be selected. Secondly, the threshold for undesirable disturbance for this specific site has to be defined and EQSs established. Different scenarios would need to be assessed with the model to check when the system goes beyond the defined EQSs.

The last steps of the modelling process are validation and calibration of the model (Fennel and Neumann, 2004). These steps are essential and without them it is impossible to know the level of accuracy of the model, to allow us to have confidence on the model. Validation is the process of comparing the output of the model with observational data. Very often modellers find problems of undersampling or insufficient data. It may be that the model is simulating a high peak during a period for which there is no observational data, for example. The process of calibration is necessary to obtain a better fitting of the simulation to the real data. It consists of adjusting the model parameters. However, this has to be done with care because there is always the risk of introducing errors to the model since the mismatch may be caused by some other reason. In addition, the number of parameters to calibrate should be limited because too many fitted parameters may lead to a decrease of the predictive potential (Fennel and Neumann, 2004).

In the past solving the differential equations of the complex models was often a problem and could slow down the process. Nowadays, with the advances of technology and all the equipment available, it is becoming easier to do research in this field and the initial problem is no longer an obstacle. Besides, the computer software is more useful and easy to use.

## 1.5 Aim and objectives

The present work aimed to develop a nutrient assimilative capacity model for the sustainable management of nutrients within the Ria Formosa lagoon. To develop this model, knowledge about the bio-chemical properties, especially nutrient and chlorophyll dynamics, of Ria Formosa was needed. Pelagic and benthic compartments of the lagoon were extensively investigated, following previous studies by Newton *et al.* (2003), Murray *et al.* (2006) and Mudge *et al.* (2007), for example.

This aim was achieved by focusing on the following specific objectives:

- **Chapter 3** - Develop an appropriate methodology for the assessment of microphytobenthos chlorophyll, as no standard methodology is currently available;
- **Chapter 4** - Assess the spatial and temporal variability of microphytobenthos in order to evaluate its appropriate use as a measure of biomass across the system;
- **Chapter 5** - Investigate the importance of microphytobenthos in the context of a shallow coastal lagoon, as Ria Formosa;
- **Chapter 5** - Evaluate the role of the microphytobenthos and benthic nutrient fluxes in the assessment of the ecological quality status of shallow water bodies;
- **Chapter 6** - Determine the yield of microphytobenthos chlorophyll from nutrients, which is expected to be one of the most important factors in the functioning of the model and the ecosystem;
- **Chapter 7** - Adapt and develop the CSTT model for a shallow coastal lagoon, incorporating an important benthic primary producer – the microphytobenthos;
- **Chapter 7** - Estimate the assimilative capacity of the system in relation to nutrient input by testing different scenarios of nutrient input conditions and assessing its effects on the bio-chemical elements of the system.

## 1.6 Thesis outline

Chapter 1 consists of a discussion about the most important general subjects involved in this thesis. The understanding of the basic aspects of the primary production is essential for the discussions about phytoplankton and microphytobenthos. Knowledge about coastal lagoons and their nutrient cycles is also very important to understand nutrient dynamics, which are discussed mainly in Chapters 5, 6 and 7. Eutrophication is one of the central phenomena of this study and therefore a general introduction is important. These topics provide the basis for a modelling approach, which is presented in Chapter 7 and introduced in the last part of Chapter 1.

Chapter 2 consists of a description of the characteristics of the Ria Formosa lagoon: climate, hydrodynamics, physico-chemical elements, socio-economy and the legal aspects that involve the lagoon system. These aspects provide a useful starting point to the understanding of this ecosystem.

Chapter 3 describes a set of experiments to determine the optimal methodology for the extraction of microphytobenthic chlorophyll. This study was essential in the work progress due to the lack of a standard methodology for benthic algae.

Chapter 4 evaluates the spatial, temporal and vertical variability of microphytobenthos in Ria Formosa. Microphytobenthos is known to be largely variable in space, being composed of several patches within the sediments. Several trends of temporal variation have also been suggested by different authors. The understanding of microphytobenthos variability is crucial for the evaluation of the usefulness of chlorophyll as a measure of biomass. It is also extremely important providing guidance on the modelling process, by the establishment of ranges of expected variations and trends.

In chapter 5 several physico-chemical and biological elements were investigated to achieve a better understanding of the system and to provide the necessary data to force and to test and improve the biogeochemical model developed in this project. In addition, the evaluation of the trophic status of the lagoon is also presented based on thresholds established by the European Environmental Agency.

Chapter 6 presents a set of laboratory experiments carried out to investigate the relationship between chlorophyll production and nutrient consumption by algae, named the yield of chlorophyll from nutrients. The yield is fundamental for eutrophication assessments and it is one of the main parameters of the model being developed.

Chapter 7 presents several steps of the development of the ecological model, representing the story of its progress and the scientific knowledge that supported the interactions until the final model was achieved. It also contains the full description of the model, presenting the conceptual, mathematical (differential equations describing the state variables) and numerical model. The assessment of different scenarios of nutrient loading that allowed the evaluation of the assimilative capacity of the system is presented. The model was also used to explore a range of scenarios that may happen in case of global climate change.

Chapter 8 presents a final discussion of the whole project results. The importance of each finding and the new questions encountered during the development of the project are placed in perspective and discussed. An analysis about the achieved and/or not achieved objectives is performed. Moreover, the new directions of future research are presented.

Chapter 1 and 2 provide the general literature review and study site description, which are essential for the development of this study, characterised by Chapters 3, 4, 5, 6 and 7 (Figure 1.14). Chapter 8 provides a general discussion involving all chapters presented in this thesis and gives indications about future studies.

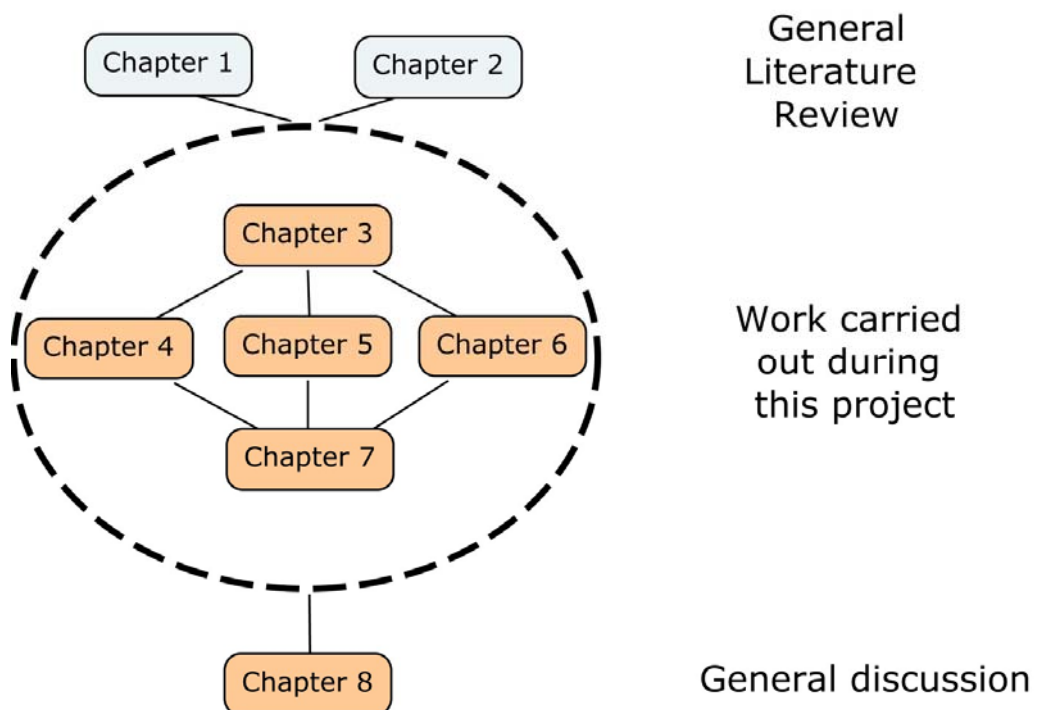


Figure 1.14 – Schematic representation of the synergies between chapters.

## CHAPTER 2

---

Study Site

---

Ria Formosa is a shallow mesotidal lagoon located in the south of Portugal (Figures 2.1 and 2.2), extending along the eastern part ( $36^{\circ}58'N$ ,  $8^{\circ}02'W$  to  $37^{\circ}03'N$ ,  $7^{\circ}32'W$ , Newton and Mudge, 2003). It has an extension of 55 km (E-W, from Ancão to Cacela) and a maximum width of 6 km (N-S, Serpa, 2005; Newton and Mudge, 2003). The lagoon covers an area of  $100\text{km}^2$  (Asmus *et al.*, 2000) with a mean depth of 1.5 m (Nobre *et al.*, 2005). The tidal range varies from 1.3 on neap tides to 3m on spring tides and the estimated maximal tidal volume of water is  $140 \times 10^6 \text{ m}^3$  (Instituto Hidrográfico, 1986).



Figure 2.1 - Geographic Location of Ria Formosa. Location of the meteorological station at São Brás de Alportel.



Figure 2.2 – Ria Formosa.

Ria Formosa is a Region of Restricted Exchange (RRE), i.e. an area which is cut off from the normal circulation of coastal waters (Newton *et al.*, 2003, Tett *et al.*, 2003). The lagoon is protected from the ocean by a sandy barrier island interrupted by seven inlets, two of which have been artificially consolidated (Newton and Mudge, 2003). It has a complex network of channels, some navigable and an extensive inter-tidal area, approximately two-thirds of the area is intertidal during low tide (Asmus *et al.*, 2000).

## **2.1 Climate**

In the south of Portugal, the climate is typically Mediterranean, with warm and dry summers and cold winters, with low rainfall. The rainfall occurs specially during 2 or 4 months.

A Portuguese meteorological database was used to obtain values of some parameters – the SNIRH database (SNIRH, 2008). These parameters include: temperature, rainfall, wind characteristics and radiation. However, there are not many stations with available data. In the area where this study took place there was just one station called *S. Brás de Alportel* which has a complete and good dataset. However, care has to be taken since this station is located uphill, at an altitude of around 200m.

Besides, the SNIRH database, some reports from national organizations were used to improve the information obtained. These organizations are DGA (*Direcção Geral do Ambiente*), DRAOT Algarve (*Direcção Regional do Ambiente e do Ordenamento do Território do Algarve*), DGPA (*Direcção Geral de Pescas e Aquicultura*). The report from Mendonça (2001) and several papers were also used to improve and complete the subject.

### **2.1.1 Temperature**

The mean air temperature in the summer is normally 25°C and in the winter is 12°C (Newton and Mudge, 2003). According to SNIRH (2008), the annual mean temperature in *São Brás* between October 2005 and March 2008 was 16.7°C (Figure 2.3).

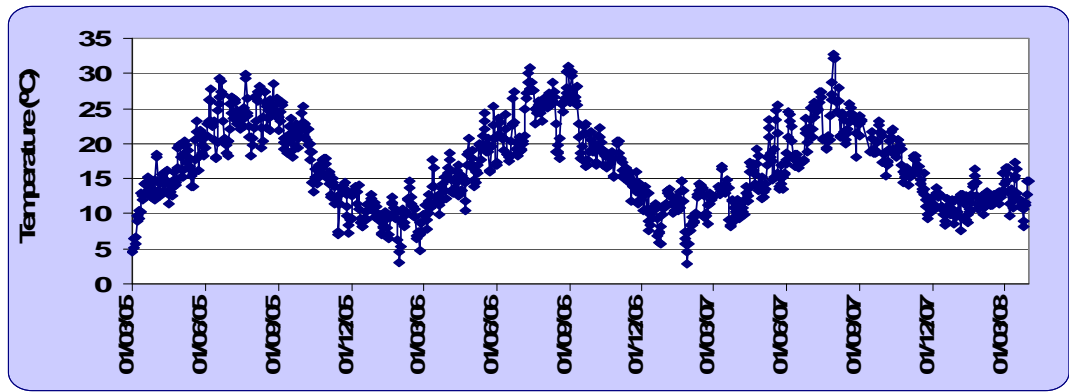


Figure 2.3 - Temporal variation of air temperature (°C) in *São Brás* from March 2005 until March 2008 (SNIRH, 2008).

### 2.1.2 Rainfall

The annual mean rainfall in Ria Formosa is from 400 to 500mm according to DGA for the years from 1931 to 1960 (Figure 2.4). The areas with the larger average of rainfall are mountains.

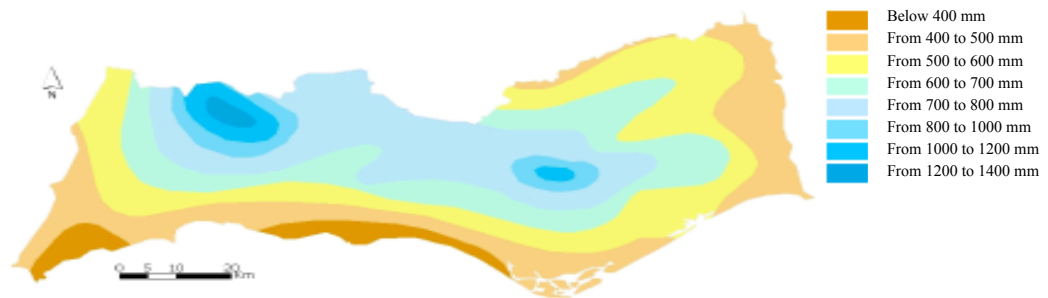


Figure 2.4 – Annual average of the rainfall from 1931 to 1960 in Algarve. Orange is below 400 mm and the blue is from 1200 to 1400 mm of rainfall (from DGA).

However, Newton and Mudge (2003) indicate a more recent annual mean of 634mm according to Instituto Hidrográfico (1981). Figure 2.5 shows the variation of the rainfall during the period between October 2006 and September 2007 in *S. Brás de Alportel* (SNIRH, 2008). The rainfall mean is 2.3mm in each day and a value of 843mm of total precipitation for the year.



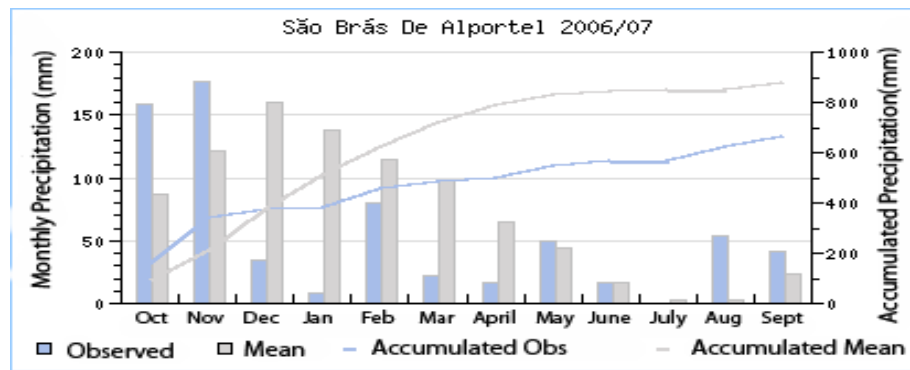


Figure 2.5 - Observed precipitation values in São Brás de Alportel and mean precipitation values (mm) in three stations: *Estoi, Quelfes and São Brás* in the period between October 2006 and September 2007 (SNIRH, 2008).

### 2.1.3 Winds

In Ria Formosa, winds from west or south-west are very common, especially during the winter. However, in the summer there is a high incidence of winds blowing from east, called the Levante winds.

### 2.1.4 Radiation

Portugal is a sunny country and the radiation intensity is very relevant for biological processes. Ria Formosa has normally more than 3100 hours of sunlight during the year (Figure 2.6) and very large values of radiation.



Figure 2.6 – Average number of sunlight hours in Algarve during the year, from 1931 to 1960 (from DGA – Atlas Digital do Ambiente).

The annual variation of the radiation is presented in Figure 2.7. It has a wave form trend with the low value, around  $200 \text{ Wh/m}^2$  during the winter, in December and the high value during summer in July of about  $8000 \text{ Wh/m}^2$  (SNIRH, 2008).

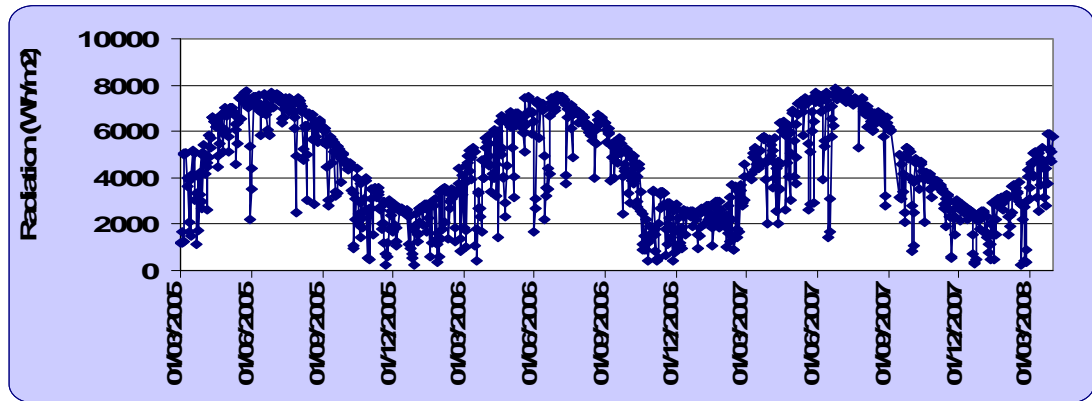


Figure 2.7 - Annual variation of the radiation ( $\text{Wh/m}^2$ ) in *São Brás* station during the period between March 2005 and March 2008 (SNIRH, 2008).

## 2.2 Hydrodynamics

The hydrodynamics of Ria Formosa are complex, resulting from its morphology and bathymetry (Figure 2.8). The tide and waves are the main forces acting in the lagoon. The freshwater input to Ria Formosa is almost negligible.

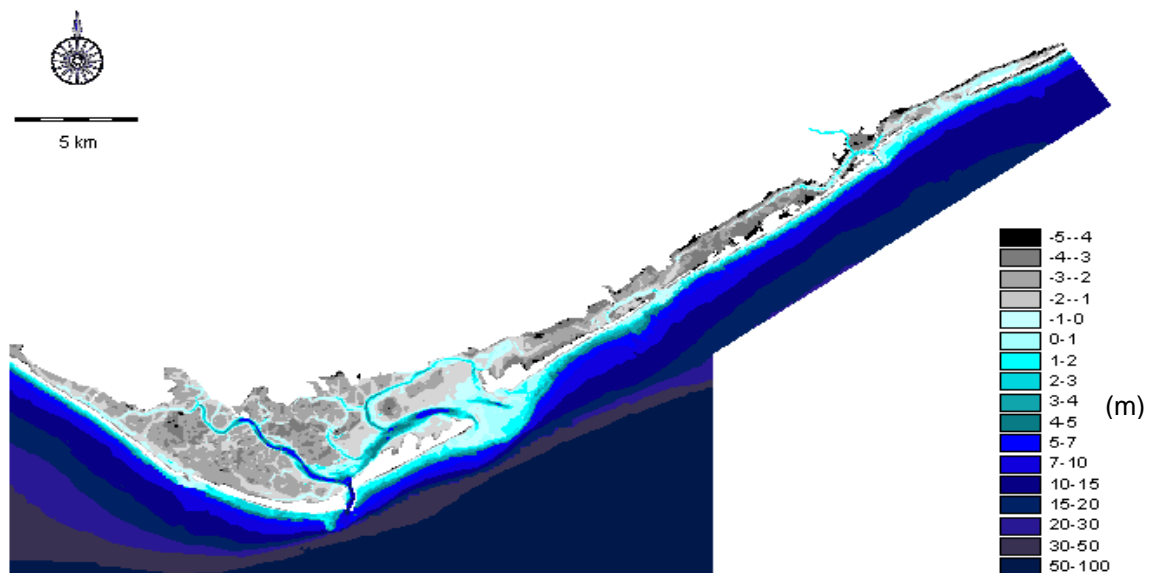


Figure 2.8 – Bathymetry of Ria Formosa (from Mendonça, 2001).

The depth of Ria Formosa is small throughout the lagoon (Mendonça, 2001). During low water a significant percentage of Ria Formosa area becomes emersed, exposing a large area of the lagoon's mudflats (Figure 2.9).

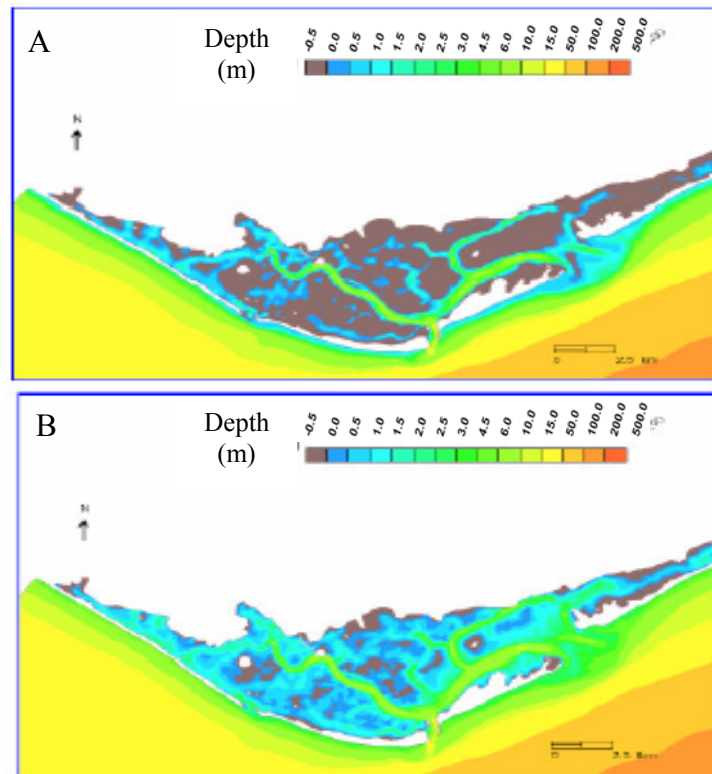


Figure 2.9 – Ria Formosa during spring low water (a) and high water (b), from Mendonça (2001).

The sub-basin of Ria Formosa has 54 water lines and only 25 of these drain directly to Ria Formosa (Figure 2.10). Five of these water streams are rivers and most of the other water lines dry out completely during summer (Newton *et al.*, 2003).



Figure 2.10 – Hydrography map of Ria Formosa area with the principal water streams (from DRAOT Algarve, 2001).

In addition, the Ria Formosa receives the product of the drainage of 85407 hectares (Rodrigues, 2004). However, since the water streams have an insignificant effect, the urban and industrial wastes are the most relevant inputs. These wastes are normally larger during the summer, when the population multiplies and they receive treatment in the urban waste water treatment plants. Most of these plants have secondary treatment or more. Faro, with a population of around 100,000 people in the summer, is the area with the larger flow from the water treatment plants, around 43 percent of the total (DRAOT Algarve, 2003). On the other hand, there are some local inputs from agriculture or golf courses.

### **2.2.1 Currents**

The currents in the inlets of Ria Formosa are very strong compared with the currents inside the lagoon. In the main channels the speed is below  $1\text{ m}\cdot\text{s}^{-1}$  and in the inlets it may be over  $2\text{ m}\cdot\text{s}^{-1}$  (Lima and Vale, 1980). However these values can be quite variable and depend on the tide, since according to Newton *et al.* (2003) the flood current velocity at Barra do Farol (main inlet southeast of Faro) is  $0.4\text{ m}\cdot\text{s}^{-1}$  and the ebb current velocity is  $0.8\text{ m}\cdot\text{s}^{-1}$  at neap tides.

### **2.2.2 Exchange with the sea**

It has been considered that Ria Formosa has a high exchange rate with the sea, having a water exchange rate of around 75% in each tide (Tett *et al.*, 2003). Asmus *et al.* (2000), indicate that the residence time is extremely low between half day and 2 days. However, some publications suggested that this could be wrong (Tett *et al.*, 2003; Mudge *et al.*, 2008). Recently, Mudge *et al.* (2008) showed that the residence time can be bigger, around 4-5 days, in some small and inner channels (Figure 2.11). The residence time (during Spring Tides) is represented at Low Water (Figure 2.11-a) and High Water (Figure 2.11-b); Mudge *et al.*, 2008). This is in agreement with Newton and Mudge (2003) who suggested that the water masses in the inner channels mostly stay there and the water being exchanged is mainly the same that comes in.

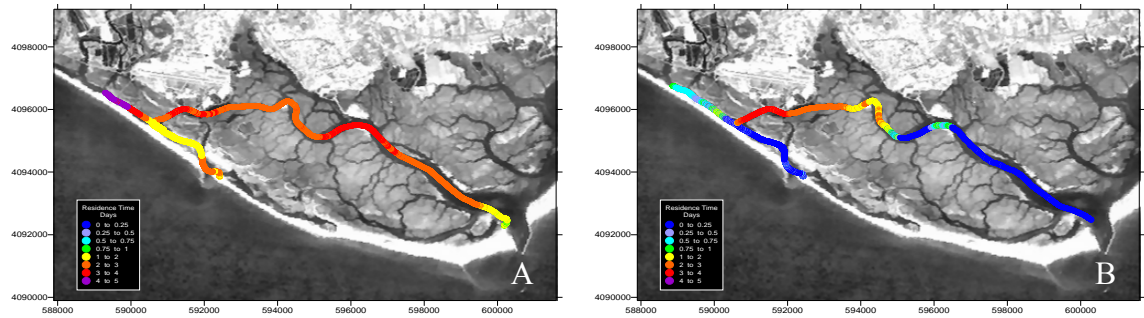


Figure 2.11 - Residence time at Low water (a) and High water (b). The scale is between 0-0,25 days (blue) to 4-5 days (purple) (Mudge *et al.*, 2008).

### 2.2.3 Stratification

Ria Formosa lagoon has a low depth, relatively strong currents and a reasonably high exchange rate, which leads to a situation of well mixed waters (Goela, 2005). During the work of Newton and Mudge (2003), most stations showed a weak or no thermal stratification.

## 2.3 Physico-chemical components

### 2.3.1 Salinity

The lagoon normally shows a difference in salinity from the winter to the summer. During the winter it is brackish and in the summer it is hypersaline. This parameter may vary from values of 13 during the winter to 36.5 in the summer (Goela, 2005). In addition, due to the water circulation pattern inside the inner channels, Newton *et al.* (2003) showed salinity differences between the water that is in the inner channels and the incoming, during low and high tide and during winter and summer (Goela, 2005). This was investigated using a CTD under a boat during the summer by Mudge *et al.* (2008). The results (Figure 2.12) confirm what was suggested previously.

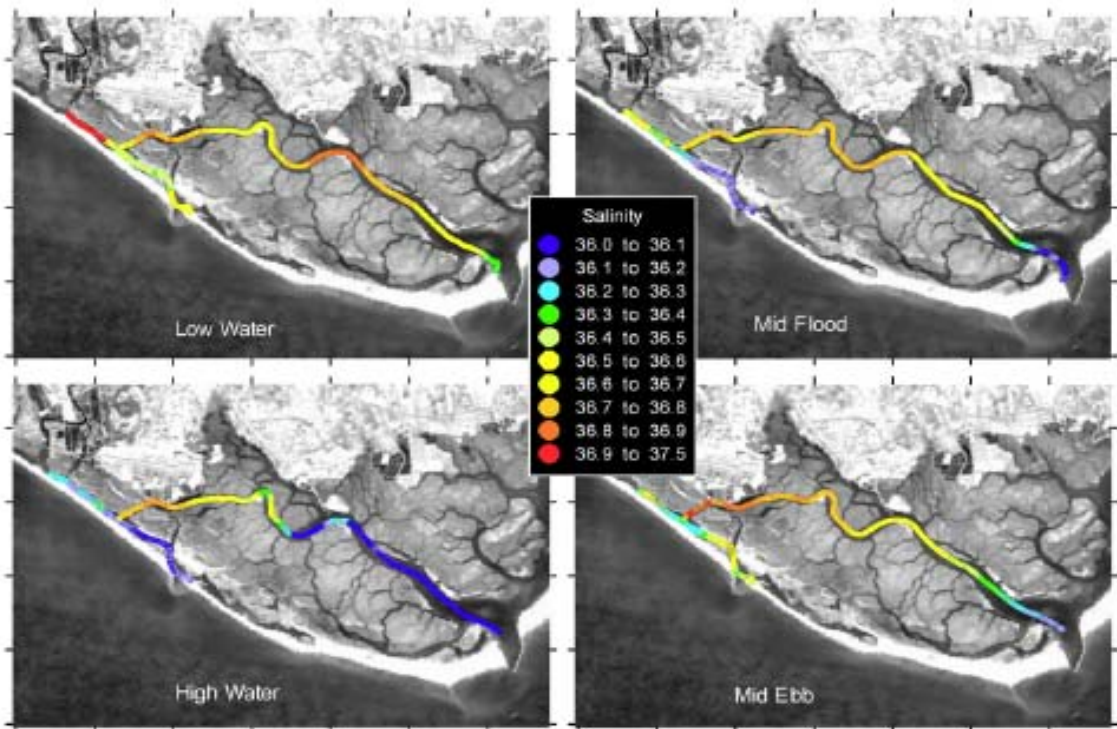


Figure 2.12 – Salinity variation during a tidal cycle in June (Mudge *et al.*, 2008).

### 2.3.2 Temperature

During the winter the temperature of the lagoon decreases mainly due to the lower air temperature and rainfall / runoff. During the summer the opposite happens. Thus, temperatures range from 12°C in the winter to 27°C in the summer (Goela, 2005).

### 2.3.3 Oxygen

According to the TICOR database (Oliveira, 2005), most of the dissolved oxygen values are above the biological stress level (5.0 mgL<sup>-1</sup>, as stated in Bricker *et al.*, 2003), especially between 6 and 10 mgL<sup>-1</sup>, which can also be seen on Figure 2.13. However, Oliveira (2005) suggested that this may have been overestimated given that most of the samples were not taken during the “low oxygen period” within the lagoon. This period is in the early morning when photosynthesis does not compensate the oxygen consumed during the night (Oliveira, 2005). A concentration of less than 2mgL<sup>-1</sup> (hypoxic level) was found by Oliveira (2005) during this period. Since the oxygen concentration is dependent on salinity and temperature, it is essential to check the oxygen saturation as well. The lower levels of the saturation found were of 20%, much lower than the 80% recognised as an indication of a healthy biota (Oliveira, 2005).

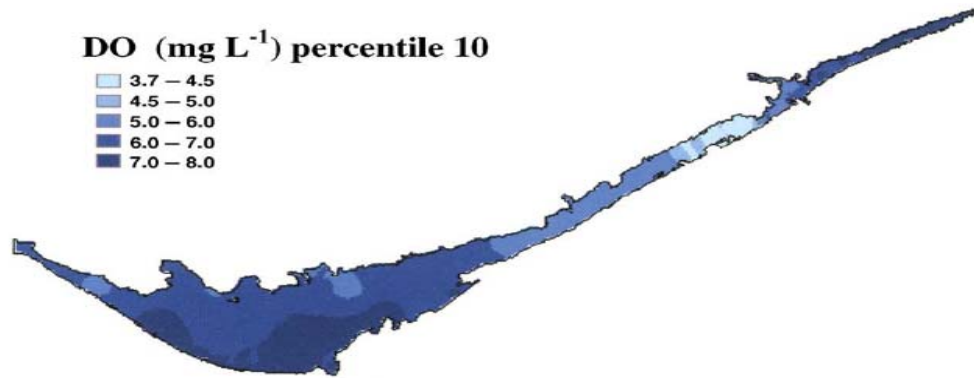


Figure 2.13 - The 10<sup>th</sup> percentile (10% lower values) of dissolved oxygen concentration ( $\text{mgL}^{-1}$ ) along the lagoon (Nobre *et al.*, 2005).

### 2.3.4 Nutrients in the water column

The nutrient concentrations within Ria Formosa have seasonal, spatial and tidal variability (Newton *et al.*, 2003). The dissolved available inorganic nitrogen (DAIN) has larger values during the winter and in the eastern part of the lagoon (Figure 2.14-a). The DAIN mean is around  $20 \mu\text{M}$ , however, in the eastern part, during the winter, values of  $150 \mu\text{M}$  have been obtained (Newton *et al.*, 2003). Although most of the population lives in the western part of the lagoon, the eastern part is rich in agriculture activities. The high concentration of DAIN in the eastern part may be caused by the runoff, especially during the winter months. However, Goela (2005) obtained DAIN concentrations much lower, around  $3 \mu\text{M}$ , throughout the lagoon. The sampling was carried out during 2005, which was an extraordinarily dry year. Data obtained by Newton *et al.* (2003), showed a clear trend where DAIN concentrations increase from late summer to winter.

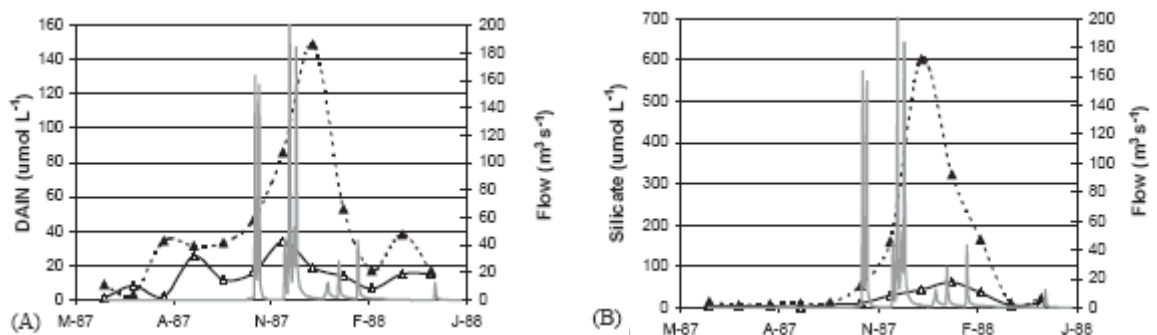


Figure 2.14 - DAIN (a) and Silicate (b) concentration means ( $\mu\text{mol.L}^{-1}$ ) in the western ( $\Delta$ , solid curve) and in the eastern ( $\blacktriangle$ , broken curve) part of the lagoon over a year, from May 1987 to April 1988 (from Newton *et al.*, 2003).

Phosphate has generally a higher concentration in the eastern part of the lagoon as well, with a peak (during late spring) of 1.4  $\mu\text{M}$ . The mean concentration is over 0.6 $\mu\text{M}$  (Newton *et al.*, 2003). The spatial variation of phosphate concentration is not as clear as for DAIN, being almost constant along the year (Goela, 2005). However it seems that higher concentrations are found during the spring (Newton *et al.*, 2003; Goela, 2005).

The mean concentration of silicate (Figure 2.14-b) is generally low during the year, except for the winter months, when it has a great increase (Newton *et al.*, 2003; Goela, 2005). The concentration varies from values near 0  $\mu\text{M}$  to 80 $\mu\text{M}$  (western part of the lagoon) and 600 $\mu\text{M}$  (in the eastern part of the lagoon; Newton *et al.*, 2003).

Goela (2005) indicated that there is a clear variation in silicate concentrations during the tidal cycle, with higher values recorded at low tide.

Based on the concentration values found by Newton *et al.* (2003) of DAIN, phosphate and silicate, the DAIN/P ratio and the DAIN/Si ratio were calculated. Combining these with the information on the nutrient concentration distribution along Ria Formosa a GIS map was created for each case (Figure 2.15 -1.). From early spring until early summer the DAIN/P ratio is close to 16 (normal Redfield ratio) or higher, which suggests a phosphorous limitation. However, Goela (2005) obtained a DAIN/P ratio of 5 during spring. This may mean that the high values found by Newton *et al.* (2003) could have been found due to an excessive concentration of DAIN, caused by a high run off.

The DAIN/Si ratio (Figure 2.15 -2.) has a small peak during the spring, suggesting some lack of silicate in the water, which may be very important for some species (Newton *et al.*, 2003). Goela (2005) also found a peak during spring months. In addition, the DAIN/Si ratio has shown a large peak in the summer (Newton *et al.*, 2003).

### **2.3.5 Nutrients in the sediments**

In shallow systems, water quality may be strongly influenced by sediment characteristics, its pore water concentrations, as well as by terrestrial or diffuse or point inputs, such as sewage. However, within lagoons with significant tidal exchange, as Ria Formosa, the effect of these inputs are normally less important.

Murray *et al.* (2006) found that for all nutrients (DIP, DOP,  $\text{NH}_4^+$ ,  $\text{NO}_3^-$ ) except nitrite, the sediment pore water concentrations are higher than their seawater concentration in Ria Formosa. Nitrite concentrations are normally very small both in the



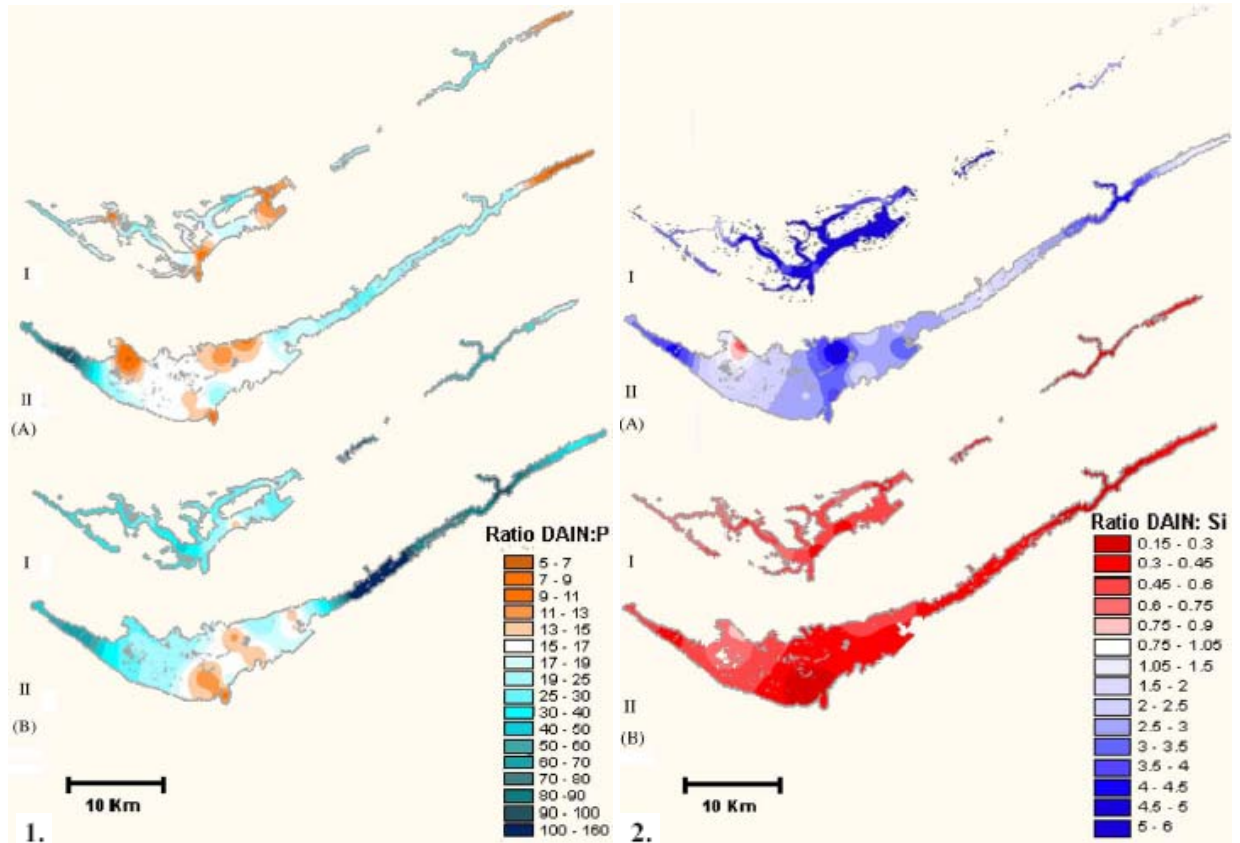


Figure 2.15 – GIS maps of the DAIN:P ratio (1.) and DAIN:Si ratio (2.), from Newton *et al.* (2003).

For the DAIN:P ratio, the orange colour suggests a N limitation and the blue/green a P limitation. For DAIN:Si ratio, the red colour suggests a N limitation and the blue a Si limitation A- Summer conditions; B- winter conditions; I – low water; II – high water.

sediment and water column. In Figure 2.16, part of the results of Murray *et al.* (2006) obtained for two sites are presented: OA - outside Ancão basin and rich in *Enteromorpha* sp. and MR - muddy site in Ancão basin. DIP concentrations ranged from almost 0-100  $\mu\text{M}$  (OA) to around 30-150  $\mu\text{M}$  (MR). Nitrite concentrations ranged from 0  $\mu\text{M}$  (OA) to 15.5  $\mu\text{M}$  (OA). Nitrate concentrations ranged from around 0  $\mu\text{M}$  (OA and MR) to around 90  $\mu\text{M}$  (MR). Ammonia concentrations ranged from 0  $\mu\text{M}$  (OA and MR) to around 1300  $\mu\text{M}$  (OA) and 700  $\mu\text{M}$  (MR).

Using Fick's First Law of Diffusion, Murray *et al.* (2006) also investigated the nutrient fluxes across the sediment-seawater interface (Figure 2.17). Except for nitrite, sediments were always a source of inorganic nutrients to the overlying seawater. DIP flux was larger in sand ( $120 \mu\text{mol.m}^{-2}.\text{h}^{-1}$ ) than in mud ( $40 \mu\text{mol.m}^{-2}.\text{h}^{-1}$ ), ammonia flux was similar both in sand (around  $290 \mu\text{mol.m}^{-2}.\text{h}^{-1}$ ) and in mud (around  $320 \mu\text{mol.m}^{-2}.\text{h}^{-1}$ ), nitrate flux was larger in mud (around  $90 \mu\text{mol.m}^{-2}.\text{h}^{-1}$ ) than in sand (around  $60 \mu\text{mol.m}^{-2}.\text{h}^{-1}$ ) and nitrite flux was larger in sand (around  $10 \mu\text{mol.m}^{-2}.\text{h}^{-1}$ ) than in mud (around  $3 \mu\text{mol.m}^{-2}.\text{h}^{-1}$ ).

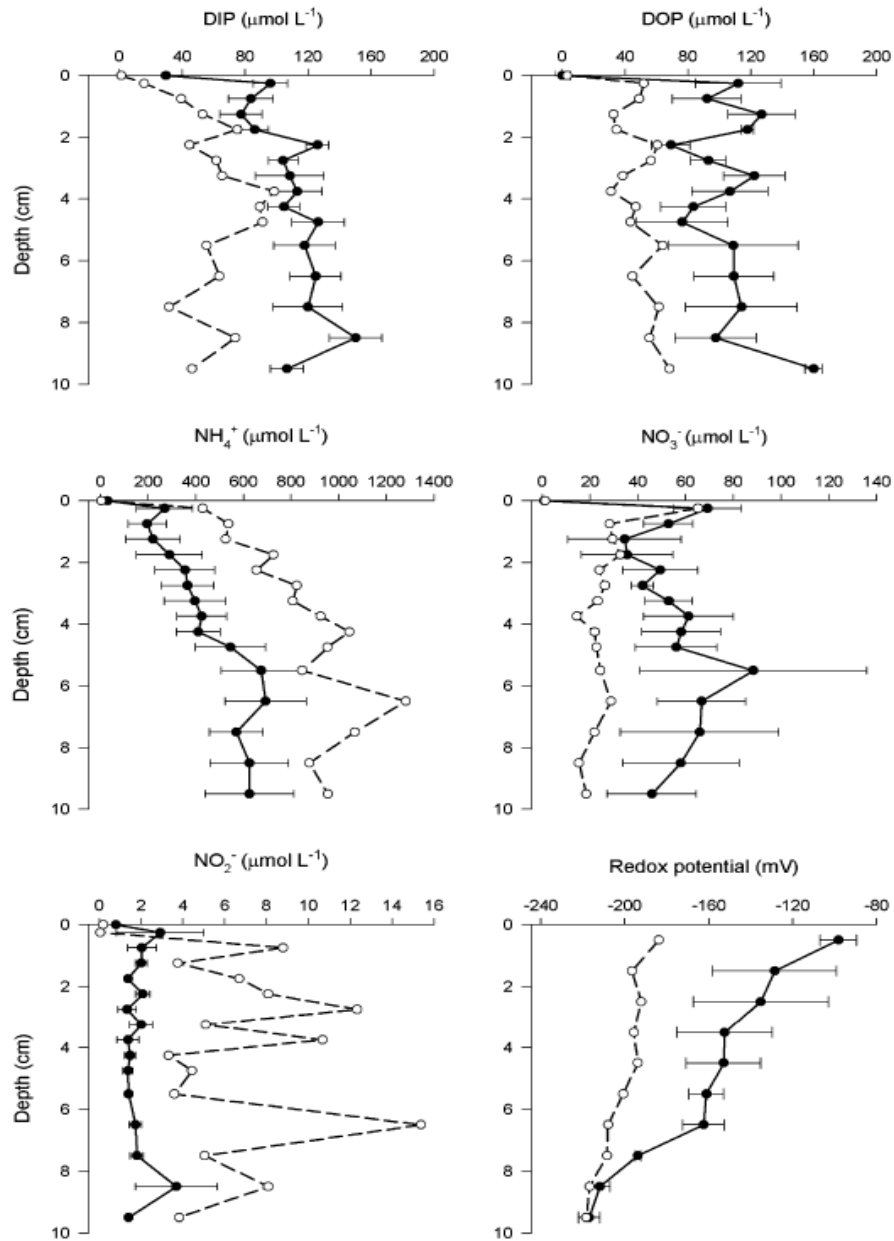


Figure 2.16 – Pore water nutrient concentrations and redox profiles until a depth of 10 cm, from muddy sediment (solid) from Ancão basin in Ria Formosa and from sand/mud sediment from outside Ancão basin (open/dashed; from Murray *et al.*, 2006).

The high value of ammonia flux for the Ancão site may be explained by the typical high rates of uptake of *Enteromorpha* sp. Organic matter resulting from the macroalgae may then contribute to an increase in ammonia by remineralisation (Murray *et al.*, 2006).

Falcão and Vale (1990) studied these fluxes in Ria Formosa during the autumn/winter and the values obtained were  $-6 \mu\text{mol.m}^{-2}.\text{h}^{-1}$  to  $96 \mu\text{mol.m}^{-2}.\text{h}^{-1}$  for DIP,  $-175 \mu\text{mol.m}^{-2}.\text{h}^{-1}$  to  $25 \mu\text{mol.m}^{-2}.\text{h}^{-1}$  for nitrate and  $0 \mu\text{mol.m}^{-2}.\text{h}^{-1}$  to  $911 \mu\text{mol.m}^{-2}.\text{h}^{-1}$  to ammonia. These are approximately within the range of variation found by Murray *et al.* (2006).

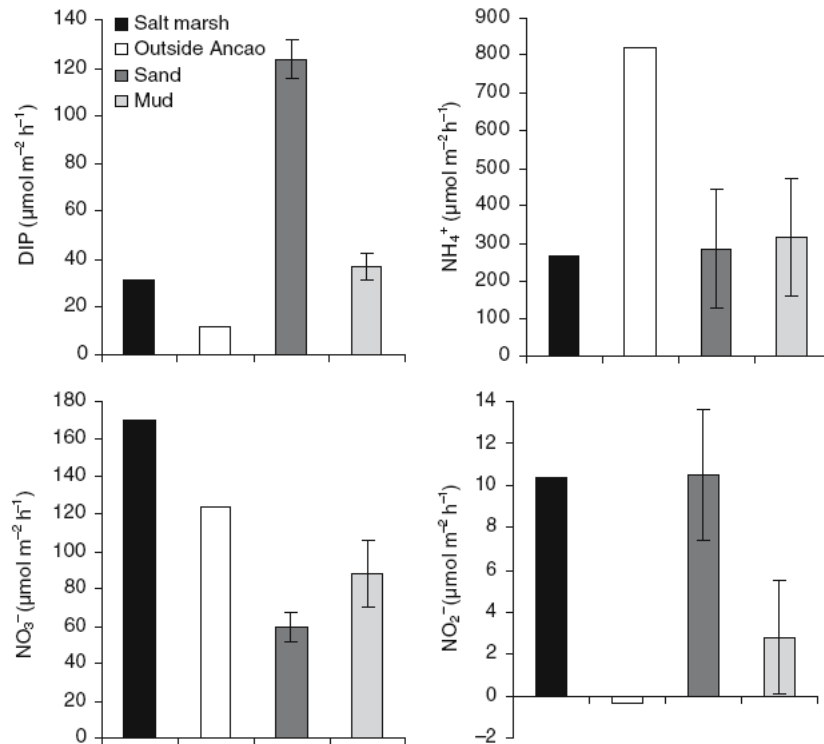


Figure 2.17 – Fluxes of nutrients across the sediment-seawater interface in the Ria Formosa on the ebb tide. Cores were taken from Ancão basin and one outside (from Murray *et al.*, 2006).

### 2.3.6 Chlorophyll in the water column

During the OAERRE project, Tett *et al.* (2003) found the maximum value of  $2\mu\text{g L}^{-1}$  of chlorophyll *a* in Ria Formosa both for summer and spring. However, high values of chlorophyll *a* were reported by Newton *et al.* (2003). In some specific parts of the lagoon, such as the inner channels, larger values can be found, as illustrated by Nobre *et al.* (2005) in Figure 2.18, representing the 90<sup>th</sup> percentile of the chlorophyll *a* concentration.

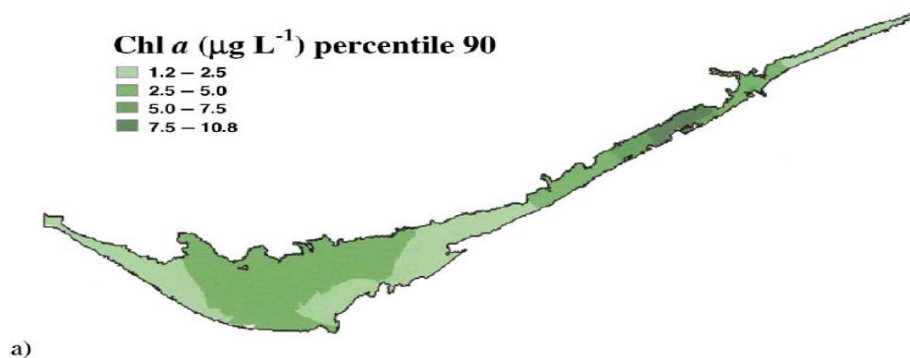


Figure 2.18 - The 90<sup>th</sup> percentile of chlorophyll *a* concentration ( $\mu\text{g L}^{-1}$ ) along the lagoon (Nobre *et al.*, 2005).

Amorim-Ferreira (1987) studied the chlorophyll *a* concentration of phytoplankton and microphytobenthos in Ria Formosa at different sites throughout the lagoon from April 1986 to July 1987 at four different times (April 1986, August 1986, November 1986 and July 1987). She found global means from 1.09  $\mu\text{g L}^{-1}$  (site in Tavira, November 1987) to 7.81  $\mu\text{g L}^{-1}$  (site in Tavira, April 1986) for phytoplankton chlorophyll. In Faro, the highest mean values were in April 1986 (4.30  $\mu\text{g L}^{-1}$ ) and November 1987 (5.20  $\mu\text{g L}^{-1}$ ).

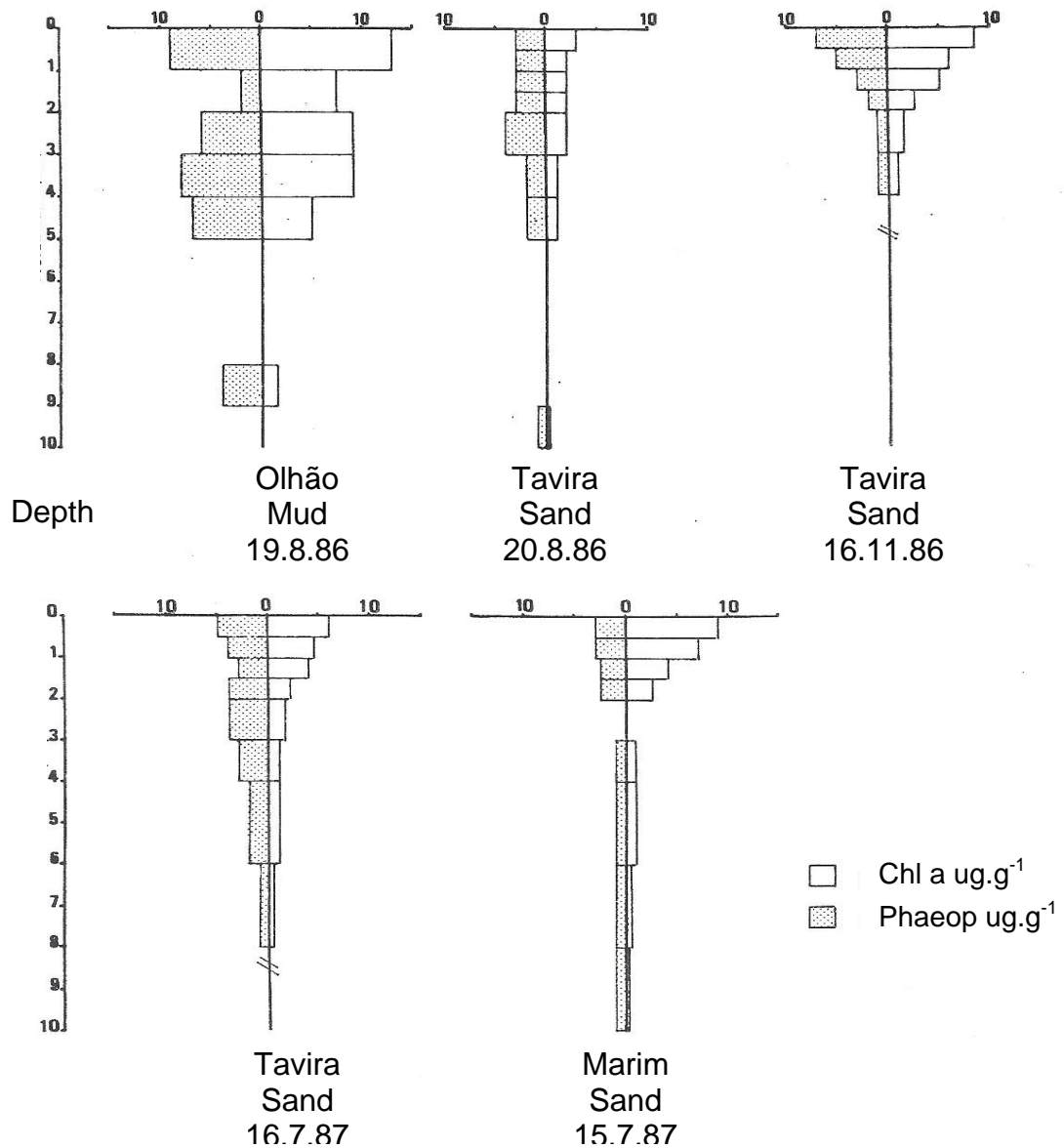


Figure 2.19 – Vertical Profiles of chlorophyll *a* ( $\mu\text{g.g}^{-1}$ ) and phaeopigments ( $\mu\text{g.g}^{-1}$ ) in several locations of Ria Formosa from August and November 1986 and July 1987 (Amorim-Ferreira, 1987).

### 2.3.7 Chlorophyll in the surface sediments

For microphytobenthos, Amorim-Ferreira (1987) obtained values of chlorophyll *a* concentration from  $4.4 \pm 1.0$  SD  $\mu\text{g.g}^{-1}$  to  $9.8 \pm 5.4$  SD  $\mu\text{g.g}^{-1}$  (global means).

The author also studied the vertical distribution of the microphytobenthos cells to a depth of 10cm (Figure 2.19). The chlorophyll *a* concentration is more or less stable (around 8  $\mu\text{g.g}^{-1}$ ) for the first 5 cms in mud (Olhão) and it decreases more rapidly in sand, just after the second cm, being more or less stable but near 0  $\mu\text{g.g}^{-1}$  until the 10cm depth.

### 2.3.8 Sediment characteristics

Some results of a grain size analysis are presented in Table 2.1. Note that the main channels were grouped with the inlets, where the currents are much stronger. This may be a relevant fact for the high percentage of sand in this category.

Table 2.1 – Grain size in the main channels / inlets and in the inner parts of the lagoon (adapted from Ribeiro et al., 2008).

Stations	Clay (%)	Silt (%)	Sand (%)
	Mean	Mean	Mean
Main channels / Inlets	0.3	0.6	99.1
Inner parts of the lagoon	7.0	71.0	22.0

The mapping of the different sediment areas was done by the Ria Formosa natural park (PNRF) and shows that the main types of sediment are sand and muddy sand (Figure 2.20).

According to Asmus *et al.* (2000), the organic matter content of the sediment varies from 1-1.4% for sandy sediment and 7-8% for muddy sediment from seagrass beds and under macroalgal cover. The same authors did not find substantial differences between the seasons.

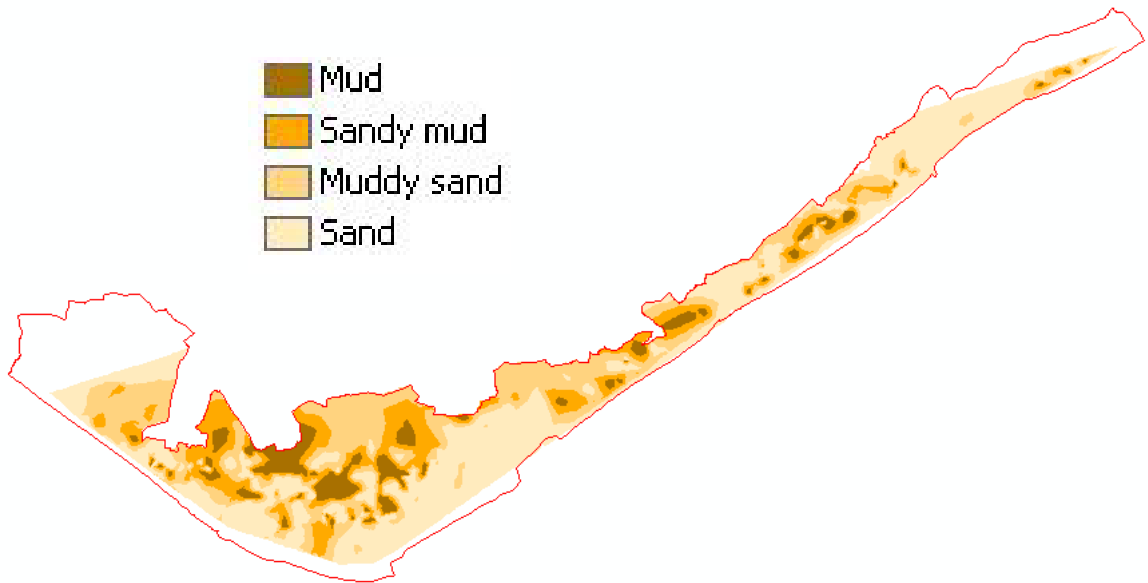


Figure 2.20 – Map of Ria Formosa showing areas and types of sediments (PNRF).

## 2.4 Socio-economy

Ria Formosa is a valuable socio-economic resource for the region. Industries linked with the lagoon such as tourism, fisheries, aquaculture and salt extraction are extremely important. The tourism is one of the most important industries in Algarve, and in Portugal. As a whole, aquaculture of shellfish (especially *Venerupis decussata* and *Cerastoderma edule*), sea bass (*Dicentrarchus labrax*) and sea bream (*Sparus aurata*) has an important role in the national production and is worth about 27.4 million Euros each year (Bernardino, 2000). DGPA reported a production of 2740 tonnes of shellfish and 542 tonnes of fish. From these values, it is important to underline that they represent 90% of the national production of *Venerupis decussata* and 81.7% of the national production of seabream (DGPA, 2008).

## 2.5 Legal considerations

Legal protection for this unique ecosystem is essential and its conservation importance is recognised by several legal instruments, both international and national. This legal background is the basis for a sustainable management of Ria Formosa.

### **2.5.1 International Context**

Ria Formosa is part of the List of Wetlands with International Importance according to the Ramsar Convention, especially because of its importance as habitat for aquatic birds (Rodrigues, 2004). Ramsar Convention was signed on February 1971 and was implemented into the Portuguese legislation by Law number 101/80 on 9<sup>th</sup> October 1980.

Ria Formosa's ecological importance was also highlighted with the Bern Convention for the Conservation of European Wildlife and Natural Habitats. The Convention is from 1979 and was adopted by the Portuguese government by law number 95/81 on 23<sup>rd</sup> July 1981 (Rodrigues, 2004).

Ria Formosa was also considered by the Wetlands Directory of the World Conservation Union (IUCN) as an area of world interest, being part of the Corine Biotopes List (CORINE/85/338/EEC).

Natura 2000 is an instrument of the European Community for nature conservation. The creation of a network of zones with special protection in accordance with two essential Directives, Habitats (92/43/EEC) and Birds (79/409/EEC), resulted in the setting up of Natura 2000 sites. Ria Formosa is one of the Portuguese sites for this network (ICN, 2007; Rodrigues, 2004).

The European Directive 2000/60/EC, known as the Water Framework Directive is another important tool for the sustainable management of Ria Formosa. The Directive was adopted in Portugal by Law number 58/2005 on 29<sup>th</sup> December 2005. This Directive has a main objective of achieving a good ecological water quality for all the EU sites by 2015.

Recently, the Marine Strategy Framework Directive was adopted by the European Union in June of 2008 (2008/25/6) to protect more effectively the marine environment across Europe. The aim is to achieve good environmental status of the European marine waters by 2021. This Directive is still not transposed into Portuguese legislation.

### **2.5.2 National Context**

A natural park was constituted in Ria Formosa by Law number 373/87 on the 9<sup>th</sup> December 1987. This law has important direct implications in Ria Formosa, as it defines its limits and the possible uses of the lagoon and surroundings. In addition,

another law was implemented in the same year, numbered 11/87. This briefly regulates aspects like noise, pollution, water and air quality and establishes the need for environmental impact studies for all projects that may have an effect in the environment. Moreover, a new tool for environmental management, the national strategy for the conservation of nature and biodiversity was also introduced in 2001 (law number 152/2001).



## **CHAPTER 3**

---

The development of an optimal methodology for the  
extraction of microphytobenthic chlorophyll

---

## **Abstract**

Benthic microalgae are important primary producers in intertidal shallow systems. Their biomass can be estimated by the assessment of chlorophyll *a* concentration. A rapid and reliable method of measuring chlorophyll *a* is by spectrophotometry. There is however, no standard protocol for the analysis of benthic chlorophyll *a*. Although the most common solvent generally used is 90% acetone, some authors showed better results with methanol and ethanol. Some pre-treatments, such as the addition of fine inert granules or ultrasound bath, have also been suggested as factors that improve the extraction efficiency. Sediment samples were collected from two sites, muddy and sandy, located within Ria Formosa (Portugal). The aim of this work was to test the effectiveness of different pre-treatments in the extraction and to develop an optimal method for chlorophyll *a* extraction and analysis. Pre-treating samples did not yield any significant differences in chlorophyll *a* extracted. Treating sediments with acetone was found to yield higher concentrations of chlorophyll *a*, both for muddy and sandy sediments. Acetone was therefore found to be the best solvent for both sediment types, with 90% being the best strength for sandy and 80% the best for muddy sediments. These differences may be related to differences in the structure of the algal communities. Six hours of extraction was found to be sufficient, since after a six hour period the extraction efficiency did not improve.

**Keywords:** microphytobenthos; chlorophyll *a*; extraction efficiency; spectrophotometry; Ria Formosa.

### 3.1 Introduction

Several techniques can be used to estimate the microphytobenthos biomass, such as: High Performance Liquid Chromatography (HPLC) pigment analysis (Brotas and Plante-Cuny, 2003; Cartaxana *et al.*, 2006), Pulse Amplitude Modulated (PAM) fluorometry (Kromkamp *et al.*, 1998; Consalvey *et al.*, 2005; Jesus *et al.*, 2005; Serôdio *et al.*, 2005) as well as chlorophyll *a* (chl *a*) extraction and analysis by spectrophotometry (Migné *et al.*, 2004; Koh *et al.*, 2007) or fluorometry (Riaux-Gobin and Bourgoïn, 2002). The first techniques (HPLC and PAM fluorometry) seem very promising but require specific knowledge and equipment. HPLC is probably the only method that really allows the measurement of the pure pigment chlorophyll *a* (Jeffrey *et al.*, 1997). Other methods may have contamination in the measurements caused by other pigments. In this work the term chl *a* will be used although it is acknowledged that this does not represent the pure pigment. Spectrophotometry and fluorometry are very useful for rapid and reliable measurements. Nevertheless, a standard method for benthic chlorophyll does not exist and extraction is a crucial step. This step has been widely discussed in the literature for phytoplankton, however for benthic algae fewer works are available (e.g. Tett *et al.*, 1978; Hagerthey *et al.*, 2006; Devesa *et al.*, 2007). No solvent can provide complete extraction efficiency, although 90% acetone has been cited as providing a reasonable value (90%, Van Leeuwe *et al.*, 2002) and has been used in the majority of algal studies (Strickland and Parsons, 1972; Garrigue, 1998; Wiltshire *et al.*, 2000; Van Leeuwe *et al.*, 2002; Tada *et al.*, 2004; Grinham *et al.*, 2007). Schagerl and Künzl (2007) discussed that dispersion in acetone was the best extraction technique for MPB extraction (Figure 3.1).

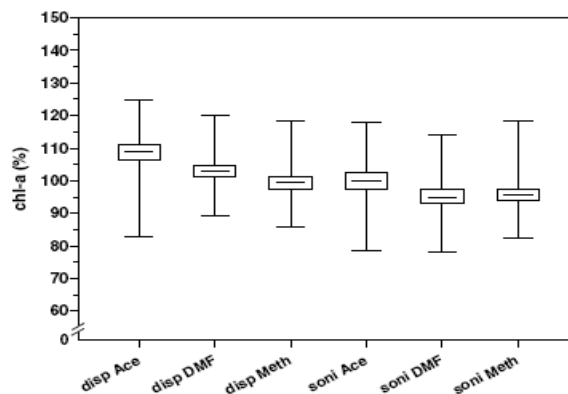


Figure 3.1 –Boxplots of the chlorophyll *a* percentage obtained by HPLC and using different extraction techniques (dispersion and sonification) and solvents (acetone, DMF and methanol; Schagerl and Künzl, 2007). The individual values of each treatment were related to the mean and expressed as a percentage.

Another important aspect and advantage of using acetone is the small amount of chlorophyll *a* derivatives that will be originated during the extraction (Ritchie, 2006; Schagerl and Künzl, 2007; Figure 3.2). In addition, the use of acetone also allows the

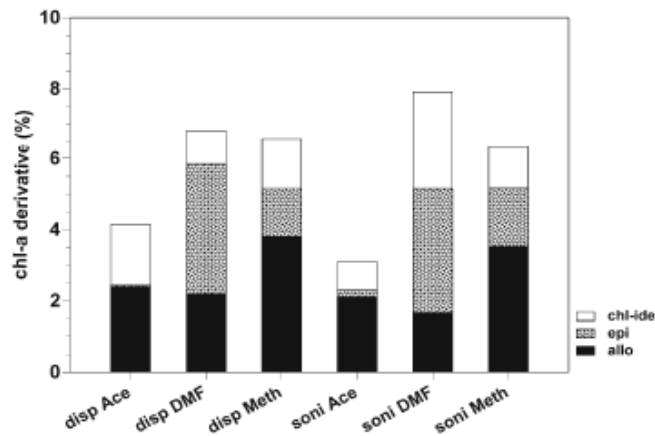


Figure 3.2 – Chlorophyll *a* derivatives percentages obtained with different extraction techniques and solvents (Schagerl and Künzl, 2007).

use of accurate spectrophotometric equations (Jeffrey *et al.*, 1997; Ritchie, 2006). Nevertheless, some authors have suggested other solvents for benthic algae such as: methanol (Tett *et al.*, 1975; Tett *et al.*, 1977; Hagerthey *et al.*, 2006; Cibic *et al.*, 2007; Devesa *et al.*, 2007) and ethanol (Sartory and Grobbelaar, 1984; Rowan, 1989; Ritchie, 2006). The equations developed for spectrophotometry using ethanol and methanol as solvents are not widely accepted and used. The efficiency of extraction varies with species composition (Wasmund *et al.*, 2006; Ritchie, 2008), therefore the methodology should be tested and adjusted for each system (see Jeffrey *et al.*, 1997). Another important aspect to take into consideration is practicality and safety. Acetone is highly flammable, narcotic in large concentrations and attacks polystyrene. This could be an issue if the cuvettes are made of this material. Ethanol is flammable as well, but safer than acetone. Furthermore, it does not attack polystyrene. Methanol is extremely toxic by inhalation or skin contact and attacks polystyrene. In addition, recent studies (Wiltshire *et al.*, 2000; Van Leeuwe *et al.*, 2002), indicated that some treatments can improve the efficiency of the benthic algae extraction, such as the addition of fine inert granules of quartz to increase the area of extraction or an ultrasound bath treatment that acts by increasing the molecular activity. Figure 3.3 represents the results obtained by Wiltshire *et al.* (2000), which show the success of the ultrasound bath as a pre-treatment.

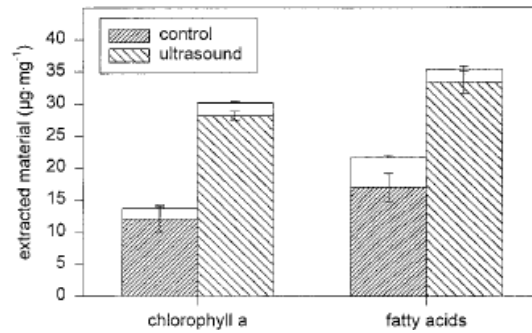


Figure 3.3 – Extraction efficiency of the ultrasound bath for chlorophyll *a* and fatty acids from *Scenedesmus obliquus*. The open bars are the results from a second extraction, which are stacked on the amounts from the first (Wiltshire *et al.*, 2000).

In studies using sediment for benthic chlorophyll measurements, freeze drying is an essential step to avoid any potential errors arising from the water content within the sediment. The freeze dryer removes the water from the sediment without changes in the structure and composition of the material. The equipment decreases the pressure inside the chamber and the direct shift from solid into a gas (sublimation) occurs.

The aim of this study was to develop an optimal methodology for chlorophyll *a* analysis of the microphytobenthos of Ria Formosa, so that it could be applied to MPB ecological investigations. A reliable and feasible (in terms of time consumption) method is essential for ecological studies, such as the assessment of spatial patchiness or seasonal cycles. The optimization was done by assessing the effectiveness of pre-treatments and testing of different solvents, concentrations and extraction times in two sediment types, mud and sand. The null hypotheses tested the non existence of differences between treatments (e.g. pre-treatment; solvent type, solvent strength).

## 3.2 Material and Methods

### 3.2.1 Standard Method

In July 2006 several sediment samples (between 600 – 800g total wet weight) were collected during low water in two intertidal areas: Ramalhete and Ponte (Figure 3.4). Ramalhete is a flat consolidated area with medium/fine sand (Table 3.1; following the classification of Holme and McIntyre, 1984). Ponte (mud) is a soft, dynamic area with ripples composed by muddy sand (following the same classification as before). Both are intercalibration sites for the implementation of the Water Framework Directive.

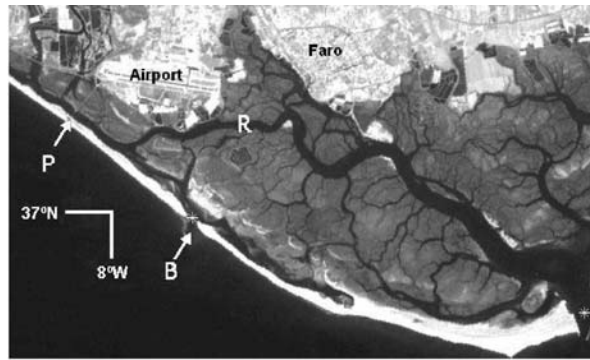


Figure 3.4 - Map of Ria Formosa showing sampling stations at P= Ponte and R = Ramalhete.

Table 3.1 - Grain size distribution (%) and organic matter (%) of samples obtained at Ramalhete (A), Ponte (mud; B) and Ponte (sand; C).

Sediment size fractions (%)	Ramalhete	Ponte (mud)	Ponte (sand)
> 1000 $\mu\text{m}$	2.21	2.49	2.04
1000 - 710 $\mu\text{m}$	6.09	1.25	2.38
710 - 500 $\mu\text{m}$	13.34	2.13	3.07
500 - 355 $\mu\text{m}$	18.79	2.54	3.67
355 - 250 $\mu\text{m}$	8.99	2.20	5.56
250 - 180 $\mu\text{m}$	3.11	3.51	12.15
180 - 125 $\mu\text{m}$	1.34	23.17	26.17
125 - 90 $\mu\text{m}$	0.53	8.39	3.65
90 - 63 $\mu\text{m}$	0.48	4.19	1.63
< 63 $\mu\text{m}$	45.12	50.13	39.68
Organic matter (%)	1.54	2.27	1.62

Samples were collected with a Petri dish of 47mm diameter and 13mm height to ensure that only the top layer, with higher chl *a* content was taken. The unit content ( $\mu\text{g}\cdot\text{g}^{-1}$ ) is in fact a concentration, according to the definition of concentration (substance mixed in another substance), but due to consistency with this specific scientific subject and previous works, it will be used as content throughout this thesis. A plastic card was used to manoeuvre underneath the sample. The samples (approximately 20) were placed in  $1\text{dm}^3$  plastic bottles wrapped in aluminium foil and were transported in a cool box to the laboratory, always protected from light and high temperatures (and thus protecting chl *a* from being degraded). As soon as possible, the plastic bottles were hand-stirred thoroughly to ensure homogeneous chl *a* content in each of them. Then, the sediment of each bottle was divided in as many homogeneous samples as necessary for the analysis (of approximately half the volume of the initial samples; see Table 3.2). Each sample was placed in  $50\text{cm}^3$  plastic tubes, covered with aluminium foil.

All samples were freeze-dried for 30 hours to avoid any potential errors arising from the water content within the sediment (Buffan-Dubau and Carman, 2000). The required time to freeze-dry samples was assessed before the beginning of this study and results are presented in the following section. This was done by weight to obtain the water loss of eighteen samples, placed in the freeze-drier, every two hours until obtaining constant weights. Eighteen samples were used because this would completely fill the freeze-drier chamber. Freeze-drying importance was tested by Buffan-Dubau and Carman (2000) and by Van Leeuwe *et al.* (2006), using methanol and acetone. Both studies clearly yielded increased extraction efficiency. The weight of the sediment was determined after freeze-drying. The solvent (90% acetone stored over sodium bicarbonate) was added to each sample, keeping a constant proportion of solvent volume to sediment weight and the tubes were agitated in the vortex. Samples were placed in the freezer at -20°C for 30 hours. Afterwards, the tubes were centrifuged for 10 min at 3000rpm. This method was adapted from Parsons *et al.* (1984) to measure chlorophyll *a* and phaeopigments. No other types of chlorophyll may be assessed. The presence of other pigments causes a small error in the estimate. This happens as well with the presence of phaeopigments in the trichromatic equations, where each type of chlorophyll may be assessed separately. The current procedure uses Lorenzen's equations (Lorenzen, 1967), however it was adapted for sediment, using weight of sediment instead of the volume of water. Ninety percent acetone (buffered with sodium bicarbonate) was centrifuged for 10 min and then placed in the Helios  $\alpha$  UV-Visible Spectrophotometer for zeroing the equipment. The wavelengths used were 663nm and 750nm according to the equation described below. Samples were measured in 1 cm pathlength spectrophotometer cells. After that, two drops of 1.2M HCl were added to the cuvette and the samples were remeasured again at 663nm and 750nm.

$$\text{Chlorophyll } a \text{ concentration } (\mu\text{g.g}^{-1}) = \frac{26,7 \times ((663-750)-(663a-750a)) \times v}{W \times l}$$

$$\text{Phaeopigments concentration } (\mu\text{g.g}^{-1}) = \frac{26,7 \times (1,7 \times (663a-750a) - (663-750)) \times v}{W \times l}$$

A663 – absorbance at 663nm

A750 – absorbance at 750nm

A663a – absorbance at 663nm after acidification

A750a – absorbance at 750nm after acidification

v – volume of acetone extract (cm<sup>3</sup>)

W – Weight of the sediment (g)

l – path length of the cuvette (cm)

Table 3.2 - Description of the methodological experiments: test of the effectiveness of pre-treatments and test for the optimal methodology.

		control	Treatment 1	Treatment 2	Treatment 3	Source of material	Subsamples	
Pre-treatments		standard	inert granules			Ponte, Jul-06, MS	5, 5	
		standard	ultrasound bath 1.5 h			Ponte, Jul-06, MS	8, 8	
	Type of solvent	standard	extract in 90% ethanol/water	extract in 95% methanol/water		Ponte, Jul-06, MS	5, 5, 5	
Optimal Methodology	Type of solvent	"	"	"		Ramalhete, Jul-06, S	5, 5, 5	
		"	"	"		Ponte, Aug-07, MS	5, 5, 5	
		"	"	"		Ponte, Aug-07, S	5, 5, 5	
		"	"	"		Ponte, Aug-07, S	5, 5, 5	
	Solvent concentration	standard	extract in 95% acetone/water	extract in 80% acetone/water	extract in 70% acetone/water		Ponte, Jul-06, MS	5, 5, 5, 5
		"	"	"	"		Ramalhete, Jul-06, S	5, 5, 5, 5
		"	"	"	"		Ponte, Aug-07, MS	5, 5, 5, 5
		"	"	"	"		Ponte, Aug-07, S	5, 5, 5, 5
	Time of extraction	standard, except extract 48 hr	extract 24 hr	extract 12 hr	extract 1 hr		Ponte, Jul-06, MS	5, 5, 5, 5
		"	"	"	"		Ramalhete, Jul-06, S	5, 5, 5, 5
		"	"	"	"		Ponte, Aug-07, MS	5, 5, 5, 5
		"	"	"	"		Ponte, Aug-07, S	5, 5, 5, 5

Obs.- Treatment as standard except if stated  
 MS - Muddy Sand      S- Sand



In August 2007, additional samples were collected following the same procedure to repeat the methodological approach. This time, 'sand' samples were collected from an area with fine sand (Table 3.1; following the classification of Holme and McIntyre, 1984) next to the area used to collect muddy sand in Ponte. The new site is similar to Ramalhete in morphological terms. This modification was carried out to ensure that any potential differences obtained in the analysis were not due to the fact that the sites were different, but were instead related to the different types of sediment.

### **3.2.2 Methodological experiments**

#### *Pre-treatments*

The effectiveness of treating the samples in the ultrasound bath was tested by submitting eight of sixteen samples to an ultrasound bath (following Wiltshire *et al.*, 2000) for 1.5 hours after the addition of the solvent as described below. The temperature was kept around 0°C. The effectiveness of fine granules in the extraction was tested by adding fine inert granules (63µm to 250µm) to five of ten muddy samples, which represented approximately 10% of the sediment weight. The granules added were collected from sediment samples from Ponte by sieving. In the laboratory, they were placed in the muffle at 475°C for 4 hours to remove the organic matter, were treated with a strong acid bath (concentrated HCl) and subsequently washed and dried. In the test of both pre-treatments 90% acetone buffered with sodium bicarbonate was used.

#### *Optimal methodology*

In order to ascertain the best solvent, three solvents were tested at the strengths recommended in the literature, namely 90% acetone (Garrigue, 1998; Miles and Sundbäck, 2000; Riaux-Gobin and Bourgoin, 2002), 90% ethanol (Sartory and Grobbelaar, 1984; Papista *et al.*, 2002) and 95% methanol (Marker, 1972). The conditions used for testing the best solvent concentrations and the best time of extraction were chosen based on an extensive review of literature. This study was performed by several steps, using the most appropriate options in the process. For example to test the optimal concentrations of the solvent, only the solvent that yielded the larger extracts of chlorophyll *a* was used. Fifteen samples were used for the solvent

test (5 per solvent), twenty samples were used for the solvent concentration test and twenty samples were used in the assessment of the time of extraction.

For samples with solvent other than 90% acetone, a 10% dilution was carried out in 90% acetone, so that the spectrophotometric equations for 90% acetone could be used. To obtain the chl *a* content ( $\mu\text{g}\cdot\text{g}^{-1}$ ), the weight of the freeze-dried sediment was used in the calculations instead of the usual volume of filtered water when studying pelagic algae.

### **3.2.3 Statistical analysis**

Data were tested for normality and homoscedasticity of variance and parametric tests conducted, as possible. Otherwise, data were transformed and re-checked. All the statistical tests and numerical analyses were carried out using Minitab software. To test the effectiveness of the use of fine granules and the ultrasound bath during the extraction a two sample T-test was carried out. To assess any differences between solvents, solvent concentrations and extraction times, one-way ANOVA tests (significance level of 0.05) were used both for sand and for mud. Multiple comparisons among pairs of means were performed using the Tukey test, when a significant difference was found with ANOVA. The Mann-Whitney non parametric test was used to compare phaeopigment contents obtained in this study, using a significance level of 0.05.

## **3.3 Results**

### **3.3.1 Freeze-drying**

The mean of weight differences of the eighteen samples used in this experiment are presented in Figure 3.5. Water loss was recorded over a 32 hours period, until sample weights were shown to be constant. Figure 3.5 shows changes in sample weight after 18 hours to 32 hours in the freeze-dryer. The first Y-value represents the difference between the initial mean weight and the weight of the sample after 18 hours in the freeze-dryer. The other Y-values represent differences in weight after consecutive 2 hours exposures in the freeze-dryer.

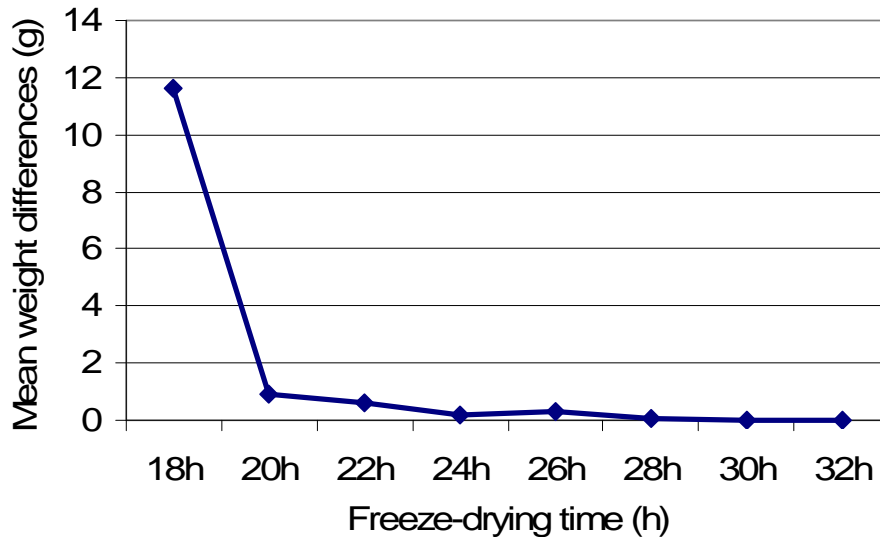


Figure 3.5 - Mean weight differences (g) along the time in the experiment. For example, the value correspondent to 20 hours is the difference between the mean weight of the samples after 18 hours and 20 hours of freeze drying.

### 3.3.2 Pre-treatments

The chl *a* contents obtained when assessing the effectiveness of the addition of fine granules were very similar (Figure 3.6 - A) both for samples with treatment (with fine granules) and with no treatment. The means obtained were  $12.29 (\pm 0.16 \text{ SE}) \mu\text{g}\cdot\text{g}^{-1}$  of chl *a* for samples with treatment and  $12.47 (\pm 0.16 \text{ SE}) \mu\text{g}\cdot\text{g}^{-1}$  of chl *a* for samples without treatment. Data were found to be normally distributed, therefore a T-test was conducted. No significant differences ( $p = 0.438$ ) were found between the two treatments.

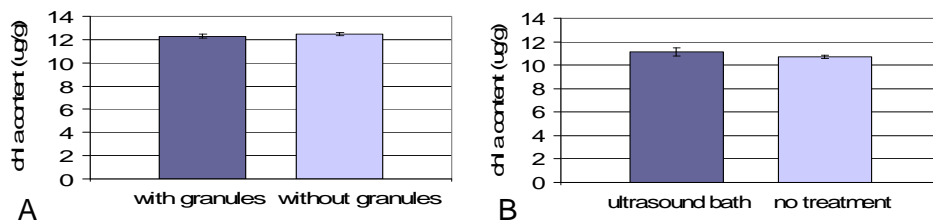


Figure 3.6 - Chlorophyll *a* contents ( $\mu\text{g}\cdot\text{g}^{-1}$ ,  $\pm$  SE) obtained in two tests: A- test of the effectiveness of the addition of fine granules in the chlorophyll *a* extraction; B- test of the effectiveness of the ultrasound bath in the chlorophyll *a* extraction.

The chl *a* contents obtained when assessing the effectiveness of the ultrasound bath were also similar (Figure 3.6 - B), for samples with treatment ( $11.10 \mu\text{g}\cdot\text{g}^{-1} \pm 0.35 \text{ SE}$ ) and with no treatment ( $10.72 \mu\text{g}\cdot\text{g}^{-1} \pm 0.13 \text{ SE}$ ). A T-test was used after a transformation of data ( $\cosine(x)$ ) and no significant differences were found ( $p = 0.379$ ) between the two conditions.

### 3.3.3 Tests for the best method for extraction

#### *Solvent*

Ethanol was the solvent which yielded the lower values of chl *a* in 2006 (mud -  $13.49 \mu\text{g}\cdot\text{g}^{-1}$ , sand -  $9.28 \mu\text{g}\cdot\text{g}^{-1}$ ) and acetone was the solvent which yielded the highest, both for mud and sand (mud -  $14.55 \mu\text{g}\cdot\text{g}^{-1}$ , sand -  $11.56 \mu\text{g}\cdot\text{g}^{-1}$ ; Figure 3.7 - A). Nevertheless, no significant differences were found (ANOVA) between the chl *a* contents obtained with different solvents for each sediment type ( $p = 0.173$  (mud);  $p = 0.069$  (sand)). In 2007, acetone was again the solvent that yielded larger chl *a* contents (Figure 3.8 - A). The smaller values were obtained using ethanol in sand ( $5.76 \mu\text{g}\cdot\text{g}^{-1}$ ) and methanol in mud ( $8.29 \mu\text{g}\cdot\text{g}^{-1}$ ). No significant differences were found (ANOVA) between the chl *a* contents obtained with different solvents for each sediment type ( $p = 0.600$  (mud);  $p = 0.935$  (sand)).

#### *Solvent concentration*

For the optimization of the method, it is also important to know the appropriate concentration of acetone. For the samples collected in 2006, an ANOVA showed significant differences between chl *a* values obtained using different acetone concentrations ( $p < 0.01$  (mud);  $p < 0.005$  (sand)). The chl *a* content obtained using different acetone concentration was lower for 70% acetone, both for mud and sand (Figure 3.7 - B). The statistical analysis for mud was carried out on transformed data ( $\cosine(x)$ ). A Tukey test was then used and significant differences were found as follows:  $90\% > 70\%$ ,  $95\%$  (sand) and  $80\% > 90\% > 70\%$  (mud). Therefore, the values of chl *a* extracted were higher using 90% acetone for sand and 80% acetone for mud.

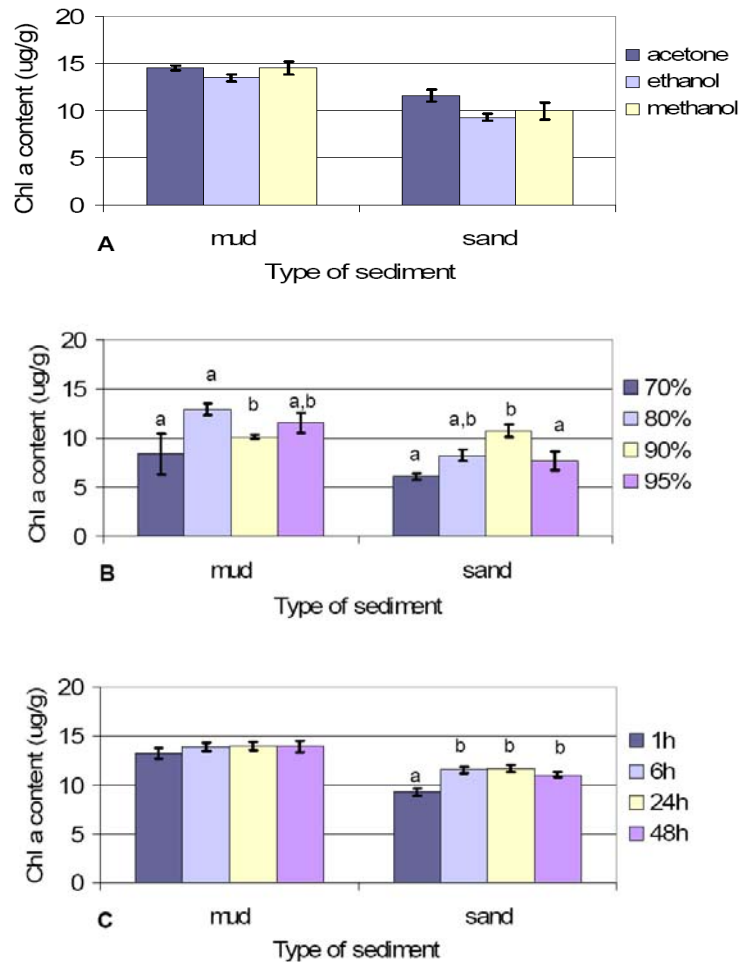


Figure 3.7 - Chlorophyll *a* contents ( $\mu\text{g}\cdot\text{g}^{-1}$ ,  $\pm$  SE) obtained in 2006 studies: A- three solvents (90% acetone, 95% methanol and 90% ethanol); B- four concentrations of the solvent, acetone at 70%, 80%, 90% and 95%; C- four extraction times (1h, 6h, 24h and 48h). The symbols a,b,c and d represent significant different groups from Tukey's test.

From the test performed in 2007 (Figure 3.8 – B), significant differences were found between treatments ( $p < 0.001$  for mud and sand; ANOVA). For both sediment types, a Tukey test showed significant differences between the results obtained using 70% acetone (lower extractions) and the other concentrations. The chlorophyll *a* content means were higher using 90% acetone for sand and 80% acetone for mud, as obtained in 2006.

#### *Extraction time*

The test of the best extraction time performed on the samples collected in 2006 showed a similar pattern for mud and sand (Figure 3.7 - C). The lower values were obtained after only one hour of extraction with the values similar for larger times of

extraction. Significant differences were found between the chlorophyll *a* values obtained with the four extraction times for sand ( $p = 0.001$ ). No significant differences were found between extraction times for mud ( $p = 0.678$ ) after a cosine (1-x) transformation. A Tukey test was used to check the temporal differences for sand and

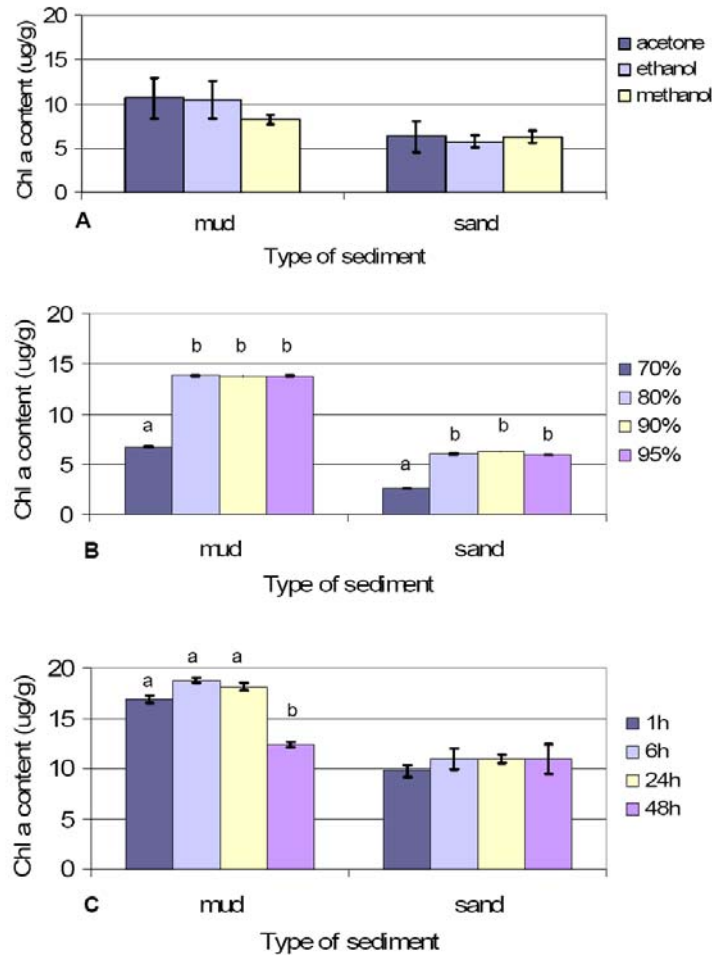


Figure 3.8 - Chlorophyll *a* contents ( $\mu\text{g}\cdot\text{g}^{-1}$ ,  $\pm$  SE) obtained in 2007 testing: A- three solvents (90% acetone, 95% methanol and 90% ethanol); B- four concentrations of the solvent, acetone at 70%, 80%, 90% and 95%; C- four extraction times (1h, 6h, 24h and 48h). The symbols a and b represent significant different groups from Tukey's test.

significant differences were found between 1 hour and all the other levels of treatment. No significant differences were found between 6h, 24h and 48h. During the 2007 test, a different pattern for mud and sand was found (Figure 3.8 - C). The results for sand were similar with the ones obtained in 2006 (sand), but no significant differences were found. The smaller mean was obtained with 1 hour of extraction. An ANOVA showed significant differences between the extraction times for mud ( $p = 0.001$ ). A Tukey test

showed significant differences between the results obtained 48 hours after the extraction (smaller) and the other levels of treatment.

### **3.3.4 Phaeopigments**

The phaeopigment contents found in the pre-treatments were high, around twice the values obtained during the other tests (Table 3.3). The ratio between phaeopigments and chlorophyll *a* was around 1, which means that contents were similar. Smaller phaeopigment contents were obtained for sandy sediments when compared with mud. Significant differences were found between phaeopigment contents from pre-treatments and other tests ( $p < 0.001$ ). Considering solely the tests for the optimal methodology, significant differences were also found between phaeopigment contents found in sand and mud ( $p < 0.001$ ).

### **3.3.5 Mud vs Sand**

Six two-sample T-tests were carried out to compare the chlorophyll *a* contents of muddy and sandy samples using all the samples of each of the 6 tests. Given that data were used for another statistical test, the Bonferroni correction was used in this analysis and a significance level of 0.025 was considered. The results showed larger values for mud with a  $p$ -value  $\leq 0.005$  for each test.

## **3.4 Discussion**

### **3.4.1 Freeze-drying**

The experiment to find the best time for freeze-drying the sediment samples showed that after 30 hours, the loss of water was almost non-existent (mean of 0.008g of difference between weights). So, it was considered that 30 hours was the appropriate time for freeze-drying. This is dependent on the equipment and its power. For example, Fowler (2006) who worked with similar material, in terms of type of sediment and weight, found that 48 hours was sufficient for freeze-drying his samples.

Table 3.3– Phaeopigment concentrations ( $\mu\text{g}\cdot\text{g}^{-1}$ ) and Phaeopigment / Chl *a* ratios observed in all tests carried out. Best option indicated in the table corresponds to the treatment that yielded the highest chl *a* concentration or simply the one recommended for future use.

	<b>Minimum</b>		<b>Maximum</b>		<b>Mean</b>		
	conc. ( $\mu\text{g}/\text{g}$ )	phaeop/ chl ratio	conc. ( $\mu\text{g}/\text{g}$ )	phaeop/ chl ratio	conc. ( $\mu\text{g}/\text{g}$ )	phaeop/ chl ratio	phaeop/chl best option
<b>Pre-treatments</b>							
Fine inerts	9.76	0.76	13.16	1.12	11.69		<b>0.95</b>
Ultrasound bath	10.63	0.86	15.53	1.49	14.5		<b>1.34</b>
<b>Optimal methodology (06)</b>							
<b>Mud</b>							
Solvent	0.26	0.2	6.79	0.48	3.9	0.23	<b>0.42 (acet)</b>
Solvent concentration	1.21	0.17	11.13	1.17	6.93	0.62	<b>0.52 (80%)</b>
Extraction time	3.89	0.29	8.43	0.718	5.85	0.43	<b>0.43 (6 h)</b>
<b>Sand</b>							
Solvent	0.05	0.01	2.89	0.32	1.2	0.12	<b>0.16 (acet)</b>
Solvent concentration	0.08	0.01	4.6	0.78	1.71	0.23	<b>0.14 (90%)</b>
Extraction time	0.03	0.02	3.02	0.38	0.14	0.15	<b>0.14 (6h)</b>
<b>Optimal methodology (07)</b>							
<b>Mud</b>							
Solvent	0.24	0.02	15.6	3.62	4.54	0.73	<b>0.6 (acet)</b>
Solvent concentration	1.25	0.19	7.75	0.55	4.59	0.37	<b>0.31 (80%)</b>
Extraction time	0.46	0.03	9.2	0.61	3.47	0.21	<b>0.15 (6h)</b>
<b>Sand</b>							
Solvent	0.11	0.02	5.43	1.1	2.14	0.64	<b>0.5 (acet)</b>
Solvent concentration	0.3	0.05	3.6	0.7	1.07	0.24	<b>0.23 (90%)</b>
Extraction time	0.13	0.01	3.18	0.34	0.99	0.1	<b>0.10 (6h)</b>



### 3.4.2 Pre-treatments

Both pre-treatments, addition of fine granules and ultrasound bath, did not show any significant differences between treated and not treated samples. The use of these methodologies was a consequence of the need to achieve a more efficient extraction of pigments, mainly by breaking down the algal cell walls. These two pre-treatments were tested by Wiltshire *et al.* (2000) in *Scenedesmus* sp. which is a ‘difficult to extract’ alga and yielded significant larger results. Although some authors such as Schagerl and Künzl (2007) have considered that cell disruption by pre-treatment is essential, others such as the present study, have found no differences with or without the treatments (Sartory and Grobbelaar, 1984; Schumann *et al.*, 2005; Hagerthey *et al.*, 2006). This may be the result of the non-existence of ‘difficult to extract’ species in Ria Formosa. Another aspect that may have improved the extraction efficiency is the freeze-drying that was performed to eliminate water dilution problems. This procedure may help the breakdown of the protein matrix of membranes and thus facilitates the penetration of the solvent (Buffan-Dubau and Carman, 2000), as well as decreasing the chlorophyllase enzyme activity by reducing the water content (Van Leeuwe *et al.*, 2006). Nevertheless, the phaeopigment content found after performing these pre-treatments suggests that no benefit comes from this approach. In addition to not improving the extraction efficiency, these pre-treatments also provided much higher chlorophyll degradation products. The comparison with the other tests, provides indication that these degradation products were a consequence of the method itself due to material handling.

### 3.4.3 Tests for the best method for extraction

#### *Solvent*

In the tests of the samples collected in 2006 and 2007, acetone yielded the largest mean value, both for mud and sand, as indicated previously by Conde *et al.* (1999), Miles and Sundbäck (2000) and Migné *et al.* (2004). Van Leeuwe *et al.* (2006) discussed how the efficiency of the extraction may be species dependent. For example, they observed an efficiency 50% higher using acetone to extract chl *a* from the diatom *Thalassiosira weissfloggi* than using methanol (Van Leeuwe *et al.*, 2006). A natural algal community is a mixture of different species that will most likely have different

individual proportions through the year. This may affect the extraction efficiency. In addition, ethanol and methanol are well known to produce chlorophyll *a* artifacts (Ritchie, 2006; Schagerl and Künzl, 2007). These artifacts are modifications of the original chlorophyll *a* pigment and have different spectral characteristics. One problem concerns the enzyme chlorophyllase that releases the phytol group of chl *a*. This enzyme is inhibited in large concentrations of acetone, while in methanol and ethanol it is still active (Ritchie, 2006). Moreover, the accepted and widely used spectrophotometric equations are a relevant point of favour to acetone (Jeffrey *et al*, 1997). The problems coming from the fact that acetone is highly flammable and does attack polystyrene are solved if acetone is handled in a fume cupboard and glass cuvettes are used. So, as discussed by Wasmund *et al.* (2006), the correct solvent to use depends on several aspects, one being the taxonomic composition of the algal community.

#### *Solvent concentration*

For the optimization of the method, it is also important to know the appropriate strength of acetone. Ninety percent acetone showed the largest means in 2006 (significant differences) and 2007 for sand. These results are in agreement with Van Leeuwe *et al.* (2006), working on microphytobenthos, as well as many others using phytoplankton. It is also a useful solvent since it has the most used spectrophotometric equations. For muddy sediment, a concentration of 80% of acetone yielded the largest contents of chlorophyll *a* for the samples of 2006 (significant differences) and 2007. This strength was initially used by Mackinney (1941). It was then used for several years and was a reference for many researchers working with algae (Margulies, 1970; Porra, 2002). Its importance decreased with new findings on extraction efficiency using different concentrations and other solvents. Our results suggest that the extraction methodology should always be adapted and optimised for each location. As stated before, community composition may be a major factor in this procedure.

#### *Extraction time*

The tests performed during 2006 and 2007, for both sandy and muddy sediments, showed that 6 hours was sufficient for an efficient extraction. The goal is to do the

extraction as quickly as possible, in order to get the maximum chlorophyll *a* possible and the minimum value of chlorophyll *a* artifacts (Hagerthey *et al.*, 2006; Van Leeuwe *et al.*, 2006). Lengthy extraction periods may increase the degradation products (Buffan-Dubau and Carman, 2000; Hagerthey *et al.*, 2006). The period needed for the chlorophyll *a* extraction also depends on the species composition, as indicated by Hagerthey *et al.* (2006). For example, using 100% acetone, Cartaxana and Brotas (2003) found a 2% difference in chlorophyll *a* results from 6 hours to a 24 hour extraction period. Buffan-Dubau and Carman (2000) found a difference of 18% for the same conditions. A difference in the communities between 2006 and 2007 might be the reason why we observed a significant decrease in the chlorophyll content in 2007 for mud. Several paths have been suggested to explain the production and degradation cycles of the chlorophyll pigments, which are commonly complex and interdependent (see for example Porra and Sheer, 2000 and Van Leeuwe *et al.*, 2006 about chlorophyll degradation). Thus, it is not possible to identify exactly what was the difference in the communities or the degradation pathway which took place in these instances. As before, taxonomic studies of algal community would be key component to understand these processes.

#### **3.4.4 Phaeopigments**

The evaluation of phaeopigment contents is especially important in sediments and particularly in mud, as they generally have a larger contribution of detritus and therefore detrital chlorophyll. If the ratio between phaeopigments and chlorophyll is high, it is likely that the main contributors of chl *a* are not living cells. The overall content of phaeopigments in these samples is considered to be relatively small. They are mainly present in muddy sediments, which was expected. Collos *et al.* (2005) indicated that all non-degraded plant systems have a phaeopigment percentage of around 4%. In their study they reported phaeopigment/chlorophyll *a* ratios from 0.17 to 1.86 (autumnal decay) for phytoplankton. Several other authors, such as Sun *et al.* (1994), Rabalais *et al.* (2004) and Reuss *et al.* (2005) reported phaeopigment/chlorophyll *a* ratios larger than 1 in sediments. This ratio can express an indication of the functional state of the algae community, being high when the community is decaying (Collos *et al.*, 2005). A ratio of 1, which means that phaeopigment and chlorophyll contents were similar, suggests that part of the chlorophyll measured was extracted from non living cells.

However, it is important to keep in mind that some methods, as ours, do not take into account the content of other types of chlorophyll, which may lead to an increased estimate of phaeopigments (Jeffrey *et al.*, 1997). For a deeper understanding, the oxygen conditions of the sediments should be known, as they might indicate if the chlorophyll *a* is accumulating in a stable form (Sun *et al.*, 1993a; Sun *et al.*, 1993b). Sun *et al.* (1993b) suggested the existence of three pools of chlorophyll *a* in sediments: bound chlorophyll *a* (nonextractable by acetone); free anoxically degradable chlorophyll *a*; and free anoxically stable chlorophyll *a*. Therefore, under anoxic conditions, non functional chlorophyll *a* may be preserved, which would result in higher estimates. Moreover, according to Sun *et al.* (1993b), chlorophyll *a* degradation is temperature dependent, being higher for high temperatures. This suggests that for sites such as Ria Formosa, where the sediments can reach very high temperatures, the chlorophyll associated with detritus should be rapidly degraded. Therefore, we do think that the ratios (<1) obtained during this study are within reasonable ranges and that most of the chlorophyll contribution is actually coming from living MPB cells.

#### **3.4.5 Mud vs Sand**

Significant differences were consistently found between the values of chlorophyll *a* in muddy and sandy sediments. Muddy sediment samples always had a larger content. These samples were taken from the top (1cm) of the sediment and this result is in accordance with the literature (Cartaxana *et al.*, 2006). These authors suggested that both mud and sand have similar chlorophyll *a* concentrations, however, in muddy sediments, cells are mainly at the top, while in sandy sediments, chlorophyll *a* is present deeper, with the concentration at the top tending to be smaller.

#### **3.5 Comments and recommendations**

Since chlorophyll *a* content has been widely used as an indicator of water quality and the trophic status of several systems (e.g. Tett *et al.*, 2003; Nobre *et al.*, 2005; Yoshiyama and Sharp, 2006), the need to obtain accurate results is extremely important. It is most likely that different algal taxa may yield different extraction efficiency (Papista *et al.*, 2002). It is worth while to investigate the biotic and abiotic characteristics of studied sites before adjusting and establishing the methodology.

Finally, for future studies on the same conditions, our recommendations are to use 90% acetone for sand and 80% acetone for mud with no pre-treatments. The extraction should be performed during 6 hours or between 6 and 24 hours.

### 3.6 References

- Brotas, V., Plante-Cuny, M. (2003). The use of HPLC pigment analysis to study microphytobenthos communities. *Acta Oecologica*, **24**, S109-S115.
- Buffan-Dubau, E., Carman, K. (2000). Extraction of benthic macroalgal pigments for HPLC analysis. *Marine Ecological Progress Series*, **204**, 203-207.
- Cartaxana, P., Brotas, V. (2003). Effects of extraction on HPLC quantification of major pigments from benthic microalgae. *Archives für Hydrobiologie*, **157**, 339-349.
- Cartaxana, P., Mendes, C.R., Van Leeuwe, M.A., Brotas, V. (2006). Comparative study on the microphytobenthic pigments of muddy and sandy intertidal pigments of the Tagus estuary. *Estuarine, Coastal and Shelf Science*, **66**, 225-230.
- Cibic, T., Blasutto, O., Hancke, K., Johnsen, G. (2007). Microphytobenthic species composition, pigment concentration, and primary production in sublittoral sediments of the Trondheimsfjord. *Phycological Society of America*, **43**, 1126-1137.
- Collos, Y., Husseini-Ratrema, J., Bec, B., Váquer, A., Hoai, T., Rougier, C., Pons, V. and Souchu, P. (2005). Pheopigment dynamics, zooplankton grazing rates and the autumnal ammonium peak in a Mediterranean lagoon. *Hydrobiologia* **550**, 83-93.
- Conde, D., Bonilla, S., Aubriot, L., de León, R., Pintos, W. (1999). Comparison of the areal amount of chlorophyll a of planktonic and attached microalgae in a shallow coastal lagoon. *Hydrobiologia*, **408/409**, 285-291.
- Consalvey, M., Perkins, R., Paterson, D., Underwood, G. (2005). PAM Fluorescence: A beginners guide for benthic diatomists. *Diatom Research*, **20**, 1-22.
- Devesa, R., Moldes, A., Díaz-Fierros, F., Barral, M. (2007). Extraction study of algal pigments in river bed sediments by applying factorial designs. *Talanta*, **72**, 1546-1551.
- Fowler, R. (2006). *Development and testing of benthic pigment analyses*. BSc(Hons) thesis. Napier University, Edinburgh, Scotland.
- Garrigue, C. (1998). Distribution and biomass of microphytes measured by benthic chlorophyll a in a tropical lagoon. *Hydrobiologia*, **385**, 1-10.
- Grinham, A., Carruthers, T., Fisher, P., Udy, J., Dinnison, W. (2007). Accurately measuring the abundance of benthic microalgae in spatially variable habitats. *Limnology and Oceanography: Methods*, **5**, 119-125.
- Hagerthey, S., Louda, G., Mongkronsri, P. (2006). Evaluation of Pigments extraction methods and a recommended protocol for periphyton chlorophyll a determination and chemotaxonomic assessment. *Journal of Phycology*, **42**, 1125-1136.
- Holme, N., McIntyre., (1984). *Methods for the study of Marine Benthos*. 2<sup>nd</sup> edition. Ed ISP Handbook 16. Blackwell Scientific Publications, 387 pp.

- Jeffrey, S., Mantoura, R., Wright, S., eds. (1997). *Phytoplankton pigments in oceanography: guidelines to modern methods*. UNESCO, Paris, 661pp.
- Jesus, B., Brotas, V., Marani, M., Paterson, D. (2005). Spatial dynamics of microphytobenthos determined by PAM fluorescence. *Estuarine and Coastal Shelf science*, **65**, 30-42
- Koh, C., Khim, J., Araki, H., Yamanishi, H., Koga, K. (2007). Within-day and seasonal patterns of microphytobenthos biomass determined by co-measurements of sediment and water column chlorophylls in the intertidal mudflat of Nanaura Sea, Ariake Sea, Japan. *Estuarine, Coastal and Shelf Science*, **72**, 42-52.
- Kromkamp, J., Barranguet, C., Peene, J. (1998). Determination of microphytobenthos PSII quantum efficiency and photosynthetic activity by means of variable chlorophyll fluorescence. *Marine Ecology Progress Series*, **162**, 45-55.
- Lorenzen, G. (1967). Determination of chlorophyll and phaeopigments: spectrophotometric equations. *Limnology and Oceanography*, **12**, 343-346.
- Mackinney, G. (1941). Absorption of light by chlorophyll solutions. *Journal of Biological Chemistry*, **140**, 315-322.
- Margulies, M. (1970). Changes in absorbance spectrum of the diatom *Phaeodactylum tricorutum* upon modification of protein structure. *Journal of Phycology*, **6**, 160-164.
- Marker, A. (1972). The use of acetone and methanol in the estimation of chlorophyll in the presence of pheophytin. *Freshwater Biology*, **2**, 361-385.
- Migné, A., Spilmont, M., Davoult, D. (2004). In situ measurements of benthic primary production during emersion: seasonal variations and annual production in the Bay of Somme (eastern English Channel, France). *Continental Shelf Research*, **24**, 1437-1449.
- Miles, A., Sundbäck, K. (2000). Diel variation in microphytobenthic productivity in areas of different tidal amplitude. *Marine Ecological Progress Series*, **205**, 11-22.
- Nobre, A.M., Ferreira, J.G., Newton, A., Simas, T., Icely, J.D., Neves, R. (2005). Management of coastal eutrophication: Integration of field data, ecosystem-scale simulations and screening models. *Journal of Marine Systems*, **56**, 375-390.
- Papista, E., Ásc, E., Böddi, B. (2002). Chlorophyll-a determination with ethanol – a critical test. *Hydrobiologia*, **485**, 191-198.
- Parsons, T., Maita, Y., Lalli, M. (1984). *A manual of chemical and biological methods for seawater analysis*. 1<sup>st</sup> edition. Pergamon Press, 105 pp.
- Porra, R., Scheer, H. (2000). <sup>18</sup>O and mass spectrometry in chlorophyll research: Derivation and loss of oxygen atoms at the periphery of the chlorophyll macrocycle during biosynthesis, degradation and adaptation. *Photosynthesis Research*, **66**, 159-175.
- Porra, R. (2002). The chequered history of the development and use of simultaneous equations for the accurate determination of chlorophylls *a* and *b*. *Photosynthesis Research*, **73**, 149-156.
- Riaux-Gobin, C., Bourgoin, P. (2002). Microphytobenthos biomass at Kerguelen's Land (Subantarctic Indian Ocean): repartition and variability during austral summers. *Journal of Marine Systems*, **32**, 295-306.

- Rabalais, N., Atilla, N., Normandeau, C., Turner, R.E. (2004). Ecosystem history of Mississippi River-influenced continental shelf revealed through preserved phytoplankton pigments. *Marine Pollution Bulletin*, **49**, 537-547.
- Reuss, N., Conley, D., Bianchi, T. (2005). Preservation conditions and the use of sediment pigments as a tool for recent ecological reconstruction in four Northern European estuaries. *Marine Chemistry*, **95**, 283-302.
- Ritchie, R. (2006). Consistent sets of spectrophotometric chlorophyll equations for acetone, methanol and ethanol solvents. *Photosynthesis Research*, **89**, 27-41.
- Richie, R. (2008). Universal chlorophyll equations for estimating chlorophylls *a, b, c* and *d* and total chlorophylls in natural assemblages of photosynthetic organisms using acetone, methanol or ethanol solvents. *Photosynthetica*, **46**, 115-126.
- Rowan, K. (1989). *Photosynthetic pigments of algae*. Cambridge University Press, Cambridge.
- Sartory, D., Globbelaar, J. (1984). Extraction of chlorophyll *a* from freshwater phytoplankton for spectrophotometric analysis. *Hydrobiologia*, **144**, 177-187.
- Serôdio, J., Vieira, S., Cruz, S., Barroso, F. (2005). Short-term variability in the photosynthetic activity of microphytobenthos as detected by measuring rapid light curves using variable fluorescence. *Journal of Marine Biology*, **146**, 903-914.
- Schagerl, M., Künzl, G. (2007). Chlorophyll *a* extraction from freshwater algae – a reevaluation. *Biologia*, **62**, 270-275.
- Schumann, R., Häubner, N., Klausch, S., Karsten, U. (2005). Chlorophyll extraction methods for the quantification of green microalgae colonizing building facades. *International Biodeterioration and Biodegradation*, **55**, 213-222.
- Strickland, J., Parsons, T. (1972). *A practical handbook of Seawater Analysis*, 2<sup>nd</sup> edition, Journal of Fisheries Research. Board of Canada. 311 pp.
- Sun, M., Lee, C., Aller, R. (1993a). Anoxic and oxic degradation of <sup>14</sup>C-labeled chloropigments and a <sup>14</sup>C-labeled diatom in Long Island Sound sediments. *Limnology and Oceanography*, **38**, 1438-1451.
- Sun, M., Lee, C., Aller, R. (1993b). Laboratory studies of oxic and anoxic degradation of chlorophyll-*a* in Long Island Sound sediments. *Geochimica et Cosmochimica Acta*, **57**, 147-157.
- Sun, M., Aller, R., Lee, C. (1994). Spatial and temporal distributions of sedimentary chloropigments as indicators of benthic processes in Long Island Sound. *Journal of Marine Research*, **52**, 149-176.
- Tada, K., Yamaguchi, H., Montani, S. (2004). Comparison of Chlorophyll *a* Concentrations Obtained with 90% Acetone and N, N-dimethylformamide Extraction in Coastal Seawater. *Journal of Oceanography*, **60**, 259-261.
- Tett, P., Kelly, M. G., Hornberger, G. (1975). A Method for the spectrophotometric measurement of chlorophyll *a* and pheophytin *a* in benthic microalgae. *Limnology and Oceanography*, **20**, 887-896
- Tett, P., Kelly, M., Hornberger, G. (1977). Estimation of chlorophyll *a* in methanol. *Limnology and Oceanography*, **20**, 579-580.
- Tett, P., Gallegos, C., Kelly, M., Hornberger, G., Cosby, B (1978). Relationships among substrate, flow, and benthic microalgal pigment density in the Mechums River, Virginia. *Limnology and Oceanography*, **23**, 785-797.

- Tett, P., Gilpin, L., Svendsen, H., Erlandsson, C.P., Larsson, U., Kratzer, S., Fouilland, E., Janzen, C., Lee, J., Grenz, C., Newton, A., Ferreira, J.G., Fernandes, T., Scory, S. (2003). Eutrophication and some European waters of restricted exchange. *Continental Shelf Research*, **23**, 1635-1671.
- Van Leeuwe, M.A., Morgan, G., Brockmann, C. (2002). HIMOM – A system of Hierarchical Monitoring Methods for assessing changes in the biological and physical state of intertidal areas – Book of protocols.
- Van Leeuwe, M., Villerius, L., Roggeveld, J., Visser, R., Stefels, J. (2006). An optimized method for automated analysis of algal pigments by HPLC. *Marine Chemistry*, **102**, 267-275.
- Wasmund, N., Topp, I., Schories, D. (2006). Optimising the storage and extraction of chlorophyll samples. *Oceanologia*, **48**, 125-144.
- Wiltshire, K. H. B., M., Möller, A., Buhtz, H. (2000). Extraction of pigments and fatty acids from the green alga *Scenedesmus obliquus* (Chlorophyceae). *Aquatic Ecology*, **34**, 119-126.
- Yoshiyama, k., Sharp, J. (2006). Phytoplankton response to nutrient enrichment in an urbanized estuary. Apparent inhibition of primary production by overeutrophication. *Limnology and Oceanography*, **51**, 424-434.



## **CHAPTER 4**

---

Seasonal, spatial and vertical variability of  
microphytobenthos

---

## Abstract

Microphytobenthos (MPB) are an important, yet highly variable, component of highly productive shallow systems and intertidal areas. Samples were collected from Ria Formosa, Portugal, to assess the temporal and spatial variability of microphytobenthic chlorophyll in two types of intertidal sediment: mud and sand. Chlorophyll pigments were measured spectrophotometrically after freeze-drying and extraction into an acetone-water mixture. The pigments were found in large quantities not only within the first centimetre of sediment, but also down to a depth of 15cm. Time-series of superficial chlorophyll measured at two sites during 2006-2007 showed no obvious seasonal peaks. A truncated Fourier series was fitted to the time-series data. Seasonality was very weak: only 5% of estimated total variance could be explained by annual cycle components up to  $3 \text{ yr}^{-1}$ , while 25% was explained by waves with periods from 14 to 91 days. The residual error about the Fourier series was partitioned into within-day variance (61%) and other components (9%). The within-day variation was made up of approximately equal contributions from (i) variability associated with sampling within sites and (ii) differences between sites. There were no significant correlations between MPB chlorophyll and tidal range, wind speed, solar irradiance, water temperature and salinity and water nutrient concentrations. Sediment type was once more confirmed to be a key factor in MPB spatial variability. These results are discussed in relation to processes controlling the distribution of benthic microalgae in Ria Formosa, and their implications considered in relation to on-going work to understand and model the role of microphytobenthos in eutrophication in such water bodies.

**Keywords:** microphytobenthos, chlorophyll *a*, spatio-temporal variability, vertical distribution, Ria Formosa.

## 4.1 Introduction

Benthic microalgae are known to be extremely variable in space (patchiness) at different scales, from centimetres to kilometres (Brotas and Plante-Cuny, 1998; Azovsky *et al.*, 2004; Jesus *et al.*, 2005). Chlorophyll *a* concentrations depend on several factors such as emersion time, distance to high water level, sediment type and sediment size. This variability has to be considered when scaling up measurements to estimate the community biomass. For example, Koh *et al.* (2006) found chlorophyll *a* (chl *a*) concentrations ranging from 13 to 300 mg.m<sup>-2</sup> in Japan. Edmunds *et al.* (2004) shows an example of how variable the microphytobenthos biomass can be in an embayment (Figure 4.1).

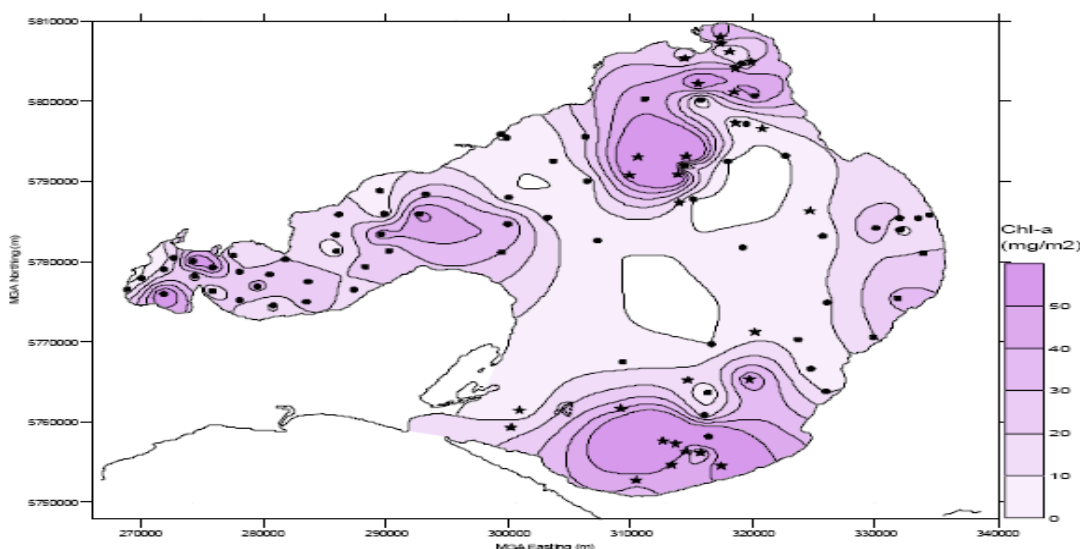


Figure 4.1 – Spatial distribution of microphytobenthos biomass (0 (white) – 50 (dark purple) mg chl.a.m<sup>-2</sup>) on the surface sediments of Port Phillip Bay (area of 2400km<sup>2</sup>; from: Edmunds *et al.*, 2004).

Hedtkamp (2005) obtained a large variation of chlorophyll *a* content within the sediment depth which was dependent on the distance from the normal high water line (0m in the graph) into the subtidal area (302m in the graph; Figure 4.2). This high variation is in agreement with Seuront and Spilmont (2002) who compiled the values of chl *a* concentration obtained in different studies. These authors reported a ratio between the maximum and minimum chl *a* that vary from 2.10 to 300.00, which illustrates its spatial heterogeneity.

MPB also exhibit a high level of temporal variability, which can explain part of the variation found. A seasonal pattern with higher values of microphytobenthos during the spring and summer has been proposed by Underwood and Kromkamp (1999). However

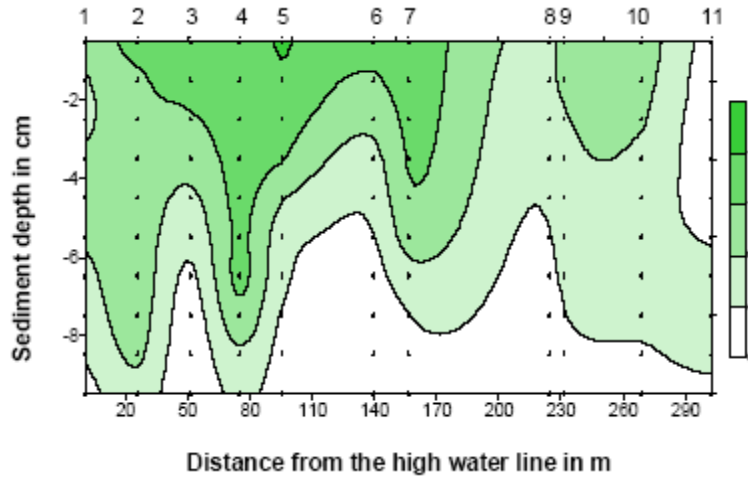


Figure 4.2 – Vertical distribution of chlorophyll *a* content ( $0 - 16 \mu\text{g.g}^{-1}$ ), in a study site of the Wadden Sea, along the transect from the normal high water line (0 m) into the subtidal (302 m at station 11; from Hedtkamp, 2005).

some authors suggest higher values of chl *a* during the winter (Koh *et al.*, 2007) or the absence of any trend (Cartaxana *et al.*, 2006; Figure 4.3). Another reason that may contribute to the reported variability is the lack of a standard extraction methodology using benthic chl *a* as a measure of MPB abundance (Defew *et al.*, 2002; Migné *et al.*, 2004; Easley *et al.*, 2005; Mitbavkar and Anil, 2005).

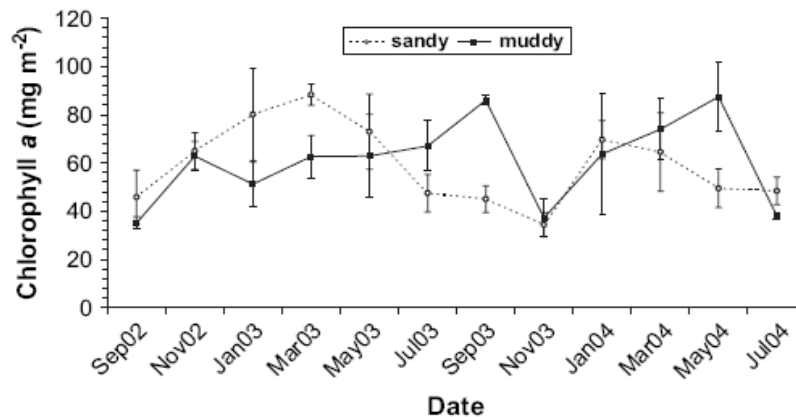


Figure 4.3 – Seasonal variation of chlorophyll *a* concentration ( $\text{mg.m}^{-2}$ ) from 2002 to 2004 for mud and sand from intertidal areas of Tagus Estuary (from Cartaxana *et al.*, 2006).

It has also been suggested that microphytobenthos could be more abundant on muddy sediment when compared with sandy sediments (Riaux-Gobin and Bourgoin, 2002; Perkins *et al.*, 2003). However, recent studies showed that microphytobenthos seems to be equally abundant both in mud and sandy areas, albeit with different vertical distributions (deeper in sand; Cartaxana *et al.*, 2006). In muddy sediments microphytobenthos is found mostly in the top 500  $\mu\text{m}$  of sediment whereas in sandy

sediment it is possible to find relatively constant concentrations down to 3mm depth (Cartaxana *et al.*, 2006). The profiles obtained by Cartaxana *et al.* (2006) from the very first part (3.5 mm) of the sediment in Tagus Estuary are shown in Figure 4.4.

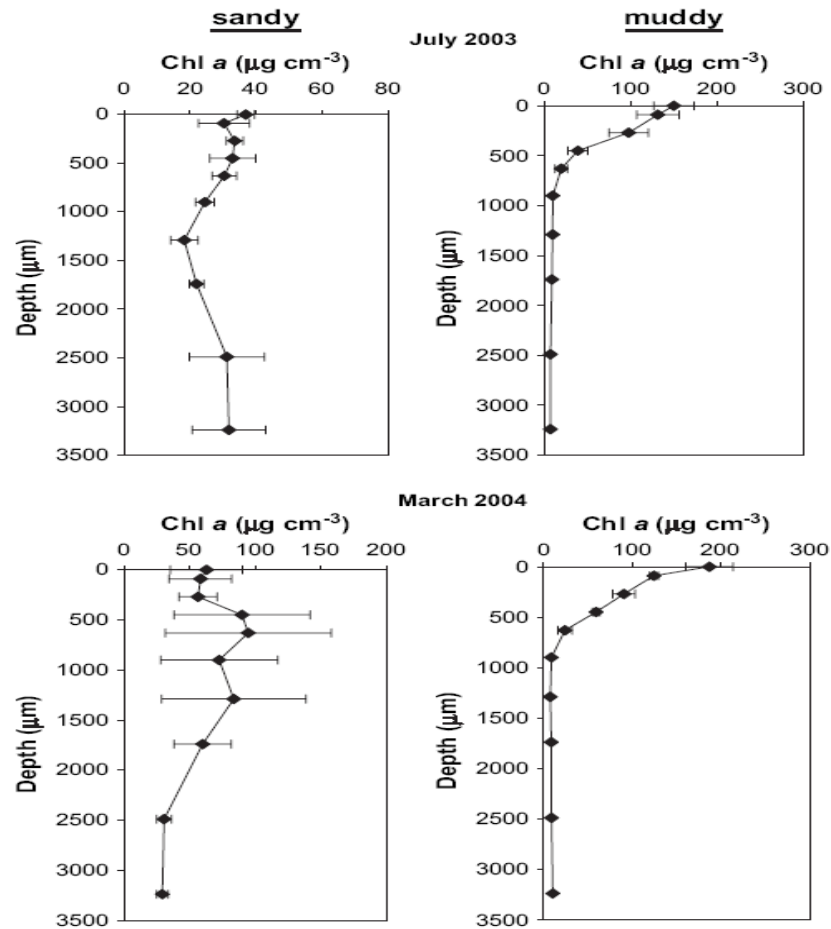


Figure 4.4 – Chlorophyll *a* concentration ( $\mu\text{g}\cdot\text{cm}^{-3}$ ) profiles for mud and sand from the Tagus Estuary (From Cartaxana *et al.*, 2006).

Hedtkamp (2005) did a similar profile study in the Wadden Sea for chlorophyll *a* (Figure 4.5). This study was done into deeper layers of sandy sediment, compared with the profiles from Cartaxana *et al.* (2006). It is shown that the concentration decreases to almost 0 approximately 6 / 8 cm depth. These profiles presented in Figure 4.5 show that minimum chlorophyll *a* content was found at 8 – 12 cm depth throughout the year (Hedtkamp, 2005). Benthic algae are found several cm down into the sediment which may result from bioturbation or active vertical migration.

The MPB is known to be mainly in the top layers (mm) of the sediment (Perkins *et al.*, 2003; Consalvey *et al.*, 2005; Easley *et al.*, 2005; Cartaxana *et al.* 2006). Serôdio *et al.* (1997) estimated the photic depth of intertidal sediments to be 270  $\mu\text{m}$ , which is likely to be a key factor in the distribution of microphytobenthic cells. Moreover, the

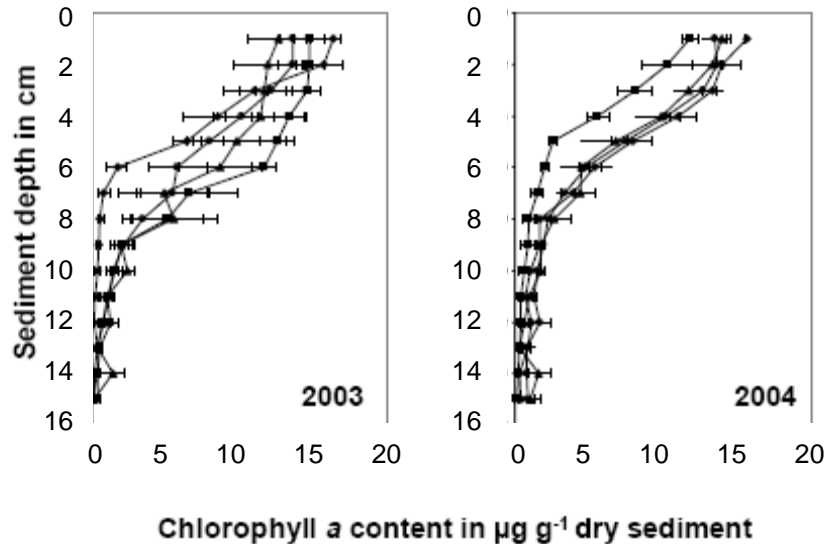


Figure 4.5 – Chlorophyll *a* content (0–20  $\mu\text{g}\cdot\text{g}^{-1}$  dry sandy sediment) profiles (0–15 cm) from Wadden Sea for the years 2003 and 2004 for 4 seasons:  $\diamond$  spring,  $\blacksquare$  summer,  $\blacktriangle$  autumn,  $\bullet$  winter (from Hedtkamp, 2005).

vertical migration of MPB in the sediment as a response to the joint stimulus of light and tide has been well documented (Serôdio *et al.*, 1997; Martins-Loução, 2003; Jesus *et al.*, 2005; Serôdio *et al.*, 2005). This phenomenon was in part suggested by the lack of any measurable photoinhibition (Underwood and Kromkamp, 1999). The patterns of vertical migration are synchronized with diurnal emersion periods (Jesus *et al.*, 2005). During the beginning of the low tide with daylight, cells can show considerable changes in biomass, accumulating at the sediment surface. At the end of the emersion period, cells tend to move downwards again. These changes in biomass over a 6h emersion period are shown in Figure 4.6. There is also another aspect of vertical migration that can be observed at shorter time scales. It has been suggested by several authors that microphytobenthos cells can be constantly migrating from the surface to deeper layers and vice-versa (Kromkamp *et al.*, 1998; Serôdio *et al.*, 2005). Colijn and de Jonge (1984) suggested that cells deeper in the sediment are not functioning, but they are viable and can restart the photosynthetic process once the sediment in the surface is removed, constituting a stock of potential primary producers.

Kromkamp *et al.* (1998) suggested that the existence of individual specimens cycling up and down within sediments can be an evolutionary advantage for cells, preventing eventual damages provoked by the excess of light, which can lead to higher rates of biofilm productivity (Consalvey *et al.*, 2005). Through this migration, they can avoid

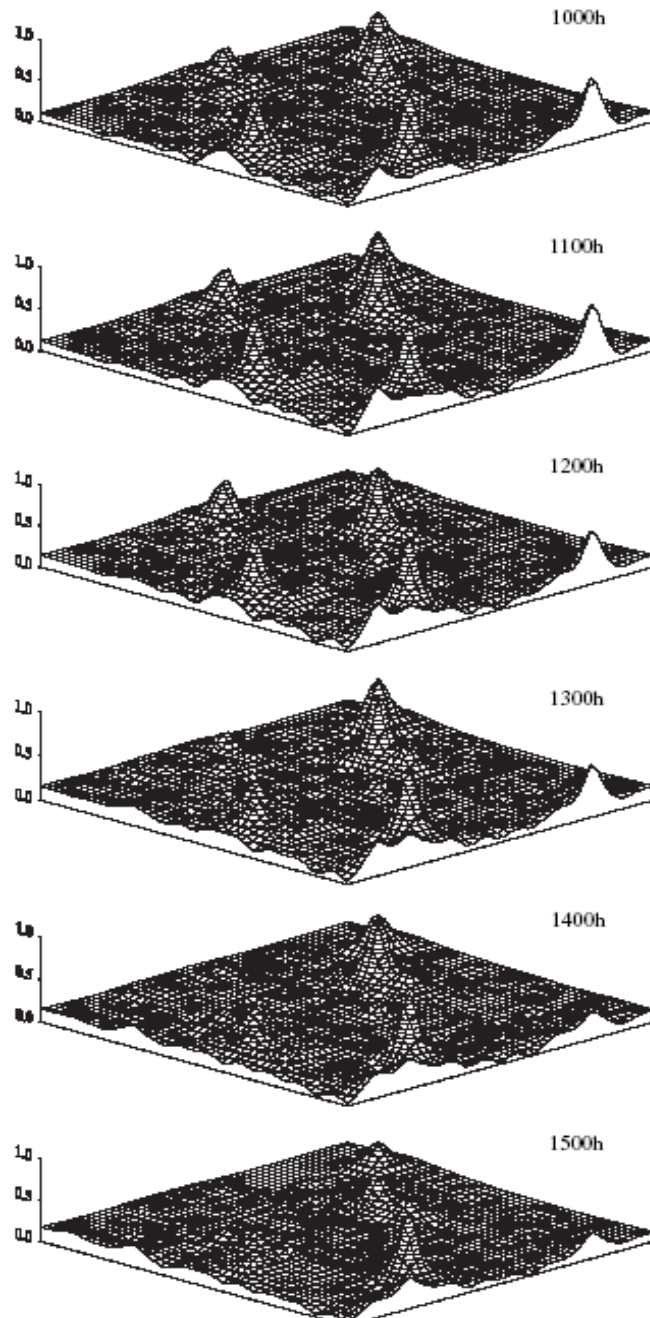


Figure 4.6 – Vertical changes of the microphytobenthos biomass throughout a 6h emersion period (from Jesus *et al.*, 2005).

re-suspension, transport to unsuitable habitats (deeper ones) and predation (Easley *et al.*, 2005).

Patchiness of microphytobenthos biomass from a microscale sampling ( $1\text{m}^2$ ) was also suggested, by authors such as Seuront and Spilmont (2002). These authors suggested that microphytobenthos exhibits a pattern that defines the fingerprints of self-organized critical state, which is defined by “the spontaneous emergence of intermittent fluctuations across a broad range of spatial and temporal scales without any “fine

tuning” necessary from outside the system”. This complex idea tries to demonstrate that microphytobenthos variability (both in space and time) does not solely depend on a specific outside factor and that there is a spontaneous and intrinsic form for cells to behave. This process is poorly understood but its knowledge may help to achieve improved estimates of microphytobenthos biomass and primary production. Although there is much knowledge about microphytobenthos migration, movement and organization, more is needed. New aspects about their behaviour have been described recently.

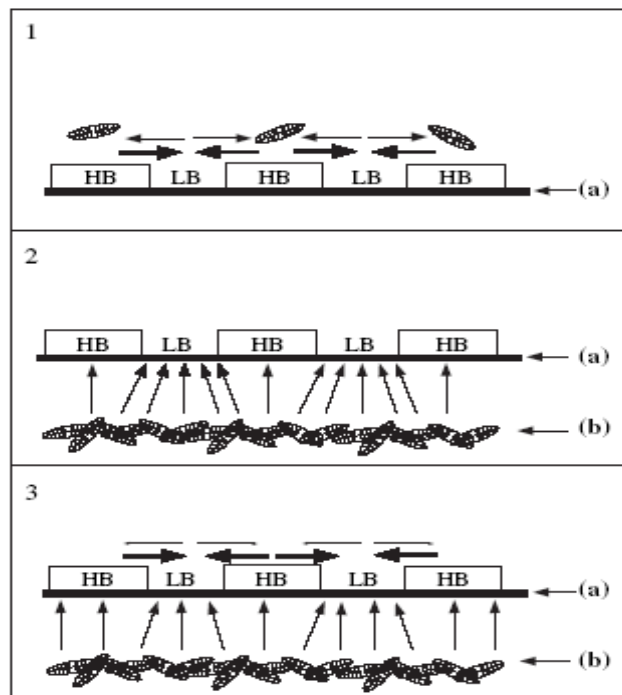


Figure 4.7 – Theoretical models for diatom migration. (a) sediment surface; (b) diatoms; (HB) high biomass; (LB) low biomass. (1) Diatoms move horizontally from HB to LB areas; (2) sub-surface diatoms migrate to LB areas; (3) homogeneous migration of the sub-surface diatoms to the surface and then a horizontal movement to LB areas. From Jesus *et al.* (2005).

Jesus *et al.* (2005) found a strong MPB biomass correlation between the chlorophyll measurements taken over a short time interval, over an emersion period (Figure 4.6). However they found a weak MPB biomass correlation before and after the immersion, which suggests some kind of lateral mobility during the tidal inundation. Jesus *et al.* (2005) suggested three conceptual theories to explain this phenomenon and they are represented in Figure 4.7. The first proposal is a lateral movement from the high biomass (HB) areas to the low biomass (LB) areas. The second is the migration of the sub-surface diatoms preferentially to LB areas. The third hypothesis is a homogeneous



migration of the sub-surface diatoms to the surface and then a horizontal movement to LB areas. The first hypothesis was excluded with observational data. The other two were not excluded but more studies are needed so that this point can be clarified (Jesus *et al.*, 2005).

This study aimed to: (1) describe and simulate the seasonal cycle of microphytobenthos in the Ria Formosa, as part of the development of a mathematical model for the nutrient-assimilative capacity of the water body; (2) determine if the MPB temporal variation is affected by environmental factors such as temperature, irradiance, salinity, tidal height, wind velocity and nutrients in the water column; (3) investigate the spatial variability, both at large and small scale due to its heterogeneity present in the lagoon, which needs to be taken into account in assessing seasonal variability observed at single sites and in testing the goodness of fit of numerical simulations; (4) investigate the vertical distribution of MPB in cores of 15cm depth. The initial hypotheses were that: 1) there was a standard temporal pattern influenced by the environmental variables; 2) there were no spatial differences in terms of chlorophyll concentrations; 3) the chlorophyll concentrations decreases from the surface to the deeper layers.

## **4.2 Material and Methods**

### **4.2.1 Sampling**

#### *Seasonal variability*

For the temporal analysis, six sediment samples were collected twice a month, from April to October of 2006 and from March 2007 until February of 2008, at two sites, where long term studies were being conducted (muddy area at Ponte and Ramalhete). Ponte is located in one of the main channels of the lagoon and has the influence of the inputs from golf courses and agriculture. Ramalhete is an area with fine sand (following Holme and McIntyre, 1984; see Table 4.1), located in an inner channel, compared with Ponte and receives the effluent from an Urban Waste Water Treatment plant. It is also affected by its proximity to the airport and recreational activities. The sediment samples were taken using a petri-dish (47mm diameter and 13mm height), covered by aluminium foil to protect them from light and placed in a cooler box, to avoid high temperatures. Several authors have used a wide number of replicates from 3 to 20, as discussed by Grinham *et al.* (2007). These authors indicated that 8 samples should be

used, less than 6 should never be considered (Figure 4.8) as discussed by Day and Quinn (1998). Six samples were taken in this study due to technical constraints.

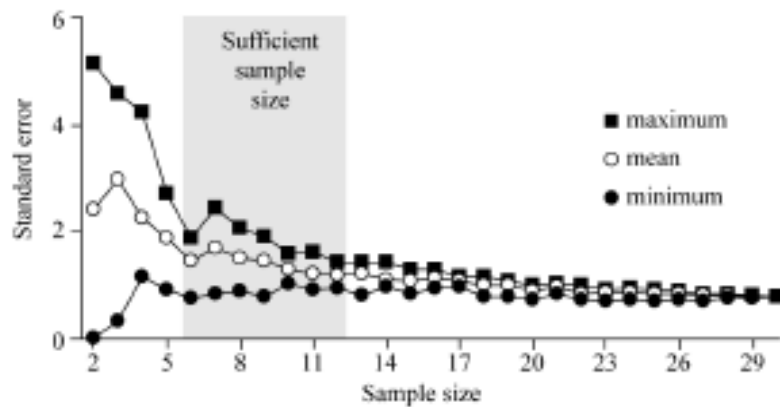


Figure 4.8 – Standard errors used to assess the sufficient sample size for abundance studies at the metres squared scale (Day and Quinn, 1998).

Table 4.1 - Grain size distribution (%) of samples obtained at Quinta do Lago, Ponte (mud), Ponte (sand), Ramalhete, Olhão, Fuzeta and Cabanas de Tavira.

Sediment size fractions (%)	Quinta do Lago	Ponte (mud)	Ponte (sand)	Ram	Olhão	Fuzeta	Cab de Tavira
> 1000 $\mu\text{m}$	2.12	2.49	2.04	2.21	2.51	1.22	2.82
1000 - 710 $\mu\text{m}$	1.64	1.25	2.38	6.09	1.94	1.32	2.10
710 - 500 $\mu\text{m}$	2.13	2.13	3.07	13.34	2.45	2.19	2.90
500 - 355 $\mu\text{m}$	2.90	2.54	3.67	18.79	3.19	3.41	4.74
355 - 250 $\mu\text{m}$	2.45	2.20	5.56	8.99	6.12	3.01	4.44
250 - 180 $\mu\text{m}$	9.64	3.51	12.15	3.11	21.93	5.05	17.79
180 - 125 $\mu\text{m}$	5.58	23.17	26.17	1.34	20.73	18.45	16.90
125 - 90 $\mu\text{m}$	12.15	8.39	3.65	0.53	6.28	15.06	5.95
90 - 63 $\mu\text{m}$	3.99	4.19	1.63	0.48	0.149	9.05	2.20
< 63 $\mu\text{m}$	57.40	50.13	39.68	45.12	34.70	41.24	40.16
Type of sediment	Muddy sand	Muddy sand	Fine sand	Fine sand	Fine sand	Fine sand	Fine sand

### *Vertical distribution*

For the vertical distribution study, three cylindrical cores (15cm depth and 8 cm of diameter) were collected in two different areas (sandy and muddy) from the site Ponte, in September 2006. The sandy station was a flat consolidated area with fine sand sediments (Table 4.1; following the classification of Holme and McIntyre, 1984). The muddy station was a soft, dynamic area with ripples with muddy sand sediments (Table 4.1; following the same classification as before). Each core was divided in 1 cm depth layers, obtaining a total of 15 layers. Then, a sample from the middle of each layer was taken using a petri-dish (described previously). Samples were protected from light and high temperatures. Due to equipment failure, one replicate from the muddy site had to be rejected during processing.

### *Spatial distribution*

For the investigation of the spatial variability at a large scale, six samples were collected from each of the six sites, which included samples from muddy and sandy sites, throughout the lagoon during one week in March of 2007. The sites are represented in Figure 4.9 and their sediment characteristics are presented in Table 4.1. The sediments taken from Ponte for this study were from muddy-sand sediments.

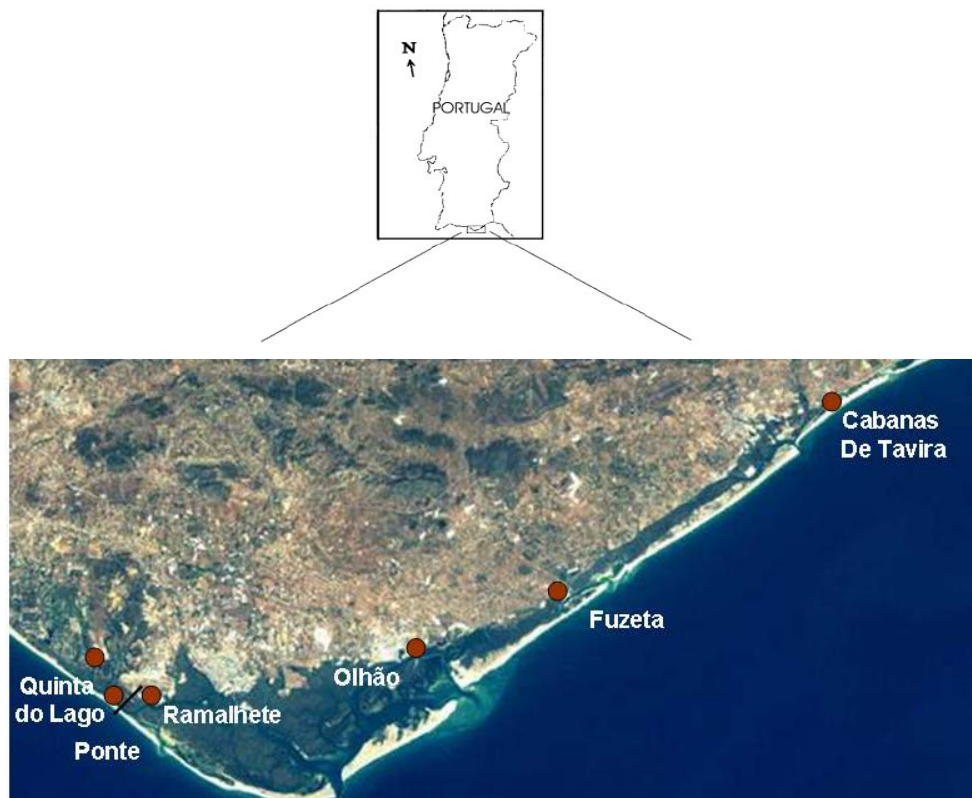


Figure 4.9 - Study area with the representation of the six study sites of this work.

For the study of the spatial variability at small scale, 30 samples were obtained randomly in July of 2006 using three quadrats of respectively the following sizes 0.3x0.3m (Figure 4.9), 0.6x0.6m and 1.2x1.2m, divided in 25 small squares (10 samples taken from each quadrat) in the two areas of the site Ponte, described above. This study was conducted using muddy sand and fine sand sediments from the same site in order to eliminate differences between sites. All the samples were taken with a petri-dish (similar to the ones described before) to ensure that only the top layer with higher chl *a* content was taken. A plastic card was used to manoeuvre underneath the sample. The samples were protected from the light and high temperatures as described above.

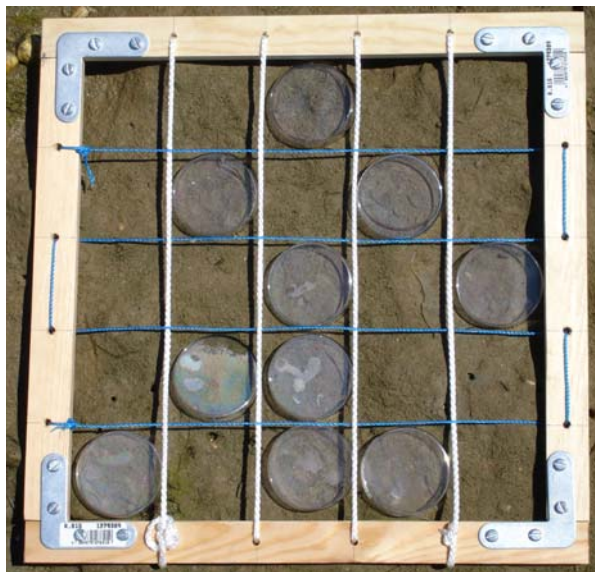


Figure 4.9 - Small quadrat used in the spatial variability at small scale study (0.3x0.3m).

#### 4.2.2 Laboratory analysis

Each sample was placed in a 50cm<sup>3</sup> plastic tube, covered by aluminium foil and frozen. All the samples were freeze-dried as recommended (see the discussion regarding this issue in Chapter 3). The weight of the sediment was taken after freeze-drying.

The spectrophotometric method, adapted from Parsons *et al.* (1984) and using Lorenzen's equations (Lorenzen, 1967), was used to measure chl *a* and phaeopigment content in the sediment samples. The procedure adopted was developed and optimised as discussed in Chapter 3. The solvent 90% acetone for sand and 80% acetone for mud, buffered with sodium bicarbonate was added to each sample in a similar proportion of solvent volume to sediment weight and the tubes were stirred in the vortex. The samples

were placed in the freezer at  $-20^{\circ}\text{C}$  for 6 hours. Before measuring chl *a* and phaeopigments by spectrophotometry, the samples were centrifuged for 10 min at 3000rpm. The spectrophotometer wavelengths used were 663nm and 750nm. A 10% dilution was done in 90% acetone for two reasons: to allow the use of spectrophotometric equations for 90% acetone in muddy samples and to decrease the solution concentration to allow a more reliable measurement. To calculate the phaeopigment and chl *a* content ( $\mu\text{g/g}$ ), the weight of sediment was used instead of the usual volume of filtered water when studying pelagic algae. Moreover, the chl *a* concentration ( $\mu\text{g}\cdot\text{cm}^{-2}$ ) was also calculated using data obtained during 2006 and 2007-08 from Ponte and Ramalhete to assess differences between chl *a* content and concentration. The sample area was known (petri-dish area) and a uniform depth distribution was assumed.

### 4.2.3 Statistical analyses

All statistical tests and numerical analyses were carried out using Minitab 14 and Matlab. Data were tested for normality and homoscedasticity of variance and parametric tests conducted, when possible, otherwise equivalent non parametric tests were used. For the analysis of the small-scale spatial distribution, an index of dispersion was calculated following Fowler et al. (1998). To test for significant differences between chlorophyll and phaeopigment contents obtained in the sandy and muddy sediments, a T-test was used. A  $\log(x)$  transformation was performed, as necessary. To assess any significant differences between chlorophyll and phaeopigment values obtained in the sandy and muddy area of Ponte in the vertical distribution study, a non parametric test was used (Mann-Whitney). An ANOVA test was carried out to assess differences between sites in the spatial variability study at large scale. Correlations between MPB and temperature, salinity, tidal height, nutrients in the water column (data on Chapter 5), irradiance (provided by the *Instituto de Metereologia*) and wind velocity (provided by *Direcção Geral de Agricultura e Pescas do Algarve*) were investigated using Pearson's coefficient.

In order to understand the temporal pattern of MPB and to explore the key factors underlying the community, an empirical model was developed and fitted to log-transformed microphytobenthic chlorophyll data. The model was:

$$\hat{y} = \bar{y} + f_M(t) + \varepsilon \quad 4.1)$$

where:

$$f_M(t) = \sum_{n=1}^{n=M} [a_n \cos(2\pi nt) + b_n \sin(2\pi nt)] \quad 4.2)$$

$$\varepsilon = \varepsilon^s + \varepsilon^{ss} + \varepsilon^t \quad 4.3)$$

The deterministic function  $\bar{y} + f_M(t)$ , describes a truncated Fourier series with  $M$  sets of sine-cosine waves. Time  $t$  is in years. The stochastic term  $\varepsilon$  is the error remaining after the Fourier series has been fitted. It contains a part,  $\varepsilon^s$  due to within-site variability, a part  $\varepsilon^{ss}$  due to variability between the sites in different parts of the lagoon, and a residual,  $\varepsilon^t$ .

The truncated Fourier series was fitted by the iterative method in Table 4.2. This non-standard approach, drawing on Chatfield (1989), was used because of the irregularity of the observed time-series, and because we wanted to fit waves whose frequencies were an integral multiple of  $1 \text{ yr}^{-1}$  without trimming or padding the observed time-series. The method in the Table satisfied two criteria: it decreased the residual sum-of-squares about the fitted series with each additional wave-pair, and it made these SOS as low as possible at each step. Iteration was halted when 26 wave-pairs had been fitted, or when the residual variance began to increase (because degrees of freedom were decreasing more than residual SOS). The frequency of  $\frac{1}{26}$  corresponds to the typical interval of 26 weeks between samplings. In order to investigate the temporal variation at each site, a Fourier series was applied to data from single sites. The error term  $\varepsilon^{ss}$  and the corresponding between-sites SOS were zero for these cases. This approach was developed and improved with contributions obtained from several discussions with myself, Prof. Paul Tett and Elisa Capuzzo. Prof. Paul Tett provided the Matlab code to perform the analysis.

A piecewise analysis of variance was then carried out to resolve spatial and temporal variability in MPB into several components. The variance explained by the Fourier series was estimated for seasonal change (represented by wave-pairs 1 to 3) and for higher-frequency temporal variation (wave-pairs 4 through  $M$ ). The residual variance after fitting the Fourier series was divided amongst the three stochastic components of the model, as shown in Table 4.5. In this table, the degrees of freedom used for each variance were calculated from  $K$  less the degrees of freedom consumed in the

calculation of the SOS. The resulting variances were then summed to give a total estimated variance, so that the percentage of this variance due to each source of variation could be set out in Table 4.5. This procedure is, of course, different from that in a formal ANOVA aimed to test the hypothesis that residual and explained variances are the same. To perform the analysis of variance, data from both Ponte and Ramalhete were pooled.

Table 4.2 – Fitting a truncated Fourier series

The first three parameters were estimated using matrix methods:

$$\begin{pmatrix} \hat{y} \\ \hat{a}_1 \\ \hat{b}_1 \end{pmatrix} = W \backslash y$$

where  $W$  contains rows  $j=1$  to  $K$  of the vector,  $(1 \cos(2\pi t_j) \sin(2\pi t_j))$ ,  $y$  is a column vector of the  $K$  observed values,  $y(t_j)$ , and ‘\’ is the Matlab ‘backslash’ operator, corresponding in the present (overdetermined) case to simultaneous parameters estimation by least-squares minimization (Anon, 1999). Parameters for higher-frequency waves were estimated iteratively:

$$\hat{a}_n = \sum_{j=1}^{j=K} y'_n(t_j) \cos(2\pi n t_j) \quad \hat{b}_n = \sum_{j=1}^{j=K} y'_n(t_j) \sin(2\pi n t_j)$$

$$y'_n(t_j) = y(t_j) - \hat{y}_{n-1}(t_j)$$

$$\hat{y}_{n-1}(t_j) = \hat{y} + \sum_{m=1}^{m=n-1} [\hat{a}_m \cos(2\pi m t_j) + \hat{b}_m \sin(2\pi m t_j)]$$

Starting from  $n = 2$ , and ceasing (with  $M = n$ ) when either  $\sigma_{res,n+1}^2 > \sigma_{res,n}^2$ , or  $n = 26$ .

res(idual) and ex(plain) sums of squares (SOS) and variances ( $\sigma^2$ ) were estimated:

$$SOS_{res,n} = \sum_{j=1}^{j=K} (y'_n(t_j))^2 \quad \sigma_{res,n}^2 = \frac{1}{df} SOS_{res,n}$$

$$SOS_{ex,n} = SOS_{all} - SOS_{res,n} \quad \sigma_{ex,n}^2 = \frac{1}{df} SOS_{ex,n}$$

$$SOS_{all} = \sum_{j=1}^{j=K} (y(t_j) - \bar{y})^2 \quad df = K - 2n - 1$$

## 4.3 Results

### 4.3.1 Seasonal variability

The variation of chl *a* content during 2006 and 2007-08 was from approximately 5  $\mu\text{g chl.g}^{-1}$  to 20  $\mu\text{g chl.g}^{-1}$  (Figures 4.10 and 4.11). The values did not show any clear trend within the years. In 2006, an overall increase was observed at Ponte during the summer, from June to September, although not consistently throughout the sampling dates. However in 2007-08, high values were not found during the summer, with no clear period of large chl *a* contents. Peaks were observed during the winter at Ponte and

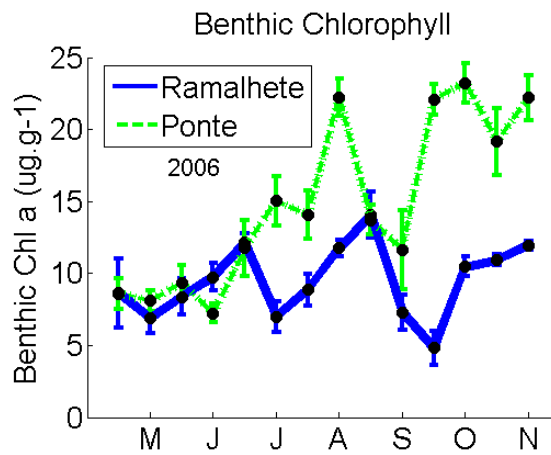


Figure 4.10 - Seasonal variation of chlorophyll *a* contents ( $\mu\text{g chl.g}^{-1} \pm \text{SE}$ ) in Ponte and Ramalhete during the year of 2006.

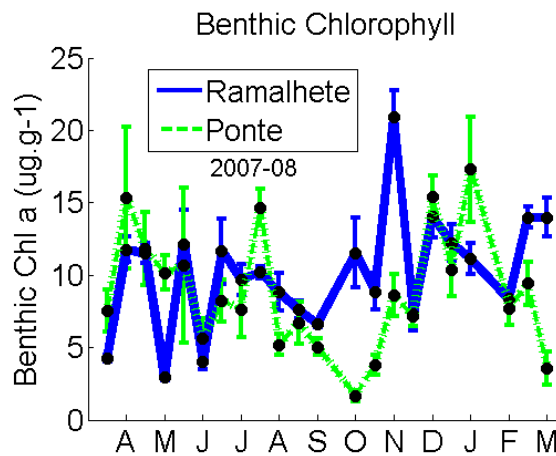


Figure 4.11 - Seasonal variation of chlorophyll *a* contents ( $\mu\text{g chl.g}^{-1} \pm \text{SE}$ ) in Ponte and Ramalhete during the year of 2007-08.



Ramalhete. Significant differences ( $p < 0.01$ ; paired T-test) were found between the chl *a* contents at Ponte and Ramalhete in 2006. Significant differences ( $p < 0.005$  against a significance level of 0.025; T-test using the Bonferroni correction for multiple tests) were also found comparing the chl *a* contents at Ponte during 2006 and 2007-08.

The range of variation of phaeopigments was from approximately  $1 \mu\text{g}\cdot\text{g}^{-1}$  to  $10 \mu\text{g}\cdot\text{g}^{-1}$  during 2006 and 2007-08 (Figures 4.12, 4.13, 4.14 and 4.15). The variation of the phaeopigment / chlorophyll *a* ratio reflected the variation of phaeopigment content throughout the years at both sites.

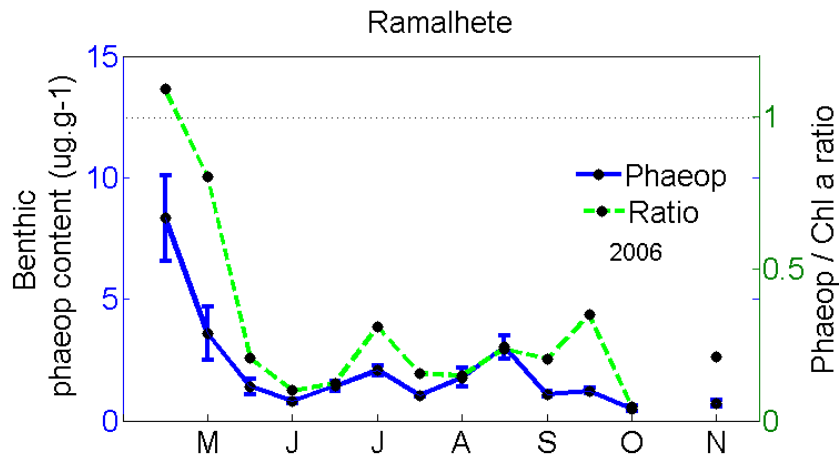


Figure 4.12 – Seasonal variation of benthic phaeopigment content ( $\mu\text{g}\cdot\text{g}^{-1} \pm \text{SE}$ ) and phaeopigment / chlorophyll *a* ratio in Ramalhete during the year of 2006.

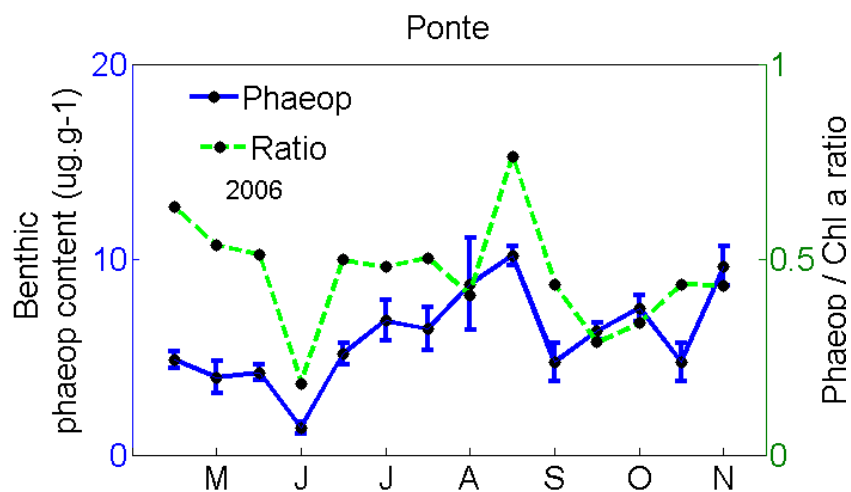


Figure 4.13 – Seasonal variation of benthic phaeopigment content ( $\mu\text{g}\cdot\text{g}^{-1} \pm \text{SE}$ ) and phaeopigment / chlorophyll *a* ratio in Ponte during the year of 2006.

Significant differences ( $p < 0.01$ ; paired T-test) were found between Ramalhete and Ponte using data from 2006 and 2007-08, after a log (x) transformation of data. Higher values were found at Ponte. The values of the phaeopigment / chlorophyll ratio were under 1 most of the time, except in a few cases. In fact, in sandy sediments (Ramalhete) it was generally under 0.5.

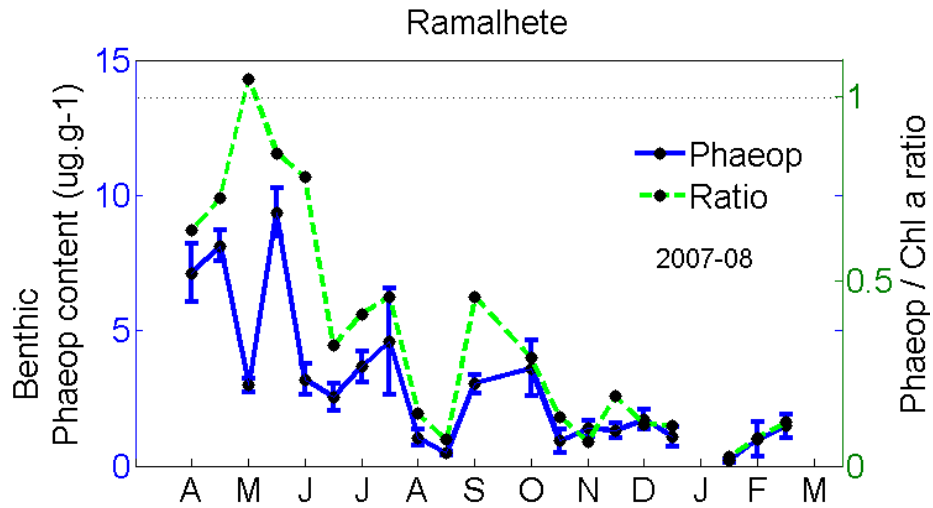


Figure 4.14 – Seasonal variation of benthic phaeopigment content ( $\mu\text{g.g}^{-1} \pm \text{SE}$ ) and phaeopigment / chlorophyll *a* ratio in Ramalhete during the year of 2007-08.

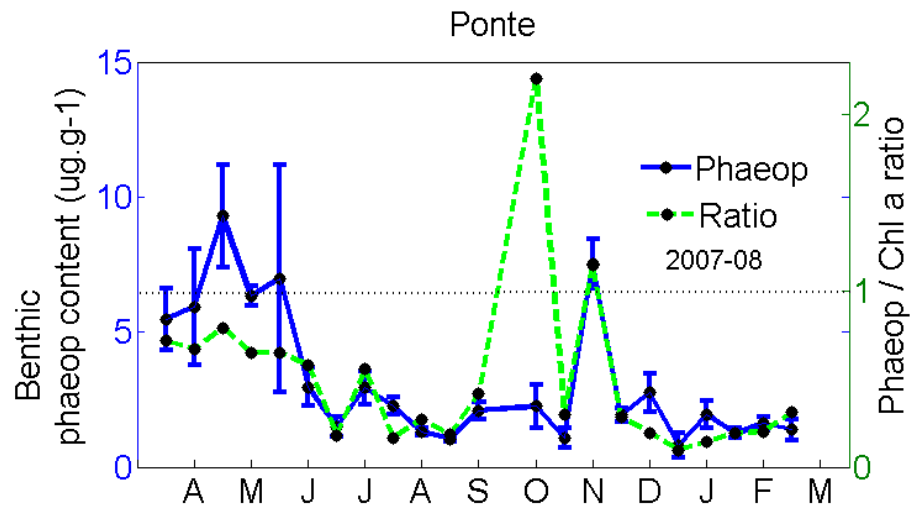


Figure 4.15 – Seasonal variation of benthic phaeopigment content ( $\mu\text{g.g}^{-1} \pm \text{SE}$ ) and phaeopigment / chlorophyll *a* ratio in Ponte during the year of 2007-08.

The calculations of the chl *a* concentrations showed similar patterns compared with the chl *a* contents both for 2006 and 2007-08 (Figures 4.16 and 4.17).

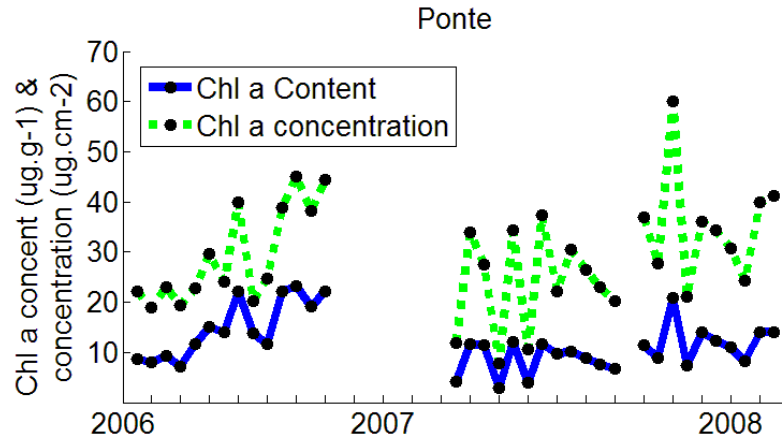


Figure 4.16 – Chlorophyll *a* content ( $\mu\text{g chl.g}^{-1}$ ) versus concentration ( $\mu\text{g chl.cm}^{-2}$ ) values of samples from Ponte during 2006 and 2007-08.

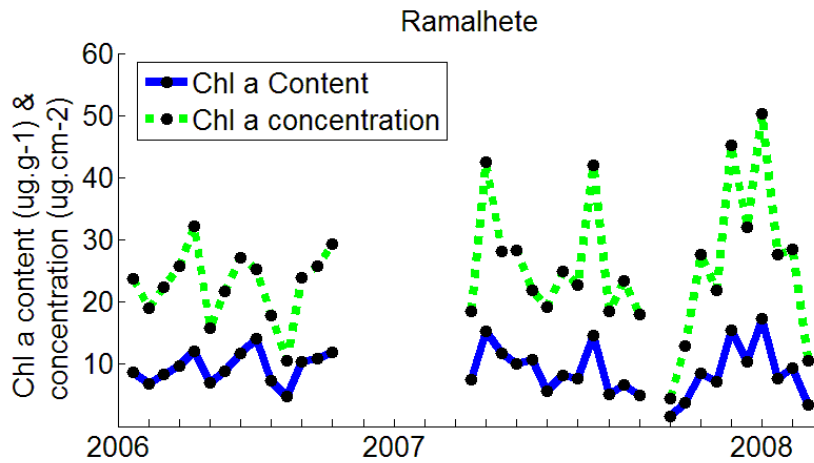


Figure 4.17 – Chlorophyll *a* content ( $\mu\text{g chl.g}^{-1}$ ) versus concentration ( $\mu\text{g chl.cm}^{-2}$ ) values of samples from Ramalhete during 2006 and 2007-08.

Pearson's correlations between microphytobenthos and temperature, salinity, tidal height, nutrients in the water column, irradiance and wind data were investigated and none were found ( $p > 0.05$ ; Table 4.3).

Fourier analysis revealed a complex and dynamic seasonal pattern of MPB at Ponte and Ramalhete (Figures 4.18 and 4.19). The best fit was obtained considering the sum of 20 wave-pairs (sin and cosine) for Ramalhete and 26 wave-pairs for Ponte. The resulting wave has a regular and constant time step and is obtained from day 1 to day 365, considering both periods altogether. Therefore, the pattern is similar for 2006, 2007 and 2008. The red dashed line is equivalent but adjusted for a time step which is

Table 4.3 – Pearson’s correlations between microphytobenthos (MPB), temperature (Temp), salinity (Sal), irradiance (Irrad), tidal height (Tide), Dissolved Available Inorganic Nitrogen (DAIN), phosphate (Phosp), Silicate and Wind velocity (Wind). Bold-italic figures are significant at  $p < 0.05$ ;  $n$  represents the number of samples.

$n=36$	MPB	Temp	Sal	Irrad	Tide	DAIN	Phosp	Silicate	Wind
MPB	1								
Temp	0.05	1							
Sal	-0.08	<b><i>0.57</i></b>	1						
Irrad	-0.06	<b><i>0.75</i></b>	<b><i>0.50</i></b>	1					
Tide	0.16	<b><i>-0.62</i></b>	<b><i>-0.37</i></b>	<b><i>-0.56</i></b>	1				
DAIN	0.02	-0.12	-0.23	-0.25	0.05	1			
Phosp	0.27	<b><i>0.49</i></b>	<b><i>0.37</i></b>	0.10	-0.25	-0.04	1		
Silicate	0.32	0.33	-0.02	0.24	-0.24	0.13	<b><i>0.45</i></b>	1	
Wind	0.05	-0.12	-0.29	0.11	-0.05	-0.07	-0.12	0.29	1

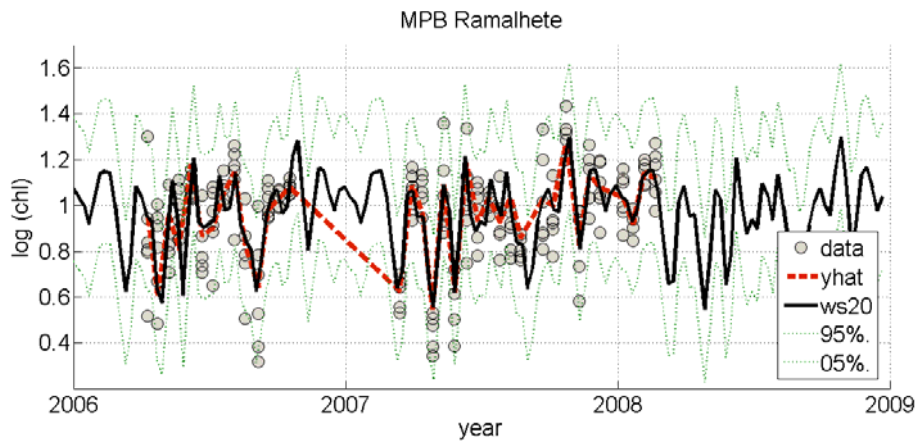


Figure 4.18 – Seasonal pattern obtained fitting 20 wave-pairs (sine and cosine) according to the Fourier series approach for Ramalhete. Transformed (log) data are presented with dots. The 5% and 95% confidence intervals are represented as dotted lines and dashed line (yhat) is the equivalent to the sum of 20 waves (ws20) but adjusted for a time step which is coincident to sampling date.

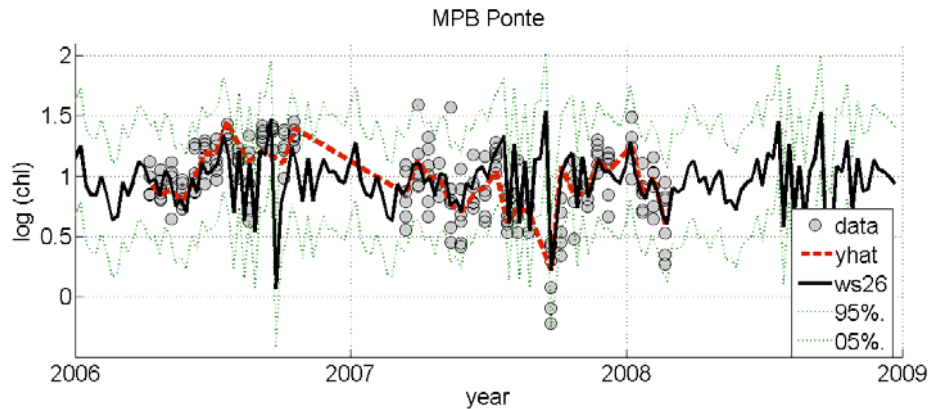


Figure 4.19 – Seasonal pattern obtained fitting 26 wave-pairs (sine and cosine) according to the Fourier series approach for Ponte. Transformed (log) data are presented with dots. The 5% and 95% confidence intervals are represented as dotted lines and dashed line (yhat) is the equivalent to the sum of 26 waves (ws26) but adjusted for a time step which is coincident to sampling date.

coincident to the sampling date. Both fits are significant at a significance level of 0.05 ( $F=5.35$ ; 40,165df, for Ramalhete;  $F=3.62$ ; 52,158df, for Ponte), although, they only explain less than half of the total variance observed in the lagoon ( $R^2$ ): 46% for Ramalhete and 39% for Ponte.

### 4.3.2 Vertical distribution

A steep decrease is seen from the first to the second centimetre in the 3 replicates from the sandy sediment (Figure 4.20). Below the second centimetre it stays almost stable, without major changes.

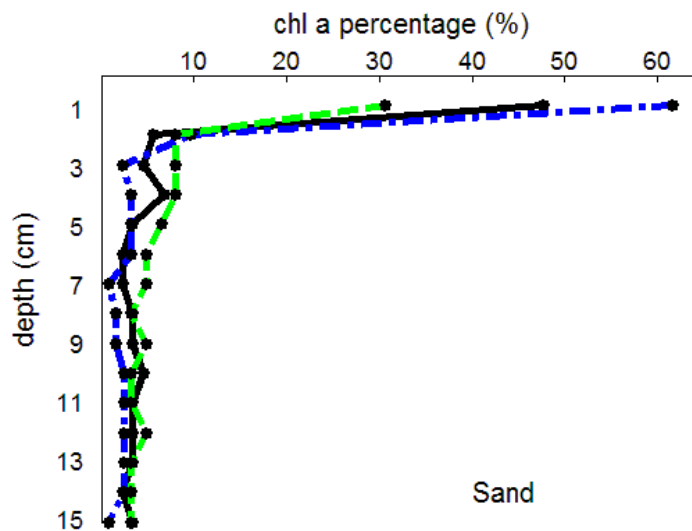


Figure 4.20 - Vertical profiles of chlorophyll *a* obtained from 3 replicates until a depth of 15cm in sand.

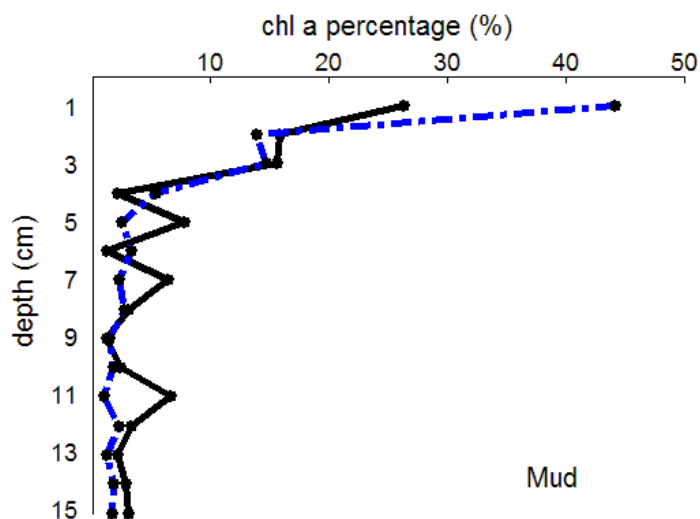


Figure 4.21 - Vertical profiles of chlorophyll *a* obtained from 2 replicates until a depth of 15cm in mud.

In the muddy sediment (Figure 4.21), although the pattern is similar, it is more dynamic, with higher chl *a* content in layer 2 and 3, when compared with the sandy site. A large difference of almost 20% was found within the first centimetre between the two replicates. However, both replicates showed higher chl *a* content within the first 3 centimetres of the core and not only within the first. Replicate 2 showed large variations along the core, with three peaks after the third centimetre. A Mann-Whitney test was used and significant differences ( $p < 0.001$ ) were found between chl *a* values obtained from sandy sediment and muddy sediment. The chl *a* content was higher in the cores of mud, with a maximum total of  $97.89 \mu\text{g chl.g}^{-1}$  against a maximum total of  $20.0 \mu\text{g chl.g}^{-1}$  in sandy sediment.

The phaeopigment / chlorophyll *a* ratio is under 1 in first layer (1cm) of sediment both in sand and mud (Figure 4.22 and 4.23). At deeper layers, ratio is above 1 for most cases. The chl peaks found at depths 5, 7 and 11 cm in one of the replicates of mud correspond to small values of the phaeopigment / chlorophyll ratio (Figure 4.23).

Significant differences ( $p < 0.001$ ; Mann-Whitney) were found between phaeopigment contents obtained from sandy and muddy sediments, considering all profiles. The phaeopigment content was higher in the muddy cores.

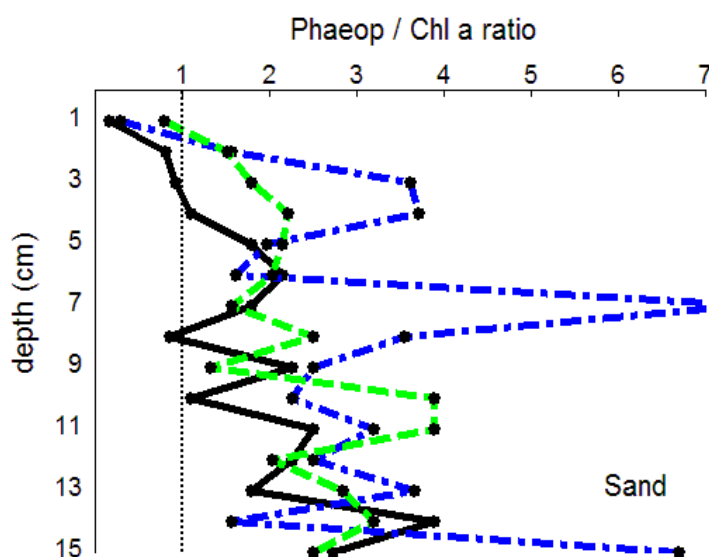


Figure 4.22 – Vertical profiles of the phaeopigment / chlorophyll *a* ratio of 3 replicated to a depth of 15cm in sand.

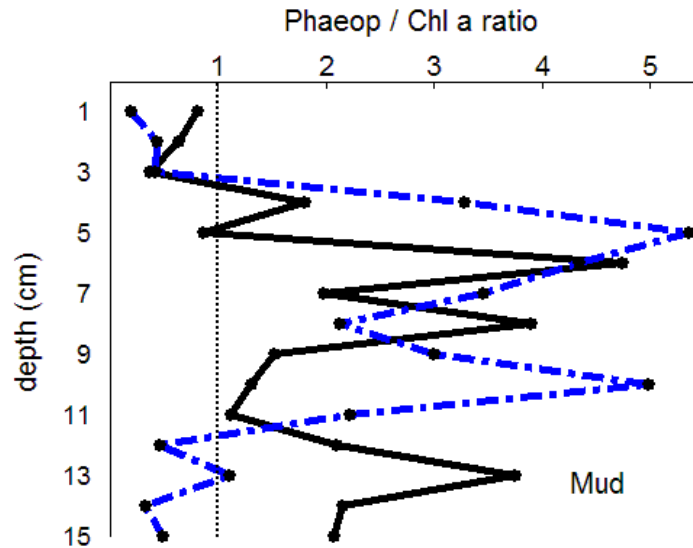


Figure 4.23 - Vertical profiles of the phaeopigment / chlorophyll *a* ratio of 3 replicated to a depth of 15cm in mud.

#### 4.3.3 Spatial variability at small scale

The chl *a* content obtained was highly variable both for mud and sand. The lower values of chl *a* content in mud were present in the samples from the smaller quadrat. In contrast, for sand the lower values were found in the samples from the medium quadrat. The index of dispersion (variance divided by the mean) was calculated in order to assess the 95% confidence zone of random dispersal. An aggregate spatial pattern was found within the largest quadrat in sand and within the medium quadrat in mud (Index of dispersion > 2; Table 4.4). Spatial patterns at other scales were found to be random (Index of dispersion between 0 and 2). For values of 0, the pattern would be regular.

Table 4.4 - Index of dispersion and spatial pattern at three different scales in sand and mud.

		Index of dispersion	Spatial Pattern
Sand	0.3 x 0.3 m	1.47	Random
	0.6 x 0.6 m	0.47	Random
	1.2 x 1.2 m	2.63	Aggregate
Mud	0.3 x 0.3 m	0.54	Random
	0.6 x 0.6 m	2.42	Aggregate
	1.2 x 1.2 m	1.62	Random

Significant differences ( $p < 0.001$ ) in total chl  $a$  (all samples taken from each site) were found between mud and sand using a T-test after a log ( $x$ ) transformation. The mean for sand was  $10.228 (\pm 0.931 \text{ SE}) \mu\text{g chl.g}^{-1}$  and for mud was  $12.667 (\pm 0.783 \text{ SE}) \mu\text{g chl.g}^{-1}$ .

#### 4.3.4 Spatial variability at large scale

The values obtained in the six sites were found to be significantly different ( $p < 0.01$ ; Figure 4.24) following an ANOVA test. The largest chlorophyll  $a$  content was found in Olhão (fine sand), a site that is 50m away from the city centre. The smallest was found in Fuzeta, a site also with fine sand sediments.

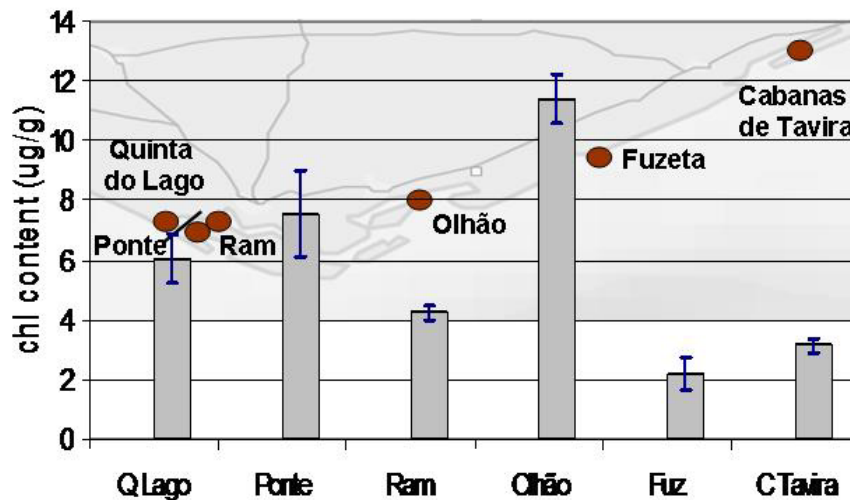


Figure 4.24 - Chlorophyll  $a$  contents ( $\mu\text{g chl.g}^{-1}$ ) in the six study sites: Quinta do Lago, Ponte, Ramalhete, Olhão, Fuzeta and Cabanas de Tavira.

A Tukey test showed that Olhão was significantly different from Ramalhete, Fuzeta and Cabanas de Tavira. Except for Olhão all the sites with the smallest values have fine sand sediments. In addition, Fuzeta and Cabanas de Tavira are located in the eastern part of the lagoon. Sites with large chlorophyll  $a$  values such as Quinta do Lago and Ponte are located in the western part of the lagoon. These two sites have muddy sand sediments.

#### 4.3.5 Analysis of variance

The most important component of the MPB variability is the within day variation (61%; Table 4.5), which is composed by two subcomponents: within-site variability



Table 4.5 – Total variance of MPB and variance of the three main components (waves, within day and residuals). Seasonal variability expressed as wave variance was decomposed in 1-3 waves variance and 4-26 waves variance. Within day variability was also decomposed in two sub-components: sampling and site variance. SOS is the sum of squares and df the degrees of freedom.

Components	Eqn.	SOS	df	$\sigma^2$	%
<b>Waves 1-26</b>	(1)	8.81	364		
	Waves 1-3 (2)	1.55	410	0.00378	5%
	Waves 4-26 (3)	7.26	371	0.01957	25%
<b>Within-day</b>	(4)	17.81	381	0.04675	61%
	Within site (5)	9.04	345	0.02620	(0.51 of 61%)
	Between sites (6)	8.77	345	0.02542	(0.49 of 61%)
<b>Residual</b>	(7)	2.22	328	0.00677	9%
	(sum of $\sigma^2$ )			0.07686	100%
<b>Totals</b>	(8)	28.84	416	0.06931	

Considering that variance is  $\sigma^2 = \text{SOS}/\text{df}$ , equations for sum of squares (SOS) and degrees of freedom (df) are provided below:

$$1) \text{SOS}_{\text{waves},M} = \text{SOS}_{\text{total}} - \text{SOS}_{\text{residual},M} \quad \text{df} = K - 2M - 1$$

$$2) \text{SOS}_{\text{waves},3} = \text{SOS}_{\text{total}} - \text{SOS}_{\text{residual},3} \quad \text{df} = K - 6 - 1$$

$$3) \text{SOS}_{\text{waves},4} = \text{SOS}_{\text{waves},26} - \text{SOS}_{\text{waves},3} \quad \text{df} = K - 46$$

$$4) \text{SOS}_{\text{whitin-day}} = \sum_{l=1}^{l=L} \sum_{i=1}^{i=I(l)} (Y_{l,i} - \bar{Y}_l)^2 \quad \text{df} = K - L$$

$$5) \text{SOS}_{\text{whitin-site}} = \text{SOS}_{\text{whitin-day}} - \text{SOS}_{\text{between-sites}} \quad \text{df} = K - S$$

$$6) \text{SOS}_{\text{between-site}} = \sum_{s=1}^{s=S} \sum_{i=1}^{i=I(s)} (Y_{s,i} - \bar{Y}_s)^2 \quad \text{df} = K - S$$

$$\text{SOS}_{\text{residual},M} = \sum_{j=1}^{j=K} (Y_j - \hat{Y}_{j,M})^2 \quad \text{df} = K - 2M - 1$$

$$7) \text{SOS}_{\text{residual}} = \text{SOS}_{\text{residual},M} - \text{SOS}_{\text{whitin-day}} \quad \text{df} = K - 2M - 1 - L$$

$$8) \text{SOS}_{\text{total}} = \sum_j (Y_j - \hat{Y})^2 \quad \text{df} = K - 1$$

$\hat{Y}_{j,n}$  is the estimate of  $Y_j$  made with a Fourier series of n wave-pairs (up to a maximum of M).  $\hat{Y}$  is the grand mean estimated as described before.

Subscript notation: sample j=1 to K, sample i=1 to I(l) on day l or i=1 to I(s) for site-day s. l=1 to L days of sampling and s=1 to S site x sampling days.

arising from differences between samples taken within few centimetres (0.51 of 61% or 31% of total) and differences, on the scale of the lagoon, between sites (0.49 of 61% or 30% of total). The Fourier analysis used a large number of waves to obtain the best fit (26 waves). Since we were interested to discuss if the solar astronomical cycles, such as the irradiance, were affecting the benthic community, the analysis was also carried out using only 3 waves, which should pick up these effects. Both analysis were significant at a significance level of 0.05 ( $F=3.08$  (52,364df) using 26 waves and  $F=3.87$  (6,410df) using 3 waves). Note that this analysis using 26 waves is different from the ones carried out to investigate the seasonal cycle. Instead of doing two different analyses for both sites, as before, this combines data and performs only one analysis. The variance explained by 1 to 3 waves was only 5% and between 4 and 26 waves was 25%, which means that the higher-frequency variability is much more important than the seasonality due to physical or astronomical cycles. The residual error, after fitting Fourier series and considering within-site and between-site spatial variation, was relatively small, only 9% of the total variance.

## **4.4 Discussion**

### **4.4.1 Seasonal variability**

The range of chl *a* variation was similar between years (5- 25  $\mu\text{g chl.g}^{-1}$  in 2006 and 2- 20  $\mu\text{g chl.g}^{-1}$  in 2007-08). Riaux-Gobin and Bourgoïn (2002) presented values of microphytobenthic chlorophyll that varied from 0.07 to 56.69  $\mu\text{g chl.g}^{-1}$  in different types of intertidal sediments in the Kerguelen Archipelago (Indian ocean). Hedtkamp (2005) found a range of chl *a* contents from 13 to 21  $\mu\text{g chl.g}^{-1}$  in the Wadden Sea. It is reasonable to consider our values as being close to the ones indicated above. However, it is not easy to compare results from different published reports. There is no homogeneity between methodologies and care has to be taken regarding the use of different units: content ( $\mu\text{g}$  of chlorophyll per unit dry weight) or concentration ( $\mu\text{g}$  of chlorophyll per area). Perkins *et al.* (2003) discussed how these different units may indicate opposite trends and patterns. However, in our study both units indicate the same pattern, probably because all samples were collected on the same tidal conditions and at the same hour.

Significant temporal variability, at periods ranging from a few weeks to a year, was found using Fourier series for both sites, Ponte and Ramalhete. This temporal variability was, however, less than half of the total variability. Discussion about seasonal patterns of MPB is present throughout the literature, however, no consensus has been achieved yet. Authors such as Brotas *et al.* (1995) reported the absence of temporal patterns in Tagus estuary and others like Underwood and Kromkamp (1999) observed higher values of MPB chlorophyll during spring and summer in estuaries. The existence of seasonality can be very difficult to assess without mathematical tools, such as the ones proposed in this study. Due to the high frequency of MPB variation and without using this mathematical approach, it would be natural to follow the hypothesis of non-existence of any defined pattern.

Temperature and irradiance are two environmental factors reported in the literature as having positive relationships with microphytobenthos (e.g. Colijn and de Jonge, 1984; Shaffer and Onuf, 1985; Cibic *et al.*, 2007). Due to the fact that microphytobenthos are photoautotrophic cells, a direct effect of the irradiance annual cycle on MPB temporal variation could be expected. However, our correlation results show that this seems not to be the case for MPB in Ria Formosa. The seasonal nature of MPB variation was investigated by the Fourier series model. The variation explained by fitting 3 waves to MPB data was as little as 5%, which shows that the variation is driven by other factors with higher annual frequency. The 3 lowest-frequency waves are expected to capture most of the astronomical variation in solar irradiance, for example. However, day-to-day changes (e.g. cloud cover) should not be included. Tidal height, salinity, wind velocity and nutrient concentrations in the water column were also not individually correlated with MPB. This supports the view that MPB variability is a result of a complex interaction of factors.

The best fit obtained in this study combines the sum of 20 wave-pairs for Ramalhete and 26 for Ponte, which confirms the involvement of high frequency variation. It is interesting to note that results represent variations with a period of 14 to 18 days. The influence of the astronomic cycles is well known in nature and there are clear examples of this phenomenon especially in the sea. These results could be interpreted to suggest that the fortnightly cycle (neap-spring tides) is the main component driving the seasonality of these benthic microalgae, with a period of 14 days. However, no significant correlation was found between tidal range and MPB chlorophyll. The tidal effect on MPB in the sediment surface was suggested to be one of the most important

drivers of their biomass concentration (Serôdio and Catarino, 1999; Jago et al., 2002; Koh et al., 2006). Serôdio and Catarino (1999) suggested that MPB is influenced by a fortnightly cycle of PAR intensity and temperature due to the neap-spring tide variation. Microphytobenthos biomass was expected to increase during neap tides, when PAR was higher due to lower turbidity. Jago et al. (2002) and Koh et al. (2006) discussed how the neap-spring tide variation may affect the algae cells resuspension. Strong currents during spring tides would generally lead to an increased resuspension of particles.

De Jonge and van Beusekom (1995) reported that the most important factor for resuspension in the Ems estuary is the wind. Although it was not significantly correlated with MPB, this factor, in combination with others, may also have an important effect in Ria Formosa and should not be excluded as one important driving force, as it might be influencing the complexity of MPB dynamics in the lagoon. In the future, a study using a more frequent sampling programme could be undertaken to explore all these issues.

Phaeopigment / chlorophyll ratios found throughout the years 2006 and 2007-08 were under 1, except in a few cases. This is in agreement with what was found and discussed in chapter 3. Sun *et al.* (1994), Rabalais *et al.* (2004) and Reuss *et al.* (2005) reported phaeopigment / chlorophyll *a* ratios larger than 1 in sediments. We do think that the ratios obtained in this study are within reasonable values. Higher contents of phaeopigments were found in muddy sediments. This was expected given the significant differences observed between sandy and muddy sediments for chlorophyll *a*. If the chlorophyll *a* content is higher in mud, chlorophyll degradation products are also expected to be higher in this type of sediment.

#### **4.4.2 Vertical distribution**

The pattern found in this study revealed an abrupt change from the top to the second centimetre, both in sand and mud. This study showed a biomass percentage of approximately 40% in the first centimetre, which is the same indicated by Méléder *et al.* (2005). The higher chl *a* content values were found on the surface (0-1cm) as stated before by Perkins *et al.* (2003), Consalvey *et al.* (2005) and Easley *et al.* (2005). Deeper, the content falls to smaller values. This variation was expected since most of the literature suggests that cells are mainly on the top of the sediment. This position is crucial for them to photosynthesize. For sand, the biomass percentage fell to less than 10% (in a depth of 5cm) and after that the values account for less than 5% of the total

chl *a* content. Muddy sediments have a similar pattern, however it is not as monotonic as for sand. The high contents seen within the first 3 cm and the non expected peaks of chlorophyll *a* for one of the replicates suggest that there are several processes influencing the distribution of chl *a*. These include disturbance of sediment by clam harvesting, dredging and tide. Another process that may be extremely important in this system is the bioturbation from benthic organisms. The cells present in the sediment might be non functional but they are viable, which means that they can start the photosynthetic process again. These results suggest that MPB can migrate deeper in the sediment to protect cells from damage, a phenomenon that is called ‘behavioural photoprotection’ by many authors (e.g. Kromkamp *et al.*, 1998 and Serôdio *et al.*, 2001). The large percentage of algae found after the first centimetre of the sediment is of great importance, since it acts as a reservoir of viable cells for the community. These results expand the knowledge already stated by recent studies (Consalvey *et al.*, 2005; Easley *et al.*, 2005; Cartaxana *et al.* 2006).

Phaeopigment / chlorophyll ratios observed in deep layers are much larger than the ones found for the surficial sediment both in the seasonal variability study and also in chapter 3. As discussed by Sun *et al.* (1993a; 1993b; 1994), chlorophyll pigments are generally degraded quickly and therefore an accumulation of phaeopigments in deep layers is expected, as observed. It is possible to observe conservation of chlorophyll pigments in deep layers but only if the oxygen (anoxia) conditions are appropriate (Sun *et al.*, 1993b; Reuss *et al.*, 2005). Chlorophyll peaks found through the vertical profile of one replicate of mud may suggest the influence of processes such as clam harvesting, dredging and bioturbation. The phaeopigment content was small, which indicates that chlorophyll was extracted from a living cell or from a recently dead cell.

#### **4.4.3 Spatial variability at small scale**

Samples taken in sand within a 0.3x0.3m and 0.6x0.6m area showed a random spatial pattern, according to the dispersion index calculated. The 1.2x1.2m study indicated an aggregate pattern. These results suggest that different MPB patches start to be visible at least in an area such as 1.2x1.2m, which include areas with high content of chl *a* and areas with low. In sandy sediments, the microphytobenthic community is usually constituted by episammic microalgae, which are attached to the grains (Mélédér *et al.*, 2005; 2007). These microalgae have a relatively homogeneous distribution in the

surface which can explain the dispersion patterns found. Within the smaller area, high values were obtained, which may be a result of sampling in a zone of high content of chlorophyll *a*, given their natural patchiness.

For muddy sediment, a random spatial pattern was found within the smallest area and an aggregate spatial pattern within the 0.6x0.6m area. This may mean that the distribution is also patchy but on a smaller scale. In fact, the mudflats are known to have epipellic microalgae (able to do vertical migration), which are responsible for the large temporal and spatial variability by forming occasional patches of high biomass (Méléder *et al.*, 2005; 2007). It is therefore likely that small grain patchiness occurs in muddy habitats which would result in the requirement of using narrower scales for the study of spatial heterogeneity in these habitats.

The patchiness of microphytobenthos was expected, as reported by Seuront and Spilmont (2002) and Jesus *et al.* (2005). Seuront and Spilmont (2002) suggested some mechanisms that may affect the dynamics of the microphytobenthic assemblage such as: tides, hydrodynamism, competition for food, grazing, migration, MPB growth or death. The patchiness cannot be explained only by abiotic factors (Méléder *et al.*, 2007). A key factor to understand this theory is the competition among species. One example is the switch from an episammic to an epipellic assemblage, which can occur if the conditions, like hydrodynamism change in mixed sediments. Jesus *et al.* (2005) showed the dynamics of microphytobenthic patches in a sample area of 0.2x0.2m during an emersion period. In their study, the presence of several patches at this scale was clear. Assemblages increased or decreased in area and biomass depending on the site. A better understanding of these phenomena is essential and further studies should be carried out, since this subject is of great relevance for MPB biomass studies.

The study of the spatial variability showed significant differences ( $p < 0.001$ ) in the superficial sediment between mud and sand. These results were expected, since differences in the surface are well documented in the literature. However, significant differences were also found in deeper sediments. The total biomass of algae along the 15cm cores was found to be five times larger in mud than in sand (there were significant differences,  $p < 0.001$ ). These results give a consistent indication that the chl *a* contents are not similar in sand and in mud as suggested by Cartaxana *et al.* (2006), supporting instead Riaux-Gobin and Bourgoïn (2002) assertion that a larger concentration should be found in mud. Algae may be more protected from desiccation in mud and the availability of nutrients should be higher in this type of sediment.

#### 4.4.4 Spatial variability at large scale

The range of chlorophyll *a* values obtained in the assessment of the spatial variability at large scale was very large (from approximately 2 to 12  $\mu\text{g chl.g}^{-1}$ ) and was approximately similar to the values obtained in other parts of this work. The microphytobenthic biomass does not seem to have a homogeneous distribution throughout the lagoon. Large chl *a* content was observed at Olhão and was significantly different from the sites with lower contents, possibly because of site proximity to discharges from the town and from aquaculture ponds located nearby. However, the possibility of natural high values due to good growth conditions or due to its small scale spatial variability have also to be considered. The low values found in the eastern part of the lagoon (Fuzeta and Cabanas de Tavira) may also be caused by specific characteristics of the sites. However, the low values found are not likely to be caused by low nutrient concentrations in the system since Newton *et al.* (2003) observed higher concentrations for the eastern part of Ria Formosa. Studies on nutrient concentrations, especially in pore water would be very useful for this discussion and should be considered in the future. Strong correlations between the microphytobenthic chl *a* and the pore water nutrients have been described by authors such as Facca and Sfriso (2007). The analysis of the community species would also provide important information.

#### 4.4.5 Analysis of variance

The MPB variability was found to be strongly influenced by the spatial heterogeneity, being the most important component of its variance (about 61% of the total variability). This component involves the small scale patchiness (sampling variation subcomponent) and the large scale patchiness (site variation subcomponent). These results confirm what is suggested by the spatial study and by several authors such as Jesus *et al.* (2005) and Méléder *et al.* (2005; 2007), a large spatial variability. Furthermore, results obtained are divergent from what was observed by Tett and Grantham (1980) for phytoplankton in a small Scottish fjord. They found that 74% of all variation (including inter-annual change and spatial patchiness on large and small scale) was explained by the seasonal cycle, which was estimated as a time-series of average (log transformed) values of 10 day intervals. Microphytobenthos tends to be much more heterogeneous in space and

therefore care has to be taken when scaling up biomass measurements. Sampling should cover as much area as possible. The fact that these benthic communities are so patchy is one of the reasons why it is so difficult to assess their seasonal cycles. In fact, when compared with the variance explained by spatial heterogeneity, the seasonal cycle only covers a smaller part, about 30%. Moreover, the variance explained with 3 wave-pairs was only 5% which suggests that the direct influence of the annual irradiance cycle is not really affecting this community. The wave resulting from 3 wave-pairs is expected to be able to pick up a cycle with 1 peak per year that is affected by other factors (noise), such as cloud cover. This could be due to the effect of turbidity in the water column, resulting from the spring-neap tide variation, as suggested by Serôdio and Catarino (1999) and discussed previously. However, this may also mean that in this shallow system, irradiance is not limiting the benthic primary producers, at least during most of the time, which has also been suggested by some authors (e.g. Catford *et al.*, 2007).

Our results suggest that most of the MPB variability throughout a 2 year period was due to small and large scale heterogeneity or variability. These results were confirmed by the analysis of variance. This analysis is essential to understand the importance of the different components to the variability obtained in the field studies. It also allows us to clearly see that the seasonality pattern is so difficult to ‘extract’ from data because it is complex itself and it is masked by the spatial heterogeneity. Nevertheless, our mathematical approach (Fourier series) proved to be a powerful tool for the assessment of community seasonality. The MPB seems to yield a pattern of variation with a period of 14 days. However, no correlation with the tidal range was observed. This warrants further investigation. Samples taken throughout a fortnight period and covering the 12-hr tidal cycle would provide useful information. Sediment type was once more confirmed to be a key factor to the spatial variability. Both analyses are of great relevance for ecological and modelling studies. Modelling benthic dynamics is complex because of the amount of interactions and processes involved in the system. Therefore, the information extracted from these studies is crucial to establish ranges of variation and give indications of patterns.



## 4.5 References

- Anon (1999). *Using Matlab (v.5.2)*. The MathWorks, Inc. Natick, Maryland.
- Azvosky, A., Chertoprod, E., Saburova, M., Polikarpov, I. (2004). Spatio-temporal variability of micro- and meiobenthic communities in a White Sea intertidal sandflat. *Estuarine Coastal and Shelf Science*, **60**, 663-671.
- Brotas, V., Cabrita, T., Portugal, A., Serôdio, J., Catarino, F. (1995). Spatiotemporal distribution of the microphytobenthos biomass in intertidal flats of Tagus estuary (Portugal). *Hydrobiologia*, **300/301**, 93-104.
- Brotas, V., Plante-Cuny, M. (1998). Spatial and temporal patterns of microphytobenthic taxa of estuarine tidal flats in the Tagus estuary using pigment analysis by HPLC. *Marine Ecology Progress Series*, **171**, 43-57.
- Cartaxana, P., Mendes, C.R., Van Leeuwe, M.A., Brotas, V. (2006). Comparative study on the microphytobenthic pigments of muddy and sandy intertidal pigments of the Tagus estuary. *Estuarine Coastal and Shelf Science*, **66**, 225-230.
- Catford, J., Walsh, C., Beardall, J. (2007). Catchment urbanization increases benthic microalgal biomass in streams under controlled light conditions. *Aquatic Science*, **69**, 511-522.
- Chatfield, C. (1989). *The analysis of Time Series: An introduction*, 4<sup>th</sup> Edition. Chapman& Hall, London. 288pp.
- Cibic, T., Blasutto, O., Hancke, K., Johnsen, G. (2007). Microphytobenthic species composition, pigment concentration, and primary production in sublittoral sediments of the Trondheimsfjord. *Phycological Society of America*, **43**, 1126-1137.
- Colijn, F., de Jonge, V. (1984). Primary production of microphytobenthos in the Sem-Dollard estuary. *Marine Ecology Progress Series*, **14**, 185-196.
- Consalvey, M., Perkins, R., Paterson, D., Underwood, G. (2005). PAM Fluorescence: A beginners guide for benthic diatomists. *Diatom Research*, **20**, 1-22.
- Day, R., Quinn, G. (1989). Comparison of treatments after an analysis of variance in ecology. *Ecological Monographs*, **59**, 433-463.
- Defew, E., Paterson, D., Hagerthey, S. (2002). The use of natural microphytobenthic assemblages as laboratory model systems. *Marine Ecology Progress Series*, **237**, 15-25.
- De Jonge, V., van Beusekom, J. (1995). Wind- and tide-induced resuspension of sediment and microphytobenthos from tidal flats in the Ems estuary. *Limnology and Oceanography*, **40**, 766-778.
- Easley, J.T., Hymel, S.N., Plante, C.J. (2005). Temporal patterns of benthic microalgal migration on a semi-protected beach. *Estuarine Coastal and Shelf Science*, **64**, 486-496.
- Edmunds, M., Beardall, J., Hart, S., Elias, J., Stojkovic-Tadic, S. (2004). *Port Phillip Bay Channel Deepening Project. Environmental Effects Statement – Marine Ecology Specialist Studies. Volume 4 : Microphytobenthos*. Australian Marine Ecology Report 161. Melbourne. 45pp.
- Facca, C., Sfriso, A. (2007). Epipellic diatom spatial and temporal distribution and relationship with the main environmental parameters in coastal waters. *Estuarine Coastal and Shelf Science*, **75**, 35-49.

- Fowler, C., Cohen, L., Jarvis, P. (1998). *Practical Statistics for Field Biology*, 2<sup>nd</sup> ed. Chichester, New York, Wiley.
- Grinham, A., Carruthers, T., Fisher, P., Udy, J., Dennison, W. (2007). Accurately measuring the abundance of benthic microalgae in spatially variable habitats. *Limnology and Oceanography: Methods*, **5**, 119-125.
- Hedtkamp, S. (2005). *Shallow subtidal sand: permeability, nutrient dynamics, microphytobenthos and organic matter*. PhD Dissertation. Kiel University, Germany.
- Holme, N.A., McIntyre, D.A. (1984). *Methods for the study of Marine Benthos*. 2<sup>nd</sup> edition. Ed ISP Handbook 16. Blackwell Scientific Publications.
- Jago, C., Jones, S.E., Latter, R.J., McCandliss, R.R., Hearn, M.R., Howarth, M.J. (2002). Resuspension of benthic fluff by tidal currents in deep stratified waters, northern North Sea. *Journal of Sea Research*, **4**, 259-269.
- Jesus, B., Brotas, V., Marani, M., Paterson, D. (2005). Spatial dynamics of microphytobenthos determined by PAM fluorescence. *Estuarine Coastal and Shelf Science*, **65**, 30-42.
- Koh, C., Khim, J., Araki, H., Yamanishi, H., Mogi, H., Koga, K. (2006). Tidal resuspension of microphytobenthic chlorophyll a in a Nanaura mudflat, Saga, Ariake Sea, Japan: flood-ebb and spring-neap variations. *Marine Ecology Progress Series*, **312**, 85-100.
- Koh, C., Khim, J., Araki, H., Yamanishi, H., Koga, K. (2007). Within-day and seasonal patterns of microphytobenthos biomass determined by co-measurement of sediment and water column chlorophylls in the intertidal mudflat of Nanaura, Saga, Ariake Sea, Japan. *Estuarine Coastal and Shelf Science*, **72**, 42-52.
- Kromkamp, J., Barranguet, C., Peene, J. (1998). Determination of microphytobenthos PSII quantum efficiency and photosynthetic activity by means of variable chlorophyll fluorescence. *Marine Ecology Progress Series*, **162**, 45-55.
- Lorenzen, G. (1967). Determination of chlorophyll and phaeopigments: spectrophotometric equations. *Limnology and Oceanography*, **12**, 343-346.
- Martins-Loução, M.A. (2003). *Fragmentos em Ecologia*. Faculdade de Ciências da Universidade de Lisboa. Escolar Editora.
- Méléder, V., Barillé, L., Rincé, Y., Morançais, M., Rosa, P., Gaudin, P. (2005). Spatio-temporal changes in microphytobenthos structure by pigment composition in a macrotidal flat (Bourgneuf Bay, France). *Marine Ecology Progress Series*, **297**, 83-99.
- Méléder, V., Rincé, Y., Barillé, L., Gaudin, P., Rosa, P. (2007). Spatiotemporal changes in microphytobenthos assemblages in a macrotidal flat (Bourgneuf Bay, France). *Journal of Phycology*, **43**, 1177-1190.
- Migné, A., Spilmont, M., Davoult, D. (2004). In situ measurements of benthic primary production during emersion: seasonal variations and annual production in the Bay of Somme (eastern English Channel, France). *Continental Shelf Research*, **24**, 1437-1449.
- Mitbavkar, S., Anil, A. (2005). Diatoms of the microphytobenthic community in a tropical intertidal sand flat influenced by monsoons: spatial and temporal variations. *Marine Biology*, **148**, 693-709.

- Newton, A., Icely, J.D., Falcão, M., Nobre, A., Nunes, J.P., Ferreira, J.G., Vale, C. (2003). Evaluation of the eutrophication in the Ria Formosa coastal lagoon, Portugal. *Continental Shelf Research*, **23**, 1945-1961.
- Parsons, T., Maita, Y., Lalli, M. (1984). *A manual of chemical and biological methods for seawater analysis*. 1<sup>st</sup> edition. Pergamon Press, 105 pp.
- Perkins, R., Honeywill, C., Consalvey, M., Austin, H., Tolhurst, T., Paterson, D. (2003). Changes in microphytobenthic chlorophyll *a* and EPS resulting from sediment compaction due to de-watering: opposing patterns in concentration and content. *Continental Shelf Research*, **23**, 575-586.
- Rabalais, N., Atilla, N., Normandeau, C., Turner, R.E. (2004). Ecosystem history of Mississippi River-influenced continental shelf revealed through preserved phytoplankton pigments. *Marine Pollution Bulletin*, **49**, 537-547.
- Reuss, N., Conley, D., Bianchi, T. (2005). Preservation conditions and the use of sediment pigments as a tool for recent ecological reconstruction in four Northern European estuaries. *Marine Chemistry*, **95**, 283-302.
- Riaux-Gobin, C., Bourgoin, P. (2002). Microphytobenthos biomass at Kerguelen's Land (Subantarctic Indian Ocean): repartition and variability during austral summers. *Journal of Marine Systems*, **32**, 295-306.
- Shaffer, G., Onuf, C. (1985). Reducing the error in estimating annual production of benthic microflora: hourly to monthly rates, patchiness in space and time. *Marine Ecology Progress Series*, **26**, 221-231.
- Serôdio, J., Silva, J., Catarino, F. (1997). Non destructive tracing of migratory rhythms of intertidal benthic microalgae using in vivo chlorophyll *a* fluorescence. *Journal of Phycology*, **33**, 542-553.
- Serôdio, J., Catarino, F. (1999). Fortnightly light and temperature variability in estuarine intertidal sediments and implications microphytobenthos primary production. *Aquatic Ecology*, **33**, 235-241.
- Serôdio, J., Marques, J., Catarino, F. (2001). Use of in vivo chlorophyll *a* fluorescence to quantify short-term variations in the productive biomass of intertidal microphytobenthos. *Marine Ecology Progress Series*, **218**, 45-61.
- Serôdio, J., Vieira, S., Cruz, S., Barroso, F. (2005). Short-term variability in the photosynthetic activity of microphytobenthos as detected by measuring rapid light curves using variable fluorescence. *Journal of Marine Biology*, **146**, 903-914.
- Seuront, L., Spilmont, N. (2002). Self-organized critically in intertidal microphytobenthos patch patterns. *Physica A*, **313**, 513-539.
- Sun, M., Lee, C., Aller, R. (1993a). Anoxic and oxic degradation of <sup>14</sup>C-labeled chloropigments and a <sup>14</sup>C-labeled diatom in Long Island Sound sediments. *Limnology and Oceanography*, **38**, 1438-1451.
- Sun, M., Lee, C., Aller, R. (1993b). Laboratory studies of oxic and anoxic degradation of chlorophyll-*a* in Long Island Sound sediments. *Geochimica et Cosmochimica Acta*, **57**, 147-157.
- Sun, M., Aller, R., Lee, C. (1994). Spatial and temporal distributions of sedimentary chloropigments as indicators of benthic processes in Long Island Sound. *Journal of Marine Research*, **52**, 149-176.
- Tett, P., Grantham, B. (1980). Variability in sea-loch phytoplankton. *Fjord Oceanography*, ed. Freeland, D.H., Farmer, D.M. & Levings, C.D., Plenum, New York, 435-438.
- Underwood, G.J.C., Kromkamp, J. (1999). Primary Production by Phytoplankton and Microphytobenthos in Estuaries. *Advances on Ecological Research*, **29**, 93-153.

## **CHAPTER 5**

---

Physico-chemical and biological elements in the water  
column and sediments

---

## **Abstract**

Coastal shallow lagoons are considered to be highly important systems, which have specific biogeochemical cycles and characteristics. The assessment of sediment-water interfaces is essential for the understanding of the nutrient dynamics and to evaluate the vulnerability to eutrophication, especially in regions of restricted water exchange (RRE), such as Ria Formosa, which have natural conditions for the accumulation of nutrients.

Water samples were collected during the years of 2006 and 2007-08 for nutrients, chlorophyll *a* and dissolved oxygen. Sediment samples were also collected for pore water nutrients and benthic chlorophyll *a*. Measurements of temperature, salinity and photosynthetic active radiation were also taken. The lagoon salinity is affected by strong rainfall events. From comparison with previous work, a decrease in the nitrogen concentration in the water column can be observed, which may indicate an improvement of the water quality. Pore water nutrient concentrations were significantly larger than in the water column. Sediment-water exchanges are considered to be the most important process in nutrient dynamics of the lagoon. Benthic chlorophyll *a* contents were also large compared with the water column chlorophyll *a* concentrations. They represent about 99% of the total chlorophyll of the system. A truncated Fourier series was fitted to chlorophyll and nutrient datasets to assess the temporal variation. A strong influence of microphytobenthos on pelagic chlorophyll seems to be indicated by the analysis. Moreover, a scenario of a high increase of temperature and sea level was evaluated and revealed the potential vulnerability of Ria Formosa to eutrophication.

**Keywords:** coastal shallow lagoons, sediments, nutrients, chlorophyll *a*, oxygen, water framework directive, Ria Formosa.

## 5.1 Introduction

The human pressure on coastal areas has been increasing during the last few decades. The inputs of nitrogen (N) and phosphorus (P) have experienced a great increase caused by anthropogenic activities (Howarth and Marino, 2006; Schindler, 2006). The use of synthetic fertilizers, animal and human wastewaters and the combustion of fossil fuels are the most important sources of nitrogen (Newton *et al.*, 2003; Howarth and Marino, 2006). Phosphorus loads are mainly a consequence of agriculture and detergent inputs (Jensen *et al.*, 2006; Schindler, 2006). As an example, the N enrichment of USA coastal waters was clearly identified as an important pollution problem. Two thirds of these waters were considered to be moderately to severely degraded due to nitrogen inputs (Bricker *et al.*, 1999; Howarth and Marino, 2006). This problem may be even greater in places where the water renewal rate is lower, such as coastal lagoons (Schindler *et al.*, 2006). These lagoons are considered Regions of Restricted Exchange (RRE) due to their physical constraints in the water exchange with the sea (Tett *et al.*, 2003). They have natural conditions for the accumulation of nutrients and therefore for the occurrence of eutrophication.

The Urban Waste Water Treatment Directive (UWWTD; CEC, 1991) which defined eutrophication as the ‘enrichment of water by nutrients especially compounds of nitrogen and phosphorus, causing an accelerated growth of algae and higher forms of plant life to produce an undesirable disturbance to the balance of organisms present in the water and the quality of the water concerned’, and the Nitrate Directive of 1991, aimed to protect against nutrients from cities and farms. The Convention for the Protection of the Marine Environment of the North-East Atlantic first established in 1992 has provided an useful approach for eutrophication assessment (OSPAR Commission, 2005). The European Union has made a great effort to develop a legal tool for the regulation of water bodies, which regardless of not considering it directly, involves the implicit concept of eutrophication. This instrument, the Water Framework Directive – WFD of 2000 (CEC, 2000) aims to reach good ecological quality of surface waters and groundwater, prevent future deterioration and thus achieve sustainable management of resources. This recent legislation has created the need to develop tools for the assessment of the quality status of water bodies. One example of this is the Assessment of Estuarine Trophic Status (ASSETS) methodology, described by Bricker *et al.* (2003), adapted to the Portuguese Tagus estuary by Ferreira *et al.* (2007) and to

the Ria Formosa lagoon by Nobre *et al.* (2005). However, the definition of undesirable disturbance is still the subject of much discussion and motivates the constant development of methodologies for the implementation of the WFD (Tett *et al.*, 2007).

The assessment of the ecological status requires a series of essential processes, such as the characterization of water bodies, the establishment of type-specific reference conditions, the intercalibration of elements, the development of monitoring programmes and finally the classification of water bodies based on Ecological Quality Ratios (EQRs; Heiskanen *et al.*, 2004). The WFD represents a significant progress towards the management of specific water bodies. For the very first time, systems may be characterized and evaluated according to their type, so that sites belonging to one specific type are more alike. The variability of biological parameters is smaller within types than between types (Heiskanen *et al.*, 2004). The ecological status of a water body is therefore evaluated by comparing measured values with site-specific reference conditions. Thus, the importance of the intercalibration of results for each specific typology is undeniable. Due to the complexity of these procedures, a Common Implementation Strategy (CIS) was developed to provide guidance on how to proceed to characterize sites, define reference conditions, implement an intercalibration exercise, etc., and finally on December 2008, the Commission Decision 2008/915/EC accomplished the harmonization of the ecological status assessment principles. For Ria Formosa, the standards for chlorophyll high-good boundary were set to be 6-8 µg/L (90%ile) and for good-moderate boundary were set to be 9-12 µg/L (90%ile; Table 5.1).

According to the WFD CIS, the assessment of the ecological status is mainly defined by the biological elements. The role of nutrients in this assessment is still unclear and

Table 5.1 – Quality status of coastal and marine waters, according to EEA (1999), OSPAR (2005) and Commission Decision (2008/915/EC).

<b>Classification</b>	<b>DAIN<sup>†</sup></b> <b>(µmol/dm<sup>3</sup>)</b>	<b>Phosphate</b> <b>(µmol/dm<sup>3</sup>)</b>	<b>Chlorophyll</b> <b>(µg.L<sup>-1</sup>)</b>	<b>Source</b>
Good	< 6.5	< 0.5	-	EEA (1999)
Fair	6.5 to 9.0	0.5 to 0.7	-	
Poor	9.0 to 16.0	0.7 to 1.1	-	
Bad	> 16.0	> 1.1	-	
Elevated concentrations	10 - 15	0.6 - 0.8	15	OSPAR (2005) <sup>‡</sup>
High – Good Boundary	-	-	6 – 8	Commission Decision (2008/915/EC)
Good – Moderate Boundary	-	-	9 – 12	

flexibility has to be taken when establishing the nutrient background levels. For example, it may be appropriate for a Member State to relax the nutrient standards if there is consistent evidence that nutrient status is less than good but the biological status is good. Given that no background levels are established for Ria Formosa and due to the importance of evaluate the evolution of the system from the 80's until now, we have used the EEA classification (EEA, 1999; Table 5.1), which was used in previous studies (Newton and Mudge, 2003; Newton *et al.*, 2003). Furthermore, efforts should be put in the assessment of the functioning of systems, as recommended by the WFD. De Jonge *et al.* (2007) discussed that most monitoring programmes have focused on structure rather than functioning of the system.

In addition, environmental elements may be used differently (Directive 2000/60/EC). For example, the phytobenthos community should only be used for the assessment of river ecological quality (WFD, Directive 2000/60/EC). However, the WFD does not include any interactions between sediments and water column in shallow enclosed coastal waters, such as the Ria Formosa lagoon. These interactions are considered very important in these systems as discussed by Falcão (1996), Falcão and Vale (2003), Murray *et al.* (2006) and Wayland *et al.* (2008). Shallow enclosed coastal systems are a good example of how important the physical and biogeochemical processes are. The water volume is spread in a large area which gives a great importance to sediments. In fact, sediments may have a determinant role influencing the quality of the water column (Murray *et al.*, 2006; Wayland *et al.*, 2008). They may act as sources or sinks of nutrients, depending on environmental conditions such as salinity, temperature and dissolved oxygen (Falcão and Vale, 1990; Falcão, 1996; Gönenç and Wolflin, 2005). The tidal exchange is also extremely important in the dynamics of each parameter. A large variation can be found in shallow lagoons from high water to low water in most of the parameters (Newton *et al.*, 2003). Moreover, light penetrates to the bottom which provides suitable conditions for the development of important benthic algal communities. Their biomass in shallow systems may be significantly larger than the phytoplankton biomass. Furthermore, their contribution to the total chlorophyll found in the water column may be up to 25% of the total annual primary production (Colijn, 1982; Colijn and de Jonge, 1984). Therefore, as discussed, the measurement of water column parameters in these systems may only provide an incomplete picture of the trophic status.



The aims of this study were to: 1) evaluate the short and long-term temporal variation of pelagic nutrients and oxygen, which are part of the physico-chemical quality elements described in the WFD as state indicators, and pelagic chlorophyll, which is part of the biological indicators relating to phytoplankton biomass; 2) assess the importance of sediments in the system dynamics in terms of nutrients and chlorophyll. The scientific hypotheses were that: 1) there were repeated temporal patterns of biological and physico-chemical elements; 2) there was an important influence on the biological elements by the environmental variables; 3) the benthic compartment was the most important component of the system, in terms of chlorophyll and nutrient concentrations.

## 5.2 Material and methods

### 5.2.1 Sampling sites and schedule

Sampling took place every two weeks, except stated, from 10<sup>th</sup> April to 18<sup>th</sup> October during 2006 and from 15<sup>th</sup> March 2007 to 20<sup>th</sup> February 2008 (Figure 5.1). Samples were collected from three sites: Ramalhete, Ponte and Beach (opposite to Ponte, in the sea side of the barrier, Figure 5.2). Beach is considered an undisturbed site or with minor anthropogenic impacts. Ponte and Ramalhete are two Water Framework Directive (WFD) sites of the intercalibration network in accordance with Directive 2000/60/EC of the European Parliament. They are in the category of coastal waters due to the insignificant input of freshwater. Ramalhete, a site with medium/fine sand sediment (Table 5.2; as in Chapter 3), receives the effluent from an Urban Waste Water Treatment Plant and is affected by its proximity to the airport and recreational activities caused mainly by boats. It is considered to be in the lower boundary of ecological quality, between Good and Moderate ecological status (Loureiro *et al.*, 2006, following Bricker *et al.*, 2003 and the ASSETS classification).

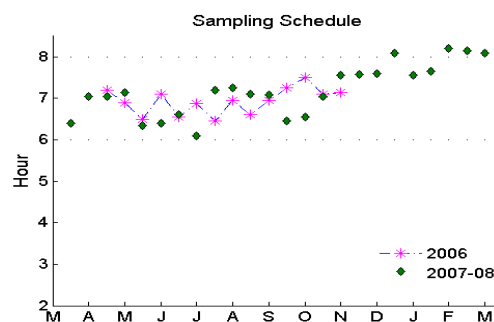


Figure 5.1 - Sampling schedule for 2006 and 2007-08.

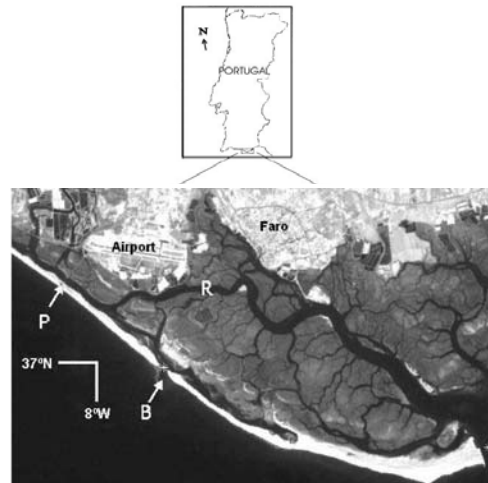


Figure 5.2 - Map of Ria Formosa showing sampling stations at P = Ponte and R = Ramalhete. The sampling station Beach is located near Ponte, but on the sea side.

Table 5.2- Grain sizes distribution (%) and organic matter (%) of samples obtained at Ramalhete and Ponte.

Sediment size fractions (%)	Ramalhete	Ponte
> 1000 $\mu\text{m}$	2.21	2.49
1000 - 710 $\mu\text{m}$	6.09	1.25
710 - 500 $\mu\text{m}$	13.34	2.13
500 - 355 $\mu\text{m}$	18.79	2.54
355 - 250 $\mu\text{m}$	8.99	2.20
250 - 180 $\mu\text{m}$	3.11	3.51
180 - 125 $\mu\text{m}$	1.34	23.17
125 - 90 $\mu\text{m}$	0.53	8.39
90 - 63 $\mu\text{m}$	0.48	4.19
< 63 $\mu\text{m}$	45.12	50.13
Organic matter (%)	1.54	2.27

Ponte, a site with muddy sand sediment (Table 5.2), has the influence of the inputs from golf courses and intense agriculture from the western part of the lagoon. However, it is one of the main channels of the lagoon and has an ecological status that goes from High to Good (Loureiro *et al.*, 2006, following Bricker *et al.*, 2003 and the ASSETS classification). Both Ramalhete and Ponte have good historical datasets.

Water samples were collected for nutrients, chlorophyll and dissolved oxygen (not at Beach during 2006) analyses and sediment samples were collected for benthic chlorophyll and pore water nutrient analyses (once a month in 2007-08) when sediment was not immersed. Measurements of salinity and temperature were taken *in situ* using a WTW conductivity meter, and Photosynthetic Active Radiation (PAR) values were also taken twice a month (see below). The sediment samples were not collected at the Beach

and the PAR measurements were also not taken at this site. This site is on the ocean coast, therefore is heavily influenced by wave action. Rainfall data were obtained from *Direcção Regional de Agricultura e Pescas do Algarve* (DRAP-Alg). The schedule was drafted so that samples could be taken during low water and early in the morning (mostly between 6 and 8 am), when the dissolved oxygen concentration is lower due to consumption by the primary producers during the night (Oliveira, 2005). Additional measurements of PAR were also taken during two days in June 2007 to cover the tidal cycle.

On the 16<sup>th</sup> June 2007 during the flood period (beginning and middle), salinity and temperature profiles were recorded in Ponte using a SeaBird 19plus CTD (Figure 5.3). The files were then uploaded using Seaterm ® software.



Figure 5.3 – CTD.

### 5.2.2 Photosynthetic Active Radiation (PAR) diffuse attenuation coefficient

Measurements were taken at Ponte and Ramalhete (P and R, Figure 5.2) every two weeks during 2007-08, using a single planar sensor and on the 13<sup>th</sup> and 14<sup>th</sup> of June 2007, using the two-bulb sensor.

#### *Single planar light sensor*

On every sampling date, PAR was measured at sea level (just submerged) and at 0.25 m of depth at Ponte and Ramalhete to obtain the PAR diffuse attenuation coefficient

using a Li-Cor (Li-192) Underwater Quantum sensor. The PAR diffuse attenuation coefficient was calculated using the Beer-Lambert Law equation:

$$K_d = \frac{-\ln\left(\frac{Ed(z_1)}{Ed(0)}\right)}{Dz} \quad 5.1)$$

where  $Ed(z)$  is the PAR measurement at  $z_1$  depth,  $Ed(0)$  is the PAR measurement when the sensor is just under the water surface,  $Dz = z_1 - 0$  m,  $K_d$  is the PAR diffuse attenuation coefficient and  $z$  is the depth.

#### *Two-bulb light sensor*

This  $K_d$  sensor is constituted by two Li-Cor Underwater Spherical Quantum sensors and a coupled CTD in the bottom (Figure 5.4). The sensor was developed by the Afbi (Agri-Food and Biosciences Institute) team in Belfast in order to assess more accurately the PAR diffuse attenuation coefficient ( $K_d$ ) and to study it during the tidal cycle. This approach aimed to make better measurements in shallow and/or turbid waters and therefore to improve the previous method used to calculate the  $K_d$ , by using profiles and instant PAR measurements at both depths. The sensor is lowered from the surface to the bottom and then taken out of the water. The distance between sensors varied between 0.25 and 0.5 m. The files were uploaded using Seaterm ® software.



Figure 5.4 – Two-bulb  $K_d$  sensor.

*Numerical approach*

Two numerical approaches were applied to datasets from the two-bulb sensor. One calculates the  $K_d$  for each optical depth using solely the instant PAR measurements recorded in that specific depth interval and at each instant. Instant  $K_d$  is calculated following the equation:

$$K_d = -\ln \left[ \frac{PAR_{bottom} \times P1P2_{ratio}}{PAR_{top}} \times \frac{1}{sp} \right] \quad (5.2)$$

$PAR_{bottom}$  and  $PAR_{top}$  are PAR measurements of the bottom and top sensor.  $P1P2_{ratio}$  is a coefficient to correct the different sensitivity of sensors. Sensor 1, which is in the top measures 1.2 times more than sensor 2.  $sp$  is the distance of separation between sensors. Medians of each optical depth were calculated and means for the whole profile were worked out. Optical depth was calculated by multiplying the real depth and the  $K_d$  estimate. Light attenuates differently through the water column, so it is essential to assess  $K_d$  at different depth intervals, according to the optical depth.

The second method performs a regression between the  $\log(x)$  transformed measurements of PAR and depth within each optical depth. The coefficient of the relationship is the  $K_d$  value.

A Matlab script was written to analyse data obtained following these two approaches (Appendix I). The script developed and improved with contributions obtained from several meetings between Elisa Capuzzo, Prof. Paul Tett and I. Prof. Paul Tett provided the Matlab code. To test whether the script was working properly, a file with test data for PAR measurements in the bottom and top sensor was produced, according to the Beer-Lambert Law described before, by another simple Matlab script. These data were produced using different values of  $K_d$  from 0.5 to 1. The script (named test script) was then used and proved to be working well (Figure 5.5). Good fit regressions were drawn to data within each optical depth as presented in the first plot in blue and red. The correspondent values of  $K_d$  are represented in the second plot in blue and red, as well. The black lines are  $K_d$  values calculated from instant measurements. The Matlab code developed to test the main analysis, allows the introduction of a term that considers seabed reflection and was used to investigate this phenomenon.

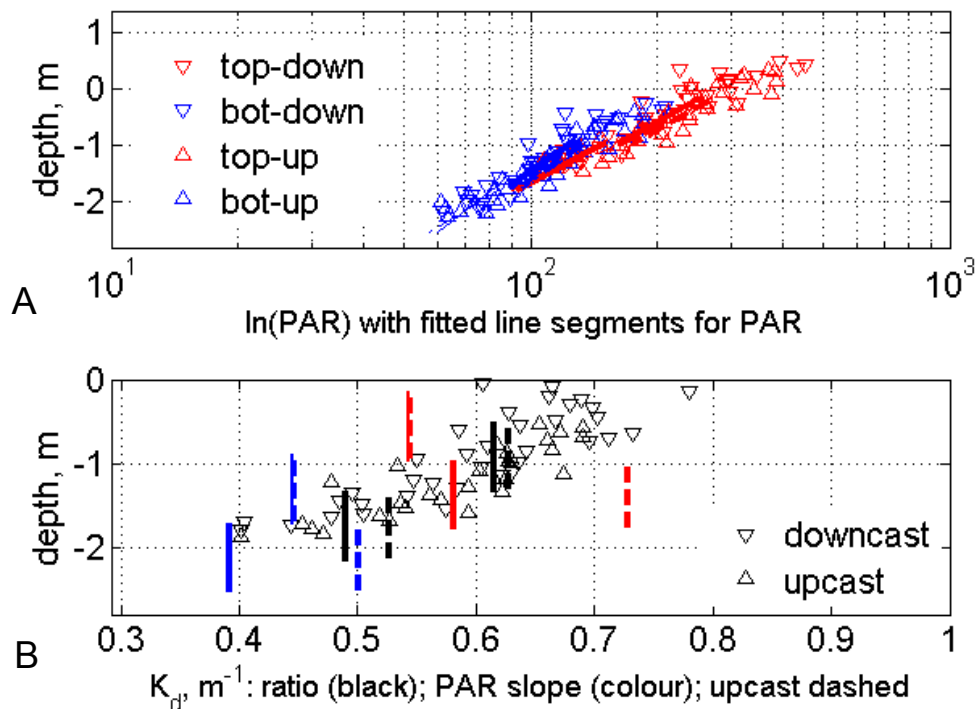


Figure 5.5 – A- Log (x) transformed PAR values created to test the Matlab script and fitted lines obtained from regression within each optical depth. B – Values of  $K_d$  obtained from regressions (colour) and instant measurements (black). Sensors: Top and bottom. Casts: down and up.

### 5.2.3 Nutrients in the water column

Three samples of  $0.5 \text{ dm}^3$  seawater were collected at each site on each sampling date. The samples were placed in a cooler box and transported to the laboratory as soon as possible. The samples were immediately analysed, if possible, or frozen at  $-20^\circ\text{C}$ . Each sample was analysed in triplicates of  $15 \text{ cm}^3$  for ammonium-nitrogen, nitrite-nitrogen, nitrate-nitrogen, orthophosphate-phosphorus and silicate-silicon following Grasshoff *et al.* (1983). The detection and quantification of these analyses are presented in Appendix I. An example of the calibration curve is also shown.

### 5.2.4 Pore water nutrients

Three sediment cores were collected at Ponte and Ramalhete once a month. The corer had a diameter of 8 cm and 10cm height. The core samples were placed in a plastic bag inside a cool box and were transported to the laboratory as soon as possible. In the laboratory random sub samples of each core were collected immediately and placed in

50 cm<sup>3</sup> plastic tubes to centrifuge for 15 minutes at 4 000rpm. The overlying water was taken from all the tubes from each site and filtered using 0.45 µm Nucleopore membranes. One sample of pore water was obtained from each site and diluted for later analysis of nutrients. Ammonium-nitrogen, nitrate-nitrogen, nitrite-nitrogen, orthophosphate-phosphorus and silicate-silicon were analysed following Grasshoff *et al.* (1983).

Nutrient fluxes ( $\phi$ ) from pore water to the water column were calculated based on the Fick's First Law of Diffusion:

$$\phi_s = -D_m \cdot \frac{\partial S}{\partial z} \cdot \frac{p}{\tau} \quad (5.3)$$

Diffusion coefficient ( $D_m$ ) values were taken from Murray *et al.* (2006),  $1.6416 \times 10^{-4} \text{ m}^2 \cdot \text{d}^{-1}$  for DAIN and  $0.71194 \times 10^{-4} \text{ m}^2 \cdot \text{d}^{-1}$  for phosphate. The concentration difference ( $\partial S$ ) was calculated by subtracting the concentrations of the water column from the pore water concentrations.  $Z$  is the sediment-water interface distance, 0.001m (thickness of the surficial benthic layer) + 0.001m (thickness of the boundary layer),  $p$  is porosity (0.5) and  $\tau$  is tortuosity of the sediment pores ( $\approx 1.4$ ; following Jackson *et al.*, 2002). Porosity was estimated considering the proportion of water lost during freeze-drying.

### 5.2.5 Pelagic chlorophyll

Three samples of 1.5 dm<sup>3</sup> of seawater were collected at each site on each sampling date. The samples were transported to the laboratory as soon as possible and 1 dm<sup>3</sup> was immediately filtered onto 47mm GF/F filters under minimal vacuum. One dm<sup>3</sup> of seawater was filtered and each filter was placed in a plastic tube covered with aluminium foil. Ten cm<sup>3</sup> of 90% acetone (buffered with sodium bicarbonate) was added to each tube. The filters were mashed up using a glass rod. The tubes were placed in a freezer at -20°C. After 24 hours, the tubes were centrifuged for 10 minutes at 3000rpm. The supernatant was decanted to a 1cm spectrophotometer cuvette and measured at 663nm and 750nm. Two drops of 1.2M HCl were added to the cuvette and the sample was measured again at both wavelengths. Chlorophyll concentrations were calculated following the Lorenzen's equations (Lorenzen, 1967).

### 5.2.6 Microphytobenthic chlorophyll

MPB samples collected for this study are the ones used in Chapter 4. However, the procedure and results are presented again due to its importance in the context of this study. Phaeopigment results were presented in Chapter 4 and are not repeated here.

Six samples of sediment were collected from Ponte and Ramalhete using a Petri-dish of 47mm diameter and 13mm height. A plastic card was used to manoeuvre underneath the sample. Samples were placed in a cooler box and protected from sunlight. They were transported to the laboratory as soon as possible. In the laboratory, they were transferred to 50 cm<sup>3</sup> plastic tubes wrapped in aluminium foil and placed in the freezer at -20°C. All samples were freeze-dried for 30 hours. The time necessary to freeze-dry the samples and the optimal procedure for benthic chlorophyll analysis of these samples were assessed previously, as described in Chapter 3. The weight of the sediment was determined after freeze-drying. The solvent 90% acetone for sand and 80% acetone for mud, buffered with sodium bicarbonate was added to each sample in a similar proportion of solvent volume to sediment weight and the tubes were stirred in the vortex. Samples were placed again in the freezer at -20°C for 6 hours. The samples were then centrifuged and measured as described in Chapter 3. A 10% dilution was carried out in 90% acetone: to allow the use of spectrophotometric equations for 80% acetone in muddy samples and to decrease the solution concentration to permit a more reliable measurement. To calculate the chl content ( $\mu\text{g/g}$ ), the dried weight of sediment was used instead of the usual volume of filtered water used in water column chlorophyll assessments.

### 5.2.6 Oxygen

Three samples of seawater were collected at each site using glass bottles. Bottles were lowered in the water, avoiding any gas bubbles. The appropriate reagents (manganese chloride and potassium iodide) were added in situ and the bottle protected from any air contact Grasshoff *et al* (1983). The bottles were transported as soon as possible to the laboratory, where they were analysed following the method presented by Grasshoff *et al* (1983;  $\text{mg.L}^{-1}$ ), which is based on the method first proposed by Winkler (1888). Oxygen saturation calculations were based on Carpenter (1966;  $\text{mmol.m}^{-3}$ ).



### 5.2.7 ECASA Sampling Week

An intensive sampling campaign was performed from the 16<sup>th</sup> October to the 20<sup>th</sup> October 2006 at Ponte and Ramalhete as part of the ECASA European Project. The objective was to study the short-time changes during a complete tidal cycle during all days (covering Low water, Flood, High Water and Ebb once per day). Measurements of temperature and salinity were taken every three hours, as described before and water samples for pelagic chlorophyll *a*, oxygen and nutrients in the water column were also collected. The protocols for nutrients, chlorophyll *a* and oxygen analysis were followed, as explained above.

### 5.2.8 Statistical analyses

All statistical tests and numerical analyses were carried out using CANOCO, Matlab and Minitab 14 softwares. Data were tested for normality and homoscedasticity of variance and parametric tests (T-test) conducted. Pearson's correlations were also carried out where appropriate.

In order to investigate the temporal variation of several components including: phytoplankton, microphytobenthos and nutrients, an empirical model was developed and fitted to log-transformed data. The model was:

$$\hat{y} = \bar{y} + f_M(t) + \varepsilon \quad (1)$$

where:

$$f_M(t) = \sum_{n=1}^{n=M} [a_n \cos(2\pi nt) + b_n \sin(2\pi nt)] \quad (2)$$

The deterministic function  $\bar{y} + f_M(t)$ , describes a truncated Fourier series with *M* sets of sine-cosine waves. Time *t* is in years. The stochastic term  $\varepsilon$  is the error remaining after the Fourier series has been fitted. It contains a part which corresponds to the within-day variability and the residual error. Detailed description of the method is presented in Chapter 4.

An analysis of variance was then carried out to assess the relative importance of the seasonal cycle (represented by wave-pairs 1 to 3), the higher-frequency temporal variation (wave-pairs 4 through *M*) and the within-day variability in each component (Table 5.8). In Table 5.8, the degrees of freedom used for each variance component

were calculated from  $K$  minus the degrees of freedom used in the calculation of the Sum of Squares (SOS). The resulting variances were then summed to give a total estimated variance, so that the percentage of this variance due to each source of variation could be set out in Table 5.8. This procedure is, of course, different from that in a formal ANOVA aimed to test the hypothesis that residual and explained variances are the same. To perform the analysis of variance inside the lagoon, data from both Ponte and Ramalhete were pooled.

In order to fulfill the objective of the assessment of relationships between elements, a multiple regression approach was performed using data from each site. A canonical correspondence analysis (CCA) was also performed using the CANOCO software. The CCA used environmental and biological elements for the analysis. Data was divided in site and month of the year (site x month/year) for all elements. Data used for the multiple regression analysis and for the canonical correspondence analysis were  $\log(x)$  transformed, except temperature, salinity and  $K_d$ , for which real values were used.

## 5.3 Results

### 5.3.1 Temperature and Salinity

Higher temperature and salinity values were found during the summer both in 2006 and 2007-08 (Figure 5.6). Beach was the site with lower values of temperatures and salinity. It was also the site that showed smaller variation throughout the years. In 2006 larger values of temperature were reached during the summer because it was a warmer period compared with 2007. The low salinity values found within the lagoon, show that rainfall episodes were strong during the winter of 2006 and 2007-08 compared with both summers. Negative Pearson's correlations were found between salinity and rainfall (considering rainfall recorded during the 4 days before) at Ponte ( $p < 0.005$ ) and Ramalhete ( $p < 0.001$ ). The last salinity recorded in 2006 was taken after two days of heavy rain. Pearson's positive correlations were found between all sites for temperature and salinity in 2007-08 ( $p < 0.05$ ) and at Ponte during 2006 ( $p < 0.05$ ). No significant differences (ANOVA) were found between temperature and salinity values at the three sites during 2006 and 2007-08 ( $p > 0.05$ ).

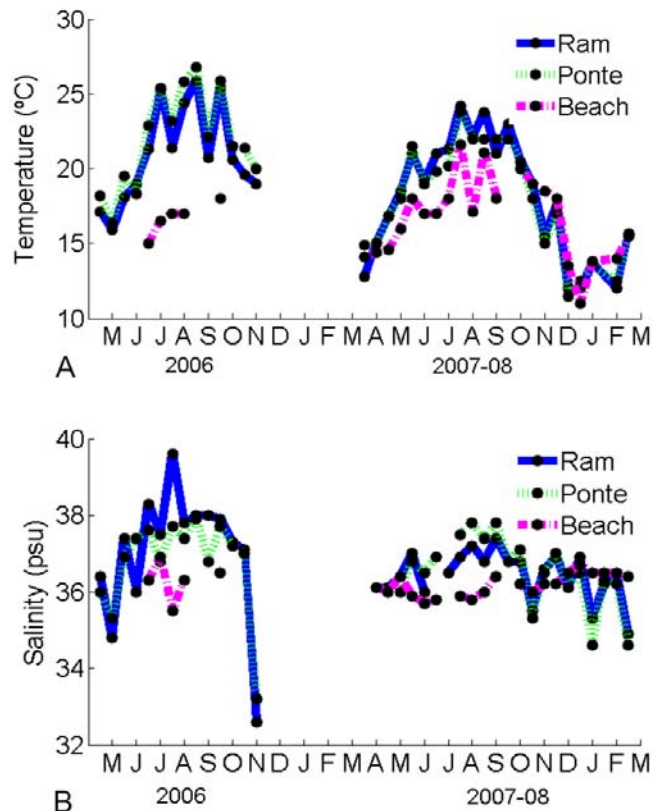


Figure 5.6 - Seasonal changes of temperature (°C; A) and salinity (psu; B) during 2006 and 2007-08 at Ramalhete, Ponte and Beach.

Profiles of temperature and salinity were recorded at Ponte on the 16<sup>th</sup> June 2007 using a CTD and results are presented in Figure 5.7 (A and B). Profile 1 corresponds to the beginning of the flooding period. Temperature and salinity are higher than the values recorded for the other profiles and decrease with depth, especially temperature (almost 1°C). The second profile corresponds to the middle of the flooding event. Temperatures dropped but are now constant with depth. The salinity is also constant with depth. Profile 3 corresponds to the final part of the flood. The temperatures and salinity values are the lowest.

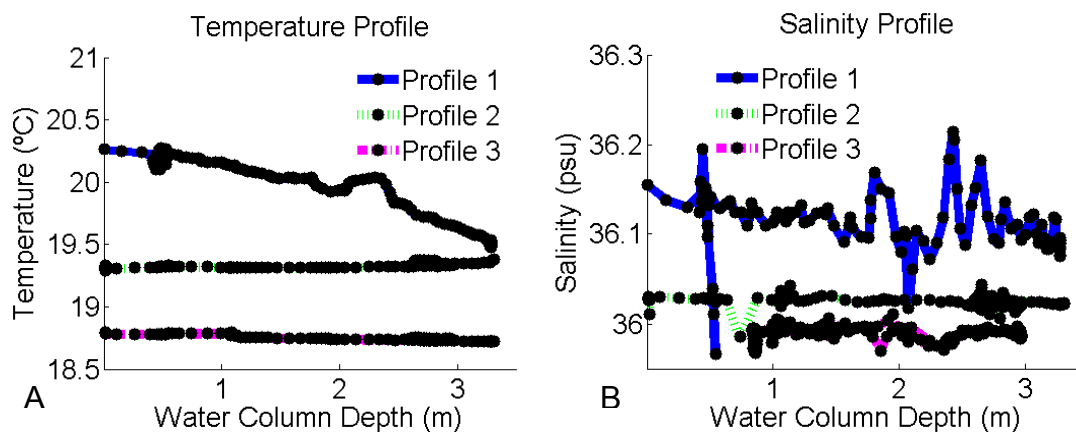


Figure 5.7 – Temperature (°C) and Salinity (psu) profiles during flood period in Ponte.

### 5.3.2 PAR diffuse attenuation coefficient

#### *Single planar light sensor*

During the period from March 07 to February 08, the values of the  $K_d$  coefficient varied from 0.25 to 1.10  $m^{-1}$ , at Ramalhete, and from 0.68 to 1.28  $m^{-1}$ , at Ponte (Table 5.3). Mean  $K_d$  values found were 0.69  $m^{-1}$ , at Ramalhete and 0.93  $m^{-1}$  at Ponte. Positive Pearson's correlations were found between values of Ponte and Ramalhete ( $p < 0.005$ ).

Table 5.3 – Mean values of the diffuse attenuation coefficient ( $m^{-1}$ ) measured at Ponte and Ramalhete with the single planar light sensor.

	$K_d (m^{-1})$	
	Ram	Ponte
<b>M</b>	0.25	0.68
<b>A</b>	0.79	0.96
<b>M</b>	0.59	0.93
<b>J</b>	0.57	0.77
<b>J</b>	0.53	1.28
<b>A</b>	-	-
<b>S</b>	0.90	1.27
<b>O</b>	0.59	1.10
<b>N</b>	1.10	1.3
<b>D</b>	-	0.96
<b>J</b>	0.66	1.17
<b>F</b>	0.90	0.75
	<b>0.69</b>	<b>0.93</b>

#### *Two-bulb light sensor*

In Ria Formosa, at Ramalhete and Ponte, the determination of the diffuse attenuation coefficient from the regression of  $\ln(x)$  transformed values of PAR against the depth of the water column was not possible due to the shallowness of the lagoon. There were insufficient measurements through the water column to conduct an accurate regression (Figure 5.8-A). The maximum depth was around 1 meter and sensors were 0.75 m apart, which only leaves an insufficient depth of less than 0.25 m to work out a profile. An example of the estimates of  $K_d$  obtained from the regression method (colour) and from the calculation of the instant  $K_d$  values (black), using dataset of profile 1 at Ponte, is represented in Figure 5.8 –B.

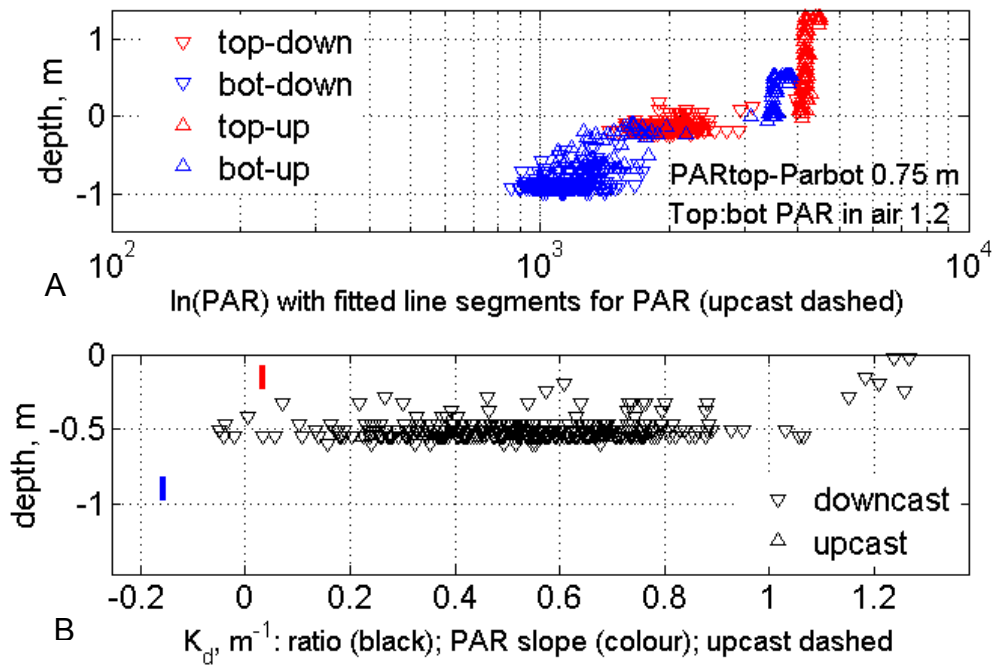


Figure 5.8 – A - Log (x) transformed PAR values measured at Ponte (Profile 1) through the water column. B – Estimates of  $K_d$  obtained from regression (colour lines) and from instant measurements (black lines).

Table 5.4 gives the  $K_d$  means obtained at Ponte and Ramalhete using only the instant measurements, as explained before. The mean  $K_d$  obtained at Ponte was  $0.55 \text{ m}^{-1}$  and was  $0.57 \text{ m}^{-1}$  at Ramalhete. Profiles 1 to 6 at Ponte were done during the flood and high water periods, as represented by the greatest depths. Profiles 7 to 9 at Ponte were recorded during the ebb period. Profile 10 at Ponte was recorded during the flood period again. Profiles 11 and 12 at Ponte were recorded during the high water period on the following day. Profiles 1 to 5 at Ramalhete were collected during low water and flood periods. No significant differences were found between  $K_d$  values obtained at Ponte and at Ramalhete ( $p > 0.05$ ).

The test script, previously described in sub-section 5.2.2, was used to evaluate the importance of the sea-bed reflection in shallow systems since the spherical light sensor responds to upwards as well as downwards light, so will underestimate  $K_d$  if lowered towards a reflecting seabed. This term was introduced in the Beer-Lambert Law equation as being 0.5, which represents a reflection of 50% of light that reaches the bottom. This value was considered as reasonable by the observation of the clear sea bottom. The result was an increase of 0.15 in the  $K_d$  estimate, which was  $0.7 \text{ m}^{-1}$  (Figure 5.9) instead of the  $0.55 \text{ m}^{-1}$  found previously (T-Test; Figure 5.9).

Table 5.4 – Greatest depths and mean  $K_d$  ( $m^{-1}$ ) of each profile at Ponte and Ramalhete. Note that the greatest depth is 0.5m larger than it should due to the space between the bottom sensor and the CTD.

Tidal conditions: Flood, High Water (HW), Ebb and Low Water (LW).

		Profile	Greatest depth	Mean $K_d$	Method
<b>Ria Formosa</b>	Flood & HW	Ponte 1	1.47	0.60	Instant
		Ponte 2	1.59	0.70	“
		Ponte 3	2.30	0.72	“
		Ponte 4	2.74	0.55	“
		Ponte 5	2.84	0.48	“
		Ponte 6	3.36	0.34	“
	Ebb	Ponte 7	3.16	0.37	“
		Ponte 8	2.61	0.40	“
		Ponte 9	2.08	0.63	“
	Flood H W	Ponte 10	2.93	0.63	“
		Ponte 11	3.50	0.55	“
		Ponte 12	3.52	0.57	“
				<b>0.55</b>	
LW & Flood	Ram 1	0.71	0.75	“	
	Ram 2	0.64	0.96	“	
	Ram 3	0.69	0.42	“	
	Ram 4	0.67	0.36	“	
	Ram 5	0.63	0.38	“	
				<b>0.57</b>	

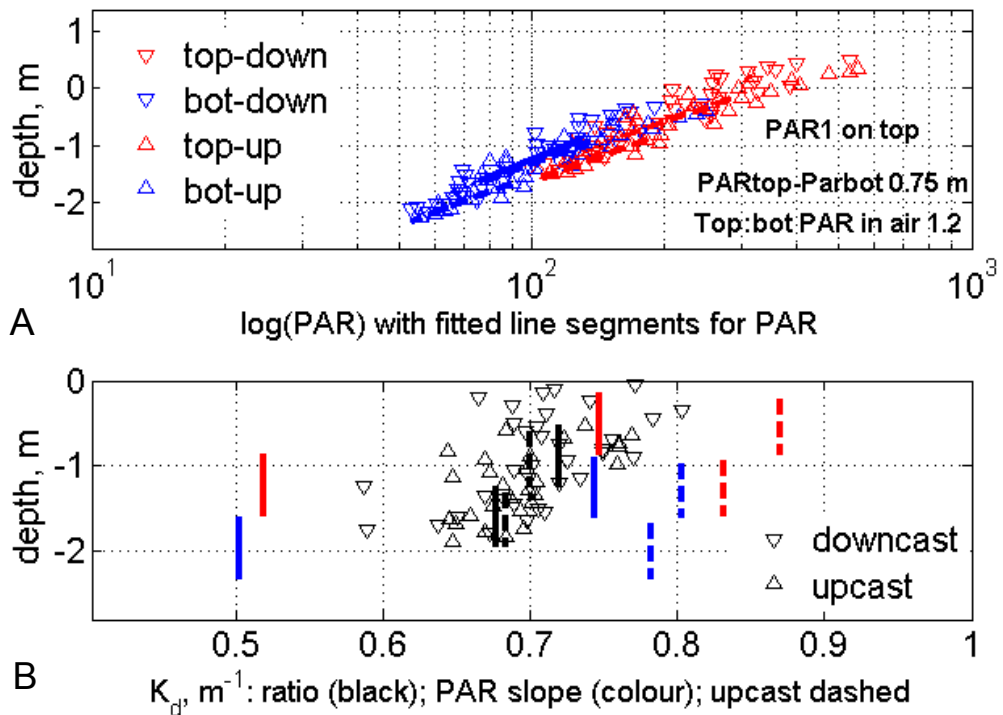


Figure 5.9 – A- Log (x) transformed PAR values created to test the Matlab script. It considers a sea-bed reflection of 0.5. B – Estimates of  $K_d$  obtained from regressions (colour) and instant measurements (black).

### 5.3.3 Nutrients

Concentrations of nitrite ranged from 0 to 0.4  $\mu\text{M}$  in 2006 and 2007-08, except on the first day of sampling, when a peak was found at the three sites (Figure 5.10-A). Positive Pearson's correlations were found between the values obtained at Ramalhete and Ponte ( $p < 0.005$  for 2006 and  $p < 0.05$  for 2007-08). Nitrite was not detectable during the summer of 2007. No significant differences were found between 2006 data and 2007-08 data (T-test,  $p > 0.05$ ).

Ammonium concentrations varied widely between 0 and 4  $\mu\text{M}$ , with three exceptions, when concentrations almost reached 6  $\mu\text{M}$  (Figure 5.10-B). In 2008, most of the concentrations observed at Beach were small, except for a peak in January 2008. Positive correlations were found between Ramalhete and Ponte in 2006 and 2007-08 ( $p < 0.005$  for 2006 and  $p < 0.05$  for 2007-08) and between Ponte and Beach in 2007-08 ( $p < 0.05$ ). No significant differences were found between data from 2006 and 2007-08 (T-test,  $p > 0.05$ ).

Concentrations of nitrate varied from 0 to 4  $\mu\text{M}$  during most of the year of 2006 and 2007-08, except in November 2007, when a peak (9  $\mu\text{M}$ ) was observed at Beach (Figure 5.10-C). Positive correlations were found between Ponte and Beach in 2006 ( $p < 0.05$ ) and between Ponte and Ramalhete in 2007-08 ( $p < 0.05$ ). No significant differences were found between data from 2006 and 2007-08 for each site (T-test,  $p > 0.05$ ).

Ramalhete was the site where the smallest concentrations of Dissolved Available Inorganic Nitrogen (DAIN) were observed (Figure 5.10-D). The variation found was from 0 to 6  $\mu\text{M}$ , except in November 2007, when the concentrations reached 9  $\mu\text{M}$  at Beach. Positive correlations were found between Ponte and Ramalhete in 2006 and 2007-08 ( $p < 0.005$  for 2006 and 2007-08).

The range of variation of phosphate was larger in 2006 (from 0.5 to 1.5  $\mu\text{M}$ ) than in 2007-08 (from 0 to 1  $\mu\text{M}$ ). Beach was the site where the smallest values were observed, especially in 2007-08 (Figure 5.10-E). Positive correlations were found between Ramalhete and Ponte and between Ramalhete and Beach in 2007-08 ( $p < 0.05$ ). Significant differences were found between data collected in 2006 and 2007-08 (T-test,  $p < 0.05$ ).

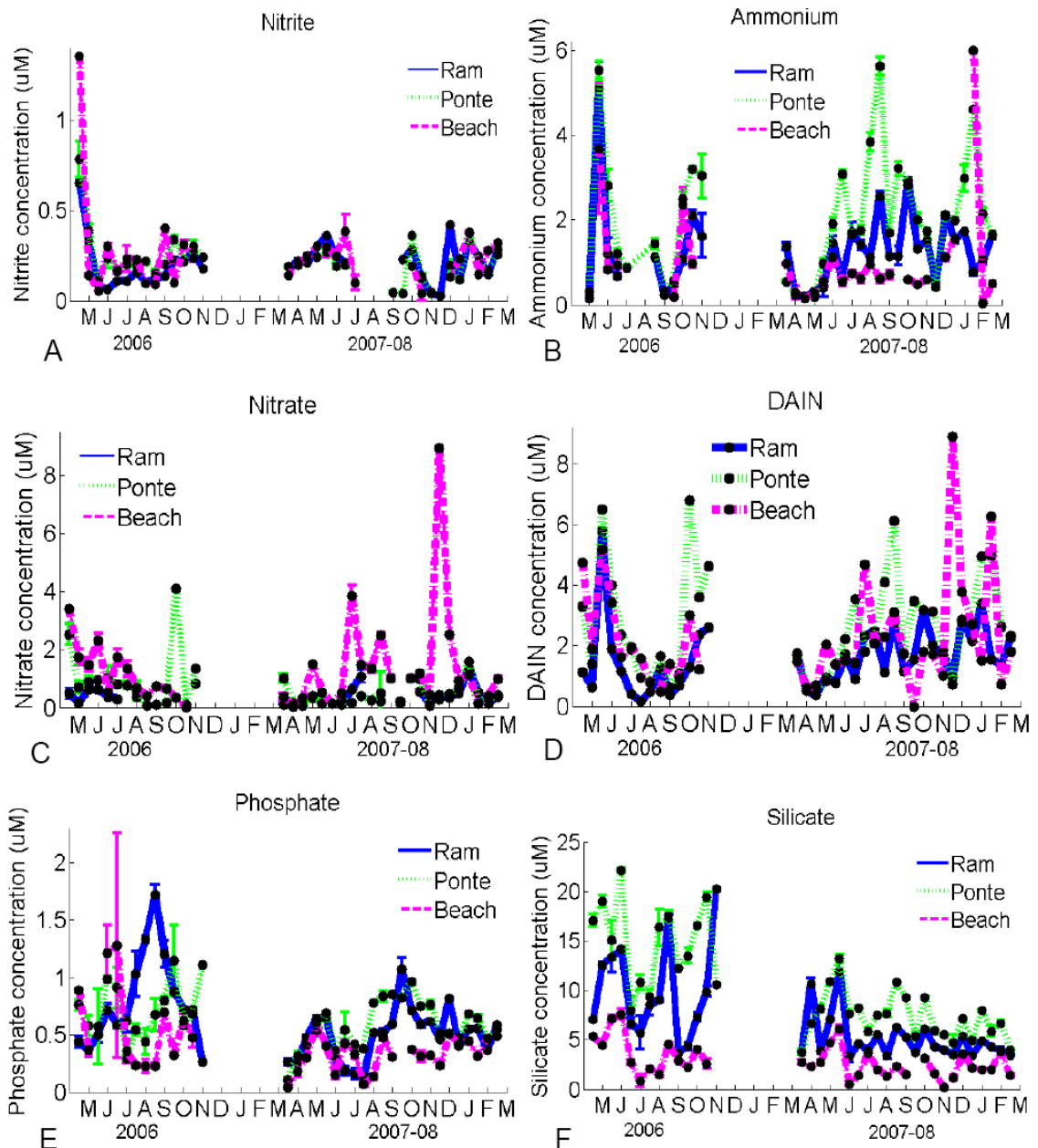


Figure 5.10 - Seasonal changes of nitrite ( $\mu\text{M}$ ; A), ammonium ( $\mu\text{M}$ ; B), nitrate ( $\mu\text{M}$ ; C), DAIN ( $\mu\text{M}$ ; D), phosphate ( $\mu\text{M}$ ; E) and silicate ( $\mu\text{M}$ ; F) in the water column during 2006 and 2007-08 at Ramalhete, Ponte and Beach.

Larger values of silicate concentrations were always found at Ponte and the smallest at Beach (Figure 5.10-F). The values varied approximately from 1 to 20  $\mu\text{M}$  in 2006 and between 1 to 15  $\mu\text{M}$  in 2007-08. Positive correlations were found between Ponte and Ramalhete in 2006 ( $p < 0.005$ ) and between all sites in 2007-08 ( $p < 0.05$ ). Significant differences were found between data collected in 2006 and 2007-08 (T-test,  $p < 0.05$ ).

The representation of the N:P ratio showed that inside the lagoon all the values are under 16, which is the reference Redfield number, except for one date (summer) at Ramalhete (Figure 5.11-A). Outside the lagoon, 4 points were found above the



reference. The N : Si ratio plot shows that inside the lagoon all the values are under 1, the Redfield reference, and outside almost all are above (Figure 5.11-B). Inside the lagoon, Si concentrations are much larger compared with N concentrations.

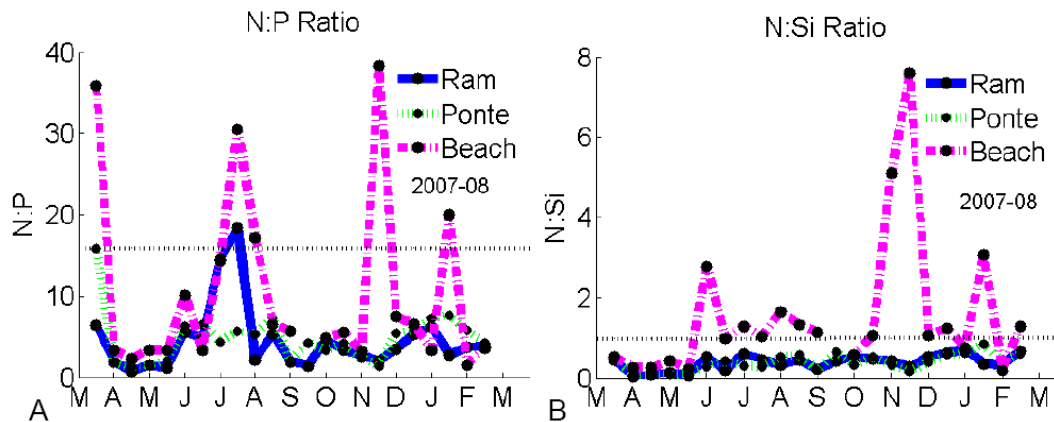


Figure 5.11 - N:P and N:Si ratios found in the water column during 2007-08 at Ramalhete, Ponte, Beach.

All the concentrations of pore water nutrients obtained in this study were considerably higher than in the water column (Figure 5.12- A to F). Actually, DAIN concentrations in the water column were just 25% of the total concentrations of nitrogen in the lagoon (pore water + water column), considering the mean concentrations of  $2.2 \mu\text{M}$  (water column) and  $412 \mu\text{M}$  (pore water) and the total volume of the water column ( $88 \times 10^6 \text{ m}^3$ ) and sediments ( $53 \times 10^6 \text{ m}^2$  and  $0.05 \text{ m}$  depth). Phosphate concentrations in the water column were estimated as being around 30% of the total and silicate concentrations around 60% of the total. Total concentrations of the water column were estimated considering mid-water values. Total concentrations of the pore water were estimated considering the area of the lagoon, the depth of the sediment layer sampled and the porosity. A significant agreement was found between the pore water nitrate values of Ponte and Ramalhete (Pearson's positive correlation:  $p < 0.05$ ). Ammonium is the compound that dominates the nitrogen reservoir of the sediment and clearly influences the Dissolved Available Inorganic Nitrogen (DAIN) concentrations. Large concentration variations were found for almost all the nutrients throughout the year 2007-08. For phosphate, the concentrations were larger during the summer and silicate also had a clear peak in August at Ramalhete. Silicate concentrations were also large during May and June.

Fluxes estimated were  $497 \mu\text{mol.m}^{-2}.\text{h}^{-1}$  for DAIN, considering a DAIN concentration difference of  $410 \text{ mmol.m}^{-3}$ , and  $37.4 \mu\text{mol.m}^{-2}.\text{h}^{-1}$  for phosphate, considering a phosphate concentration difference of  $72 \text{ mmol.m}^{-3}$ .

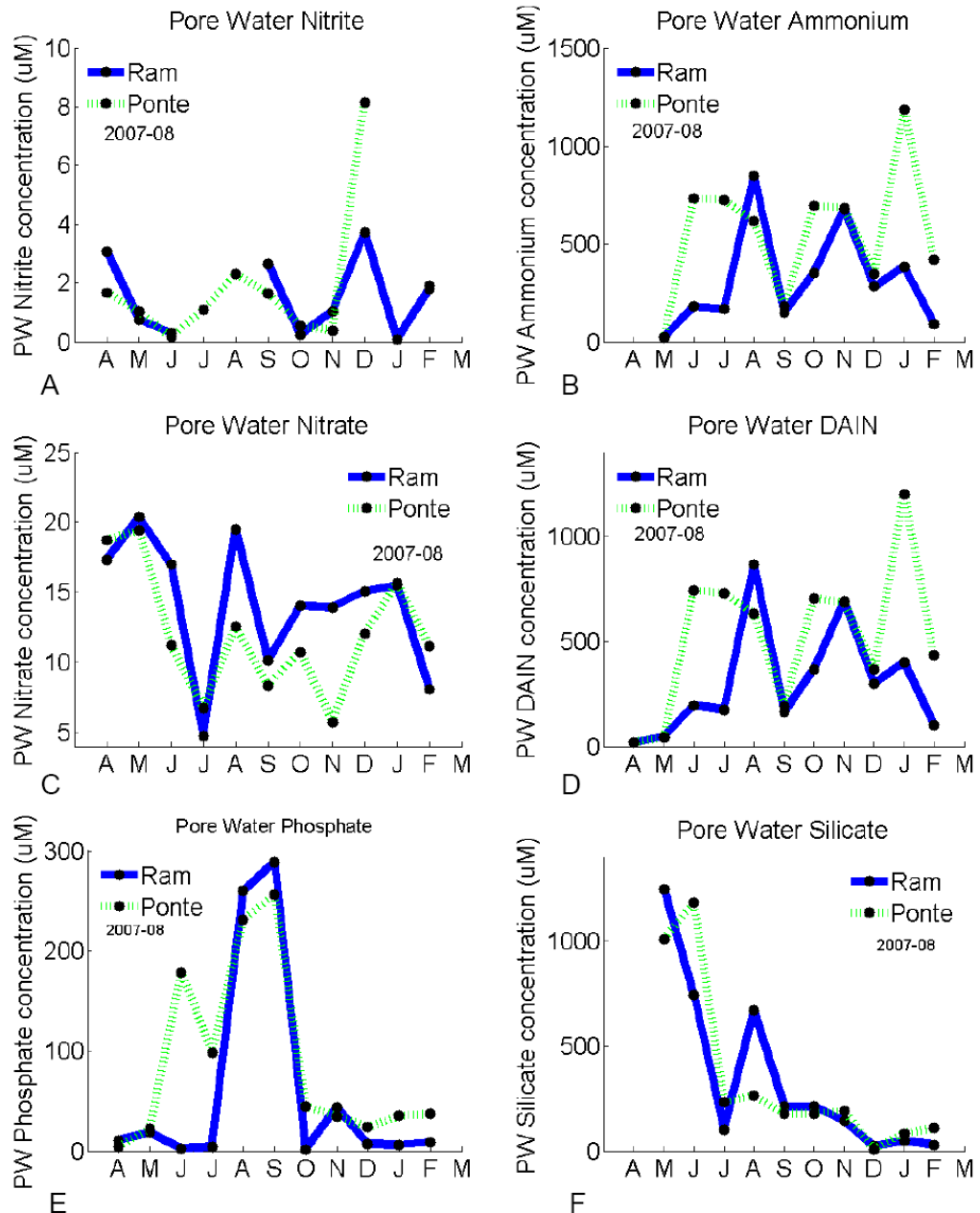


Figure 5.12 - Seasonal changes of nitrite ( $\mu\text{M}$ ; A), ammonium ( $\mu\text{M}$ ; B), nitrate ( $\mu\text{M}$ ; C), DAIN ( $\mu\text{M}$ ; D), phosphate ( $\mu\text{M}$ ; E) and silicate ( $\mu\text{M}$ ; F) in the pore water during 2007-08 at Ramalhete and Ponte.

### 5.3.4 Chlorophyll

During 2006, low concentrations of pelagic chlorophyll *a* were found during the summer (Figure 5.13-A). However, the same trend was not found in 2007. Actually, a slight and constant decrease in the concentrations was found after June until February 2008. The concentration peaks found in 2006 were much higher than the ones found in 2007-08. The 90 %ile of chlorophyll *a* found at Ponte and Beach in 2006 was below 5

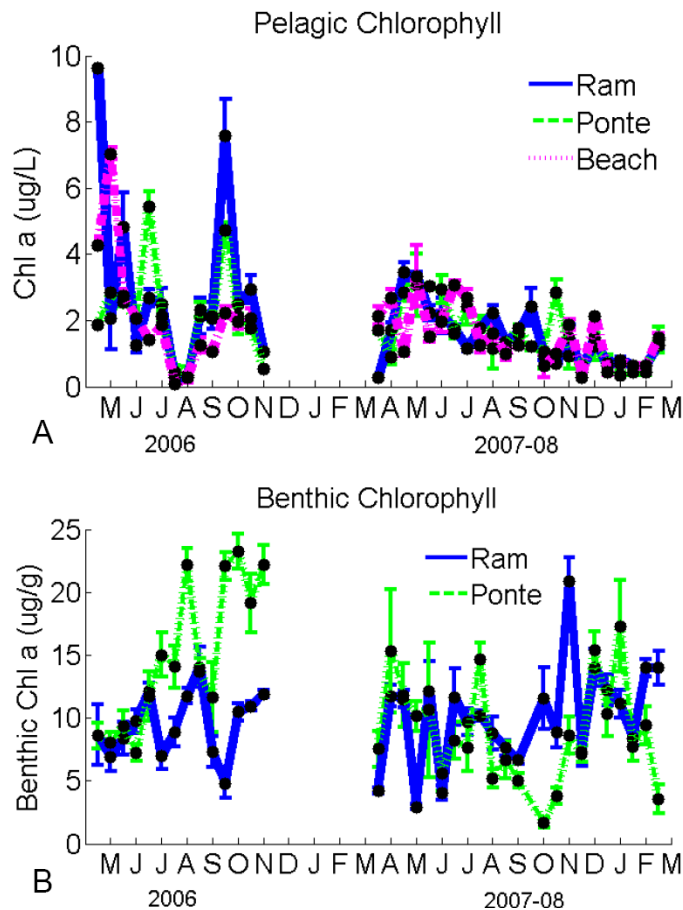


Figure 5.13 - Seasonal changes of pelagic chlorophyll *a* ( $\mu\text{g}\cdot\text{L}^{-1}$ ; A) and benthic chlorophyll ( $\mu\text{g}\cdot\text{g}^{-1}$ ; B) during 2006 and 2007-08 at Ramalhete, Ponte and Beach.

$\mu\text{g}/\text{L}$  and at Ramalhete was  $7.6 \mu\text{g}/\text{L}$ . In 2007, the 90%ile found at the three sites was below  $3 \mu\text{g}/\text{L}$ .

No clear pattern of variation can be pointed out for the benthic chlorophyll *a* content found in 2006 and 2007-08 (Figure 5.13-B). Large values were obtained during the summer of 2006 (from June to September) and after October of 2006, at Ponte. However, in 2007-08, Ramalhete showed the larger values, although similar to the values observed at Ponte. The smallest values were observed at Ponte during the autumn and late winter of 2007-08.

No significant Pearson's correlations were found ( $p > 0.05$ ) in 2006 and 2007-08 between the pelagic and benthic chlorophyll *a* concentrations for each site. In 2006, no significant correlations were found between pelagic and benthic chl *a* and the nitrite, nitrate, DAIN, phosphate and silica concentrations, except for a positive correlation between the nitrite concentration and pelagic chlorophyll *a* concentration for Ramalhete ( $p < 0.05$ ). In 2007, significant negative correlations were found between pelagic chl *a* and ammonium and DAIN in Ponte and Ramalhete ( $p < 0.05$ ). No significant

correlations were found between the benthic and pelagic chlorophyll and pore water nutrients ( $p > 0.05$ ) for the period 2007-08.

In addition, the total pelagic chlorophyll concentrations of the system at mid water were calculated by multiplying the concentration by the volume. Total benthic concentrations were also calculated, considering that sediment surface is approximately constituted by 50% of sandy sediments and 50% of muddy sediments (Serpa *et al.*, 2007). Concentrations of pelagic chlorophyll were converted to  $\text{mg}/\text{m}^2$  units in order to be easily comparable with MPB concentrations. Pelagic chlorophyll amounts of about 132 Kg (or  $2.49 \text{ mg}/\text{m}^2$ ) and benthic chlorophyll amounts of around 14250 Kg (or  $269 \text{ mg}/\text{m}^2$ ) were estimated for the whole lagoon, which indicates that pelagic chlorophyll is around 1% of the total chlorophyll existent in the lagoon.

### 5.3.5 Oxygen

Inside the lagoon, lower concentrations of Dissolved Oxygen were generally found during the summer and autumn (Figure 5.14). Ramalhete was the site where the lowest summer values were found, being almost  $4 \text{ mg}\cdot\text{l}^{-1}$  or between 60 and 80% of saturation. During the winter, larger values were found at Ramalhete. However, small values were also observed (55%). Ponte showed occasionally similar small values during the summer as well. The majority of saturation percentages at Ponte in 2007-08 were between 60 and 90%. The 10%ile at Ponte and Ramalhete during 2006 and 2007-08 was less than  $5 \text{ mg}\cdot\text{L}^{-1}$ . Supersaturation (100-130%) was observed during the winter of 2006 at both sites and at Ponte on summer and autumn. In 2007-08, supersaturation values were only observed at Beach.

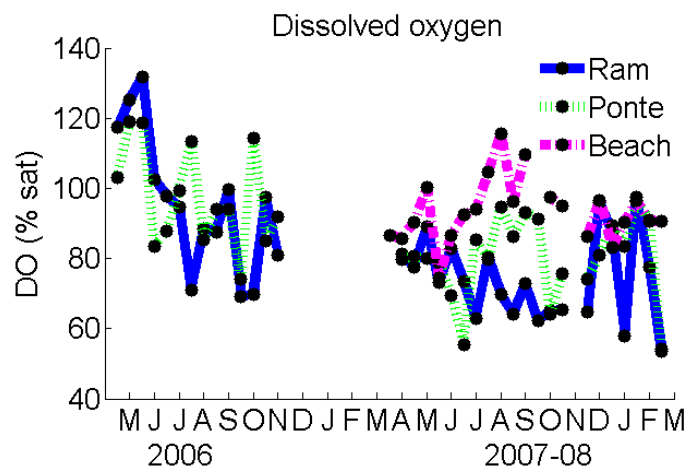


Figure 5.14 - Seasonal changes of Dissolved Oxygen (% saturation) during 2006 and 2007-08 at Ramalhete, Ponte and Beach.

Significant Pearson's correlations were found between the Dissolved Oxygen concentrations of Ponte and Ramalhete during 2006 ( $p < 0.05$ ) and 2007-08 ( $p < 0.005$ ). Significant correlations were also found between Ponte and Beach ( $p < 0.05$ ) but not between Ramalhete and Beach ( $p > 0.05$ ). As expected, significant negative Pearson's correlations were found between Temperature and Dissolved Oxygen in Ponte and Ramalhete ( $p < 0.05$ ).

### 5.3.6 ECASA Sampling Week

An increase of around 1°C in temperature seems to occur during the flood / HW at Ponte (Figure 5.15-A). At low water the temperature is lower. At Ramalhete the changes are similar but with some delay. The temperature is always lower at low water and the values are smaller at Ramalhete than at Ponte probably because of the greater heat loss in the inner channels. The largest values are found during the ebb period, just after the high water time. The changes from the highest to the lowest values are around 2°C.

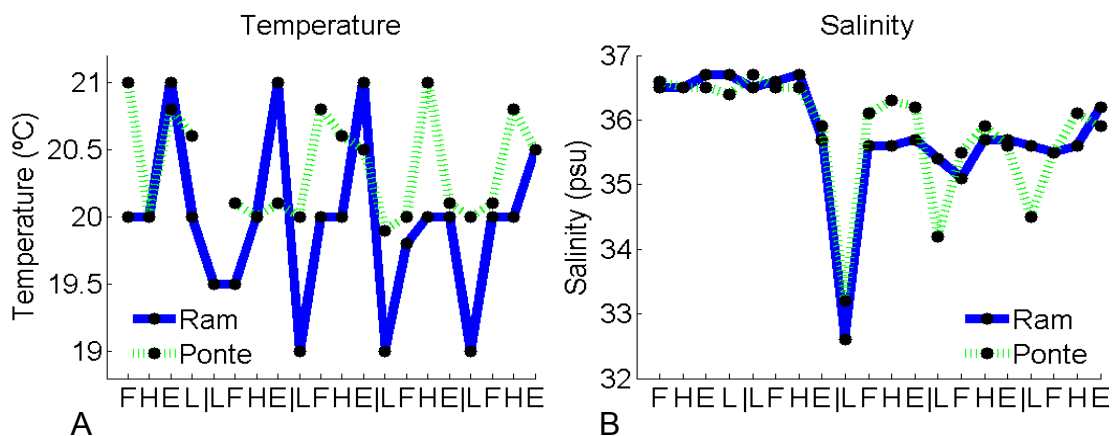


Figure 5.15 – Temperature (°C) and salinity (psu) values at Ramalhete and Ponte during the intensive campaign from 16<sup>th</sup> to 20<sup>th</sup> October 2006. Tidal conditions: Flood (F), High water (H), Ebb (E) and Low water (L).

The salinity was constant during the first days of sampling: 16<sup>th</sup> and 17<sup>th</sup> October (Figure 5.15-B). The lower value found on the 18<sup>th</sup> is due to a heavy rain that occurred during the night of the 17<sup>th</sup> and early in the morning of the 18<sup>th</sup>. During the following days some periods of rain occurred again. This is visible by the smaller changes in salinity at Ponte.

The larger values of nitrite were found during low water both at Ponte and Ramalhete. The concentrations at Ponte and Ramalhete are similar throughout the sampling period.

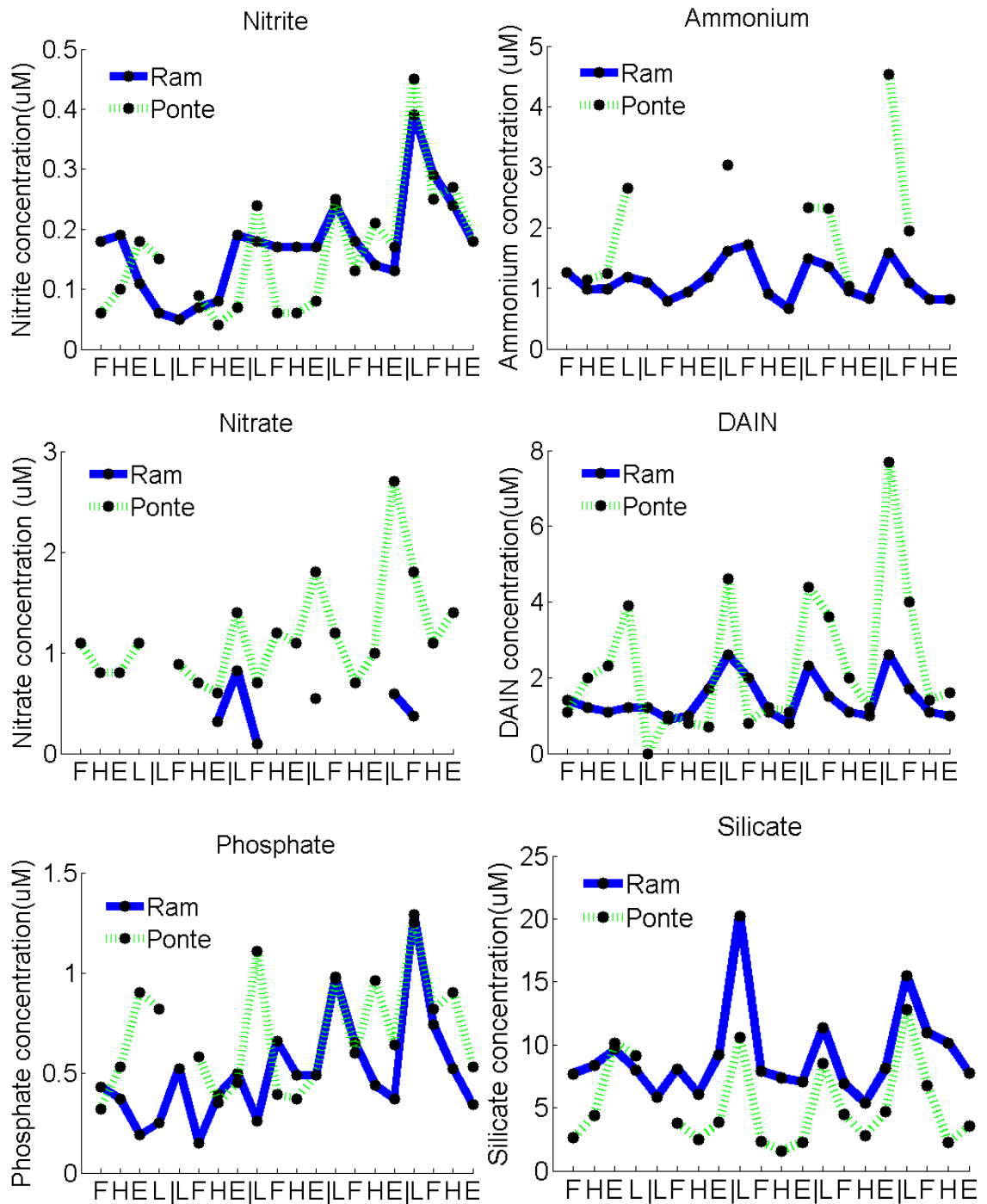


Figure 5.16 – Nitrite, Ammonium, Nitrate, DAIN, Phosphate and Silicate concentrations ( $\mu\text{M}$ ) at Ramalhete and Ponte during the intensive campaign from 16<sup>th</sup> to 20<sup>th</sup> of October 2006. Tidal conditions: Flood (F), High water (H), Ebb (E) and Low water (L).

Positive Pearson correlation was found between the two sites ( $p < 0.005$ ). The values of ammonium were larger during low water both at Ramalhete and Ponte (Figure 5.16). The largest values were found at Ponte. The nitrate values were larger at Ponte. Large values

were also found during low water at Ponte and Ramalhete. The values at Ramalhete were so low that most of them were below the quantification and detection limits of the analysis. The trend of DAIN concentrations shows clearly the trend of the nitrogen in the lagoon. Its concentration is larger during low water and the values at Ponte are larger than in Ramalhete. Positive correlation was also found between the concentrations found in both sites ( $p < 0.001$ ) Phosphate did not have any clear trend contrary to what was found for the other nutrients. The agreement between the phosphate values found at Ponte and at Ramalhete was not as good as found before (no correlation:  $p > 0.05$ ). Larger silicate concentrations were found during low water and at Ramalhete. A positive correlation between sites was also found for this component ( $p < 0.001$ ).

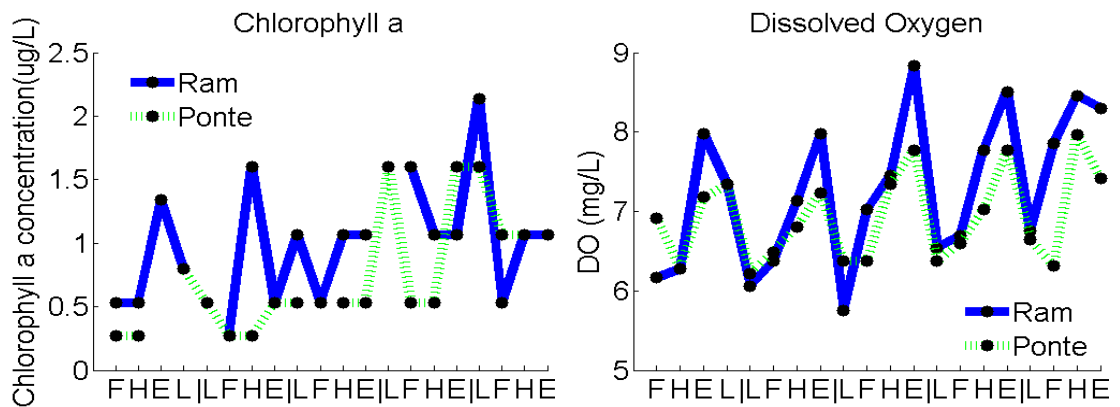


Figure 5.17 -Pelagic chlorophyll *a* concentrations ( $\mu\text{g/L}$ ) and Dissolved Oxygen ( $\text{mg.L}^{-1}$ ) at Ponte and Ramalhete during the intensive campaign from 16<sup>th</sup> to 20<sup>th</sup> October 2006. Tidal conditions: Flood (F), High water (H), Ebb (E) and Low water (L).

The values of pelagic chlorophyll found during this sampling period were between 0 and around  $2 \mu\text{g.L}^{-1}$ . There is no clear trend for concentrations at Ramalhete and it seems that Ponte had larger values during low water. No correlations were found between Ramalhete and Ponte and between the chlorophyll values of Ramalhete and nutrient concentrations ( $p > 0.05$ ). Positive correlations were found between the chl concentrations found in Ponte and nitrogen (DAIN and nitrite) concentrations ( $p < 0.01$ ).

The pattern of variation of the dissolved oxygen is similar both at Ponte and at Ramalhete. The smaller values were always found during low water, which was early in the morning every day. The differences between the smaller values and the largest were about  $2 \text{mg.L}^{-1}$  at Ponte and  $3 \text{mg.L}^{-1}$  at Ramalhete.

### 5.3.7 Statistical analyses

#### Temporal variation

Table 5.8 – Total variance of MPB and phytoplankton (as examples) and variance of the three main components (waves, within day and residuals). Temporal variability expressed as wave variance was decomposed in 1-3 waves variance and 4-26 waves variance.

	Components	Eqn.	SOS	df	$\sigma^2$	%	
<b>Microphytobenthos</b>	<b>Waves 1-26</b>	(1)	8.81	364			
	Waves 1-3	(2)		1.55	410	0.00378	5%
	Waves 4-26	(3)		7.26	371	0.01957	25%
	<b>Within-day</b>	(4)	17.81	381	0.04675	61%	
	<b>Residual</b>	(5)	2.22	328	0.00677	9%	
	(sum of $\sigma^2$ )					0.07686	100%
<b>Totals</b>	(6)	28.84	416	0.06931			
<b>Phytoplankton</b>	<b>Waves 1-23</b>	(1)	15.09	150			
	Waves 1-3	(2)		8.42	190	0.04432	31.15%
	Waves 4-23	(3)		6.67	157	0.04248	29.9%
	<b>Within-day</b>	(4)	5.944	161	0.0369	25.9%	
	<b>Residual</b>	(5)	2.117	114	0.01857	13.05%	
	(sum of $\sigma^2$ )					0.14227	100%
<b>Totals</b>	(6)	23.15	196	0.1181			

Considering that variance is  $\sigma^2 = \text{SOS}/\text{df}$ , equations for sum of squares (SOS) and degrees of freedom (df) are provided below:

- 1)  $SOS_{waves,M} = SOS_{total} - SOS_{residual,M}$   $df = K - 2M - 1$
- 2)  $SOS_{waves,3} = SOS_{total} - SOS_{residual,3}$   $df = K - 6 - 1$
- 3)  $SOS_{waves,4} = SOS_{waves,M} - SOS_{waves,3}$   $df = K - 2M_{M-3}$
- 4)  $SOS_{within-day} = \sum_{l=1}^{l=L} \sum_{i=1}^{i=I(l)} (Y_{l,i} - \bar{Y}_l)^2$   $df = K - L$
- $SOS_{residual,M} = \sum_{j=1}^{j=K} (Y_j - \hat{Y}_{j,M})^2$   $df = K - 2M - 1$
- 5)  $SOS_{residual} = SOS_{residual,M} - SOS_{within-day}$   $df = K - 2M - 1 - L$
- 6)  $SOS_{total} = \sum_j (Y_j - \bar{Y})^2$   $df = K - 1$

$\hat{Y}_{j,n}$  is the estimate of  $Y_j$  made with a Fourier series of n wave-pairs (up to a maximum of M).  $\bar{Y}$  is the grand mean estimated as described in Chapter 4  
 Subscript notation: sample j=1 to K, sample i=1 to I(l) on day l. l=1 to L days of sampling.



Fourier analysis revealed a complex and dynamic temporal pattern of the tested elements inside and outside the lagoon (Figure 5.18-A to D). The best fit for MPB was

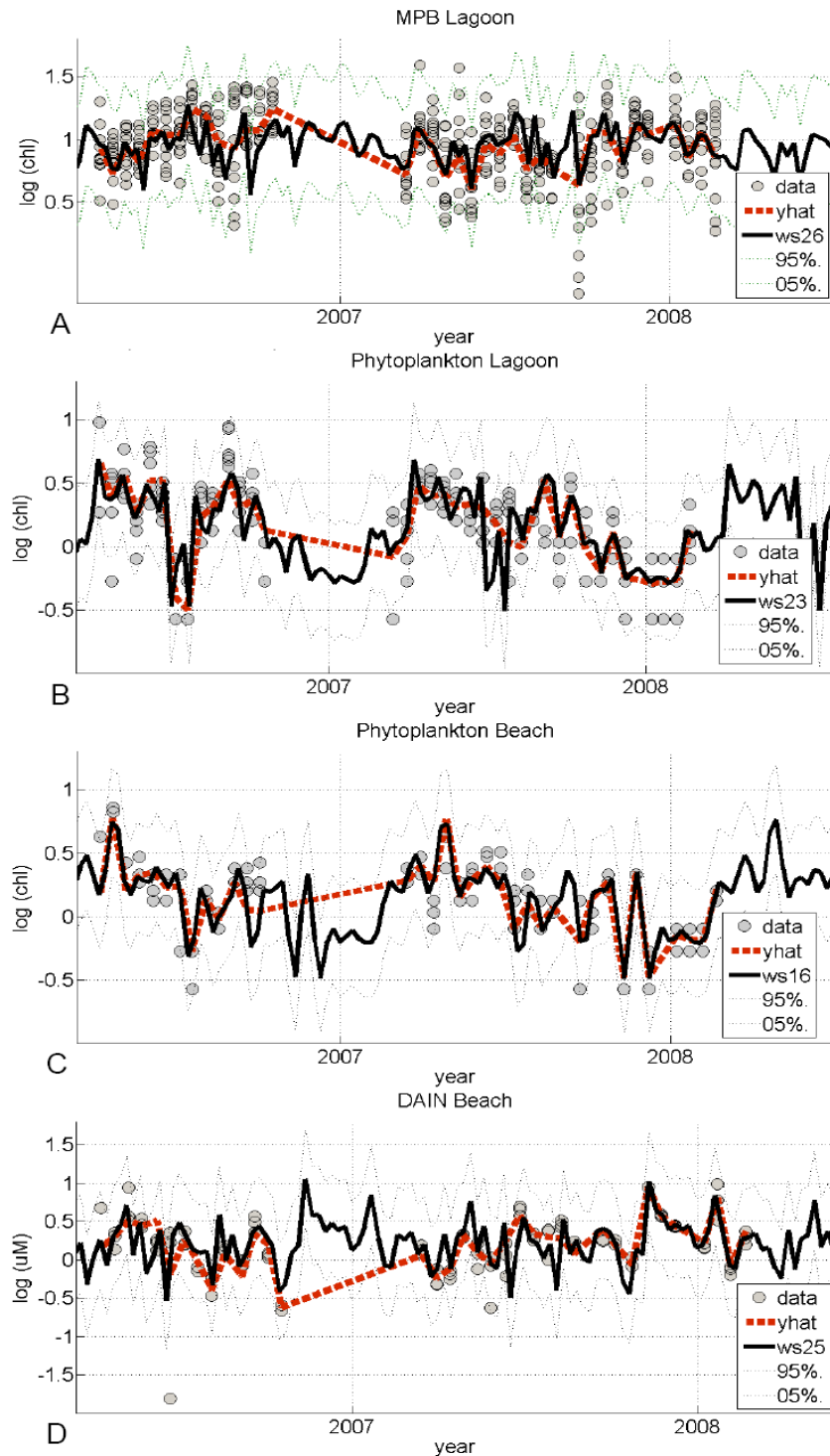


Figure 5.18 - Seasonal pattern obtained fitting sine and cosine wave-pairs according to the Fourier series approach to MPB data (A), phytoplankton data (B and C) and DAIN data (D). Transformed (log) data are presented with dots. The 5% and 95% confidence intervals are represented as dotted lines and dashed line (yhat) is the equivalent to the sum of 26 waves (ws26) but adjusted for a time step which is coincident to sampling date.

obtained considering the sum of 26 wave-pairs (sin and cosine). Fits are significant at a significance level of 0.05, which was used for all analyses ( $F=3.08$  (52,364df) using 26 waves and  $F=3.87$  (6,410df) using 3 waves). The seasonal cycle (1-3 waves) explained only 5% of the variability and the higher-frequency temporal variation explained 25% of the variation (4-26 waves; Table 5.8). Fitting 26 waves to MPB data means that variability is explained by waves with variation periods of 14 days. Within-day variability which includes spatial heterogeneity explained 61% of the variability.

The best fit for phytoplankton inside the lagoon was obtained using 23 wave-pairs. Temporal cycle, considering the seasonal (1-3 waves) and higher frequency temporal variation (4-23 waves) explained around 61% of the variability (Table 5.8). Fits were significant at the same significance level ( $F=6.10$ (46,150df) using 23 waves and  $F=18.10$ (6,190df) using 3 waves). Within-day variability explained around 26% of the variability. This approach was also applied to phytoplankton and DAIN data from outside the lagoon. In both cases, fits were significant and the residual error was high (40.5% for phytoplankton and 30.2% for DAIN) mainly because of the smaller number of samples involved. The temporal variation was responsible for around 50% of the variability for both. However, for phytoplankton the seasonal variation (1-3 waves) explained 22% of the variability and for DAIN just 4.5% of the variability. A linear regression was performed between the output of the Fourier analysis for MPB and phytoplankton and DAIN, inside the lagoon. A significant regression ( $p < 0.05$ ) was obtained between phytoplankton and MPB, explaining approximately 3.2% of the variability. No significant regression was obtained using DAIN ( $p > 0.05$ ).

### *Multiple regression*

Multiple regression approach revealed a significant relationship between phytoplankton and nitrite, temperature and oxygen at Ramalhete and between MPB and

Table 5.9 – Multiple regression of phytoplankton and microphytobenthos at Ramalhete, Ponte and Beach.

Note that all data, except temperature are  $\log(x)$  transformed.

		Equation	R <sup>2</sup>	p-value
<b>Ram</b>	Phyto	$Phyto = -1.64 + 0.681NO_2 + 0.0502Temp + 1.830O_2$	47.2	<b>0.001</b>
	MPB	$MPB = 0.866 + 0.307NH_{4, sed} + 0.283Si_{sed}$	82.8	<b>0.002</b>
<b>Ponte</b>	Phyto	$Phyto = 0.788 - 0.649MPB$	12.4	<b>0.035</b>
	MPB	$MPB = -0.301 + 0.0192Temp + 1.19O_2$	11.8	0.054
<b>Beach</b>	Phyto	No significant regression found	-	-

ammonium and silicate in pore water (Table 5.9). The most important components were dissolved oxygen for phytoplankton, explaining 18.2% of the variability and pore water silicate, explaining 43.6% of the variability. At Ponte a significant relationship was only found between phytoplankton and microphytobenthos, although explaining just 12.4% of the variability. No significant relationships were found at Beach. Data are  $\log(x)$  transformed except for temperature.

### Canonical Correspondence analysis

The CCA revealed four significant environmental variables (salinity, silicate, ammonium and diffuse attenuation coefficient ( $K_d$ )) involved in the measurements of phytoplankton and microphytobenthos at Ramalhete, Ponte and Beach (Figure 5.19). Salinity was the most important variable, explaining 12% of the 19% of variability explained by the canonical axes. Data are divided by site and also month of year and are  $\log(x)$  transformed, except salinity and  $K_d$ . A clear separation between data collected at Beach during 2006 and 2007-08 is observed. Moreover, all samples collected at Ponte and Ramalhete are plotted together and separated from all samples collected at Beach.

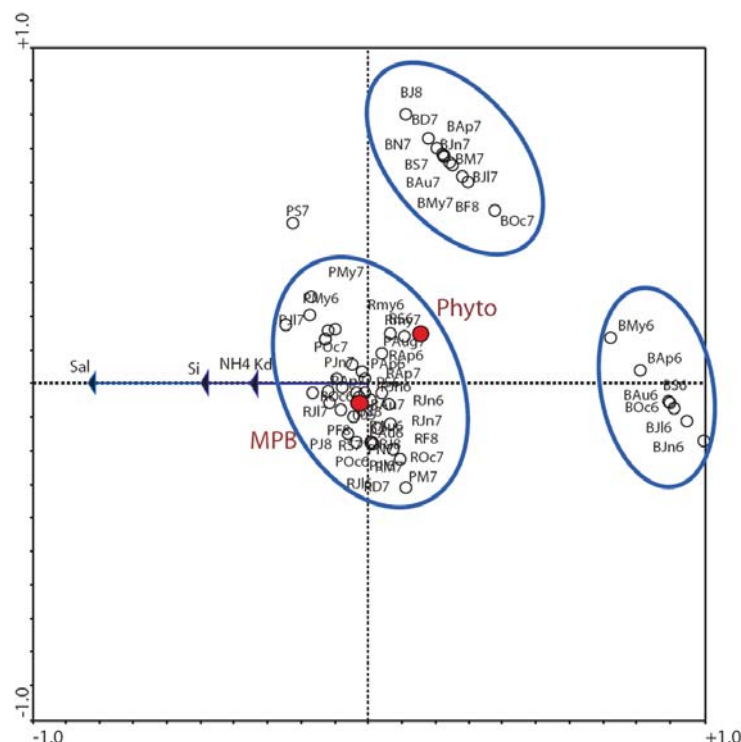


Figure 5.19 – Canonical correspondence Analysis (CCA) plot obtained using four significant environmental components (salinity, silicate, ammonium and  $k_d$  coefficient) and two variables (phytoplankton and microphytobenthos) at three sites (Ramalhete, Ponte and Beach).

The Monte Carlo tests indicated the significance of the analysis,  $p$ -value = 0.005. Considering the first two axes, the cumulative percentage of variance of phytoplankton and microphytobenthos was 54.4%.

## **5.4 Discussion**

### **5.4.1 Temperature and salinity**

The salinity values presented in this study confirm the inclusion of Ria Formosa in the category of coastal water, according to the Water Framework Directive (C.E.C., 2000). The influence of freshwater is not dominant in this system, as discussed previously by Newton and Mudge (2003), Newton *et al.* (2003) and Loureiro *et al.* (2006). Salinity is closely related to temperature inside Ria Formosa. Typically, salinity is higher during the warm summer due to evaporation and lower in the cooler winter due to freshwater inputs from rainfall and runoff (Loureiro *et al.*, 2006). Our results show clearly how the rainfall can affect salinity. During the winter of 2007-08 lower salinity values, when compared with outside, were found after rainfall episodes. Temperature follows the same pattern with large values during the summer and smaller during the winter. It is of interest to highlight that freshwater inputs do not seem to affect the temperature of the lagoon. Probably, because the solar heating of water and sediments is stronger in the summer.

The salinity profiles showed no stratification at Ponte. Slight decreases were found especially in Profile 1. The difference was of about 0.075 psu. This decrease was caused by the entrance of less saline seawater in the lagoon. The range of variation was very high for each depth which indicates the mixing of the water column. Regarding the temperature profiles, the differences found were larger. The decrease of temperatures in Profile 1 was of about 1°C due to the entrance of cold water from outside. This difference in three meters of depth is not sufficient to have stratification, i.e. a thermocline. Goela (2005) indicated no stratification in the lagoon and Newton and Mudge (2003) also found weak or no thermal stratification.

### **5.4.2 PAR Diffuse Attenuation coefficient**

The variation found in the  $K_d$  values observed with the single planar light sensor, represent the temporal variation in the lagoon. High values are a consequence of the higher concentrations of particles (such as chlorophyll and suspended particular matter, for example) in the water column (Bowers *et al.*, 2000; Branco and Kremer, 2005; Bowers and Binding, 2006; Devlin *et al.*, 2008) or a different balance of particles. It is likely that the most important component for light attenuation varies throughout the year in Ria Formosa. SPM is influenced by atmospheric conditions, as winds will affect the re-suspension of sediments, as well as by the rainfall events, that will increase the run-off (Kostoglidis *et al.*, 2005; Obrador and Pretus, 2008). Chlorophyll is mainly affected by nutrient concentrations and light availability. The lagoon is characterized by complex dynamics, involving all its components. The fact that Ponte shows a higher mean  $K_d$  than Ramalhete might express the higher influence of currents and run-off at this site, which is a main channel, compared with Ramalhete.

Profiles recorded at Ponte and Ramalhete, clearly express differences of light attenuation between low and high water. A shallow region of restricted exchange, as Ria Formosa, is expected to have higher concentrations of suspended particles due to the run-off and re-suspension of sediments than the open ocean (Obrador and Pretus, 2008). Therefore, a decrease of light attenuation is expected during the flood and high water periods due to the dilution in clear water (Lund-Hansen, 2004; Devlin *et al.*, 2008).

The increase of 0.15 in  $K_d$  was very interesting. The shallowness of the system means that a significant part of the incident light will reach the bottom and be reflected (Ackleson, 2003). Bottom reflection is therefore an important phenomenon that should be taken in account when studying shallow waters. Reflected light will be available again for phytoplankton and turns the water clearer. The two-bulb light sensor was spherical and because of that it would also record the reflected light from the sea-bed. The influence of the reflected light in the flat sensor (single planar light sensor) should be smaller because the sensor was only recording light reaching from above. This essential change may explain the differences observed between  $K_d$  values obtained with the flat and spherical sensors. Our two-bulb light sensor provides more accurate  $K_d$  values due to the fact that PAR measurements are collected at the same time. It also represents well the available light in the water column. Nevertheless, if the main aim of an investigation is to study the light attenuation due to particle concentrations, a correction for bottom reflection should be used or the flat sensor should be considered.

### 5.4.3 Nutrients in the water column and sediments

In 2006, two clear peaks of DAIN were found in spring and in autumn. The first peak was caused by high ammonium concentrations (5  $\mu\text{M}$ ) at Ramalhete and Ponte and the second was caused by high nitrate concentrations (4  $\mu\text{M}$ ) in Ponte. These peaks are likely to be a consequence of the runoff from the surrounding areas, as confirmed by the small values of salinity. In 2007-08 several DAIN peaks were observed throughout the year at Beach (caused by nitrate and ammonium) and Ponte (caused again by ammonium). The ammonium peak observed in January was also found at Beach (6  $\mu\text{M}$ ) and Ponte (5  $\mu\text{M}$ ). In this case, the source of ammonium seems to be the seawater and not runoff. The nitrite, nitrate, ammonium and therefore DAIN concentrations are apparently very similar to each other during 2006 and 2007-08, except when peaks are observed. The phosphate concentrations in 2006 and 2007-08 seem to be slightly larger in the summer. An increase in the concentration was expected due to the larger use of detergents by the increased population during this period. Ramalhete also shows high values of phosphate, probably because of its location, near to the water treatment plant, which only has secondary treatment. Silicate concentrations found during both sampling periods were relatively large, compared to the other nutrients. They are clearly larger in Ponte, probably because of the greater influence of freshwater input on this site, compared with Ramalhete that is an inner channel.

These results are not totally in agreement with previous work. Newton *et al.* (2003) showed much larger values of DAIN concentration in the western part of the lagoon, where our study was focused (see Table 5.10). Newton and Mudge (2005) also obtained larger values of nitrate concentrations, much larger than the ones obtained in the present study. The same authors also found silicate measurements at some sites which were 10 times larger. However, data used in both studies were collected in late 80's, prior to the opening of the artificial inlet in the west part of the lagoon, which caused an important change to the water exchange in this part of the lagoon. Despite the proximity to towns, the source of these large concentrations was attributed to runoff (Newton and Mudge, 2005). Loureiro *et al.* (2006) found slightly larger nitrate values, however much more similar to the values reported here. Loureiro's work was carried out under the same conditions existent today, i.e., after the inlet opening. Much has been discussed in the literature about the export or import character of the lagoon for nutrients (e.g. Newton *et al.*, 2003, Newton and Mudge, 2005). Except for silicate, the similar values obtained for

the different sites, Ramalhete, Ponte and Beach do not allow a clear assessment of possible relationships and evaluation of sources, given the distinctness of the sites. Silicate concentrations are clearly and consistently larger inside the lagoon in 2006 and 2007-08. Therefore, the lagoon may be considered as exporting this nutrient. Occasional exports / imports of nitrogen compounds also take place whenever there is a peak in the concentrations, but it is not persistent. The nitrate peaks found in Beach during 2007 were probably caused by natural upwelling events. The lagoon also seems to be exporting phosphate to outside. The unexpected small values of nitrate and DAIN are also of great interest. They could be a result of a larger demand from an increased biomass of algae or could also be due to the improvement of the water quality by the decrease of nitrogen inputs in the lagoon or the increase of seawater exchange stimulated by the new inlet.

One of the elements considered in the WFD to assess the ecological quality is the ‘nutrient condition’, which should not only include the concentrations but also ratios between nutrients. The N:P ratio values obtained are mostly below the Redfield ratio inside the lagoon, which may indicate a nitrogen limitation in this system. Although the use of this ratio to evaluate the limiting nutrient is still a subject of great discussion, especially in presence of large concentrations, this can be a useful indicator (Falcão, 1996; EEA, 1999; Newton *et al.*, 2003; Neill, 2005; Kim *et al.*, 2007). Nitrogen limitation is also supported by previous experimental studies such as Edwards *et al.* (2005) and Loureiro *et al.* (2005, 2008). The N : Si ratio, which can be very important for organisms with silicate requirements such as diatoms, reflects clearly the large and available concentrations of silicate inside the lagoon compared with nitrogen. Outside the lagoon, the ratio can have high values, which may be expressed as a silicate limitation during upwelling events. This can influence the algal species composition and balance.

The concentrations of all nutrients studied here were significantly larger in the pore water than in the water column (Table 5.10). These results have been largely reported in the literature for coastal systems in general, but also for Ria Formosa (Lerat *et al.*, 1990; Forja *et al.*, 1994; Falcão, 1996; Murray *et al.*, 2006; Serpa *et al.*, 2007; Wayland *et al.*, 2008). The larger concentrations observed in the sediments suggest that the production is faster than the release to the water column, which can happen by molecular diffusion, tide influence or bioturbation, for example (Di Toro, 2001; Falcão, 1996; Murray *et al.*, 2006). Falcão (1996) and Serpa *et al.* (2007) observed larger values of ammonium

during the summer in Ria Formosa. Our results agree with this pattern but these high values were sustained after summer. The increase of ammonium in the summer is mainly due to the increase of the microbial process, which is temperature dependent (Falcão, 1996; Gönenç and Wolflin, 2005). The large concentrations observed may therefore be a consequence of the high temperatures after the summer in Portugal. The

Table 5.10 – Mean nutrient concentrations and nutrient fluxes obtained in several studies at Ria Formosa.

	Source	NO <sub>2</sub> <sup>-</sup>	NO <sub>3</sub> <sup>-</sup>	NH <sub>4</sub> <sup>+</sup>	PO <sub>4</sub> <sup>3-</sup>	SiO <sub>2</sub>	Units	N:P	Months
Water Column	Newton <i>et al.</i> (2003)		20.0		0.7	40	µM	> 16	June 87 – May 88
	Loureiro <i>et al.</i> (2006)	0.13	4.1	1.15	0.49	4.0	µM	12.0	June 01 - July 02
	Present study	0.19	0.72	1.27	0.54	6.58	µM	6.4	April 06 – March 08
Pore Water	Falcão (1996)*	-	15	100	10	150	µM	-	May 93 – March 94
	Murray <i>et al.</i> (2006)*	2	50	400	100	-	µM	≈ 4.5	June – August 04
	Serpa <i>et al.</i> (2007)*		35	155	25	-	µM	≈ 7.6	March – December
	Present study	1.47	13.02	437.9	73.5	343.8	µM	≈ 6	March 07 – March 08
Fluxes Sediment-Water column	Serpa <i>et al.</i> (2007)	-		41.6	2.9	-	µmol. m <sup>-2</sup> .h <sup>-1</sup>		July – September
	Murray <i>et al.</i> (2006)		412		≈ 50	-	µmol. m <sup>-2</sup> .h <sup>-1</sup>		August 04
	Present study		497		37.4		µmol. m <sup>-2</sup> .h <sup>-1</sup>		March 07 – March 08

\* - Concentrations found in muddy samples

concentrations of the nitrogen compounds found were larger than the ones found by Falcão (1996) and similar to the concentrations found by Murray *et al.* (2006), except for ammonium, which are slightly larger. The larger phosphate concentrations found in the summer were also reported by Falcão (1996) although in a smaller magnitude. The phosphate is accumulated during the winter and released in the summer, affected by anoxia. Temperature is also a factor that affects the release of silicate, so larger concentrations are normally observed in the summer, as reported by Falcão (1996). The results here reported show larger concentrations in late spring and summer in accordance with what was previously discussed, except at Ramalhete in June/July. The large pore water nutrient concentrations result in a need to quantify the molecular diffusion to evaluate the role of sediments in water column quality (Table 5.10). Falcão (1996) and Murray *et al.* (2006) used the Fick law of diffusion to calculate the molecular diffusion. The largest value for ammonium obtained by Falcão (1996) was



97.5  $\mu\text{mol.m}^{-2}.\text{h}^{-1}$ . Murray *et al.* (2006) obtained a maximum that was almost ten times larger, 821  $\mu\text{mol.m}^{-2}.\text{h}^{-1}$ . For nitrate+nitrite, Falcão (1996) found the maximum value of 45.25  $\mu\text{mol.m}^{-2}.\text{h}^{-1}$ , while Murray *et al.* (2006) found a maximum of 170  $\mu\text{mol.m}^{-2}.\text{h}^{-1}$  just for nitrate. Our results (means) are very similar with results obtained by Murray *et al.* (2006) and confirm the importance of these fluxes to the lagoon system. For phosphate, the maximum obtained by Murray *et al.* (2006) was 123  $\mu\text{mol.m}^{-2}.\text{h}^{-1}$  and the range was from 10  $\mu\text{mol.m}^{-2}.\text{h}^{-1}$ . Falcão (1996) observed a maximum of 35.5  $\mu\text{mol.m}^{-2}.\text{h}^{-1}$ . Once more, our results were similar to Murray *et al.* (2006), as stated in Table 5.10. For silicate the maximum obtained by Falcão (1996) was 162.60  $\mu\text{mol.m}^{-2}.\text{h}^{-1}$ . These values give clear indication of the importance of sediments, when compared with the measured concentrations. Falcão (1996) also estimate the total balance of nutrients in Ria Formosa and showed how the water-sediment exchange is the principal component.

#### 5.4.5 Pelagic and Benthic Chlorophyll

The pelagic chlorophyll *a* concentrations observed in Ria Formosa are within the range found previously by Falcão (1996), Falcão and Vale (2003) and Newton *et al.* (2003). These values are actually smaller than the concentrations found in other European RREs (Tett *et al.*, 2003). However, during 2006, occasional peaks were observed in spring and late summer. In both sampling periods, the concentrations were smaller in the winter, when the radiation decreases. In the summer of 2006, a strong decrease was observed, which may be related with an increase in the grazing pressure (Alpine and Cloern, 1992; Loureiro *et al.*, 2006). The non-existence of any positive strong correlation with nutrients in the water column indicates that several processes may affect the chl *a*, such as the re-suspension of benthic algae.

The range of variation of benthic chlorophyll was approximately within the range reported for Ria Formosa (Amorim-Ferreira, 1987) and for other sites (Hedtkamp, 2005 and Riaux-Gobin and Bourgoïn, 2002). Contents of chlorophyll *a* seem to be larger now than in 1987 (Amorim-Ferreira, 1987). This increase is in agreement and may be supported by the larger pore water concentrations (Facca and Sfriso, 2007) in comparison with the ones found in the past (Falcão, 1996), especially for ammonium which is preferentially taken up by microphytobenthos.

The estimates of the pelagic chlorophyll percentage of the total chlorophyll in the system, presented here, confirm the importance of the benthic microalgae for the uptake of nutrients and as a source of chlorophyll to the water column by re-suspension. Moreover, shellfish grazing may be responsible for such low concentrations of pelagic chlorophyll. Sobral (1995) presented clearance rates for the clam *Ruditapes decussata* of  $0.7 \text{ L.h}^{-1}.\text{ind}^{-1}$ , which represents around 90% of the shellfish production in the lagoon. Clearance rates correspond to a specific water volume that shellfish are able to clear in a certain period of time. Falcão and Vale (1990) reported a standard density of  $90 \text{ ind.m}^{-2}$ . Considering the total biomass of the lagoon, it was estimated that clams are responsible for the loss of 90% of the phytoplankton biomass in one single day.

#### **5.4.6 Dissolved Oxygen**

The warmer periods are critical for Dissolved Oxygen, because it decreases with increased values of temperature. Moreover, the oxygen saturation percentages are extremely important to express oxygen availability in this temperature and salinity variable system. In general terms, the observed saturation percentages confirmed the conclusions obtained from the dissolved oxygen concentrations. As expected, the lower values were obtained in the summer period both in 2006 and 2007-08. The critical DO value is variable for different organisms, but generally  $5 \text{ mg.l}^{-1}$  is considered critical (biological stress) for most vertebrates (Bricker *et al.*, 2003). Especially in 2007-08, the smallest values were obtained at Ramalhete ( $4\text{-}5 \text{ mg.l}^{-1}$  and 60-80% of oxygen saturation) and the largest at Beach ( $6\text{-}8 \text{ mg.l}^{-1}$  and 80-120% of oxygen saturation). At Ramalhete most of the values were under the critical value after May (below  $5 \text{ mg.l}^{-1}$  and 80% of oxygen saturation). These extremely low values are in agreement with Mudge *et al.* (2007) but not with Falcão (1996) and Falcão and Vale (2003). The divergence may be due to the time of sampling. Both our results and those of Mudge *et al.* (2007) were obtained early in the morning, when the oxygen levels are lower due to respiration and oxidation overnight (Mudge *et al.*, 2007). Newton and Mudge (2005) also presented lower percentages of oxygen saturation during low water. In addition to being affected by the smaller exchange rate, the water in the inner channel Ramalhete may also be influenced by the oxygen consuming effluents (Mudge *et al.*, 2007).

### 5.4.7 ECASA Intensive Sampling Week

The intensive sampling week in Ria Formosa had the objective of studying the short-time changes during a complete tidal cycle. The variations of temperature showed a constant pattern, with high values during flood / high water at Ponte and during the ebb at Ramalhete. This suggests that the water in the sea was a little warmer than inside the lagoon during this period. Newton and Mudge (2003) also found warmer temperatures during high water, especially in the main channels of the lagoon. The salinity measurements showed clearly the intense rain that occurred on the 17<sup>th</sup> / 18<sup>th</sup> October and following days. The direct and indirect freshwater input caused by rain has a significant effect in the conditions inside Ria Formosa. In case of several days with intense rain, it may be a stress factor for life in the lagoon. These events also contribute to consolidate the idea of the low influence of freshwater to the lagoon, as discussed before and by Loureiro *et al.* (2006), Newton *et al.* (2003) and Newton and Mudge (2003).

The ammonium concentrations were larger during low tide and apparently were not affected by the intense rain. Nitrate and nitrite showed larger concentrations during low tide and were probably affected by the rain, since from the 18<sup>th</sup> until the end of the sampling period the concentrations increased. As discussed above, the nitrogen compounds are mainly added to the lagoon by runoff. The fact that DAIN concentrations were larger during low water gives an extra indication that the lagoon may be exporting nutrients and is in agreement with Falcão (1996) and Newton *et al.* (2003).

Silicates showed a large increase on the 18<sup>th</sup> October, just after the more intense episode of rain, which suggests that the silicate concentration is affected by runoff. Moreover, it is clear that Ria Formosa is exporting silicate, because its concentration value is much larger during low water and small during high water, which was discussed above and also verified by Goela (2005). For phosphate slight increases in the concentrations were found after 18<sup>th</sup> at Ramalhete, however, it is not clear enough to suppose its origin. At Ponte there were not any clear differences.

The concentration of pelagic chlorophyll was relatively constant during the sampling period. However, a slight pattern showing large values during low water seems to indicate that seawater has smaller chlorophyll a concentrations than inside the lagoon. Chlorophyll a concentrations at Ponte and Ramalhete showed strong correlations with

DAIN concentrations. This could be an indirect indication that nitrogen is the limiting compound in Ria Formosa and reinforce the ideas discussed above and by Edwards *et al.* (2005) and Loureiro *et al.* (2005). The measurements of dissolved oxygen showed the pattern of low values in early morning during low water, as indicated by previous studies (Oliveira, 2005). The range of variation is similar with the results obtained throughout the year of 2006 and 2007-08.

#### **5.4.8 Temporal variation**

This approach was developed to investigate the influence of seasonality in a highly variable component, microphytobenthos, as discussed in Chapter 4. Given the usefulness of this analysis it was applied to other elements. The Fourier series revealed that the seasonal variation (1-3 waves) only explained 5% of the MPB variability in MPB and that most of it was explained by the spatial heterogeneity (61%). This shows almost a non existence of direct influence of astronomical elements such as the irradiance cycle, which has a standard variation of a 1 sine and cosine wave-pair per year. Fortnightly tidal cycles, which have a variation of 14 days, and wind effect, are indicated by the literature to have a strong effect in MPB dynamics (Chapter 4). Not surprisingly, phytoplankton has a stronger influence of the seasonal variation (1-3 waves; 31%) when compared with MPB. Spatial heterogeneity is also smaller as phytoplankton tends to mix in the water column. An interesting point is the high percentage (30%) of variability explained by the higher frequency temporal variation (4 to 23 waves). This may indicate that MPB is affecting chl a concentrations in the water column, as suggested by Lucas *et al.* (2001) and de Jonge and van Beusekom (1995), for example. Re-suspension of benthic algal cells, which are present in high concentrations, would have an important impact on phytoplankton measurements especially in shallow waters. This is also supported by the linear regression performed using the output of the Fourier analysis, which showed a significant relationship between phytoplankton and microphytobenthos.

Outside the lagoon, there is no direct influence of MPB on phytoplankton. However, measurements may also be affected by the chlorophyll export from the lagoon. Therefore, the effect of the high-frequency variation is expected to be attenuated. It is indeed observed that the best fit was obtained using just 16 waves, which is less than for phytoplankton inside the lagoon. The Fourier analysis was also conducted with DAIN

values at Beach to show that the higher-frequency temporal variation of phytoplankton is being affected by elements other than DAIN concentrations, which revealed a variation with higher-frequency. Moreover, the influence of the seasonal variation (1-3 waves) is very small (4.5%) as expected.

#### **5.4.9 Multiple regression**

The strong relationship between microphytobenthos and two nutrients (ammonium and silicate) of the pore water provides another indication of the factors that are driving MPB biomass. Besides not being directly affected by the irradiance cycle or not without considering other factors, MPB is strongly influenced and can be predicted by nitrogen and silicate within sediments. This result is extremely important since it represents about 83% of the total variability explained. In fact, a strong relationship between benthic chlorophyll and pore water nutrients was previously indicated and discussed by Facca and Sfriso (2007) for Venice lagoon. The great importance of nutrients in supporting the benthic microalgae biomass should be further investigated in the future.

The prediction of phytoplankton from MPB biomass is also very interesting. Although representing a small percentage of the variability, this supports the result of the Fourier analysis and suggests again the importance of the re-suspension of benthic algal cells for the total chlorophyll in the water column.

#### **5.4.10 Canonical correspondence analysis**

The CCA analysis expressed relationships between all three sites and the associated environment variables used to express differences and similarities. The multiple regression focused on the relationships found at each site. CCA pooled the whole dataset and extracts the information. The CCA plot revealed that the phytoplankton and microphytobenthos measurements at Ponte and Ramalhete during 2006 and 2007-08 and at Beach during 2007-08 were approximately equally influenced by salinity (the most important environmental variable), silicate, ammonium and  $k_d$ . The difference between samples at Beach in 2006 was larger. Samples collected at Beach are separated from Ponte and Ramalhete mainly because of microphytobenthos, which was assessed only in the last two sites. Unfortunately, the dataset obtained during this study did not

allow a more informative analysis due to the fact that we are only dealing with two biological variables and therefore all the environmental variables are within the x-axis.

#### **5.4.11 Assessment of the quality status of Ria Formosa**

The assessment of the quality status of this lagoon system, in terms of nutrients, followed the EEA (1999) and the OSPAR (2005) classifications (Table 5.1). This was an attempt at clarifying the system given that no nutrient background concentrations or thresholds exist at the moment for Ria Formosa. Harmonized methodologies at the EU level should be followed in the future and the role of nutrients in the assessment of the ecological status has to be clarified. Moreover, mathematical models should be optimised and used as important tools to establish reference conditions. Using EEA standards also allows a comparison with the nutrient status found in previous papers. According to our results the quality status of Nitrate+Nitrite was never worse than 'Fair' in 2006 and 2007-08 (following EEA, 1999). In fact, in 2006 it was always classified as 'Good'. This represents an improvement on water quality, compared with the results of Newton *et al.* (2003). In 2006 the quality status based on phosphate was most of the time 'Fair' or 'Poor'. However in 2007-08 it was most of the time 'Good' or 'Fair', which was the same as described by Newton *et al.* (2003). Following the OSPAR classification (OSPAR, 2005), DAIN concentrations are 'below elevated level' and phosphate concentrations are 'above elevated level'.

Following the criteria provided by the Commission Decision 2008/915/EC, Ria Formosa had high ecological quality in 2006 and 2007, except at Ramalhete in 2006, when the phytoplankton element indicated that it was within the high to good boundary (EC, 2008). Under OSPAR procedure (OSPAR, 2005), the chlorophyll measurements in the lagoon were 'below elevated concentrations'.

The overall classification of Ria Formosa following the OSPAR procedure would seem to be a 'Potential Problem Area' in terms of eutrophication. The phosphate concentrations are above the threshold and oxygen levels indicate oxygen deficiency in the lagoon. However, since the limiting element is considered to be nitrogen, the elevated concentrations of phosphate may not have a significant expression in the eutrophication process. It is not clear that the oxygen deficiency is a result of nutrient-stimulated production in the Ria Formosa.

It is now expected that the assessment of the ecological quality would rely on the investigation of the structure and functioning of an ecosystem, as indicated by the Habitat and Species Directive, the OSPAR convention, the Water Framework Directive and more recently the EU Marine Strategy (de Jonge *et al.*, 2006). Much has been made on the structure, however the evaluation of the ecosystem functioning has still much to progress.

#### **5.4.12 Implications within the WFD**

The first problematic issue to be addressed here is related to the definition of surface water categories within the WFD, especially the transitional and coastal waters (CEC, 2000). Transitional waters are defined in the WFD as ‘bodies of surface waters in the vicinity of river mouths which are partially saline in character as a result of their proximity to coastal waters but which are substantially influenced by freshwater’ (CEC, 2000). Coastal waters are then defined as ‘surface water on the landward side of the line, every point of which is at a distance of one nautical mile on the seaward side from the nearest point of the baseline from which the breadth of territorial waters is measured, extending where appropriate up to the outer limit of transitional waters’ (CEC, 2000). Salinity and morphology are the obvious criteria used for these definitions. Several European countries have classified their coastal lagoons as transitional waters due to the important freshwater input and due to the fact that they are not open coastal waters (e.g. Spain and Italy; Basset *et al.*, 2006). As already discussed by McLusky and Elliott (2007), there are some unclear situations, such as the Baltic Sea, which has brackish waters and still is considered within the coastal waters typology and some coastal lagoons such as Ria Formosa, which are clearly not open coastal waters but at the same time not measurably influenced by freshwater inputs and still are considered within the coastal waters typology. The distinction between the different categories should be ecologically relevant. Following the salinity criterion Ria Formosa is correctly classified. However, being within the coastal waters category means that no monitoring of fish communities is needed. The high ecological importance of the lagoon as a nursery system for fish communities (Santos and Monteiro, 1997) is therefore not considered.

Secondly, it is important to discuss the relevance of our findings, in terms of the importance of sediments to the implementation plans of the WFD. The ecological status

of coastal water bodies is required to be assessed under the WFD guidelines, following physico-chemical and biological criteria. The annex V of the WFD specifies the ‘physico-chemical quality elements’ as pelagic nutrient concentrations, oxygen concentration and transparency and of three ‘biological quality elements’ as phytoplankton, macroalgae and angiosperms, and benthic invertebrate fauna. Therefore, no monitoring on microphytobenthos, as well as nutrients within the benthic system is expected. Our study indicates that most of the primary productive capacity lies on the microalgae community living in the sediment surface. It is also within the sediments where the main stock of nutrients within the lagoon is. The standard monitoring programmes required by the implementation of the Directive, may fail to track relevant changes in the nutrient conditions and dynamics, as well as the algal responses to them.

#### **5.4.13 Future consequences and scenarios in case of global warming**

The importance of global warming in the near future is becoming clear and consensual within the scientific community (e.g. Kerr *et al.*, 2008; Lloret *et al.*, 2008). The increase of seawater temperature and level may have a strong influence in coastal shallow lagoons. Moreover, global warming will also change the hydrological cycle and increase precipitation in the northern and central Europe, as discussed by Lloret *et al.* (2008) and indicated by IPCC (2007). These factors are likely to contribute to an increase of light attenuation. If these effects are strong enough, lighted bottoms of shallow lagoons may lose a significant part of the benthic algal community. As discussed throughout this study, these communities are essential to control nutrient dynamics of the system by taking up large amounts of nutrients both from the water column and from the sediments. If due to light limitation, benthic algal communities disappear, the flux of nutrients from the sediments may increase dramatically and lead to eutrophication (Figure 5.20). Furthermore, the increase of temperature complicates even more the scenario since it allows an increase of the ammonium concentration within the sediments. The microbial activity involved is temperature dependent. In addition, temperature also increases the release of phosphate and silicate from sediments (Gönenç and Wolflin, 2005). Therefore, shallow lagoons should be evaluated in terms of ecological quality with care since they may be very vulnerable to eutrophication.



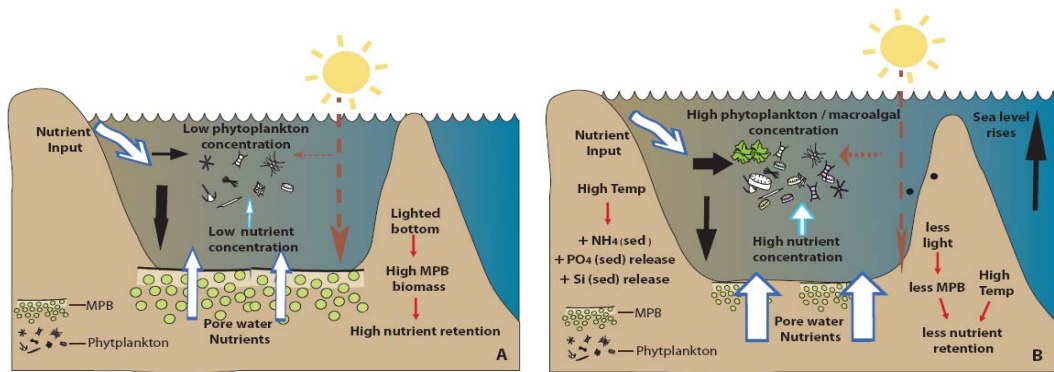


Figure 5.20 – Scheme of the lagoon system: A- current status and B – in case of global warming (higher temperatures and higher sea level). Adapted from Lloret *et al.* (2008).

## 5.5 Conclusions

The quality status of the water column in Ria Formosa is still considered to be lower than the main objective ('Good' status) defined by the Water Framework Directive for 2015, following EEA (1999) classification. Nevertheless, an improvement in water quality was observed, compared with previous published results. This may be due to an increase of the benthic algal community, which contributes to the nutrient retention in the sediments and uptakes nutrients from the water column. Nevertheless, this assessment is merely indicative and present conditions should be re-evaluated against site specific reference conditions. The microphytobenthos communities are extremely important in this system, not only because of nutrient dynamics, but also because they strongly affect the chlorophyll concentrations in the water column by re-suspension. They represent the majority of photosynthetic elements, being responsible for about 99% of the chlorophyll of the system. In a scenario of a large temperature and sea level increase, MPB community could deteriorate due to light limitation. This would have a strong impact in the nutrient concentration of the water column and consequently in the phytoplankton populations. Nutrient fluxes from sediments would be greater and fewer nutrients would be removed from the water column by benthic algae. This cascade of processes would reveal the vulnerability of the shallow lagoon to eutrophication. The small levels of dissolved oxygen observed in the morning may be critical for faunal populations and should be closely followed. The release of nutrients from sediments may also be influenced by oxygen concentration. This problem is even greater in the inner channels of the lagoon, where the residence time of water is longer leading to a decrease in oxygen.

Due to the importance of pore water nutrients and benthic algal communities, the implementation plan of the Water Framework Directive should be carefully planned as it may fail to track nutrient-driven changes amongst the primary producers. In addition, due to the extreme low values of DO and similarly with what was already suggested by Ferreira et al. (2007), shorter sampling intervals, compared with the 3 months proposed by the WFD, could be considered.

## 5.6 References

- Ackleson, S. (2003). Light in shallow waters: a brief research review. *Limnology and Oceanography*, **48**, 323-328.
- Alpine, A., Cloern, J. (1992). Trophic interaction and direct physical effects control phytoplankton biomass and production in an estuary. *Limnology and Oceanography*, **37**, 946-955.
- Amorim-Ferreira, A. (1987). *Contribuição para o estudo do fitoplâncton e microalgas epibênticas em viveiros de amêijoas (*Tapes decussatus* (L.)) da Ria Formosa*. First degree thesis in Biology, University of Lisbon.
- Basset, A., Sabetta L., Fonnesu, A., Mouillot, T., Chi, D., Viaroli, P., Giordani, G., Reizopoulou, S., Abbiati, M., Carrada, G. (2006). Typology in Mediterranean transitional waters: new challenges and perspectives. *Aquatic Conservation: Marine and Freshwater Ecosystems*. **16**, 441-455.
- Bowers, D., Harker, G., Smith, P, Tett, P. (2000). Optical properties of a Region of Freshwater Influence (The Clyde Sea). *Estuarine, Coastal and Shelf Science*, **50**, 717-726.
- Bowers, D., Binding, C. (2006). The optical properties of mineral suspended particles: A review and synthesis. *Estuarine, Coastal and Shelf Science*, **67**, 219-230.
- Branco, A., Kremer, J. (2005). The relative importance of chlorophyll and colored dissolved organic matter (CDOM) to the prediction of the diffuse attenuation coefficient in shallow estuaries. *Estuaries*, **28**, 643-652.
- Bricker, S., Clement, C., Pirhalla, D., Orlando, S., Farrow, D. (1999). *National Estuarine Eutrophication Assessment. Effects of Nutrient Enrichment in the Nation's Estuaries*. National ocean Service, Silver Spring, MD, USA, 71 pp.
- Bricker, S., Ferreira, JG., Simas, T. (2003). An integrated methodology for assessment of estuarine trophic status. *Ecological Modelling*, **169**, 39-60.
- Carpenter, J. (1966). New measurements of oxygen solubility in pure and natural water. *Limnology and Oceanography*, **11**, 264-277.
- C.E.C. (1991). *Council Directive of 21 May 1991 concerning urban wastewater treatment (91/271/EEC)*. Official Journal of the European Communities, L135 of 30.5.91, 40–52.

- C.E.C. (2000). *Council Directive of 23 October 2000, establishing a framework for Community action in the field of water policy (2000/60/EC)*. Official Journal of the European Communities, L327 of 22.12.2000, 1-72.
- Colijn, F. (1982). Light absorption in the waters of the Ems-Dollard estuary and its consequences for the growth of phytoplankton and microphytobenthos. *Netherlands Journal of Sea Research*, **15**, 196-216.
- Colijn, F., de Jonge, V. (1984). Primary production of microphytobenthos in the Sem-Dollard estuary. *Marine Ecology Progress Series*, **14**, 185-196.
- De Jonge, V., van Beusekom, J. (1995). Wind- and tide-induced resuspension of sediment and microphytobenthos from tidal flats in the Ems estuary. *Limnology and Oceanography*, **40**, 766-478.
- De Jonge, Elliott, M., Brauer, V. (2006). Marine Monitoring: Its shortcomings and mismatch with the EU's Water Framework Directive.. *Marine Pollution Bulletin*, **53**, 5-19.
- De Jonge, V. (2007). Toward the application of ecological concepts in the EU coastal water management. *Marine Pollution Bulletin*, **55**, 407-414.
- Devlin, M., Barry, J., Mills, D., Gowen, R., Foden, J., Sivyer, D., Tett, P. (2008). Relationships between suspended particulate material, light attenuation and sechi disk in UK marine waters. *Estuarine, Coastal and Shelf Science*, **79**, 429-439.
- Di Toro, D. (2001). *Sediment Flux Modeling*. J. Wiley and Sons., New York. 624pp.
- European Communities, 2008. *Commission Decision 2008/915/EC*, Official Journal of the European Communities, **L332**, 20-44.
- Edwards, V., Icelly, J., Newton, A., Webster, R., 2005. The yield of chlorophyll from nitrogen: a comparison between the shallow Ria Formosa and the deep oceanic conditions at Sagres along the southern coast of Portugal. *Estuarine, Coastal and Shelf Science*, **62**, 391-403.
- EEA (1999). *Nutrients in European ecosystems. Topic Report N. 4/1999*. European Environmental Agency, 156pp.
- Facca, C., Sfriso, A. (2007). Epipelagic diatom spatial and temporal distribution and relationship with the main environmental parameters in coastal waters. *Estuarine Coastal and Shelf Science*, **75**, 35-49.
- Falcão, M., Vale, C. (1990). Study of the Ria Formosa ecosystem: benthic nutrient remineralization and tidal variability of nutrients in the water. *Hydrobiologia*, **207**, 137-146.
- Falcão, M. (1996). *Dinâmica dos Nutrientes na Ria Formosa: efeitos da interação da laguna com as suas interfaces na reciclagem do azoto, fósforo e sílica*. PhD Thesis. University of Algarve.
- Falcão, M., Vale, C. (2003). Nutrient dynamics in a coastal lagoon (Ria Formosa, Portugal): The importance of lagoon-sea water exchanges on the biological productivity. *Ciencias Marinas*, **29**, 425-433.
- Ferreira, J.G., Vale, C., Soares, C.V., Salas, F., Stacey, P.E., Bricker, S.B., Silva, M.C., Marques, J.C. (2007). Monitoring of coastal and transitional waters under the E.U. Water Framework Directive. *Environmental monitoring and assessment*, **135**, 195-216.

- Forja, J., Blasco, J., Gómez-Parra (1994). Spatial and seasonal variation of in situ benthic fluxes in the Bay of Cadiz (South-west Spain). *Estuarine, Coastal and Shelf Science*, **39**, 127-141.
- Goela, P. (2005). *Plano Teórico de Monitorização da Ria Formosa segundo a Directiva Quadro da Água*. Thesis of Chemistry, Algarve University.
- Gönenç, I., Wolflin, J. (2005). *Coastal lagoons: ecosystem processes and modeling for sustainable use and development*. CRC Press. 500pp.
- Grasshoff, K., Ehrhardt, M., Kremling, K. (1983). *Methods of seawater analysis*. Verlag Chemie, Weilheim: 419pp.
- Hedtkamp, S. (2005). *Shallow subtidal sand: permeability, nutrient dynamics, microphytobenthos and organic matter*. PhD Thesis. Kiel University.
- Heiskanen, A., van de Bund, W., Cardoso A.C., Nõges, P., 2004. Towards good ecological status of surface waters in Europe – interpretation and harmonisation of the concept. *Water Science and Technology*, **49**, 169-177.
- Howarth, R., Marino, R. (2006). Nitrogen as the limiting nutrient for eutrophication in coastal marine ecosystem: Evolving views over three decades. *Limnology and Oceanography*, **51**, 364-376.
- IPCC (2007). *Climate Change 2007: The Physical Science Basis. Contribution of Working Group I to the Fourth Assessment Report of the Intergovernmental Panel on Climate Change* [Solomon, S., Qin, D., Manning, M., Chen, Z., Marquis, M., Averyt, K., Tignor, M., Miller, H. (eds.)]. Cambridge University Press. Cambridge, United Kingdom and New York, NY, USA, 996pp.
- Jackson, P., Briggs, K., Flint, R., Holyer, R., Sandidge J. (2002). Two- and three-dimensional heterogeneity in carbonate sediments using resistivity imaging. *Marine Geology*, **182**, 55-76.
- Jensen, J.P., Pederson, A.R., Jeppensen, E., Søndergaard, M. (2006). An empirical model describing the seasonal dynamics of phosphorus in 16 shallow eutrophic lakes after external loading reduction. *Limnology and Oceanography*, **51**, 791-800.
- Kerr, R. (2008). Global warming throws some curves in the Atlantic Ocean. *Science*, **322**, 515.
- Kim, H., Hwang, S., Shin, J., An, K., Yoon, C.G. (2007). Effects of limiting nutrients and N:P ratios on the phytoplankton growth in a shallow hypertrophic reservoir. *Hydrobiologia*, **581**, 255-267.
- Kostoglidis, A., Pattiaratchi, C., Hamilton, D. (2005). CDOM and its contribution to the underwater light climate of a shallow, microtidal estuary in south-western Australia. *Estuarine, Coastal and Shelf Science*, **63**, 469-477.
- Lerat, Y., Lasserre, P., Corre, P. (1990). Seasonal changes in pore water concentrations of nutrients and their diffusive fluxes at the sediment-water interface. *Journal of Experimental Marine Biology and Ecology*, **135**, 135-160.
- Lloret, J., Marín, A., Marín-Guirao, L. (2008). Is coastal lagoon eutrophication likely to be aggravated by global climate change? *Estuarine, Coastal and Shelf Science*, **78**, 403-412.
- Lorenzen G (1967) Determination of chlorophyll and phaeopigments: spectrophotometric equations. *Limnology and Oceanography*, **12**, 343–346.

- Loureiro, S., Newton, A., Icery, J. (2005). Microplankton composition, production and upwelling dynamics in Sagres (SW Portugal) during the summer of 2001. *Scientia Marina*, **69**, 323-341.
- Loureiro, S., Newton, A., Icery, J. (2006). Boundary conditions for the European Water Framework Directive in the Ria Formosa lagoon, Portugal (physico-chemical and phytoplankton quality elements). *Estuarine, Coastal and Shelf Science*, **67**, 382-398.
- Loureiro, S., Newton, A., Icery, J. (2008). Enrichment experiments and primary production at Sagres (SW Portugal). *Journal of Experimental Marine Biology and Ecology*, **359**, 118-125.
- Lucas, C., Banham, C., Holligan, P. (2001). Benthic-pelagic Exchange of microalgae at a tidal flat, taxonomic analysis. *Marine Ecology Progress Series*, **212**, 39-52.
- Lund-Hansen, L. (2004). Diffuse attenuation coefficients  $K_d$  (PAR) at the estuarine North Sea-Baltic Sea transition: time-series, partitioning, absorption and scattering. *Estuarine, Coastal and Shelf Science*, **61**, 251-259.
- McLusky, D.S., Elliott, M. (2007). Transitional water : A new approach, semantics or just muddying the waters? *Estuarine, Coastal and Shelf Science*, **71**, 359-363.
- Mudge, S., Icery, J., Newton, A. (2007). Oxygen depletion in relation to water residence times. *Journal of Environmental Monitoring*, **9**, 1194-1198.
- Murray, L., Mudge, S., Newton, A., Icery, J. (2006). The effect of benthic sediments on dissolved nutrient concentrations and fluxes. *Biochemistry*, **81**, 159-178.
- Neil, M. (2005). A method to determine which nutrient is limiting for plant growth in estuaries waters – at any salinity. *Marine Pollution Bulletin*, **50**, 945-955.
- Newton, A., Mudge, S. (2003). Temperature and salinity regimes in a shallow, mesotidal lagoon, the Ria Formosa, Portugal. *Estuarine, Coastal and Shelf Science*, **57**, 73-85.
- Newton, A., Icery, J.D., Falcão, M., Nobre, A., Nunes, J.P., Ferreira, J.G., Vale, C. (2003). Evaluation of the eutrophication in the Ria Formosa coastal lagoon, Portugal. *Continental Shelf Research*, **23**, 1945-1961.
- Newton, A., Mudge, S. (2005). Lagoon-sea exchanges, nutrient dynamics and water quality management of Ria Formosa (Portugal). *Estuarine, Coastal and Shelf Science*, **62**, 405-414.
- Obrador, B., Pretus, J. (2008). Light regime and components of turbidity in a Mediterranean coastal lagoon. *Estuarine, Coastal and Shelf Science*, **77**, 123-133.
- Oliveira, P. (2005). *Análise e Monitorização do Oxigénio na Ria Formosa*. First Degree Thesis in Oceanography, Algarve University.
- OSPAR Commission, 2005. *Common procedure for the identification of the eutrophication status of the OSPAR marine area*, OSPAR Convention for the protection of the marine environment of the north-east Atlantic, 36pp.
- Riaux-Gobin, C., Bourgoin, P. (2002). Microphytobenthos biomass at Kerguelen's Land (Subantarctic Indian Ocean) : repartition and variability during austral summers. *Journal of Marine Systems*, **32**, 295306.

- Santos, M., Monteiro, C. (1997). The Olhão artificial reef system (south Portugal): Fish assemblages and fishing yield. *Fisheries Research*, **30**, 33-41.
- Schindler, D. (2006). Recent advances in the understanding and management of eutrophication. *Limnology and Oceanography*, **51**, 356- 363.
- Serpa, D., Falcão, M., Duarte, P., Fonseca, L.C., Vale, C. (2007). Evaluation of ammonium and phosphate release from intertidal and subtidal sediments of a shallow coastal lagoon (Ria Formosa – Portugal): a modelling approach. *Biochemistry*, **82**, 291-304.
- Sobral, P. (1995). *Ecophysiology of Ruditapes Decussatus*. New University of Lisbon, PhD Thesis, 187pp.
- Tett, P., Gilpin, L., Svendsen, H., Erlandsson, C.P., Larsson, U., Kratzer, S., Fouilland, E., Janzen, C., Lee, J., Grenz, C., Newton, A., Ferreira, J.G., Fernandes, T., Scory, S. (2003). Eutrophication and some European waters of restricted exchange. *Continental Shelf Research*, **23**, 1635-1671.
- Tett, P., Gowen, R., Mills, D., Fernandes, T., Gilpin, L., Huxham, M., Kennington, K., Read, P., Service, M., Wilkinson, M., Malcom, S. (2007). Defining and detecting undesirable disturbance in the context of marine eutrophication. *Marine Pollution Bulletin*, **55**, 1-6.
- Wayland, D., Megson, D.P., Mudge, S., Icely, J., Newton, A. (2008). Identifying the source of nutrient contamination in a lagoon system. *Environmental Forensics*, **9**, 231-239.
- Winkler, L.W. (1888). Die Bestimmung des in Wasser gelosten Sauerstoffes. *Berichte der Deutschen Chemischen Gesellschaft*, **21**, 2842-2855.

## **CHAPTER 6**

---

The yield of microphytobenthic chlorophyll from nitrogen:  
enriched experiments in microcosms

---

## Abstract

The yield of phytoplankton chlorophyll from nitrogen has proved to be a useful parameter in the study of eutrophication of coastal waters. It represents the main relationship or link between chlorophyll formation and nutrient consumption. This is the first time that it has been estimated for microphytobenthos. Six sediment cores were collected from Ria Formosa with an acrylic cylinder and cork stoppers were placed on the bottom. Water samples were also collected in large containers and prepared (filtered and enriched) to be pumped on top of the sediment inside the acrylic cylinders, which are the incubators of the experiments. Incubators were isolated to avoid water exchanges and placed in large tanks full of water to maintain stable conditions of temperature. Three experiments were conducted in May and September of 2007. They were run for 5 to 9 days in a continuous diluted nutrient enriched system. One of the experiments was carried out with half the incubators in dark conditions to evaluate the nutrient fluxes between the sediment and the water column, when no algal growth is expected. Nutrient fluxes from muddy sediments into the water column were estimated to be  $0.1015 \mu\text{mol}\cdot\text{cm}^{-2}\cdot\text{d}^{-1}$  for nitrogen,  $-0.0015 \mu\text{mol}\cdot\text{cm}^{-2}\cdot\text{d}^{-1}$  for phosphorus,  $0.1395 \mu\text{mol}\cdot\text{cm}^{-2}\cdot\text{d}^{-1}$  for silicon. The yield of chlorophyll was determined to be between 3.7 and  $4.1 \mu\text{gchl}\cdot(\mu\text{mol N})^{-1}$  from nitrogen and between 4.0 and  $4.8 \mu\text{gchl}\cdot(\mu\text{mol Si})^{-1}$  from silicon in muddy sediments. It was not possible to determine the yield from phosphorus. These values are higher than for phytoplankton which may be due to physiological reasons or due to the presence of a smaller fraction of microheterotrophs, which would divert nutrients. For sand, smaller yields were obtained but mainly because the values of the sediment fluxes used were the ones obtained for mud, which are higher than they are likely to be for sand. This extra input of nutrients is considered to be taken up by algae and therefore decrease the value of the microphytobenthic yield.

**Keywords:** Chlorophyll, nitrogen, microphytobenthos, yield, microcosm, eutrophication, CSTT model, Ria Formosa,



## 6.1 Introduction

Eutrophication in marine coastal waters has been identified in recent years as a potential serious environmental problem (Howard and Marino, 2006; Nixon, 1995), especially in enclosed areas with restricted exchange such as Ria Formosa (Tett *et al.*, 2003). Eutrophication events have become more prevalent within the increased use of nitrogen and phosphorus-rich compounds, such as detergents, fertilizers and discharge of wastewaters (Bricker *et al.*, 1999; Jensen *et al.*, 2006; Howarth and Marino, 2006; Schindler, 2006). Pelagic chlorophyll concentration has been used for several years as an indicator of eutrophication (Tett *et al.*, 2003; Nobre *et al.*, 2005; Yoshiyama and Sharp, 2006). It is therefore of great importance to assess accurately the relationship between nitrogen concentration, uptake by algae and algal growth in coastal waters. This relationship portrays the rate of chlorophyll production from a known amount of nutrient. It has been investigated by several authors due to its importance in predicting and preventing eutrophication events (e.g. Gowen *et al.*, 1992; Edwards *et al.*, 2003; 2005). The quantification of this relationship can be done in terms of the yield of algal chlorophyll from nitrogen ( $q$ ), which is considered to be the limiting nutrient in temperate coastal waters of the North Atlantic (e.g. Taylor *et al.*, 1995a; 1995b; Edwards *et al.*, 2003; Tett *et al.*, 2003; Mills *et al.*, 2004). This yield is crucial for the development of models such as Comprehensive Studies Task Team (CSTT) that simulates the nutrient and chlorophyll conditions and predicts eutrophication (CSTT, 1994; 1997; Tett *et al.*, 2003).

Given that the yield of chlorophyll from nitrogen is the relationship between chlorophyll change or production ( $\Delta X$ ), and nutrient change or consumption ( $\Delta S$ ), so that,  $q = \Delta X / -\Delta S$ , the heterotrophs' fraction may strongly influence the  $q$  estimate. Fouilland *et al.* (2007) suggested that heterotrophs may take up around 25% of the available nitrate and ammonium therefore lead to smaller  $q$  values than expected. Microheterotrophs are present in marine waters and have been studied especially in the water column (e.g. Glibert, 1982; Tett and Wilson, 2000; Lee *et al.*, 2002; Tett and Lee, 2005).

Several methods may be used to study the algal growth in response to nutrient enrichment and simultaneously, the yield of chlorophyll from nutrients (Edwards *et al.*, 2003; Escaravage *et al.*, 1996; Jones *et al.*, 1978). Methodologies may range from *in situ* experiments, conducted in open waters, to *ex situ* experiments, which are carried

out in the laboratory. *In situ* experiments have to be controlled and enclosed. Otherwise, the added nutrients will be diluted in the seawater and the chlorophyll will dissipate as well, leading to an inability to calculate of the yield  $q$ . *Ex situ* experiments are much more easily controlled. However, these studies may miss some important aspects of the natural ecosystems, such as the hydrodynamics, for example. Care has to be taken, as much as possible, to ensure that no other factors that may interfere with natural processes are added to the experimental design. There are two kinds of experimental approach (Edwards, 2001): batch cultures, which are closed systems with no replacement of water, and continuous diluted cultures, which are open systems and allow the addition of enriched water at the same rate each day and the removal of the same volume per day. According to the same authors, the second option is better because it avoids the accumulation of metabolites and the effects of the deterioration of the culture, which may complicate the analysis of nutrient limitation.

Gowen *et al.* (1992) investigated the yield using data sets from natural sites in Scotland on which they carried out regression analyses. A median yield of about  $1.1 \mu\text{g chl.}(\mu\text{mol N})^{-1}$  was observed by these authors. Gowen *et al.* (1992) had to rely on the assumption that there were no differences in the uptake and use of the different forms of nitrogen and that the result in terms of phytoplankton growth would be the same. Another assumption was that the yield was not dependent on the physiological state of cells and community structure (during blooms, for example). They observed a high range of variation in the yields obtained at each site. The range of variation was even larger between sites. Edwards *et al.* (2003; 2005) continued Gowen *et al.*'s work and performed microcosm experiments using continuous diluted culture techniques (Figure 6.1). The aim was to investigate and evaluate the yield under controlled conditions, where light, temperature and background nutrient concentrations could be recorded and controlled. This approach should result in a reduction in the range of variation. The set up included a reservoir containing the enriched water and a sump container which stored the water removed from the reactor. Filtered air was added through a tube which also added the enriched water. An independent channel was used to collect samples every two days. The results of these experiments showed that a value of around  $1 \mu\text{g chl.}(\mu\text{mol N})^{-1}$  is appropriate for modelling proposes. Edwards *et al.* (2003) used a nitrogen level for the enrichment that corresponds to the limit of eutrophication for British waters ( $12 \mu\text{M}$ ; Tett *et al.*, 2003). This level is extremely useful to study algal growth as a response to nutrient enrichment in waters. In their results, Edwards *et al.*

(2003) could clearly identify three different phases for phytoplankton growth. Phase I, when the growth and the yield were in their maximum, corresponds to the first two days. Phase II corresponds to the rapid decline of the yield, between day 2 and 4. Phase III corresponds to the stabilization of the yield (equilibrium). The periods in which these processes would occur greatly depend on the species composition and their interactions with the system.

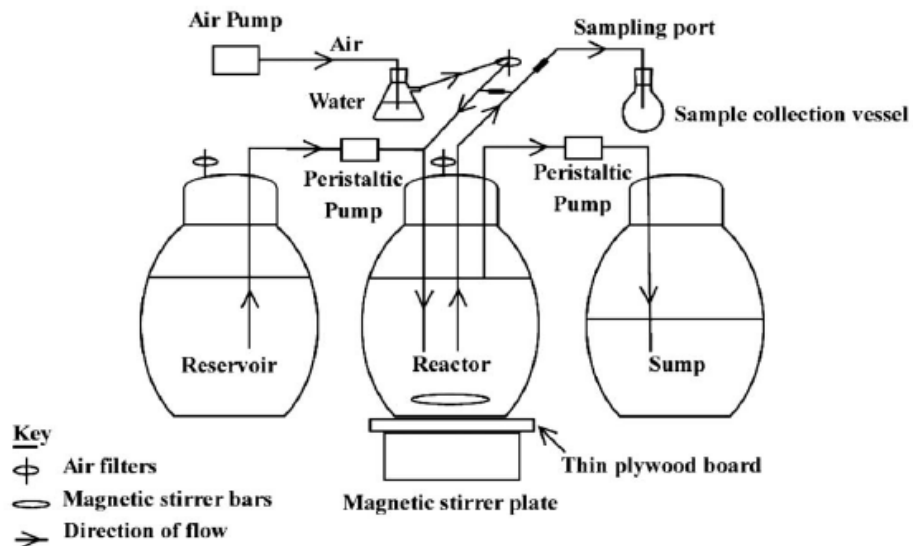


Figure 6.1 – Microcosm apparatus used by Edwards *et al.* (2003; 2005).

Recent work by Li *et al.* (2008) showed a value of  $1 \mu\text{g chl } (\mu\text{mol N})^{-1}$  for phytoplankton yield obtained from regression analyses and using values on hourly and weekly timescales. The relationship obtained between nutrients and chlorophyll was very strong. The method was similar to what Gowen *et al.* (1992) used and revealed interesting similar results.

The yield  $q$  of chlorophyll from nitrogen or phosphorus is also determined by physiological processes since it is specific for each species. Therefore, the results and conclusions taken from previous studies with phytoplankton cannot necessarily be applied directly to benthic microalgae. Large differences are found between the species composition and the physiology of phytoplankton and microphytobenthos (Aberle-Malzahn, 2004). Microphytobenthos (MPB) are generally found living in well established biofilms and, according to Costello and Chisholm (1981) the algal growth rate can be higher for cells with large cell size, which is the case of MPB. Moreover, the temporal variability of communities needs to be taken into consideration. The algal community may change through the year according to environmental conditions, so it is likely that the yield  $q$  may change seasonally.

Another important aspect discussed by Edwards (2001) is the interaction between primary producers and grazers and the effects of remineralisation. In the case of monoculture experiments all these aspects are not considered in the experiment and the study is clearly not recreating the ecosystem. Therefore, microcosm experiments using natural, heterogeneous communities may be the best way to obtain more realistic results. This is especially important in the study of the yield of microphytobenthos. Since they live within the sediment layers, it is desirable to disturb them as little as possible. Therefore, it is not possible to eliminate grazers without considering the use of chemical products that could compromise the results. Estimates of these processes should be obtained when possible, to understand the interactions occurring throughout the experiment.

The importance of sediments in coastal shallow lagoons was fully discussed in Chapter 5. The water is spread over a large area of sediments, which are rich in nutrient concentrations and well illuminated. The microphytobenthos represents the majority of chlorophyll pigments found in the lagoon, when compared with phytoplankton and as discussed in Chapter 5. Therefore, it is of great importance for the assessment of eutrophication to perform the investigation of the yield of chlorophyll from nutrients by these benthic microalgae. However, the analysis of microphytobenthos chlorophyll dynamics is complicated and requires the use of a complex set of equations to describe growth processes. This set of equations is part of a theory of microphytobenthos dynamics developed and improved for modelling purposes (full description and explanation of how it was achieved is presented in Chapter 7).

Microphytobenthos growth is considered to be either nutrient or light limited. The relationships and processes involved in light and nutrient limited growth are discussed below, and parameterized in terms of equations that will be used in this chapter in calculation of fluxes and in Chapter 7 as part of a formal mathematical model.

### **6.1.1 Nutrient limited growth**

It is assumed that microphytobenthos cells are distributed in the sediment surface and within the sediment, as indicated by several studies (e.g. Underwood and Paterson, 2003; Cartaxana *et al.*, 2006). The cells placed in the sediment surface should be able to take nutrients up from the water column. Cells within the sediment should be able to take nutrients up by intercepting a sediment nutrient flux that is independent of algal

biomass. The nutrient limited growth is calculated considering only nitrogen, because it has been indicated as the limiting nutrient in Ria Formosa. This was discussed mainly in Chapter 5 where there are several citations of others' work. After obtaining the values of the biomass increase or community growth ( $\mu X$ , Equation 6.1), these were used in the calculation of the phosphorus and silicon yields. The nutrient limited increase of microphytobenthos biomass ( $\mu X$ ) is therefore dependent on the nutrient flux from the sediment and nutrient supply from the water column:

$$\mu X = q.(c_2.\phi_s + c_4\phi_w) \quad (\mu\text{g chl.cm}^{-2}.\text{d}^{-1}) \quad (6.1)$$

Where  $c_2$  is the proportion of the sediment nutrient flux that is captured by benthic algae, which depends on algal biomass;  $\phi_s$  is the nutrient flux from the sediment into the water column, which is estimated by the term *flux*, described below;  $c_4$  is the proportion of the water nutrient that is captured by benthic algae, which again, depends on algal biomass; and  $\phi_w$  is the nutrient flux from the water column to algae on the surface of the sediment. MPB biomass in this experimental work was measured as  $\mu\text{g chl.cm}^{-2}$  and therefore units in this Chapter are in agreement with it and different from what is presented in Chapter 7. The yield  $q$  is essential for this equation but it is one of the aims of this study. For this intermediate calculation, a  $q$  estimate was used following:

$$q = {}^X q_a^N .(1 - \eta_b) \quad (\mu\text{g chl.}\mu\text{mol}^{-1}) \quad (6.2)$$

Where  ${}^X q_a^N$  is the algal yield of chlorophyll from nitrogen in pure cultures. The value used in this study ( $6 \mu\text{g chl} (\mu\text{mol})^{-1}$ ) was the maximum value obtained by Edwards *et al.* (2005) in Portugal and Gowen *et al.* (1992) for pelagic algae. Maximum values were considered because it was expected that benthic algae established in biofilms are larger in size than the pelagic algae and would have larger values of yield. There are not many available works in the literature about this topic. Costello and Chisholm (1981) discuss how the growth of benthic algae (larger in size) is greater than the growth of pelagic cells, at the same conditions. Moreover, benthic microalgae would have to be adapted to light limitation within the sediments and have increased chlorophyll concentrations in the thylakoids (Falkowski and Raven, 2007).  $\eta_b$  is the ratio of the benthic microheterotroph to total microbenthic (carbon) biomass. The value of 0.125 was taken from Tett and Lee (2005).

The water column nutrient flux ( $\phi_w$ ) is assumed to result from molecular diffusion across the benthic boundary layer or viscous layer, which separates the sea-bed from the main part of the water column. It was estimated following:

$$\phi_w = D_m \cdot \left. \frac{\partial S}{\partial z} \right|_{bbl} \quad (\mu\text{mol} \cdot \text{cm}^{-2} \cdot \text{d}^{-1}) \quad (6.3)$$

Where  $D_m$  is the coefficient of molecular diffusion for small particles at the prevailing temperature. The value ( $1.648 \times 10^{-8} \text{ cm}^2 \cdot \text{d}^{-1}$  for Nitrogen) used in this study was taken from Murray *et al.* (2006). The gradient of nutrient concentration was estimated from:

$$\left. \frac{\partial S}{\partial z} \right|_{bbl} \approx \max \left( 0, \frac{S_w - S_0}{h_{bbl}} \right) \quad (6.4)$$

Where  $S_w$  is the nutrient concentration in the water column,  $S_0$  is the notional concentration ( $> 0$ ) at algal cell walls. In principle, it is less than  $S_w$  because of the uptake by cells and it cannot fall too close to zero, which would lead to the termination of trans-wall nutrient transport. It was considered to be  $1 \mu\text{M}$  for Dissolved Available Inorganic Nitrogen (DAIN).  $h_{bbl}$  is the thickness of the benthic boundary layer, which depends on the sea-bed roughness and the flow velocity. The value considered for  $h_{bbl}$  (0.1 cm) is between the range proposed by Di Toro (2001) and Murray *et al.* (2006). It would be standard to place a negative symbol before the coefficient of molecular diffusion in Equation 6.3. In this case, the flux will be positive for a inflow into the cells.

The intercepted fraction of the benthic nutrient flux,  $c_2$ , can be calculated using a nutrient absorption cross-section parameter,  $a_s^*$  ( $0.3 \text{ cm}^2 \cdot (\mu\text{g chl})^{-1}$ ), estimated considering diatom cell dimension taken from Jesus (2005), analogous to the light absorption cross-section, which will be described below.

$$c_2 = (1 - e^{-a_s^* \cdot (1-c_3) \cdot X}) \quad (6.5)$$

Where  $c_3$  (0.3) is the proportion of microphytobenthos on the surface of the sediment, considering that microphytobenthos is distributed within the sediment and migrate vertically due to the effect of light and tide. The intercepted fraction of the water column flux ( $c_4$ ) was estimated using a similar equation to the one for  $c_2$ , but considering the proportion of MPB cells on the surface and not the  $(1 - c_3)$  term.

### 6.1.2 Light limited growth

The net photosynthetic production limited by light depends on capture of light, conversion factors and losses due to respiration of cells. Hence (Tett et al., 2007):

$$\mu X = k.c_l.I_s.\Phi.\chi - r.X \quad (\mu\text{g chl.cm}^{-2}.\text{d}^{-1}) \quad (6.6)$$

Where  $k$  ( $86.4 \text{ s.d}^{-1}$ ) converts units from  $\text{s}^{-1}$  to  $\text{d}^{-1}$  and from  $\text{ng}$  to  $\mu$ ;  $c_l$  is the fraction of PAR absorbed by benthic algae, described below;  $I$  is the PAR at the sea-bed ( $\mu\text{E.m}^{-2}.\text{s}^{-1}$ );  $\Phi$  is the photosynthetic yield ( $50 \text{ ng-at C fixed.}(\mu\text{E photons absorbed})^{-1}$ );  $\chi$  is  $0.4 \mu\text{g chl.}(\mu\text{g-at organic C})^{-1}$ ; and  $r$  is the respiration rate (below).

The algal fraction of PAR,  $c_l$ , is the part of light that reaches the sea-bed and is used in algal photosynthesis. Pigments that capture this fraction of light, compete with algal non-photosynthetic pigments and sediment particles for light. The influence of these ‘Optically Active Constituents’ can be described by the sum of products of their absorption cross-sections and concentrations. Algal pigments and particulate matter ( $PM$ ) are the only constituents that will be considered in the study. This theory is standard for water column (Kirk, 1994) and its application to the sediments is proposed here. The most important difference is that light is likely to attenuate much more strongly in sediments than in the water column.  $h_b$  is defined here as the thickness of the layer in which 99% of photons are absorbed, corresponding to the euphotic zone in the water column. The thickness of the layer was assessed by placing freeze-dried sediment in a plastic chamber. A light source was placed on the top of the sediment and a light sensor below the sample (Figure 6.2). It was concluded that 99% of the photons would be absorbed in around 1 mm layer.

It is also assumed that all particles that influence the light absorption are uniformly

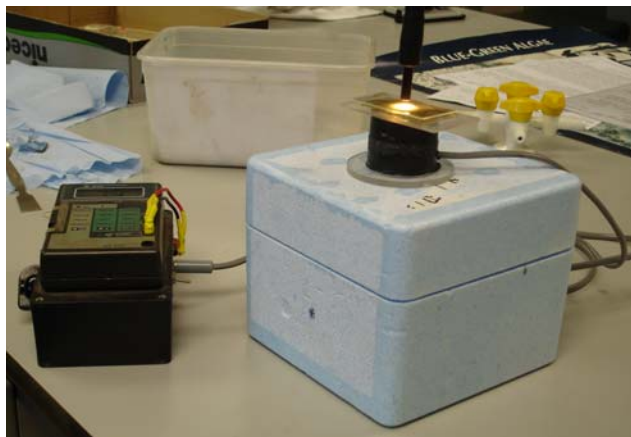


Figure 6.2 – Sediment layer (1mm) in a plastic cell. Light source is placed in the top of the cell and the light sensor just below.

distributed within the sediment, except the fraction  $c_3$  of cells that are in the surface. The fraction of PAR taken by algae may be estimated following (Tett et al., 2007):

$$c_1 = \frac{a_{PH} \cdot h_b}{a \cdot h_b} \cdot (1 - R) + (1 - e^{-a_{PH,s}}) \cdot R \quad (6.7)$$

where:

$$a_{PH} = (1 - c_3) \cdot a_{PH}^* \cdot X \cdot h_b^{-1} \quad (\text{cm}^{-1}) \quad (6.8)$$

$$a_{PH,s} = c_3 \cdot a_{PH}^* \cdot X \cdot h_b^{-1} \quad (\text{cm}^{-1}) \quad (6.9)$$

$$a = (1 - c_3) \cdot (a_{PH}^* + a_{NP}^*) \cdot X \cdot h_b^{-1} + a_{PM}^* \cdot PM \quad (\text{cm}^{-1}) \quad (6.10)$$

$$PM = \rho_s \cdot (1 - p) \quad (\mu\text{g} \cdot \text{cm}^{-3}) \quad (6.11)$$

Where  $a_{PH}^*$  is the absorption cross-section ( $0.2 \text{ cm}^2 \cdot (\mu\text{g chl})^{-1}$ ) of photosynthetic pigments. It describes the ability of chlorophyll and other accessory pigments to harvest photons for photosynthetic processes.  $a_{NP}^*$  is the absorption cross-section ( $0.2 \text{ cm}^2 \cdot (\mu\text{g})^{-1}$ ) of photoprotective pigments, such as carotenoids and degraded photosynthetic pigments, which do not lead to photosynthesis.  $a_{PM}^*$  is the absorption cross-section ( $0.0004 \text{ cm}^2 \cdot (\mu\text{g})^{-1}$ ) taken from Devlin *et al.* (2008) of particulate matter in the sediment.  $\rho_s$  is the density of dry and compact sediment ( $1000 \mu\text{g} \cdot \text{cm}^{-3}$ ),  $p$  is porosity of superficial sediment (0.5) and  $R$  is the reflected proportion (considered to be 0.5) of PAR by the sediment or sea-bed *albedo*.

Equation 6.7 describes the fraction of light that is taken by algae within the sediment. This term is likely to be small due to the rapid attenuation of light in sediments. Light-absorption is likely to be dominated by sediment particles.

The objectives of this study were: 1) to investigate the nutrient dynamics across the sediment-water interface in a series of microcosms, 2) to determine the nutrient fluxes from the sediment to the water column and 3) to determine the yield of chlorophyll from nitrogen, phosphorus and silicon for microphytobenthos in Ria Formosa. To achieve these goals an experimental device, a microcosm or reactor, was implemented.

The hypotheses were that: 1) Edwards' approach could be modified to get a value of the MPB yield; 2) there would be an increase of MPB chlorophyll related to a decrease in the nitrogen concentration; 3) estimates of nutrient fluxes were similar to the ones obtained in Chapter 5; 4) estimates for MPB yield were higher than for phytoplankton; 5) similar estimates of yield in sandy and muddy sediments would be obtained.



This chapter is complex since the work involved several approaches to reach one of its main aims: the estimate of the yield of microphytobenthos chlorophyll from nitrogen. Therefore, a diagram was constructed to illustrate the main components of the chapter and the steps followed (Figure 6.3). In the introduction, the importance and the usefulness of the yield were discussed, as well as its ecological and physiological aspects. Previous studies and methodologies followed were presented. Moreover, an introduction to essential aspects of microphytobenthos growth was also presented. This is part of the model of microbenthic processes that will be used to estimate  $q$  and is represented in orange in Figure 6.3. In the methods section, detailed descriptions of the experiments are provided and the first part of the numerical analysis is shown. This first

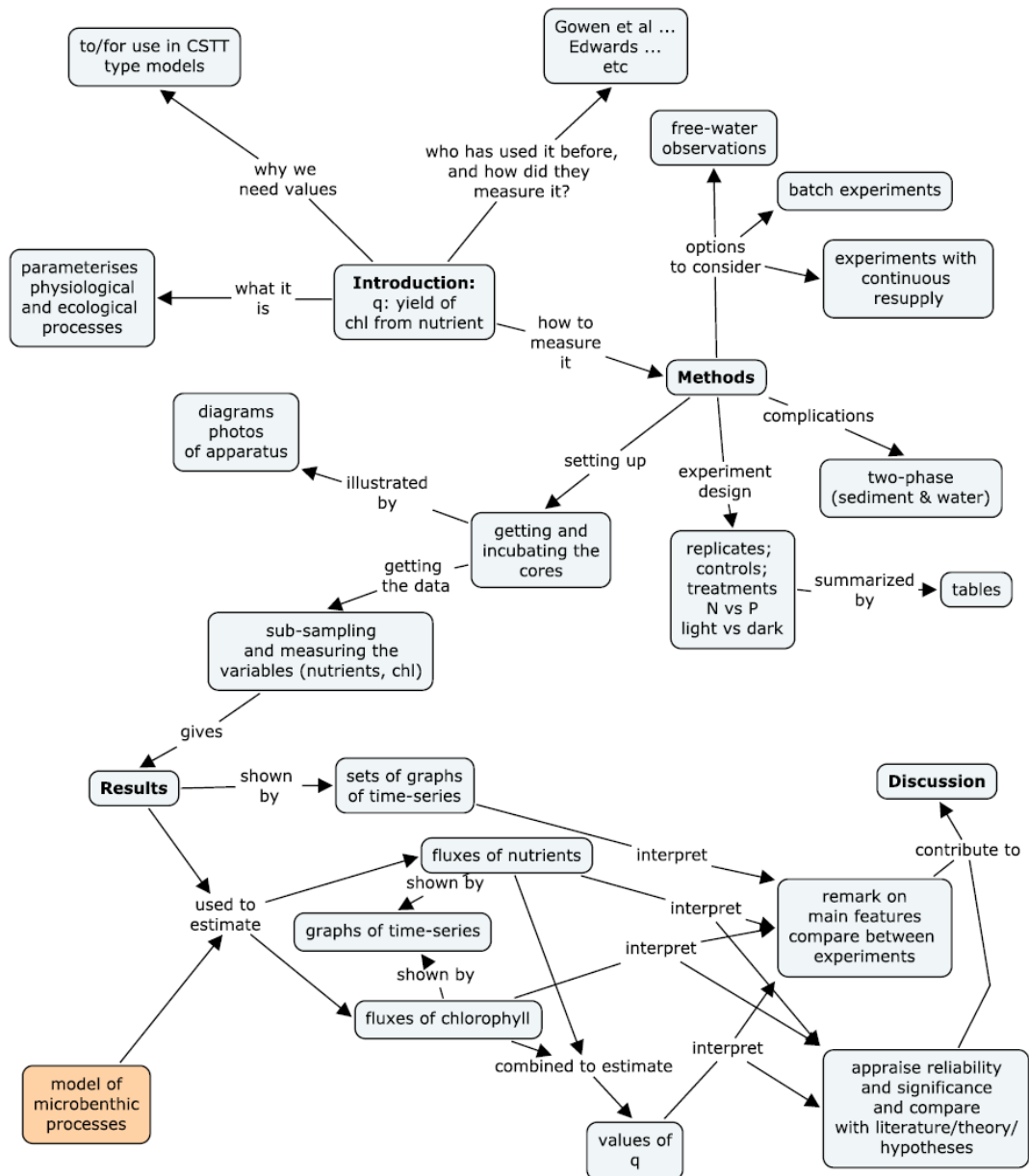


Figure 6.3 – Components and actions of each section of this chapter.

part consists in a set of equations used to describe nutrient and chlorophyll dynamics within the incubators. However, an important component is needed to carry out calculations, which is the microphytobenthos growth. This is the part of the microphytobenthic model, of which detailed description is provided above. Results from the observed nutrient and chlorophyll concentrations are provided as time-series graphs. These values were used to estimate changes of nutrients and chlorophyll and additionally, the yield.

## 6.2 Material and methods

Three different experiments were carried out for this study. Experiments started on the 4<sup>th</sup> May 2007, 24<sup>th</sup> May 2007 and 16<sup>th</sup> September 2007. A pilot study was run on the 18<sup>th</sup> April 2007 to ensure that the experimental device was working properly. Sediment and water samples were always collected during low water in Ria Formosa, at the site Ponte (P in Figure 6.4). Samples were then transported to Sagres (in the southern west of Portugal) to a warehouse due to the availability of the required conditions of space and environmental control (e.g. light, temperature).

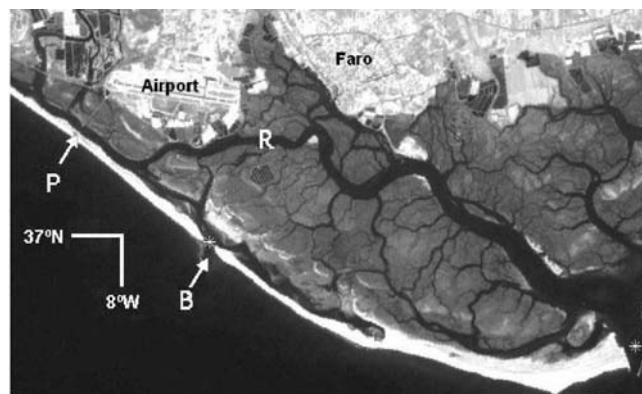


Figure 6.4 – Map of Ria Formosa representing the station Ponte (P).

### 6.2.1 Water and sediment collection

For each experiment 6 cores of sediment were collected using the cylindrical part of the incubator and using a shovel and a plastic sheet underneath down to a depth of around 5 cm (Figure 6.5).



Figure 6.5– Equipment for the sampling.

The cork stoppers were immediately placed under each core in the field to avoid disturbing the sample (Figures 6.6- B). Stoppers were previously covered by parafilm to ensure the non-existence of leaking. The sediment was placed in cold boxes to protect from light and avoid the increase in temperature.



Figures 6.6– A - Sampling the sediment cores. B – Placing the cork stoppers.

Furthermore, seventy litres of water were also collected in large containers. All the material collected was transported to a warehouse in Sagres, where it was possible to run the experiment in controlled conditions.

### 6.2.2 Microcosm

For this experiment, the experimental approach adopted by Edwards (2003; 2005) was followed and adjusted to the objectives and aims of this work. The reactor used in this work is much more complex because we have to deal with an extra sediment layer that has to be disturbed as little as possible.

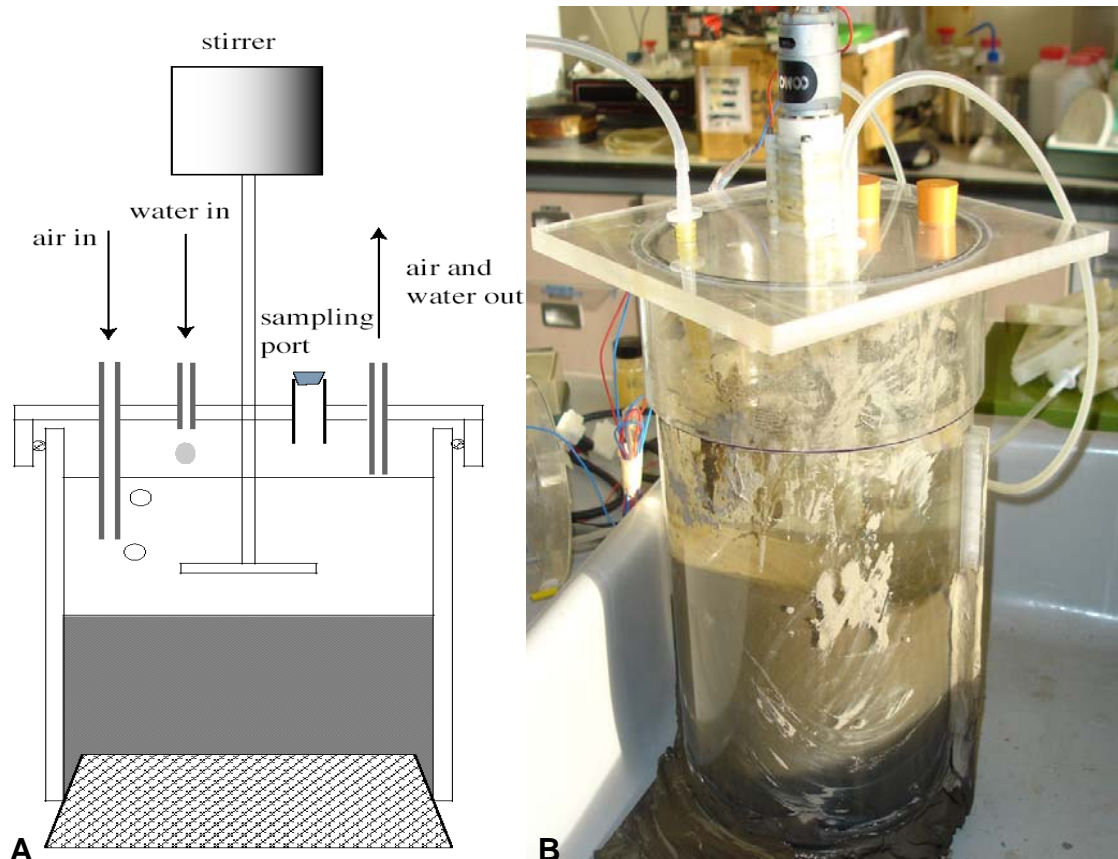


Figure 6.7 – A - Theoretical scheme and B – picture of the microcosm with additional tubing.

The design consists in an acrylic cylinder of 25cm height and 15 cm diameter, an acrylic cap with 6 holes: 2 sampling ports, one air entry, one water entry, one way out to water and air and a hole for placing the stirrer (Figure 6.7). The cylinder has a cork stopper at the bottom. This stopper was completely covered in parafilm to avoid any leaching of water. It is also important to avoid any exchanges between the microcosm and the water of the tank where the microcosms were placed (see below). The aim of the cap was to stop air and water exchanges. All the others holes are not permeable to gas and water, except the sampling port during the sampling periods. I thank John Kinross for his help building the microcosms.

### 6.2.3 Experiments

The first run was essential to test all the equipment involved and to ensure that everything was working properly. Small losses of water were found during the first days, but after a reinforcement of the coverage with parafilm the problem was solved. The level of water outside and inside the incubators was also adjusted. The set up implemented is represented in Figure 6.8. The only main difference between this diagrammatic representation and reality is that for the third experiment it was used two tanks during the experiments to place the six (3+3) incubators in total. One tank was under light conditions and the second tank was under dark conditions. A peristaltic pump pumped the water in from reservoirs and a vacuum pump took out the excess water every 10 minutes so that the volume was constant throughout the experiment.

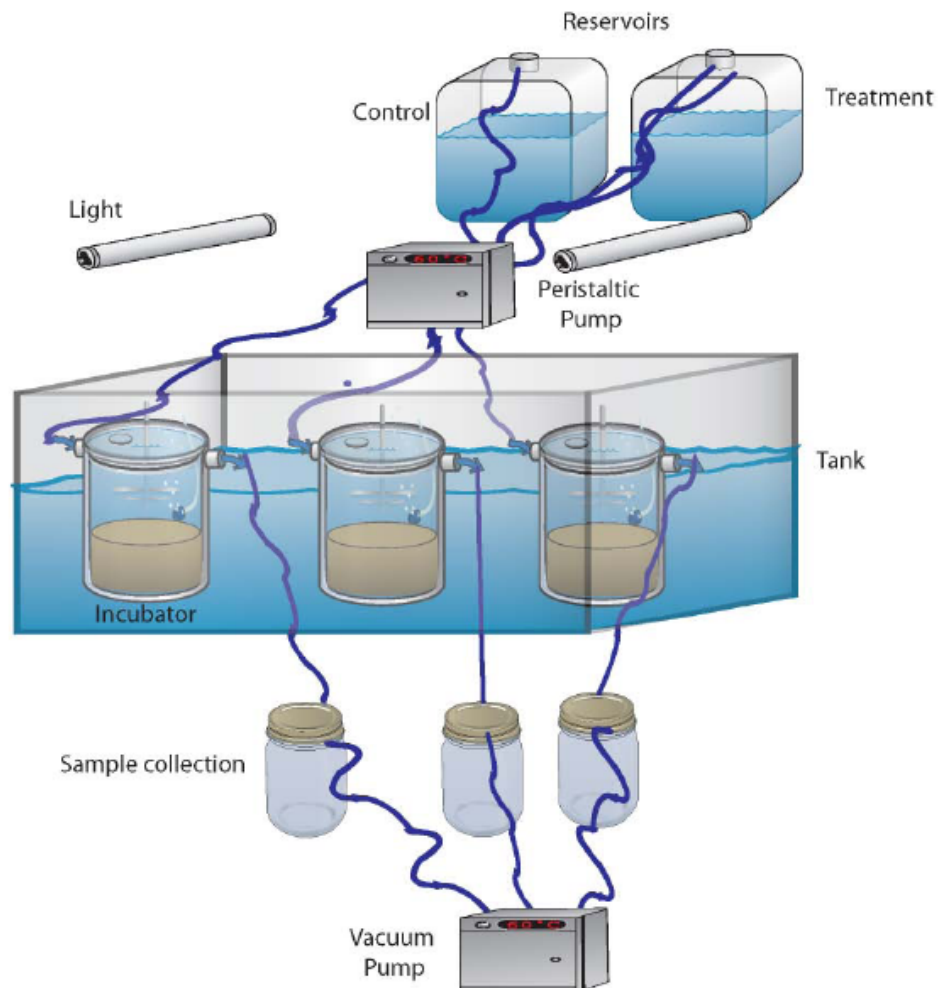


Figure 6.8 – Schematic representation of the experimental set up.

This experiment was conducted under diluted continuous culture conditions, which means that the system was open, so it continuously received new inputs of nutrients. In addition, a similar volume of water was removed from the incubator. Influxes and outfluxes to and from the incubators were done at the same rate, so that the volume inside was kept constant. Continuous cultures are preferred to batch cultures. In batch cultures, the growth can stop as nutrients become depleted and metabolites are produced much more rapidly, as the culture deteriorates. Continuous cultures ensure the nutrient availability throughout the experiment and dilute the metabolites. It allows cultures to reach equilibrium.

### *Laboratory work*

Once at Sagres, the cork stoppers were impermeabilized again with parafilm and tape. This was done, as discussed before, to avoid exchange of water between the incubators and the water present in the surrounding tank, to maintain constant conditions. The 70 L of water were then filtered using two cartridge filters from Cole Parmer Instruments Co: 25  $\mu\text{m}$  and 0.2  $\mu\text{m}$ . This step was done in order to eliminate algae, fauna and bacteria present in the water. The water was divided in different 20L bottles to prepare the different nutrient conditions. An adaptation of the Guillard's F/2 medium recipe (Guillard and Ryther, 1962; Guillard, 1975) was used to reach the final concentration of each condition (Full information included in Appendix II) for silica, phosphate and nitrate. Each 20L were used to fill one of four reservoirs.

The incubators were filled with around 1.5 / 1.7 L of enriched seawater, prepared previously, and placed in the tank. All the tubing connections were done and the holding tank was filled (Figure 6.9). The water was pumped into each incubator by a peristaltic pump at a rate of 0.5L per day. A vacuum system was used to remove the excess water in the incubator, every 10 minutes, in order to keep a constant volume. Air bubbles were pumped inside each incubator to ensure adequate aeration. The air was filtered with a cotton-wool filter. The glass stirrer was prepared to spin in a relatively low velocity. This was done to avoid disturbing the sediment and water within the incubator. The tank was covered to ensure that the lamps used were the only light source. The mean light was as high as possible, and it was much higher than what was used by Edwards (2001). In May, during midday on a sunny day the light measured in the field was around  $1100 \mu\text{mol}\cdot\text{s}^{-1}\cdot\text{m}^{-2}$ .

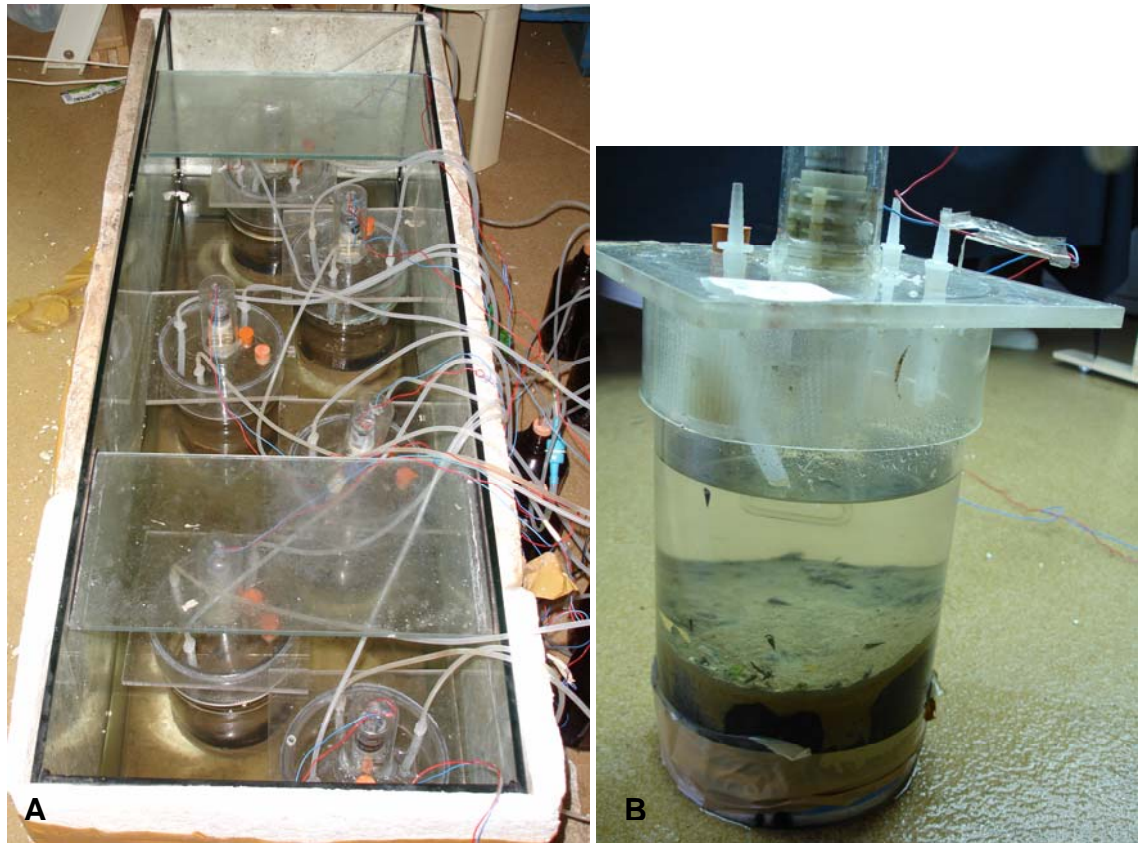


Figure 6.9 – A - Experimental tank and B –device.

A temperature sensor was introduced in the tank to record the temperature variation throughout the second and third experiment. Besides that, temperature and salinity were checked every day to ensure good conditions throughout the experiment. PAR was also checked twice during the experiment with a Li-Cor (Li-192) Underwater Quantum sensor, in the beginning and in the middle of the experimental period. The mean light intensity, mean temperature, daylength and salinity were as similar as possible to the natural conditions and are described below.

#### *Experiment zero*

The pilot study was performed using muddy sediment, which was collected on the 18<sup>th</sup> April 2007. Two different nutrient treatments were prepared as described for the first experiment (see below). Two control incubators (1 per treatment) and four treatment incubators (two per treatment) were used. The light regime used was also the same as described for the first experiment. The experiment was run for 9 days.

Results of this pilot study are not presented here because the set up revealed some problems. Small losses of water from the incubators were discovered during the first days. The water level inside the incubators was higher than outside and it started to decrease. There was a leaking problem and also possible water exchanges between the incubator and the tank. Reinforcement in the coverage of the incubators with parafilm was done in order to resolve the problem. The experiment continued and the problem was solved. The water level in the tank was adjusted and it proved to be working properly.

### *First Experiment*

This experiment was performed using sandy sediment which was collected on the 4<sup>th</sup> May 2007. It was planned to have two different treatments with two incubators each (four incubators in total) and one control for each treatment (two incubators). The treatments consisted of enriched waters with phosphate limitation and with nitrogen limitation in regards to the Redfield ratio of 16:1 (N:P; Table 6.1). The nitrate concentrations followed previous similar studies (Edwards, 2001). Silica concentrations were larger than the ones suggested by the Redfield Ratio of approximately 1:1 (Si:N; Lane *et al.*, 2004), however it was decided to use this concentrations since silica requirements of the benthic algae are likely to be larger than those of pelagic algae, since benthic diatoms typically have thicker cell walls (Tett, personal comment). Incubator 1 had enriched water in agreement with the ‘Control N-lim’ of Table 6.1. Incubator 2 had enriched water in agreement with ‘Control P-lim’, incubators 3 and 4 had enriched water according to the ‘N-limitation’ and incubators 5 and 6 had ‘P-limitation’.

Table 6.1 – Nutrient concentrations of enriched water in the reservoirs and seawater concentrations for the first experiment.

Incubators	conditions	nutrient concentration ( $\mu\text{M}$ )			
		N	P	Si	N:P
Inc. 1	Control N-lim	0	1.8	30	
Inc. 2	Control P-lim	18	0	30	
Inc. 3,4	N - limitation	12	1.8	30	< 16:1
Inc. 5, 6	P- limitation	18	0.3	30	> 16:1
	Seawater 1st Exp	0.159	0.264	7.965	< 16:1



The experiment was run for 9 days. Table 6.2 describes the conditions found in the tank during the period of the experiment. Lamps were programmed to switch on and off according to what is described in the table.

Table 6.2 – Daylength in terms of daylight and night hours, mean light, temperature and salinity during the first experiment.

Experiment	Daylength (hours D:N)	Mean Light ( $\mu\text{mol.s}^{-1}\text{m}^{-2}$ )	Temperature ( $^{\circ}\text{C}$ )		Salinity (psu)	
			Initial	Final	Initial	Final
1 <sup>st</sup> Exp	14:10	105.31	17.5	19.75	36.2	36.3

### *Second Experiment*

This experiment was performed with muddy sediment, which was collected on the 24<sup>th</sup> May 2007. The treatments used during this experiment were exactly the same as previously. The nutrient concentrations of enriched water were the same and were similarly distributed in the incubators. The only difference was the larger nutrient concentrations found in seawater (Table 6.3).

Table 6.3 – Seawater concentrations for the second experiment.

Incubators	conditions	nutrient concentration ( $\mu\text{M}$ )			
		N	P	Si	N:P
Inc. 1	Control N-lim	0	1.8	30	
Inc. 2	Control P-lim	18	0	30	
Inc. 3, 4	N - limitation	12	1.8	30	< 16:1
Inc. 5, 6	P- limitation	18	0.3	30	> 16:1
	Seawater 2nd Exp	0.751	0.603	7.826	< 16:1

The experiment was run for 9 days. Table 6.4 describes the conditions found in the tank during the period of the experiment.

Table 6.4 – Daylength in terms of daylight and night hours, mean light, temperature and salinity during the second experiment.

Experiment	Daylength (hours D:N)	Mean Light ( $\mu\text{mol.s}^{-1}\text{m}^{-2}$ )	Temperature ( $^{\circ}\text{C}$ )		Salinity (psu)	
			Initial	Final	Initial	Final
2 <sup>nd</sup> Exp	14:10	109.53	18.1	20.5	36.4	36.6

The temperature sensor reported a slight and gradual increase of about 2°C of the temperature during the period of the experiment (Figure 6.10). A clear increase in the temperature during the light period was followed by a decrease during the night period every day.

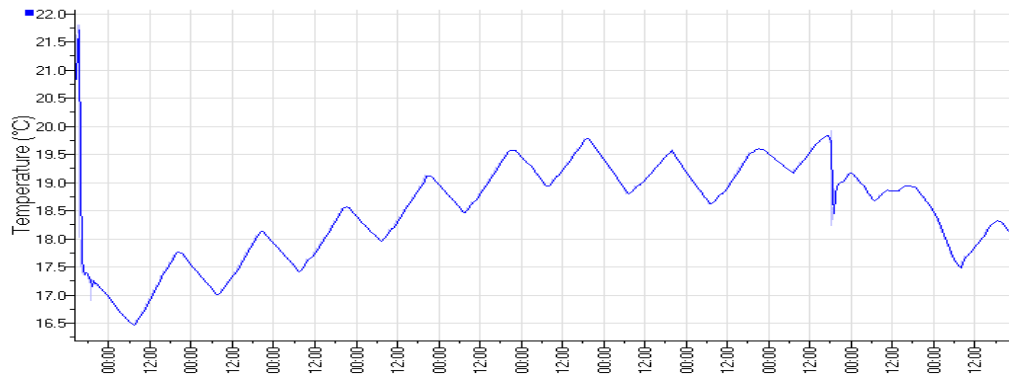
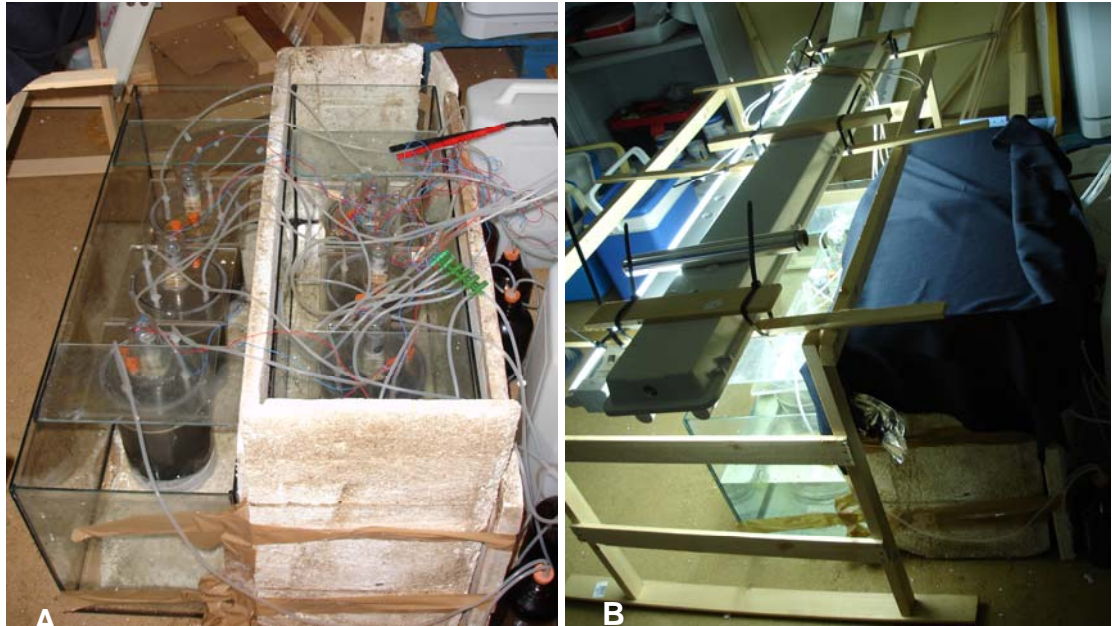


Figure 6.10 – Temperature variation during the second experiment. The last peak around 19.75°C corresponds to the end of experiment.

### *Third Experiment*

The experiment was repeated one more time on the 16<sup>th</sup> September 2007 using mud. This experiment was done in a slightly different way. This time, the aim of the experiment was to study the differences in the nutrient fluxes and  $q$  value in incubators exposed to light and dark conditions. Theoretically, without light photosynthesis will not happen, so it could be easier to determine the effect of pore water – water column fluxes and other processes, like denitrification or mineralisation on water column nutrient concentrations. It became clear that the experiment should be repeated because of the unexpected variation of nutrients during the first two experiments. To ensure complete darkness, the incubators were placed in two different tanks and one of them was completely covered (Figure 6.11).



Figures 6.11– Tanks with dark (A) and light conditions (B).

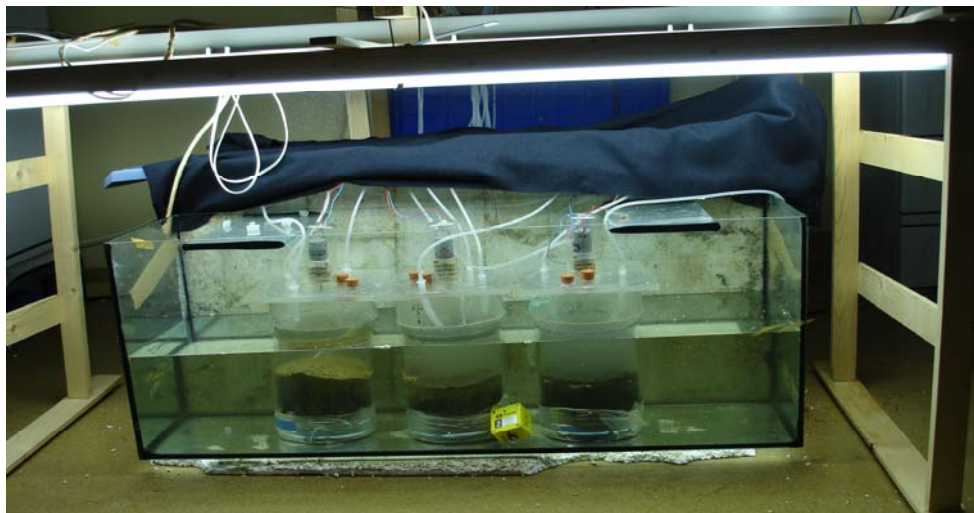


Figure 6.12 – Tanks with dark and light conditions.

The experiment was run for 5 days. Table 6.5 describes the conditions found in the tank during the period of the experiment.

Table 6.5 – Daylength in terms of daylight and night hours, mean light, temperature and salinity during the third experiment.

Experiment	Daylength (hours D:N)	Mean Light ( $\mu\text{mol}\cdot\text{s}^{-1}\cdot\text{m}^{-2}$ )	Temperature ( $^{\circ}\text{C}$ )		Salinity (psu)	
			Initial	Final	Initial	Final
3 <sup>rd</sup> Exp - Light	14:10	107.46	18.7	22.4	36.5	36.6
3 <sup>rd</sup> Exp - Dark	0:24	4.09	18.8	21.8	36.4	36.6

There was one control incubator in each tank, incubator 1 under light conditions and incubator 2 under dark conditions, and two incubators with the same nutrient concentrations (incubators 3 and 4 – light conditions; incubators 5 and 6 – dark conditions; Table 6.6). This experiment was done only with the concentrations correspondent to the N-limitation because the other experiments showed indications of N limitation. Furthermore, data collected in Ria Formosa also indicated this limitation, as discussed in Chapter 3.

Table 6.6 –Nutrient concentrations of enriched water and seawater concentrations.

Incubators	conditions	nutrient concentration ( $\mu\text{M}$ )			
		N	P	Si	N:P
Inc. 1, 2	Control N-lim	0	1.8	30	
Inc. 3, 4, 5, 6	N - limitation	12	1.8	30	< 16:1
	Seawater 3rd Exp	2.207	0.555	8.201	< 16:1

The temperature sensor reported the daily variation of temperatures during the light exposure and darkness of the tank (Figure 6.13).

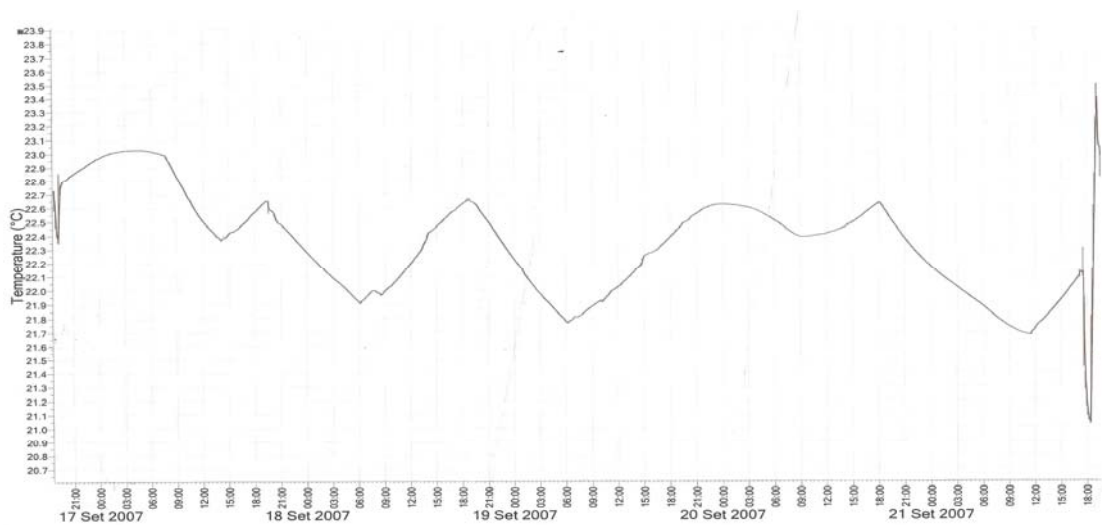


Figure 6.13 – Temperature variation during the third experiment in the tank with light.

The daily pattern of temperature variation was not so clear in the tank without light. However, small variations were found in the same period of the peaks in the other tank (Figure 6.14).



Figure 6.14 – Temperature variation during the third experiment in the tank without light.

### 6.2.4 Sample collection

At the beginning of all the experiments (day 0), sediment samples were collected before the addition of the initial enriched water using a syringe of about 1cm diameter until a depth of approximately 1cm (Figure 6.15). Water samples were also collected. Afterwards, sediment samples were collected using the same device through the sampling ports every day. Water samples were obtained via the action of the vacuum system, described previously, and were collected in 6 glass bottles of 0.5L, every day.



Figure 6.15 – Material used to collect sediment from the incubators.

### 6.2.5 Methods used for sample analysis

#### *Nutrients*

Samples were immediately analysed, if possible, or frozen at  $-20^{\circ}\text{C}$ . Each sample was analysed in triplicates of  $15\text{ cm}^3$  for ammonium-nitrogen, nitrite-nitrogen, nitrate-

nitrogen, ortophosphate-phosphorus and silicate-silicon following Grasshoff *et al.* (1983). The detection and quantification of these analyses are presented in Appendix I. An example of the calibration curve is also shown.

### *Benthic Chlorophyll*

The procedure followed was the same described previously in Chapters 3, 4 and 5, except that the plastic tubes used in this study were smaller, of 10 cm<sup>3</sup>. The plastic tubes were wrapped in aluminium foil and placed in the freezer at -20°C. All the samples were freeze-dried for 30 hours. The weight of the sediment was determined after freeze-drying. The solvent, 90% acetone for sand and 80% acetone for muddy samples, buffered with sodium bicarbonate, was added to each sample in a similar proportion of solvent volume to sediment weight and the tubes were stirred in the vortex, as discussed in Chapter 3. The samples were placed again in the freezer at -20°C for 6 hours. The samples were then centrifuged and chlorophyll measured as described in Chapter 3. However, a 10% dilution was done in 90% acetone. This was done to allow the use of spectrophotometric equations for 90% acetone in muddy samples and to decrease the solution concentration to permit a more reliable measurement. To calculate the chl *a* content (µg/g), the weight of dry sediment was used instead of the usual volume of filtered water.

### **6.2.6 Analysis of fluxes – Numerical approach**

An analysis of the nutrient concentrations in the water column obtained during the experiments is not sufficient to obtain the required information to discuss the nutrient dynamics and fluxes existent in the incubators. The dynamics are complex and involve a large number of processes such as diffusion of nutrients, mineralisation of particles and denitrification, for example. As stated before, the concentrations in the pore water of sediments are likely to be much higher than the concentrations in the water column, even considering nutrient enrichment. From the first experiments carried out, it was possible to acknowledge the difficulty to assess the amount of chlorophyll produced by algae from nutrients. Concentrations of some nutrients were increasing greatly in the water column and no realistic assumptions could be made about nutrient fluxes from the sediments because all processes were happening at the same time, most specifically,

nutrient fluxes and nutrient uptake by algae. Therefore, a new approach was carried out during the third experiment to assess the nutrient fluxes by limiting the algal growth and therefore algal uptake of nutrients. This was achieved by forcing algae to be in dark conditions during the period of the experiment. This approach provided realistic values of nutrient fluxes, or diffusion, that would always happen during these experiments and facilitate the analysis of results of the first and second experiment. Other processes, such as denitrification or nitrification, are not considered in this analysis due to the additional complexity that would be introduced.

A Matlab programme was then created and developed to evaluate all the processes and calculate changes of nutrients, chlorophyll and the yield of chlorophyll from nitrogen (Appendix II). This resulted from a close collaboration between Ana Brito and Prof. Paul Tett. The yield ( $q$ ) was determined from the changes of chlorophyll concentration ( $X$ ) divided by the changes of nutrient concentration due to consumption ( $S$ ; nutrient consumption or uptake):

$$q = \frac{\Delta X}{-\Delta S} \text{ (}\mu\text{g chl.}\mu\text{mol}^{-1}\text{)} \quad (6.12)$$

As discussed above, the nutrient dynamics inside the incubators are complex. Moreover, the chlorophyll dynamics are also complicated due to the fact that the sediment is undisturbed and therefore contains grazers.

The main concept of the numerical script used in the analysis of the results is to describe nutrient changes from the nutrient input of reservoirs ( $res$ ; enriched water), from the fluxes that may occur between sediment and water column ( $flux$ ) and from the uptake of nutrient by algae ( $uptake$ ):

$$\frac{\partial S}{\partial t} = res + flux - uptake \text{ (}\mu\text{mol N.cm}^{-2}\text{.d}^{-1}\text{)} \quad (6.13)$$

In order to determine the flux term for Equation 6.13, the final results from the third experiment, under dark conditions, have to be used in the beginning of the numerical analysis to obtain the mean nutrient flux for nitrogen, phosphorus and silicon, which will be used throughout the study. For the incubators under dark conditions, it is considered that no algal growth is possible and therefore, no algal nutrient uptake takes place. Thus:

$$flux = \frac{\partial S}{\partial t} - res \quad (6.14)$$

The term *uptake*, which is actually what is consumed by the microphytobenthos to grow, is the important term that will be used to calculate the yield.

In addition, chlorophyll changes are calculated from the observed chlorophyll change ( $\Delta X$ ) and the loss term of chlorophyll grazed in the incubators ( $L.X$ ):

$$\frac{\partial X}{\partial t} = \Delta X + L.X \text{ (}\mu\text{g chl.cm}^{-2}\text{.d}^{-1}\text{)} \quad (6.15)$$

To determine the loss rate ( $L$ ), it was considered that the system was in equilibrium between loss and growth of microphytobenthos, during the last days of the experiment. Contents of microphytobenthic chlorophyll did not generally increase after 3 days of the experiment. In a few cases, there was actually a decrease. Therefore, it was considered that all new algal chlorophyll produced was grazed by organisms present inside the incubators. So, it was considered that:

$$L.X = \mu X \quad (6.16)$$

Where  $\mu X$  is the microphytobenthos growth. In previous versions of the analysis of microphytobenthic chlorophyll dynamics, growth was calculated using equations considering the specific growth rate. However, it was concluded that the best approach is to work with the increase in algal biomass ( $\mu\text{g chl.cm}^{-2}\text{.d}^{-1}$ ) instead of with relative growth rates ( $\text{d}^{-1}$ ). In the equation,  $\mu X$  is a single term (and not the product  $\mu.X$ ). This topic will be discussed and described in detail in Chapter 7. So, for the purpose of this Chapter, growth is dependent on nutrients ( $\mu S$  - nutrient limited growth) and light ( $\mu I$  - light limited growth):

$$\mu X = \min(\mu S, \mu I) \text{ (}\mu\text{g chl.cm}^{-2}\text{.d}^{-1}\text{)} \quad (6.17)$$

The approach considered to obtain the microphytobenthos growth ( $\mu X$ ) was described previously, in the introduction section. The theory of the microphytobenthos growth used for these calculations was developed for modelling purposes and applied here.

### 6.2.7 Statistical analysis

Statistical tests were carried out using Minitab 14 software. Data were tested for normality and homoscedasticity of variance and parametric tests (ANOVA) conducted. Multiple comparisons among pairs of means were performed using the Tukey test, when a significant difference was found with ANOVA.



## 6.3 Results

### 6.3.1 Observed concentrations

#### *First Experiment*

Concentrations of microphytobenthos chlorophyll in incubator 1 (Control N –limitation) were stable during the experiment, around  $5 \mu\text{g chl.g}^{-1}$  (Figure 6.16- A). In incubator 2 (Control P-limitation), MPB concentrations dropped to around  $2.5 \mu\text{gchl.g}^{-1}$ . Concentrations of silicate were always large, but smaller than the ones in the enriched water. Nitrogen concentrations were small in incubator 1 and a slight increase was found on day 7. In incubator 2, the large nitrogen concentration added and found in the beginning of the experiment decreased in the end, with a slight increase during the last 2 days. Phosphate concentrations were always extremely small in both incubators.

Nitrate and phosphate concentrations were small in incubators 3 and 4 (N-limitation; Figure 6.16-C,D). However, ammonium concentration increased during the experiment. Silicate concentrations were most of the time smaller than in the enriched water. Chlorophyll concentrations did not show any increase during the period.

Phosphate concentrations were larger in incubators 5 and 6 (P-limitation; Figure 6.16-E,F). They were not consumed during the experiment. Nitrate concentrations were larger in the beginning, which is in agreement with the enriched water added, but its concentration rapidly decreased. Silicate concentration of incubator 5 was not presented because it reached values of  $150 \mu\text{M}$ . Larger concentrations of silicate than the ones in the enriched water were found in these two incubators during the experiment. Again, chlorophyll concentration was relatively stable around  $5 \mu\text{g chl.g}^{-1}$ .

#### *Second Experiment*

Phosphate and nitrate concentrations were very small in incubator 1 (Control N-limitation) which is in agreement with the enriched water (Figure 6.17-A). Incubator 2 (Control P-limitation) received nitrate enriched water, however concentrations also dropped rapidly. Furthermore, a great increase in ammonium was found in both

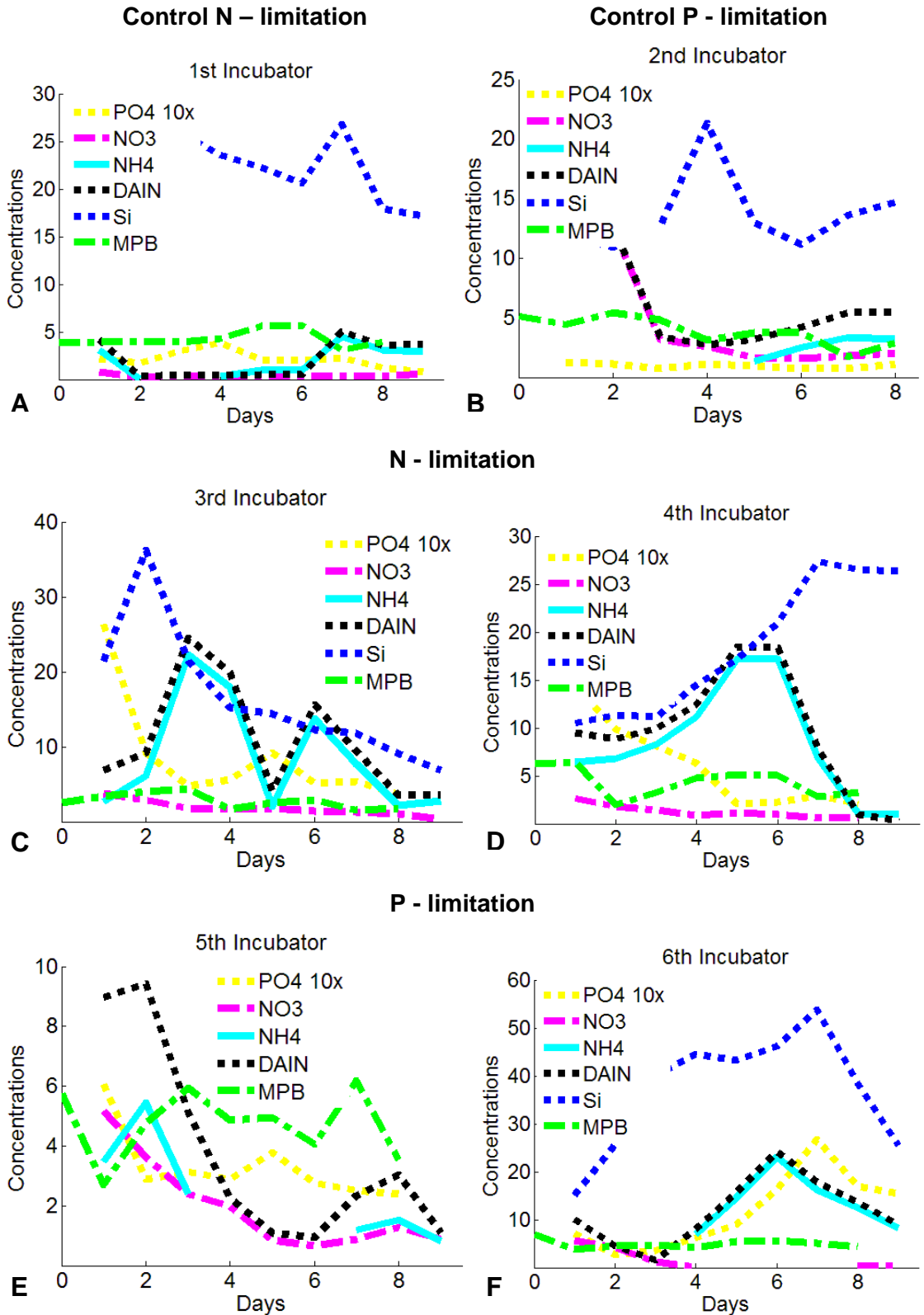


Figure 6.16 – Concentrations of nitrate, ammonium, DAIN, silicate, phosphate ( $\mu\text{M}$ ) and microphytobenthic chlorophyll ( $\mu\text{g chl.g}^{-1}$ ) in incubator 1 (A), 2 (B), 3 (C), 4 (D), 5 (E) and 6 (F), during the first experiment (sand). Incubators 1 and 2 are both controls for N-limitation and P-limitation. Incubators 3 and 4 have N-limitation and incubators 5 and 6 have P-limitation. Concentrations of Si in Incubator 5 were very high (approximately  $170 \mu\text{M}$ ) and were not included due to resolution.

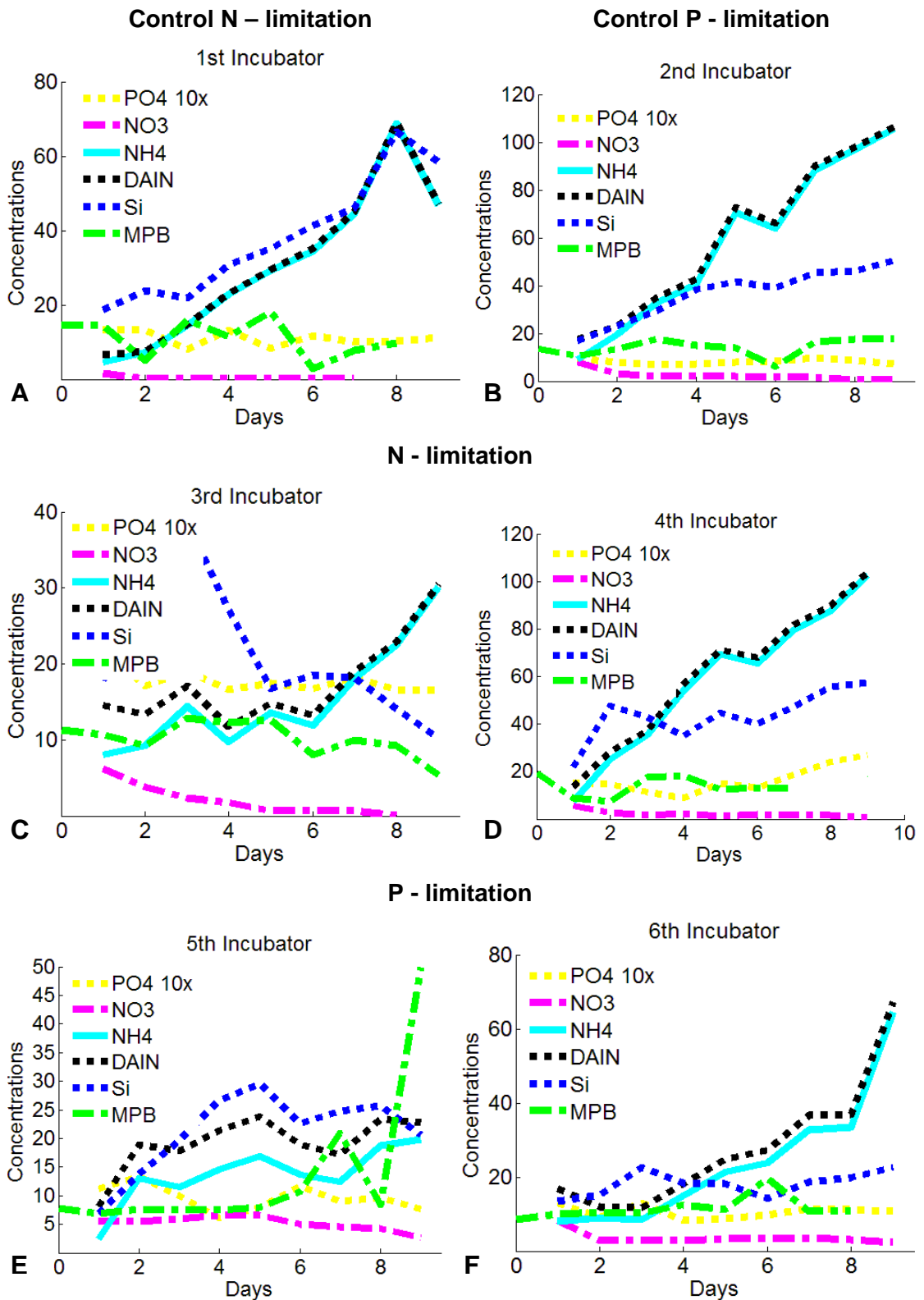


Figure 6.17– Concentrations of nitrate, ammonium, DAIN, silicate, phosphate ( $\mu\text{M}$ ) and microphytobenthic chlorophyll ( $\mu\text{g chl.g}^{-1}$ ) in incubator 1 (A), 2 (B), 3 (C), 4 (D), 5 (E) and 6 (F), during the second experiment (mud). Incubators 1 and 2 are both controls for N-limitation and P-limitation.

Incubators 3 and 4 have N-limitation and incubators 5 and 6 have P-limitation.

incubators during the period of the experiment. Chlorophyll concentrations varied, especially in incubator 1, but always around the same concentration. No increase in chlorophyll concentration was found. Silicate concentrations were also large and increased during the experiment.

Nitrate concentrations dropped almost to zero in incubators 3 and 4 (N-limitation; Figure 6.17-C,D). Phosphate concentrations also dropped in incubator 4 but were stable in incubator 3. Ammonium concentrations increased greatly again. Chlorophyll concentrations were relatively constant.

Nitrate concentrations were not totally depleted in incubators 5 and 6 (P-limitation; Figure 6.17-E,F). Phosphate concentrations were very small, which was in agreement with the enriched water. Silicate concentrations were similar to the ones in the enriched water. Ammonium concentrations increased again, strongly in incubator 6.

### *Third Experiment*

Silicate concentrations increased in incubator 1 (control N - light conditions) and 2 (Control N - dark conditions; Figure 6.18). However, in incubator 1, the concentrations started to drop on day 3. Nitrate and phosphate concentrations decreased down to almost 0. Ammonium concentrations increased slightly in both incubators during the experiment. Chlorophyll concentrations were relatively constant.

Silicate concentrations increased during the experiment but were never larger than the ones of the enriched water in incubators 3 and 4 (N limitation - light conditions; Figure 6.18-C,D). Nitrate, phosphate and ammonium concentrations decreased during the experiment to small values. Chlorophyll concentrations were similar during the period of the experiment and in both incubators.

Silicate concentrations also increased and reached concentrations larger than 30  $\mu\text{M}$  in incubators 5 and 6 (N limitation - dark conditions; Figure 6.18-E,F). Ammonium concentrations strongly increased during the experiment. Nitrate and phosphate concentrations decreased in both incubators. Chlorophyll concentrations increased slightly in incubator 6.

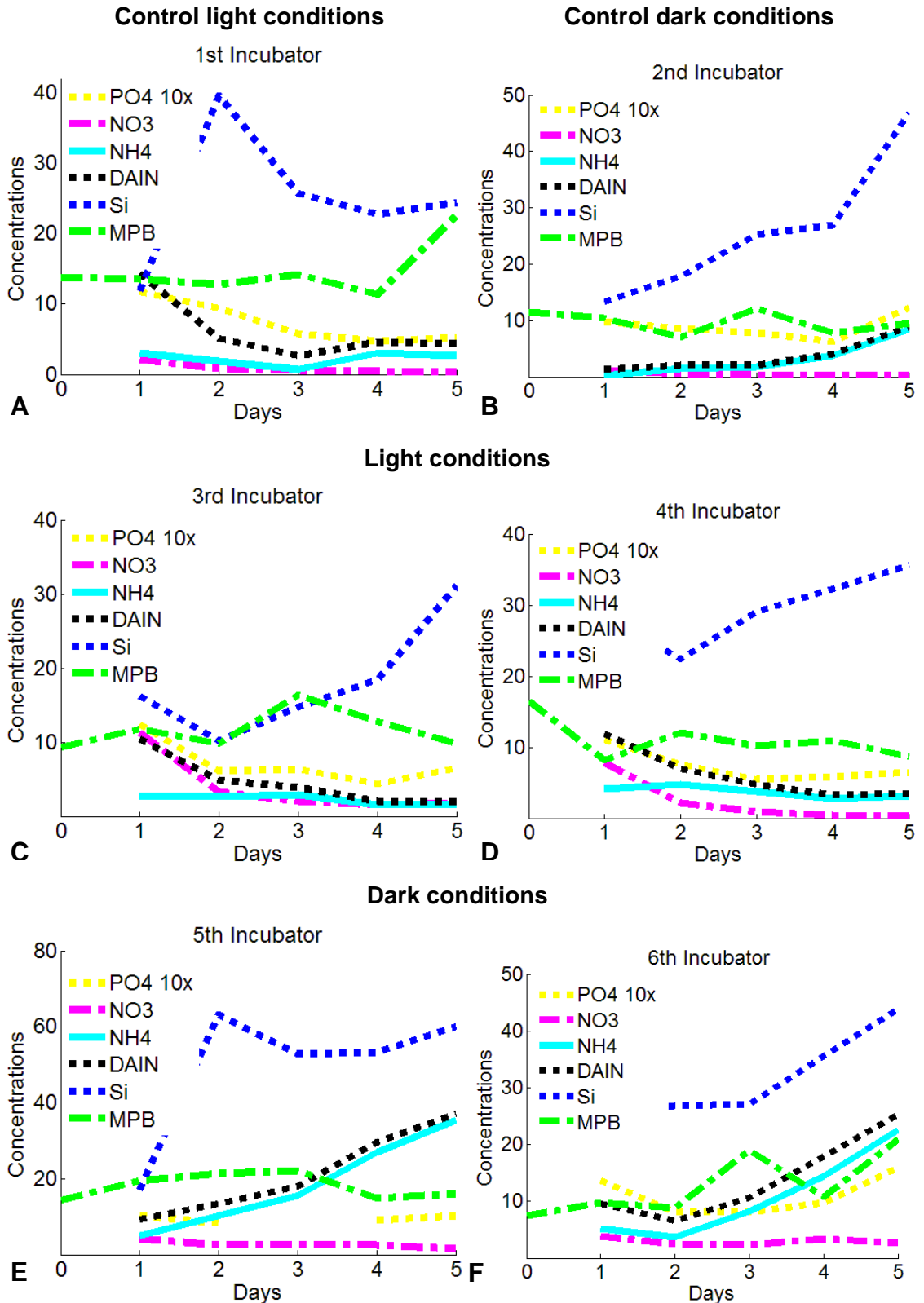


Figure 6.18– Concentrations of nitrate, ammonium, DAIN, silicate, phosphate ( $\mu\text{M}$ ) and microphytobenthic chlorophyll ( $\mu\text{g chl.g}^{-1}$ ) in incubator 1 (A), 2 (B), 3 (C), 4 (D), 5 (E) and 6 (F), during the third experiment (mud). Incubators 1 and 2 are both controls for light and dark conditions. Incubators 3 and 4 were under light conditions and incubators 5 and 6 were under dark conditions. Each one of the six incubators have a N-limitation nutrient regime.

### 6.3.2 Nutrient fluxes

During dark conditions, nutrients are not being consumed by algae because there is no photosynthesis or growth. Therefore, concentrations in the water column are expected to increase due to the flux from the sediment to the water column. Nitrogen concentrations in the water column increased in both incubators after the second day, as represented by positive fluxes (Figure 6.19). Positive fluxes represent the flux from sediment to the water column and negative fluxes, from the water column to the sediment. Phosphorus concentrations decreased, as represented by negative fluxes during the whole experiment, except on the last day in incubator 2. Silicon concentrations increased during most of the experiment, except few exceptions, when the fluxes were negative.

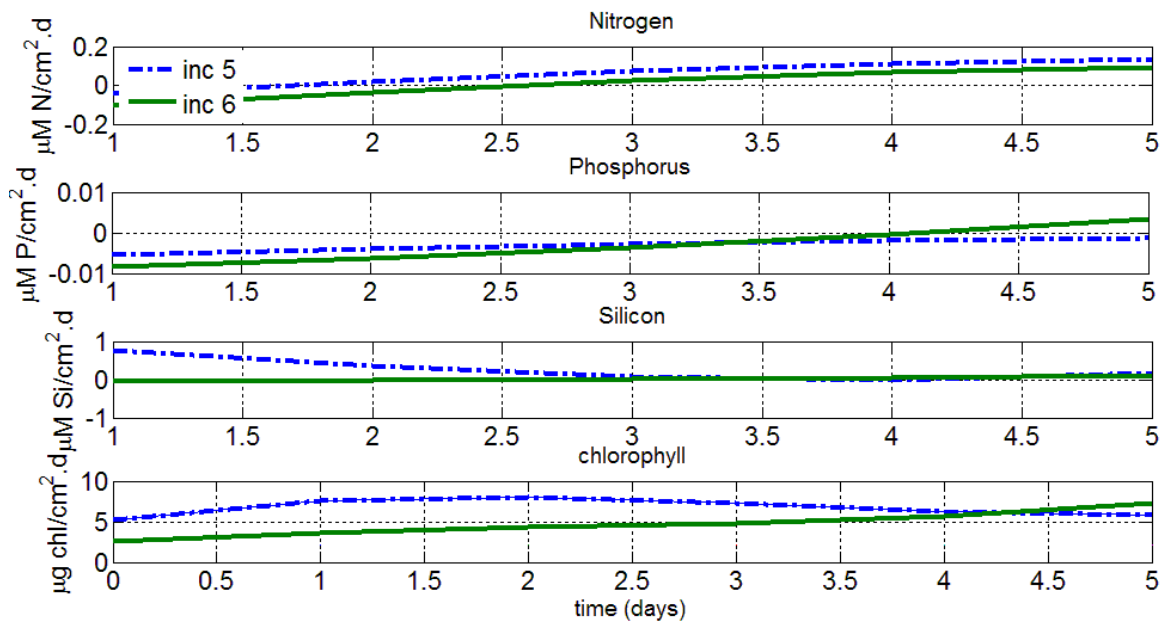


Figure 6.19 – Nutrient fluxes between sediment and water column of nitrogen, phosphorus and silicon, observed during the third experiment under dark conditions (incubators 5 and 6). Chlorophyll changes through the experiment are also presented.

Nutrient fluxes were estimated as described in the methods section, using nutrient concentrations obtained at dark conditions (Table 6.7). Fluxes were estimated considering solely the nutrient fluxes of the last two days of the experiment. Conditions are considered to be more stable at the end of the experiment, compared to the beginning. One negative value of silicon flux was excluded from these estimates.

Table 6.7 – Mean values of sediment – water column nutrient fluxes ( $\mu\text{mol} \cdot \text{cm}^{-2} \cdot \text{d}^{-1}$ ) obtained from experiment in dark conditions.

Nitrogen	Phosphorus	Silicon	Units
0.1015	-0.0015	0.1395	$\mu\text{mol} \cdot \text{cm}^{-2} \cdot \text{d}^{-1}$

Nitrogen and phosphorus fluxes were negative during the whole third experiment in light conditions (Figure 6.20). Silicon fluxes were positive during the last days of the experiment.

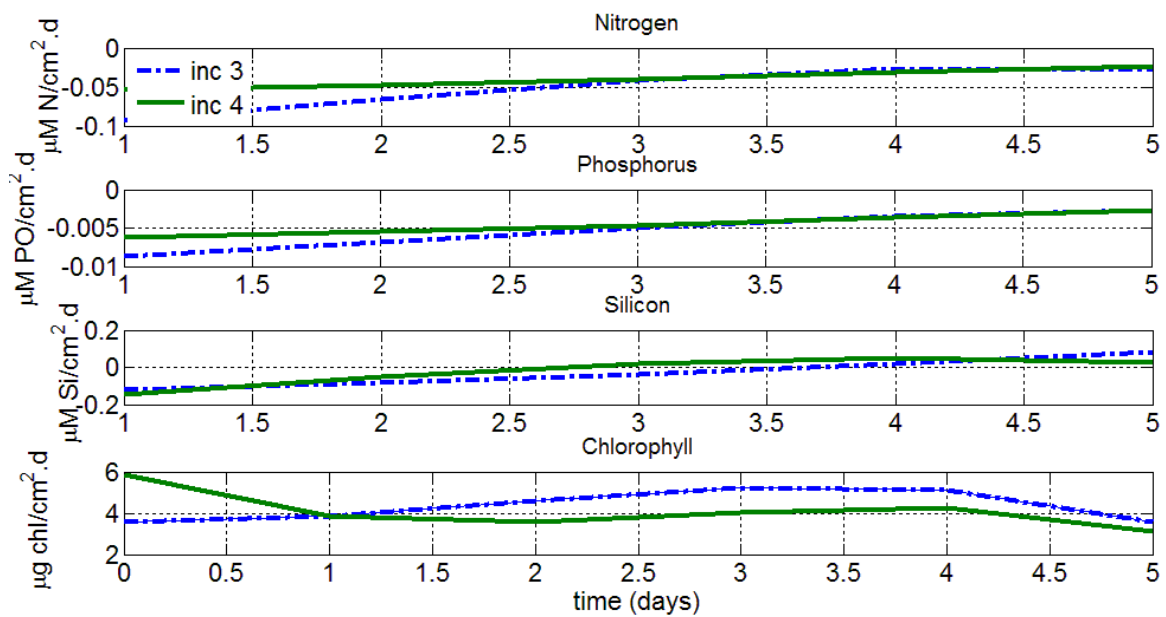


Figure 6.20 – Nutrient fluxes between sediment and water column of nitrogen, phosphorus and silicon, observed during the third experiment under light conditions (incubators 3 and 4) . Chlorophyll changes through the experiment are also presented.

### 6.3.3 Yields of chlorophyll from nutrients

The nutrient uptake for DAIN, phosphate and silicate were calculated for all experiments, following Equation 6.13 and using the nutrient fluxes values estimated above at dark conditions. Chlorophyll change was also estimated, following Equation 6.15, and used to assess the yield of chlorophyll from each nutrient (Table 6.8). Daily values of nutrient uptake and chlorophyll change from each incubator were used to calculate the yield. A matrix of yield values was obtained for each incubator and the range of yields are presented in Table 6.8. Yields from phosphate were omitted because

they are not correct. They were obtained using negative values of phosphate flux or chlorophyll change.

Significant differences between the yields from nitrogen obtained in the experiments were found ( $p < 0.005$ ; ANOVA). A Tukey test revealed that yields obtained in the second experiment (P limitation) were larger and significantly different from the yields obtained in the first experiment (N and P limitation) and in the second experiment (N limitation). No significant differences were found between the yields obtained in the second experiment (P limitation) and in the third experiment (at light conditions). No significant differences were also found between the yields from silicon obtained in the experiments ( $p > 0.05$ ; ANOVA).

Table 6.8 – Range of values and means of the yield ( $\mu\text{gchl.}(\mu\text{mol})^{-1}$ ) of chlorophyll from DAIN, and silicate obtained from the three experiments.

Sediment Type	Experiment	Yields	
		DAIN	Silicate
Sand	1 <sup>st</sup> – N limitation	0.82 – 9.39	0.54 – 3.67
	mean	3.5	1.71
	1 <sup>st</sup> – P limitation	0.33 – 6.44	0.22 – 9.57
	mean	2.54	4.77
Mud	2 <sup>nd</sup> - N limitation	1.66 – 4.61	0.66 – 8.9
	mean	3.65	4.773
	2 <sup>nd</sup> – P limitation	0.728 – 12.99	0.5 – 13.10
	mean	8.9	4.896
Mud	3 <sup>rd</sup> – Light	0.27 – 7.11	0.21 – 6.8
	mean	4.11	4.03

## 6.4 Discussion

### 6.4.1 Observed concentrations

The observed increase of nitrogen concentrations in incubators 1 of the first and second experiment was initially surprising. Incubator 1 of each experiment did not have any addition of nitrogen and therefore, the increase observed had to be caused by the nutrient dynamics in the incubator, within the sediment. The nitrogen increase was



mainly caused by ammonium concentrations and was especially evident in the second experiment, using mud. Sandy sediment is considered to have smaller concentrations of nutrients, especially ammonium, as discussed in Chapter 5, and by authors such as Murray *et al.* (2006) and Serpa *et al.* (2007). The smaller amount of organic matter in sandy sediments is probably the main reason for smaller ammonium concentrations. This was the first indication of the importance of sediment processes such as mineralisation, diffusion or nitrification (Gönenç and Wolflin, 2005). The increase in ammonium concentration was also evident in incubator 2 of the first and second experiments, especially during the last days. Nitrate concentration decreased through the experiment and ammonium concentration increased. Phosphate concentrations did not show any great change during the experimental periods. Actually, phosphate concentrations were always relatively small. For silicate, large concentrations were found in some incubators, especially in the second experiment. Concentrations were even larger than the ones added in the enriched water. This means, that as for nitrogen, there should be an additional source of silicate to the water column, the sediment. Another interesting point of these results was the balance between phosphate and nitrogen. If a large concentration of nitrate is present in the system, it will decrease rapidly to values of around 0. The same did not happen for phosphate. Concentrations of phosphate were relatively stable during experiments and were sometimes larger than nitrate. The N:P ratio throughout the experiments was most of the time under 16:1 (Redfield ratio), even in the incubators set up with phosphorus limitation, which suggests a nitrogen limitation of the system. Although these changes are very informative, further studies would be useful and necessary to accurately conclude on the nutrient limitation because it is not possible to establish direct associations between nutrient changes and the increase or the stabilization of chlorophyll in the system due to its high variability and patchiness. It is relatively easy to have an indication of which nutrient is limiting the primary production using microcosms with different nutrient regimes and no additional factors of nutrient and chlorophyll variation as done by Taylor *et al.* (1995; 1995b) and Edwards *et al.* (2003; 2005).

It is extremely difficult to understand microphytobenthos chlorophyll dynamics just by evaluating the observed concentrations during the experiments. Microphytobenthos is highly variable in space as discussed in Chapter 4. It became clear that results from these experiments would have to be analysed in other terms, by developing a system of equations that would help to assess interactions between nutrient and chlorophyll

dynamics, as described in the methods section. Edwards *et al.* (2003; 2005) who estimated for the first time the yield of chlorophyll from nitrogen for phytoplankton, were able to calculate directly the nutrient and chlorophyll changes in their microcosms mainly because it was not as complex as this one. Nutrient concentrations were homogeneous in their system and did not have sediments or any other such factor influencing its concentration. Chlorophyll concentrations were also homogeneous in the system. There were no grazers in their system that could also contribute to concentration changes.

The third experiment was carried out to investigate the nutrient fluxes between the sediment and the water column, using the principle that under dark conditions, no growth would occur and therefore microphytobenthos would not take nutrients up from the sediment and water column. In theory, it would allow an assessment of any differences between the nutrient concentrations in the water column in light and dark conditions. In fact, we consider this experiment to be a success because it expresses everything we were expecting. Nitrogen concentrations increased greatly in dark conditions and decreased in light conditions. The large change allowed the estimation of nutrient fluxes for nitrogen, phosphorus and silicon. It is interesting to note that the main increase of ammonium concentrations started after day 2. Incubators 2 and 6 are good examples of this phenomenon. In incubator 5 the increase started in day 1 but it was greater after day 2.

It is documented in the literature (see Björk-Ramberg, 1985 and Fan and Glibert, 2005, for example) that even in darkness, algae may continue to take nutrients up for a short period, which can happen at a similar or smaller rate, compared to the dynamics in light conditions. Edwards (2001) and Edwards *et al.* (2003) also observed a great uptake of nitrogen by algae, and a consequent great increase of phytoplankton chlorophyll concentration, during the first two days after enrichment of experiments in a microcosm. After day 2, the uptake of nitrogen and the phytoplankton chlorophyll growth decreased and became stable after day 3 or 5. However, this variation is associated with a different process. In the beginning of the experiment, phytoplankton reached a maximum of chlorophyll at day 2, due to the high concentration of nutrients. Then, it decayed and reached equilibrium. The fact that the nutrient concentration did not increase in the first days under dark conditions in the current study, indicates that our results should be discussed as a mixture of several effects, at least during the first days of the experiment, when nutrient uptake is still expected. Moreover, the third

experiment also yielded interesting results regarding microphytobenthos chlorophyll dynamics. Despite being a small difference and considering the high spatial variability in microphytobenthos, an increase of chlorophyll concentration could be observed, especially in incubators 5 and 6. An increase of microphytobenthos was not expected because growth should not happen at dark conditions. This change however can be simply explained by the theory of algal photoacclimation (Geider *et al.*, 1997; Falkowski and Raven, 2007). At extremely low light levels, cells tend to increase their chlorophyll concentration within the thylakoid membranes, which become larger, thicker and with more layers. This corresponds to a great energy cost to each cell, but represents a great effort to increase the light harvesting rate of the chloroplast (Falkowski and Raven, 2007). Thus, as cells increase the number of pigments per membrane, each molecule becomes less effective at light absorption because self-shading of pigments occurs, although globally it brings benefits (Figure 6.21). It is therefore not possible to consider that the increase of MPB chlorophyll is directly related to the decrease in nitrogen concentrations, as hypothesized initially.

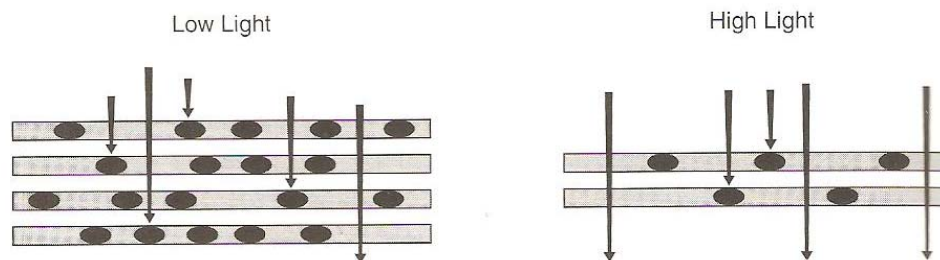


Figure 6.21 – Chloroplast ultrastructure at different light regimes (from Falkowski and Raven, 2007).

#### 6.4.2 Nutrient fluxes

Due to the fact that nitrogen concentrations in the water column were increasing more greatly at the end of the experiment and that some algal nutrient uptake could occur during the first days, it was decided to calculate the nutrient fluxes for the last two days of the experiment, when processes should be more stabilised.

The nitrogen flux estimated from this experiment was  $0.1015 \mu\text{mol}\cdot\text{cm}^{-2}\cdot\text{d}^{-1}$ . This value is extremely similar to the one proposed by Serpa *et al.* (2007) at about  $0.104 \mu\text{mol}\cdot\text{cm}^{-2}\cdot\text{d}^{-1}$ . Serpa *et al.* (2007) measured the nutrient concentrations in pore water and following the Fick's Law of diffusion, estimated the flux. This result is extremely interesting since it contradicts what was presented in Chapter 5 and thus leads to the rejection of the initial hypothesis of similar estimates. Following the same law used by

Murray *et al.* (2006) and Serpa *et al.* (2007), and considering pore water concentrations measured during this project, our estimates were ten times larger, at around  $1.176 \mu\text{mol}\cdot\text{cm}^{-2}\cdot\text{d}^{-1}$  and in agreement with Murray *et al.* (2006), who also presented similar results.

There are several factors that may explain this divergence of results. First, there is a conceptual difference in the calculations of fluxes between Murray's and Serpa's studies, due to the use of different layer thicknesses. Other possibilities such as the existence of denitrification have also to be considered.

The main difference between Serpa's and Murray's calculation, which can indeed lead to such difference, was the thickness of the layer involved in the diffusion, 2 cm for Serpa *et al.* (2007) and 2.5 mm for Murray *et al.* (2006) who followed Hopkinson's study to support their choice (Hopkinson *et al.*, 1999). Our calculations also used a thickness of 2 mm as explained before, in Chapter 5, and as recommended by Di Toro (2001), who stated that the sediment-water interface has 1 to 5 mm. This layer thickness is considered to be within the range, which means that the reason for the difference of results obtained in this study and by Murray *et al.* (2006) may be elsewhere.

One possibility is that not all the nitrogen was reaching the water column. This may be caused by the continuous uptake of nitrogen by algae to compensate for the chlorophyll production due to photoacclimation. The other possibility is that processes such as denitrification have a great importance and are not being considered in these calculations. Denitrification is higher at high temperatures, which Ria Formosa experiences, due to the higher microbial activity. Further studies on processes that may influence nutrient fluxes should be carried out in the future for a better understanding of these phenomena. It is extremely hard to ascertain which estimate is more accurate without having further information but if the difference is caused by natural biogeochemical process and not by unexpected algal uptake, estimates obtained from this experiment would be more accurate because they represent the system in a more realistic way. If none of these possibilities explain the difference, the existence of a thicker interface layer could also be considered and fully investigated.

The phosphate flux observed in these experiments was negative. This is again in contradiction to what was presented in Chapter 5, which was positive, and what is discussed by Murray *et al.* (2006) and Serpa *et al.* (2007). Our flux estimates were calculated following the Fick's Law of diffusion, as for nitrogen. Murray *et al.* (2006) and Serpa *et al.* (2007) also used the same law. This difference is probably due to the

fact that adsorption to sediments is not considered in calculations. Serpa *et al.* (2007) considered this process in their calculations and that may be the reason why their estimate was small. But, as before, they considered a thick interface layer, which would automatically decrease the value. The most reasonable possibility is that the adsorption phenomenon has great importance in phosphate dynamics.

The silicate flux estimate of  $0.1395 \mu\text{mol}\cdot\text{cm}^{-2}\cdot\text{d}^{-1}$  was within the range of values obtained in the study of Baric *et al.* (2002), who observed a maximum flux value of  $0.267 \mu\text{mol}\cdot\text{cm}^{-2}\cdot\text{d}^{-1}$  for the Adriatic Sea.

### 6.4.3 Yields of chlorophyll from nutrients

The yield of chlorophyll from nitrogen found for muddy sediments (second and third experiments) ranged from 0.27 to  $12.99 \mu\text{gchl}\cdot(\mu\text{molN})^{-1}$ . Significant higher values were obtained in the incubator with the phosphorus limitation. This was expected because in this case, the amount of available nitrogen was larger. Cells would have a luxurious uptake of nitrogen which would lead to a ‘high growth phase’, as discussed by Edwards *et al.* (2003). These phases normally express the highest yields of chlorophyll from nitrogen. Nevertheless, since it is considered that the system is nitrogen limited, as discussed here, in Chapter 5 and by Tett *et al.* (2003) for example, the estimates obtained with nitrogen limitation are considered to be more realistic. Therefore, the yield should be between 3.65 to  $4.11 \mu\text{gchl}\cdot(\mu\text{molN})^{-1}$ . These estimated mean values are within the range of values observed by Gowen *et al.* (1992) and Edwards *et al.* (2005) for phytoplankton, although the values used by them were much smaller, around  $1 \mu\text{gchl}\cdot(\mu\text{molN})^{-1}$ . As hypothesized and discussed above, larger values of yield were expected for benthic algae, which are normally established in biofilms and are larger in size, because their growth is more rapid than for pelagic algae, as discussed by Costello and Chisholm (1981), for example. Other aspects of the eco-physiology of the system may also be associated with these higher values of yield. The nitrogen may be less diverted to microheterotrophs, which also uptake nutrients, due to smaller biomasses (Fouilland *et al.*, 2007). The fraction of heterotrophs, compared with photoautotrophic cells may be smaller. This would imply the effective use of a larger amount of nitrogen to produce chlorophyll. Note that it was not possible to distinguish in this work between nitrogen that was used by microalgae or microheterotrophs. The observed change would

always be the same, but if less is taken by heterotrophs, more is used by algae and higher values of yield are observed.

The values of yield obtained from the first experiment are slightly smaller. These were obtained from sandy sediment and the nitrogen flux value used was the one estimated for mud. According to the Equation 6.13, this means that the uptake was larger than it was supposed to be due to a larger value of flux and the yield estimates are smaller than they ought to be. Sandy sediments have a smaller content of organic matter and are reported in the literature as having smaller nutrient fluxes (Murray *et al.*, 2006, Serpa *et al.*, 2007, for example). Therefore, values of  $q$  obtained are not as correct as the ones obtained for mud and should be somewhat larger. The same principle is valid for the yield of chlorophyll from silicon. The values for silicon are within a reasonable range, similar to the ones obtained for nitrogen. Although these values are extremely useful to study natural communities, they are very hard to interpret because they strongly depend on the structure of the community and the proportion of diatoms, which need higher amounts of silicate to grow. The values for phosphorus are not presented because they are not correct. A negative flux value was used in the calculations, which means that, according to the Equation 6.13, a smaller value for the uptake was considered. Consequently, the value of the yield, which represents the amount of chlorophyll obtained from a specific nutrient, is higher than it should be. Further studies dealing with adsorption processes would be able to follow this approach and improve the estimate of the yield of chlorophyll from phosphorus.

In these experiments, the three phases with different values of yield, presented and discussed by Edwards *et al.* (2003) were not found (Figures 6.22 and 6.23). On day 2, a great increase of chlorophyll and a great decrease of nitrate are observed by Edwards *et al.* (2003). This is reflected in the values of the yield obtained for the same period. Although it is difficult to identify the reasons for this without further studies, it is reasonable to expect a stable community in terms of nutrient uptake. Nutrient concentrations within the sediment are high in Ria Formosa as discussed in Chapter 5 and by Murray *et al.* (2006) and Serpa *et al.* (2007). Since nutrient availability is much higher for microphytobenthos, compared to phytoplankton, a great increase in nutrient uptake and algal growth could be expected for phytoplankton but not necessarily for MPB.

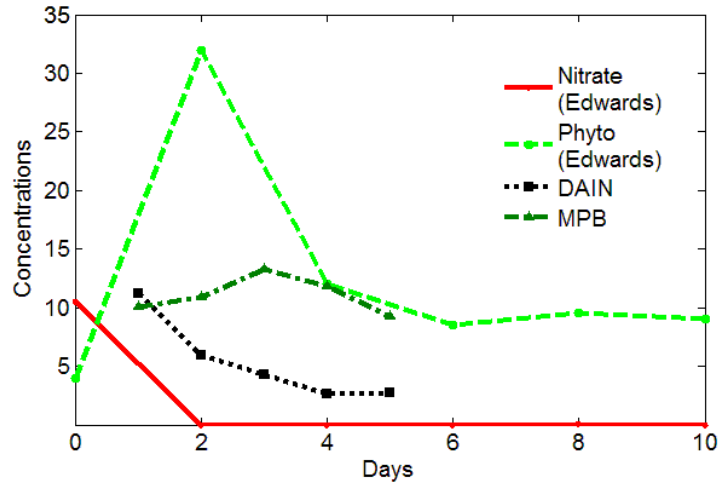


Figure 6.22 - Nutrient and phytoplankton chlorophyll concentrations (red- $\mu\text{M}$  and light green- $\mu\text{g.l}^{-1}$ ) within the reactor from Edwards *et al.* (2003) and DAIN and MPB concentrations (black-  $\mu\text{M}$  and green-  $\mu\text{g.g}^{-1}$ ).

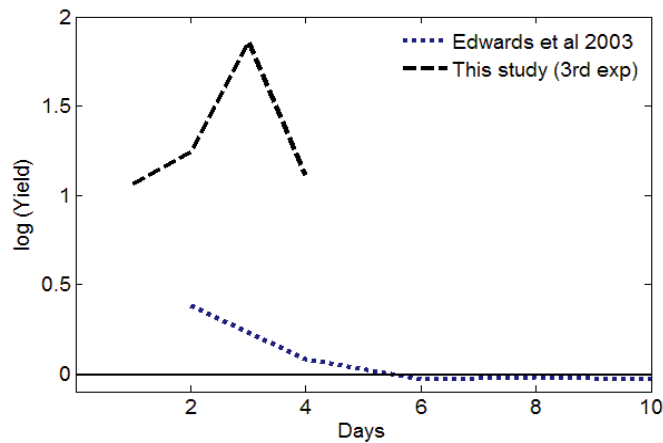


Figure 6.23 – Log-transformed values of the yield of chlorophyll from nitrogen ( $\mu\text{g Chl.}\mu\text{mol N}^{-1}$ ), from Edwards *et al.* (2003; blue) and from the third experiment (black).

## 6.5 Conclusions

The first two experiments carried out to study the yield of chlorophyll from nutrients following the approach of Edwards *et al.* (2003; 2005) provided results that were too complex and difficult to analyse. Concentrations in the water column increased greatly, especially ammonium. Therefore the need for specific experiments to assess nutrient fluxes between sediments and water column was evident. Estimated fluxes of nitrogen under dark conditions were much smaller than the fluxes calculated in Chapter 5, using the Fick's Law of diffusion. Several factors may be influencing the results, such as the uptake of nitrogen by algae or the great importance of processes such as the denitrification. Further studies (e.g. species identification; microcosm experiments to

investigate fluxes) should be carried out to assess these phenomena. Negative phosphorus fluxes and the adsorption process should also be fully assessed to provide improved estimates. Estimates of the yield of chlorophyll from nitrogen in muddy sediments, range from 3.65 to 4.11  $\mu\text{gchl} (\mu\text{molN})^{-1}$  and from 4.03 to 4.78 for the yield from silicon. These values are higher than for phytoplankton which may be due to physiological reasons or due to a smaller fraction of microheterotrophs, which would divert fewer nutrients. No estimate of the yield from phosphorus was obtained because according to our numerical approach, the negative flux influences the amount of phosphorus consumed by algae, decreasing it and leading to large, and incorrect values of yields. Further biochemical experimental studies on phosphorus adsorption to the sediment are essential to obtain an accurate estimate.

Accurate estimates of the yield of benthic chlorophyll from nutrients will be essential for the addition of another primary producer compartment, the microphytobenthos to eutrophication models, such as the dynamic CSTT model being developed in this project.

## 6.6 References

- Aberle-Malzahn, N. (2004). *The microphytobenthos and its role in aquatic food webs*. PhD Thesis. Kiel University.
- Baric, A., Kuspilic, G., Matijevic, S. (2002). Nutrient (N, P, Si) fluxes between marine sediment and water column in coastal and open Adriatic. *Hydrobiologia*, **475/476**, 151-159.
- Björk-Ramberg, A. (1985). Uptake of phosphate and inorganic nitrogen by a sediment-algal system in a subarctic lake. *Freshwater biology*, **15**, 175-183.
- Bricker, S., Clement, C., Pirhalla, D., Orlando, S., Farrow, D. (1999). *National Estuarine Eutrophication Assessment. Effects of Nutrient Enrichment in the Nation's Estuaries*. National ocean Service, Silver Spring, MD, USA, 71 pp.
- Cartaxana, P., Mendes, C.R., Van Leeuwe, M.A., Brotas, V. (2006). Comparative study on the microphytobenthic pigments of muddy and sandy intertidal pigments of the Tagus estuary. *Estuarine Coastal and Shelf Science*, **66**, 225-230.
- Costello, J., Chisholm, S. (1981). The influence of cell size on the growth rate of *Thalassiosira weissflogii*. *Journal of Plankton Research*, **3**, 415-419.
- CSTT (Comprehensive Studies Task Team) (1994). *Comprehensive studies for the purposes of Article 6 of DIR 91/271 EEC, the Urban Waste Water Treatment Directive*. Published for the Comprehensive Studies Task Team of Group Coordinating Sea Disposal Monitoring by the Forth River Purification Board, Edinburgh.



- CSTT (Comprehensive Studies Task Team) (1997). *Comprehensive Studies for the Purposes of Article 6 and 8.5 of Directive 91/271 ECC, the Urban Waste Water Treatment Directive..* Report prepared for the UK Urban Waste Water Treatment Directive Implementation Group and Environmental departments by the Group Co-ordinating Sea Disposal Monitoring, 2<sup>nd</sup> edition, UK. Department of the environment for Northern Ireland, the Environment Agency, the Scottish Environment Protection Agency and the Water Services Association. Edinburgh: SEPA. 60 pp.
- Devlin, M., Barry, J., Mills, D., Gowen, R., Foden, J., Sivyer, D., Tett, P. (2008). Relationships between suspended particulate material, light attenuation and sechi disk in UK marine waters. *Estuarine, Coastal and Shelf Science*, **79**, 429-439.
- Di Toro, D. (2001). *Sediment Flux Modeling*. J. Wiley and Sons., New York. 624pp.
- Edwards, V. (2001). *The yield of marine phytoplankton chlorophyll from dissolved inorganic nitrogen under eutrophic conditions*. PhD Thesis. Napier University, Edinburgh.
- Edwards, V., Tett, P., Jones, K. (2003). Changes in the yield of chlorophyll *a* from dissolved available inorganic nitrogen after an enrichment event – applications for predicting eutrophication in coastal waters. *Continental Shelf Research*, **23**, 1771-1785.
- Edwards, V., Icelly, J., Newton, A., Webster, R. (2005). The yield of chlorophyll from nitrogen: a comparison between the shallow Ria Formosa lagoon and the deep oceanic conditions at Sagres along the southern coast of Portugal. *Estuarine, Coastal and Shelf Science*, **62**, 391-403.
- Escaravage, V., Prins, T., Smaal, A., Peeters J. (1996). The response of phytoplankton communities to phosphorus input reduction in mesocosm experiments. *Journal of Experimental Marine Biology and Ecology*, **198**, 55–79.
- Falkowski, P., Raven, J. (2007). *Aquatic Photosynthesis*. 2<sup>nd</sup> Edition. Princeton University Press.
- Fan, C., Glibert, P. (2005). Effects of light on nitrogen and carbon uptake during a *Prorocentrum minimum* bloom. *Harmful Algae*, **4**, 629-641.
- Fouilland, E., Gosselin, M., Rivkin, R.B., Vasseur, C., Mostajir, B. (2007). Nitrogen uptake by heterotrophic bacteria and phytoplankton in Arctic surface waters. *Journal of Plankton Research*, **29**, 369-376.
- Geider, R., MacIntyre, H., Kana, T. (1997). Dynamic model of phytoplankton growth and acclimation: responses of the balanced growth rate and the chlorophyll *a*:carbon ratio to light, nutrient limitation and temperature. *Marine Ecology Progress Series*, **148**, 187-200.
- Glibert, P.M. (1982). Regional studies of daily, seasonal and size fraction variability in ammonium remineralisation. *Marine Biology*, **70**, 209-220.
- Gönoç, I., Wolflin, J. (2005). *Coastal lagoons: ecosystem processes and modeling for sustainable use and development*. CRC Press. 500pp.
- Gowen, R., Tett, P., Jones, K. (1992). Predicting marine eutrophication: the yield of chlorophyll from nitrogen in Scottish coastal waters. *Marine Ecology Progress Series*, **85**, 153-161.
- Grasshoff, K., Ehrhardt, M., Kremling, K. (1983). *Methods of seawater analysis*. Verlag Chemie, Weilheim: 419pp.
- Guillard, R., Ryther, J. (1962). Studies of marine planktonic diatoms. I. *Cyclotella nana* Hustedt and *Detonula confervacea* Cleve. *Canadian Journal of Microbiology*, **8**, 229-239.

- Guillard, R.R.L. (1975). Culture of phytoplankton for feeding marine invertebrates. pp 26-60. In: Smith, W., Chanley, M. (eds.) *Culture of Marine Invertebrate Animals*. Plenum Press, New York, USA.
- Hopkinson, C., Giblin, A., Tucker, J., Garritt, R. (1999). Benthic metabolism and nutrient cycling along an estuarine salinity gradient. *Estuaries*, **22**, 863-881.
- Howarth, R., Marino, R. (2006). Nitrogen as the limiting nutrient for eutrophication in coastal marine ecosystem: Evolving views over three decades. *Limnology and Oceanography*, **51**, 364-376.
- Jensen, J.P., Pederson, A.R., Jeppensen, E., Søndergaard, M. (2006). An empirical model describing the seasonal dynamics of phosphorus in 16 shallow eutrophic lakes after external loading reduction. *Limnology and Oceanography*, **51**, 791-800.
- Jesus, B. (2005). *Ecophysiology and spatial distribution of microphytobenthic biofilms*. PhD Thesis, University of Lisbon, 225pp.
- Jones, K.J., Tett, P., Wallis, A.C., Wood, B.J.B. (1978). Investigation of a nutrient-growth model using a continuous culture of natural phytoplankton. *Journal of the Marine Biological Association of the United Kingdom* **58**, 923-941.
- Kirk, J. (1994). *Light and Photosynthesis in Aquatic Ecosystems*. 2<sup>nd</sup> Edition. Cambridge University Press.
- Lane, R., Day, J., Justic, D., Reyes, E., Marx, B., Day, J., Hyfield, E. (2004). Changes in the stoichiometric Si, N and P ratios of Mississippi River water diverted through coastal wetlands to the Gulf of Mexico. *Estuarine, Coastal and Shelf Science*, **60**, 1-10.
- Lee, J-Y., Tett, P., Jones, K., Jones, S., Luyten, P., Smith, C., Wild-Allen, K. (2002). The PROWQM physical-biological model with benthic-pelagic coupling applied to the northern North Sea. *Journal of Sea Research*, **48**, 287-331.
- Li, W., Lewis, M., Harrison, W. (2008). Multiscalarity of the nutrient-chlorophyll relationship in coastal phytoplankton. *Estuaries and Coasts*, doi:10.1007/s12237-008-9119-7.
- Mills, M., Ridame, C., Davey, M., La Roche, J., Geider, R. (2004). Iron and phosphorus co-limit nitrogen fixation in the eastern tropical North Atlantic. *Nature*, **429**, 292-294.
- Murray, L., Mudge, S., Newton, A., Icely, J. (2006). The effect of benthic sediments on dissolved nutrient concentrations and fluxes. *Biochemistry*, **81**, 159-178.
- Nixon, S. (1995). Coastal marine eutrophication: a definition, social causes, and future concerns. *Ophelia*, **41**, 199-219.
- Nobre, A.M., Ferreira, J.G., Newton, A., Simas, T., Icely, J.D., Neves, R. (2005). Management of coastal eutrophication: Integration of field data, ecosystem-scale simulations and screening models. *Journal of Marine Systems*, **56**, 375-390.
- Schindler, D. (2006). Recent advances in the understanding and management of eutrophication. *Limnology and Oceanography*, **51**, 356- 363.
- Serpa, D., Falcão, M., Duarte, P., Fonseca, L.C., Vale, C. (2007). Evaluation of ammonium and phosphate release from intertidal and subtidal sediments of a shallow coastal lagoon (Ria Formosa – Portugal): a modelling approach. *Biochemistry*, **82**, 291-304.

- Taylor, D., Nixon, S., Granger, S., Buckley, B., McMahon, J., Lin, H. (1995a). Responses of coastal lagoon plant communities to different forms of nutrient enrichment- a mesocosm experiment. *Aquatic Botany*, **52**, 19-34.
- Taylor, D., Nixon, S., Granger, S., Buckley, B. (1995b). Nutrient limitation and the eutrophication of coastal lagoons. *Marine Ecology Progress Series*, **127**, 235-244.
- Tett, P., Wilson, H. (2000). From biochemical to ecological models of marine microplankton. *Journal of Marine Systems*, **25**, 431-446.
- Tett, P., Gilpin, L., Svendsen, H., Erlandsson, C.P., Larsson, U., Kratzer, S., Fouilland, E., Janzen, C., Lee, J., Grenz, C., Newton, A., Ferreira, J.G., Fernandes, T., Scory, S. (2003). Eutrophication and some European waters of restricted exchange. *Continental Shelf Research*, **23**, 1635-1671.
- Tett, P., Lee, J-Y. (2005). N:Si ratios and the 'balance of organisms': PROWQM simulations of the northern North Sea. *Journal of Sea Research*, **54**, 70-91.
- Tett, P., Portilla, E., Inall, M., Gillibrand, P., Gubbins, M., Amundrod, T. (2007). *Modelling the Assimilative Capacity of Sea Lochs (Final Report on SARF 012)*. Napier University, 1-29.
- Underwood, G., Paterson, D. (2003). The importance of extracellular carbohydrate production by marine epipelagic diatoms. *Advances in Botanical Research*, **40**, 183-240.
- Yoshiyama, K., Sharp, J. (2006). Phytoplankton response to nutrient enrichment in an urbanized estuary: Apparent inhibition of primary production by overeutrophication. *Limnology and Oceanography*, **51**, 424-434.

## **CHAPTER 7**

---

Biogeochemical model for the sustainable management of  
nutrients within the Ria Formosa

---

## **Abstract**

Ria Formosa is a Region of Restricted Exchange and therefore is cut off from the normal circulation of coastal waters. Furthermore, it is subject to several anthropogenic activities that can lead to an increase in nutrients and potentially to eutrophication.

Previous studies have shown the importance of the benthic compartment, specifically the microphytobenthos and pore water nutrients in this shallow coastal lagoon. A dynamic version of the CSTT model, the dCSTT-MPB model, has been developed coupling the benthic and pelagic components of the system to assess its assimilative capacity. The usefulness of the benthic components was assessed during the development process. The model predicts a large biomass of microphytobenthos, as observed in the Ria Formosa, which strongly influences the pelagic chlorophyll concentration by resuspension. However, algae concentrations in the water column are relatively small due to the high flushing rate of the lagoon. The microphytobenthos community is mainly supported by nutrients in the pore water.

A sensitivity analysis has revealed that the factors associated with the benthic compartment were the most important and sensitive to changes. The porosity, benthic chlorophyll recycling, loss of microphytobenthos due to grazing and the yield of microphytobenthic chlorophyll from nitrogen, investigated in the previous Chapter, were some of the most important parameters. Moreover, the factors associated with the decay of particulate organic nitrogen were also as important as the ones described before.

**Keywords:** Microphytobenthos, assimilative capacity, CSTT model, eutrophication, Ria Formosa,

## 7.1 Introduction

Historically, the complexity of the first models developed during the last century greatly increased, mainly due to computer technology improvements (Jørgensen and Bendoricchio, 2001). The first complex eutrophication models were developed for rivers, where eutrophication assessment itself was more focused. Rapidly, eutrophication models were also derived for coastal and marine systems, mainly in regions that suffered from nutrient enrichment due to point (e.g. sewage, aquaculture farms) and diffuse (agriculture run-off, for example) sources. However, it was difficult to have an extensive knowledge of ecological components and processes of each system and soon this became the most important limitation of models. Finding the appropriate complexity of models and having a good and robust dataset became a requirement.

Several different models may be used and developed to evaluate different parts or components of an ecosystem. The definition of the model structure is crucial and depends on the objective of the study. The UK's 'Comprehensive Studies Task Team' (CSTT, 1994; 1997) suggested the definition of three scales to study the effect of waste discharges, as represented in Figure 7.1.

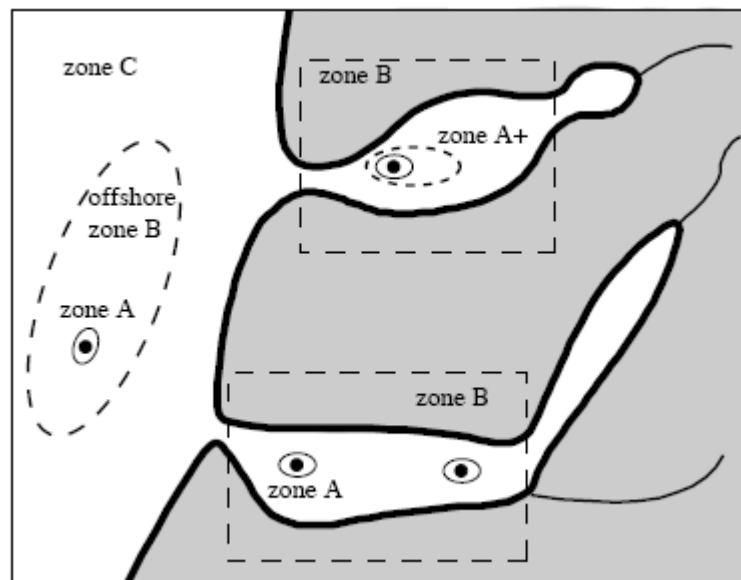


Figure 7.1 – Scales A, B and C proposed by the CSTT (CSTT, 1994).

DEPOMOD (Cromey *et al.*, 2002) is an example of a model that operates on the zone A scale, which corresponds to the area immediately around a point source, such as a fish farm. This model has been widely used for the assessment of the effects of sinking

waste on the seabed. Waters at this scale have generally a residence time of few hours. Waters on the zone C scale have a residence time of weeks to months and include the sum of wastes from all zones B. The ERSEM model, which is a complex ecosystem model (see details below in this section), is an example of a model that operates on this zone C scale. The CSTT model works on the zone B scale. The residence time of waters is of a few days to weeks, sufficient for an algal response to nutrient enrichment. This kind of model can be coupled to a physical model to track particle movement and therefore be transformed into a model that operates on the zone C scale.

The model being developed in this work is based on the CSTT model (CSTT, 1994; CSTT, 1997), which was described in the first chapter of this thesis. The CSTT model was created to be a steady-state model, assessing only the worst-case scenario. This type of model, called a screening-model, may be extremely important for a rapid system evaluation (Bricker *et al.*, 2003; Tett *et al.*, 2003 and Nobre *et al.*, 2005). The results are normally very clearly interpreted and understood. Moreover, it allows the application of the model by persons, regulators or institutions without deep background knowledge. This simple CSTT model was applied to the Ria Formosa to assess the trophic status of the lagoon during the European Project OAERRE (Tett *et al.*, 2003). No clear trend consistent with eutrophication was found. However, work undertaken in Ria Formosa has provided conflicting evidence on its trophic status (Tett *et al.*, 2003; Newton *et al.*, 2003; Nobre *et al.*, 2005). Although certain areas within the Ria suffer from nutrient enrichment, hypoxia and algal mats, pelagic eutrophication symptoms do not tend to be apparent (Newton *et al.*, 2003). Using a hybrid approach (ASSETS which is a simple, screening model for the ASSESSment of Estuarine Trophic Status, and an ecosystem model) Nobre *et al.* (2005) suggested that eutrophication symptoms are not present in the water column, although an excessive growth of macroalgae and dissolved oxygen fluctuations (in the bottom) were observed in areas with low water exchange (Newton and Icely, 2006). These symptoms can have important ecological consequences with adverse effects on sustainability, i.e., with the resulting impairment of environmental quality within the lagoon, and therefore a possible impact on biodiversity, fisheries and aquaculture (Fernandes *et al.*, 2002). Shallow systems such as Ria Formosa should be considered differently from other coastal systems. The influence of sediments is crucial for nutrient and chlorophyll dynamics as discussed in Chapter 3 and by Falcão (1996), Newton *et al.* (2003), Newton and Mudge (2005), Murray *et al.* (2006). The benthic compartment has not been convincingly incorporated into the assessments so far. The

most important source of nutrients to the lagoon dynamics is considered to be the sediments (Falcão, 1996). Moreover, microbenthic algal communities are of great importance. They can contribute up to 50% of the total carbon budget (Underwood and Kromkamp, 1999). In chapter 4 and 5 the importance and large biomass was described and discussed intensively. Alvera-Azcárate *et al.* (2003) also showed that the phytobenthos may play a significant role in nitrogen balance, which is considered to be the limiting nutrient within the Ria Formosa (see discussion in chapter 5).

The results obtained from the application of the simple CSTT model to Ria Formosa suggested its inaccuracy regarding this specific system. The observed maximum value of pelagic chlorophyll *a* was twice the predicted (Tett *et al.*, 2003). This discrepancy indicates that the model was not well adapted to this particular system and clearly needed improvement. The results obtained represented an underestimation. Some important questions were pointed out at this stage to explain the discrepancy. Tett *et al.* (2003) suggested that this could be caused by the application of a box model (with well-mixed waters) to a heterogeneous system. Recently, results from this study confirmed that the water column is well mixed (see chapter 5). This was also suggested by Newton and Mudge (2003). The exchange rate used in the CSTT model was of about 50-75% per tide, which is now considered too high. Mudge *et al.* (2008) observed that the residence time in some inner channels of the lagoon may be up to 3-4 days, or even more. Therefore, the nutrients may remain longer in the system and may be used for algal growth. Another point that was suggested, for example by Alvera-Azcárate *et al.* (2003), Newton *et al.* (2003) and Tett *et al.* (2003) is the lack of an important benthic primary producer in this shallow system and its interaction with the water column.

Models dealing with the biological (e.g. algal communities) and chemical (e.g. nutrient) components of a system, and the interactions between sediment and water are considered biogeochemical models. These models work with mass or concentration units and imply the conservation of mass (Jørgensen and Bendoricchio, 2001). They are important tools to obtain useful predictions of the trophic status of a system. They allow the assessment of potential impacts arising from biological or chemical changes, such as the increase of nutrient inputs. The increase of nutrients may be caused by the implementation in an aquaculture farm or a new golf course. These models allow comparison of the system to limits recommended by international and national legislation, such as the Water Framework Directive. Therefore, the simplicity of models and their easy application is of great interest in the management of coastal systems.



Several other models have been developed to study the ecological quality of water bodies, considering the interactions of the sediment – water interface, such as ERSEM (Baretta *et al.*, 1995; Ebenhöh *et al.*, 1997; Blackford, 2002) or the one developed by Murray and Parslow (1997), for example. In addition to being complex models, they are very important in providing guidance on the development of coupled (pelagic and benthic) interactions.

The ERSEM model is the European Regional Seas Ecosystem Model. It was developed to simulate the seasonal cycling of carbon, nitrogen, phosphorus and silicon in the pelagic and benthic food webs in the North Sea. It considers the zoobenthos, benthic microalgae and benthic nutrients (Figure 7.2). In the initial version, the primary producers component consisted of two phytoplankton groups, diatoms and flagellates (Ebenhöh *et al.*, 1995). More recently, Blackford (2002) added the microphytobenthos to the ERSEM model in a shallow system, where the seabed is illuminated and important for primary production. Blackford (2002) reported that microphytobenthos does not have a significant impact on the Adriatic system, but it does have at shallow sites, where it significantly contributes to nutrient and carbon cycling.

Murray and Parslow (1997) developed a complex model incorporating 16 state variables for both water column and sediments, representing nutrients, algae, detritus

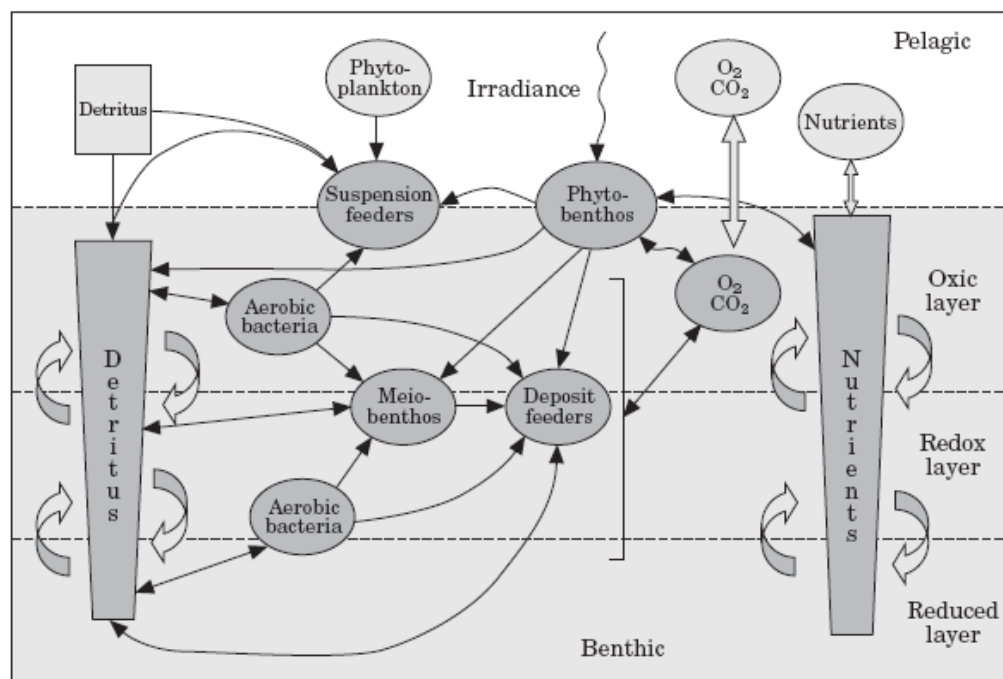


Figure 7.2 – Conceptual diagram of the ERSEM model with phytobenthos, showing state variables and fluxes (from Blackford, 2002).

and animals. Since their site was shallow, they thought it would be important to include a microphytobenthos component. The model revealed the importance of the water column and sediments interaction and denitrification (Murray and Parslow, 1997). Both models recognize the importance of coupling the benthic and pelagic interactions and processes. The studies of Murray and Parslow (1997) and Blackford (2002) also represent some of the first attempts to incorporate the microphytobenthos as a primary producer in shallow systems.

Accurate simulations are difficult to obtain in sediments. Blackford (2002) indicates that his results are to be used only in a qualitative manner due to uncertainties about key parameters and results. Murray and Parslow (1997) do not address the question of the temporal variation of microphytobenthos and acknowledge the need of further studies on MPB dynamics. In contrast, good agreement between model results and observations are generally expected for phytoplankton models, such as the LESV model (Portilla *et al.*, 2009). Phytoplankton is subject to strong seasonal cycles of illumination and it also experiences the strong influence of boundary conditions, which in the case of the LESV model are well-known. MPB in Ria Formosa express a complex temporal variation (Chapter 4) and are less influenced by boundary conditions.

The modelling process should start with the definition of the problem. This is the first step and the most important one (Jørgensen and Bendoricchio, 2001). The model focus also needs to be bound by constituents of space, time and subsystems. It is crucial to try to get the big picture of the processes needed for the model. However, it is most likely that the procedure is not correct at the first attempt. The modelling process is an iterative procedure and the main model may be reconsidered and changed during the development process. The modelling process generally covers three major procedures during and after the construction of the model itself which are verification, calibration and validation (Jørgensen and Bendoricchio, 2001). Verification is the first logical test of the model. Does it make sense? Is it consistent? Is it explaining observations? The second procedure is an attempt to find the best parameter values for a good fit of the model with the observations. Validation should reveal how good the agreement between predictions and observations is. It is a critical step. In addition, an additional analysis may be carried out to help understand the dynamics of the model: the sensitivity analysis. It basically consists in the analysis of the effects due to a change in parameter values with a known magnitude, for example  $\pm 10\%$  or  $\pm 50\%$ . This knowledge is extremely important to assess which parameters are most important in defining the

results of the model and on what parameters most effort should be concentrate to derive robust data (Jørgensen and Bendoricchio, 2001).

The aim of this study is to develop a simple and dynamic biogeochemical model based on the dynamic version of CSTT (dCSTT; Laurent *et al.*, 2006) which will allow accurate predictions and the assessment of the trophic status of the lagoon through time. It will also be used as an important tool to evaluate the usefulness of specific indicators and to assess the assimilative capacity of the system.

The structure of this chapter is slightly different from the other chapters. The development process was done by steps, with the aim of finding the simplest and most accurate way to explain the dynamics of Ria Formosa. Therefore, the most important steps or stages of the model will be presented as part of the development process (Figure 7.3). The model was developed sequentially from Stage 1 to 4. In stage 1 the importance of MPB is investigated and pore water nutrients are considered to be crucial to support the community. In stage 2, pore water nutrients are included, however, the approach taken was found not to be enough to support MPB. In stage 3, dissolved oxygen was included due to its potential importance to investigate eutrophication and ecological quality but it was abandoned because the expected results were not obtained. Therefore, the model was returned to stage 2 and was then developed directly to stage 4 by changing the approach of MPB growth. The options made will be explained and the directions taken will be supported by existent knowledge. Each stage will be fully described, explaining why those components were chosen and the scale at which the work is being conducted. The model will be described in three main parts according to what is recommended by Tett *et al.* (2007): conceptual, mathematical and numerical model. The conceptual model is our theoretical view of the relationships existent within the system. This has an associated error that derives from our incapacity of describing perfectly the systems we want to study. The mathematical model is represented by differential equations that describe the processes and the relationships of each component of the system (state variables). The numerical model is the application of sets of data and forcing variables to our mathematical model. The results of each stage will be presented and discussed. This will be repeated for each development stage. This model resulted from a scientific modelling process rather than an engineering modelling process. The former corresponds to the development phase, with formulation and rejection of scientific hypotheses. The latter is aimed at making a model that is reliable in prediction, based on existent models and using data for the calibration process as an

essential step to provide a good agreement between model output and data. The most important hypotheses tested in the development process are described in each section.

Finally, the chapter presents results from the stage 4 model - an analysis of its sensitivity to the values of some parameters and an application to estimate the capacity of the Ria Formosa to assimilate nutrients without perceived harm to the ecosystem. The estimated assimilative capacity will be indicative rather than definitive because this work is not the final stage in developing a nutrient cycling model for a complex ecosystem such as the Ria. The work did, however, lead to insights into the system's functioning. It is for that reason that the developmental stages are fully presented and scrutinised.

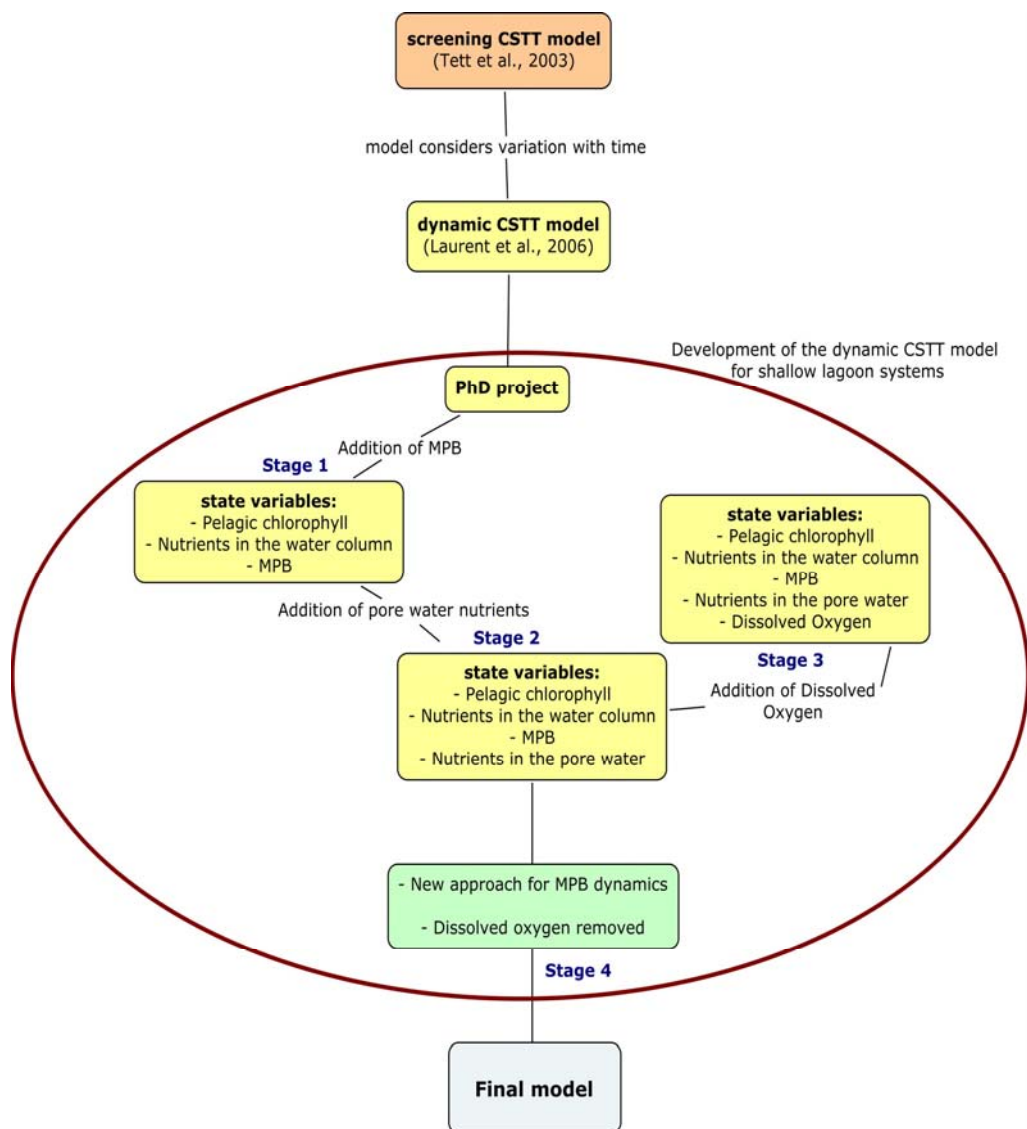


Figure 7.3 – Scheme of the model development process. Two published models, the CSTT (Tett *et al.*, 2003) and the dCSTT (Laurent *et al.*, 2006) were the basis for the new model. The development of this new model is considered inside the red circle, illustrating the four different stages of the model development.

## 7.2 Development of the model

The model being developed is considered to be a box model, as represented in Chapter 1 – Figure 1.2. It considers the Ria Formosa as one single box, vertically and spatially homogeneous. Processes are considered in this model as daily means. Therefore, and due to the tidal cycle existent in the lagoon, the water volume and depth of the water column used in the model corresponds to mid-water conditions. The model intends to simulate the whole lagoon and as such the surface area considered corresponds to the total lagoon area. The standard units of this dynamic model are milligrams or milimoles, metres and days.

A general equation can be presented to describe one or more state variables ( $Y$ ) of the dCSTT-MPB or similar models such as the LESV model presented by Portilla *et al.* (2009). Hence:

$$\frac{\partial Y}{\partial t} = -\nabla \phi_Y + \beta_Y + \frac{\partial \Gamma_Y}{\partial V} \quad (7.1)$$

The first term ( $-\nabla \phi_Y$ ) is the divergence of physical transport fluxes at a point. It represents the physical transport and gives the rate of change of the variable as a result of a set of water exchanges. In a spatially complex model, the physical transport may occur along three axes and result from different processes, such as advection and diffusion. This term is also used to describe fluxes and interactions between the water column and sediment layers. In this single box model, the physical term represents the exchange of a certain state variable with the sea, along exclusively one axis, plus vertical interactions with sediments, when considered. Thus for nutrients:

$$-\nabla \phi_Y = E(S_0 - S) \quad (7.2)$$

Where  $E$  is the exchange rate ( $d^{-1}$ ), which will be described below in this section and  $S$  corresponds to the nutrient concentration ( $mmol.m^{-3}$ ) in the water column. The subscript 0 refers to the concentrations outside the lagoon.

The bio-chemical term ( $\beta_Y$ ) consists of the biological and chemical transformations of the state variable, such as growth or loss. The final term ( $\partial \Gamma_Y / \partial V$ ) gives the input/flux to the system, such as a water treatment plant or a fish farm, for example, or the loss to the farm of the state variable. The inputs have origin from local

anthropogenic or land-derived sources. In this model, a possible solution for  $\partial\Gamma_Y/\partial V$ , as a daily variation of the influx of nutrients to the water column is:

$$\frac{\partial\Gamma_Y}{\partial V} = \frac{si}{V} \quad (7.3)$$

Where  $si$  corresponds to the total amount of nutrient inputs ( $\text{mmol.d}^{-1}$ ) to the water column, except fluxes from sediments, and  $V$  is the volume ( $\text{m}^3$ ) of the lagoon. We separate the gamma term from the flux divergence because the gamma term is not associated with significant flows of water. In this case, the gamma term corresponds to the local anthropogenic and/or land-derived inputs. Some state variables may be described by only part of the equation, i.e. with some terms having no representation. This is what happens with the benthic state variables, such as microphytobenthos, which do not have any significant exchange with the sea, but may have a sediment-water exchange due to resuspension.

The development of a model raises issues of notation. It is essential that all variables are well defined and described. It is also desirable that the notation system follows the standards or conventions of the scientific discipline in which it operates. For simplicity and logical sequence, notation used by the simple CSTT model (CSTT, 1994; 1997) and subsequent models, such as dCSTT (Laurent *et al.*, 2006) and LESV (Tett *et al.*, 2007), will be generally followed. Some adjustments will also be made, as necessary.

### 7.2.1 Stage 1 – Addition of the benthic primary producer component

The first step towards the development of this new dynamic model was to introduce a new compartment, the benthic algae, to the two already existent in the previous models, limiting nutrients in the water column and pelagic chlorophyll *a*. This was done by starting from the dynamic CSTT model that already provides a simulation output through time (Laurent *et al.*, 2006). The reasons that support this step were discussed above. DAIN was used as the limiting nutrient, since it is considered to be the limiting nutrient in the lagoon (see chapter 5; Tett *et al.*, 2003). The aim of this improvement is to give an extra term for a chlorophyll source to achieve predictions similar to the observed values. The hypothesis that the benthic compartment, the microphytobenthos, represents the majority of the chlorophyll stock existent in this shallow lagoon is

considered here. This model works on the water body scale, just within the lagoon area, which is where the eutrophication events could be problematic.

### 7.2.1.1 Conceptual model

The conceptual model deals with a homogeneous box representing the lagoon and its state variables. Figure 7.4 represents the processes involved. The box has an exchange term with the sea, in the water column for all pelagic variables.

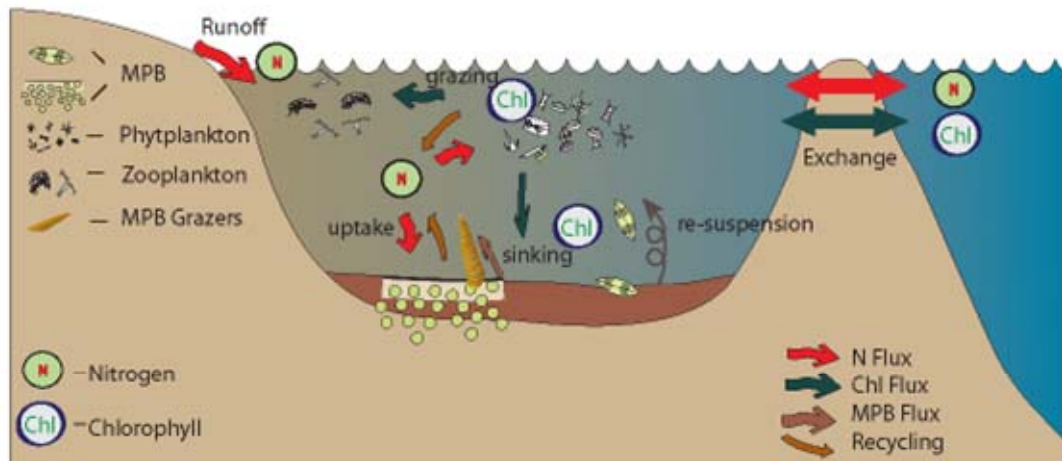


Figure 7.4 – Diagram representation of the conceptual model. Illustration symbols from the Integration and Application Network (<http://ian.umces.edu>).

### 7.2.1.2 Mathematical model

The mathematical model is constituted by three differential equations, one for each state variable:  $S$  (limiting nutrient in the lagoon),  $X_p$  (pelagic chlorophyll inside the lagoon) and  $X_b$  (microphytobenthic chlorophyll inside the lagoon).

$$\frac{\partial S}{\partial t} = E.(S_0 - S) - \frac{\mu_b X_b}{q_b.H} - \frac{\mu_p X_p}{q} + e.L_p \cdot \frac{X_p}{q} + e_b \cdot \frac{L_g X_b}{q_b.H} + \frac{S_i}{V} \quad (7.4)$$

(mmol.m<sup>-3</sup>.d<sup>-1</sup>)

$$\frac{\partial X_p}{\partial t} = E.(X_0 - X_p) + \mu_p X_p - L_p X_p + \frac{L_{br} X_b}{H} - \frac{sk}{H} X_p \quad (7.5)$$

(mg chl.m<sup>-3</sup>.d<sup>-1</sup>)

$$\frac{\partial X_b}{\partial t} = \mu_b X_b - L_g X_b + sk X_p - L_{br} X_b \quad (7.6)$$

(mg chl.m<sup>-2</sup>.d<sup>-1</sup>)

The subscript  $0$  (outside) always refers to the concentrations in the sea and the subscript  $i$  refers to inputs, in this case of nutrients ( $S_i$ ,  $\text{mmol.d}^{-1}$ ) to the box. The subscript  $b$  refers to microphytobenthos.  $E$  is the exchange rate of waters between the inside and outside of the lagoon ( $\text{d}^{-1}$ ),  $V$  is the volume of the lagoon ( $\text{m}^3$ ),  $e$  is the fraction of grazed nitrogen that is recycled,  $q$  is the yield of chlorophyll from nutrients ( $\text{mg chl.mmol}^{-1}$ ),  $H$  is the mean depth of the lagoon (m),  $L_p$  is phytoplankton loss rate ( $\text{d}^{-1}$ ),  $\mu$  is phytoplankton growth rate ( $\text{d}^{-1}$ ),  $L_{br}$  is the loss rate of microphytobenthos chlorophyll to the water column ( $\text{d}^{-1}$ ),  $L_g$  is the grazing rate ( $\text{d}^{-1}$ ) and  $sk$  is the sinking rate ( $\text{d}^{-1}$ ) of phytoplankton.

### 7.2.1.3 Numerical model

To solve these differential equations it is necessary to use numerical integration. For this, the initial and boundary conditions must be known. The exchange with the sea is an important physical process in this system. The numerical model is composed of sets of expressions which define the relationships between state variables, forcing variables and boundary conditions. In fact, it is in the numerical model stage when the specific information and data about the study site are applied.

#### **Physical Model – the $-\nabla\phi_Y$ terms**

##### *Exchange*

Ria Formosa is a mesotidal lagoon. Tides are semidiurnal, i.e., with two high tides and two low tides per day. The lagoon is shallow and it was estimated by Tett *et al.* (2003) that 50 to 75% of the water in the lagoon is exchanged in each tide, which corresponds to a residence time of about 0.5 days. Mudge *et al.* (2008), after an extensive study of temperature and salinity, observed a mean residence time of approximately 2.4 days in the lagoon. This exchange is therefore key in the understanding of the dynamics of the state variables in this model. Mudge *et al.* (2008) estimated residence time considering a box system in which salinity is dependent on freshwater influx, evaporative losses and mixing with adjacent waters. During the summer the freshwater inflow is negligible. Therefore, an increase in salinity values, compared with sea is expected due to evaporation. The following method was considered to estimate residence time:



$$\text{Residence time} = \frac{\Delta S}{S_0 \cdot Ev} \quad (\text{days}) \quad (7.7)$$

$\Delta S$  is the difference in salinity between the inlet ( $S_0$ ) and the measured salinity at any point, and  $Ev$  is the proportion of the water column evaporated per day.

#### *Sinking and resuspension of algae*

Pelagic chlorophyll cells sink to the bottom. This loss term is defined as the chlorophyll concentration ( $\text{mg chl.m}^{-3}$ ) times a sinking constant ( $\text{m.d}^{-1}$ ) divided by the mean depth (m). In this model, a default value of  $1 \text{ m.d}^{-1}$  for the sinking constant was used (Mann and Lazier, 1996). This process influences MPB chlorophyll concentration as well, since it constitutes an inflow of chlorophyll to the sediment surface. This input is defined by the pelagic chlorophyll ( $\text{mg chl.m}^{-3}$ ) times the sinking constant ( $\text{m.d}^{-1}$ ).

Microphytobenthos cells on the sediment surface are subject to several potential losses. One loss is by the grazing of snails and other surface feeders. They may also be elevated into the water column during immersion. Since benthic microalgae are heavier than water and since they lie within a viscous layer, suspension should not be frequent. However, irregularities in the sea-bed disrupt the smooth flow and may originate small eddies. These eddies have a vertical component and once in contact with the biofilm, it may lift up cells. The result may solely be a saltation, in which cells would move along the sea-bed rather than being lifted into the water column. In other cases, cells would be taken up into regions of stronger turbulence in which the upwards motions exceed the sinking speed. In order to improve the model, the sinking of benthic microalgae cells should also be considered. Obviously, benthic and pelagic cells have different sinking speeds due to their different size and weight. Therefore the addition of another state variable, representing the benthic algae suspended in the water column would be a logical improvement in the future. It was not considered in this work due to difficulties in the implementation and validation of results, since no data are available.

**Bio-chemical Model – the  $\beta_Y$  terms***Recycling*

Nutrient concentration in the water column is influenced by two input flows from recycling. These processes are generally defined by the term  $\frac{e.L.X}{q}$ , one for pelagic chlorophyll and the other for MPB chlorophyll.  $e$  is the proportion of grazed nitrogen that is recycled and has the value of 0.5 (Laurent *et al.*, 2006).

*Uptake of nutrients by algae*

The conversion of nutrients to algal chlorophyll is very important in this model. It is one of the most important links in terms of eutrophication assessment. It is now widely accepted that algae growth may be nutrient-controlled. The growth depends mainly on the limiting nutrient content inside the cell. However, this leads to complex cell-quota models and there is a simpler way to establish this link. The alternative is the ratio of chlorophyll formed from the limiting nutrient assimilated –  $q$ , which is discussed below. So, the loss term can be simply defined for pelagic algae as:

$$uptake = \frac{\mu_p \cdot X_p}{q} \quad (\text{mmol.m}^{-3}.\text{d}^{-1}) \quad (7.8)$$

*Biological Production*

For both equations of chlorophyll concentration the growth is the product of the instantaneous value of chlorophyll concentration for a specific time ( $t$ ) times its growth rate for that specific time.

The growth rate is either nutrient limited or light limited and the function that defines this relationship is:

$$\text{If}(muI < muS)\text{then}(muI)\text{Else}(muS) \quad (\text{d}^{-1}) \quad (7.9)$$

$muI$  is the light-limited growth rate and  $muS$  is the nutrient-limited growth rate.

The growth rate of primary producers can switch from being nutrient-limited to being light-limited. This dependency depends on prevailing conditions. According to the

theory, during the winter (for example) the nutrient concentration may be much higher than needed by the algae, but the light is maybe not sufficient for an optimal growth. So, the model takes into account the smaller growth rate based on the limiting factor.

The nutrient-limited growth rate for algae follows the Monod model (Monod, 1942):

$$\mu(S) = \frac{\mu_{max} \cdot S}{K_s + S} \quad (\text{d}^{-1}) \quad (7.10)$$

$K_s$  is the half saturation concentration ( $\text{mmol} \cdot \text{m}^{-3}$ ) and  $\mu_{max}$  is the maximum growth rate ( $\text{d}^{-1}$ ).  $\mu_{max}$  is the instantaneous rate coefficient to be used in the algae growth equation.  $K_s$  is defined as the concentration at which the rate is one-half the maximum (Kremer and Nixon, 1978). The effect of smaller values of  $K_s$  is to steepen the rate of ascent to  $\mu_{max}$  (Figure 7.5). If  $S$  is much larger than  $K_s$ , algae will grow because the term  $\frac{S}{K_s + S}$  approaches 1. If  $S$  decreases to values much smaller than  $K_s$ , then the growth will stop because the term will approach 0. The Monod model has some weaknesses such as the fact that it considers an average value that counts for the global algae population, independently of what species are being considering and the fact that it deals with a single nutrient limitation (Kremer and Nixon, 1978). For pelagic and microbenthic algae, the value of  $K_s$  used for nitrate was  $2 \text{ mmol} \cdot \text{m}^{-3}$  taken from Laurent *et al.* (2006). For pelagic and microbenthic algae the value used of  $\mu_{max}$  was  $1 \text{ d}^{-1}$ , obtained from Laurent *et al.* (2006).

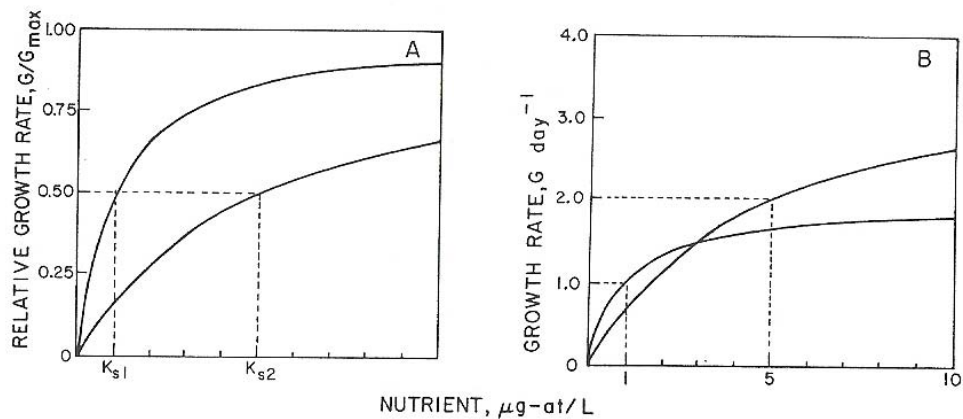


Figure 7.5 – Hyperbolic response of phytoplankton growth to a limiting nutrient. In the normalized representation (A) the species 1 (with lower  $K_s$ ) is dominant. However in the representation (B) species 2 grows faster at nutrient levels above  $3 \mu\text{g} \cdot \text{L}^{-1}$ .

Typically, the relationship between photosynthesis and irradiance is defined as a curve (Dring, 1992; Parsons *et al.*, 1984). However, a linear relationship may be acceptable (Tett, 1990). The light-limited growth rate can be defined as:

$$\mu(I) = \alpha(I - I_c) \quad (\text{d}^{-1}) \quad (7.11)$$

$I_c$  is the compensation irradiance, its value of  $5 \mu\text{Em}^{-2}\text{s}^{-1}$  was taken from Tett *et al.* (2003).  $\alpha$  is the photosynthetic efficiency parameter  $(\mu\text{Em}^{-2}\text{s}^{-1})^{-1}.\text{d}^{-1}$  and corresponds to the initial slope of the Photosynthesis-Irradiance (P-I) curve illustrated in Chapter 1 (Figure 1.2).  $\alpha$  can be calculated following:

$$\alpha = \frac{P_m}{I_k} \quad (\mu\text{Em}^{-2}\text{s}^{-1})^{-1}.\text{d}^{-1} \quad (7.12)$$

$P_m$  is the maximum photosynthetic rate and  $I_k$  is the saturation irradiance. The value of  $0.006 (\mu\text{Em}^{-2}\text{s}^{-1})^{-1}.\text{d}^{-1}$  for  $\alpha$  was taken from Tett *et al.* (2003) and used for pelagic and benthic algae.

### *Irradiance*

Photosynthetically active radiation (PAR, 400-750 nm) is 0.42 to 0.5 of the solar energy flux (Tett, 1990). Irradiance is crucial in this model because it clearly has an important obvious effect on the algae growth. Mean PAR on the water column ( $\bar{I}$ ) can be defined as (Tett *et al.*, 2003):

$$\bar{I} = (1 - m_0).m_1.m_2.I_0 \cdot \frac{1 - e^{-K_d.H}}{K_d.H} \quad \mu\text{E}.\text{m}^{-2}.\text{s}^{-1} \quad (7.13)$$

$I_0$  is the 24-hour mean of solar radiation (all wavelengths) at ground level ( $\text{W}.\text{m}^{-2}$ ),  $m_0$  corrects mean PAR for sea-surface reflection (albedo),  $m_1$  converts solar radiation to PAR photons and  $m_2$  deals with losses additional to those of Beer-Lambert decay.  $K_d$  is a crucial site-specific property, the PAR diffuse attenuation coefficient. The Beer-Lambert Law describes the exponential decrease of the irradiance with depth, as the photons are absorbed and scattered by water:

$$I_H = I_S.e^{-K_d.H} \quad \text{or} \quad \frac{I_H}{I_S} = e^{-K_d.H} \quad (7.14)$$

$I_H$  is the irradiance at a given depth and  $I_S$  is the irradiance at the sea-surface.

The 24-hour mean of solar irradiance ( $I_0$ ) used in this stage was the summer mean of about  $700 \mu\text{E} \cdot \text{m}^{-2} \cdot \text{s}^{-1}$ . This value is considered to be the normal irradiance found during the summer period in Ria Formosa. The  $K_d$  value used was initially similar for the water column and surface sediments and was about  $0.7 \text{ m}^{-1}$ . This was taken from observations in Ria Formosa (Chapter 5).

The mean PAR at the bottom of the aquatic system ( $\bar{I}_m$ ) is different and is defined in this model as:

$$\bar{I}_m = (1 - m_0) \cdot m_1 \cdot m_2 \cdot I_0 \cdot e^{-K_d \cdot H} \mu\text{E} \cdot \text{m}^{-2} \cdot \text{s}^{-1} \quad (7.15)$$

For an illustrative purpose, since a mean value for  $I_0$  was used rather than the yearly dataset, the variation of water column and bed irradiance throughout the year is presented in Figure 7.6. Irradiance values at the sediment surface are slightly lower than in the water column because the radiation has to cross the water layer to reach the sediment.

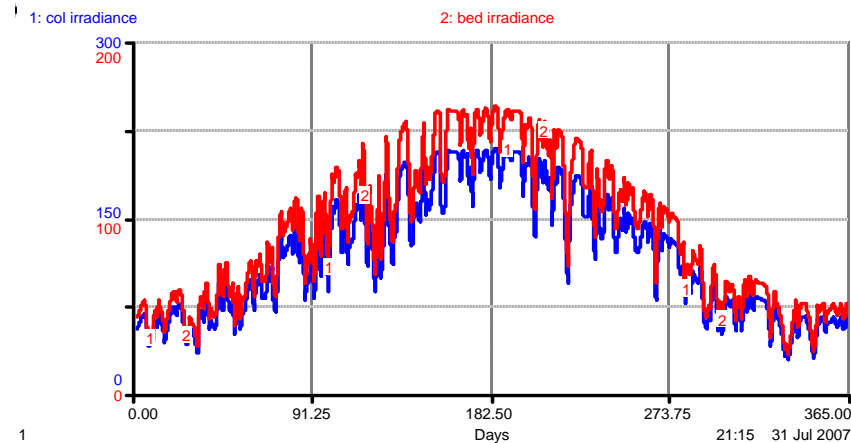


Figure 7.6– Daily mean values of PAR ( $I$ ;  $\mu\text{E} \cdot \text{m}^{-2} \cdot \text{s}^{-1}$ ) in the water column (blue; 0-300  $\mu\text{E} \cdot \text{m}^{-2} \cdot \text{s}^{-1}$ ) and at the sediment surface (red; 0-200  $\mu\text{E} \cdot \text{m}^{-2} \cdot \text{s}^{-1}$ ) from 1995 to 2004.

### *The yield of chlorophyll from nutrient*

The yield of pelagic chlorophyll from assimilated nitrogen,  $q$ , was investigated by Gowen *et al.* (1992), Edwards (2001), and Edwards *et al.* (2003, 2005). This parameter was an important tool for the assessment of eutrophication using the CSTT model. It did allow the calculation of chlorophyll concentration resulting from the conversion of all

available nitrogen. The yield  $q$  is determined by physiological responses of phytoplankton to environmental conditions (Edwards, 2001). The conditions are variable between species or ecosystems.

Gowen *et al.* (1992) carried out regressions between chlorophyll and DAIN data from observations. They found significant relationships and the range of slopes was from 0.25 to 4.4 mg chl. (mmol N)<sup>-1</sup>, with a median value of 1.05 mg chl. (mmol N)<sup>-1</sup>. Edwards *et al.* (2003; 2005) conducted several studies using microcosms, tending towards steady state, and found similar yield values. These findings supported Gowen *et al.* (1992). It was this median value that the CSTT used in its model (Tett *et al.*, 2003). Furthermore, several other studies have investigated this subject (e.g. Sosik and Mitchell, 1994).

In a closed system, the uptake of limiting nutrient from water to form new chlorophyll may be calculated by:

$$q = -\frac{\Delta X}{\Delta S} \quad (\text{mg chl. (mmol N)}^{-1}) \quad (7.16)$$

In this model, the value of 1.1 mg chl.(mmol N)<sup>-1</sup> proposed by Tett *et al.* (2003) was used for pelagic algae. For benthic chlorophyll, a value of 4 mg chl.(mmol N)<sup>-1</sup> was used. This value was obtained from my own previous studies, described in Chapter 6.

### *Algal Loss*

The algal loss component depends on a constant loss rate of 0.15 d<sup>-1</sup> which defines the loss by grazing and mortality. This term has implications for both pelagic and benthic chlorophyll. In addition, there are also other loss terms due to sinking of pelagic algae and resuspension of benthic algae, which is described above.

### **Discharges/Inputs to the water column - the $\Gamma_Y$ terms**

This part of the model is only composed of nutrient inputs from local anthropogenic or land-derived sources, as explained before by Equation 7.3.

#### 7.2.1.4 Methodology

This model was initially developed using STELLA ® software due to its simplicity, the efficiency, and the visual representation, which is frequently used to illustrate the model. In STELLA the integration method has to be chosen by the user between the Euler's method and the Runge-Kutta. Euler's method uses first order functions to perform approximations and is advised when there is a switch function in the model. The growth rate is such a function (can be light limited or nutrient limited, see above). However, Runge-Kutta, which employs higher order functions, is more precise.

In STELLA it is necessary to choose one time-step that is the same until the end of the run. To determine the best time-step to use, the model was run for several times and the outputs compared. A time-step of  $0.125 \text{ d}^{-1}$  was used in this stage. The STELLA diagram of the model is represented in Appendix III. Despite its complexity, it is useful to understand the fluxes of each state variable. The equations describing the relationships between them are placed below the diagram. The description of variables and parameters used in the model is presented in Table 7.1. The parameter values were taken from the literature. Efforts were made to obtain the most appropriate values for each parameter. However, in some cases, specific parameters were not available, especially for microphytobenthos. In these cases, values for phytoplankton were taken. This is expressed in parameter tables as 'adapted'.

The initial data used to run the model and boundary conditions are described in Table 7.2. The initial value of the limiting nutrient (DAIN) corresponds to the mean of data collected during 2006 and 2007-08. The nutrient concentration outside the lagoon also corresponds to the mean of both periods. The initial value for pelagic chlorophyll corresponds to the average obtained during the same periods, inside the lagoon. It was considered to use as boundary condition a value between what was observed in the sea and what was found by Tett *et al.* (2003), who indicated a concentration of  $0 \text{ mgchl.m}^{-3}$ . For the benthic chlorophyll, a value of  $270 \text{ mg chl. m}^{-2}$  was used as the initial value, which corresponds to the average observed during both periods.

Table 7.1 –Parameters used in the model for stage 1.

Parameter	Description	Value	Units	Source
$S_0$	Seawater nutrient concentration	2.3	mmol.m <sup>-3</sup>	data
$S_i$	Nutrient input from all sources except sea	78 x 10 <sup>6</sup>	mmol.d <sup>-1</sup>	Tett <i>et al.</i> (2003)
$X_0$	Seawater Chlorophyll concentration	1.75	mg chl.m <sup>-3</sup>	Tett <i>et al.</i> (2003) and data
$E$	Exchange rate	0.5	d <sup>-1</sup>	Tett <i>et al.</i> (2003)
$V$	Volume of Ria Formosa	88 x 10 <sup>6</sup>	m <sup>3</sup>	Tett <i>et al.</i> (2003)
$H$	Mean depth of Ria Formosa	1.5	m	Tett <i>et al.</i> (2003)
$q$	Chlorophyll yield from limiting nutrient (N)	1.1	mg chl. mmol <sup>-1</sup>	Tett <i>et al.</i> (2003)
$q_b$	MPB chlorophyll yield from limiting nutrient	4	mg chl. mmol <sup>-1</sup>	Chapter 6
$e$	Proportion of grazed nutrient that is recycled	0.5		Laurent <i>et al.</i> (2006)
$e_b$	Proportion of grazed nutrient that is recycled for MPB	0.5		Adapted from Tett <i>et al.</i> (2003)
$L_p$	Loss rate of phytoplankton due to pelagic grazers	0.15	d <sup>-1</sup>	Adapted from Tett <i>et al.</i> (2003)
$L_{br}$	Loss rate of MPB due to benthic resuspension	0.15	d <sup>-1</sup>	Adapted from Tett <i>et al.</i> (2003)
$sk$	Sinking rate of pelagic chlorophyll	1	m.d <sup>-1</sup>	Mann and Lazier (1996)
$L_g$	Loss rate of MPB due to grazing	0.15	d <sup>-1</sup>	Adapted from Blackford (2002)
$I_c$	Compensation irradiance	5	μEm <sup>-2</sup> s <sup>-1</sup>	Tett <i>et al.</i> (2003)
$\alpha$	Photosynthetic efficiency	0.006	(μEm <sup>-2</sup> s <sup>-1</sup> ) <sup>-1</sup> .d <sup>-1</sup>	Tett <i>et al.</i> (2003)
$I_0$	24-hour mean of solar radiation	700	μE.m <sup>-2</sup> .s <sup>-1</sup>	data
$K_d$	PAR diffuse attenuation coefficient	0.7	m <sup>-1</sup>	Chapter 5
$m_0$	Correction of mean PAR for sea-surface reflection	0.06		Tett <i>et al.</i> (2003)
$m_1$	Conversion of solar radiation to PAR photons	0.46 x 4.15	μE.J <sup>-1</sup>	Tett <i>et al.</i> (2003)
$m_2$	Additional losses to those of Beer-Lambert decay	0.37		Tett <i>et al.</i> (2003)
$\mu_{max}$	Maximum relative growth rate	1	d <sup>-1</sup>	Laurent <i>et al.</i> (2006)
$\mu_{max,b}$	Maximum relative growth rate for MPB	1	d <sup>-1</sup>	Adapted from Laurent <i>et al.</i> (2006)
$k_s$	Half-saturation concentration	2	mmol.m <sup>-3</sup>	Laurent <i>et al.</i> (2006)
$k_{s,b}$	Half-saturation concentration for MPB	2	mmol.m <sup>-2</sup>	Adapted from Laurent <i>et al.</i> (2006)

Table 7.2 – Initial values of state variables and their boundary conditions for stage 1.

Symbol		Initial values	Boundary conditions
$S$	Nutrient concentration	2.1 mmol.m <sup>-3</sup>	2.3 mmol.m <sup>-3</sup>
$X$	Chlorophyll concentration	2 mg chl. m <sup>-3</sup>	1.75 mg chl. m <sup>-3</sup>
$X_b$	MPB chlorophyll concentration	270 mg chl. m <sup>-2</sup>	

### 7.2.1.5 Results

The model simulation of the three state variables for a period of 365 days is represented in Figure 7.7. All the simulations followed the conditions indicated above, unless stated.



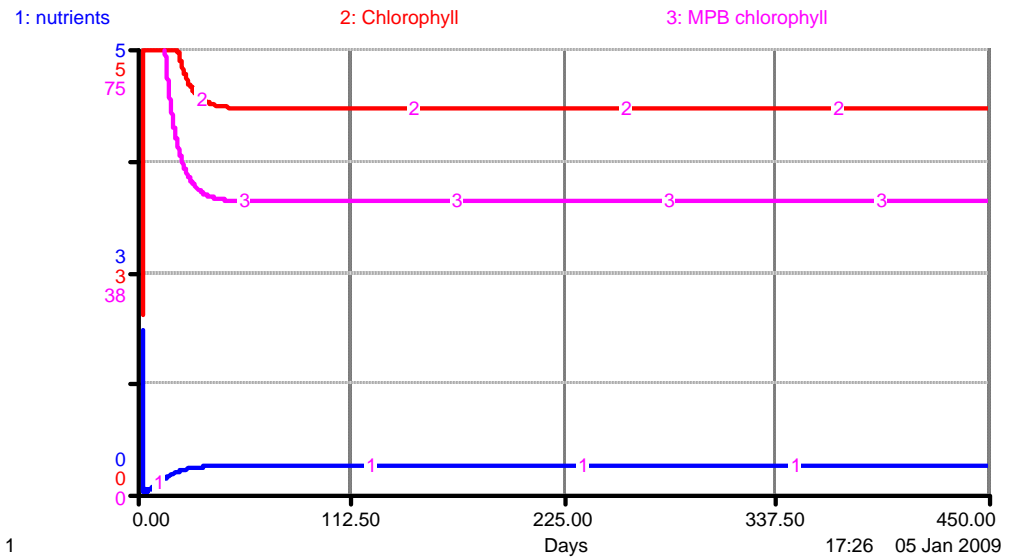


Figure 7.7 – Simulation of DAIN (blue;  $\text{mmol.m}^{-3}$ ), pelagic (red;  $\text{mg chl.m}^{-3}$ ) and benthic chlorophyll (pink;  $\text{mg chl.m}^{-2}$ ) concentrations during a period of 365 days.

The system reaches equilibrium at the beginning of the simulation and stays stable until day 365. DAIN concentration in the water column was predicted to be just above  $0.5 \text{ mmol.m}^{-3}$ . The pelagic chlorophyll concentration stays around  $4.3 \text{ mg chl.m}^{-3}$  and the benthic chlorophyll concentration around  $50 \text{ mg chl.m}^{-2}$ .

During this period of 365 days, the growth rate used by the model is the nutrient limited growth rate since it has smaller values compared with the light part. The 24-hour mean of solar irradiance used in this simulation was for the summer.

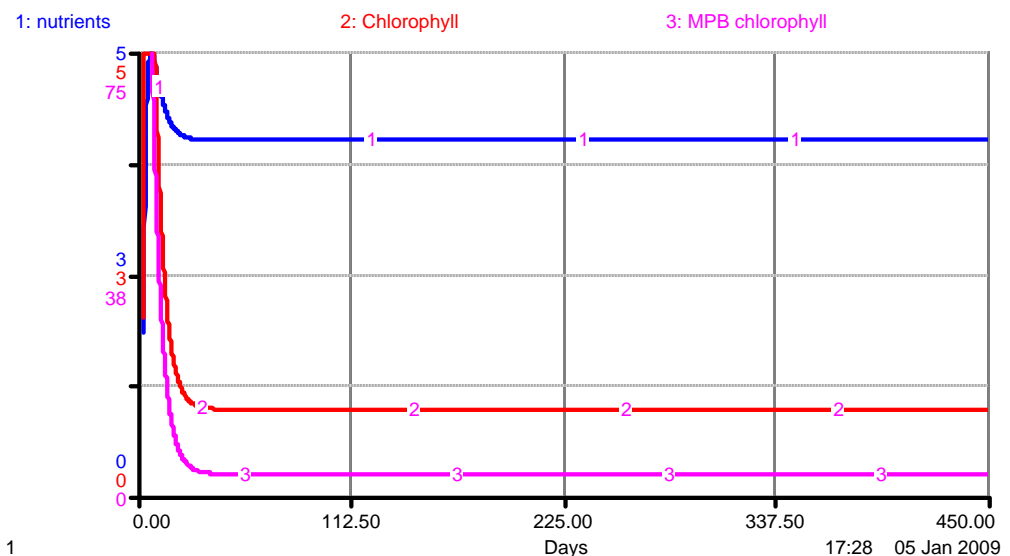


Figure 7.8 – Simulation of DAIN (blue;  $\text{mmol.m}^{-3}$ ), pelagic (red;  $\text{mg chl.m}^{-3}$ ) and benthic chlorophyll (pink;  $\text{mg chl.m}^{-2}$ ) concentrations during a period of 365 days over the same conditions, except for the 24-hour mean of solar irradiance.

The simulation was repeated with the same conditions, except the 24-hour mean of solar radiation, which was changed for the winter value ( $100 \mu\text{E}\cdot\text{m}^{-2}\cdot\text{s}^{-1}$ ). The growth did become light limited (via the light equations) and the output is represented in Figure 7.8. The algal growth was significantly smaller and so were chlorophyll concentrations. DAIN concentrations are also higher. However, during most of the year the solar irradiance is much higher than the winter value. Therefore, the first simulation, using the summer solar irradiance value, will be preferentially explored.

The model is clearly underestimating the microphytobenthos chlorophyll concentration in this system (Figure 7.9). Observations are more than 10 times the simulated ones. For DAIN and Pelagic chlorophyll observations the range of variation is not exactly within the predicted (Figure 7.10). For DAIN a slight underestimation seems to be present and for pelagic chlorophyll a slight overestimation seems to be present.

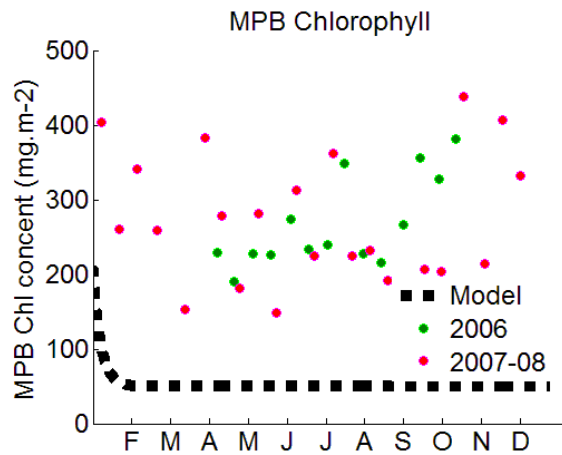


Figure 7.9 - Observed values of Microphytobenthos chlorophyll ( $\text{mg chl}\cdot\text{m}^{-2}$ ) concentrations found in 2006 and 2007-08 versus the model simulation.

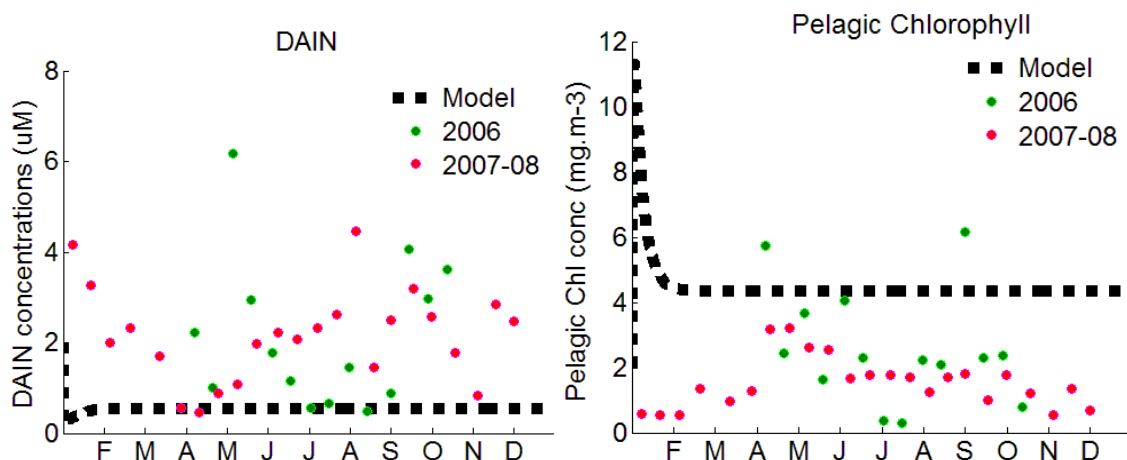


Figure 7.10 - Observed values of DAIN ( $\mu\text{M}$  or  $\text{mmol}\cdot\text{m}^{-3}$ ) and pelagic chlorophyll ( $\text{mg chl}\cdot\text{m}^{-3}$ ) concentrations found in 2006 and 2007-08 versus the model simulation.

### 7.2.1.6 Discussion

The model output does not predict the natural variability of the state variables considered for this system. This is mainly due to the lack of time-series data of forcing variables. These forcing variables are crucial to create a dynamic model and to incorporate specific information/data about the system. Dynamic models, which provide predictions showing intrinsic variability, are desirable for a correct understanding of processes. As shown in the results, by changing the 24-hour mean of solar irradiance from the summer to the winter value, a great variation of the output was obtained. The model could be improved with the addition of a complete time-series of the irradiance values throughout the year. DAIN concentrations were larger in the second simulation due to the decrease in nitrogen incorporation by algae. Actually the knowledge of which process limits the algal growth is extremely important for an appropriate eutrophication assessment. It is also essential for the selection of ecosystem indicators.

The addition of forcing variables to the model would result in more accurate predictions of DAIN and pelagic chlorophyll concentrations. The addition of a new state variable, microphytobenthic chlorophyll concentration, did not result in a more accurate model. The improvement of the model obtained was clearly not enough to satisfy our objectives. The larger values of MPB found in the lagoon do not have enough nutrients in the water column to support them. The growth seems to be nutrient limited through almost all year and the nutrients in the water column are scarce.

The goodness of the fit was not evaluated for this step due to the non-existence of variability in the model output. The plot showing the observed values against the model output would be a representation of a straight and constant line, such as in Figures 7.9 and 7.10. The observation values would vary just in one axis and not in two, as desired.

### **7.2.2 Stage 2 – Addition of pore nutrients as a state variable**

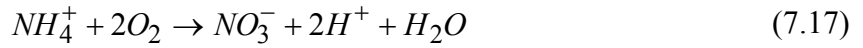
It is imperative to provide forcing data in order to obtain a model with the ability to predict the natural variability of the system, as discussed above. Although the STELLA software allows the addition of this time-series of data, it has some constraints in the manipulation of the long sets of data and in the simulation itself. Data have to be copied directly to the program, one by one. Besides that, if we desire to work with a simulation of larger periods, all the forcing variables have to be manually changed accordingly.

Mainly for this reason the model was transferred to other software, Matlab. It allows the addition of datasheets and the use of these as desired, by just changing a simple command. Moreover, some of the original datasheets obtained for Ria Formosa were not in the final format and needed transformation, which was very easy to do in Matlab. Furthermore, this software is much more powerful. The graphical representation obtained is better and can be manipulated. Another characteristic of Matlab that can be considered an advantage is the integration method, which is more precise by allowing the use of non-fixed time-steps.

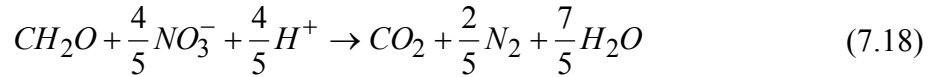
Another improvement was the addition of an alternative source of nutrients for microphytobenthos to test if the microphytobenthic cells are mainly supported by nutrients from the pore water. Stage 1 was important since it led to the realisation that the large concentrations of benthic chlorophyll could not be reached using the small nutrient concentrations in the water column. Nutrients in the pore water were therefore considered to be the fourth state variable of the model. As discussed in previous chapters, pore water nutrients play an important role in shallow water systems such as Ria Formosa. Moreover, their large concentrations (compared with the water column) were repeatedly suggested as associated with large benthic chlorophyll concentrations (e.g. Sundbäck and Granéli, 1988; Magni and Montani, 2006; Facca and Sfriso, 2007).

Modelling nutrients in pore water involves a good understanding and knowledge about nutrient dynamics in the surface sediment layers. Sediments have a large capacity to storage organic matter and nutrients (Jørgensen and Richardson, 1996). Sediments receive particulate organic matter mainly by sedimentation. They are part of an important regulation process and are characterized by having a large microbial activity. The organic material is primarily mineralized by aerobic microorganisms, however this depends on sediment type and other conditions (Jørgensen and Richardson, 1996). Only a thin layer beneath the surface is oxic and the position of oxic-anoxic interface may change throughout the year.

Chemical reactions take place in the pore water, which interacts with the water column by diffusion (Di Toro, 2001). Typically, pore water has large concentrations of ammonia, which is a direct result from the mineralization of Particulate Organic Nitrogen (PON), in a process called diagenesis. Ammonia can then be transformed into nitrate in the presence of oxygen, by nitrification (Di Toro, 2001):



Nitrate can be converted into gaseous nitrogen by denitification, where  $CH_2O$  is the electron donor to the reaction (Equation 7.18; Jørgensen and Richardson, 1996):



There is also an exchange process of pore water nutrients (ammonia, nitrate, silica, etc.) with the water column by diffusion and particle mixing. The diffusion follows the Fick's Law of mass transport by molecular diffusion. The flux is proportional to the concentration gradient (Di Toro, 2001).

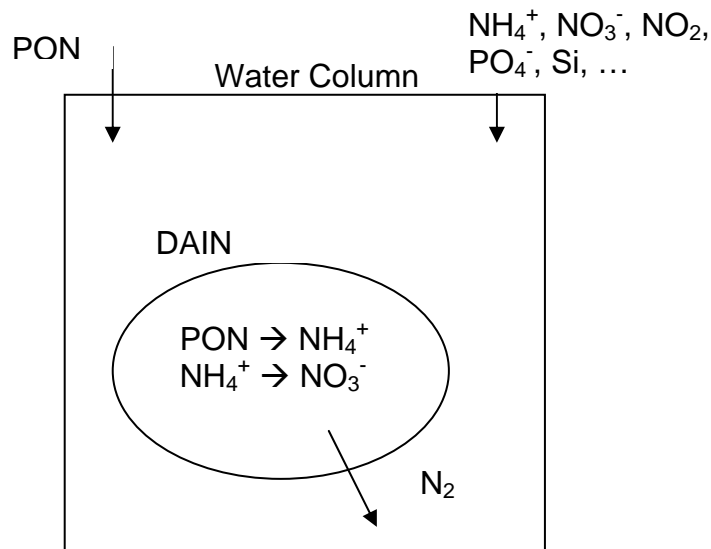


Figure 7.11 – Scheme of nutrient dynamics in the sediment.

The scheme presented in Figure 7.11 is the representation of the model processes and it is a simplification of the Di Toro model (Di Toro, 2001). This author considered two different layers in the sediment: the oxic and anoxic. He also considers the different processes of diagenesis, nitrification and diffusion, for example. The same was done for different nutrients. Di Toro's model is much more complex than the one developed in here. The dCSTT-MPB model considers the total concentration of DAIN, so nitrification was not considered directly in the model because it does not affect the DAIN concentration.

## 7.2.2.1 Conceptual model

The conceptual model is similar with the one presented before. However, the box representing the lagoon has now another state variable, nutrients in the pore water. In addition, relationships and processes involved are also described in Figure 7.12.

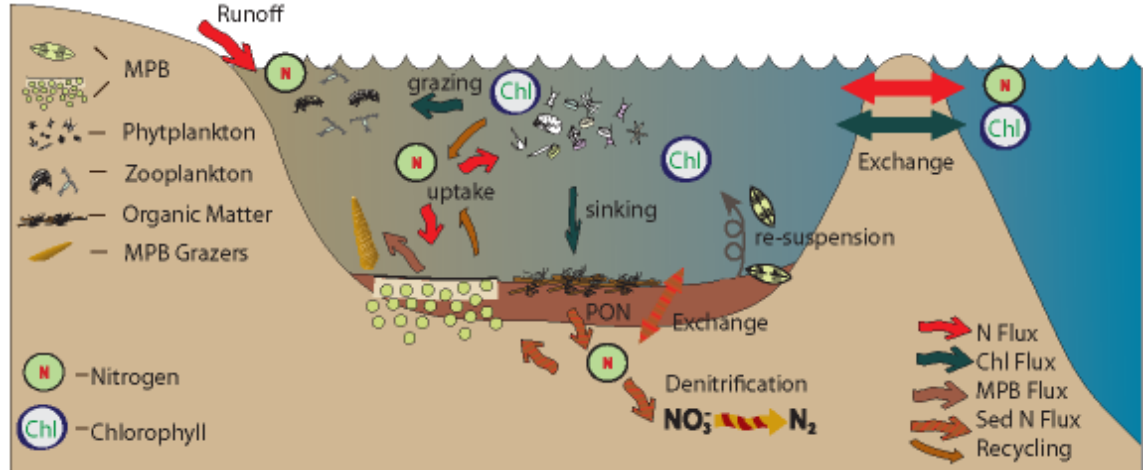


Figure 7.12 – Diagram representation of the conceptual model. Illustration symbols from the Integration and Application Network (<http://ian.umces.edu>).

## 7.2.2.2 Mathematical model

The mathematical model is constituted by four differential equations, one for each state variable:  $S$  (limiting nutrient in the lagoon),  $X_p$  (pelagic chlorophyll inside the lagoon),  $X_b$  (microphytobenthic chlorophyll inside the lagoon) and  $S_{sed}$  (pore water limiting nutrient).

$$\frac{\partial S}{\partial t} = E.(S_0 - S) - \frac{\mu_p \cdot X_p}{q} + e.L_p \cdot \frac{X_p}{q} + \frac{S_i}{V} + \frac{S_{sed} - S}{h_s} \cdot \frac{D_m \cdot p}{\tau \cdot H} \quad (\text{mmol} \cdot \text{m}^{-3} \cdot \text{d}^{-1}) \quad (7.19)$$

$$\frac{\partial X_p}{\partial t} = E.(X_0 - X_p) + \mu_p \cdot X_p - L_p \cdot X_p + \frac{L_{br} \cdot X_b}{H} - \frac{sk}{H} \cdot X_p \quad (\text{mg chl} \cdot \text{m}^{-3} \cdot \text{d}^{-1}) \quad (7.20)$$

$$\frac{\partial X_b}{\partial t} = \mu_b \cdot X_b - L_g \cdot X_b + sk \cdot X_p - L_{br} \cdot X_b \quad (\text{mg chl} \cdot \text{m}^{-2} \cdot \text{d}^{-1}) \quad (7.21)$$

$$\frac{\partial S_{sed}}{\partial t} = \frac{e_b \cdot L_g \cdot X_b}{h_s \cdot q_b \cdot p} + \frac{N \cdot d}{p} + \frac{S - S_{sed}}{h_s} \cdot \frac{D_m}{h_s \cdot \tau} - den \cdot S_{sed} - \frac{\mu_b \cdot X_b}{q_b \cdot p} \quad (\text{mmol} \cdot \text{m}^{-3} \cdot \text{d}^{-1}) \quad (7.22)$$

The subscript 0 (outside) always refers to the concentrations in the sea and the subscript i refers to inputs, in this case of nutrients ( $S_i$ ,  $\text{mmol}\cdot\text{d}^{-1}$ ) to the box (lagoon). The subscript p refers to phytoplankton and b to the microphytobenthos.  $E$  is the exchange rate of waters between inside and outside the lagoon ( $\text{d}^{-1}$ ),  $V$  is the volume ( $\text{m}^3$ ),  $e$  is the fraction of grazed nitrogen that is recycled,  $q$  is the yield of chlorophyll from nutrients ( $\text{mg chl}\cdot\text{mmol}^{-1}$ ),  $H$  is the mean depth of the lagoon (m),  $L_p$  is phytoplankton loss rate ( $\text{d}^{-1}$ ),  $\mu$  is phytoplankton growth rate ( $\text{d}^{-1}$ ),  $L_{br}$  is the loss rate of microphytobenthos chlorophyll to the water column ( $\text{d}^{-1}$ ) and  $L_g$  is the MPB grazing rate ( $\text{d}^{-1}$ ). In the equation for pore water nutrients,  $N$  is the particulate organic nitrogen concentration ( $\text{mmol}\cdot\text{m}^{-3}$ ) in the sediment,  $h_s$  is the thickness of the sediment layer considered (m),  $d$  is the decay rate of  $N$  ( $\text{d}^{-1}$ ) in the sediment,  $p$  is porosity (percentage) of the sediment,  $D_m$  is the diffusion coefficient ( $\text{m}^2\cdot\text{d}^{-1}$ ) between pore water and water column,  $\tau$  is tortuosity and  $den$  is the denitrification coefficient ( $\text{d}^{-1}$ ).

### 7.2.2.3 Numerical model

#### **Physical Model – the $-\nabla\phi_Y$ terms**

Nutrient fluxes from the sediment to the water column were added and resuspension of benthic chlorophyll was improved.

#### *Flux of pore water nutrients to the water column*

The outflux term of nutrients ( $\text{mmol}\cdot\text{m}^{-3}\cdot\text{d}^{-1}$ ) from pore water to the water column is defined by  $\frac{S - S_{sed}}{h_s} \cdot \frac{D_m}{h_s \cdot \tau}$ . Nutrient concentrations within the sediments are reported in the literature to be much higher than nutrient concentrations in the water column (e.g. Murray *et al.*, 2006; Serpa *et al.*, 2007). Therefore, an influx from the sediments to the water column is expected. The coefficient of diffusion ( $D_m$ ) was taken from Murray *et al.* (2006). The thickness ( $h_s$ ) of the layer of sediments considered in this model is 5 cm, which corresponds to the depth of the samples collected. Tortuosity ( $\tau$ ) value was taken from Jakson *et al.* (2002).

The equation of the influx of pore water nutrients into the water column is slightly different. State variables are in the opposite position because the flux is now positive. It

also has to deal with the dilution in the water column. Thus, the influx can be defined by the following equation:

$$\frac{S_{sed} - S}{h_s} \cdot \frac{D_m \cdot P}{\tau \cdot H} \quad (\text{mmol.m}^{-3}.\text{d}^{-1}) \quad (7.23)$$

### *Sinking and resuspension of algae*

The sinking process of pelagic algae is the same as in stage 1. However, the resuspension of microphytobenthos was divided in two different processes: the resuspension caused by the wind action and the resuspension caused by the tidal action. Thus, the MPB loss due to resuspension ( $L_{br}$ ):

$$L_{br} = r_{tide} + r_{wind} \quad (\text{d}^{-1}) \quad (7.24)$$

Resuspension caused by the neap-spring tidal variation is a sinusoidal curve representing the tidal cycle. The loss rates used both for the tidal and the wind effects were adjusted to observations. For tidal effect it is around 5% per day. Thus:

$$r_{tide} = \sin(48 \cdot \pi \cdot t / 365 + 162) \cdot 0.002 + 0.05 \quad (\text{d}^{-1}) \quad (7.25)$$

$t$  is time in days.

The re-suspension by wind is the product of the multiplication of the relative effect of winds (obtained dividing daily values by the yearly maximum observed) times a ‘loss rate by wind’ ( $\text{d}^{-1}$ ). This MPB loss corresponds to an input of chlorophyll in the water column, i.e., in the pelagic chlorophyll, that is obtained dividing the MPB water column total loss by the mean depth ( $\text{mg chl.m}^{-3}$ ). Thus:

$$r_{wind} = \left( \frac{w}{w_{\max}} \right) \cdot 0.1 \quad (\text{d}^{-1}) \quad (7.26)$$

### *Winds*

Wind velocity ( $\text{m.s}^{-1}$ ) data were used to describe one part of the water column loss of microphytobenthos (see above) caused by wind action. This information was obtained



from the European Project OAERRE database for the years between 1990 and 2002 (Caetano *et al.*, 2002). The initial file contained several values per day and a script similar to the one used for irradiance was used to bin them into daily means (Appendix III). The final file, which is used by the main routine deals with daily means over the 12 year period. The daily means were also transformed in order to obtain the squared daily values of wind velocity (Figure 7.14). This was done to facilitate its use in the model.

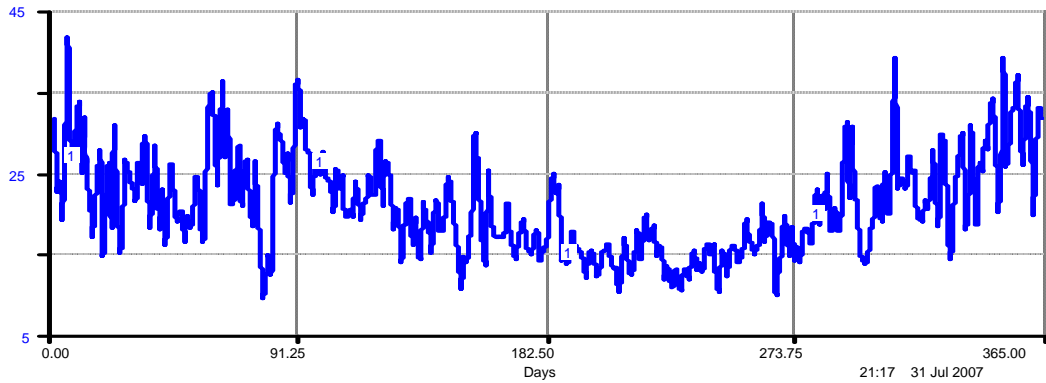


Figure 7.14 – Daily means of squared wind velocity from 1990 to 2002 over 365 days.

### **Bio-chemical Model – the $\beta_Y$ terms**

#### *Recycling*

Pelagic nutrient concentration in this stage has only one input flow from recycling of pelagic chlorophyll. This process is the same as described in Stage 1. The recycling term from microphytobenthos chlorophyll is now added to the nitrogen concentration in the pore water. It is more likely that the end products of benthic grazers stay in the sediment. The process is now described:

$$\frac{e_b \cdot L_g \cdot X_b}{q_b \cdot p \cdot h_s} \quad (\text{mmol} \cdot \text{m}^{-3} \cdot \text{d}^{-1}) \quad (7.27)$$

#### *Uptake of nutrients by algae*

The conversion of nutrients into chlorophyll in the water column is the same as in Stage 1. However, the new state variable, nutrients in pore water, also has a conversion

term to microphytobenthos. The equation is very similar to the one for nutrients in the water column and is described below:

$$uptake_b = \frac{\mu_b \cdot X_b}{q_b \cdot p \cdot h_s} \quad (\text{mmol} \cdot \text{m}^{-3} \cdot \text{d}^{-1}) \quad (7.28)$$

### *Biological Production*

For pelagic chlorophyll the equations remain the same. Slight differences are described for benthic algae. Nutrients from pore water are the ones considered for the equation of the nutrient-limited growth rate. Therefore, the benthic algae will have much more nutrient available for their growth. Hence:

$$\mu_b(S) = \frac{\mu_{\max,b} \cdot S_{sed}}{K_s + S_{sed}} \quad (\text{d}^{-1}) \quad (7.29)$$

The value of  $\mu_{\max}$  used for pelagic chlorophyll and for microphytobenthos was  $1 \text{ d}^{-1}$ . For pelagic  $K_s$  the value of  $2 \text{ mmol} \cdot \text{m}^{-3}$  for nitrogen was used, taken from Laurent *et al.* (2006) and for MPB a larger value was used,  $10 \text{ mmol} \cdot \text{m}^{-3}$  for nitrogen. Eppley *et al.* (1969) and Baird *et al.* (2003) suggested that the half saturation constant of benthic algae may be larger than for phytoplankton.

### *Irradiance*

The functions used for irradiance are the ones described for stage 1. However, cloud cover data obtained from the *Instituto de Meteorologia de Portugal* was used to determine the 24-hour mean of solar irradiance ( $I_0$ ). This was done using an algorithm based on the equations suggested by Kirk (1994). The script is presented in Appendix III. The output of the script (Figure 7.13) is a time series for 365 days of the 24-hour mean of PAR at sea-surface in  $\mu\text{E} \cdot \text{m}^{-2} \cdot \text{s}^{-1}$ .

The  $K_d$  value used for the water column was similar to that used in stage 1 and discussed in Chapter 5.

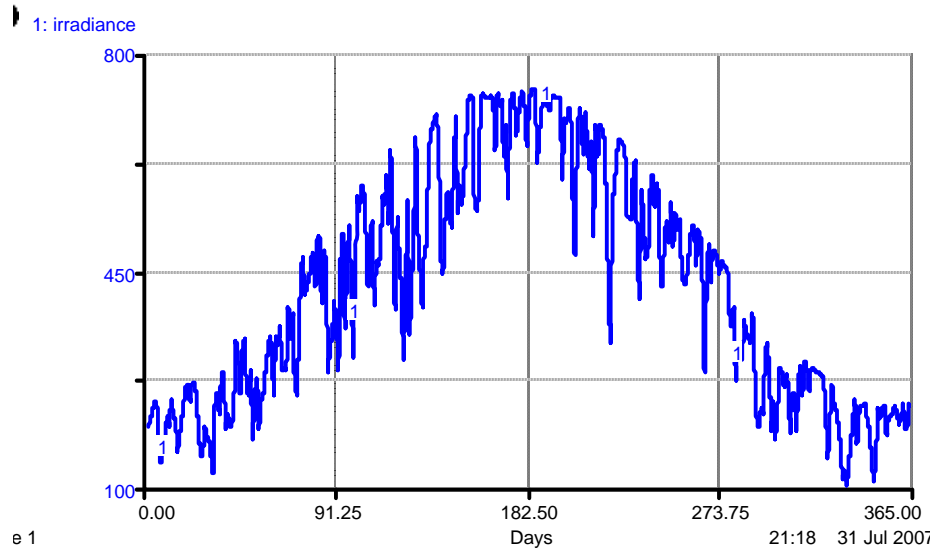


Figure 7.13 – Daily mean values of PAR at sea-surface ( $I_0$ ;  $\mu\text{E}\cdot\text{m}^{-2}\cdot\text{s}^{-1}$ ) from 1995 to 2004.

### *The yield of chlorophyll from nutrient*

The yield of chlorophyll from nutrients is the same as described previously, in stage 1.

### *Algal Loss*

Algal loss equations are the same as before (stage 1).

### *Denitrification*

Denitrification is the process of reducing nitrate and nitrite into gaseous nitrogen, which makes it less available to organisms. In this model, a denitrification coefficient of 0.01 was considered (Murray and Parslow, 1997). The loss of nutrients from the pore water is 1% per day.

### *Mineralisation of organic nitrogen*

There is also an input of nutrients to the pore water from the particulate organic nitrogen ( $N$ ) which was considered to be  $100 \text{ mmol}\cdot\text{m}^{-3}$  (Serpa *et al.*, 2007). The flux is defined as:

$$\frac{N \cdot d}{p} \quad (\text{mmol}\cdot\text{m}^{-3}\cdot\text{d}^{-1}) \quad (7.30)$$

The decay rate was considered to be  $0.1 \text{ d}^{-1}$  and porosity 0.5 (percentage). The concentrations of particulate organic nitrogen were based on Serpa *et al.* (2007). The value presented by Serpa *et al.* (2007) is for the total organic nitrogen and was reduced to be applied to this model. Moreover, PON has labile and refractory fractions. Refractory fractions are generally the main part and are normally neglected because they are not soluble or hydrolysable.

### **Discharges/Inputs to the water column - the $\Gamma_Y$ terms**

This part of the model is only composed of nutrient inputs from local anthropogenic or land-derived sources, as explained before by Equation 7.3.

#### 7.2.2.4 Methodology

The model was transferred to Matlab software, which is more powerful in data handling and allows a wider exploration of the graphical output of the model. The Matlab numerical integration function used was ode23, which is based in the Runge-Kutta integration method. This method is more precise than the Euler's method used in STELLA. Moreover, it is a one-step solver, which means that this solver only needs the solution immediately preceding the time point. Some other solvers of the ode family also need other solution points of the simulation. This means that the simulation would be time consuming, which ode23 avoids. In addition, this solver also chooses the best time-step to use in the simulation, which can be considered an advantage compared to fixed time-step in STELLA. The model is described in three scripts (m-files), which are ana.m, csttfunction.m and parameters.m, that are computed in Matlab simultaneously (Figure 7.15). The scripts are presented in Appendix III. The m-file ana.m includes the main commands for loading forcing variables, running the solver and plotting and saving the output. The m-file csttfunction.m has the description of the differential equations and all the equations involved in the model. The list of parameters used and their correspondent values are present in file parameters.m. Table 7.3 presents the values of the parameters used in the model.

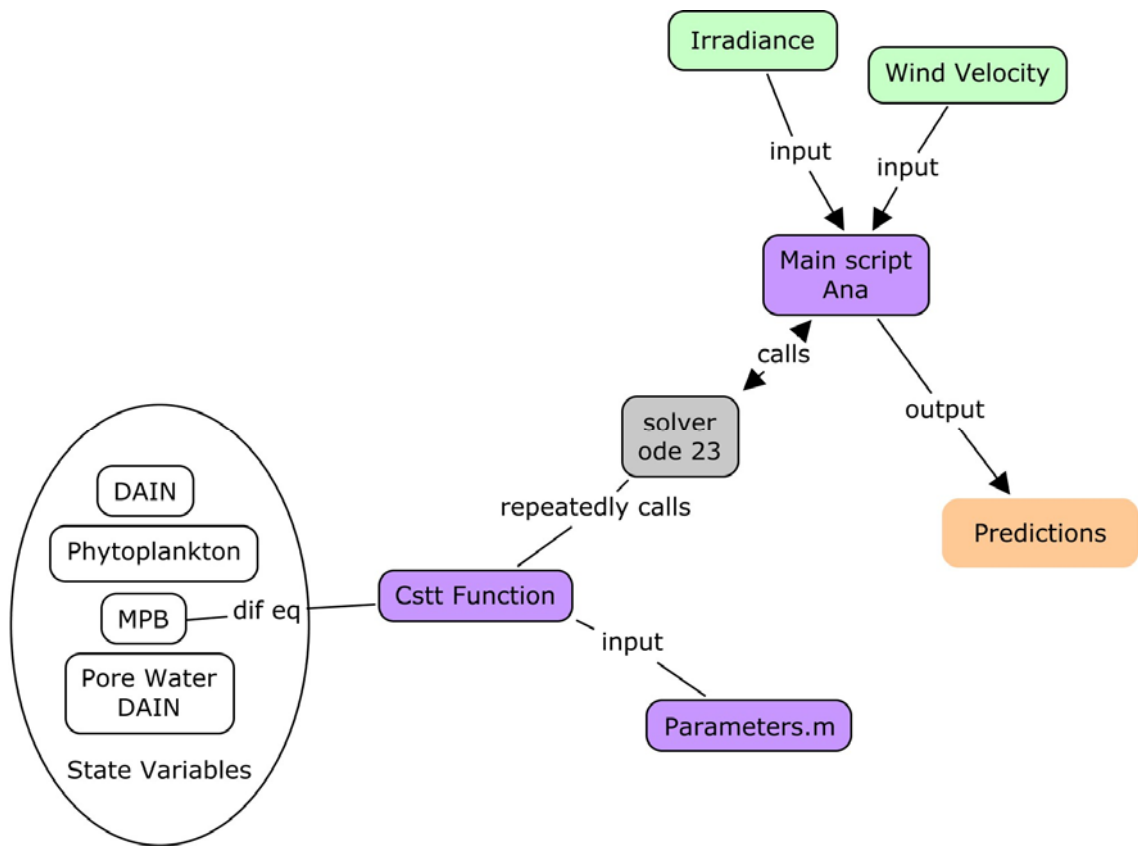


Figure 7.15 – Scheme of the functioning of files involved in the model.

The initial data used to run the model and boundary conditions are described in Table 7.3. The initial value of the limiting nutrient (DAIN) corresponds to the mean of data collected during 2006 and 2007-08. The nutrient concentration outside the lagoon also corresponds to the mean of both periods. The initial value for pelagic chlorophyll corresponds to the average obtained during the same periods, inside the lagoon. As boundary condition a value between what was observed in the sea and what was found by Tett *et al.* (2003), who indicated a concentration of  $0 \text{ mgchl.m}^{-3}$ , was used. For the benthic chlorophyll, a value of  $270 \text{ mg chl. m}^{-2}$  was used as the initial value, which corresponds to the average observed during both periods. The initial value used for pore water nutrients was  $100 \text{ mmol.m}^{-3}$ , taken from literature (e.g. Serpa *et al.*, 2007). Some parameters, such as the decay of N ( $d$ ), were ‘adjusted’ to observations, which means that the value used was the one that allowed the best correspondence with data.

Table 7.3 –Parameters used in the model for stage 2.

Parameter	Description	Value	Units	Source
$S_0$	Seawater nutrient concentration	2.3	mmol.m <sup>-3</sup>	data
$S_i$	Nutrient input from all sources except sea	78 x 10 <sup>6</sup>	mmol.d <sup>-1</sup>	Tett <i>et al.</i> (2003)
$X_0$	Seawater Chlorophyll concentration	1.75	mg chl.m <sup>-3</sup>	Tett <i>et al.</i> (2003) and data
$E$	Exchange rate	0.5	d <sup>-1</sup>	Tett <i>et al.</i> (2003)
$V$	Volume of Ria Formosa	88 x 10 <sup>6</sup>	m <sup>3</sup>	Tett <i>et al.</i> (2003)
$H$	Mean depth of Ria Formosa	1.5	m	Tett <i>et al.</i> (2003)
$q$	Chlorophyll yield from limiting nutrient (N)	1.1	mg chl. mmol <sup>-1</sup>	Tett <i>et al.</i> (2003)
$q_n$	MPB chlorophyll yield from limiting nutrient	4	mg chl. mmol <sup>-1</sup>	Chapter 6
$e$	Proportion of grazed nutrient that is recycled	0.5		Laurent <i>et al.</i> (2006) Adapted from
$e_b$	Proportion of grazed nutrient that is recycled for MPB	0.5		Laurent <i>et al.</i> (2006) Adapted from
$L_p$	Pelagic chlorophyll loss rate	0.15	d <sup>-1</sup>	Tett <i>et al.</i> (2003)
$sk$	Sinking rate of pelagic chlorophyll	1	m.d <sup>-1</sup>	Mann and Lazier (1996) Adapted from
$L_g$	Grazing rate	0.15	d <sup>-1</sup>	Blackford (2002)
$I_0$	24-hour mean of solar radiation		μE.m <sup>-2</sup> .s <sup>-1</sup>	data
$K_d$	PAR diffuse attenuation coefficient	0.7	m <sup>-1</sup>	Chapter 5
$I_c$	Compensation irradiance	5	μEm <sup>-2</sup> s <sup>-1</sup>	Tett <i>et al.</i> (2003)
$\alpha$	Photosynthetic efficiency	0.006	(μEm <sup>-2</sup> s <sup>-1</sup> ) <sup>-1</sup> .d <sup>-1</sup>	Tett <i>et al.</i> (2003)
$m_0$	Correction of mean PAR for sea-surface reflection	0.06		Tett <i>et al.</i> (2003)
$m_1$	Conversion of solar radiation to PAR photons	0.46 x 4.15	μE.J <sup>-1</sup>	Tett <i>et al.</i> (2003)
$m_2$	Additional losses to those of Beer-Lambert decay	0.37		Tett <i>et al.</i> (2003)
$\mu_{max}$	Maximum relative growth rate	1	d <sup>-1</sup>	Laurent <i>et al.</i> (2006) Adapted from
$\mu_{max,b}$	Maximum relative growth rate for MPB	1	d <sup>-1</sup>	Laurent <i>et al.</i> (2006)
$k_s$	Half-saturation concentration	2	mmol.m <sup>-3</sup>	Laurent <i>et al.</i> (2006) Adapted from
$k_{s,b}$	Half-saturation concentration for MPB	10	mmol.m <sup>-3</sup>	Laurent <i>et al.</i> (2006)
$N$	Particulate Organic Nitrogen	100	mmol.m <sup>-3</sup>	Serpa <i>et al.</i> (2007)
$d$	Decay rate of N	0.1	d <sup>-1</sup>	Adjusted
$\tau$	Tortuosity of sediment pores	1.3	-	Jackson <i>et al.</i> (2002)
$p$	Porosity	0.5	-	data
$D_m$	Diffusion coefficient	1.66 x 10 <sup>-4</sup>	m <sup>2</sup> .d <sup>-1</sup>	Murray <i>et al.</i> (2006) Adapted from Murray and Parslow (1997)
$den$	Denitification rate	0.01	d <sup>-1</sup>	
$hs$	Thickness of the pore water sediment layer	0.05	m	data

Table 7.4 – Initial values of state variables and their boundary conditions for stage 2.

Symbol		Initial values	Boundary conditions
S	Nutrient concentration	2.1 mmol.m <sup>-3</sup>	2.3 mmol.m <sup>-3</sup>
X <sub>p</sub>	Chlorophyll concentration	2 mg chl. m <sup>-3</sup>	1.75 mg chl. m <sup>-3</sup>
X <sub>b</sub>	MPB chlorophyll concentration	270 mg chl. m <sup>-2</sup>	
S <sub>sed</sub>	Pore water nutrient concentration	100 mmol.m <sup>-3</sup>	

Statistical assessments of the goodness of the fit were done using the least squares regression. Comparisons were done between model simulations and observations.

Observation data consist of two sets of data obtained during this project, from 2006 and 2007-08.

### 7.2.2.5 Results

The model simulation of the four state variables for a 730 day period is presented in Figure 7.16 (A and B). The predictions of DAIN concentrations in the water column and pelagic chlorophyll concentrations are small compared with the other variables, so they are presented in a separate plot (Figure 7.16 -B). The pelagic chlorophyll and DAIN in the water column have relatively stable values during spring, summer and autumn. However, during the winter, the values of pelagic chlorophyll decrease and the values of DAIN increase. The same was found for benthic chlorophyll and DAIN in pore water, but in larger proportions.

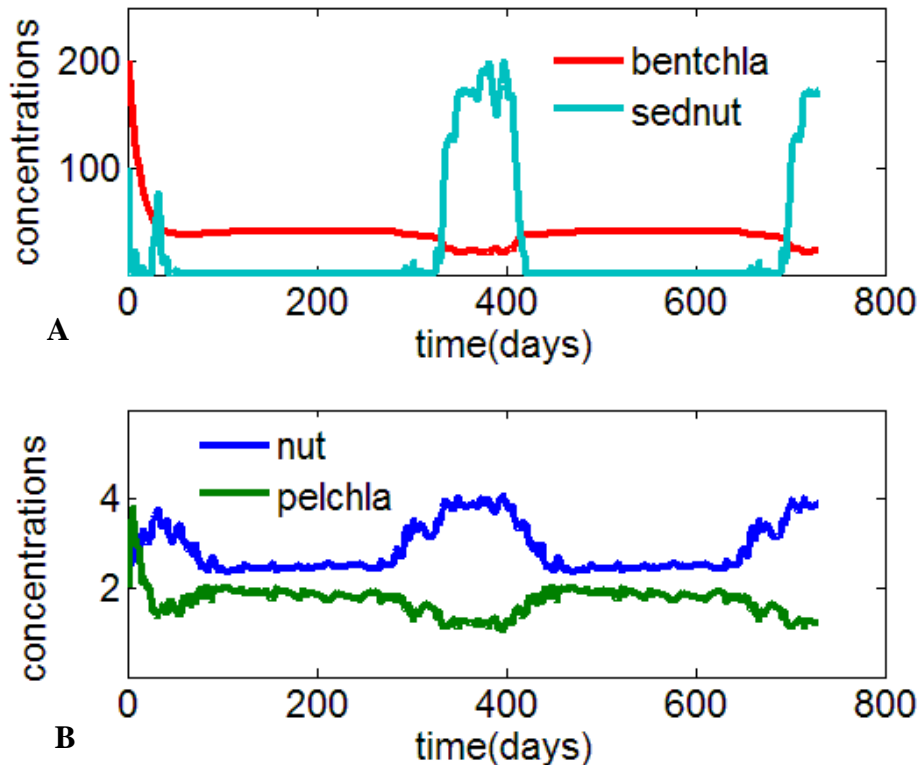


Figure 7.16 (A and B) – Simulation of DAIN (blue;  $\text{mmol.m}^{-3}$ ) in the water column, pelagic (green;  $\text{mg chl.m}^{-3}$ ) and benthic chlorophyll (red;  $\text{mg chl.m}^{-2}$ ) and DAIN in pore water (light blue;  $\text{mmol.m}^{-3}$ ) concentrations during a period of 730 days.

The model predicts constant concentrations of DAIN in the water column during the year, except for winter. Predictions are within the range of variation found in Ria Formosa, however, during spring, summer and autumn, observations showed a large

variation which is not explained by the model (Figure 7.17). For pelagic chlorophyll, the model also predicts relatively constant values for the whole year, except the winter, when they are slightly smaller. The benthic chlorophyll (MPB) is clearly underestimated by the model (Figure 7.18). Moreover, the observed variability throughout the year is not predicted by the model. The model also clearly underestimates DAIN concentrations in pore water. Furthermore, the model predicted an increase of DAIN in the winter, which was not observed.

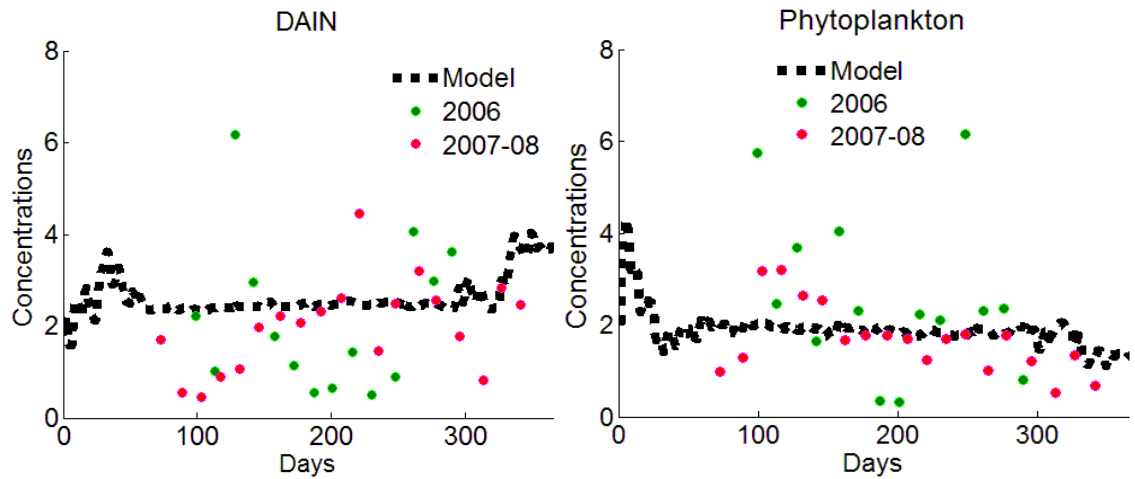


Figure 7.17 – Concentrations of DAIN and pelagic chlorophyll observed (2006 and 2007-08;  $\text{mmol.m}^{-3}$  and  $\text{mg chl.m}^{-3}$ ) and predicted by the model for Ria Formosa.

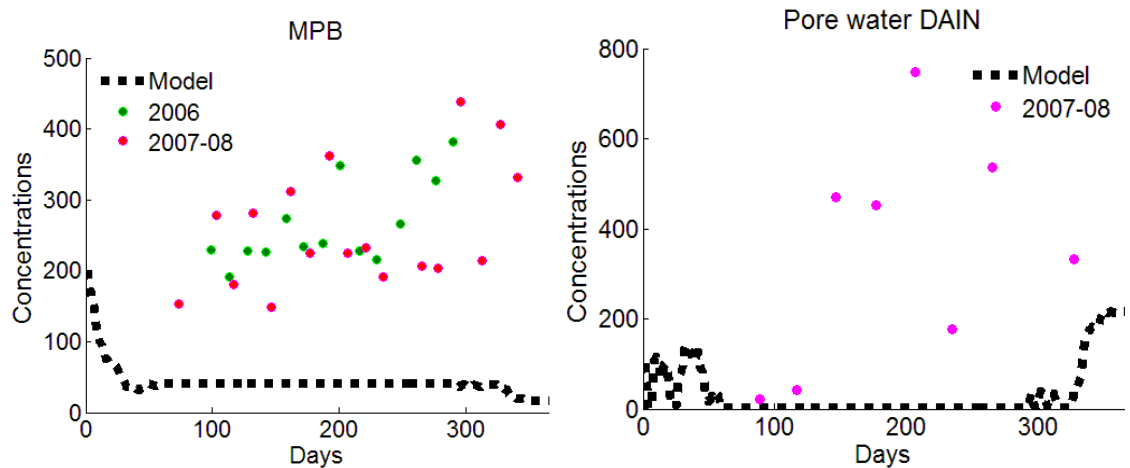


Figure 7.18 – Concentrations of MPB and pore water DAIN observed (2006 and 2007-08;  $\text{mg chl.m}^{-2}$  and  $\text{mmol.m}^{-3}$ ) and predicted by the model for Ria Formosa.

### *Model validation*

For an appropriate assessment of the agreement between data collected and the model output, a regression analysis should be performed. Several methods may be used for the regression. In this case the least square of means analysis was done. This provides



information on the goodness of the fit of the model. The perfect agreement would result in the line described by the equation  $y = x$ . These plots were done using values obtained in 2006 (Figure 7.19) and 2007-08 (Figure 7.20). The values of  $R^2$ , the determination coefficient, were also calculated. These values can vary from 0, which is the worst agreement to 1, which corresponds to a total agreement between data. Slopes of DAIN and phytoplankton in 2007-08 were close to one. The regression of phytoplankton presented in Figure 7.20 was significant ( $p < 0.05$ ). All the others were not significant ( $p > 0.05$ ).

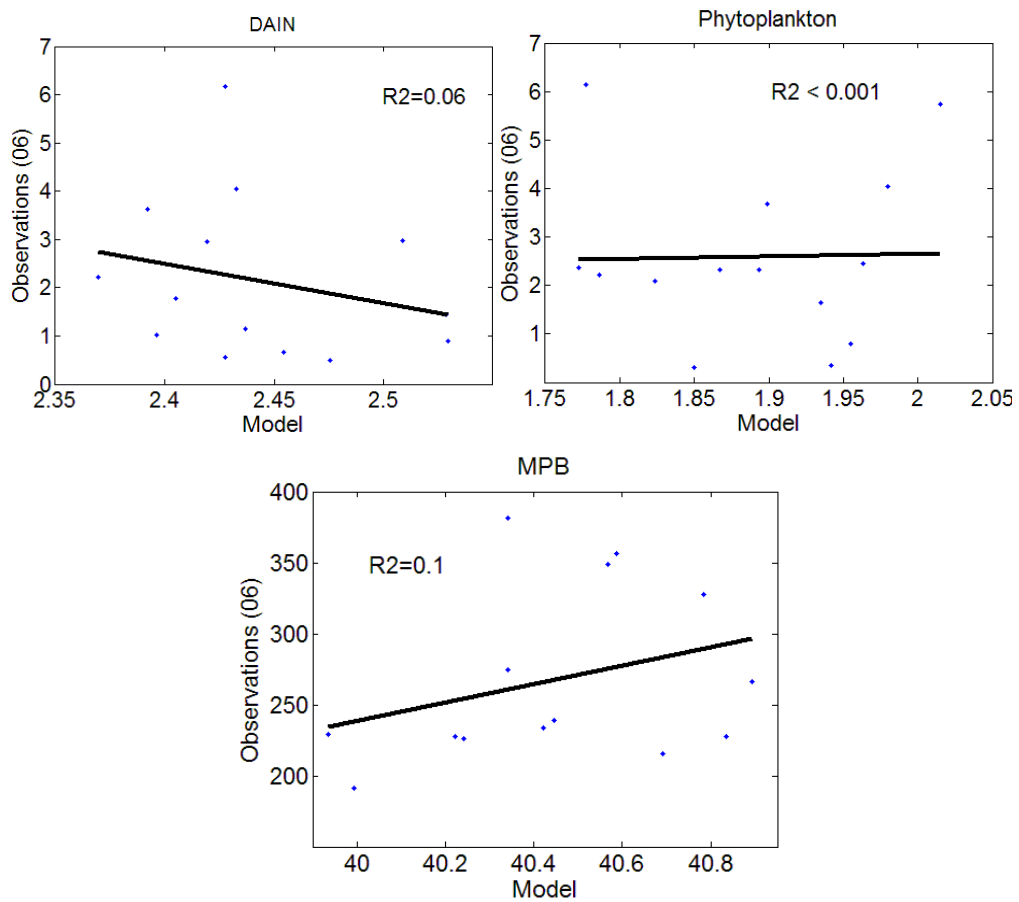


Figure 7.19– Scatter plots of the observed values versus predicted values using 2006 data. The determination coefficient is shown in each plot.

#### 7.2.2.6 Discussion

The addition of forcing variables gave some of the desired variability to the model. The predictions are now more dynamic and reflect the trends of the forcing variables and their interaction. Nevertheless, the improvement is still insufficient due to the small expression of the variability in the final simulation of the model. It is clear that data contain much more variation throughout the year. A small decrease in pelagic and

benthic chlorophyll concentrations was observed during the winter. However, the same trend is not expressed by the observed data. This occurs due to the switch between the limiting growth rate, which is nutrient limited during almost all of the year and light limited during the winter. Growth rates for this system need to be reviewed since they are not contributing to obtain of good predictions of chlorophyll concentration. The hypothesis of not having a limiting growth rate in the winter may be considered. Nitrogen concentrations are larger during this period and the irradiance values in the lagoon may be large enough to allow a normal growth. The range of variation in model's prediction is adequate for the water column but not for sediments. The model is clearly underestimating both benthic chlorophyll and nutrients. Therefore, there is a clear indication that the model is not adequate to describe this benthic system. It needs to be improved.

Finally, the equations for DAIN concentration in the pore water must also be reviewed. The nitrogen concentration from Particulate Organic Nitrogen (PON) is insufficient to maintain a relatively large concentration in the sediments.

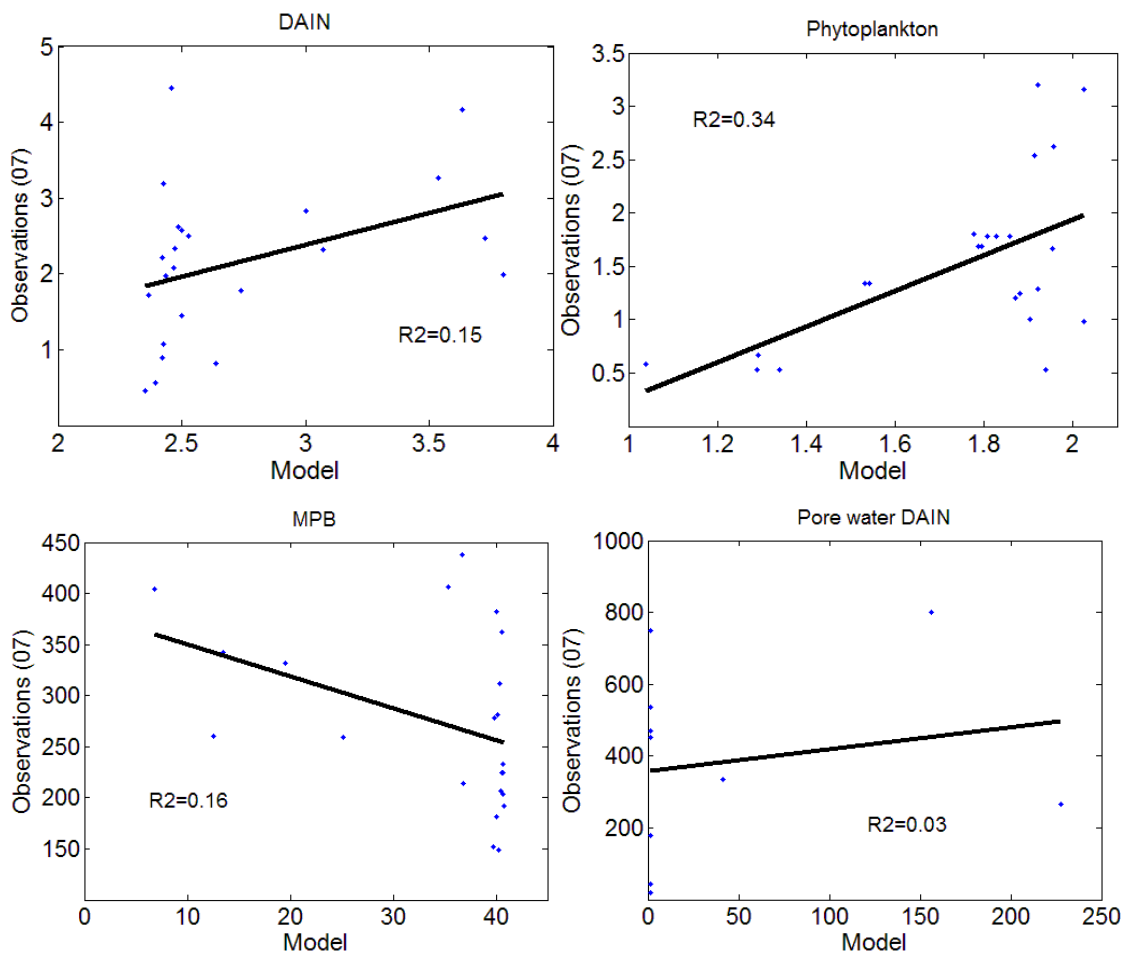


Figure 7.20 - Scatter plots of the observed values versus predicted values using 2007-08 data. The determination coefficient is shown in each plot.

All the results of  $R^2$  calculations show weak agreements ( $R^2 \leq 0.34$ ) between observed and predicted values. Despite of some slopes that were around 1, this assessment indicates that the model should be improved, since it does not explain or predict completely the observations. Therefore, other processes in the system should be considered or those in Stage 2 should be redefined.

### 7.2.3 Stage 3 – Addition of other important component of the system – Oxygen

During the development of the model and practical work, another important component of this lagoon system was considered. Low concentrations of dissolved oxygen were found by Oliveira (2005) early in the morning, at dawn. These findings encouraged continuous monitoring of this variable throughout the year. The concentration of dissolved oxygen could be an important tool / indicator to assess the trophic status of a system. The relationships between, and implications of, low oxygen concentrations and eutrophication are well known. So, a fifth state variable, dissolved oxygen in the water column was added to the model.

#### 7.2.3.1 Conceptual model

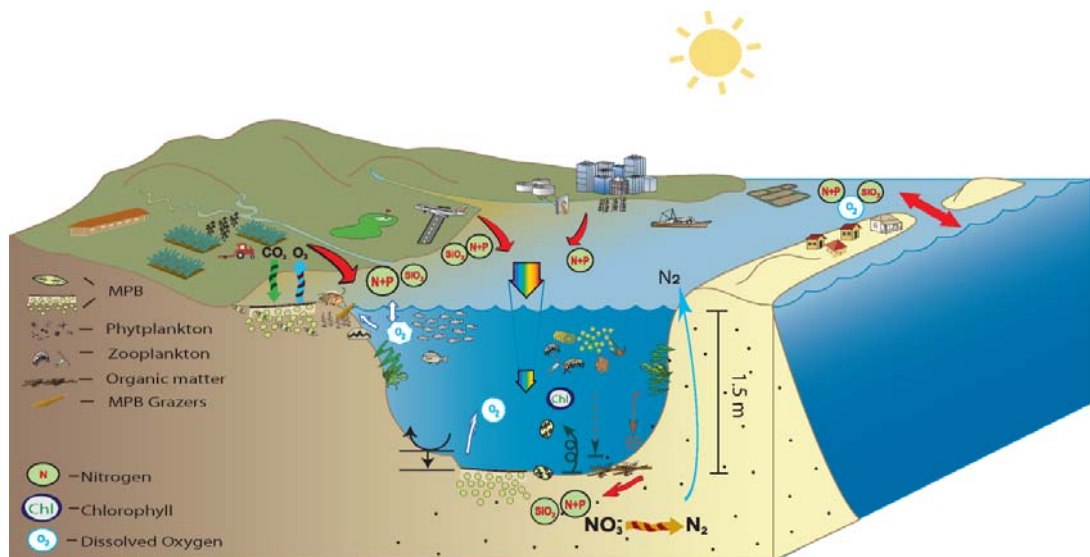


Figure 7.21 – Scheme representation of the Ria Formosa system. Illustration symbols from the Integration and Application Network (<http://ian.umces.edu>).

Ria Formosa system is a lagoon with several sources of nutrients as represented in Figure 7.21. The exchange with the sea takes place at some points of connection.

The conceptual model is similar to the ones previously presented. However, the box representing the lagoon has now another state variable, the dissolved oxygen. In addition, relationships and processes involved are also described in Figure 7.22.

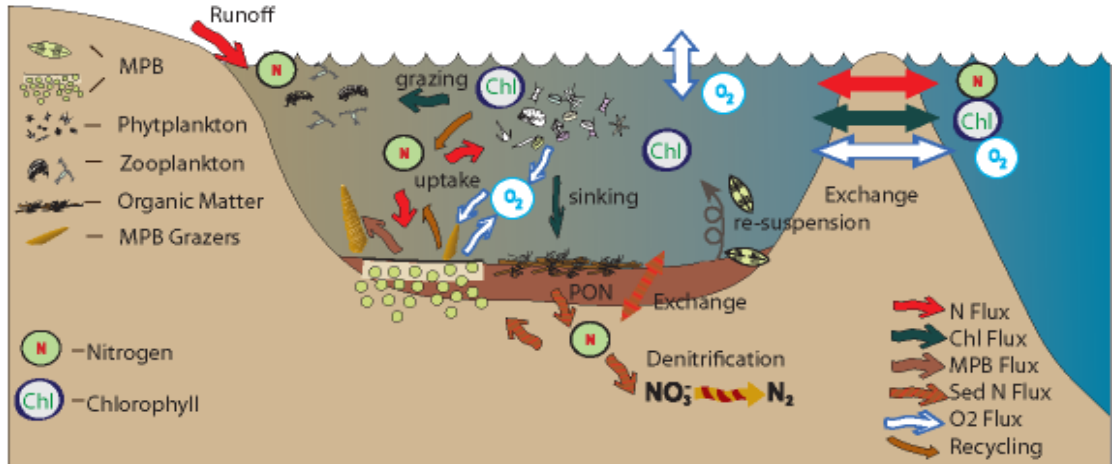


Figure 7.22 – Diagram representation of the conceptual model. Illustration symbols from the Integration and Application Network (<http://ian.umces.edu>).

### 7.2.3.2 Mathematical model

The mathematical model is now composed by five differential equations, one for each state variable:  $S$  (limiting nutrient in the lagoon),  $X$  (pelagic chlorophyll inside the lagoon),  $X_b$  (microphytobenthic chlorophyll inside the lagoon),  $S_{sed}$  (pore water limiting nutrient) and  $DO$  (dissolved oxygen).

$$\frac{\partial S}{\partial t} = E.(S_0 - S) - \frac{\mu_p \cdot X_p}{q} + e.L_p \cdot \frac{X_p}{q} + \frac{S_i}{V} + \frac{S_{sed} - S}{h_s} \cdot \frac{D_m \cdot p}{\tau \cdot H} \quad (\text{mmol} \cdot \text{m}^{-3} \cdot \text{d}^{-1}) \quad (7.31)$$

$$\frac{\partial X_p}{\partial t} = E.(X_0 - X_p) + \mu_p \cdot X_p - L_p \cdot X_p + \frac{L_{br} \cdot X_b}{H} - \frac{sk}{H} \cdot X_p \quad (\text{mg chl} \cdot \text{m}^{-3} \cdot \text{d}^{-1}) \quad (7.32)$$

$$\frac{\partial X_b}{\partial t} = \mu_b \cdot X_b - L_g \cdot X_b + sk \cdot X_p - L_{br} \cdot X_b \quad (\text{mg chl} \cdot \text{m}^{-2} \cdot \text{d}^{-1}) \quad (7.33)$$

$$\frac{\partial S_{sed}}{\partial t} = \frac{e_b \cdot L_g \cdot X_b}{q_b \cdot p} + \frac{N \cdot d}{p} + \frac{S - S_{sed}}{h_s} \cdot \frac{D_m}{h_s \cdot \tau} - den \cdot S_{sed} - \frac{\mu_b \cdot X_b}{q_b \cdot p} \quad (\text{mmol} \cdot \text{m}^{-3} \cdot \text{d}^{-1}) \quad (7.34)$$

$$\frac{\partial DO}{\partial t} = \frac{w.(DOI - DO)}{H} + E.(DO_0 - DO) + c.dc.(\mu_p.X_p + \frac{\mu_b.X_b}{H}) - \frac{R_o}{H} \quad (7.35)$$

(mmol.m<sup>-3</sup>.d<sup>-1</sup>)

*DOI* is the oxygen saturation concentration at a given temperature and salinity, *w* is air exchange rate (m.d<sup>-1</sup>), *DO<sub>0</sub>* is the reference concentration (outside the lagoon; mmol.m<sup>-3</sup>), *dc* is a coefficient to transform mg chl into mmol C (2.27), *c* is the coefficient to transform mmol C into mmol O<sub>2</sub> (12.69) and *R<sub>o</sub>* is the biological oxygen demand per meter square (mmol.m<sup>-2</sup>.d<sup>-1</sup>).

### 7.2.3.3 Numerical model

#### **Physical Model – the $-\nabla\phi_\gamma$ terms**

The physical model did not suffer any modification, except the addition of new parts of the DO model.

#### *Exchange of oxygen*

The state variable *DO* has an exchange term with the sea, defined as:

$$E.(DO_0 - DO) \quad (7.36)$$

It is the same expression as used before for nutrient and pelagic chlorophyll exchange and used the same rate *E*. Dissolved Oxygen outside (*DO<sub>0</sub>*) was obtained through an interpolation of the values obtained during 2006 outside the lagoon.

#### *Dissolved Oxygen outside (DO<sub>0</sub>) and Dissolved Oxygen inside (DOI)*

In this model, the state variable *DO* has an exchange term with the sea. Seawater oxygen concentration is equated always in comparison with the oxygen concentration inside the lagoon. *DO<sub>0</sub>* was calculated from oxygen concentration measured in the samples collected at beach sampling site during 2006. The time-series represented in Figure 7.23 was achieved by an interpolation of data. The oxygen saturation

concentration of a sample is dependent on the temperature and salinity of the water. A script (Appendix III) was used to transform the oxygen concentrations measured during 2006 into oxygen saturation concentrations  $DO_o$  and  $DOI$  (Figure 7.23). The  $DOI$  was then used in the aeration term of the  $DO$  differential equation.

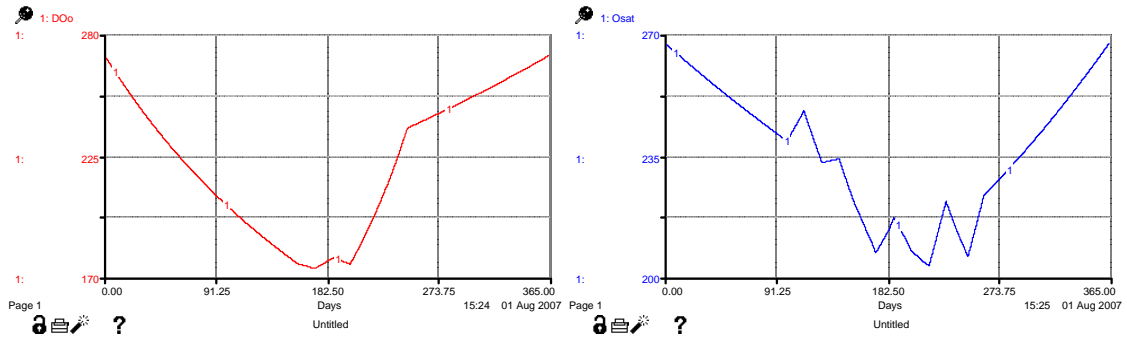


Figure 7.23– Seawater oxygen concentration (red;  $\text{mmol.m}^{-3}$ ) throughout the year 2006 and oxygen saturation concentration inside the lagoon (blue;  $\text{mmol.m}^{-3}$ ) through the year 2006.

### **Bio-chemical Model – the $\beta_Y$ terms**

The components of the bio-chemical model of stage 2 were kept unchanged, except for the equations of the fifth state variable (dissolved oxygen).

#### *DO production by algae*

$DO$  has an obvious input resulting from algal photosynthesis in Ria Formosa. It is possible to convert the amount of chlorophyll  $a$  into the amount of dissolved oxygen produced by two coefficients ( $c$  and  $d$ ) presented in the formula:

$$c \cdot dc \cdot \left( \mu_p \cdot X_p + \frac{\mu_b \cdot X_b}{H} \right) \quad (7.37)$$

$dc$  is the coefficient used to convert mg chl into mmol C and was taken from Geider (1987) and Tett and Wilson (2000). It has the value of 2.27.  $c$  is the coefficient used to convert mmol C into mmol  $O_2$ . The value used was 2.69 (Ambrose *et al.*, 2006).

#### *Aeration*

Aeration of waters depends on the re-aeration velocity ( $w$ ;  $\text{m.d}^{-1}$ ) and the difference between the saturation concentration at a given salinity and temperature ( $DOI$ ), and the dissolved oxygen concentration in the lagoon ( $DO$ ), according to the following equation:

$$\frac{w.(DOI - DO)}{H} \quad (7.38)$$

$DOI$  was computed using observed values of salinity and temperature recorded at Ria Formosa during 2006. The procedure of Carpenter (1966) was followed and the script is shown in Appendix III, as described before. Re-aeration follows Tett and Walne (1995).

The re-aeration velocity is defined by (Figure 7.24):

$$w = \text{daylength}.kw.W^2 \quad (7.39)$$

$Daylength$  is considered to be  $86400 \text{ s.d}^{-1}$ ,  $kw$  is a coefficient and has the value of  $3 \times 10^{-5} \text{ m}^{-1}.\text{s}$  (Liss, 1988) and  $W$  is the wind velocity ( $\text{m.s}^{-1}$ ) of Ria Formosa.

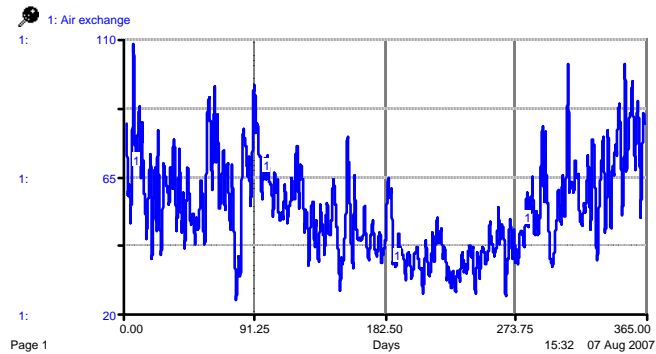


Figure 7.24 – Air Exchange rate ( $\text{m.d}^{-1}$ ) throughout one year.

### *Biological Oxygen Demand*

Within shallow lagoons an important loss of oxygen is organismal oxygen uptake. This loss is defined as:

$$\frac{R_o}{H} \quad (7.40)$$

The biological Oxygen Demand ( $R_o$ ) considered in this model is of  $40 \text{ mmol.m}^2.\text{d}^{-1}$  since it is assumed that Ria Formosa has a high concentration of organisms using this  $DO$ , such as bacteria and other animals (Falcão *et al.*, 1991).

### **Discharges/Inputs to the water column - the $\Gamma_Y$ terms**

The components of this part of the model were kept unchanged.

#### 7.2.3.4 Methodology

As stated before, the model is described in three scripts (m files) that are computed in Matlab simultaneously. The scripts are presented in Appendix III. The scripts comprise the main commands for loading forcing variables, running the solver and plotting and saving the output. They also have the description of the differential equations and all the equations involved in the model. The description of variables and parameters used in the model is presented in Table 7.5 and the initial data used to run the model and boundary conditions are described in Table 7.6.

The initial value of the limiting nutrient (DAIN) corresponds to the annual mean of data collected during 2006 and 2007-08. The nutrient concentration outside the lagoon also corresponds to the mean of both periods. The initial value for pelagic chlorophyll corresponds to the average obtained during the same periods in the lagoon. A value between what was observed in the sea and what was found by Tett *et al.* (2003), who indicated a concentration of  $0 \text{ mgchl. m}^{-3}$  was used as boundary condition. For the benthic chlorophyll, a value of  $270 \text{ mg chl. m}^{-2}$  was used as the initial value. The initial value for pore water nutrients used was  $100 \text{ mmol.m}^{-3}$ , taken from the literature (e.g. Serpa *et al.*, 2007). The initial value for dissolved oxygen was  $100 \text{ mmol.m}^{-3}$ , which is within the range of the maximum values of dissolved oxygen measured at Ria Formosa.

Statistical assessment of the goodness of the fit was carried out using least squares regressions. Comparisons were done between model simulations and observations. Observed data consist of two sets of data obtained during this project, from 2006 and 2007-08.



Table 7.5 – Variables and parameters used in the model for stage 3.

Parameter	Description	Value	Units	Source
$S_0$	Seawater nutrient concentration	2.3	mmol.m <sup>-3</sup>	data
$S_i$	Nutrient input from all sources except sea	$78 \times 10^6$	mmol.d <sup>-1</sup>	Tett <i>et al.</i> (2003)
$X_0$	Seawater Chlorophyll concentration	1.75	mg chl.m <sup>-3</sup>	Tett <i>et al.</i> (2003) and data
$E$	Exchange rate	0.5	d <sup>-1</sup>	Tett <i>et al.</i> (2003)
$V$	Volume of Ria Formosa	$88 \times 10^6$	m <sup>3</sup>	Tett <i>et al.</i> (2003)
$H$	Mean depth of Ria Formosa	1.5	m	Tett <i>et al.</i> (2003)
$q$	Chlorophyll yield from limiting nutrient (N)	1.1	mg chl. mmol <sup>-1</sup>	Tett <i>et al.</i> (2003)
$q_n$	MPB chlorophyll yield from limiting nutrient	4	mg chl. mmol <sup>-1</sup>	Chapter 6
$e$	Proportion of grazed nutrient that is recycled	0.5		Laurent <i>et al.</i> (2006) Adapted from
$e_b$	Proportion of grazed nutrient that is recycled for MPB	0.5		Laurent <i>et al.</i> (2006) Adapted from
$L_p$	Pelagic chlorophyll loss rate	0.15	d <sup>-1</sup>	Tett <i>et al.</i> (2003)
$sk$	Sinking rate of pelagic chlorophyll	1	m.d <sup>-1</sup>	Mann and Lazier (1996) Adapted from
$L_g$	Grazing rate	0.15	d <sup>-1</sup>	Blackford (2002)
$I_0$	24-hour mean of solar radiation		μE.m <sup>-2</sup> .s <sup>-1</sup>	data
$K_d$	PAR diffuse attenuation coefficient	0.7	m <sup>-1</sup>	Chapter 5
$I_c$	Compensation irradiance	5	μEm <sup>-2</sup> .s <sup>-1</sup>	Tett <i>et al.</i> (2003)
$\alpha$	Photosynthetic efficiency	0.006	(μEm <sup>-2</sup> .s <sup>-1</sup> ) <sup>-1</sup> .d <sup>-1</sup>	Tett <i>et al.</i> (2003)
$m_0$	Correction of mean PAR for sea-surface reflection	0.06		Tett <i>et al.</i> (2003)
$m_1$	Conversion of solar radiation to PAR photons	$0.46 \times 4.15$	μE.J <sup>-1</sup>	Tett <i>et al.</i> (2003)
$m_2$	Additional losses to those of Beer-Lambert decay	0.37		Tett <i>et al.</i> (2003)
$\mu_{max}$	Maximum relative growth rate	1	d <sup>-1</sup>	Laurent <i>et al.</i> (2006) Adapted from
$\mu_{max,b}$	Maximum relative growth rate for MPB	1	d <sup>-1</sup>	Laurent <i>et al.</i> (2006)
$k_s$	Half-saturation concentration	2	mmol.m <sup>-3</sup>	Laurent <i>et al.</i> (2006) Adapted from
$k_{s,b}$	Half-saturation concentration for MPB	10	mmol.m <sup>-3</sup>	Laurent <i>et al.</i> (2006)
$N$	Particulate Organic Nitrogen	100	mmol.m <sup>-3</sup>	Serpa <i>et al.</i> (2007)
$d$	Decay rate of N	0.1	d <sup>-1</sup>	Adjusted
$p$	Porosity	0.5	-	data
$D_m$	Diffusion coefficient	$1.66 \times 10^{-4}$	m <sup>2</sup> .d <sup>-1</sup>	Murray <i>et al.</i> (2006) Adapted from Murray and Parslow (1997)
$den$	Denitification rate	0.01	d <sup>-1</sup>	
$hs$	Thickness of the pore water sediment layer	0.05	m	data
$W$	Wind velocity	-	m.s <sup>-1</sup>	data
$c$	Coefficient to transform mmol C into mmol O <sub>2</sub>	2.69		Ambrose <i>et al.</i> (2006) Geider (1987) and Tett and Wilson (2000)
$dc$	Coefficient to transform mg chl into mmol C	2.27		
$R_0$	Biological oxygen demand	40	mmol.m <sup>-3</sup> .d <sup>-1</sup>	Falcão <i>et al.</i> (1991)
$DOI$	Oxygen saturation concentration	-	mmol.m <sup>-3</sup>	data
$DO_0$	Seawater oxygen concentration	-	mmol.m <sup>-3</sup>	data

Table 7.6 – Initial values of each state variable of the model and boundary conditions.

Symbol		Initial values	Boundary conditions
S	Nutrient concentration	2.1 mmol.m <sup>-3</sup>	2.3 mmol.m <sup>-3</sup>
X	Chlorophyll concentration	2 mg chl. m <sup>-3</sup>	1.75 mg chl. m <sup>-3</sup>
$X_m$	MPB chlorophyll concentration	270 mg chl. m <sup>-2</sup>	
$S_{sed}$	Pre water nutrient concentration	100 mmol.m <sup>-3</sup>	
DO	Dissolved Oxygen concentration	100 mmol.m <sup>-3</sup>	

## 7.2.3.5 Results and Model validation

The part of the model used to predict pelagic and benthic nutrients and chlorophyll was the same as presented in Stage 2 and therefore results are the same. Dissolved oxygen predictions are novel (Figure 7.25–C). Higher concentrations are found during the winter and lower during the summer.

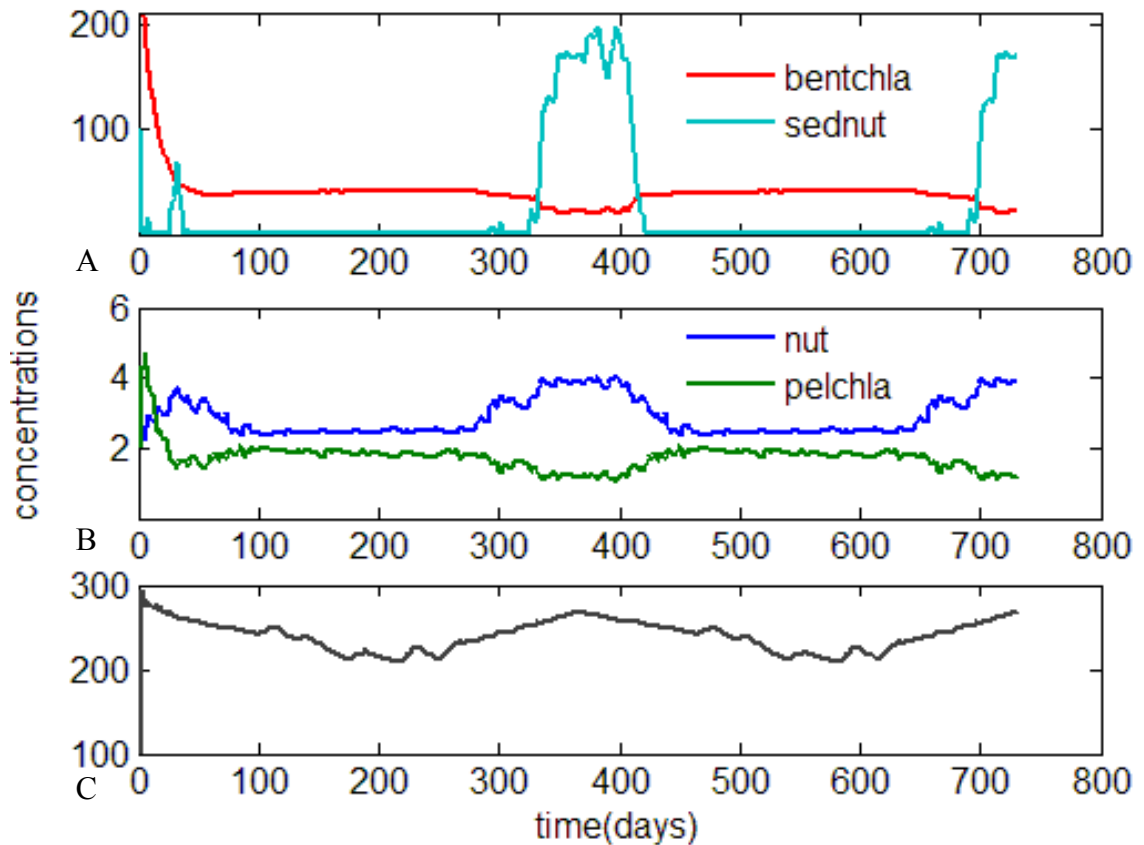


Figure 7.25 A- Simulation of benthic chlorophyll (red;  $\text{mg chl.m}^{-2}$ ) and DAIN in pore water (light blue;  $\text{mmol.m}^{-3}$ ); B- DAIN in the water column (blue;  $\text{mmol.m}^{-3}$ ) and pelagic chlorophyll (green;  $\text{mg chl.m}^{-3}$ ); C- dissolved oxygen (dark brown;  $\text{mmol.m}^{-3}$ ) concentrations during a period of 730 days.

Dissolved oxygen concentrations observed in Ria Formosa during the period of 2007-08 were much lower than the ones predicted by the model (Figure 7.26-A). The model also clearly overestimates this variable. Moreover, concentrations seem to vary throughout the year, around the same values. The model simulates a different pattern of variability, with lower values during the summer. The agreement between the simulation and data is also very small (Figure 7.26-B). The regression was not significant ( $p > 0.05$ ).

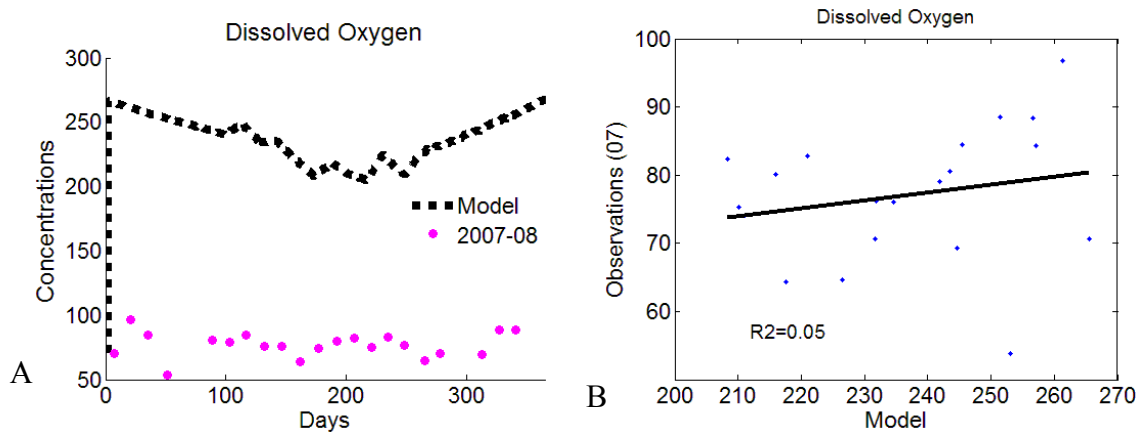


Figure 7.26 (A and B) – A- Concentrations of dissolved oxygen (2007-08;  $\text{mmol.m}^{-3}$ ) and predicted by the model for Ria Formosa. B- Scatter plot of the observed values versus predicted values using 2007-08 data. The determination coefficient is shown in the plot.

### 7.2.3.6 Discussion

The model predicts lower dissolved oxygen concentrations during the summer. This is in agreement with the main relationship between the dissolved oxygen saturation and concentrations, which are closely linked to salinity and temperature concentrations, as described above. For higher values of temperature and salinity, the concentration of dissolved oxygen decreases. This model considers solely the exchange of oxygen between the water column and the air and between the lagoon and the sea. It also considers the production of oxygen by algae and consumption. However, it does not consider the specific characteristics of the lagoon and water circulation, especially in the inner parts of the lagoon. Moreover, the measured values of oxygen are from the period of the day when the concentrations are supposed to be the lowest. In contrast, the model is simulating daily means, which may enlarge the differences.

This model considers the lagoon as a well-mixed box. In the case of oxygen, the critical situations are mainly found in the inner channels, as discussed in Chapter 5. Lower values of dissolved oxygen were presented at Ramalhete, which is located at an inner channel, compared with Ponte, which is located at one of the main channels. The oxygen model may be very useful for the assessment of the environmental quality of water bodies. However, in the case of Ria Formosa, this should be applied and adapted to specific cases and locations.

#### 7.2.4 Stage 4 – New approach to MPB dynamics – Final dCSTT-MPB model

The approach used in the previous stages, considers the ‘physiological’ property of microphytobenthos, which involves the specific growth rate, i.e., cell growth and division. It simulated nutrient concentrations of pore water close to zero for a significant part of the year, which is not correct since high concentrations of DAIN in pore water were observed in Ria Formosa and reported by several authors, as described and discussed in Chapter 5. Therefore, the growth approach was changed to test if the prediction can be improved in relation to the previous approach (Monod), as used for phytoplankton, which was applied by Laurent *et al.* (2006).

Part of the biological term, the MPB growth, of the general equation of the model can be written as:

$$\frac{\partial X_b}{\partial t} \frac{1}{X_b} = \mu \quad (7.41)$$

or

$$\frac{\partial X_b}{\partial t} = \mu X_b \quad (7.42)$$

The first equation emphasises the specific growth rate ( $d^{-1}$ ) and the second emphasises the product  $\mu X$ , which represents the growth and is a flux ( $mg\ chl.m^{-2}.d^{-1}$ ). Note that  $\mu X$  is not the product of  $\mu \cdot X$ , but is instead the biomass increase. The second approach directs attention to the flow of ecological resources that gives rise to the flux. It corresponds to the *ecological* approach, in contrast with the *physiological*. Therefore, the general equation for microphytobenthic chlorophyll ( $X_b$ , units:  $mg\ chl.m^{-2}$ ) is written in flux terms:

$$\frac{\partial X_b}{\partial t} = (\mu X)_b - (LX)_b + \phi_x \quad (mg\ chl.m^{-2}.d^{-1}) \quad (7.43)$$

The term  $\phi_x$  represents the net flux (gain or loss) that results from the resuspension of benthic algae to the water column and the deposition of algal cells from the water column to the sediment. This topic was described and discussed previously.

### 7.2.4.1 Conceptual model

The Ria Formosa system is a lagoon with several sources of nutrients as represented in Figure 7.27. The exchange with the sea is done in some points of connection with the sea, as described before.

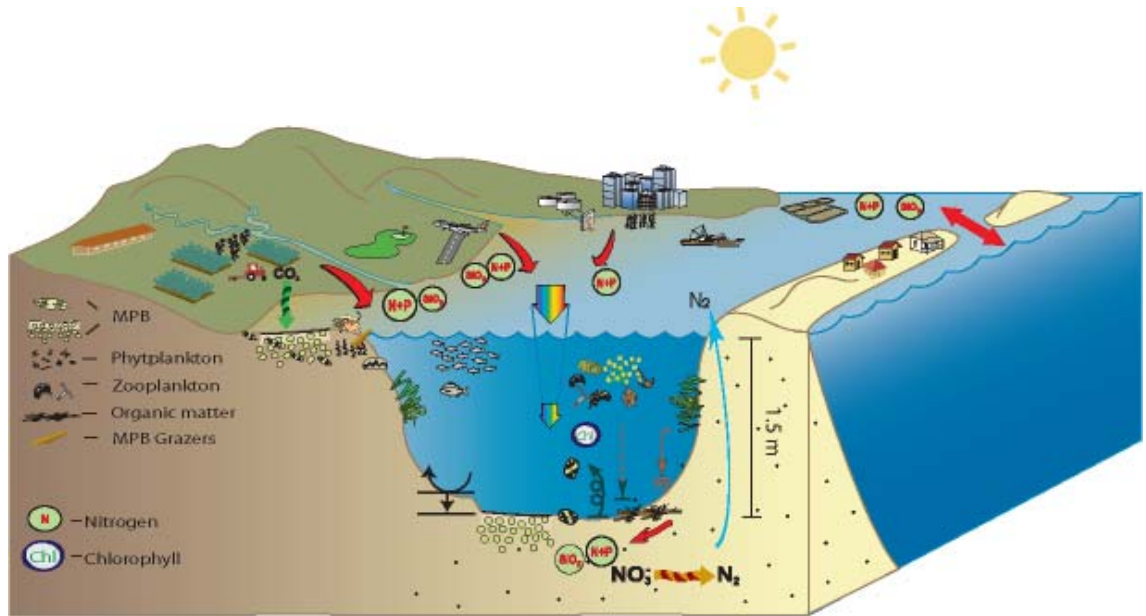


Figure 7.27 – Scheme representation of the Ria Formosa system.

The conceptual model is similar to the ones presented before. However, the box representing the lagoon has now one less state variable, the dissolved oxygen. In addition, relationships and processes involved are also described in Figure 7.28. Although relationships involve approximately the same components, the mathematical equations that define those relationships suffered modifications.

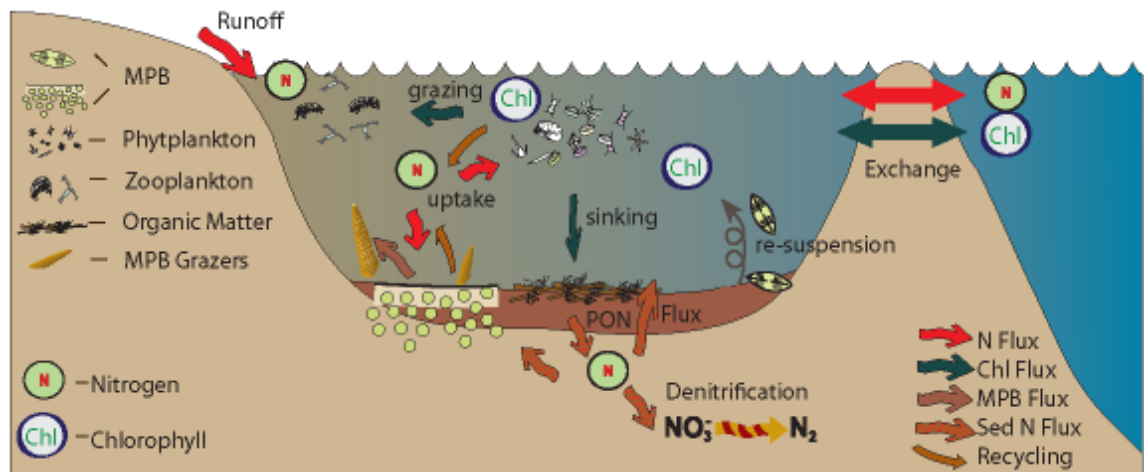


Figure 7.28 – Diagram representation of the conceptual model.

## 7.2.4.2 Mathematical model

The mathematical model is now constituted by four differential equations, one for each state variable: S (limiting nutrient in the lagoon),  $X_p$  (pelagic chlorophyll inside the lagoon),  $X_b$  (microphytobenthic chlorophyll inside the lagoon) and  $S_{sed}$  (pore water limiting nutrient).

$$\frac{\partial S}{\partial t} = E.(S_0 - S) - \frac{\mu_p \cdot X_p}{q} + e.L_p \cdot \frac{X_p}{q} + e.L_{bf} \cdot \frac{X_p}{q} + \frac{S_i}{V} + \frac{\phi_s - \frac{\mu X_b}{q_b}}{H} \quad (7.44)$$

(mmol.m<sup>-3</sup>.d<sup>-1</sup>)

$$\frac{\partial X_p}{\partial t} = E.(X_0 - X_p) + \mu_p \cdot X_p - (L_p + L_{bf}) \cdot X_p + \frac{c_3 \cdot L_{br} \cdot X_b}{H} - \frac{sk}{H} \cdot X_p \quad (7.45)$$

(mg chl.m<sup>-3</sup>.d<sup>-1</sup>)

$$\frac{\partial X_b}{\partial t} = \mu X_b - L_g \cdot X_b + sk \cdot X_p - c_3 \cdot L_{br} \cdot X_b \quad (7.46)$$

(mg chl.m<sup>-2</sup>.d<sup>-1</sup>)

$$\frac{\partial S_{sed}}{\partial t} = \frac{e_b \cdot L_g \cdot X_b}{h_s \cdot p} + \frac{(1-e) \cdot L_{bf} \cdot X_p}{q \cdot p} \cdot \frac{V}{A \cdot h_s} + \frac{N_a \cdot d}{A \cdot h_s \cdot p} - den \cdot S_{sed} - \frac{\phi_s}{h_s \cdot p} \quad (7.47)$$

(mmol.m<sup>-3</sup>.d<sup>-1</sup>)

Where  $\phi_s$  is the nutrient flux from the sediments to the water column, which is assumed to result from molecular diffusion,  $L_{bf}$  is the loss rate of phytoplankton due to filter-feeders (d<sup>-1</sup>),  $c_3$  is the MPB fraction located at the sediment surface and  $N_a$  is the particulate organic nitrogen in mmol. The positive value of the  $\phi_s$  flux corresponds to a flux into the water column.

## 7.2.4.3 Numerical model

**Physical Model – the  $-\nabla\phi_Y$  terms**

The resuspension of benthic algae and sinking of pelagic algae components were kept unchanged from the previous stages. There is, however, a major change in the concept of microphytobenthos distribution and therefore resuspension, In this stage, there is only a fraction of the community,  $c_3$ , that is located at the sediment surface, as described

below. Following this approach, only this fraction will suffer the effects of wind and tide and be suspended to the water column.

Nutrient fluxes between sediments and water column are described below due to their relevance to the biological model.

### **Bio-chemical Model – the $\beta_Y$ terms**

Substantial modifications were done to the biological model due to the new *ecological* approach to describe microphytobenthos growth, which comprises the relationship between biomass increase and the fluxes of photons ( $I$ , from previous sections), nutrients ( $\phi$ , mostly from within the sediment) and a function of the temperature ( $\theta$ ).

Thus:

$$\mu X_b = \min[f(\phi), f(I), f(\theta)] \quad (\text{mg chl.m}^{-2}.\text{d}^{-1}) \quad (7.48)$$

The function  $f(\theta)$  sets an upper limit in algal physiology to the rate of biomass production. It can be expanded as:

$$f(\theta) = \mu(\theta).X_b \quad (7.49)$$

The nutrient limited growth rate, controlled by algal physiology and considering a temperature of 20°C follows the approach described by Lee *et al.* (2003). The growth rate can be described as:

$$\mu(\theta) = \mu_{\max(20)} \cdot Q_{10}^{\left(\frac{T_i - 20}{10}\right)} \quad (7.50)$$

Where  $\mu_{\max(20)}$  is the maximum growth rate at a temperature of 20°C,  $Q_{10}$  is a multiplicative factor that represents the increase to the double of metabolic activity due to an increase of 10°C in temperature and  $T_i$  is the temperature observed in the Ria. This general equation follows previous studies by Droop (1968), Eppley and Strickland (1968) and Eppley (1972). Equation 7.50 is also used to describe the phytoplankton growth rate at this stage, so that phytoplankton is also dependent on temperature.

It is important to note that if these fluxes are independent of biomass, as they are considered, growth rate must decrease as biomass increases. Biomass should stabilize at a level at which growth, consuming all available limiting factors, is balanced by losses due to grazing by meiobenthos, macrobenthos and resuspension to water column:

$$\mu X_b = L.X_b \quad (7.51)$$

*Nutrient Limited Growth*

It is well accepted that microphytobenthos cells are present in the sediment surface and within the sediment (see for example, Underwood and Paterson, 2003; Cartaxana *et al.*, 2006). Cells in the top of the sediment should be able to take nutrients up from the water column, whereas cells within the sediment will take nutrients from the pore water. Therefore, the nutrient limited increase of microphytobenthos depends on nutrient flux from the sediment and nutrient supply from the water column. Thus:

$$\mu X_b = q_b \cdot (c_2 \cdot \phi_s + c_4 \phi_w) \quad (\text{mg chl.m}^{-2} \cdot \text{d}^{-1}) \quad (7.52)$$

Where  $c_2$  is the proportion of the sediment flux that is captured by benthic algae, which depends on algal biomass,  $\phi_s$  is the nutrient flux from the sediment into the water column,  $c_4$  is the proportion of the water nutrient that is captured by benthic algae, which again, depends on algal biomass, and  $\phi_w$  is the nutrient flux from the water column to algae on the surface of the sediment. The yield  $q_b$  for microphytobenthos was estimated in chapter 6 and is used in this modelling approach.

Equation 7.52 assumes that the source of nutrients for MPB cells within the sediment comes from algal interception of a fixed sediment nutrient flux. This flux is originated by initial remineralisation of organic matter in the seabed, which is independent of algal processes.

The benthic nutrient flux ( $\phi_s$ ) is assumed to result from molecular diffusion in sediment pore water, following:

$$\phi_s = D_m \cdot \frac{\partial S}{\partial z} \Big|_{ss} \cdot \frac{p}{\tau} \quad (\text{mmol.m}^{-2} \cdot \text{d}^{-1}) \quad (7.53)$$

Where  $D_m$  is the coefficient of molecular diffusion for small particles at the prevailing temperature,  $p$  is sediment porosity and  $\tau$  is the tortuosity of sediment pores, which corresponds to the ratio of the mean path through pores across the superficial layer to the vertical distance  $h_b$  (thickness of the superficial layer).

The nutrient gradient in the superficial sediment is positive when the concentration in the pore water is higher than that in the water column resulting in a flux into the water column. It was calculated following:

$$\frac{\partial S}{\partial z} \Big|_{ss} = \frac{S_s - S_w}{h_b + h_{bbl}} \quad (7.54)$$



Where  $S_s$  is the concentration in the pore water, just beneath the superficial layer and  $S_w$  is the nutrient concentration in the water column.  $h_b$  is the thickness of the superficial layer and  $h_{bbl}$  is the thickness of the benthic boundary layer, which depends on the sea-bed roughness and the flow velocity. A standard value of 1mm for  $h_{bbl}$  was used. This is within the range of values used by Di Toro (2001) and Murray *et al.* (2006). It would be standard to place a negative symbol before the coefficient of molecular diffusion in Equation 7.53. In this case, the flux will be positive for an inflow to the water column.

The water column nutrient flux ( $\phi_w$ ) is assumed to result from molecular diffusion across the benthic boundary layer or viscous layer, which separates the sea-bed from the main part of the water column. It was estimated following:

$$\phi_w = D_m \cdot \left. \frac{\partial S}{\partial z} \right|_{bbl} \quad (\text{mmol.m}^{-2}.\text{d}^{-1}) \quad (7.55)$$

$$\left. \frac{\partial S}{\partial z} \right|_{bbl} \approx \max \left( 0, \frac{S_w - S_0}{h_{bbl}} \right) \quad (7.56)$$

Where  $S_w$  is the nutrient concentration in the water column,  $S_0$  is the notional concentration ( $> 0$ ) at algal cells. In principle, it is less than  $S_w$  because of the uptake by cells and it cannot fall too close to zero, which would lead to the termination of trans-wall nutrient transport. It was considered to be 1  $\mu\text{M}$  for DAIN. It would be standard to place a negative symbol before the coefficient of molecular diffusion in Equation 7.55. In this case, the flux will be positive for an inflow to the cell.

The intercepted fraction of the benthic nutrient flux,  $c_2$ , can be calculated using a nutrient absorption cross-section parameter,  $a_s^*$ , estimated considering diatom cell dimension taken from Jesus (2005), analogous to the light absorption cross-section, which will be described below. Thus:

$$c_2 = (1 - e^{-a_s^* \cdot (1-c_3) \cdot X_b}) \quad (7.57)$$

Where  $c_3$  is the proportion of microphytobenthos on the surface of the sediment, considering that microphytobenthos is distributed within the sediment and migrate vertically due to the effect of light and tide. The intercepted fraction of the water column flux ( $c_4$ ) can be estimated using a similar equation:

$$c_4 = (1 - e^{-a_s^* \cdot c_3 \cdot X_b}) \quad (7.58)$$

There is an important conceptual difference between the benthic nutrient flux and the water column nutrient flux. The benthic flux is a real flux and the part  $(1-c_2) \cdot \phi_s$ , not

consumed by algae, but instead goes directly to the water column nutrient stock. The other is a potential flux and only the part consumed by algae is realized. The unused  $(1 - c_4) \cdot \phi_w$  does not happen.

### *Light Limited Growth*

The net photosynthetic production limited by light depends on capture of light, conversion efficiencies and losses due to respiration of cells. Hence:

$$\mu X_b = k \cdot c_1 \cdot I_s \cdot \Phi \cdot \chi - r \cdot X_b \quad (\text{mg chl.m}^{-2} \cdot \text{d}^{-1}) \quad (7.59)$$

Where  $k$  converts units from  $\text{s}^{-1}$  to  $\text{d}^{-1}$  and from  $\text{ng}$  to  $\text{mg}$ .  $c_1$  is the fraction of PAR absorbed by benthic algae, described below,  $I_s$  is the PAR at the sea-bed,  $\Phi$  is the photosynthetic yield,  $\chi$  is a conversion factor ( $\text{mg chl.}(\text{mg-at organic C})^{-1}$ ) and  $r$  is the respiration rate (below).

### *Optical Properties*

The algal pigments that capture the fraction of PAR used for photosynthesis have to compete with other ‘Optically Active Constituents’ (OAC), mainly non-photosynthetic pigments and sediment particles. The thickness of the superficial layer ( $h_b$ ), corresponding to the euphotic zone of the sediment, was assessed experimentally in the laboratory as presented in Chapter 6.

It is also assumed that all particles that influence the light absorption are uniformly distributed within the sediment, except for the fraction  $c_3$  of cells that are on the sediment surface. The fraction of PAR captured by algae may be estimated following:

$$c_1 = \frac{a_{PH} \cdot h_b}{a \cdot h_b} \cdot (1 - R) + (1 - e^{-a_{PH,s}}) \cdot R \quad (7.60)$$

where:

$$a_{PH} = (1 - c_3) \cdot a_{PH}^* \cdot X \cdot h_b^{-1} \quad (\text{cm}^{-1}) \quad (7.61)$$

$$a_{PH,s} = c_3 \cdot a_{PH}^* \cdot X \cdot h_b^{-1} \quad (\text{cm}^{-1}) \quad (7.62)$$

$$a = (1 - c_3) \cdot (a_{PH}^* + a_{NP}^*) \cdot X \cdot h_b^{-1} + a_{PM}^* \cdot PM \quad (\text{cm}^{-1}) \quad (7.63)$$

$$PM = \rho_s \cdot (1 - p) \quad (\text{mg.m}^{-3}) \quad (7.64)$$

Where  $a_{PH}^*$  is the absorption cross-section of photosynthetic pigments. It describes the ability of chlorophyll and other accessory pigments to harvest photons for photosynthetic processes.  $a_{NP}^*$  is the absorption cross-section of photoprotective pigments, such as carotenoids and degraded photosynthetic pigments, which do not lead to photosynthesis.  $a_{PM}^*$  is the absorption cross-section of particulate matter in the sediment.  $\rho_s$  is the density of dry and compact sediment,  $p$  is porosity of superficial sediment and  $R$  is the reflected proportion of PAR from the sediment or sea-bed *albedo*.

Equation 7.60 describes the fraction of light that is taken by algae within the sediment. This term is likely to be small due to the rapid attenuation of light in sediments. Light-absorption is likely to be dominated by sediment particles.

#### *Microphytobenthic respiration*

The microphytobenthic respiration ( $r$ ) is assumed to include a basal ( $r_0$ ) and a growth dependent ( $b \cdot \mu$ ) component. Thus:

$$r = r_0 + b \cdot \mu \quad (7.65)$$

The two parameters involved in the equation, the basal respiration ( $r_0$ ) and the respiration slope ( $b$ ), were calculated from autotroph and heterotroph parameters as described in the microplankton model (Tett *et al.*, 2007). Hence:

$$r_0 = r_{0,a} \cdot (1 - \eta) + r_{0,h} \cdot \eta \cdot (1 + b_a) \quad (7.66)$$

$$b = b_a \cdot (1 + b_h \cdot \eta) + b_h \cdot \eta \quad (7.67)$$

Where  $r_{0,a}$  is algal basal respiration rate,  $r_{0,h}$  is the heterotroph basal respiration rate,  $\eta$  is the heterotroph fraction,  $b_a$  is the slope of graphical relationship between algal respiration and growth rate;  $b_h$  is the slope of graphical relationship between heterotroph respiration and growth rate.

*Vertical Migration and Surface Fraction*

The surface fraction specifies the proportion of microphytobenthos able to take up nutrient from the water column. Several studies have reported the vertical migration of microalgae due to the joint stimulus of tide and light (e.g. Serôdio *et al.*, 1997; Jesus *et al.*, 2005; Serôdio *et al.*, 2005). Microalgae tend to preferentially migrate to the sediment surface during daylight and as water level falls.

The above implies that the value of  $c_3$  is a complicated function of time in the tidal cycle, time of day, height relative to low water. In addition, the type of sediment is also likely to be important. The CSTT-MPB model works with daily values and does not resolve processes within the diel cycle. Therefore, a single value that averages all processes is needed. Considering that Ria Formosa has approximately 12 hours of light per day (half day; fraction  $c_5$ ) and that the lagoon has semidiurnal tides, which means that the sediment is exposed at different levels during almost one third of the day (fraction  $c_6$ ),  $c_3$  may be estimated following:

$$c_3 = c_5 \cdot c_6 \quad (7.68)$$

*Two-part Light Limited Growth Function*

The light limited growth equation described previously (Equation 7.59) considers solely a single value for sea-bed illumination. This refers to a conceptual model in which Ria Formosa is a permanently-filled box, in which the water depth is the average  $H$ . Equation 7.75 describes the PAR that reaches the sea bed. However, Ria Formosa experiences different water levels according to the tidal cycle, which may strongly affect the radiation in the sediment surface. Furthermore, according to Equation 7.59, MPB cells present in the top, or within the sediment, would always experience  $I_s$ . However, as discussed previously, we are assuming that microalgae cells migrate into the sediment surface during part of the day. Under these conditions, cells are exposed to  $I_0$  rather than  $I_s$ . This consideration implies that a two-part light limited function should be used. Equation 7.59 becomes:

$$\mu X_b = k \cdot (c_{1s} \cdot I_0 + c_{1b} \cdot I_s) \cdot \Phi \chi - r \cdot X_b \quad (\text{mg chl.m}^{-2} \cdot \text{d}^{-1}) \quad (7.69)$$

Where  $c_{1s}$  is the proportion of the photons in  $I_0$  absorbed by algae on the sediment surface,  $c_{1b}$  is the proportion of the photons in  $I_s$  absorbed by algae inside the sediment.  $c_{1s}$  can be estimated following:

$$c_{1s} = (1 - e^{-a_{PH,s}.h_b}).R \quad (7.70)$$

where

$$a_{PH,s} = c_3.a_{PH}^*.X_b.h_b^{-1} \quad (\text{m}^{-1}) \quad (7.71)$$

$c_{1b}$  can be estimated following:

$$c_{1b} = \frac{a_{PH,s}.h_b}{a.h_b}.(1 - R) \quad (7.72)$$

where

$$a_{PH,b} = (1 - c_3).a_{PH}^*.X_b.h_b^{-1} \quad (\text{m}^{-1}) \quad (7.73)$$

$$a = (1 - c_3).(a_{PH}^* + a_{NP}^*).X_b.h_b + a_{PM}^*.PM \quad (\text{m}^{-1}) \quad (7.74)$$

The  $I_0$  is the 24-hr mean surface PAR and  $I_s$  is now the 24-hr PAR on the top of the sediment, averaged over the lagoon. Assuming that each depth interval corresponds to an equal proportion of sea-bed, then this mean PAR can be equated with the mean PAR in the water column when the Ria is flooded, so that  $h_{hw} = V_{hw} / A$ , where  $V_{hw}$  and  $h_{hw}$  are the volume and depth of water contained in the Ria at high tide and A is the high-tide area. Then:

$$I_s = (1 - m_0).m_1.m_2.I_0 \cdot \frac{1 - e^{-K_d.h_{hw}}}{K_d.h_{hw}} \quad (\mu\text{E.m}^{-2}.\text{s}^{-1}) \quad (7.75)$$

The depth  $h_{hw}$  might be greater or less than  $H$ , depending on the relative area of the Ria above mid-water.  $K_d$  is the average attenuation coefficient for the lagoon and the parameter  $m_2$  takes account of losses by surface reflection and hyper exponential decay.

*Mineralisation of organic nitrogen*

The input terms of nutrients to the water column remained unchanged. However, the input of particulate organic nitrogen was changed to be expressed in mmol and not in concentration. The term in the differential equation is now:

$$\frac{\frac{N_a.d}{A.h_s}}{\rho} \quad (\text{mmol.m}^{-3}.\text{d}^{-1}) \quad (7.76)$$

This modification allows the use of a more accurate value.

**Discharges/Inputs to the water column - the  $\Gamma_Y$  terms**

The components of this part of the model were kept unchanged.

**Further considerations***Conservation of matter*

It is a basic requirement of this model that it conserves quantities. This means that, for any state variable, the sum of fluxes over a year must equal the difference between the end and initial amounts. There are further implications when a quantity exchanges between several state variables, such as nitrogen. Global nutrient budgets are generally slightly more complex to describe than the global chlorophyll budget of the lagoon. Pelagic and benthic chlorophyll are linked solely by processes of resuspension and deposition of cells. The chlorophyll amount that is lifted to the water column is distributed throughout the water column. It is a purely physical process and there is no change in quantities. Therefore, there is no need to include the resuspension / deposition in the global equation for total chlorophyll ( $X_T$ ):

$$X_T = X_b + X_p.H \quad (\text{mg.m}^{-2}) \quad (7.77)$$

or

$$\frac{\partial X_T}{\partial t} = (\mu X_b - L_g X_b) + (\mu_p.X_p.H + (-L_p - L_{bf}).X_p.H + E.(X_0 - X_p).H) \quad (7.78)$$

(mg.m<sup>-2</sup>.d<sup>-1</sup>)

The global equation for nitrogen in Ria Formosa can be described as the sum of both equations for nitrogen in the water column and within sediments:

$$S_T = S + S_{sed} \quad (\text{mmol.m}^{-3}) \quad (7.79)$$

The most important issue in the nutrient budget is to close it as far as possible. The model is considering a realistic dynamic of nutrients and of the effects of nutrient enrichment by eliminating undesirable forms of nutrient loss from the system. An example of these losses are the amount of chlorophyll, and indirectly, nutrients lost due to grazing because only a percentage of these, correspondent to the parameter  $e$ , are immediately recycled. This closure of the system may be done at several levels. The model can assume that all chlorophyll losses are immediately recycled. Biologically, this means that all nitrogen content of the phytoplankton grazed will be immediately excreted and recycled into the global nutrient budget. Alternatively, a new state variable for particulate organic nitrogen (PON) could be added to the model. This variable would receive all the losses not immediately recycled. After grazing, part of the grazed material would be immediately recycled and the other part would go directly to the PON stock. Here in this model, the pelagic chlorophyll grazed by filter-feeders ( $L_{bf}$ ) is completely recycled, the portion  $e$  goes to the water column and the remainder,  $1-e$ , goes to the pore water. However, only the  $e$  portions of the grazed MPB and pelagic chlorophyll ( $L_g$  and  $L_p$ ) are immediately recycled.

#### *Microphytobenthos maximum biomass*

Following the new approach described here, the maximum possible values of microphytobenthos biomass, according to the ecological properties of growth, can be easily estimated for each nutrient and light limited growth. Considering the nutrient limited growth, the maximum biomass possible is obtained considering that all the benthic and the water column nutrient flux is captured by algae. Combining equation 7.51 and equation 7.52, gives:

$$X_{b,\max(S)} = \frac{q_b \cdot (\phi_s + \phi_w)}{L_g + L_{br}} \quad (\text{mg chl.m}^{-2}) \quad (7.80)$$

Replace  $\mu X$  by  $LX$  in Equation 7.52, then solve for  $X$ .

The same calculation may be carried out for the light limited growth. To calculate the upper limit to biomass, the equation has to consider that all available photons are captured by algae. Thus:

$$X_{b,\max(I)} = \frac{k.(c_3.I_0 + (1 - c_3).I_s).\Phi.\chi}{L.(1 + b) + r_0} \quad (\text{mg chl.m}^{-2}) \quad (7.81)$$

Replace  $\mu X$  by  $LX$  in Equation 7.69, then solve for  $X$ . Equation 7.65 allows  $L(=\mu)+r$  to be re-written as  $L(1+b)+r_0$ .

#### 7.2.4.4 Methodology

As stated before, the model is described in three scripts (m files) that are computed in Matlab simultaneously. The scripts are presented in Appendix III. The description of parameters used in the model is presented in Table 7.7 and the initial data used to run the model and boundary conditions are described in Table 7.8 .

The initial values used for the state variables were the same used and discussed before.

Statistical assessment of the goodness of fit was carried out using least squares regressions. Comparisons were done between model simulations and observations. Observation data consist of two sets of data obtained during this project, from 2006 and 2007-08. This statistical assessment is essential for model validation. It provides information on how good and accurate the model is.

#### 7.2.4.5 Results

The new model approach resulted in new and more appropriate predictions of the variables considered. DAIN and pelagic chlorophyll concentrations are within the range of variation observed in Ria Formosa and presented in Chapter 5 (Figure 7.29). DAIN varies from 2 to 10 mmol.m<sup>-3</sup> and pelagic chlorophyll around 2 mg chl.m<sup>-3</sup>. Benthic microalgal predicted concentrations are now within the expected range (200 to 300 mg chl.m<sup>-2</sup>). However, the lower values predicted during the winter were not observed in the lagoon. This is due to the fact that the growth changes from nutrient limited (throughout the year) to light limited. The pore water DAIN concentrations, which vary from 120 to 135 mmol.m<sup>-3</sup>, are strongly affected by the MPB concentrations, and are



Table 7.7 –Parameters used in the model for stage 4.

Parameter	Description	Value	Units	Source
$S_0$	Seawater nutrient concentration	2.3	mmol.m <sup>-3</sup>	Data
$S_i$	Nutrient input from all sources except sea	78 x 10 <sup>6</sup>	mmol.d <sup>-1</sup>	Tett <i>et al.</i> (2003)
$X_0$	Seawater Chlorophyll concentration	1.75	mg chl.m <sup>-3</sup>	Tett <i>et al.</i> (2003) and data
$E$	Exchange rate	0.5	d <sup>-1</sup>	Tett <i>et al.</i> (2003)
$V$	Volume of Ria Formosa	88 x 10 <sup>6</sup>	m <sup>3</sup>	Tett <i>et al.</i> (2003)
$V_{hw}$	Volume of Ria Formosa (high water)	140 x 10 <sup>6</sup>	m <sup>3</sup>	Mudge <i>et al.</i> (2008)
$A$	Area of Ria Formosa	53 x 10 <sup>6</sup>	m <sup>2</sup>	Newton and Mudge (2003)
$H$	Mean depth of Ria Formosa	1.5	m	Tett <i>et al.</i> (2003)
$q$	Chlorophyll yield from limiting nutrient (N)	1.1	mg chl. mmol <sup>-1</sup>	Tett <i>et al.</i> (2003)
$q_b$	MPB chlorophyll yield from limiting nutrient	4	mg chl. mmol <sup>-1</sup>	Chapter 6
$e$	Proportion of grazed nutrient that is recycled	0.5	-	Laurent <i>et al.</i> (2006)
$e_b$	Proportion of grazed nutrient that is recycled for MPB	0.5	-	Adapted from Laurent <i>et al.</i> (2006)
$L_p$	Loss rate of phytoplankton due to pelagic grazers	0.05	d <sup>-1</sup>	Adapted from Tett <i>et al.</i> (2003)
$L_{bf}$	Loss rate of phytoplankton due to filter-feeders	0.9	d <sup>-1</sup>	Data & Sobral (1995)
$L_g$	Loss rate of MPB due to grazing	0.1	d <sup>-1</sup>	Adapted from Blackford (2002)
$sk$	Sinking rate of pelagic chlorophyll	1	m.d <sup>-1</sup>	Mann and Lazier (1996)
$c_3$	Proportion of MPB on the sediment surface	0.15	-	estimated <sup>f</sup>
$N_a$	Particulate Organic Nitrogen	5 x 10 <sup>8</sup>	mmol	Serpa <i>et al.</i> (2007)
$d$	Decay rate of N	0.1	d <sup>-1</sup>	Adjusted
$p$	Porosity	0.5	-	data
$D_m$	Diffusion coefficient	1.66 x 10 <sup>-4</sup>	m <sup>2</sup> .d <sup>-1</sup>	Murray <i>et al.</i> (2006)
$\tau$	Tortuosity of sediment pores	1.3	-	Jackson <i>et al.</i> (2002)
$Den$	Denitification rate	0.01	d <sup>-1</sup>	Adapted from Murray and Parslow (1997)
$h_b$	Thickness of the superficial sediment layer	0.001	m	Chapter 6
$h_{bbi}$	Thickness of the benthic boundary layer	0.001	m	Di Toro (2001) and Murray <i>et al.</i> (2006)
$h_s$	Thickness of the pore water sediment layer	0.05	m	data
$\Phi$	Photosynthetic yield	40	nmol C.μE <sup>-1</sup>	Tett <i>et al.</i> (2007)
$\chi$	Conversion factor	0.4	mg chl.(mg-at organic C) <sup>-1</sup>	Tett <i>et al.</i> (2007)
$k$	Conversion factor	8.64 x 10 <sup>-2</sup>	s.d <sup>-1</sup> .mili(nano) <sup>-1</sup>	Tett <i>et al.</i> (2007)
$R$	Proportion of reflected PAR from sea-bed	0.5	-	Chapter 5
$K_d$	PAR diffuse attenuation coefficient in the lagoon	0.7	m <sup>-1</sup>	Chapter 5
$m_2$	Corrects for losses due to the surface reflection and hyperexponential decay	0.7	-	Tett <i>et al.</i> (2003)
$a_s^*$	‘Nutrient absorption cross-section’	0.03	m <sup>2</sup> .mg <sup>-1</sup>	estimated
$a_{PH}^*$	Absorption cross-section of photosynthetic pigments	0.02	m <sup>2</sup> .mg <sup>-1</sup>	Tett <i>et al.</i> (2007)
$a_{NP}^*$	Absorption cross-section of photoprotective pigments	0.02	m <sup>2</sup> .mg <sup>-1</sup>	Tett <i>et al.</i> (2007)
$a_{PM}^*$	Absorption cross-section of particulate matter	3 x 10 <sup>-6</sup>	m <sup>2</sup> .mg <sup>-1</sup>	Devlin <i>et al.</i> (2008)
$\rho_s$	Density of dry sediment	2.16 x 10 <sup>9</sup>	mg.m <sup>-3</sup>	data
$c_5$	MPB fraction that takes part of vertical migration	0.5	-	data
$c_6$	Exposed sediment surface fraction	0.3	-	data
$\mu_{max}$	Maximum relative growth rate	1	d <sup>-1</sup>	Laurent <i>et al.</i> (2006)
$\mu_{max(20)}$	MPB maximum growth rate at 20°C	1.2	d <sup>-1</sup>	Lee <i>et al.</i> (2003)
$Q_{10}$	Multiplicative factor that represents the increase to the double of metabolism activity due to an increase of 10°C in temperature	2		Lee <i>et al.</i> (2003)
$T_i$	Temperature		°C	data
$r_{0,a}$	Algal basal respiration rate	0.05	d <sup>-1</sup>	Tett <i>et al.</i> (2007)
$r_{0,h}$	Heterotroph basal respiration rate	0.03	d <sup>-1</sup>	Tett <i>et al.</i> (2007)
$b_a$	Slope of graph of algal respiration on growth rate	0.5	-	Tett <i>et al.</i> (2007)

$b_h$	Slope of graph of heterotroph respiration on growth rate	1.5	-	Tett <i>et al.</i> (2007)
$\eta$	Heterotroph fraction	0.125	-	Tett <i>et al.</i> (2007)

Table 7.8 – Initial values of each state variable of the model and boundary conditions.

Symbol		Initial values	Boundary conditions
S	Nutrient concentration	2 mmol.m <sup>-3</sup>	2.3 mmol.m <sup>-3</sup>
X	Chlorophyll concentration	2 mg chl. m <sup>-3</sup>	1.75 mg chl. m <sup>-3</sup>
X <sub>b</sub>	MPB chlorophyll concentration	200 mg chl. m <sup>-2</sup>	
S <sub>sed</sub>	Pore water nutrient concentration	100 mmol.m <sup>-3</sup>	

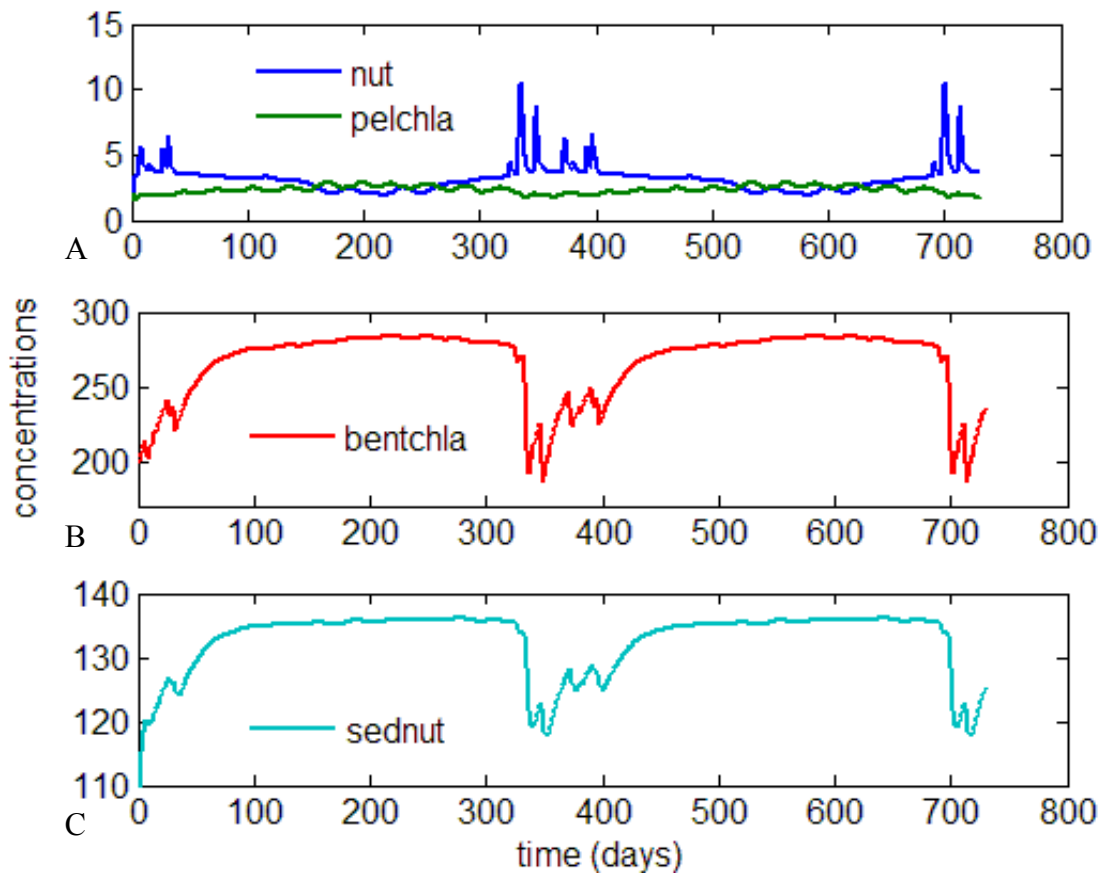


Figure 7.29– A- Simulation of DAIN (blue; mmol.m<sup>-3</sup>) in the water column, pelagic chlorophyll (green; mgchl.m<sup>-3</sup>), B- benthic chlorophyll (red; mg chl.m<sup>-2</sup>),and C- DAIN in pore water (light blue; mmol.m<sup>-3</sup>) during a period of 730 days.

also lower during the winter due to the decrease in recycled MPB chlorophyll.

Both pore water DAIN and benthic chlorophyll are very variable through the year (Figure 7.30). MPB has a high spatial variability and therefore it is expected that the observed concentrations vary, with a high standard deviation throughout the year, around a specific value.

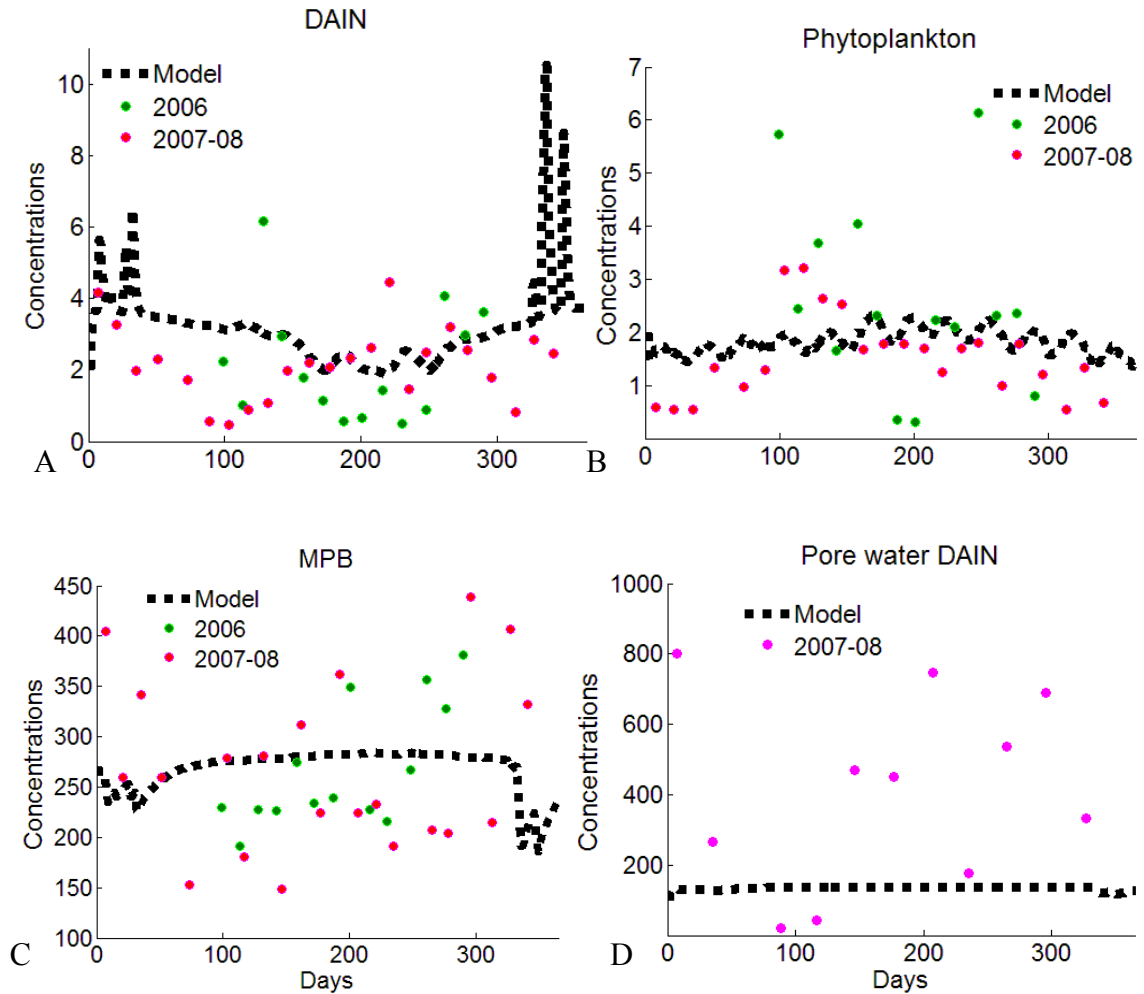


Figure 7.30 – A- Concentrations of DAIN (2006 and 2007-08;  $\text{mmol.m}^{-3}$ ) and predictions by the model for Ria Formosa, B- Concentrations of pelagic chlorophyll (2006 and 2007-08;  $\text{mgchl.m}^{-3}$ ) and predictions by the model, C- Concentrations of MPB chlorophyll (2006 and 2007-08;  $\text{mg chl.m}^{-2}$ ) and predictions by the model and D- Concentrations of Pore water DAIN (2007-08;  $\text{mmol.m}^{-3}$ ) and predictions by the model.

As presented before in this section, this new approach to the microphytobenthos dynamics, allows the calculation of the maximum possible value of chlorophyll concentration. According to the model simulation, the maximum value is of  $417 \text{ mg chl.m}^{-2}$ , defined by the light limited growth rate, which is the one allowing higher values of chlorophyll concentration.

#### *Model validation*

The goodness of the fit was investigated by carrying out a linear regression using the least squares method. The statistical coefficient of determination ( $R^2$ ) provides a measure of how good the model is. This procedure was done using data collected during the year

of 2006 (Figure 7.31) and was repeated using the data from 2007-08 (Figure 7.32). This analysis showed that the model agreement with data is weak using data from both periods. In some cases, such as for phytoplankton, the regression line has a negative slope, which contradicts expectations. This represents an increase in the model output and a decrease in the observations. A good fit should express a simultaneous increase both in the model output and observed data, as for microphytobenthos (Figure 7.31). Slopes of DAIN in 2006 and MPB in 2007-08 were close to one. However, all the regression analyses conducted were not significant ( $p > 0.05$ ).

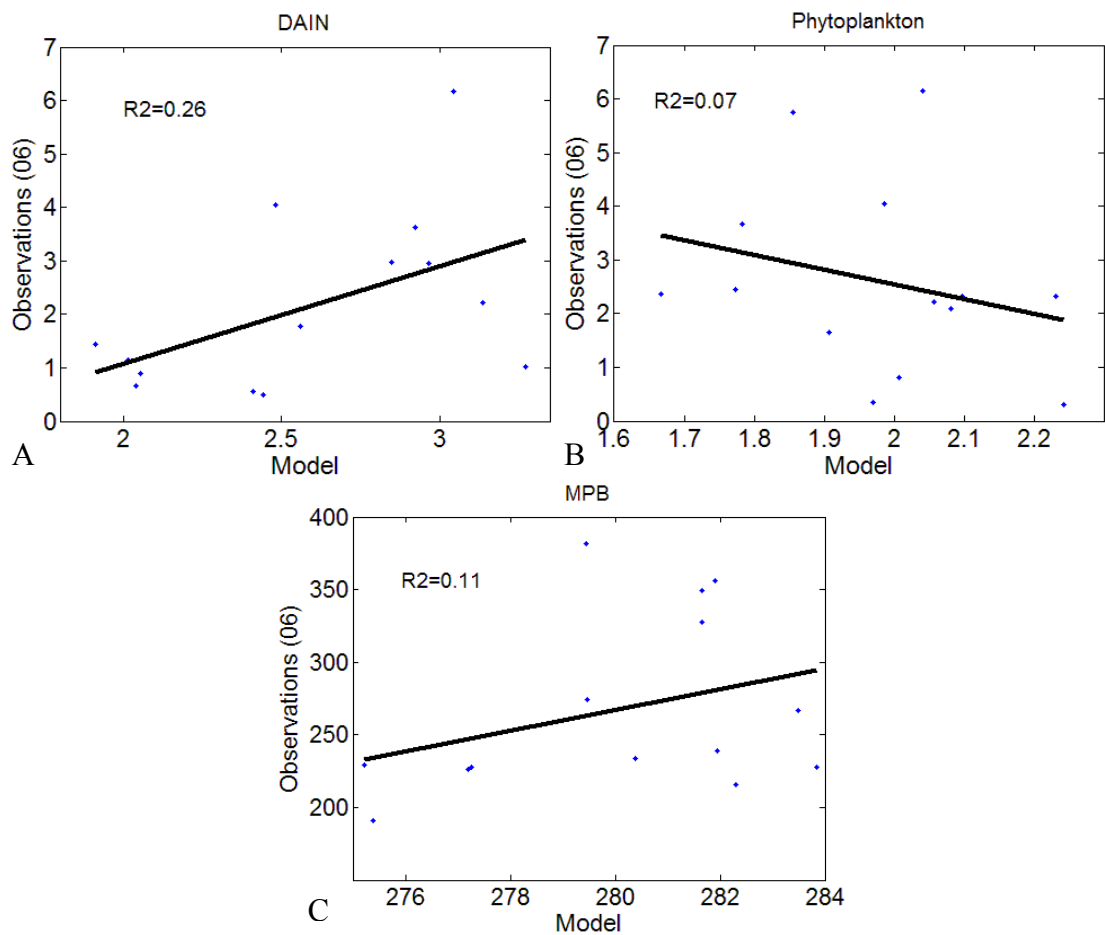


Figure 7.31 - Scatter plot of the observed values versus predicted values for DAIN (A), Phytoplankton (B) and MPB (C), using 2006 data. The determination coefficient is shown in each plot.

These results have to be carefully analysed. First, it is important to recall that the model output is within the appropriate range of natural variation. The regression analysis does not consider this point. Moreover, for components which are highly variable both in space and time, such as the microphytobenthos, as discussed in chapter 4 and 5, small values of the coefficient of determination may be expected. It is extremely difficult and complex to simulate the small-spatial-scale and the short-time variability of these components and this was not the aim of this model. In addition, it is

important to indicate that data were not used directly to calibrate and adjust the model to real conditions. This point is important since it could significantly improve the goodness of fit. For this approach it is important to have different datasets, so that the one used to calibrate the model is not the same used for the model validation. Data used were limited and did not allow this approach.

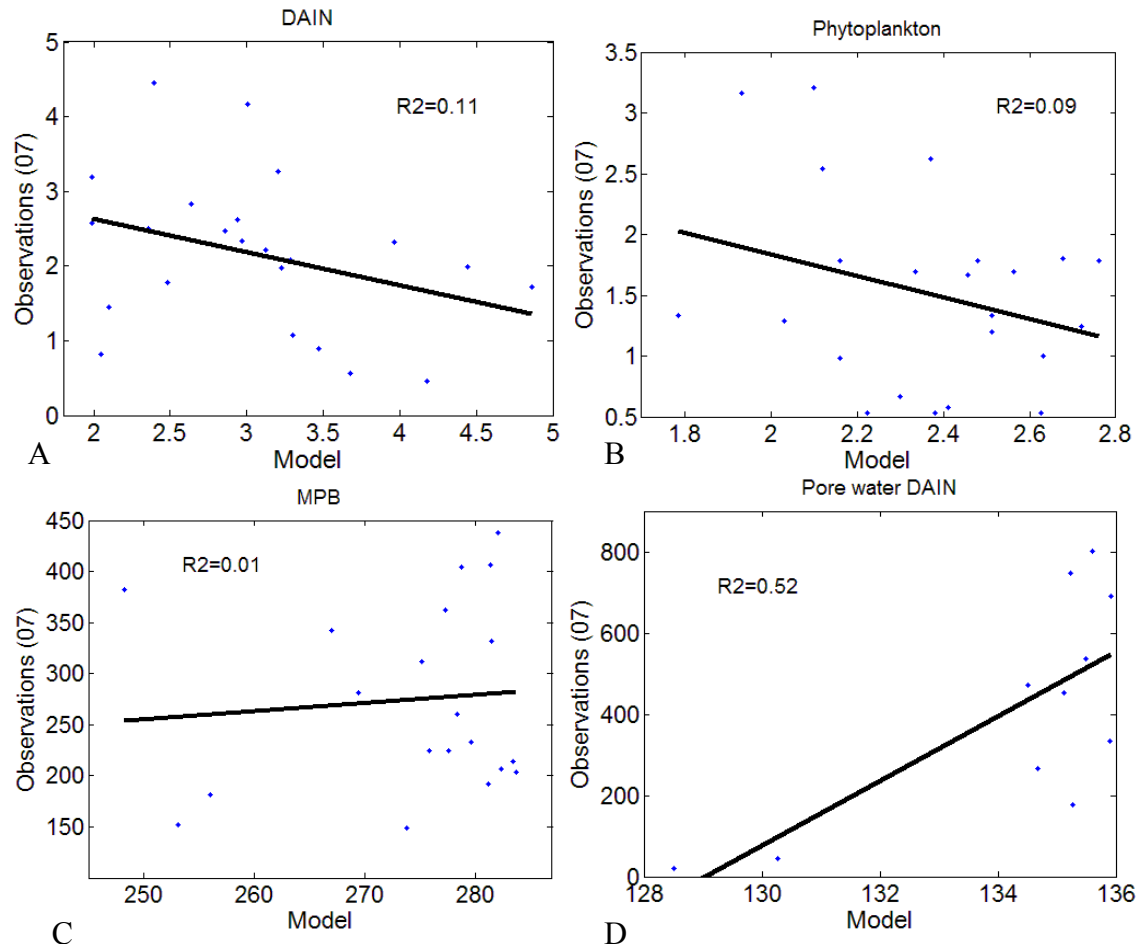


Figure 7.32 - Scatter plot of the observed values versus predicted values for DAIN (A), Phytoplankton (B), MPB (C) and pore water DAIN (D), using 2007-08 data. The determination coefficient is shown in each plot.

#### 7.2.4.6 Discussion

DAIN concentrations in the water column are closely dependent on run-off and diffuse sources. The model developed predicts values within the range of the observed variation, although they are much more stable than the observations. Moreover, the range of variation predicted is in accordance with the results obtained by Serpa *et al.* (2007) using a biogeochemical model just for nutrients and considering the denitrification process. This system has complex interactions and is influenced by

stochastic events, which are difficult to predict, especially without considering complex meteorological models. The model reflects well the variable character of the pelagic chlorophyll, which is mainly influenced by the resuspension of benthic chlorophyll, especially by the action of spring and neap tides. This is clear in the output due to the periodicity of the peaks. As discussed in Chapter 5, microphytobenthos are considered to have a major role in the dynamics of chlorophyll. The high flushing rate of the lagoon, as well as the large grazing pressure by benthic organisms, also estimated in Chapter 5, leads to a strong reduction in the phytoplankton biomass, which is compensated by the resuspension of benthic algae. Due to the large concentration of benthic chlorophyll, as observed and predicted by the model, a small rate of daily resuspension (around 0.5 to 1% of the fraction  $c_3$  of the microphytobenthos community) is sufficient to keep the system within these conditions. The importance of the pelagic and benthic coupling in shallow lagoons, like Ria Formosa should be further explored. In the future, shellfish models could be coupled to this dynamic CSTT model and processes such as resuspension should be fully evaluated.

The high pore water DAIN concentrations are the major source of nutrients for the large microphytobenthic algal community as evidenced by the data obtained when assembling the model. Given the nutrient flux from the sediments to the water column, the microphytobenthos always have a large amount of available resources for growth. However, if the benthic chlorophyll concentrations drop for any reason, i.e. lower MPB biomass, the nutrient flux into the water column increases strongly. This is what happens in the model during the winter. Following the discussions in Chapter 5, in the case of a global change of climate, a large number of changes could take place within the lagoon. If the turbidity of the water column increases due to a rise of sea level and increased precipitation, the sea bed will be less illuminated and the microphytobenthos biomass would decay. The model developed here supports the hypothesis of the degradation of the environmental quality of the lagoon, in the face of a climate change.

There are other important components of the system that were not considered in the approach adopted, such as the macroalgae. It could be very important to consider the addition of this element, which could also provide important information for the benthic nutrient component. This would be very helpful to explore different scenarios in the case of climate change. Pore water DAIN depends on a daily input of particulate organic nitrogen. Unfortunately, there are no consistent data that can be used in this model. An important supplier of organic matter may be the macroalgae community.

Therefore, by including this community, a novel set of important relationships could be evaluated. Furthermore, it is interesting to note that the maximum observed chlorophyll concentrations were always under the maximum predicted by the light limited growth, except for one observation.

The evaluation of the accuracy of the model is complex and should be carried out carefully. Cloern and Jassby (2008) have reported the absence of repeated temporal variations of phytoplankton over 150 sites located at land-sea interfaces. They suggest that the interactions between the processes that affect phytoplankton are very complex and unclear. It is therefore very difficult to predict accurately the temporal variation of primary producers in coastal areas. In the development of this model, it was especially difficult to deal with the conflict between keeping the model as simple as possible and improving it to be as accurate as needed. The main goal of this work was to develop a simple model to provide a better understanding of this system, which could be used for management purposes. Some of the suggested possible improvements of this model, such as the inclusion of a different state variable for Particulate Organic Nitrogen (PON), were considered during this work. However, some of them were too complex to include in this project and for others, there were no available data to proceed. For academic and research purposes, they should be explored in the future.

It is interesting to note that Murray and Parslow (1997) and Blackford (2002), both studying shallow locations, indicate a strong light limitation for microphytobenthos growth, much more important than nutrient limitation. Pore water nutrients provide a rich source of nitrogen for benthic algae. However, the model developed here did not express a strong light limitation. In fact, there are few periods in the year, mainly during the winter, when this is observed. This is the reason why the model simulates a decrease in the microphytobenthic chlorophyll concentrations during the winter. However, this was not observed in the lagoon. The concentrations of benthic chlorophyll were fairly similar throughout the year. The sites studied by Murray and Parslow (1997) and Blackford (2002) are in higher latitudes and waters may have different optical properties that may attenuate light. Blackford (2002) also indicated a seasonal variation of microphytobenthos which presented higher values during the summer. Both studies suggested the importance of microphytobenthos in benthic-pelagic interactions, especially in the dynamics of nutrients.

## 7.3 Sensitivity analysis

### 7.3.1 Introduction

Mathematical models of marine ecosystems have been extensively used to investigate the functioning of these complex systems, as management tools to predict assimilative capacities or eutrophication, and supporting the decision-making process (Tett *et al.*, 2003; Laurent *et al.*, 2006; Campolongo *et al.*, 2007). The analysis of uncertainty and sensitivity of the model are recognized as essential steps in the model development process, but not commonly implemented (Campolongo *et al.*, 2007; Cossarini and Solidoro, 2008; Portilla *et al.*, 2009). Uncertainty in the results is caused by errors in the formulation of the model, in the parameter values used and in the boundary or forcing conditions (Portilla *et al.*, 2009). Sensitivity analysis (SA) is essential to identify the critical processes and parameters of the model and should be carried out during the development of the model to help the building process (Cossarini and Solidoro, 2008). Moreover, SA is also a powerful tool in the understanding of ecosystem functioning since it allows the determination of parameter ranks and therefore provides an indication of the ranks and importance of processes.

The sensitivity analysis approach was used throughout the development process to help understanding the interactions between the components of this lagoon system and to make decisions of which processes to include. Here, only the final assessment is shown due to clarity and relevance for future improvements of the model and the understanding of ecosystem functioning.

Several sensitivity analysis strategies exist, ranging from the methods that decompose the total output variance into the contributions of each input factor, to other types of global sensitivity, where the whole range of variations is explored, down to the simplest techniques that evaluate the variation caused by changing One factor At a Time (OAT; Kohberger *et al.*, 1978; Campolongo *et al.*, 2007; Cossarini and Solidoro, 2008; Saltelli *et al.*, 2008). Here, a screening sensitivity analysis was applied, based on a randomised one-at-a-time parameter change design, described by Kohberger *et al.* (1978) and Morris (1991), and revised by Campolongo *et al.* (2007). The effects of changing one factor are assessed using an indicator,  $\mu$ , for the overall influence of the factor on the final output of the model (Campolongo *et al.*, 2007; Portilla *et al.*, 2009). A high value



of  $\mu$  indicates that the input factor has an overall influence in the model results (Morris, 1991; Campolongo *et al.*, 2007).

### 7.3.2 Methodology

For the assessment of the sensitivity of the dCSTT-MPB model, two different approaches were used. The first approach is based on the OAT approach in Campolongo *et al.* (2007) and considers the overall effect of a parameter change to the model output without standardizing it, which means that state variables with higher magnitudes can be more affected. The second approach is part of the method proposed by Kohberger *et al.* (1978) and involves the standardization of the model output, which means that the variable magnitude is no longer important.

#### 7.3.2.1 Relative Absolute Change

Each model factor  $X_i$  with  $i=1, \dots, k$ , was assumed to vary across  $p$  selected levels in the space of the input factors. The levels covered  $\pm 50\%$  of the initial parameter value, as exemplified in Figure 7.33.

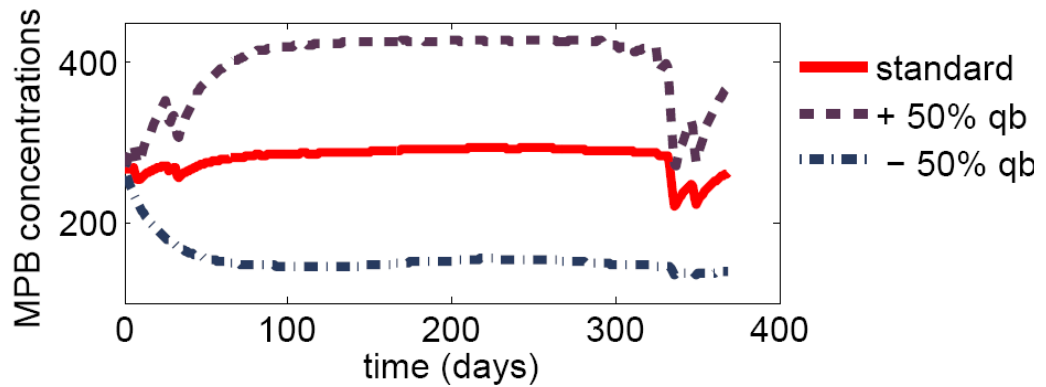


Figure 7.33 – Model output for MPB chlorophyll concentrations: standard simulation, +50% of the  $q_b$  parameter, and – 50% of the  $q_b$  parameter.

For a given value of  $X$ , the effect of the  $i$ th impact factor is defined as:

$$d_i = \frac{f(X + \Delta X_i) - f(X)}{\Delta X_i / X_i} \quad (7.82)$$

Where  $\Delta X_i / X_i$  is a value in  $\{1/(p-1), \dots, 1-1/(p-1)\}$  and  $p$  is the number of levels considered in the assessment, which in this case is a value from the set  $\{-0.5, \dots, 0.5\}$  (Campolongo *et al.*, 2007). The indicator  $\mu$  is likely to involve Type II errors, i.e. not considering an important factor rather than Type I errors, i.e. considering a factor as influential when it is not (Campolongo *et al.*, 2007). The  $d_i$  distribution may contain positive and negative elements resulting from the increase or decrease of the input factor value. These elements may cancel each other out and thus producing incorrectly a low value of  $\mu$ , indicating a negligible effect. Therefore, Campolongo *et al.* (2007) suggested the use of  $\mu^*$  which is the estimate of the mean of the distribution of the absolute values. This indicator provides sufficient information for an adequate parameter ranking (Campolongo *et al.*, 2007). For the assessment of the most important factor, parameters were ranked following the  $\mu^*$  indicator. Scores under the 50<sup>th</sup> quantile of all the effects considered were not included in the evaluation.

### 7.3.2.2 Standardized Change

This approach is similar to the previous one, except that the variation in the model output due to the parameter change is now standardized, which is done by dividing it by the standard output of the model with no change ( $f(X)$ ). Thus:

$$d_i = \frac{(f(X + \Delta X_i) - f(X)) / f(X)}{\Delta X_i / X_i} \quad (7.83)$$

The levels of parameter change for this analysis were  $\pm 50\%$ . The indicator  $\mu^*$  was calculated for each state variable and each parameter. A variation from 0 to 1 of  $\mu^*$  indicates that the model is insensitive to the parameter change. A value of 1 indicates a direct relationship between the model and the parameter change. Values above 1 indicate that the model is sensitive to the change of parameter. The values of  $\mu^*$  were used instead of the ranks, used on the previous approach.

### 7.3.3 Results and discussion

The input factors that caused the largest change in the model simulation, following the first approach, are represented in Figure 7.34 by dark colours. Results clearly indicate that variations in all input factors have a greater effect on the benthic

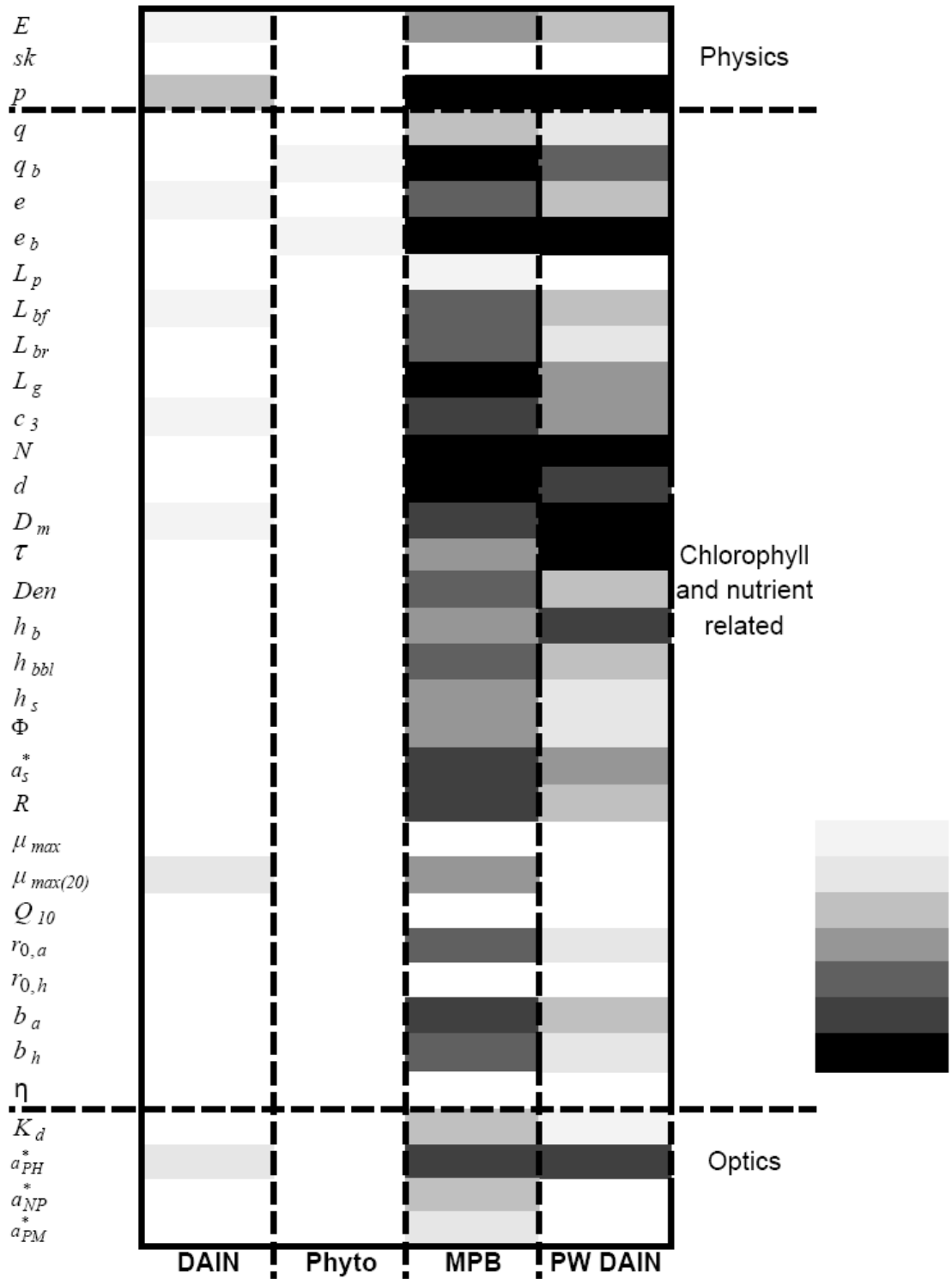


Figure 7.34 – Parameter change effect as a function of the state variables. The darker the colour the higher the score of  $\mu^*$  indicator. Scores under the 50<sup>th</sup> quantile of all of the effects considered were not included.

components of the system, on both the microphytobenthos and the pore water nutrients. This is due to the fact that the concentrations of the benthic elements are one or two orders of magnitude higher than the concentrations simulated for pelagic elements. The

physical characteristics of this lagoon system are important in the model. Variations in the exchange rate (E) produce a high variation in the output of DAIN concentration in the water column. However, this fact is masked due to the importance of the benthic compartments. If the exchange rate is lower than the normal, the nutrient concentrations in the water column will increase because of the accumulation of nutrients. Porosity ( $p$ ) is another input factor that is extremely important both for pelagic and benthic compartments. This factor is essential for the flux equations, having a great impact in the diffusion of nutrients from the sediments to the water column and therefore in the amount of nutrient that is captured by microphytobenthos (Equation 7.53). It also affects the MPB growth by interfering with the uptake of nutrients by MPB. Regarding the group of factors that include the chlorophyll and nutrient related factors, it is clear that the parameters directly associated with benthic processes are the ones that cause the largest variations. The yield of MPB chlorophyll from nutrients ( $q_b$ ) has a key role in the calculation of the MPB chlorophyll concentration by the model. The yield of chlorophyll from nutrients was previously identified as a key factor for phytoplankton by Portilla *et al.* (2009) using a different version of the CSTT model (LESV model) which only considers the pelagic compartments. The benthic chlorophyll fraction that is recycled ( $e_b$ ) is also critical in this model both for MPB and pore water nutrients. If the value of the  $e_b$  factor is higher than the original value, the amount of matter that will be recycled rises and leads to an increase in the pore water concentrations. This is favourable for an increase in the MPB concentrations, as well. The loss rate of MPB due to grazing ( $L_g$ ) has a direct effect on MPB chlorophyll concentrations. All the other input factors with large effects on the benthic components have a close relationship with pore water concentrations and fluxes, such as the nitrogen input ( $N$ ), the decay rate ( $d$ ), the diffusion coefficient ( $D_m$ ) and tortuosity ( $\tau$ ). The absorption cross section of photosynthetic pigments ( $a_{PH}^*$ ) is the only input factor from the 'optics' group that has a relatively high effect on the model output. A higher value of this input factor would lead to an increase of the photosynthetic efficiency of MPB.

The parameters that caused the largest impact in the model, following the second approach, are represented in Figure 7.35. The results are similar to the ones obtained with the previous approach. It is clear that porosity ( $p$ ) is a parameter to which the model is highly sensitive, also indicated previously. In fact, porosity has the largest impact on all the state variables of the model. The yield of microphytobenthic chlorophyll from nitrogen ( $q_b$ ) was also confirmed as an important parameter for MPB,

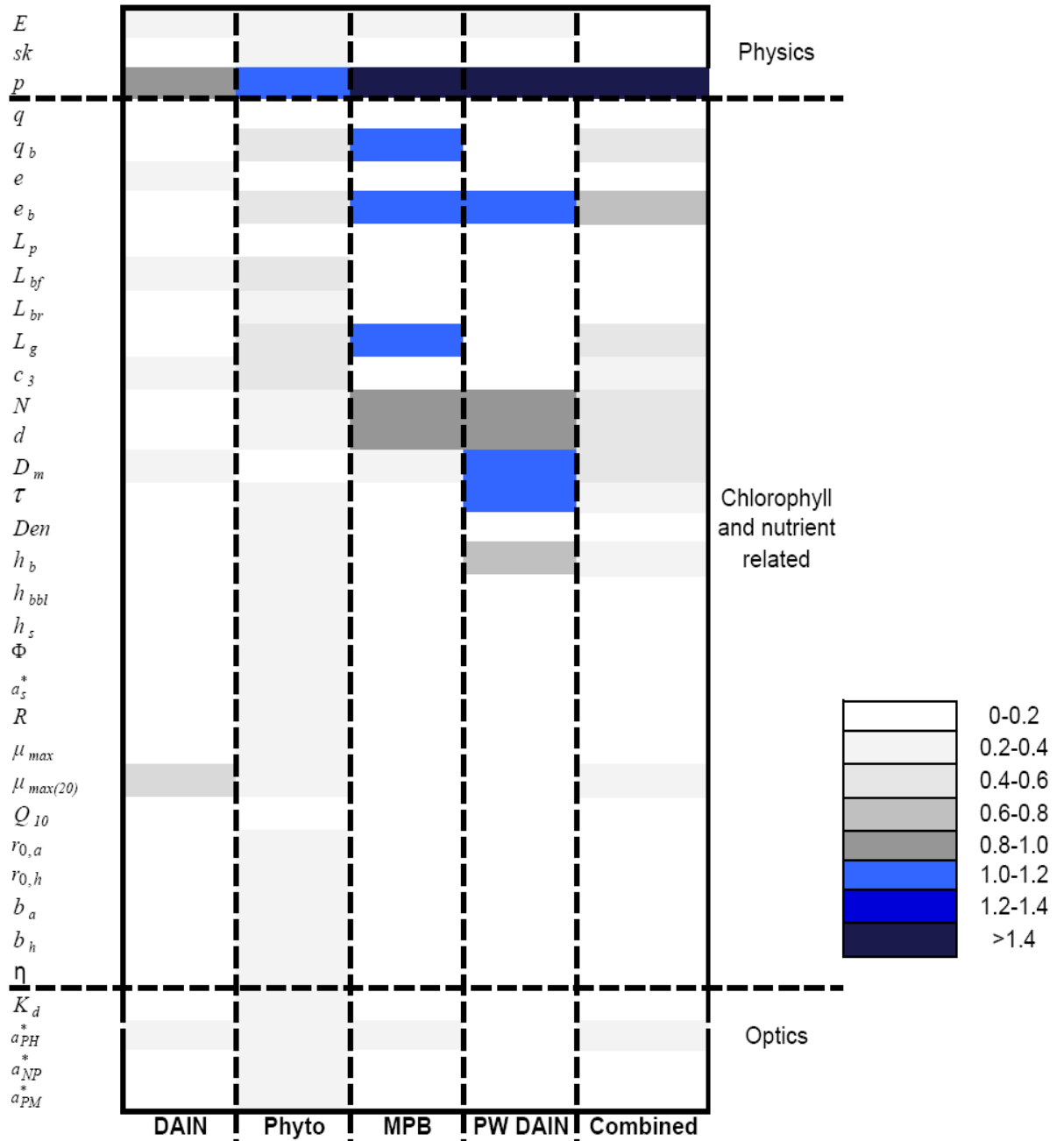


Figure 7.35 – Parameter change effect as a function of the state variables, represented as the  $\mu^*$  indicator values. The darkest colour correspond to the highest value of the  $\mu^*$  indicator.

as well as the benthic chlorophyll fraction that is recycled ( $e_b$ ), which has also an important effect on pore water nutrient concentrations. The parameters that are linked to the nutrient fluxes such as the diffusion coefficient ( $D_m$ ) and tortuosity ( $\tau$ ) have also an important effect on the benthic variables, as indicated previously. Finally, it is interesting to note that combining the four state variables, the model becomes only sensitive to one parameter, porosity, which has a strong effect on the model output.

Given the importance of these factors, they should be carefully evaluated in future applications of this model. Porosity is easily evaluated by field and laboratorial work, as done here, and should always be assessed. This project also provided useful experimental results to support the value of the yield of microphytobenthic chlorophyll from nutrients. Similar evaluations have also been carried out in the past for pelagic communities (e.g. Edwards *et al.*, 2003; 2005). Further work on nutrient recycling and grazing pressure should be seriously considered in the future to improve the understanding of the system. Not surprisingly, the optical parameters did not show a strong effect on the model output. The analysis of the model output and field data indicate that photosynthetic communities do not have a strong dependence on light, because light does not seem to be limiting the algal growth (both pelagic and benthic) in this shallow lagoon. This was also discussed in Chapter 4 and 5.

#### **7.4 Estimating Assimilative Capacity**

The assimilative capacity of a system is its ability to accommodate waste products without breaching any of the Ecological Quality Objectives (ECoQOs) defined for the specific area, in this case, the Ria Formosa lagoon. As presented in Chapter 1, the assimilative capacity of a system was defined by GESAMP (1986) as “*a property of the environment defined as its ability to accommodate a particular activity or rate of activity without unacceptable impacts*”. The current practice is to use the ECoQOs to define what is desirable (Laurent *et al.*, 2006). However, no Ecological Quality Objectives have yet been defined and established for Portuguese waters, and more specifically to the Ria Formosa lagoon. In current study, the standards suggested by Crane *et al.* (2006) and Tett *et al.* (2007) for DAIN (winter values -  $10\mu\text{M}$  or  $10\text{mmol}\cdot\text{m}^{-3}$ ) and phytoplankton chlorophyll (spring/summer values -  $10\text{mg}\cdot\text{m}^{-3}$ ) concentrations were taken and applied. This approach is merely illustrative due to the fact that the model still needs to be improved. This dCSTT-MPB reveals a weak agreement between model output and data from the lagoon. In addition, in the future this analysis should be performed with specific reference conditions and ECoQOs for Ria Formosa, as required by the Water Framework Directive.

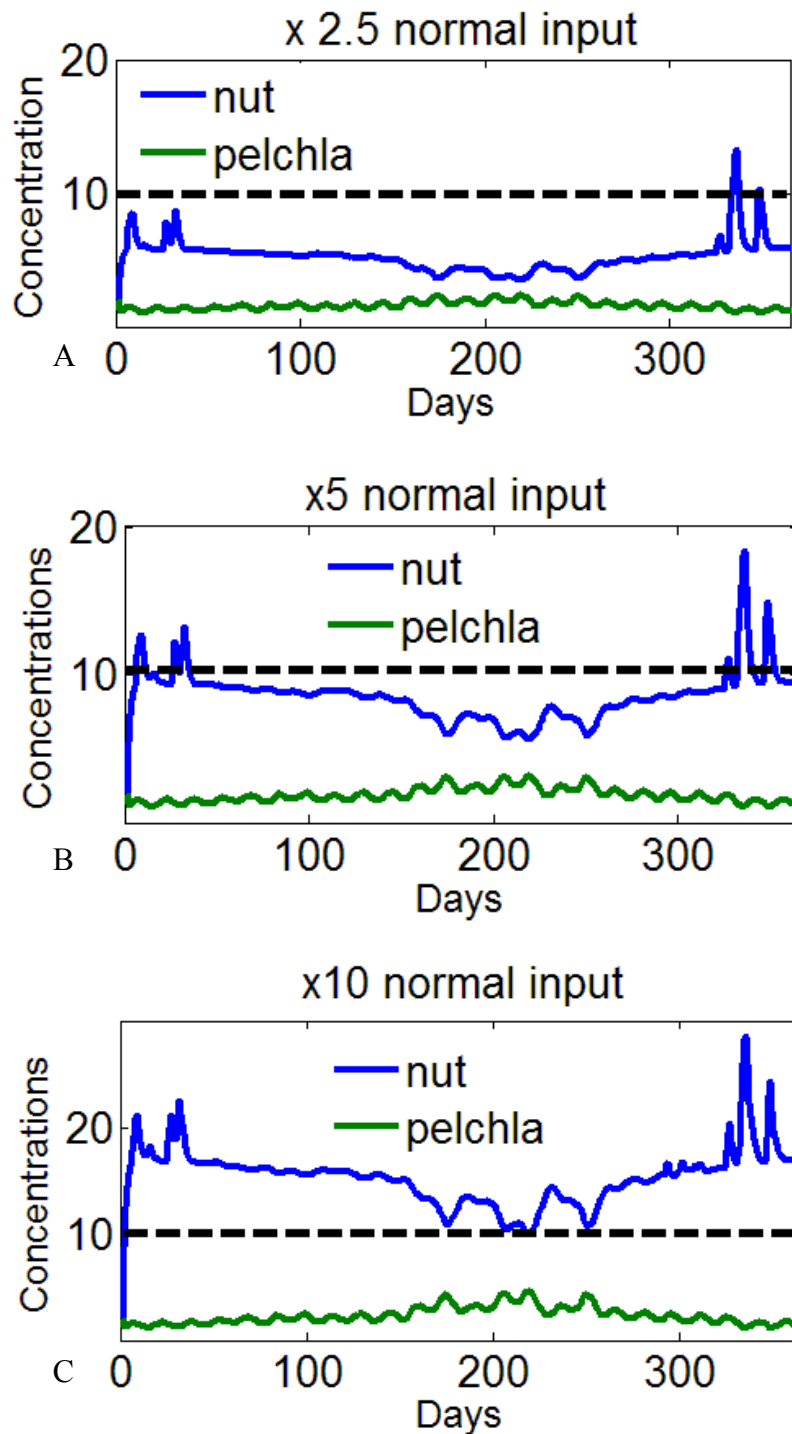


Figure 7.36 - Model output for DAIN ( $\text{mmol.m}^{-3}$ ) and pelagic chlorophyll ( $\text{mg chl.m}^{-3}$ ) concentrations with nitrogen input increased by a factor of 2.5 (A), 5 (B) and 10 (C). Threshold for DAIN and pelagic chlorophyll concentrations is shown in each figure (black dashed line).

A series of simulations were carried out in which the nitrogen input ( $S_i$ ) to the lagoon system was increased by a factor of 2.5, 5 and 10. The output of these simulations are presented in Figures 7.36 and 7.37. Figures include the threshold for DAIN and pelagic chlorophyll concentrations, indicated previously. The threshold for DAIN

concentrations was reached and exceeded by doubling the amount of nitrogen inputs to the lagoon, as illustrated in Figure 7.38. Enrichment of nutrient concentrations in the lagoon did not produce a clear reaction from the algal community. Pelagic chlorophyll concentrations remained far below the threshold during all the simulations performed (Figure 7.39). Benthic chlorophyll concentrations increased significantly with an increase of nitrogen input by a factor of 10 (Figure 7.40). In summary, the DAIN threshold was breached by doubling the nitrogen input and the pelagic chlorophyll threshold was not reached, even with an increase of nitrogen input by a factor of 10.

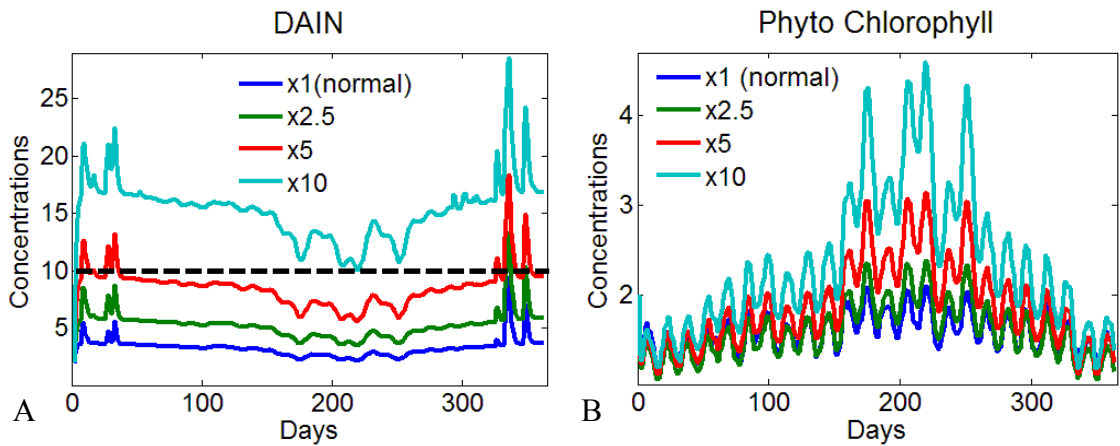


Figure 7.37 - DAIN concentration (A;  $\text{mmol.m}^{-3}$ ) and pelagic chlorophyll concentration (B;  $\text{mg chl.m}^{-3}$ ) variations using different multipliers of the nitrogen input parameter (2.5, 5 and 10)

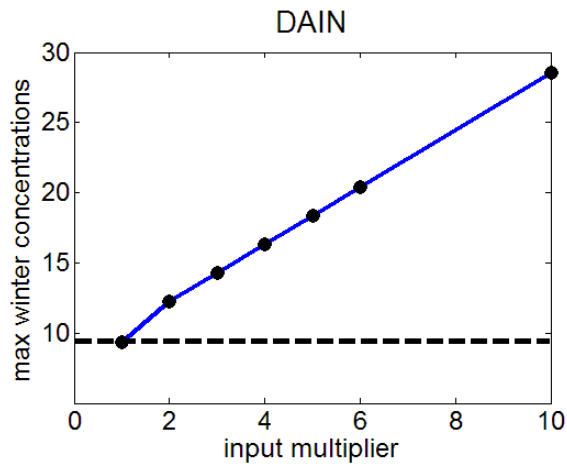


Figure 7.38 - Estimation of the assimilative capacity for the indicator DAIN ( $\text{mmol.m}^{-3}$ ). Threshold is represented by a black and dashed line.



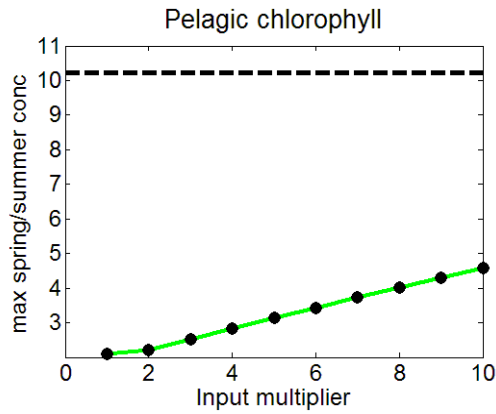


Figure 7.39 - Estimation of the assimilative capacity for indicator pelagic chlorophyll (mg chl.m<sup>-3</sup>). Threshold is represented by a black and dashed line.

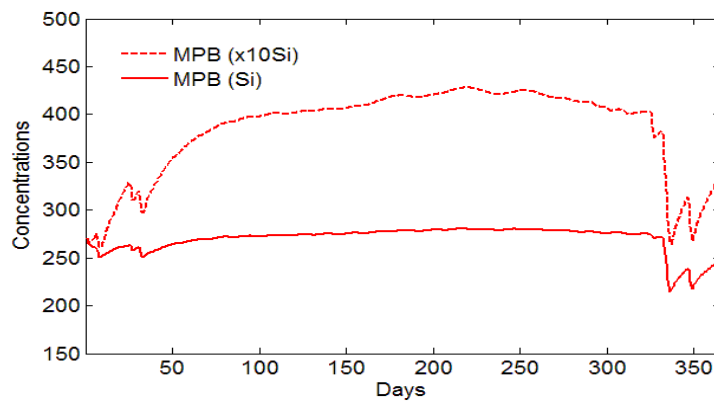


Figure 7.40 - MPB chlorophyll concentrations (mg chl.m<sup>-2</sup>) obtained using an increased nitrogen input by a factor of 10.

Another interesting point to investigate is the effect of nitrogen enrichment on the nitrogen fluxes simulated by the model (Figure 7.41). Note that the physical term is separated into the water exchange with the sea (*Physic*) and the interactions or nutrient fluxes between the sediment and the water column (*Inter*). The nutrient input  $S_i$  is represented as *Input*. During the winter period, a positive flux to the water column occurs due to the fact that the model predicts a decrease in MPB chlorophyll concentrations and therefore an increase in the nitrogen flux from the sediments to the water column. This flux does not seem to be affected by nutrient enrichment at this scale. A negative flux is present during the whole year, especially during the spring / summer due to the nitrogen uptake by algae for growth. This flux is much stronger in a scenario of nitrogen enrichment. The physical fluxes are also strongly affected by an increase in the nitrogen concentrations because the water exchange between the water body of the lagoon and the sea is higher. A nutrient enrichment in Ria Formosa would lead to a strong increase in nutrient concentrations in the water column. The lagoon

would behave as a source of nutrients to the sea by exporting an important amount of nitrogen. The uptake of nitrogen by pelagic and benthic algae would increase strongly (Figure 7.41B), but little response on pelagic communities is seen (Figure 7.39). This fact is expected because the extra nitrogen would go preferentially to the MPB due to their high chlorophyll concentrations. This increase in uptake is important because it leads to an increase in the MPB chlorophyll concentrations (Figure 7.40).

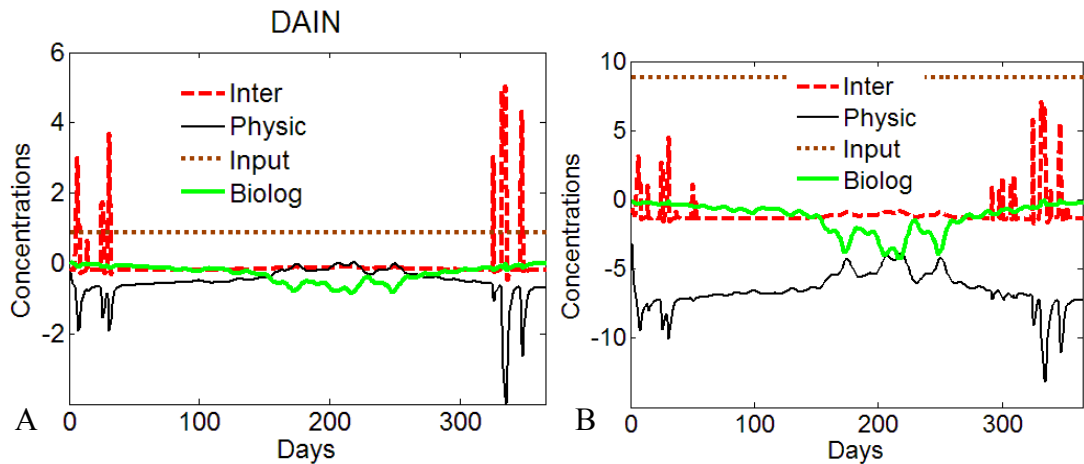


Figure 7.41 - Fluxes of DAIN concentrations ( $\text{mmol.m}^{-3}$ ) caused by the physical model, the bio-chemical model, the interactions between sediments and the water column and the nitrogen input. A – normal nitrogen input; B – increase of nitrogen input by a factor of 10.

## 7.5 Exploration of different scenarios

Mathematical models are powerful tools to explore ecosystems under different scenarios. Therefore, the dCSTT-MPB model developed here was used to investigate the repercussions on the lagoon ecological quality of some variations of its parameters, simulating potential future events. This was done by analysing the model output against the ECoQOs for DAIN and pelagic chlorophyll concentrations, as before. The thresholds are also represented in each figure. This analysis is, once more, merely illustrative due to the weak agreement between model output and data and the lack of specific ECoQOs for Ria Formosa. The scenario considered here was a global climate change that would lead to sea level rise and an increase in temperature to the regions close to the Mediterranean basin (IPCC, 2007). This climate change would also lead to an increase in precipitation in the northern areas of Europe, which could also increase the turbidity of lagoons due to the stronger run-off. So, in the case of sea level rise, it would be expected that MPB would absorb a smaller proportion of photons, which means that  $c_l$  would be smaller.  $c_l$  is defined by the Equations 7.70 and 7.72 and is

dependent on the absorption cross section ( $a_{PH}^*$ ). This parameter ( $a_{PH}^*$ ) was then changed to 0.01 (50% reduction) to simulate this scenario. In the future, it would be useful to assess exactly how much this reduction should be per each meter of sea level rise. This reduction of 50% may be exaggerated. As shown in Figure 7.42, this reduction would lead to a stronger light limitation and would lead to a relevant increase of DAIN concentrations in the water column, breaching the established threshold.

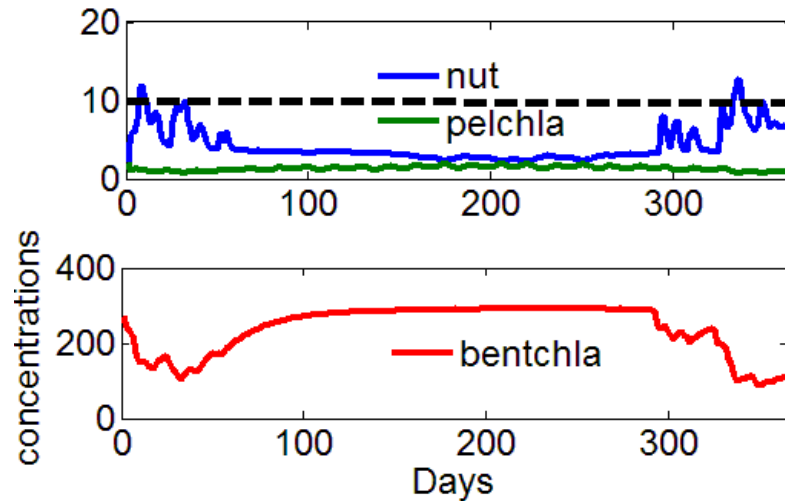


Figure 7.42 - Model output for DAIN ( $\text{mmol.m}^{-3}$ ), pelagic chlorophyll ( $\text{mg chl.m}^{-3}$ ) and MPB chlorophyll ( $\text{mg chl.m}^{-2}$ ) concentrations with smaller value of  $c_1$  obtained by decreasing the  $a_{PH}^*$  parameter to 0.01. Threshold for DAIN and pelagic chlorophyll concentrations is shown (black dashed line).

If the sea level rises another potential effect on the MPB community is the decrease of the proportion of MPB cells on the sediment surface, since they tend to be within the sediment when they are immersed. Therefore, to simulate this, the  $c_3$  parameter was

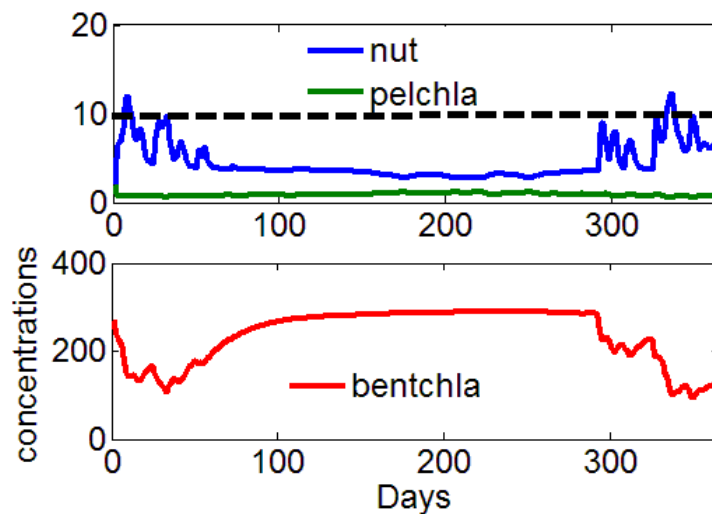


Figure 7.43 - Model output for DAIN ( $\text{mmol.m}^{-3}$ ), pelagic chlorophyll ( $\text{mg chl.m}^{-3}$ ) and MPB chlorophyll ( $\text{mg chl.m}^{-2}$ ) concentrations with smaller value of  $c_3$  parameter to 0.05. Threshold for DAIN and pelagic chlorophyll concentrations is shown (black dashed line).

reduced to 0.05 (from 0.15). Figure 7.43 presents the result of this simulation, showing once more, a decrease in the MPB community during the winter. As for the previous simulation, this would lead to an increase in the DAIN concentrations in the water column, breaching the threshold. If both effects, reduced  $a_{PH}^*$  and  $c_3$  parameters are combined, the effect on MPB community is stronger (Figure 7.44). This would lead to much higher DAIN concentrations in the water column, breaching the threshold not only during the winter but also during the autumn.

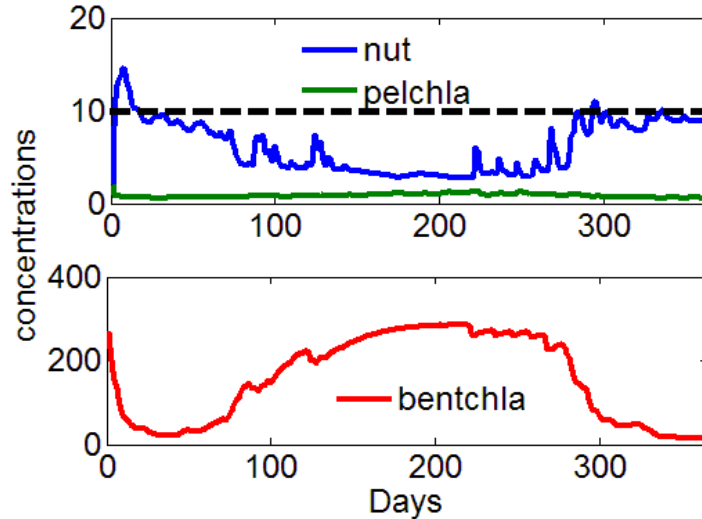


Figure 7.44 - Model output for DAIN ( $\text{mmol.m}^{-3}$ ), pelagic chlorophyll ( $\text{mg chl.m}^{-3}$ ) and MPB chlorophyll ( $\text{mg chl.m}^{-2}$ ) concentrations with a smaller value of  $c_1$  obtained by decreasing the  $a_{PH}^*$  parameter to 0.01, combined with a smaller value of parameter  $c_3$  to 0.05. Threshold for DAIN and pelagic chlorophyll concentrations is shown (black dashed line).

Finally, the effects of an increase in water temperature by  $2^\circ\text{C}$  were also simulated (Figure 7.45). There were no effects on the MPB chlorophyll concentration, except on the first few days. However, the phytoplankton was favoured by the temperature. Because no effects were observed on the MPB community, there were no effects on the diffusion of nutrients from the sediments to the water column which could increase the DAIN concentrations in the water column. Effects could be expected on the diffusion of ammonium from the sediments but they are not considered in this model. As discussed in Chapters 1 and 5, an increase in temperature would lead to an increase in ammonium concentrations in the sediments because the microbial activity would be favoured.

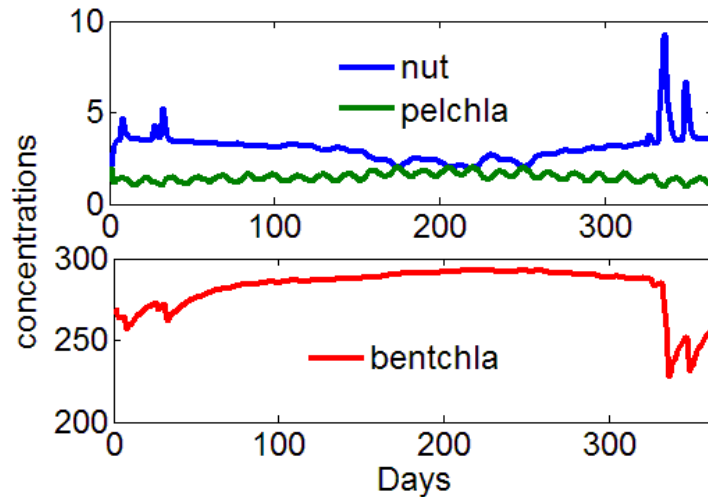


Figure 7.45 - Model output for DAIN ( $\text{mmol.m}^{-3}$ ), pelagic chlorophyll ( $\text{mg chl.m}^{-3}$ ) and MPB chlorophyll ( $\text{mg chl.m}^{-2}$ ) concentrations with higher values of temperature, considering an increase of  $2^{\circ}\text{C}$ . Threshold for DAIN and pelagic chlorophyll concentrations is shown (black dashed line).

Concluding, our dCSTT-MPB model suggests what was discussed at the end of Chapter 5. A sea level increase may lead to a decrease in the MPB community which would affect the DAIN concentrations in the water column due to stronger diffusion of nitrogen. This fact in itself would represent the breach of the DAIN threshold but no response is seen in the phytoplankton. The large concentrations of DAIN dissociated from an algal response would not be considered as an evidence of undesirable impacts.

## 7.6 Final considerations

Through the development of this dCSTT-MPB model, hypotheses were tested and results presented. The model revealed the importance of the microphytobenthos in terms of chlorophyll concentrations, compared to pelagic producers. The microphytobenthos represent around 99% of the total chlorophyll of the system, as discussed before. Pore water nutrients also assumed a crucial role in the system dynamics by supporting the microphytobenthos community. These nutrients may also be released into the water column and subsequently have a great impact on the nutrient concentration of the water body. The sediments of Ria Formosa lagoon represent an important stock of chlorophyll and nutrients to the lagoon. Through sensitivity analysis, the most important factors to this model were revealed. The yield of chlorophyll from nitrogen is one of the most important factors, as expected. This result provided more confidence in the experimental design used to estimate this factor. The modelling process also indicated that the standard Monod approach for microphytobenthos growth was not the most

appropriate and a flux-orientated method was implemented. The model provided an indication that in the case of nutrient enrichment, little response would be expected in the algal communities. Moreover, if for any reason the microphytobenthos biomass decreases, the model predicts a strong increase in the winter nutrient concentrations of the water column, due to an increase in the diffusion.

## 7.7 References

- Alvera-Azcárate, A., Ferreira, J.G., Nunes, J.P. (2003). Modelling eutrophication in mesotidal and macrotidal estuaries. The role of intertidal seaweeds. *Estuarine and Coastal Shelf Science*, **57**, 715-724.
- Ambrose, R., Martin, J., Wool, T. (2006). *WASP7 Benthic Algae -Model Theory and User's Guide*. Environmental Protection Agency, USA, 32pp.
- Baird, M., Walker, S., Wallace, B., Webster, I., Parslow, J. (2003). The use of mechanistic description of algal growth and zooplankton grazing in an estuarine eutrophication model. *Estuarine, Coastal and Shelf Science*, **56**, 685-695.
- Baretta, J., Ebenhöf, W., Ruardij, P. (1995). The European Region Seas Ecosystem Model, a Complex Marine Ecosystem Model. *The Netherlands Journal of Sea Research*, **33**, 233-246.
- Blackford, J. (2002). The Influence of Microphytobenthos on the Northern Adriatic Ecosystem: A Modelling Study. *Estuarine, Coastal and Shelf Science*, **55**, 109-123.
- Bricker, S., Ferreira, J.G., Simas, T. (2003). An integrated methodology for the assessment of estuarine trophic status. *Ecological Modelling*, **169**, 39-60.
- Caetano, M., Ferreira, J.G., Icely, J., Newton, A., Nunes, J.P., Vale, C. (2002). *Ria Formosa*. In: Gilpin, L., Tett, P. (Eds.) OAERRE Sites Description Report. Napier University, Edinburgh.
- Campolongo, F., Cariboni, J., Saltelli, A. (2007). An effective screening design for sensitivity analysis of large models. *Environmental Modelling and Software*, **22**, 1509-1518.
- Carpenter, J. (1966). New measurements of oxygen solubility in pure and natural water. *Limnology and Oceanography*, **11**, 264-277.
- Cartaxana, P., Mendes, C.R., Van Leeuwe, M.A., Brotas, V. (2006). Comparative study on the microphytobenthic pigments of muddy and sandy intertidal pigments of the Tagus estuary. *Estuarine Coastal and Shelf Science*, **66**, 225-230.
- Cloern, J., Jassby, A. (2008). Complex seasonal patterns at the land-sea interface. *Ecology Letters*, **11**, 1294-1303.
- Cossarini, G., Solidoro, C. (2008). Global sensitivity analysis of a trophodynamic model of the Gulf of Trieste. *Ecological Modelling*, **212**, 16-27.
- Crane, M., Warr, S., Codling, I., Power, B. (2006). *Review of Environmental Quality Standards (EQSs) for Use in Assimilative Capacity Model Development*. Watts & Crane Associates, Faringdon, Oxfordshire.
- Cromey, C.J., Nickell, T.D., Black, K.D. (2002). DEPOMOD - modelling the deposition and biological effects of waste solids from marine cage farms. *Aquaculture*, **214**, 211-239.

- CSTT (Comprehensive Studies Task Team), (1994). *Comprehensive studies for the purposes of Article 6 of DIR 91/271 EEC, the Urban Waste Water Treatment Directive*. Published for the Comprehensive Studies Task Team of Group Coordinating Sea Disposal Monitoring by the Forth River Purification Board, Edinburgh.
- CSTT (Comprehensive Studies Task Team), (1997): *Comprehensive Studies for the Purposes of Article 6 and 8.5 of Directive 91/271 ECC, the Urban Waste Water Treatment Directive*, 2<sup>nd</sup> edn. Report prepared for the UK Urban Waste Water Treatment Directive Implementation Group and Environmental departments by the Group Co-ordinating Sea Disposal Monitoring. UK. Department of the environment for Northern Ireland, the Environment Agency, the Scottish Environment Protection Agency and the Water Services Association. Edinburgh: SEPA. 60 pp.
- Devlin, M., Barry, J., Mills, D., Gowen, R., Foden, J., Sivyer, D., Tett, P. (2008). Relationships between suspended particulate material, light attenuation and sechi disk in UK marine waters. *Estuarine, Coastal and Shelf Science*, **79**, 429-439.
- Di Toro, D. (2001). *Sediment Flux Modeling*. J. Wiley and Sons., New York. 624pp.
- Dring, M.J. (1992). *The Biology of Marine Plants*. Cambridge university Press. 199p.
- Droop, M. (1968). Vitamin B<sub>12</sub> and marine ecology, IV: the kinetics of uptake, growth and inhibition in *Monochrysis lutheri*. *Journal of the Marine Biological Association of the UK*, **48**, 689-733.
- Ebenhöh, W., Kohlmeier, C., Radford, P. (1995). The benthic biological submodel in the European Seas Ecosystem Model. *Netherlands Journal of Sea Research*, **33**, 423-452.
- Ebenhöh, W., Baretta-Bekker, J.G., Baretta, J.W. (1997). The primary production module in the marine ecosystem model ERSEM II, with emphasis on the light forcing. *Journal of Sea Research*, **38**, 173-193.
- Edwards, V. (2001). *The yield of marine phytoplankton chlorophyll from dissolved inorganic nitrogen under eutrophic conditions*. PhD thesis, Napier University, Edinburgh.
- Edwards, V., Tett, P., Jones, K. (2003). Changes in the yield of chlorophyll *a* from dissolved available inorganic nitrogen after an enrichment event – applications for predicting eutrophication in coastal waters. *Continental Shelf Research*, **23**, 1771-1785.
- Edwards, V., Icely, J., Newton, A., Webster, R. (2005). The yield of chlorophyll from nitrogen: a comparison between the shallow Ria Formosa lagoon and the deep oceanic conditions at Sagres along the southern coast of Portugal. *Estuarine Coastal and Shelf Science*, **62**, 391-403.
- Eppley, R., Strickland, D. (1968). Kinetics of marine phytoplankton growth. In: *Advances in the Microbiology of the Sea*. Droop, M., Wood, E., eds, Academic Press, New York, 23-62.
- Eppley, R., Rogers, J., McCarthy, J., 1969. Half saturation constants for uptake of nitrate and ammonium by marine phytoplankton. *Limnology and Oceanography*, **14**, 912-920.
- Eppley, R. (1972). Temperature and phytoplankton growth in the sea. *Fishery Bulletin*, **70**, 1063-1085.
- Falcão, M., Pissarra, J. Cavaco, M. (1991). *Características químico-biológicas da Ria Formosa: análise de um ciclo anual (1985-1986)*. Boletim do Instituto Nacional de Investigação das Pescas, 16, 5-21.
- Falcão, M. (1996). *Dinâmica dos Nutrientes na Ria Formosa: efeitos da interação da laguna com as suas interfaces na reciclagem do azoto, fósforo e sílica*. PhD Thesis. University of Algarve.
- Facca, C., Sfriso, A. (2007). Epipellic diatom spatial and temporal distribution and relationship with the main environmental parameters in coastal waters. *Estuarine Coastal and Shelf Science*, **75**, 35-49.

- Fernandes, T.F., Eleftheriou, A., Ackefors, H., Eleftheriou, M., Ervik, A., Sanchez-Mata, A., Scanlon, T., White, P., Cochrane, S., Pearson, T.H., Read, P.A. (2002). *The Management of the Environmental Impacts of Marine Aquaculture*. Aberdeen, UK: Scottish Executive, ISBN: 0 9532838 8 7.
- Geider, R.J. (1987). Light and temperature dependence of the carbon to chlorophyll a ratio in microalgae and cyanobacteria: Implications for physiology and growth of phytoplankton. *New Phytologist*, **106**, 1-34.
- GESAMP (IMO/FAO/UNESCO-IOC/WMO/WHO/IAEA/UN/UNEP Joint Group of Experts on the Scientific Aspects of Marine Environmental Protection), (1986). *Environmental Capacity: an Approach to Marine Pollution Prevention*. Report of the study GESAMP 30. Rome, Italy: FAO. 49 pp.
- Gowen, R., Tett, P., Jones, K. (1992). Predicting marine eutrophication : the yield of chlorophyll from nitrogen in Scottish coastal phytoplankton. *Marine Ecology Progress Series*, **85**, 153-161.
- IPCC (2007). *Climate Change 2007: The Physical Science Basis*. Contribution of Working Group I to the Fourth Assessment Report of the Intergovernmental Panel on Climate Change [Solomon, S., Qin, D., Manning, M., Chen, Z., Marquis, M., Averyt, K., Tignor, M., Miller, H. (eds.)]. Cambridge University Press. Cambridge, United Kingdom and New York, NY, USA, 996pp.
- Jackson, P., Briggs, K., Flint, R., Holyer, R., Sandidge, J. (2002). Two- and three-dimensional heterogeneity in carbonate sediments using resistivity imaging. *Marine Geology*, **182**, 55-76.
- Jesus, B. (2005). *Ecophysiology and spatial distributin of microphytobenthic biofilms*. PhD Thesis, University of Lisbon, 225pp.
- Jesus, B., Brotas, V., Marani, M., Paterson, D. (2005). Spatial dynamics of microphytobenthos determined by PAM fluorescence. *Estuarine Coastal and Shelf Science*, **65**, 30-42.
- Jørgensen, B., Richardson, K. (1996). *Eutrophication in coastal marine ecosystems*. American Geophysical Union, Coastal and Estuarine Studies 52, Washington, D.C. 273pp.
- Jørgensen, S., Bendoricchio, G. (2001). *Fundamentals of Ecological Modelling*. Third Edition. Elsevier Science, Oxford.530pp.
- Kirk, J. (1994). *Light and photosynthesis in aquatic ecosystems*. 2<sup>nd</sup> Edition. Cambridge University Press. 528pp.
- Kohberger, R., Scavia, D., Wilkinson, J. (1978). A method for parameter sensitivity analysis in differential equation models. *Water Resources Research*, **14**, 25-29.
- Kremer, J., Nixon, S. (1978). *A Coastal Marine Ecosystem*. New York: Springer-Verlag Berlin Heidelberg. 271 pp.
- Laurent, C., Tett, P., Fernandes, T.F., Gilpin, L., Jones, K. (2006). A Simple Assimilative Capacity Model for Fjordic Environments. *Journal of Marine Systems*, **61**, 149-164.
- Lee, J-Y., Tett, P., Kim, K-R. (2003). Parameterising a microplankton model. *Journal of the Korean Society of Oceanography*, **38**, 185-210.
- Liss, P. (1988). Tracers of air-sea gas exchange. *Philosophical Transactions of the Royal Society of London*, **325**, 93–103.
- Magni, P., Montani, S. (2006). Seasonal patterns of pore-water nutrients, benthic chlorophyll a and sedimentary AVS in a macrobenthos-rich tidal flat. *Hydrobiologia*, **571**, 297-311.
- Mann, K., Lazier, J. (1996). *Dynamics of marine ecosystems :biological-physical interaction in the ocean*. 2<sup>nd</sup> edition. Blackwell Science, Oxford, 480 pp.



- Monod, J. (1942). Recherches sur la croissance des cultures bactériennes (Studies on the growth of bacterial cultures), *Actualités Scientifique et Industrielles*, **911**, 1–215.
- Morris, M. (1991). Factorial Sampling Plans for Preliminary Computational Experiments. *Technometrics*, **33**, 161 - 174.
- Mudge, S., Icely, J., Newton, A. (2008). Residence times in a hypersaline lagoon: using salinity as a tracer. *Estuarine, Coastal and Shelf Science*, **77**, 278-284.
- Murray, A., Parslow, J. (1997). *Port Philip Bay Integrated Model: Final Report*. CSIRO Environmental Projects Office, Australia, 215 pp.
- Murray, L., Mudge, S., Newton, A., Icely, J. (2006). The effect of benthic sediments on dissolved nutrient concentrations and fluxes. *Biochemistry*, **81**, 159-178.
- Newton, A., Mudge, S. (2003). Temperature and salinity regimes in a shallow, mesotidal lagoon, the Ria Formosa, Portugal. *Estuarine, Coastal and Shelf Science*, **57**, 73-85.
- Newton, A., Icely, J.D., Falcão, M., Nobre, A., Nunes, J.P., Ferreira, J.G., Vale, C. (2003). Evaluation of the eutrophication in the Ria Formosa coastal lagoon, Portugal. *Continental Shelf Research*, **23**, 1945-1961.
- Newton, A., Mudge, S., 2005. Lagoon-sea exchanges, nutrient dynamics and water quality management of Ria Formosa (Portugal). *Estuarine, Coastal and Shelf Science*, **62**, 405-414.
- Newton, A., Icely, J.D. (2006). Oceanographic Applications to Eutrophication in Tidal, Coastal Lagoons, the Ria Formosa, Portugal. *Journal of Coastal Research*, **SI39**, 1346-1350.
- Nobre, A.M., Ferreira, J.G., Newton, A., Simas, T., Icely, J.D., Neves, R. (2005). Management of coastal eutrophication: Integration of field data, ecosystem-scale simulations and screening models. *Journal of Marine Systems*, **56**, 375-390.
- Oliveira, P. (2005). *Análise e Monitorização do Oxigénio na Ria Formosa*. First Degree Thesis in Oceanography, Algarve University.
- Parsons, T., Maita, Y., Lalli, M. (1984). *A manual of chemical and biological methods for seawater analysis*. 1<sup>st</sup> edition. Pergamon Press, 105 pp.
- Portilla, E., Tett, P., Gillibrand, P., Inall, M. (2009). Description and sensitivity analysis for the LESV model: water quality variables and the balance of organisms in a fjordic region of restricted exchange. *Ecological Modelling*, in press.
- Saltelli, A., Chan, K., Scott, E. (2008). *Sensitivity Analysis*. 1<sup>st</sup> edition, John Wiley and Sons, 475pp.
- Serôdio, J., Silva, J., Catarino, F. (1997). Non destructive tracing of migratory rhythms of intertidal benthic microalgae using in vivo chlorophyll *a* fluorescence. *Journal of Phycology*, **33**, 542-553.
- Serôdio, J., Vieira, S., Cruz, S., Barroso, F. (2005). Short-term variability in the photosynthetic activity of microphytobenthos as detected by measuring rapid light curves using variable fluorescence. *Journal of Marine Biology*, **146**, 903-914.
- Serpa, D., Falcão, M., Duarte, P., Fonseca, L.C., Vale, C. (2007). Evaluation of ammonium and phosphate release from intertidal and subtidal sediments of a shallow coastal lagoon (Ria Formosa – Portugal): a modelling approach. *Biochemistry*, **82**, 291-304.
- Sobral, P. (1995). *Ecophysiology of Ruditapes Decussatus*. New University of Lisbon, PhD Thesis, 187pp.

- Sosik, H., Mitchell, B. (1994). Effects of temperature on growth, light absorption, and quantum yield in *Dunaliella tertiolecta* (Chlorophyceae). *Journal of Phycology*, **30**, 833–840.
- Sundbäck, K., Graneli, W. (1988). Influence of microphytobenthos on nutrient flux between sediment and water: a laboratory study. *Marine Ecology Progress Series*, **43**, 63-69.
- Tett, P. (1990). The Photic Zone. In: *Light and Life in the Sea*, ed. Herring, P.J., Campbell, A.K., Whitfield, M. & Maddock, L., Cambridge University Press, 59-87.
- Tett, P., Walne, A. (1995). Observations and simulations of hydrography, nutrients and plankton in the southern North Sea. *Ophelia*, **42**, 371-416.
- Tett, P., Wilson, H. (2000). From biogeochemical to ecological models of marine microplankton. *Journal of Marine Systems*, **25**, 431-466.
- Tett, P., Gilpin, L., Svendsen, H., Erlandsson, C.P., Larsson, U., Kratzer, S., Fouilland, E., Janzen, C., Lee, J., Grenz, C., Newton, A., Ferreira, J.G., Fernandes, T., Scory, S. (2003). Eutrophication and some European waters of restricted exchange. *Continental Shelf Research*, **23**, 1635-1671.
- Tett, P., Portilla, E., Inall, M., Gillibrand, P., Gubbins, M., Amundrod, T. (2007). *Modelling the Assimilative Capacity of Sea Lochs (Final Report on SARF 012)*. Napier University, 1-29.
- Underwood, G.J.C., Kromkamp, J. (1999). Primary Production by Phytoplankton and Microphytobenthos in Estuaries. *Advances in Ecological Research*, **29**, 93-153.
- Underwood, G., Paterson, D. (2003). The importance of extracellular carbohydrate production by marine epipelagic diatoms. *Advances in Botanical Research*, **40**, 183-240.

## **CHAPTER 8**

---

General Discussion

---

## 8.1 General considerations

The ultimate aim of this research project was to progress towards the development of an assimilative capacity model for the sustainable management of nutrients within the Ria Formosa lagoon. The development of a biogeochemical model is a difficult and complex process. This was done by improving the dynamic version of the CSTT model and by adapting it to the Ria Formosa shallow system. The first natural step to improve the model was the addition of a benthic primary producer – the microphytobenthos (MPB). This component was considered to be key in the dynamics of Ria Formosa by previous studies such as Newton *et al.* (2003) and Tett *et al.* (2003). The estimate of the yield of the microphytobenthos chlorophyll from nitrogen ( $q$ ), carried out in Chapter 6, is novel and was used in this step. Gowen *et al.* (1992) first estimated (*in situ*) and proposed the use of the parameter in the CSTT model. Edwards *et al.* (2003) developed an experimental approach to obtain this estimate. This thesis includes the first application of Edwards' concept to MPB and the first use of a benthic microcosm to estimate  $q$ . Other parameters, associated with the new approach to describe MPB growth, were also used for the first time and were derived from data, such as  $c_3$ , the proportion of MPB chlorophyll on the sediment surface. Through the process of developing the model, important ecological questions were raised, hypotheses tested and new directions for the model were taken. The microphytobenthos was confirmed to be the most important chlorophyll source within the system, when compared to phytoplankton, confirming the initial hypothesis. A key primary productive capacity of the Ria lies in this community of benthic microalgae, which live within the sediment. The importance of the pore water nutrients was also revealed by the model, being essential to support the MPB community. The new approach to describe MPB growth developed in this project is also an important achievement. Only by considering the real fluxes of nutrients and photons it is possible to predict accurately the increase of MPB biomass.

The final stage of this model is able to predict chlorophyll and nutrient concentrations that are correctly within the range of natural variation. However, the model's capacity to simulate temporal variation accurately is less effective. Cloern and Jassby (2008) have reported the absence of repeated temporal patterns of phytoplankton over 150 sites located at land-sea interfaces. They indicate that the interactions between the processes that affect phytoplankton are very complex and unclear. It is very difficult, therefore, to

predict the temporal variation of primary producers at land-sea interfaces. Therefore, despite not providing perfect agreements between model simulations and observations, the dCSTT-MPB model can certainly be used illustratively.

Several specific studies were needed to achieve the main aim of this project, which was the development of a nutrient assimilative capacity model for the sustainable management of nutrients within the Ria Formosa lagoon. These included essential development steps such as the assessment of the optimal methods for the measurement of MPB chlorophyll, as well as, the assessment of temporal variation in nutrients and chlorophyll and the estimation of the yield of benthic chlorophyll from nitrogen. The major aspects of these studies are considered and discussed here.

The development of an optimal methodology for the extraction of microphytobenthic chlorophyll was a crucial step in the development of the subsequent steps, carried out during this project (Chapter 3). Earlier in this project, it was decided that the lack of a standard methodology for chlorophyll extraction was critical and efforts should be made to address this gap. The results presented here indicate that the procedure should be different for muddy and sandy sediments, which may be a consequence of different microphytobenthos assemblages at each sediment type. The objectives of this study were achieved by accepting or rejecting the scientific hypotheses, following the results obtained in the experimental work. Results from this study provide a simple methodology for the assessment of the microphytobenthos chlorophyll stock in the Ria Formosa.

Currently there are also other techniques that allow accurate *in situ* and/or *ex situ* measurements of microphytobenthos chlorophyll from an undisturbed sediment (e.g. Jesus *et al.*, 2005; Serôdio *et al.*, 2005). These techniques are based in the application of a recently developed Pulse Amplitude Modulated (PAM) fluorometry method. This approach was first developed for the study of the physiological status of higher plants and then adapted for phytoplankton and microphytobenthos in the 90's. These techniques allow the evaluation of the very top layer of the sediment, the photic layer, where most of the microphytobenthos community is likely to be (Serôdio *et al.*, 2005). This is important because it allows the measurement of the active chlorophyll, which is nowadays considered to be the proxy of the Photosynthetic Active Biomass (PAB; Guarini *et al.*, 2000). However, for studies like the one presented here, where the focus of interest is the total stock and not the PAB, simple procedures such as the one proposed here are more appropriate as they allow their use for routine monitoring and so

may be more appropriate for use by environmental regulators, as indicators of trophic status. Furthermore, these techniques allow the comparison of results with previous and similar studies (e.g. Brotas *et al.*, 1995; de Jong and de Jonge, 1995; Buffan-Dubau and Carman, 2000).

Knowledge about the temporal, spatial and vertical variability of MPB is also critical for the understanding of the microphytobenthic community itself and also for the adaptation of the model developed here (Chapter 4). Spatial patchiness of microphytobenthos was revealed by the small-scale studies. According to the results presented here, the MPB cells are more widespread in sand than in mud, where they are more aggregated in patches. The studies on spatial variability provide an indication of the appropriateness of the sampling programme. The scientific hypothesis of no spatial differences in terms of the chlorophyll concentration was therefore refuted. It is interesting to note that MPB cells are mainly (40%) found in the top centimetre as previously indicated by Consalvey *et al.* (2005) and Méléder *et al.* (2005). After the first centimetre, the percentage of chlorophyll falls abruptly to smaller values, confirming the initial working hypothesis. Nevertheless, MPB chlorophyll may be found through a profile of 15 cm depth.

The analysis of the total variance revealed that the most important component driving the microphytobenthos variance is the spatial variability. Results from this analysis clearly indicate that the seasonality pattern is so difficult to ‘extract’ from data because it is complex in itself and it is masked by the spatial heterogeneity. The small importance of seasonality (which only explains 5% of the variance) and the large importance of the spatial variability clearly indicate how difficult it is to develop a model that is able to predict accurately the temporal variation of the microphytobenthic chlorophyll without including the complex and unclear interactions which define the spatial distribution of MPB within the sediment. This area would need to be addressed further in the future. The analysis of the MPB temporal pattern by the application of the truncated Fourier series mathematical approach is novel and proved to be a powerful tool for the assessment of the community seasonality. The scientific hypothesis of the existence of a standard temporal pattern considered was therefore tested and could not be rejected.

The assessment of the nutrient and chlorophyll concentrations in the water column and within the sediments allowed the evaluation of the importance of the sediments for this shallow coastal lagoon. As presented and discussed in Chapter 5, the benthic

microphytic system comprises around 99% of the total lagoon chlorophyll (considering only the planktonic and benthic micro primary producers) and approximately 75% of the total nitrogen present in the system. As indicated previously by Falcão (1996), the high pore water nutrient concentrations would result in large fluxes of nutrients from the sediments to the water column. The objectives of this work were achieved here since the importance of the benthic compartment was demonstrated.

The molecular diffusion of nitrogen was estimated as being around  $497 \mu\text{mol.m}^{-2}.\text{h}^{-1}$ , which is similar to the values provided by Murray *et al.* (2006) for Ria Formosa. This value is indicative of the effects that these fluxes may have in the water column, where the concentrations of dissolved available inorganic nitrogen are between 2-3  $\mu\text{M}$  throughout the year. Falcão (1996) estimated the total balance of nutrients in Ria Formosa and showed that the exchange between the sediments and the water column is the principal input of nitrogen into the water column. Nevertheless, nitrogen concentrations in the water column remain relatively low. This fact is likely to be related to the existence of the important communities of benthic microalgae in the sediments that take up large amounts of nutrients to live and grow and also to the high flushing rate.

An improvement of the water quality seems to have occurred in the Ria Formosa lagoon system, compared to the results obtained from measurements done in the past and presented by Newton *et al.* (2003), for example. The increase in seawater exchange due to the opening of a new inlet near the sites studied in this project and also by Newton *et al.* (2003), is likely to be a key factor. Nevertheless, the lagoon seems to act as a source of nutrients, especially considering silicate, to the seawater outside the system. According to the analysis of the N:P and N:Si ratios, the lagoon does not seem to suffer from phosphate or silicate limitation. All the obtained values were below the standard Redfield ratios.

The application of the mathematical approach (truncated Fourier Series) used in Chapter 4 to phytoplankton data from the Ria Formosa revealed a stronger influence of the seasonal variation, when compared to the benthic compartment. The use of 1 to 3 wave-pairs explained around 31% of the variance, which is much higher than the 5% obtained for MPB. Nonetheless, the percentage of the variance explained by the seasonal variation is still low when compared with the seasonality found in more strongly seasonally variable environments, in terms of light, such as Scotland. This was presented and discussed by Tett and Grantham (1980). Moreover, the high frequency

temporal variation (4 to 23 waves) explained a further 30% of the variability. This may indicate that MPB affects chl *a* concentration in the water column, as suggested by Lucas *et al.* (2001) and de Jonge and van Beusekom (1995), for example. Re-suspension of benthic algal cells, which are present in high concentrations, would have an important impact on phytoplankton measurements especially in shallow waters. This is also supported by the significant relationship found between pelagic and benthic chlorophyll, which allows the prediction of pelagic chlorophyll concentrations using MPB data by a multiple regression approach. Recently, Cloern and Jassby (2008) have analysed the seasonal variation of phytoplankton at several sites, with temperate climate, located at the land-sea interface. They indicate the absence of predictable seasonal patterns because of the complexity of interactions existent in these specific sites, which is in accordance with the results presented throughout this project. Despite the interesting results obtained with the application of the truncated Fourier Series, these dynamics should be further investigated in the future using long time-series to confirm what was observed. Nevertheless, the proposed objectives were achieved with the influence of the environmental and biological elements on the temporal variation of microphytobenthos and phytoplankton proposed and discussed.

The results obtained from the microcosms (Chapter 6) revealed much smaller nitrogen fluxes than the ones obtained by applying the Fick's Law of diffusion, as done in Chapter 5. Therefore, the hypothesis of similar estimates provided by these two different approaches was rejected. In these experiments, the fluxes were estimated considering the nutrient changes in the water column. Changes would be a result of the input of nutrients from the reservoir and the input of nutrients from the sediments. No uptake of nutrients should have taken place because the fluxes were assessed in dark conditions, when no algal growth should occur. These results represent the amount of nitrogen that reaches the water column and not only the potential flux that could occur. These fluxes may be more realistic than the ones obtained in Chapter 5 because they consider the natural processes that might occur within the sediments, such as denitrification, which may remove part of the nitrogen from the flux and therefore contribute to a decrease in nitrogen concentration in the water column.

The yield of chlorophyll from nitrogen is considered to be a key parameter in algal growth. Portilla *et al.* (2009) recently described a new dynamic version of the CSTT model for the effects of nutrient enrichment on phytoplankton. The sensitivity analysis of the model showed that the yield was one of the most important factors for the



mathematical simulation of phytoplankton growth using a new version of the dynamic CSTT model (LESV model). It is therefore expected that the same factor would also be important for benthic microalgae. The experiments conducted to evaluate this parameter revealed that the microphytobenthic yield, considering nitrogen as the nutrient, would range from 3.65 to 4.11  $\mu\text{gchl} \cdot (\mu\text{molN})^{-1}$ . These estimated mean values are within the range of values observed by Gowen *et al.* (1992) and Edwards *et al.* (2005) for phytoplankton, but are much higher than the standard value used by them, which was around  $1\mu\text{gchl} \cdot (\mu\text{molN})^{-1}$ , confirming the initial working hypothesis.

The sensitivity analysis of the dCSTT-MPB model has shown that the yield of microphytobenthos chlorophyll from nitrogen was a key and sensitive factor for the model (Chapter 7). In addition, porosity, nutrient recycling rate and MPB loss rate due to grazing were also revealed as key to this model. The assimilative capacity analysis for the Ria Formosa, using the model, indicated that higher land-derived nitrogen inputs, twice the ones existent now, are sufficient to breach a DAIN threshold of  $10\text{ mmol} \cdot \text{m}^{-3}$ . Nevertheless, little response of pelagic algal communities to nutrient enrichment is predicted by the model, indicating that the Ria Formosa system is very resistant (unsensitive) to eutrophying effects of nutrient enrichment, according to the model. A chlorophyll threshold of  $10\text{ mgchl} \cdot \text{m}^{-3}$  was not achieved by increasing the nitrogen input by a factor of 10. The model was also used to explore future possible scenarios, such as climate change, involving the increase of sea level and temperatures. Results from the simulation indicate a decrease in the biomass of the MPB community, which is directly associated with an increase in the nutrient flux from the sediment to the water column and an increase in water column nutrient concentrations.

This study confirmed the importance of the microphytobenthos in this coastal shallow lagoon (Figure 8.1). The nutrient flux from the sediments to the water column is the main source of nitrogen to the pelagic system. The microphytobenthic community has a

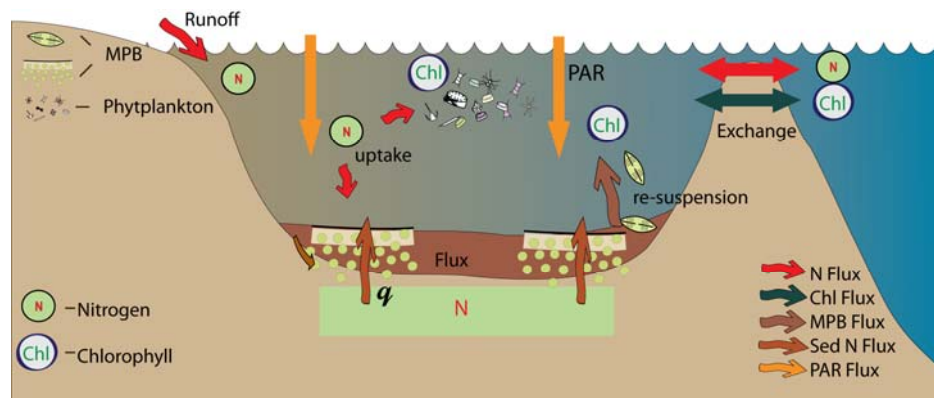


Figure 8.1 - Scheme of the most important fluxes and components of the Ria Formosa system.

key role in intercepting these nutrients, which support the high concentrations of benthic chlorophyll. MPB are also essential, acting as a buffer, and avoiding the increase in nutrient concentrations in the water column. Therefore, healthy MPB communities can be crucial in the prevention of eutrophication. However, if they decay or disappear, the system may be at risk. According to these findings, in the case of a change that affects MPB, the vulnerability to eutrophication of the Ria Formosa lagoon may be high. Moreover, this study also suggested the importance of the MPB resuspension, as discussed previously.

The scientific findings presented here revealed that the ecological quality of complex systems such as Ria Formosa is difficult to evaluate. The importance of the use of integrated assessments is outstanding. The Water Framework Directive (WFD) is a powerful tool for the management of water bodies. However, care has to be taken in the implementation of the Directive. The definition of surface water categories should have an ecological meaning. Ria Formosa is defined as part of coastal waters, which means that its importance as a nursery system for fish communities is not considered. Moreover, the primary production potential of the lagoon system is located mainly in the sediments, as discussed previously. However, according to annex V of the WFD, no monitoring of microphytobenthos and pore water nutrients is expected. It would be important to understand the dynamics of these components. Changes in the nutrient conditions of the lagoon and the algal response to them may be neglected.

## **8.2 Overview and Future studies**

A research project is a dynamic process in which several hypotheses are tested and more are raised from the process itself. The responses to the scientific questions are often partial solutions to ecological problems. Therefore, from this project, several questions remained unanswered and opened new windows for future research. From the methodological studies, it was unclear why two different optimal procedures were derived for sandy and muddy sediments. The available literature has indicated that a difference in the microphytobenthic assemblages could lead to this effect. This should be further investigated. In this project, chlorophyll *a* measurements were done using the spectrophotometry method. However, High Performance Liquid Chromatography (HPLC) pigment analysis could be used in the future to confirm and improve results. HPLC is the only method that really allows the measurement of the pure pigment

chlorophyll *a* and could help bridge the gap between the simple method used in this work and the use of fluorescence probes, as HPLC can show how much of the total extractable pigment is potentially photosynthetically active (ie. is chlorophyll *a* and not chlorophyllides or phaeophorbides).

Further investigation of the environmental factors that influence and drive the microphytobenthic temporal and spatial variability, as well as how these factors interact, is still required. From the scientific literature, it is indicated that the microphytobenthos is affected by a complex interaction of several biotic and abiotic factors. Further experimental work in this area would be key to improve our understanding of microphytobenthos dynamics. The results presented here, especially from the truncated Fourier method, seem to indicate an influence of the tidal cycle on the microphytobenthos dynamics. However, further studies are required, especially on a shorter time scale, to investigate the effects throughout the tidal cycle, which were not covered by this project. This could be done by using modern techniques such as the Pulse Amplitude Modulated (PAM) fluorometry which allows *in situ* studies. This technique may have a key role in the understanding of MPB dynamics at short spatial and temporal scales.

The nutrient fluxes in shallow lagoons such as Ria Formosa have been investigated by several authors. However, large differences up to a factor of 10 are still found, even within the same sites, as discussed previously. The processes involved in the nutrient interactions between sediments and the water column, such as denitrification, have to be clarified so that accurate estimates can be obtained. The incubators used for the experimental design presented in Chapter 6 could be used to investigate denitrification. This could be done by evaluating the fluxes.

The temporal patterns of primary producers in Ria Formosa are still weakly understood and therefore their full prediction not possible at this stage. As discussed by Cloern and Jassby (2008), the dynamics of phytoplankton at the land-sea interface are extremely complex and patterns are not necessarily repeated across different sites and years. This leads to a great difficulty in the development of accurate mathematical models for primary producers, and consequently also for nutrients. Therefore, the investigation and the understanding of these patterns and their causes are essential to improve predictions. Moreover, the inclusion of other components in the model, such as shellfish, macroalgae or seagrasses would be likely to contribute to better predictions or at least to a better understanding of the system.

## **CHAPTER 9**

---

Global Reference List

---

- Aberle-Malzahn, N. (2004). *The microphytobenthos and its role in aquatic food webs*. PhD Thesis. Kiel University.
- Ackleson, S. (2003). Light in shallow waters: a brief research review. *Limnology and Oceanography*, **48**, 323-328.
- Adir, N., Zer, H., Shoshat, S., Ohad, I. (2003). Photoinhibition: A historical perspective. *Photosynthesis Research*, **76**, 343-370.
- Alpine, A., Cloern, J. (1992). Trophic interaction and direct physical effects control phytoplankton biomass and production in an estuary. *Limnology and Oceanography*, **37**, 946-955.
- Alvera-Azcárate, A., Ferreira, J.G., Nunes, J.P. (2003). Modelling eutrophication in mesotidal and macrotidal estuaries. The role of intertidal seaweeds. *Estuarine and Coastal Shelf Science*, **57**, 715-724.
- Ambrose, R., Martin, J., Wool, T. (2006). *WASP7 Benthic Algae -Model Theory and User's Guide*. Environmental Protection Agency, USA, 32pp.
- Amorim-Ferreira, A. (1987). *Contribuição para o estudo do fitoplâncton e microalgas epibênticas em viveiros de amêijoia (Tapes decussatus (L.)) da Ria Formosa*. First degree thesis in Biology, University of Lisbon.
- Anon (1999). *Using Matlab (v.5.2)*. The MathWorks, Inc. Natick, Maryland.
- Asmus, R., Sprung, M., Asmus, H. (2000). Nutrient fluxes in intertidal communities of a South European lagoon (Ria Formosa) – similarities and differences with a northern Wadden Sea bay (Sylt-Rømø Bay). *Hydrobiologia*, **436**, 217-235.
- Azvosky, A., Chertoprod, E., Saburova, M., Polikarpov, I. (2004). Spatio-temporal variability of micro- and meiobenthic communities in a White Sea intertidal sandflat. *Estuarine Coastal and Shelf Science*, **60**, 663-671.
- Bachmann, R., Cloern, J., Heckey, R., Schindler, D. (2006). Eutrophication of freshwater and marine ecosystems. *Limnology and Oceanography*, **51** (1, part 2), 351–800.
- Baird, M., Walker, S., Wallace, B., Webster, I., Parslow, J. (2003). The use of mechanistic description of algal growth and zooplankton grazing in an estuarine eutrophication model. *Estuarine, Coastal and Shelf Science*, **56**, 685-695.
- Baretta, J., Ebenhöh, W., Ruardij, P. (1995). The European Region Seas Ecosystem Model, a Complex Marine Ecosystem Model. *The Netherlands Journal of Sea Research*, **33**, 233-246.
- Baretta-Bekker, J., Baretta, J., Ebenhöh, W. (1997). Microbial dynamics in the marine ecosystem model ERSEM II with decoupled carbon assimilation and nutrient uptake. *Journal of Sea Research*, **38**, 195-211.
- Baric, A., Kuspilic, G., Matijevic, S. (2002). Nutrient (N, P, Si) fluxes between marine sediment and water column in coastal and open Adriatic. *Hydrobiologia*, **475/476**, 151-159.
- Bartoli, M., Nizzoli, D., Viaroli, P. (2003). Microphytobenthos activity and fluxes at the sediment-water interface: interactions and spatial variability. *Aquatic Ecology*, **37**, 341-349.
- Basset, A., Sabetta L., Fonnesu, A., Mouillot, T., Chi, D., Viaroli, P., Giordani, G., Reizopoulou, S., Abbiati, M., Carrada, G. (2006). Typology in Mediterranean transitional waters: new challenges and perspectives. *Aquatic Conservation: Marine and Freshwater Ecosystems*. **16**, 441-455.
- Bernardino, F. (2000). Review of aquaculture development in Portugal. *Journal of Applied Ichthyology*, **16**, 196-199.

- Björk-Ramberg, A. (1985). Uptake of phosphate and inorganic nitrogen by a sediment-algal system in a subarctic lake. *Freshwater biology*, **15**, 175-183.
- Blackford, J. (2002). The influence of microphytobenthos on the Northern Adriatic Ecosystem: A modelling study. *Estuarine Coastal and Shelf Science*, **55**, 109-123.
- Blanchard, G., Paterson, D., Stal, L., Richard, P., Galois, R., Huet, V., Kelly J., Honeywill, C. De brouwer, J., Dyer, K., Christie, M., Seguignes, M. (2000). The effect of geomorphological structures on potential biostabilisation by microphytobenthos on intertidal mudflats. *Continental Shelf Research*, **20**, 1243-1256.
- Borja, A., Franco, J., Perez, V. (2000). A marine biotic index to establish the ecological quality of soft-bottom benthos within European Estuarine and Coastal Environments. *Marine Pollution Bulletin*, **40**, 1100–1114.
- Bowers, D., Harker, G., Smith, P, Tett, P. (2000). Optical properties of a Region of Freshwater Influence (The Clyde Sea). *Estuarine, Coastal and Shelf Science*, **50**, 717-726.
- Bowers, D., Binding, C. (2006). The optical properties of mineral suspended particles: A review and synthesis. *Estuarine, Coastal and Shelf Science*, **67**, 219-230.
- Branco, A., Kremer, J. (2005). The relative importance of chlorophyll and colored dissolved organic matter (CDOM) to the prediction of the diffuse attenuation coefficient in shallow estuaries. *Estuaries*, **28**, 643-652.
- Bricker, S., Clement, C., Pirhalla, D., Orlando, S., Farrow, D. (1999). *National Estuarine Eutrophication Assessment. Effects of Nutrient Enrichment in the Nation's Estuaries*. National ocean Service, Silver Spring, MD, USA, 71 pp.
- Bricker, S., Ferreira, JG., Simas, T. (2003). An integrated methodology for assessment of estuarine trophic status. *Ecological Modelling*, **169**, 39-60.
- Brotas, V., Cabrita, T., Portugal, A., Serôdio, J., Catarino, F. (1995). Spatiotemporal distribution of the microphytobenthos biomass in intertidal flats of Tagus estuary (Portugal). *Hydrobiologia*, **300/301**, 93-104.
- Brotas, V., Plante-Cuny, M. (1998). Spatial and temporal patterns of microphytobenthic taxa of estuarine tidal flats in the Tagus estuary using pigment analysis by HPLC. *Marine Ecology Progress Series*, **171**, 43-57.
- Brotas, V., Plante-Cuny, M. (2003). The use of HPLC pigment analysis to study microphytobenthos communities. *Acta Oecologica*, **24**, S109-S115.
- Buffan-Dubau, E., Carman, K. (2000). Extraction of benthic macroalgal pigments for HPLC analysis. *Marine Ecological Progress Series*, **204**, 203-207.
- Caetano, M., Ferreira, J.G., Icely, J., Newton, A., Nunes, J.P., Vale, C. (2002). *Ria Formosa*. In: Gilpin, L., Tett, P. (Eds.) OAERRE Sites Description Report. Napier University, Edinburgh.
- Cahoon, L. (1999). The role of benthic microalgae in neritic ecosystems. *Oceanography and Marine Biology: an Annual Review*, **37**, 47– 86.
- Campolongo, F., Cariboni, J., Saltelli, A. (2007). An effective screening design for sensitivity analysis of large models. *Environmental Modelling and Software*, **22**, 1509-1518.
- Carpenter, J. (1966). New measurements of oxygen solubility in pure and natural water. *Limnology and Oceanography*, **11**, 264-277.

- Cartaxana, P., Brotas, V. (2003). Effects of extraction on HPLC quantification of major pigments from benthic microalgae. *Archives für Hydrobiologie*, **157**, 339-349.
- Cartaxana, P., Mendes, C.R., Van Leeuwe, M.A., Brotas, V. (2006). Comparative study on the microphytobenthic pigments of muddy and sandy intertidal pigments of the Tagus estuary. *Estuarine, Coastal and Shelf Science*, **66**, 225-230.
- Casas, B., Varela, M., Bode, A. (1999). Seasonal Succession of Phytoplankton species on the coast of A Coruña (Galicia, northwest Spain). *Instituto Español de Oceanografía*, **15**(1-4), 413-429.
- Catford, J., Walsh, C., Beardall, J. (2007). Catchment urbanization increases benthic microalgal biomass in streams under controlled light conditions. *Aquatic Science*, **69**, 511-522.
- Chatfield, C. (1989). *The analysis of Time Series: An introduction*, 4<sup>th</sup> Edition. Chapman & Hall, London.
- C.E.C. (1991). *Council Directive of 21 May 1991 concerning urban wastewater treatment (91/271/EEC)*. Official Journal of the European Communities, L135 of 30.5.91, 40-52.
- C.E.C. (2000). *Council Directive of 23 October 2000, establishing a framework for Community action in the field of water policy (2000/60/EC)*. Official Journal of the European Communities, L327 of 22.12.2000, 1-72.
- Cibic, T., Blasutto, O., Hancke, K., Johnsen, G. (2007). Microphytobenthic species composition, pigment concentration, and primary production in sublittoral sediments of the Trondheimsfjord. *Phycological Society of America*, **43**, 1126-1137.
- Costanza, R. (1992). *Towards an operational definition of health*. In *Ecosystem Health - New Goals for Environmental Management* (eds R. Costanza, B. Norton & B.D. Haskell), pp. 603, 239-256. Inland Press, Washington D.C.
- Costello, J., Chisholm, S. (1981). The influence of cell size on the growth rate of *Thalassiosira weissflogii*. *Journal of Plankton Research*, **3**, 415-419.
- Cloern, J. (2001). Our evolving conceptual model of the coastal eutrophication problem. *Marine Ecology Progress in Series*, **210**, 223-253.
- Cloern, J., Jassby, A. (2008). Complex seasonal patterns at the land-sea interface. *Ecology Letters*, **11**, 1294-1303.
- Colijn, F. (1982). Light absorption in the waters of the Ems-Dollard estuary and its consequences for the growth of phytoplankton and microphytobenthos. *Netherlands Journal of Sea Research*, **15**, 196-216.
- Colijn, F., de Jonge, V. (1984). Primary production of microphytobenthos in the Sem-Dollard estuary. *Marine Ecology Progress Series*, **14**, 185-196.
- Collos, Y., Husseini-Ratrema, J., Bec, B., Váquer, A., Hoai, T., Rougier, C., Pons, V. and Souchu, P. (2005). Pheopigment dynamics, zooplankton grazing rates and the autumnal ammonium peak in a Mediterranean lagoon. *Hydrobiologia* **550**, 83-93.
- Conde, D., Bonilla, S., Aubriot, L., de León, R., Pintos, W. (1999). Comparison of the areal amount of chlorophyll a of planktonic and attached microalgae in a shallow coastal lagoon. *Hydrobiologia*, **408/409**, 285-291.
- Consalvey, M., Perkins, R., Paterson, D., Underwood, G. (2005). PAM Fluorescence: A beginners guide for benthic diatomists. *Diatom Research*, **20**, 1-22.
- Cossarini, G., Solidoro, C. (2008). Global sensitivity analysis of a trophodynamic model of the Gulf of Trieste. *Ecological Modelling*, **212**, 16-27.

- Crane, M., Warr, S., Codling, I., Power, B. (2006). *Review of Environmental Quality Standards (EQSs) for Use in Assimilative Capacity Model Development*. Watts & Crane Associates, Faringdon, Oxfordshire.
- Cromey, C.J., Nickell, T.D., Black, K.D. (2002). DEPOMOD - modelling the deposition and biological effects of waste solids from marine cage farms. *Aquaculture*, **214**, 211-239.
- CSTT (Comprehensive Studies Task Team) (1994). *Comprehensive studies for the purposes of Article 6 of DIR 91/271 EEC, the Urban Waste Water Treatment Directive*. Published for the Comprehensive Studies Task Team of Group Coordinating Sea Disposal Monitoring by the Forth River Purification Board, Edinburgh.
- CSTT (Comprehensive Studies Task Team) (1997). *Comprehensive Studies for the Purposes of Article 6 and 8.5 of Directive 91/271 ECC, the Urban Waste Water Treatment Directive..* Report prepared for the UK Urban Waste Water Treatment Directive Implementation Group and Environmental departments by the Group Co-ordinating Sea Disposal Monitoring, 2<sup>nd</sup> edition, UK. Department of the environment for Northern Ireland, the Environment Agency, the Scottish Environment Protection Agency and the Water Services Association. Edinburgh: SEPA. 60 pp.
- Day, R., Quinn, G. (1989). Comparison of treatments after an analysis of variance in ecology. *Ecological Monographs*, **59**, 433-463.
- De Brouwer, J., Stal, L. (2001). Short-term dynamics in microphytobenthos distribution and associated extracellular carbohydrates in surface sediments of an intertidal mudflat, *Marine Ecology Progress Series*, **218**, 33-44.
- De Brouwer, J., Wolfstein, K., Stal., L. (2002). Physical characterization and diel dynamics of different fractions of extracellular polysaccharides in an axenic culture of a benthic diatom. *European Journal of Phycology*, **37**, 37-44.
- Defew, E., Paterson, D., Hagerthey, S. (2002). The use of natural microphytobenthic assemblages as laboratory model systems. *Marine Ecology Progress Series*, **237**, 15-25.
- DGPA (2008). Direcção Geral das Pescas e Aquicultura. Website: [www.dgpa.min.agricultura.pt](http://www.dgpa.min.agricultura.pt). Consulted on October 2008.
- De Jong, D., de Jonge, V. (1995). Dynamics and distribution of microphytobenthic chlorophyll-a in the western Scheldt estuary (SW Netherlands). *Hydrobiologia*, **311**, 21-30.
- De Jonge, V., van Beusekom, J. (1992). Contribution of resuspended microphytobenthos to total phytoplankton in the Ems Estuary and its possible role for grazers. *Netherlands Journal of Sea Research*, **30**, 91-105.
- De Jonge, V., van Beusekom, J. (1995). Wind- and tide-induced resuspension of sediment and microphytobenthos from tidal flats in the Ems estuary. *Limnology and Oceanography*, **40**, 766-778.
- De Jonge, V., Elliot, M., Orive, E. (2002). Causes, historical development, effects and future challenges of a common environmental problem: eutrophication. *Hydrobiologia*, **475/476**, 1-19.
- De Jonge, Elliott, M., Brauer, V. (2006). Marine Monitoring: Its shortcomings and mismatch with the EU's Water Framework Directive.. *Marine Pollution Bulletin*, **53**, 5-19.
- De Jonge, V. (2007). Toward the application of ecological concepts in the EU coastal water management. *Marine Pollution Bulletin*, **55**, 407-414.



- Devesa, R., Moldes, A., Díaz-Fierros, F., Barral, M. (2007). Extraction study of algal pigments in river bed sediments by applying factorial designs. *Talanta*, **72**, 1546-1551.
- Devlin, M., Barry, J., Mills, D., Gowen, R., Foden, J., Sivyer, D., Tett, P. (2008). Relationships between suspended particulate material, light attenuation and sechi disk in UK marine waters. *Estuarine, Coastal and Shelf Science*, **79**, 429-439.
- Di Toro, D. (2001). *Sediment Flux Modeling*. J. Wiley and Sons., New York. 624pp.
- DRAOT - Direção Regional do Ambiente e do Ordenamento do Território do Algarve (2001). *Dados relativos às cheias ocorridas em 2000/2001 na Região do Algarve*.
- DRAOT - Direção Regional do Ambiente e do Ordenamento do Território do Algarve, Divisão de Monitorização Ambiental (2003). *Recursos Hídricos na Região do Algarve*.
- Dring, M.J. (1992). *The Biology of Marine Plants*. Cambridge university Press. 199p.
- Droop, M. (1968). Vitamin B<sub>12</sub> and marine ecology, IV: the kinetics of uptake, growth and inhibition in *Monochrysis lutheri*. *Journal of the Marine Biological Association of the UK*, **48**, 689-733.
- Easley, J.T., Hymel, S.N., Plante, C.J. (2005). Temporal patterns of benthic microalgal migration on a semi-protected beach. *Estuarine Coastal and Shelf Science*, **64**, 486-496.
- European Communities, 2008. *Commission Decision 2008/915/EC*, Official Journal of the European Communities, **L332**, 20-44.
- Ebenhöh, W., Kohlmeier, C., Radford, P. (1995). The benthic biological submodel in the European Seas Ecosystem Model. *Netherlands Journal of Sea Research*, **33**, 423-452.
- Ebenhöh, W., Baretta-Bekker, J.G., Baretta, J.W. (1997). The primary production module in the marine ecosystem model ERSEM II, with emphasis on the light forcing. *Journal of Sea Research*, **38**, 173-193.
- Edmunds, M., Beardall, J., Hart, S., Elias, J., Stojkovic-Tadic, S. (2004). *Port Phillip Bay Channel Deepening Project. Environmental Effects Statement – Marine Ecology Specialist Studies. Volume 4 : Microphytobenthos*. Australian Marine Ecology Report 161. Melbourne. 45pp.
- Edwards, V. (2001). *The yield of marine phytoplankton chlorophyll from dissolved inorganic nitrogen under eutrophic conditions*. PhD Thesis. Napier University, Edinburgh.
- Edwards, V., Tett, P., Jones, K. (2003). Changes in the yield of chlorophyll *a* from dissolved available inorganic nitrogen after an enrichment event – applications for predicting eutrophication in coastal waters. *Continental Shelf Research*, **23**, 1771-1785.
- Edwards, V., Icelly, J., Newton, A., Webster, R., 2005. The yield of chlorophyll from nitrogen: a comparison between the shallow Ria Formosa and the deep oceanic conditions at Sagres along the southern coast of Portugal. *Estuarine, Coastal and Shelf Science*, **62**, 391-403.
- EEA (1999). *Nutrients in European ecosystems. Topic Report N. 4/1999*. European Environmental Agency, 156pp.
- EEA (2006). *European Environmental Agency – Information for improving Europe's environment*. <http://glossary.eea.europa.eu>. Consulted on October 2006.
- Elliott, M., Burdon, D., Hemingway, K., Apitz, S., 2007. Estuarine, coastal and marine ecosystem restoration: confusing management and science – A revision of concepts. *Estuarine, Coastal and Shelf Science*, **74**, 349-366.
- EPA (2007). *U S environmental Protection Agency*. Website: <http://www.epa.gov/owow/wetlands/vital/protection.html>. Consulted on August 2007

- Eppley, R., Strickland, D. (1968). Kinetics of marine phytoplankton growth. In: *Advances in the Microbiology of the Sea*. Droop, M., Wood, E., eds, Academic Press, New York, 23-62.
- Eppley, R., Rogers, J., McCarthy, J., 1969. Half saturation constants for uptake of nitrate and ammonium by marine phytoplankton. *Limnology and Oceanography*, **14**, 912-920.
- Eppley, R. (1972). Temperature and phytoplankton growth in the sea. *Fishery Bulletin*, **70**, 1063-1085.
- Escaravage, V., Prins, T., Smaal, A., Peeters J. (1996). The response of phytoplankton communities to phosphorus input reduction in mesocosm experiments. *Journal of Experimental Marine Biology and Ecology*, **198**, 55–79.
- Facca, C., Sfriso, A. (2007). Epipelagic diatom spatial and temporal distribution and relationship with the main environmental parameters in coastal waters. *Estuarine Coastal and Shelf Science*, **75**, 35-49.
- Falcão, M., Vale, C. (1990). Study of the Ria Formosa ecosystem: benthic nutrient remineralization and tidal variability of nutrients in the water. *Hydrobiologia*, **207**, 137-146.
- Falcão, M., Pissarra, J. Cavaco, M. (1991). *Características químico-biológicas da Ria Formosa: análise de um ciclo anual (1985-1986)*. Boletim do Instituto Nacional de Investigação das Pescas, 16, 5-21.
- Falcão, M. (1996). *Dinâmica dos Nutrientes na Ria Formosa: efeitos da interação da laguna com as suas interfaces na reciclagem do azoto, fósforo e sílica*. PhD Thesis. University of Algarve.
- Falcão, M., Vale, C. (2003). Nutrient dynamics in a coastal lagoon (Ria Formosa, Portugal): The importance of lagoon–sea water exchanges on the biological productivity. *Ciencias Marinas*, **29**, 425-433.
- Falkowski, P.G., Davis, C.S. (2004) Natural Proportions, *Nature*, **431**, 131.
- Falkowski, P., Raven, J. (2007). *Aquatic Photosynthesis*. 2<sup>nd</sup> Edition. Princeton University Press.
- Fan, C., Glibert, P. (2005). Effects of light on nitrogen and carbon uptake during a *Prorocentrum minimum* bloom. *Harmful Algae*, **4**, 629-641.
- Fasham, M. (1984). *Flows of energy and materials in marine ecosystems: theory and practice*. NATO Scientific Affairs Division [by] Plenum Press.
- Fennel, W., Neumann, T. (2004). *Introduction to the Modelling of Marine Ecosystems*. Elsevier Science and Technology. 230pp.
- Fernandes, T.F., Eleftheriou, A., Ackefors, H., Eleftheriou, M., Ervik, A., Sanchez-Mata, A., Scanlon, T., White, P., Cochrane, S., Pearson, T.H., Read, P.A. (2002). *The Management of the Environmental Impacts of Marine Aquaculture*. Aberdeen, UK: Scottish Executive, ISBN: 0 9532838 8 7.
- Ferreira, J.G., Vale, C., Soares, C.V., Salas, F., Stacey, P.E., Bricker, S.B., Silva, M.C., Marques, J.C. (2007). Monitoring of coastal and transitional waters under the E.U. Water Framework Directive. *Environmental monitoring and assessment*, **135**, 195-216.
- Forja, J., Blasco, J., Gómez-Parra (1994). Spatial and seasonal variation of in situ benthic fluxes in the Bay of Cadiz (South-west Spain). *Estuarine, Coastal and Shelf Science*, **39**, 127-141.
- Fouilland, E., Gosselin, M., Rivkin, R.B., Vasseur, C., Mostajir, B. (2007). Nitrogen uptake by heterotrophic bacteria and phytoplankton in Arctic surface waters. *Journal of Plankton Research*, **29**, 369-376.
- Fowler, C., Cohen, L., Jarvis, P. (1998). *Practical Statistics for Field Biology*, 2<sup>nd</sup> ed. Chichester, New York, Wiley, 260pp.

- Fowler, R. (2006). *Development and testing of benthic pigment analyses*. BSc(Hons) thesis. Napier University, Edinburgh, Scotland.
- Garrigue, C. (1998). Distribution and biomass of microphytes measured by benthic chlorophyll a in a tropical lagoon. *Hydrobiologia*, **385**, 1-10.
- Geider, R.J. (1987). Light and temperature dependence of the carbon to chlorophyll a ratio in microalgae and cyanobacteria: Implications for physiology and growth of phytoplankton. *New Phytologist*, **106**, 1-34.
- Geider, R., MacIntyre, H., Kana, T. (1997). Dynamic model of phytoplankton growth and acclimation: responses of the balanced growth rate and the chlorophyll a:carbon ratio to light, nutrient limitation and temperature. *Marine Ecology Progress Series*, **148**, 187-200.
- GESAMP (IMO/FAO/UNESCO-IOC/WMO/WHO/IAEA/UN/UNEP Joint Group of Experts on the Scientific Aspects of Marine Environmental Protection), (1986). *Environmental Capacity: an Approach to Marine Pollution Prevention*. Report of the study GESAMP 30. Rome, Italy: FAO. 49 pp.
- Gillibrand, P., Turrell, W. (1997). The use of simple models in the regulation of the impact of fish farms on water quality in Scottish sea lochs. *Aquaculture*, **159**, 33 – 46
- Glibert, P.M. (1982). Regional studies of daily, seasonal and size fraction variability in ammonium remineralisation. *Marine Biology*, **70**, 209-220.
- Gowen, R., Tett, P., Jones, K. (1992). Predicting marine eutrophication: the yield of chlorophyll from nitrogen in Scottish coastal waters. *Marine Ecology Progress Series*, **85**, 153-161.
- Goela, P. (2005). *Plano Teórico de Monitorização da Ria Formosa segundo a Directiva Quadro da Água*. Thesis of Chemistry, Algarve University.
- Göncü, I., Wolflin, J. (2005). *Coastal lagoons: ecosystem processes and modeling for sustainable use and development*. CRC Press. 500pp.
- Granéli, E., Olsson, P., Carlsson, P., Granéli, W., Nylander, C. (1993). Weak “Top-down” control of dinoflagellate growth in the coastal Skagerrat. *Journal of Plankton Research*, **15**, 213-237.
- Grasshoff, K., Ehrhardt, M., Kremling, K. (1983). *Methods of seawater analysis*. Verlag Chemie, Weinheim, 419pp.
- Gray, J., Elliott, M. (2009). *Ecology of Marine Sediments*. 2<sup>nd</sup> Edition. Oxford University Press, 225pp.
- Grinham, A., Carruthers, T., Fisher, P., Udy, J., Dinnison, W. (2007). Accurately measuring the abundance of benthic microalgae in spatially variable habitats. *Limnology and Oceanography: Methods*, **5**, 119-125.
- Guarini, J.M., Blanchard, G.F., Bacher, C., Gros, P., Riera, P., Richard, P., Gouleau, D., Galois, R., Prou, J., Sauriau, P.G. (1998). Dynamics of spatial patterns of microphytobenthic biomass: inferences from a geostatistical analysis of two comprehensive surveys in Marennes-Oléron Bay (France): results from a geostatistical approach. *Marine Ecology Progress Series*, **166**, 131-141.
- Guarini, J.M., Blanchard, G.F., Gros, P. (2000). Quantification of the microphytobenthic primary production in European intertidal mudflats – a modelling approach. *Continental Shelf Research*, **20**, 1771-1788.
- Guillard, R., Ryther, J. (1962). Studies of marine planktonic diatoms. I. *Cyclotella nana* Hustedt and *Detonula confervacea* Cleve. *Canadian Journal of Microbiology*, **8**, 229-239.
- Guillard, R.R.L. (1975). Culture of phytoplankton for feeding marine invertebrates. pp 26-60. In: Smith, W., Chanley, M. (eds.) *Culture of Marine Invertebrate Animals*. Plenum Press, New York, USA.

- Hagerthey, S., Louda, G., Mongkronsri, P. (2006). Evaluation of Pigments extraction methods and a recommended protocol for periphyton chlorophyll a determination and chemotaxonomic assessment. *Journal of Phycology*, **42**, 1125-1136.
- Hall, D., Rao, K. (1999). *Photosynthesis (Studies in Biology)*. 6<sup>th</sup> Edition. Cambridge University Press, 214pp.
- Hedtkamp, S. (2005). *Shallow subtidal sand: permeability, nutrient dynamics, microphytobenthos and organic matter*. PhD Dissertation. Kiel University, Germany.
- HELCOM (2005). *Minutes of the first meeting of the project 'Development of tools for the thematic eutrophication assessment (HELCOM EUTRO)*, 26–27 January 2005, Helsinki, 21 pp.
- Hein, M., Pedersen, M., Sand-Jensen, K. (1995). Size-dependent nitrogen uptake in micro- and macroalgae. *Marine Ecology Progress Series*, **118**, 247–253.
- Heiskanen, A., van de Bund, W., Cardoso A.C., Nõges, P., 2004. Towards good ecological status of surface waters in Europe – interpretation and harmonisation of the concept. *Water Science and Technology*, **49**, 169-177.
- Hickman, C., Roberts, L., Larson, A. (2001). *Integrated principles of zoology*, 11<sup>th</sup> edition. McGraw- Hill. 897pp.
- Holme, N., McIntyre, D.A. (1984). *Methods for the study of Marine Benthos*. 2<sup>nd</sup> edition. Ed ISP Handbook 16. Blackwell Scientific Publications, 387 pp.
- Hopkinson, C., Giblin, A., Tucker, J., Garritt, R. (1999). Benthic metabolism and nutrient cycling along an estuarine salinity gradient. *Estuaries*, **22**, 863-881.
- Howarth, R., Marino, R. (2006). Nitrogen as the limiting nutrient for eutrophication in coastal marine ecosystem: Evolving views over three decades. *Limnology and Oceanography*, **51**, 364-376.
- ICN (2007). *Instituto da Conservação da Natureza, Parque Natural da Ria Formosa*. <http://www.icn.pt> . Consulted October 2007.
- Instituto Hidrográfico (1981). *Roteiro da Costa do Algarve*, Lisboa, Instituto Hidrográfico, 141 pp.
- Instituto Hidrográfico (1986). *Marés 81/82 Ria de Faro. Estudo das marés de oito estações da Ria de Faro*. Lisboa, Instituto Hidrográfico, (Rel.FT-MC-4/86), 13pp.
- IPCC (2007). *Climate Change 2007: The Physical Science Basis*. Contribution of Working Group I to the Fourth Assessment Report of the Intergovernmental Panel on Climate Change [Solomon, S., Qin, D., Manning, M., Chen, Z., Marquis, M., Averyt, K., Tignor, M., Miller, H. (eds.)]. Cambridge University Press. Cambridge, United Kingdom and New York, NY, USA, 996pp.
- Irigoién, X., Castel, J. (1997). Light limitation and chlorophyll distribution in a highly turbid estuary: the Gironde (SW France). *Estuarine Coastal and Shelf Science*, **44**, 507-517.
- Jackson, P., Briggs, K., Flint, R., Holyer, R., Sandidge J. (2002). Two- and three-dimensional heterogeneity in carbonate sediments using resistivity imaging. *Marine Geology*, **182**, 55-76.
- Jago, C., Jones, S.E., Latter, R.J., McCandliss, R.R., Hearn, M.R., Howarth, M.J. (2002). Resuspension of benthic fluff by tidal currents in deep stratified waters, northern North Sea. *Journal of Sea Research*, **4**, 259-269.
- Jeffrey, S., Mantoura, R., Wright, S., eds. (1997). *Phytoplankton pigments in oceanography: guidelines to modern methods*. UNESCO, Paris, 661pp.

- Jensen, J.P., Pederson, A.R., Jeppesen, E., Søndergaard, M. (2006). An empirical model describing the seasonal dynamics of phosphorus in 16 shallow eutrophic lakes after external loading reduction. *Limnology and Oceanography*, **51**, 791-800.
- Jesus, B. (2005). *Ecophysiology and spatial distribution of microphytobenthic biofilms*. PhD Thesis, University of Lisbon, 225pp.
- Jesus, B., Brotas, V., Marani, M., Paterson, D. (2005). Spatial dynamics of microphytobenthos determined by PAM fluorescence. *Estuarine and Coastal Shelf Science*, **65**, 30-42
- Joint Nature Conservation Committee (2007). Website: <http://www.jncc.gov.uk/>. Consulted on November 2007.
- Jones, K.J., Tett, P., Wallis, A.C., Wood, B.J.B. (1978). Investigation of a nutrient-growth model using a continuous culture of natural phytoplankton. *Journal of the Marine Biological Association of the United Kingdom* **58**, 923-941.
- Jørgensen, B., Richardson, K. (1996). *Eutrophication in coastal marine ecosystems*. American Geophysical Union, Coastal and Estuarine Studies 52, Washington, D.C. 273pp.
- Jørgensen, S., Bendoricchio, G. (2001). *Fundamentals of Ecological Modelling*. Third Edition. Elsevier Science, Oxford. 530pp.
- Karr, E., Sattley, M., Jung, D., Madigan, M., Achenbach, L. (2003). Remarkable Diversity of the phototrophic Purple Bacteria in a Permanently Frozen Antarctic Lake. *Applied and Environmental Microbiology*, **69**(8), 4910-4914.
- Kemp, W., Sampou, P., Caffrey, J., Mayer, M. (1990). Ammonium recycling versus denitrification in Chesapeake Bay sediment. *Limnology and Oceanography*, **35**(7), 1545.
- Kerr, R. (2008). Global warming throws some curves in the Atlantic Ocean. *Science*, **322**, 515.
- Kim, H., Hwang, S., Shin, J., An, K., Yoon, C.G. (2007). Effects of limiting nutrients and N:P ratios on the phytoplankton growth in a shallow hypertrophic reservoir. *Hydrobiologia*, **581**, 255-267.
- Kirk, J. (1994). *Light and Photosynthesis in Aquatic Ecosystems*. 2<sup>nd</sup> Edition. Cambridge University Press, 528pp.
- Koh, C., Khim, J., Araki, H., Yamanishi, H., Mogi, H., Koga, K. (2006). Tidal resuspension of microphytobenthic chlorophyll a in a Nanaura mudflat, Saga, Ariake Sea, Japan: flood-ebb and spring-neap variations. *Marine Ecology Progress Series*, **312**, 85-100.
- Koh, C., Khim, J., Araki, H., Yamanishi, H., Koga, K. (2007). Within-day and seasonal patterns of microphytobenthos biomass determined by co-measurements of sediment and water column chlorophylls in the intertidal mudflat of Nanaura Sea, Ariake Sea, Japan. *Estuarine, Coastal and Shelf Science*, **72**, 42-52.
- Kohberger, R., Scavia, D., Wilkinson, J. (1978). A method for parameter sensitivity analysis in differential equation models. *Water Resources Research*, **14**, 25-29.
- Kostoglidis, A., Pattiaratchi, C., Hamilton, D. (2005). CDOM and its contribution to the underwater light climate of a shallow, microtidal estuary in south-western Australia. *Estuarine, Coastal and Shelf Science*, **63**, 469-477.
- Kremer, J., Nixon, S. (1978). *A Coastal Marine Ecosystem*. New York: Springer-Verlag Berlin Heidelberg. 271 pp.

- Kromkamp, J., Barranguet, C., Peene, J. (1998). Determination of microphytobenthos PSII quantum efficiency and photosynthetic activity by means of variable chlorophyll fluorescence. *Marine Ecology Progress Series*, **162**, 45-55.
- Lane, R., Day, J., Justic, D., Reyes, E., Marx, B., Day, J., Hyfield, E. (2004). Changes in the stoichiometric Si, N and P ratios of Mississippi River water diverted through coastal wetlands to the Gulf of Mexico. *Estuarine, Coastal and Shelf Science*, **60**, 1-10.
- Laurent, C., Tett, P., Fernandes, T.F., Gilpin, L., Jones, K. (2006). A Simple Assimilative Capacity Model for Fjordic Environments. *Journal of Marine Systems*, **61**, 149-164.
- Lee, J-Y., Tett, P., Jones, K., Jones, S., Luyten, P., Smith, C., Wild-Allen, K. (2002). The PROWQM physical-biological model with benthic-pelagic coupling applied to the northern North Sea. *Journal of Sea Research*, **48**, 287-331.
- Lee, J-Y., Tett, P., Kim, K-R. (2003). Parameterising a microplankton model. *Journal of the Korean Society of Oceanography*, **38**, 185-210.
- Legendre, L., Rassoulzadegan, F. (1995). Plankton and nutrient dynamics in marine waters. *Ophelia*, **41**, 153-172.
- Lerat, Y., Lasserre, P., Corre, P. (1990). Seasonal changes in pore water concentrations of nutrients and their diffusive fluxes at the sediment-water interface. *Journal of Experimental Marine Biology and Ecology*, **135**, 135-160.
- Li, W., Lewis, M., Harrison, W. (2008). Multiscalarity of the nutrient-chlorophyll relationship in coastal phytoplankton. *Estuaries and Coasts*, doi:10.1007/s12237-008-9119-7.
- Lima, C., Vale, C. (1980). *Alguns dados físicos, químicos e bacteriológicos sobre a Ria Formosa*. *Boletim do instituto Nacional de Investigação das Pescas*, 5-25pp.
- Liss, P. (1988). Tracers of air-sea gas exchange. *Philosophical Transactions of the Royal Society of London*, **325**, 93-103.
- Lloret, J., Marín, A., Marín-Guirao, L. (2008). Is coastal lagoon eutrophication likely to be aggravated by global climate change? *Estuarine, Coastal and Shelf Science*, **78**, 403-412.
- Lorenzen, G. (1967). Determination of chlorophyll and phaeopigments: spectrophotometric equations. *Limnology and Oceanography*, **12**, 343-346.
- Loureiro, S., Newton, A., Icery, J. (2005). Microplankton composition, production and upwelling dynamics in Sagres (SW Portugal) during the summer of 2001. *Scientia Marina*, **69**, 323-341.
- Loureiro, S., Newton, A., Icery, J. (2006). Boundary conditions for the European Water Framework Directive in the Ria Formosa lagoon, Portugal (physico-chemical and phytoplankton quality elements). *Estuarine, Coastal and Shelf Science*, **67**, 382-398.
- Loureiro, S., Newton, A., Icery, J. (2008). Enrichment experiments and primary production at Sagres (SW Portugal). *Journal of Experimental Marine Biology and Ecology*, **359**, 118-125.
- Lucas, C., Banham, C., Holligan, P. (2001). Benthic-pelagic Exchange of microalgae at a tidal flat, taxonomic analysis. *Marine Ecology Progress Series*, **212**, 39-52.
- Lund-Hansen, L. (2004). Diffuse attenuation coefficients  $K_d$  (PAR) at the estuarine North Sea-Baltic Sea transition: time-series, partitioning, absorption and scattering. *Estuarine, Coastal and Shelf Science*, **61**, 251-259.

- Lundkvist, M., Gangelhof, U., Lunding, J., Flindt, M. (2007). Production and fate of extracellular polymeric substances produced by benthic diatoms and bacteria: A laboratory study. *Estuarine, Coastal and Shelf Science*, **75**, 337-346.
- MacIntyre, H., Geider, R., Miller, D. (1996). Microphytobenthos: the ecological role of the “secret garden” of unvegetated shallow-water marine habitats. I. Distribution, abundance and primary production. *Estuaries*, **19**, 186-201.
- Mackinney, G. (1941). Absorption of light by chlorophyll solutions. *Journal of Biological Chemistry*, **140**, 315-322.
- Magni, P., Montani, S. (2006). Seasonal patterns of pore-water nutrients, benthic chlorophyll *a* and sedimentary AVS in a macrobenthos-rich tidal flat. *Hydrobiologia*, **571**, 297-311.
- Mann, K., Lazier, J. (1996). *Dynamics of marine ecosystems :biological-physical interaction in the ocean*. 2<sup>nd</sup> edition. Blackwell Science, Oxford, 480 pp.
- Margulies, M. (1970). Changes in absorbance spectrum of the diatom *Phaeodactylum tricornutum* upon modification of protein structure. *Journal of Phycology*, **6**, 160-164.
- Marker, A. (1972). The use of acetone and methanol in the estimation of chlorophyll in the presence of pheophytin. *Freshwater Biology*, **2**, 361-385.
- Martins-Loução, M.A. (2003). *Fragmentos em Ecologia*. Faculdade de Ciências da Universidade de Lisboa. Escolar Editora.
- McLusky, D.S., Elliott, M. (2004). *The Estuarine Ecosystem: ecology, threats and management*. Third edition. Oxford University Press, Oxford, 214pp.
- McLusky, D.S., Elliott, M. (2007). Transitional water : A new approach, semantics or just muddying the waters? *Estuarine, Coastal and Shelf Science*, **71**, 359-363.
- Méléder, V., Barillé, L., Rincé, Y., Morançais, M., Rosa, P., Gaudin, P. (2005). Spatio-temporal changes in microphytobenthos structure by pigment composition in a macrotidal flat (Bourgneuf Bay, France). *Marine Ecology Progress Series*, **297**, 83-99.
- Méléder, V., Rincé, Y., Barillé, L., Gaudin, P., Rosa, P. (2007). Spatiotemporal changes in microphytobenthos assemblages in a macrotidal flat (Bourgneuf Bay, France). *Journal of Phycology*, **43**, 1177-1190.
- Mendonça, A. (2001). *Simulação da hidrodinâmica de maré na Ria Formosa com um modelo de elementos finitos*. Relatório de apresentação do tema do trabalho de fim de curso, Instituto Superior Técnico.
- Migné, A., Spilmont, M., Davoult, D. (2004). In situ measurements of benthic primary production during emersion: seasonal variations and annual production in the Bay of Somme (eastern English Channel, France). *Continental Shelf Research*, **24**, 1437-1449.
- Miles, A., Sundbäck, K. (2000). Diel variation in microphytobenthic productivity in areas of different tidal amplitude. *Marine Ecological Progress Series*, **205**, 11-22.
- Mills, M., Ridame, C., Davey, M., La Roche, J., Geider, R. (2004). Iron and phosphorus co-limit nitrogen fixation in the eastern tropical North Atlantic. *Nature*, **429**, 292-294.
- Mitbavkar, S., Anil, A. (2005). Diatoms of the microphytobenthic community in a tropical intertidal sand flat influenced by monsoons: spatial and temporal variations. *Marine Biology*, **148**, 693-709.

- Monod, J. (1942). Recherches sur la croissance des cultures bactériennes (Studies on the growth of bacterial cultures), *Actualités Scientifique et Industrielles*, **911**, 1–215.
- Monte-Luna, d., Brook, P., Zetina-Rejón, M., Cruz-Escalona, H. (2004). The carrying capacity of ecosystems. *Global Ecology and Biogeography*, **13**, 485–495.
- Morris, M. (1991). Factorial Sampling Plans for Preliminary Computational Experiments. *Technometrics*, **33**, 161 - 174.
- Morris, E. (2005). *Quantifying Primary Production of Microphytobenthos: Application of optical methods*. PhD Thesis. Rijksuniversiteit Groningen, Groningen.
- Mudge, S., Icelly, J., Newton, A. (2007). Oxygen depletion in relation to water residence times. *Journal of Environmental Monitoring*, **9**, 1194-1198.
- Mudge, S., Icelly, J., Newton, A. (2008). Residence times in a hypersaline lagoon: using salinity as a tracer. *Estuarine, Coastal and Shelf Science*, **77**, 278-284.
- Murray, A., Parslow, J. (1997). *Port Philip Bay Integrated Model: Final Report*. CSIRO Environmental Projects Office, Australia, 215 pp.
- Murray, L., Mudge, S., Newton, A., Icelly, J. (2006). The effect of benthic sediments on dissolved nutrient concentrations and fluxes. *Biochemistry*, **81**, 159-178.
- Neil, M. (2005). A method to determine which nutrient is limiting for plant growth in estuaries waters – at any salinity, *Marine Pollution Bulletin*, **50**, 945-955.
- Newton, A., Mudge, S. (2003). Temperature and Salinity regimes in a shallow, mesotidal lagoon, the Ria Formosa, Portugal. *Estuarine Coastal and Shelf Science*, **57**, 73-85.
- Newton, A., Icelly, J.D., Falcão, M., Nobre, A., Nunes, J.P., Ferreira, J.G., Vale, C. (2003). Evaluation of the eutrophication in the Ria Formosa coastal lagoon, Portugal. *Continental Shelf Research*, **23**, 1945-1961.
- Newton, A., Mudge, S. (2005). Lagoon-sea exchanges, nutrient dynamics and water quality management of Ria Formosa (Portugal). *Estuarine Coastal and Shelf Science*, **62**, 405-414.
- Newton, A., Icelly, J.D. (2006). Oceanographic Applications to Eutrophication in Tidal, Coastal Lagoons, the Ria Formosa, Portugal. *Journal of Coastal Research*, **SI39**, 1346-1350.
- Nielson, B., Cronin, L. (1981). *Estuaries and Nutrients*. Humana Press, Totowa.
- Nixon, S. (1995). Coastal marine eutrophication: a definition, social causes, and future concerns. *Ophelia*, **41**, 199-219.
- Nobre, A.M., Ferreira, J.G., Newton, A., Simas, T., Icelly, J.D., Neves, R. (2005). Management of coastal eutrophication: Integration of field data, ecosystem-scale simulations and screening models. *Journal of Marine Systems*, **56**, 375-390.
- Nybakken, J.W. (1997). *Marine Biology: An Ecological Approach*, 4th ed. New York: Harper & Row, Publishers, 481pp.
- Obrador, B., Pretus, J. (2008). Light regime and components of turbidity in a Mediterranean coastal lagoon. *Estuarine, Coastal and Shelf Science*, **77**, 123-133.
- Officer, C., Ryther, J. (1980). The possible importance of silicon in marine eutrophication. *Marine Ecology Progress Series*, **3**, 83.
- Oliveira, P. (2005). *Análise e Monitorização do Oxigénio na Ria Formosa*. First Degree Thesis in Oceanography, Algarve University.



- OSPAR (2001). *Draft Common Assessment Criteria and their Application within the Comprehensive Procedure of the Common Procedure*. Meeting of the Eutrophication Task Group, London, 9-11 October 2001, Annex5. Ospam Convention For The Protection of The Marine Environment of The North-East Atlantic.
- OSPAR Commission, 2005. *Common procedure for the identification of the eutrophication status of the OSPAR marine area*, OSPAR Convention for the protection of the marine environment of the north-east Atlantic, 36pp.
- Painting, S.J., Devlin, M.J., Rogers, S.I., Mills, D.K., Parker, E.R., & Rees, H.L. (2005). Assessing the suitability of OSPAR EcoQOs for eutrophication vs ICES criteria for England and Wales. *Marine Pollution Bulletin*, **50**, 1569-1584.
- Papista, E., Ásc, E., Böddi, B. (2002). Chlorophyll-a determination with ethanol – a critical test. *Hydrobiologia*, **485**, 191-198.
- Parsons, T., Maita, Y., Lalli, M. (1984). *A manual of chemical and biological methods for seawater analysis*. 1<sup>st</sup> edition. Pergamon Press, 105 pp.
- Paterson, D.M., Tolhurst, T., Kelly, J., Honeywill, C., de Deckere, E., Huet, V., Shayler, S., Black, K., de Brouwer, J., Davidson, I. (2000). Variations in the sediment properties Skeffling mudflat, Humber Estuary, UK. *Continental Shelf Research*, **20**, 1373-1396.
- Perkins, R., Honeywill, C., Consalvey, M., Austin, H., Tolhurst, T., Paterson, D. (2003). Changes in microphytobenthic chlorophyll *a* and EPS resulting from sediment compaction due to de-watering: opposing patterns in concentration and content. *Continental Shelf Research*, **23**, 575-586.
- Porra, R., Scheer, H. (2000). <sup>18</sup>O and mass spectrometry in chlorophyll research: Derivation and loss of oxygen atoms at the periphery of the chlorophyll macrocycle during biosynthesis, degradation and adaptation. *Photosynthesis Research*, **66**, 159-175.
- Porra, R. (2002). The chequered history of the development and use of simultaneous equations for the accurate determination of chlorophylls *a* and *b*. *Photosynthesis Research*, **73**, 149-156.
- Portilla, E., Tett, P., Gillibrand, P., Inall, M. (2009). Description and sensitivity analysis for the LESV model: water quality variables and the balance of organisms in a fjordic region of restricted exchange. *Ecological Modelling*, in press.
- Press, F., Siever, R. (2000). *Understanding Earth*, 3<sup>rd</sup> edition. W.H. Freeman and Company. 573 pp.
- Rabalais, N., Atilla, N., Normandeau, C., Turner, R.E. (2004). Ecosystem history of Mississippi River-influenced continental shelf revealed through preserved phytoplankton pigments. *Marine Pollution Bulletin*, **49**, 537-547.
- Raven, P., Evert, R., Eichhorn, S. (1999). *Biology of Plants*, 6<sup>th</sup> Edition. W.H. Freeman and Company. 944pp.
- Redfield, A., Ketchum, B., Richards, F. (1963). *The influence of organisms on the composition of seawater*. In M. N. Hill [ed.], *The sea*, v. 2. Interscience.
- Reuss, N., Conley, D., Bianchi, T. (2005). Preservation conditions and the use of sediment pigments as a tool for recent ecological reconstruction in four Northern European estuaries. *Marine Chemistry*, **95**, 283-302.

- Riaux-Gobin, C., Bourgoin, P. (2002). Microphytobenthos biomass at Kerguelen's Land (Subantarctic Indian Ocean): repartition and variability during austral summers. *Journal of Marine Systems*, **32**, 295-306.
- Ribeiro, J., Monteiro, C., Monteiro, P., Bentes, L., Coelho, R., Gonçalves, J., Lino, P., Erzini, K. (2008). Long-term changes in fish communities of the Ria Formosa coastal lagoon (southern Portugal) based on two studies made 20 years apart. *Estuarine, Coastal and Shelf Science*, **76**, 57-68.
- Riley, G. (1946). Factors controlling phytoplankton populations on Georges Bank. *Journal of Marine Research*, **6**, 54-73.
- Ritchie, R. (2006). Consistent sets of spectrophotometric chlorophyll equations for acetone, methanol and ethanol solvents. *Photosynthesis Research*, **89**, 27-41.
- Richie, R. (2008). Universal chlorophyll equations for estimating chlorophylls *a,b,c* and *d* and total chlorophylls in natural assemblages of photosynthetic organisms using acetone, methanol or ethanol solvents. *Photosynthetica*, **46**, 115-126.
- Rodrigues, A. (2004). *Plano de Ordenamento do Parque Natural da Ria Formosa - Estudos de Caracterização*, Volume I. ICN – Instituto da Conservação da Natureza.
- Rosenberg, G., Ramus J. (1984). Uptake of inorganic nitrogen and seaweed surface area : volume ratios. *Aquatic Botany*, **19**, 65-72.
- Rowan, K. (1989). *Photosynthetic pigments of algae*. Cambridge University Press, Cambridge.
- Sartory, D., Globbelaar, J. (1984). Extraction of chlorophyll *a* from freshwater phytoplankton for spectrophotometric analysis. *Hydrobiologia*, **144**, 177-187.
- Saltelli, A., Chan, K., Scott, E. (2008). *Sensitivity Analysis*. 1<sup>st</sup> edition, John Wiley and Sons, 475pp.
- Santos, M., Monteiro, C. (1997). The Olhão artificial reef system (south Portugal): Fish assemblages and fishing yield. *Fisheries Research*, **30**, 33-41.
- Schagerl, M., Künzl, G. (2007). Chlorophyll *a* extraction from freshwater algae – a reevaluation. *Biologia*, **62**, 270-275.
- Schumann, R., Häubner, N., Klausch, S., Karsten, U. (2005). Chlorophyll extraction methods for the quantification of green microalgae colonizing building facades. *International Biodeterioration and biodegradation*, **55**, 213-222.
- Schindler, D. (2006). Recent advances in the understanding and management of eutrophication. *Limnology and Oceanography*, **51**, 356- 363.
- Seitzinger, S. (1988). Denitrification in freshwater and coastal marine ecosystems: Ecological and geochemical significance. *Limnology and Oceanography*, **33**, 702 – 724.
- Serpa, D. (2005). Macroalgae (*Enteromorpha spp.* And *ulva spp.*) Primary productivity in the Ria Formosa lagoon. MSc thesis, New University Of Lisbon, 75 pp.
- Serpa, D., Falcão, M., Duarte, P., Fonseca, L.C., Vale, C. (2007). Evaluation of ammonium and phosphate release from intertidal and subtidal sediments of a shallow coastal lagoon (Ria Formosa – Portugal): a modelling approach. *Biochemistry*, **82**, 291-304.
- Serôdio, J., Silva, J., Catarino, F. (1997). Non destructive tracing of migratory rhythms of intertidal benthic microalgae using in vivo chlorophyll *a* fluorescence. *Journal of Phycology*, **33**, 542-553.
- Serôdio, J., Catarino, F. (1999). Fortnightly light and temperature variability in estuarine intertidal sediments and implications microphytobenthos primary production. *Aquatic Ecology*, **33**, 235-241.

- Serôdio, J., Marques, J., Catarino, F. (2001). Use of in vivo chlorophyll *a* fluorescence to quantify short-term variations in the productive biomass of intertidal microphytobenthos. *Marine Ecology Progress Series*, **218**, 45-61.
- Serôdio, J., Vieira, S., Cruz, S., Barroso, F. (2005). Short-term variability in the photosynthetic activity of microphytobenthos as detected by measuring rapid light curves using variable fluorescence. *Journal of Marine Biology*, **146**, 903-914.
- Seuront, L., Spilmont, N. (2002). Self-organized critically in intertidal microphytobenthos patch patterns. *Physica A*, **313**, 513-539.
- Shaffer, G., Onuf, C. (1985). Reducing the error in estimating annual production of benthic microflora: hourly to monthly rates, patchiness in space and time. *Marine Ecology Progress Series*, **26**, 221-231.
- Smith, V. (2006). Responses of estuarine and coastal marine phytoplankton to nitrogen and phosphorus enrichment. *Limnology and Oceanography*, **51** (1 part 2), 377-384.
- SNIRH (2008). *Sistema Nacional de informação de Recursos Hídricos*. Available: <http://snirh.inag.pt/>. Consulted on October 2008.
- Sobral, P. (1995). *Ecophysiology of Ruditapes Decussatus*. New University of Lisbon, PhD Thesis, 187pp.
- Sosik, H., Mitchell, B. (1994). Effects of temperature on growth, light absorption, and quantum yield in *Dunaliella tertiolecta* (Chlorophyceae). *Journal of Phycology*, **30**, 833-840.
- Stigebrandt, A. (2001). FJORDENV—a water quality model for fjords and other inshore waters. Report C40. Earth Sciences Centre, Göteborg University, Göteborg.
- Strickland, J., Parsons, T. (1972). *A practical handbook of Seawater Analysis*, 2<sup>nd</sup> edition, Journal of Fisheries Research. Board of Canada. 311 pp.
- Summerhayes, C.P., Thorpe, S.A. (1996). *Oceanography: An illustrated guide*. Manson Publishing, London. 352pp.
- Sun, M., Lee, C., Aller, R. (1993a). Anoxic and oxic degradation of <sup>14</sup>C-labeled chloropigments and a <sup>14</sup>C-labeled diatom in Long Island Sound sediments. *Limnology and Oceanography*, **38**, 1438-1451.
- Sun, M., Lee, C., Aller, R. (1993b). Laboratory studies of oxic and anoxic degradation of chlorophyll-a in Long Island Sound sediments. *Geochimica et Cosmochimica Acta*, **57**, 147-157.
- Sun, M., Aller, R., Lee, C. (1994). Spatial and temporal distributions of sedimentary chloropigments as indicators of benthic processes in Long Island Sound. *Journal of Marine Research*, **52**, 149-176.
- Sundbäck, K., Graneli, W. (1988). Influence of microphytobenthos on nutrient flux between sediment and water: a laboratory study. *Marine Ecology Progress Series*, **43**, 63-69.
- Sundbäck, K., Miles, A., Göransson, E. (2000). Nitrogen fluxes, denitrification and the role of microphytobenthos in microtidal shallow-water sediments: an annual study. *Marine Ecology Progress Series*, **200**, 59-76.
- Tada, K., Yamaguchi, H., Montani, S. (2004). Comparison of Chlorophyll *a* Concentrations Obtained with 90% Acetone and N, N-dimethylformamide Extraction in Coastal Seawater. *Journal of Oceanography*, **60**, 259-261.
- Taylor, D., Nixon, S., Granger, S., Buckley, B., McMahon, J., Lin, H. (1995a). Responses of coastal lagoon plant communities to different forms of nutrient enrichment- a mesocosm experiment. *Aquatic Botany*, **52**, 19-34.

- Taylor, D., Nixon, S., Granger, S., Buckley, B. (1995b). Nutrient limitation and the eutrophication of coastal lagoons. *Marine Ecology Progress Series*, **127**, 235-244.
- Tett, P., Kelly, M. G., Hornberger, G. (1975). A Method for the spectrophotometric measurement of chlorophyll *a* and pheophytin *a* in benthic microalgae. *Limnology and Oceanography*, **20**, 887-896
- Tett, P., Kelly, M., Hornberger, G. (1977). Estimation of chlorophyll *a* in methanol. *Limnology and Oceanography*, **20**, 579-580.
- Tett, P., Gallegos, C., Kelly, M., Hornberger, G., Cosby, B (1978). Relationships among substrate, flow, and benthic microalgal pigment density in the Mechums River, Virginia. *Limnology and Oceanography*, **23**, 785-797.
- Tett, P., Grantham, B. (1980). Variability in sea-loch phytoplankton. *Fjord Oceanography*, ed. Freeland, D.H., Farmer, D.M. & Levings, C.D., Plenum, New York, 435-438.
- Tett, P., Heaney, S., Droop, M.R. (1985). The redfield ration and phytoplankton growth rate. *Journal of Marine Biology Association*, **65**, 487-504.
- Tett, P. (1990). The Photic Zone. In: *Light and Life in the Sea*, ed. Herring, P.J., Campbell, A.K., Whitfield, M. & Maddock, L., Cambridge University Press, 59-87.
- Tett, P., Walne, A. (1995). Observations and simulations of hydrography, nutrients and plankton in the southern North Sea. *Ophelia*, **42**, 371-416.
- Tett, P., Wilson, H. (2000). From biochemical to ecological models of marine microplankton. *Journal of Marine Systems*, **25**, 431-446.
- Tett, P., Gilpin, L., Svendsen, H., Erlandsson, C.P., Larsson, U., Kratzer, S., Fouilland, E., Janzen, C., Lee, J., Grenz, C., Newton, A., Ferreira, J.G., Fernandes, T., Scory, S. (2003). Eutrophication and some European waters of restricted exchange. *Continental Shelf Research*, **23**, 1635-1671.
- Tett, P., Lee, J-Y. (2005). N:Si ratios and the 'balance of organisms': PROWQM simulations of the northern North Sea. *Journal of Sea Research*, **54**, 70-91.
- Tett, P., Portilla, E., Inall, M., Gillibrand, P., Gubbins, M., Amundrod, T. (2007a). *Modelling the Assimilative Capacity of Sea Lochs (Final Report on SARF 012)*. Napier University, 1-29.
- Tett, P., Gowen, R., Mills, D., Fernandes, T., Gilpin, L., Huxham, M., Kennington, K., Read, P., Service, M., Wilkinson, M., Malcom, S. (2007b). Defining and detecting undesirable disturbance in the context of marine eutrophication. *Marine Pollution Bulletin*, **55**, 1-6.
- Thronsen, J., Hasle, G.R., Tangen, K. (2007). *Phytoplankton of Norwegian Coastal Waters*. 1<sup>st</sup> Edition, Almatel Forlag AS, 341pp.
- Tolhurst, T., Jesus, B., Brotas, V., Paterson, D. (2003). Diatom migration and sediment armouring – an example from the Tagus Estuary, Portugal. *Hydrobiologia* **503**, 183-193.
- Tonolla, M., Peduzzi, R., Hahn, D. (2005). Long Term Population Dynamics of Phototrophic Sulfur Bacteria in the Chemocline of Lake Cadagno, Switzerland. *Applied and Environmental Microbiology*, **71** (7), 3544-3550.
- Yallop, M., De Winder, B., Paterson, D., Stal, L. (1994). Comparative structure, primary production and biogenic stabilization of cohesive and non-cohesive marine sediments inhabited by microphytobenthos. *Estuarine, Coastal and Shelf Science*, **39**, 565 - 582.

- Underwood, G., Paterson, D. (1993). Seasonal changes in diatom biomass, sediment stability and biogenic stabilisation in the Severn Estuary, UK. *Journal of the Marine Biological Association of the United Kingdom*, **73**, 871-8879.
- Underwood, G.J.C., Kromkamp, J. (1999). Primary Production by Phytoplankton and Microphytobenthos in Estuaries. *Advances in Ecological Research*, **29**, 93-153.
- Underwood, G., Paterson, D. (2003). The importance of extracellular carbohydrate production by marine epipelagic diatoms. *Advances in Botanical Research*, **40**, 183-240.
- Underwood, G.J.C., Perkins, R.G., Consalvey, M.C., Hanlon, A.R.M., Oxborough, K., Baker, N.R., Paterson, D.M. (2005). Patterns in microphytobenthic primary productivity: Species-specific variation in migratory rhythms and photosynthetic efficiency in mixed-species biofilms. *Limnology and Oceanography*, **50**(3), 755-767.
- Van Leeuwe, M.A., Morgan, G., Brockmann, C. (2002). HIMOM – A system of Hierarchical Monitoring Methods for assessing changes in the biological and physical state of intertidal areas – Book of protocols.
- Van Leeuwe, M., Villerius, L., Roggeveld, J., Visser, R., Stefels, J. (2006). An optimized method for automated analysis of algal pigments by HPLC. *Marine Chemistry*, **102**, 267-275.
- Verhulst, P.F., (1838). Notice sur la loi que la population poursuit dans son accroissement. *Correspondance mathématique et physique*, **10**, 113–121.
- Wasmund, N., Topp, I., Schories, D. (2006). Optimising the storage and extraction of chlorophyll samples. *Oceanologia*, **48**, 125-144.
- Wayland, D., Megson, D.P., Mudge, S., Icely, J., Newton, A. (2008). Identifying the source of nutrient contamination in a lagoon system. *Environmental Forensics*, **9**, 231-239.
- Williams, P.J., Thomas, D.N., Reynolds, C.S. (2002). Phytoplankton Productivity: Carbon assimilation in marine and freshwater ecosystems. Blakwell Publishing
- Wiltshire, K. H. B., M., Möller, A., Buhtz, H. (2000). Extraction of pigments and fatty acids from the green alga *Scenedesmus obliquus* (Chlorophyceae). *Aquatic Ecology*, **34**, 119-126.
- Winkler, L.W. (1888). Die Bestimmung des in Wasser gelosten Sauerstoffes. *Berichte der Deutschen Chemischen Gesellschaft*, **21**, 2842-2855.
- Yoshiyama, k., Sharp, J. (2006). Phytoplankton response to nutrient enrichment in an urbanized estuary. Apparent inhibition of primary production by overeutrophication. *Limnology and Oceanography*, **51**, 424-434.

---

## **Appendixes**

---

# **Appendix I**

---

Additional information for Chapter 5

---

The appendix I is divided in two parts. The first covers the detection and quantification limits and an example of a calibration curve used for nutrient analysis. The second is composed by script files which were used to treat data from the Li-Cor Underwater Spherical Quantum Sensor. The scripts allowed the verification of data and the determination of the diffuse attenuation coefficient ( $K_d$ ).

## First part

Limits of detection and quantification were calculated according to the Portuguese recommendations for good laboratory practices, described in the 'Relacre' guide (Table I.1). The limits using were calculated using a series of blanks, in this case 30, measured throughout the period of work and in an independent way. The equations used were:

$$LD= X_0+K.\sigma_0 \quad LQ= X_0+10.\sigma_0$$

$X_0$  is the mean of the blanks,  $\sigma_0$  is the standard deviation associated to  $X_0$ .  $K$  is a constant that depends on the confidence level of a Gaussian distribution of errors. In this case, the value used was 3.3, correspondent to a confidence level of 99.7%.

Table I.1 – Limits of Detection and Quantification of the analysis.

<b>Nutrient</b>	<b>Mean (x)</b>	<b>Standard deviation (st)</b>	<b>Limit of Detection</b>	<b>Limit of Quantification</b>
<b>Ammonium</b>	0.0017	0.0041	0.0153	0.0428
<b>Nitrite</b>	-0.0002	0.0025	0.0080	0.0248
<b>Nitrate</b>	0.0011	0.0038	0.0136	0.0388
<b>Phosphate</b>	0.0006	0.0015	0.0054	0.0152
<b>Silicate</b>	0.0005	0.0020	0.0071	0.0205

A calibration curve was determined for all the analyses performed. The nutrient concentrations involved in the calibration curve are always adjusted to the range of



concentrations found previously in the field. An example of calibration curve for nitrite is given in table I.2. The correspondent equation and  $R^2$  are given in Figure I.1.

**Table I.2 – Absorbance value vs nitrite concentrations.**

<b>Concentrations Nitrite</b>	<b>Abs</b>
0	0
0	0.002
0	0.001
0.1	0.028
0.1	0.028
0.1	0.028
0.25	0.063
0.25	0.063
0.25	0.061
0.5	0.126
0.5	0.127
0.5	0.126
1	0.252
1	0.256
1	0.256

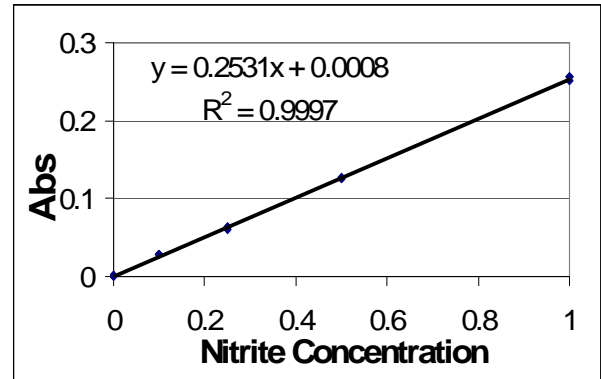


Figure I.1 – Calibration curve, equation and  $R^2$  measured values for nitrite

## Second part

To determine the  $K_d$  values from data collected by the two-bulb light sensor, the scripts UWLight0.m and UWLight1.m were used. The first is useful to check if the input data is correct. If everything is working properly in this script, then the second one is used. The script UWLight1.m gives an output plot showing the mean  $K_d$  values found for each cast.

First script – UWLight0.m

```
% script UWLight0
% checks data for UWLight1
% PT, 16 June 07
%
clear all;% all variables
close all;% figure windows
%
prog_name='UWLight0';
%
dfn='Ramal15.txt';% default file name
```

```

defPontop=1;% normal - PAR1 on top of PAR2
defsepd=0.75;% metres separation between sensors
defP2above=0.5; % second sensor above depth sensor, m
%
% set current working directory
cd('/SeShaT/Edinburgh - Napier/PhD/KdMeter Matlab scripts');% for
Mac OSX
% cd('C:\MATLABR11\PT-ENV');%or some such - for Windows
%
fprintf('\n%s\n', '-----');
fprintf('%s\n', strcat([prog_name ' started at: ' datestr(now)]));
fprintf('%s\n', ...
        'Outputs selected data for 1 lifeform OR species at a time');
fprintf('%s\n', 'abort with ctrl-C, ctrl-break or <apple>-<.>');
fprintf('%s\n\n', strcat(['Current directory is ' pwd]));
%
% request name and read data file, which must be in current directory
fprintf('\n');
tfname=input(strcat(...
             ['Enter data file name, <RET> or just <RET> for default [' ...
             dfname ']: ']), 's');
if isempty(tfname), tfname=dfname; end
% sensor configuration
fprintf('%s\n', ...
        'PAR sensor configuration; 1 for PAR1 on top, 2 for PAR2 --');
Pontop=input(strcat(['PAR sensor on top [' ...
                    num2str(defPontop) ' ] :']));
if isempty(Pontop), Pontop=defPontop; end
fprintf('%s\n', ...
        'Enter parameter values; <RET> alone gives default --');
sepd=input(strcat(['Sensor separation [' ...
                  num2str(defsepd) ' m ] :']));
if isempty(sepd), sepd=defsepd; end
P2above=input(strcat(['Bottom sensor above CTD, [' ...
                    num2str(defP2above) ' , m ] :']));
if isempty(P2above), P2above=defP2above; end
% load file and put data into columns
Idata=load(tfname);
depth=Idata(:,2);
time=Idata(:,8);
% find maximum depth for time split
btime=max(time(depth==max(depth)));% want one value only!
timedown=time(time<btime);
timeup=time(time>btime);
maxdepth=max(depth);
fprintf('\n\n%s', strcat(['Greatest (raw) depth of CTD was ' ...
                        num2str(maxdepth) ' m']));
depthdown=depth(time<btime);
depthup=depth(time>btime);
if Pontop<1.5,
    PARTopdown=Idata(time<btime,3);
    PARbotdown=Idata(time<btime,4);
    PARTopup=Idata(time>btime,3);
    PARbotup=Idata(time>btime,4);
else % sensors have been swapped, so
    PARTopdown=Idata(time<btime,4);
    PARbotdown=Idata(time<btime,3);
    PARTopup=Idata(time>btime,4);
    PARbotup=Idata(time>btime,3);
end
% calculate calibration values for this cast
endtime=max(time);% seconds
decktime=endtime-10;

```

```

decktime2=endtime-3;
endtimeindex=time>decktime1 & time<decktime2;
zdeck=mean(depth(endtimeindex));
fprintf('\n%s',...
    strcat(['CTD depth reading in air was ' num2str(zdeck) ' m']));
if zdeck >0, mess='I.e., slightly under the water surface';
else mess='I.e. slightly above the water surface'; end
fprintf('\n%s', mess);
if Pontop<1.5,
    PARTopend=mean(Idata(endtimeindex,3));
    PARbotend=mean(Idata(endtimeindex,4));
else
    PARTopend=mean(Idata(endtimeindex,4));
    PARbotend=mean(Idata(endtimeindex,3));
end
P1P2=PARTopend/PARbotend;
fprintf('\n%s',...
    strcat(['PARTop/PARbot in air was ' num2str(P1P2) ' m']));
NS=length(depth(endtimeindex));
fprintf('\n%s\n',...
    strcat(['Number of samples : ' num2str(NS) '.']));
%
% diagrams =====
%
fprintf('\n%s', 'Starting to plot part 1 .....');
subplot(2,1,1);% depth against time
plot(time, -(depth-P2above-sepd), 'r.', ...
    time, -(depth-P2above), 'b.', time, -depth, 'k. ');
hold on
plot([decktime1 decktime1],ylim, 'k-', ...
    [decktime2 decktime2],ylim, 'k-');
grid on;
if Pontop<1.5,
    mess1='PARTop P1'; mess2='PARbot P2';
else
    mess1='PARTop P2'; mess2='PARbot P1';
end
xlabel('time, s');
ylabel('raw depth, m');
title(strcat(['Data source:' tfn ]), 'FontWeight', 'bold');
legend(mess1, mess2, 'CTD', 'Location', 'SouthEast');
%
fprintf('\n%s\n', 'Starting to plot part 2 .....');
subplot(2,1,2); % PAR against time
semilogy(timedown, PARTopdown, 'rv', timedown, PARbotdown, 'bv' );
hold on
semilogy(timeup, PARTopup, 'r^', timeup, PARbotup, 'b^' );
plot([decktime1 decktime1],ylim, 'k-', ...
    [decktime2 decktime2],ylim, 'k-');
grid on;
xlabel('time, s');
ylabel('log(PAR)');
title(strcat(['plotted by ' prog_name ' on ' date ';' ]));
legend('top-down', 'bot-down', 'top-up', 'bot-up',...
    'Location', 'SouthEast');
%
%
fprintf('\n%s\n', '*****');
fprintf('%s\n', strcat(['End of ' prog_name ' at: ' datestr(now)]));
fprintf('%s\n\n', '*****');
%
%end

```

## Second script – UWLight1.m

```

% script UWLight1
% processes output from AFBI Kd meter
% this version assumes all data either numeric or starts with '%'
% PT, 6-15 June 07
%
clear all;% all variables
close all;% figure windows
%
prog_name='UWLight1';
%
dfn='Ponte02.txt';% default file name
%
defsepd=0.75;% metres separation between sensors
defP1P2=1.2;% on deck ratio of top to bottom PAR sensor outputs
defP2above=0.5;% second sensor above depth sensor, m
defzdeck=0.2;% depth (m) reading on deck (depth increasing
positive)
odstart=0.5;% ignore downcast data from shallower optical depth
odstop=0.1;% ignore upcast data from shallower optical depth
odstep=0.5;% extract Kd statistics for these od increments
defPontop=1;% normal - PAR1 on top of PAR2
% set [default] output type; alternatives are 'ai', 'ps', 'pdf'
pt='pdf';% set defpt for default and then query
%
% set current working directory
cd('/SeShaT/Edinburgh - Napier/PhD/Kd meter MATLAB scripts');% for
Mac OSX
% cd('C:\MATLABR11\PT-ENV');%or some such - for Windows
%
fprintf('\n%s\n', '-----');
fprintf('%s\n', strcat([prog_name ' started at: ' datestr(now)]));
fprintf('%s\n', ...
'Outputs selected data for 1 lifeform OR species at a time');
fprintf('%s\n', 'abort with ctrl-C, ctrl-break or <apple>-<.>');
fprintf('%s\n\n', strcat(['Current directory is ' pwd]));
%
% set parameters
fprintf('%s\n', ...
'Enter parameter values; <RET> alone gives default --');
zdeck=input(strcat(['On-deck CTD depth reading [' ...
num2str(defzdeck) ', m] :']));
if isempty(zdeck), zdeck=defzdeck; end
fprintf('%s\n', ...
'PAR sensor configuration; 1 for PAR1 on top, 2 for PAR2 --');
Pontop=input(strcat(['PAR sensor on top [' ...
num2str(defPontop) '] :']));
if isempty(Pontop), Pontop=defPontop; end
% this value merely acts on data columns
sepd=input(strcat(['Sensor separation [' ...
num2str(defsepd) ' m] :']));
if isempty(sepd), sepd=defsepd; end
P2above=input(strcat(['Bottom sensor above CTD, [' ...
num2str(defP2above) ', m] :']));
if isempty(P2above), P2above=defP2above; end
P1P2=input(strcat(['On-deck ratio top:bottom PAR [' ...
num2str(defP1P2) '] :']));
if isempty(P1P2), P1P2=defP1P2; end
%
zcorrKd=P2above+sepd/2;

```

```

zcorrstop=P2above+sepd;
%
% request name and read data file, which must be in current directory
fprintf('\n');
tf=input(strcat(...
    ['Enter data file name, <RET> or just <RET> for default [' ...
    dfn ': ']),'s');

if isempty(tf), tf=dfn; end
Idata=load(tf);
time=Idata(:,8);
depth=Idata(:,2)-zdeck;% corrected
% find maximum depth for time split
btime=max(time(depth==max(depth)));% want one value only!
fprintf('\n%s',...
    strcat(['Greatest depth of CTD was ' num2str(max(depth)) '
m']));
depthdown=depth(time<btime);
depthup=depth(time>btime);
% get the PAR data and calculate some Kds
% assume that all downcast samples have both sensors in water
% but some upcast samples taken with one or two sensors in air
if Pontop<1.5,
    PARTopdown=Idata(time<btime,3);
    PARbotdown=Idata(time<btime,4);
    PARTopup=Idata(time>btime,3);
    PARbotup=Idata(time>btime,4);
else % sensors have been swapped, so
    PARTopdown=Idata(time<btime,4);
    PARbotdown=Idata(time<btime,3);
    PARTopup=Idata(time>btime,4);
    PARbotup=Idata(time>btime,3);
end
Kd12down=-log((PARbotdown*P1P2)./PARTopdown)/sepd;
PARTopupwater=PARTopup(depthup>zcorrstop);
PARbotupwater=PARbotup(depthup>zcorrstop);
Kd12up=-log((PARbotupwater*P1P2)./PARTopupwater)/sepd;
meanKd=mean([Kd12down; Kd12up]);
odmax=round(meanKd*max(depth));
% now calculate for down-cast
rowdown=ceil(2*(odmax-odstart));
bestKddown=zeros(rowdown,3);
regKddown=zeros(rowdown,4);
regdowntop=zeros(rowdown,4);
regdownbot=zeros(rowdown,4);
od=odstart;
fprintf('\n%s', 'Processing downcast ...');
while od<odmax,
    % start with bottom sensor odstart below surface
    ztop=od/meanKd+P2above;
    zbot=(od+odstep)/meanKd+P2above;
    odi=round((od-odstart)/odstep)+1;
    fprintf('%s', strcat(num2str(odi),'...'));
    whichdepth=depthdown>=ztop & depthdown<=zbot;
    % get the Kd12 and depths within this od range, and find median
Kd12
    Kd12downlocal=Kd12down(whichdepth);
    bestKddown(odi,:)= [ztop zbot median(Kd12downlocal)];
    % regression (Down, ln(PAR) on depth -----
    depthdownlocal=depthdown(whichdepth);
    PARbotdownlocal=PARbotdown(whichdepth);
    PARTopdownlocal=PARTopdown(whichdepth);
    if (max(depthdownlocal)-
min(depthdownlocal))*meanKd>(odstep/3),

```

```

        pPb=polyfit(-depthdownlocal, log(PARbotdownlocal), 1);
        pPt=polyfit(-depthdownlocal, log(PARtopdownlocal), 1);
        regKddown(odi,:)=[ztop zbot pPb(1) pPt(1)];% for Kd
        regdowntop(odi,:)=...
        [ztop zbot exp(pPt(2)-pPt(1)*ztop) exp(pPt(2)-
pPt(1)*zbot)];
        regdownbot(odi,:)=...
        [ztop zbot exp(pPb(2)-pPb(1)*ztop) exp(pPb(2)-
pPb(1)*zbot)];
        else
            regKddown(odi,:)=[ztop zbot NaN NaN];
            regdowntop(odi,:)=[ztop zbot NaN NaN];
            regdownbot(odi,:)=[ztop zbot NaN NaN];
        end % of regression -----
        od=od+odstep;
    end
% now calculate for upcast
    rowup=ceil(2*(odmax-odstop));
    bestKdup=zeros(rowup,3);
    regKdup=zeros(rowup,4);
    reguptop=zeros(rowup,4);
    regupbot=zeros(rowup,4);
    od=odstop;
    fprintf('\n%s', 'Processing upcast ...');
    while od<odmax,
        % stop with bottom sensor just below surface
        ztop=od/meanKd+P2above;
        zbot=(od+odstep)/meanKd+P2above;
        odi=round((od-odstop)/odstep)+1;
        fprintf('%s', strcat(num2str(odi),'...'));
        whichdepth=(depthup>=ztop & depthup<=zbot);
        whichdepthwater=...
            (depthup>=ztop & depthup<=zbot & depthup>zcorrtop);
        % get the Kd12 and depths within this od range, and find median
Kd12
        Kd12uplocal=Kd12up(whichdepthwater);
        bestKdup(odi,:)=[ztop zbot median(Kd12uplocal)];
        % regression (Up, ln(PAR) on depth -----
        depthuplocal=depthup(whichdepth);
        PARbotuplocal=PARbotup(whichdepth);
        PARTopuplocal=PARTopup(whichdepth);
        if (max(depthuplocal)-min(depthuplocal))*meanKd>(odstep/3),
            pPb=polyfit(-depthuplocal, log(PARbotuplocal), 1);
            pPt=polyfit(-depthuplocal, log(PARTopuplocal), 1);
            regKdup(odi,:)=[ztop zbot pPb(1) pPt(1)];
            reguptop(odi,:)=...
            [ztop zbot exp(pPt(2)-pPt(1)*ztop) exp(pPt(2)-
pPt(1)*zbot)];
            regupbot(odi,:)=...
            [ztop zbot exp(pPb(2)-pPb(1)*ztop) exp(pPb(2)-
pPb(1)*zbot)];
        else
            regKdup(odi,:)=[ztop zbot NaN NaN];
            reguptop(odi,:)=[ztop zbot NaN NaN];
            regupbot(odi,:)=[ztop zbot NaN NaN];
        end % of regression -----
        od=od+odstep;
    end
%
% diagrams =====
%
    fprintf('\n%s', 'Starting to plot part 1 .....');
    subplot(2,1,1);% PAR against depth

```

```

semilogx(PARtopdown, -(depthdown-zcorrtop), 'rv',...
        PARbotdown, -(depthdown-P2above), 'bv' );
hold on
semilogx(PARtopup, -(depthup-zcorrtop), 'r^',...
        PARbotup, -(depthup-P2above), 'b^' );
% for downcast PAR/depth
od=odstart;
while od<odmax,
    odi=round((od-odstart)/odstep)+1;
    X1=[regdowntop(odi,3) regdowntop(odi,4)];
    Y1=[regdowntop(odi,1) regdowntop(odi,2)]-zcorrtop;
    if min(Y1)>0,
        semilogx(X1,-Y1, 'r-', 'Linewidth', 1);
    end % otherwise, don't plot values from air
    X1=[regdownbot(odi,3) regdownbot(odi,4)];
    Y1=[regdownbot(odi,1) regdownbot(odi,2)]-P2above;
    if min(Y1)>0,
        semilogx(X1,-Y1, 'b-', 'Linewidth', 1);
    end % otherwise, don't plot values from air
    od=od+odstep;
end
% for upcast PAR/depth
od=odstop;
while od<odmax,
    odi=round((od-odstop)/odstep)+1;
    X1=[reguptop(odi,3) reguptop(odi,4)];
    Y1=[reguptop(odi,1) reguptop(odi,2)]-zcorrtop;
    if min(Y1)>0,
        semilogx(X1,-Y1, 'r--', 'Linewidth', 1);
    end % otherwise, don't plot values from air
    X1=[regupbot(odi,3) regupbot(odi,4)];
    Y1=[regupbot(odi,1) regupbot(odi,2)]-P2above;
    if min(Y1)>0,
        semilogx(X1,-Y1, 'b--', 'Linewidth', 1);
    end % otherwise, don't plot values from air
    od=od+odstep;
end
% add the labels and parameter values
grid on;
xlabel('ln(PAR) with fitted line segments for PAR (upcast
dashed)');
ylabel('corr. depth, m');
title(strcat(['Data source:' tfn ]), 'FontWeight', 'bold');
legend('top-down', 'bot-down', 'top-up', 'bot-up',...
        'Location', 'SouthEast');
Xt=1.1*min(xlim);
Yt=max(ylim)-min(ylim);
if Pontop<1.5, mess='PAR1 on top'; else mess='PAR2 on top'; end
text(Xt, max(ylim)-0.1*Yt, mess);
text(Xt, max(ylim)- 0.2*Yt, ...
    strcat(['PARTop-Parbot ' num2str(sepd) ' m']));
text(Xt, max(ylim)- 0.3*Yt, ...
    strcat(['Parbot-CTD ' num2str(P2above) ' m']));
text(Xt, max(ylim)- 0.4*Yt, ...
    strcat(['CTD in air reads ' num2str(zdeck) ' m']));
text(Xt, max(ylim)- 0.5*Yt, ...
    strcat(['Top:bot PAR in air ' num2str(P1P2)]));
%
fprintf('\n%s\n', 'Starting to plot part 2 .....');
subplot(2,1,2); % Kd against depth, ignoring air values
plot(Kd12down, -(depthdown-zcorrKd), 'kv');
hold on
plot(Kd12up, -(depthup(depthup>zcorrtop)-zcorrKd), 'k^');

```

```

if meanKd>0, xlim([0 2.0*meanKd]); end
    % otherwise errors - don't constrain
grid on;
xlabel ...
('K_{d}, m^{-1}: ratio (black); PAR slope (colour); upcast dashed');
ylabel('corr. depth, m');
title(strcat(['plotted by ' prog_name ' on ' date ';'']));
% for downcast Kd estimates
od=odstart;
while od<odmax,
    odi=round((od-odstart)/odstep)+1;
    X1=[bestKddown(odi,3) bestKddown(odi,3)];
    Y1=[bestKddown(odi,1) bestKddown(odi,2)]-zcorrKd;
    if min(Y1)>0,
        plot(X1,-Y1, 'k-', 'Linewidth', 2);
    end % otherwise, don't plot values from air
    X1=[regKddown(odi,3) regKddown(odi,3)];
    Y1=[regKddown(odi,1) regKddown(odi,2)]-P2above;
    if min(Y1)>0,
        plot(X1,-Y1, 'b-', 'Linewidth', 2);
    end % otherwise, don't plot values from air
    X1=[regKddown(odi,4) regKddown(odi,4)];
    Y1=Y1-sepd;
    if min(Y1)>0,
        plot(X1,-Y1, 'r-', 'Linewidth', 2);
    end % otherwise, don't plot values from air
    od=od+odstep;
end
% for upcast Kd estimates
od=odstop;
while od<odmax,
    odi=round((od-odstop)/odstep)+1;
    X1=[bestKdup(odi,3) bestKdup(odi,3)];
    Y1=[bestKdup(odi,1) bestKdup(odi,2)]-zcorrKd;
    if min(Y1)>0,
        plot(X1,-Y1, 'k--', 'Linewidth', 2);
    end % otherwise, don't plot values from air
    X1=[regKdup(odi,3) regKdup(odi,3)];
    Y1=[regKdup(odi,1) regKdup(odi,2)]-P2above;
    if min(Y1)>0,
        plot(X1,-Y1, 'b--', 'Linewidth', 2);
    end % otherwise, don't plot values from air
    X1=[regKdup(odi,4) regKdup(odi,4)];
    Y1=Y1-sepd;
    if min(Y1)>0,
        plot(X1,-Y1, 'r--', 'Linewidth', 2);
    end % otherwise, don't plot values from air
    od=od+odstep;
end
legend('downcast', 'upcast', 'Location', 'SouthEast');
%
% output diagram
printname=strcat(prog_name,tfname(1:length(tfname)-4));
orient tall
ofn=strcat(printname, '.',pt);
switch pt
    case 'ai'
        print('-dill', ofn);
    case 'pdf'
        print('-dpdf', ofn);
    case 'ps'
        print('-dpsc2', ofn);
end

```



```
    fprintf(strcat(['\n==== graph saved as ' ofn '\n\n']));  
%  
fprintf('\n%s\n', '*****');  
fprintf('%s\n', strcat(['End of ' prog_name ' at: ' datestr(now)]));  
fprintf('%s\n\n', '*****');  
%  
%end
```

## **Appendix II**

---

Additional information for Chapter 6

---

### II-1. Guillard's F/2 Medium Recipe

The medium used was an adaptation of the Guillard's F/2 Medium Recipe and was prepared for 1000 cm<sup>3</sup> of water. Table II.1 represents the recipe that was used to produce enriched water with concentrations of 12 µM of nitrogen, 1.8 µM of phosphate and 30 µM of silicate, which corresponds to the nitrate limited medium.

Table II.1 – Adaptation of the Guillard's F/2 Medium recipe for nitrate limited medium.

	Amounts per 1000cm <sup>3</sup>
NaNO <sub>3</sub> (12 µM)	0.00102g
NaH <sub>2</sub> PO <sub>4</sub> .2H <sub>2</sub> O (1.8 µM)	0.0028g
Vitamin Mix	1cm <sup>3</sup>
Trace Elements	1cm <sup>3</sup>
Na <sub>2</sub> SiO <sub>3</sub> (30 µM)	0.003663g
<b>Trace Elements</b>	
Na <sub>2</sub> EDTA	0.8386g
FeCl <sub>3</sub> .6H <sub>2</sub> O	0.6059g
CuSO <sub>4</sub> .5H <sub>2</sub> O	0.0019g
ZnSO <sub>4</sub> .7H <sub>2</sub> O	0.0042g
CoCl <sub>2</sub> .6H <sub>2</sub> O	0.0019g
MnCl <sub>2</sub> .4H <sub>2</sub> O	0.0346g
Na <sub>2</sub> MO <sub>4</sub> .2H <sub>2</sub> O	0.0012g
<b>Vitamin Mix</b>	
Cyanocobalamin (vitamin B12)	0.000096g
Thiamine HCl (vitamin B1)	0.0192g
Biotin	0.000096g

For the other combinations, calculations were made. For larger quantities, the amounts indicated in this recipe should be multiplied by the number of cm<sup>3</sup> wanted. The amounts of trace elements and vitamins were calculated proportionally to the silicate concentration, which is the element clearly in excess.

First, the nitrogen and the phosphate were added to the water and then the trace elements and the vitamin mix. The volume was then made up to 1000 cm<sup>3</sup> with filtered natural seawater. The pH was adjusted to 3.0 – 4.0 with HCl and then the silicate was added. Finally pH was adjusted to 8.0 with NaOH or HCl.

## II-2. Analysis of Fluxes of *Q* Experiment

A MATLAB routine was created and developed to analyse the nutrient and chlorophyll changes. It is composed by two scripts: the main one, which is the MLM.m file; and the associated script, the MUX.m file. The main script is divided in two parts, the first where data is loaded and polynomial curves are fitted and the second where the nutrient fluxes and changes are calculated and yields are estimated. The script MUX.m was used to assess the growth and loss of microphytobenthos. These processes are essential to calculate chlorophyll changes, as described in Chapter 6. The main script was run initially to estimate nutrient fluxes in dark conditions. After that, these fluxes were saved in a file which is loaded by the script on the next run. The second run calculates the growth, loss, nutrient and chlorophyll changes and simultaneously the yields. The routine development was a result of a close collaboration between Ana Brito and Prof. Paul Tett.

- Main script MLM.m

```
% Script MLM.m
%
% Reads a single file of stacked data, containing one or
% more replicates of the same treatment
% -----
% Initial stuff
clear all;% all variables
close all;% figure windows
%
global polychlcm2 chl Nchange NExChange polyN mvol marea muX uSm uIm
...
uSmsee uImsee N qN qNt fiN phiPOdark

prog_name='MLM';
%
dfn='Ana356.txt';% default file name - user asked to change
% set output type; alternatives are 'ai', 'ps', 'pdf'
pt='pdf';
% If dark conditions, only phi is estimated.
% If light conditions, only q is calculated using dark fluxes
```

```

%
% options - use default value when option = 0, fit when option = 1
options = [1 1 1 0 0 0]
% for muX LX q(N,P,Si) phiN phiP phiSi
% muX calculated as muX using function MUX
% LX calculated from muX
% can't estimate q and phi at same time
%
% PARAMETERS FOR MICROCOSM EXPERIMENTS =====
% ADJUST AS NECESSARY - OR, IN FUTURE, READ SOME FROM DATA FILE
% standard units are Litres for volume and cm^2 for area
% reactor sediment and area parameters
mdia = 15.0;% (internal) diameter (cm) of microcosm reactor
marea = pi*(mdia/2)^2;% cm^2 (pi is a Matlab constant)
sdia = 1.0;% sample diameter (cm)
nsample = 1;% samples/day for mpb chl
sample = nsample * pi*(sdia/2)^2;% cm^2 of sediment removed each day
sprop = sample/marea;% proportion of sediment area removed each day
sddens = 2.7;% g/cm^2 density of dry sediment
spore = 0.4;% sediment porosity
swdens = sddens*(1-spore) + 1.0*spore;% g/cm^2 density wet sediment
% reactor water and volume parameters
mvol = 1.5;% volume (litres) of water in microcosm reactor
DV = 0.5;% Litres/day pumped from reservoir & displaced from reactor
E = DV/mvol;% daily exchange rate
% reservoir concentrations, mu-molar
SrN = 12.0;% DAIN
SrP = 1.8;% DIP
SrSi = 30.0;% DSi
% illumination parameters
Ilight = 105.0; % PAR (muE m-2 s-1) when light is 'on'
%Ilight = 4.0; % PAR (muE m-2 s-1) when light is 'off'
hrlight = 14; % hours out of 24 during which light is 'on'
I = Ilight * hrlight/24; % 24-hr mean PAR muE m-2 s-1
% -----
% trial parameter values
% -----
% mu = 0.3; % mpb relative growth rate, d-1
defmu = [0 0;0 0;0 0;0 0;0 0]; % default mpb relative growth rate, d-1,
in dark
defL = 0.0; % exp 3, dark incubations
e = 0.5; % proportion of recycled nutrient (maybe differs N, P, Si)
%
defqN = 2.1; % mu-g chl/mu-mol N == can be changed by muI2
defqP = 5.0; % mu-g chl/mu-mol P == not used in this script version
defqSi = 0.8; % mu-g chl/mu-mol Si == can be changed afte muI2
%
etapb = 0.2; % guess at heterotroph content of microphytobenthos
% =====
%
fprintf('\n%s\n', '-----');
fprintf('%s\n', strcat([prog_name ' started at: ' datestr(now)]));
fprintf('%s\n', ...
        'Plots (benthic) microcosm data and calculates budget');
fprintf('%s\n', 'abort with ctrl-C, ctrl-break or <apple>-<.>');
fprintf('%s\n\n', strcat(['Current directory is ' pwd]));
%
% request name and read data file, which must be in current directory
fprintf('\n');
tfn=input(strcat(...
        ['Enter data file name, <RET> or just <RET> for default [' ...
        dfn ']: ']),'s');
if isempty(tfn), tfn=dfn; end

```

```

%
% PART 1 - LOAD THE DATA AND PLOT IT =====
%
% load file and put stacked data into unstacked columns
Mdata=load(tfn);
incubator=Mdata(:,2);
Iset=unique(incubator);
nj=length(Iset);
for j=1:nj,
    % extract data for incubator i
    i=Iset(j);
    day(:,j)=Mdata(ismember(incubator, i),1);
    nitrate(:,j)=Mdata(ismember(incubator, i),3);
    nitrite(:,j)=Mdata(ismember(incubator, i),4);
    silicate(:,j)=Mdata(ismember(incubator, i),5);
    phosphate(:,j)=Mdata(ismember(incubator, i),6);
    ammonium(:,j)=Mdata(ismember(incubator, i),7);
    mpbchl(:,j)=Mdata(ismember(incubator, i),8);
    DAIN(:,j)=nitrate(:,j)+nitrite(:,j)+ammonium(:,j);
end
ndays=length(day);

%
% fit polynomial to observations
%
polydegree=3;
pcoeffSi=zeros(polydegree+1,nj);
for j=1:nj,
    % Nitrogen
    Ndata=isfinite(DAIN(:,j));
    if length(DAIN(Ndata,j))>polydegree,
        pcoeffN(:,j)=...
            polyfit(day(Ndata,j), DAIN(Ndata,j), polydegree);
    else
        pcoeffN(1,j)=NaN;
    end
    polyN(:,j)=polyval(pcoeffN(:,j), day(:,j));
    % Phosphate
    POdata=isfinite(phosphate(:,j));
    if length(phosphate(POdata,j))>polydegree,
        pcoeffPO(:,j)=...
            polyfit(day(POdata,j), phosphate(POdata,j), polydegree);
    else
        pcoeffPO(1,j)=NaN;
    end
    polyPO(:,j)=polyval(pcoeffPO(:,j), day(:,j));
    % Silicate
    Sidata=isfinite(silicate(:,j));
    if length(silicate(Sidata,j))>polydegree,
        pcoeffSi(:,j)=...
            polyfit(day(Sidata,j), silicate(Sidata,j), polydegree);
    else
        pcoeffSi(1,j)=NaN;
    end
    polySi(:,j)=polyval(pcoeffSi(:,j), day(:,j));
    % -----
    chldata=isfinite(mpbchl(:,j));
    if length(mpbchl(chldata,j))>polydegree,
        pcoeffchl(:,j)=...
            polyfit(day(chldata,j), mpbchl(chldata,j), polydegree);
    else
        pcoeffchl(1,j)=NaN;
    end
    polychl(:,j)=polyval(pcoeffchl(:,j), day(:,j));

```

```

end
%
% first set of graphs -----
%
% legend labels
lab=num2str(Iset); % add to it with strvcat ...
% different symbol and poly-fit line for each (up to 6) microcosm
plotsymb=['o'; 's'; '^'; 'v'; '*'; '+'];
plotpoly=['-r'; '-b'; '-g'; ':r'; ':b'; ':g'];
plotpoly2=['--b'; '--g'; '-.r'; '-.b'; '-.g'];
%
figure(1);
%
% First subplot DAIN
subplot(4,1,1);
for j=1:nj,
    plot (day(:,j), DAIN(:,j), strcat('-k',plotsymb(j)));
    hold on;
    plot (day(:,j), polyN(:,j), plotpoly(j,:));
    % legend(lab, 'Location', 'NorthWest');
end
plot ([min(day(:,j)) max(day(:,j))], [SrN SrN], '--k');% reservoir
grid on;
ylabel('\muM DAIN');
title(strcat(['Microcosm experiment data from ' tfn ';']));

% Second subplot Phosphate
subplot(4,1,2);
for j=1:nj,
    plot (day(:,j), phosphate(:,j), strcat('-k',plotsymb(j)));
    hold on;
    plot (day(:,j), polyPO(:,j), plotpoly(j,:));
end
plot ([min(day(:,j)) max(day(:,j))], [SrP SrP], '--k');% reservoir
grid on;
ylabel('\muM PO4');
title(...
'curves: fitted polynomials; dashed lines: reservoir concs.');
```

```

% Third subplot silicate
subplot(4,1,3);
for j=1:nj,
    plot (day(:,j), silicate(:,j), strcat('-k',plotsymb(j)));
    hold on;
    plot (day(:,j), polySi(:,j), plotpoly(j,:));
    % legend(lab, 'Location', 'NorthWest');
end
plot ([min(day(:,j)) max(day(:,j))], [SrSi SrSi], '--k');%
reservoir
grid on;
ylabel('\muM Silicate');
title(strcat(['Microcosm experiment data from ' tfn ';']));

% Fourth Subplot Chlorophyll
subplot(4,1,4);
for j=1:nj,
    plot (day(:,j), mpbchl(:,j), strcat('-k',plotsymb(j)));
    hold on;
    plot (day(:,j), polychl(:,j), plotpoly(j,:));
end
grid on;
xlabel(strcat ...

```

```

        (['time, days -- plotted by ' prog_name ' on ' date '.']));
ylabel('\mug chl gdw^{-1}');
title( ['Exchange rate = ' num2str(E, 2) ' d^{-1}']);
%
% output first diagram
printname=strcat(prog_name,tfn(1:length(tfn)-4),'F1');
orient tall
ofn=strcat(printname, '.',pt);
switch pt
    case 'ai'
        print('-dill', ofn);
    case 'pdf'
        print('-dpdf', ofn);
    case 'ps'
        print('-dpsc2', ofn);
end
fprintf(strcat(['\n===== first graph saved as ' ofn '\n']));
fprintf('%s\n', 'Contains data and fitted polynomials.');
```

%  
 % PART 2 - DYNAMICS (RELATED TO SEDIMENT AREA) =====  
 %  
 % Our aim in this part is to 1) calculate the nutrient fluxes from  
 % third experiment at dark conditions, 2) calculate q using estimated  
 % fluxes and changes of nutrients in the reservoir. Following:  
 %  
 % Yield of chlorophyll from nutrient:  
 % (1)  $q = \Delta X / \Delta S$  (mug chl/mumol)  
 %  
 % Rate of change of nutrient (S) in each microcosm:  
 % (2)  $dS/dt = res + phi - uptake$  (mu-mol/cm<sup>2</sup>.d)  
 %  
 % where  
 % X is chlorophyll measured per cm<sup>2</sup> of sediment  
 % S is nutrient concentration (mu-molar) measured in the water  
 % ΔS is the change of nutrient concentration due to consumption  
 % (uptake)  
 % res is reservoir concentration, mu-molar  
 % phi is 'dark' sediment nutrient flux, mu-mol/cm<sup>2</sup>.d  
 %=====

```

%load fluxes obtained during darkness on 4th experiment
load darkfluxes.mat
%Convert matrix into scalar value, using the last days of the exp
fiNt=phiNt;
fiN=mean(mean(fiNt(4:5,:)))
fiPt=phiPdark;
fiP=mean(mean(fiPt(4:5,1)))
fiSit=phiSidark;
fiSi=mean(mean(fiSit(5:5,:)))
%=====
uSmsee=NaN(6,2);
uImsee=NaN(6,2);
for j=1:nj,
    % convert chl from mu-g/gdrwt to mu-g/cm2
    % sddens is g/cm^3 density of dry sediment
    polychlcm2(:,j) = polychl(:,j)./sddens;
end
for j=1:nj,
    % do the fitting from the chl data in mu-g/gdrwt
    chlchange(:,j) = diff(polychl(:,j));% n ==> n-1
    % observation vector length needs to go to n-1, so
    polychlshort(:,j) = polychl(2:length(polychl(:,j)),j);
    corrchlchange(:,j) = (chlchange(:,j)./polychlshort(:,j)) + sprop;
    chlchangecm2(:,j)=chlchange(:,j)./sddens;

```



```

end
% The term 'ExChange' is calculated next
%
fa=1; fb=[0.5 0.5];% for 2-point moving average
for j=1:nj,
% -----
NfromResraw(:,j)=E.*(SrN-polyN(:,j));
NfromRessmooth(:,j)=filter(fb,fa,NfromResraw(:,j));
% preserves n, so
NfromRes(:,j)=NfromRessmooth(2:length(NfromRessmooth(:,j)),j);
Nchange(:,j)=diff(polyN(:,j));% n ==> n-1
NExChange(:,j)=(Nchange(:,j) - NfromRes(:,j))*mvol/marea;
% -----
% Adding phosphate instead of silicate.
POfromResraw(:,j)=E.*(SrP-polyPO(:,j));
POfromRessmooth(:,j)=filter(fb,fa,POfromResraw(:,j));
% preserves n, so
POfromRes(:,j)=POfromRessmooth(2:length(POfromRessmooth(:,j)),j);
POchange(:,j)=diff(polyPO(:,j));% n ==> n-1
POExChange(:,j)=(POchange(:,j) - POfromRes(:,j))*mvol/marea;
% Silicate
SifromResraw(:,j)=E.*(SrSi-polySi(:,j));
SifromRessmooth(:,j)=filter(fb,fa,SifromResraw(:,j));
% preserves n, so
SifromRes(:,j)=SifromRessmooth(2:length(SifromRessmooth(:,j)),j);
Sichange(:,j)=diff(polySi(:,j));% n ==> n-1
SiExChange(:,j)=(Sichange(:,j) - SifromRes(:,j))*mvol/marea;
end
% Preparing variables for function MUX
% Checking if matrices have equal number of lines and columns
chl=polychlcm2((2:ndays),:);
N=polyN((2:ndays),:);

if options(1) > 0.5,
% calculate (microphytobenthic) growth rate
[muX defqN] = MUX(I, etapb, 1);
defqSi = 0.75*defqN;
else
muX = defmu; % muX=0;
end
if options(2) > 0.5,
% Loss is considered to be the same as growth, as if they were in
% equilibrium
LX=muX
else
LX=defmu; % L=0;
end
for j=1:nj,
% calculate the 'biological' nutrient terms, just for info
betachlnut(:,j) = muX(:,j) - e.*LX(:,j);
end
%
% estimate phi for darkness and q for light experiments for each
% nutrient
%
if options(4) > 0.5,
% estimate phiN
% In dark conditions, nutrients in the water column will increase,
% if there is a positive flux and no growth
% If dS/dt= phi + reservoir input ; phi = dS/dt - reservoir input
% So, phi = NExChange
qN = defqN;

```

```

        for j=1:nj,
            phiNtd(:,j) = NExChange(:,j);
        end
        phiN = mean(mean(phiNtd(ndays-2:ndays-1,:)))
    else
        phiN=defphiN;
    if options(3) > 0.5,
        % estimate qN
        % q = chl change/ nutconsumption
        % chl change = observed chl change + L*X
        % Nut cons = phi(dark)-phi(light)
        for j=1:nj,
            chlch=chlchangecm2(:,:)+LX(:,:); % ugchl.cm-2.d-1
            chlc=mean(mean(chlch));
            fiNmean=mean(mean(fiN));
            nutcons=fiN+(-NExChange)
            % calculate qN
            qN=chlch(:,:)./nutcons(:,:);
            qNfinal=mean(mean(qN));
        end
    else
        qN = defqN;
    end
end
%
if options(5) > 0.5,
    % estimate phiP
    % In dark conditions, nutrients in the water column will increase,
    % if there is a positive flux and no growth
    % If dS/dt= phi + reservoir input ; phi = dS/dt - reservoir input
    % So, phiP = POExChange
    for j=1:nj,
        phiPOdark(:,j) = POExChange(:,j);%
    end
    phiP = mean(mean(phiPOdark(ndays-2:ndays-1,1)))
else
    phiP=defphiP
if options(3) > 0.5,
    % estimate qP
    chlch=chlchangecm2(:,:)+LX(:,:); % ugchl.cm-2.d-1
    chlc=mean(mean(chlch));
    fiPmean=mean(mean(fiP));
    nutconsP=fiP+(-POExChange);
    % calculate q
    qP=chlch(:,:)./nutconsP(:,:);
    qPfinal=mean(mean(qP));
else
    qP = defqP;
end
end
if options(6) > 0.5,
    % estimate phiSi
    % In dark conditions, nutrients in the water column will increase,
    % if there is a positive flux and no growth
    % If dS/dt= phi + reservoir input ; phi = dS/dt - reservoir input
    % So, phiSi = SiExChange
    for j=1:nj,
        phiSidark(:,j) = SiExChange(:,j);%
    end
    phiSi = mean(mean(phiSidark(ndays-1:ndays-1,:)))
else
    phiSi=defphiSi
if options(3) > 0.5,

```

```

        % estimate qSi
        chlch=chlchangecm2(:,:)+LX(:,:); % ugchl.cm-2.d-1
        chlc=mean(mean(chlch));
        fiPmean=mean(mean(fiP));
        nutconsSi=fiSi+(-SiExchange);
        % qSi
        qSi=chlch(:,:)./nutconsSi(:,:);
        qSifinal=mean(mean(qSi));
    else
        qSi = defqSi;
    end
end
%
% second set of graphs -----
%
figure(2);
timelinezero=[min(min(day)) max(max(day))];
ld=length(day);
% First subplot
subplot(4,1,1);
    for j=1:nj,
        plot (day(2:ld,j), NExchange(:,1:2));
    end
grid on;
title(['...
    'Fluxes (per unit sediment area) estimated from data in ' ...
    tfn ';'']);
ylabel('\muM N/cm^2.d');
legend('inc 1', 'inc 2', 'Location', 'Best');
yrange = max(ylim)-min(ylim);
tpos = min(ylim) + 0.4*yrange;
if options(4) > 0.5,
    messflux = 'phi, sed. flux (fit) = ';
    messsq = 'q = ';
else
    messflux = 'phi, sed. flux = ';
    if options(3) > 0.5,
        messsq = 'q(fit) = ';
    else
        messsq = 'q = ';
    end
end
text(0.2, tpos, [messflux num2str(phiN, 2) ...
    ' \muM N/cm^2.d']);
tpos = min(ylim) + 0.3*yrange;
% Second subplot
subplot(4,1,2);
    for j=1:nj,
        plot (day(2:ld,j), POExchange(:,1:2));
    end
grid on;
ylabel('\muM PO/cm^2.d');
yrange = max(ylim)-min(ylim);
tpos = min(ylim) + 0.4*yrange;
if options(5) > 0.5,
    messflux = 'phi, sed. flux (fit) = ';
    messsq = 'q = ';
else
    messflux = 'phi, sed. flux = ';
    if options(3) > 0.5,
        messsq = 'q(fit) = ';
    else
        messsq = 'q = ';
    end
end

```

```

        end
    end
    text(0.2, tpos, [messflux num2str(phiP, 2) ...
        ' \muM PO/cm^2.d']);
    tpos = min(ylim) + 0.3*yrange;
    text(0.2, tpos, [messsq num2str(defqP, 2) ...
        ' \mug chl/\mu-g at PO']);
% Third subplot
subplot(4,1,3);
    for j=1:nj,
        plot (day(2:ld,j), SiExChange(:,1:2));
    end
    grid on;
    ylabel('\muM Si/cm^2.d');
    yrange = max(ylim)-min(ylim);
    tpos = min(ylim) + 0.4*yrange;
    if options(6) > 0.5,
        messflux = 'phi, sed. flux (fit) = ';
        messsq = 'q = ';
    else
        messflux = 'phi, sed. flux = ';
        if options(3) > 0.5,
            messsq = 'q(fit) = ';
        else
            messsq = 'q = ';
        end
    end
    end
    text(0.2, tpos, [messflux num2str(phiSi, 2) ...
        ' \muM PO/cm^2.d']);
    tpos = min(ylim) + 0.3*yrange;
    text(0.2, tpos, [messsq num2str(defqSi, 2) ...
        ' \mug chl/\mu-g at Si']);
% Fourth Subplot
subplot(4,1,4);
    for j=1:nj,
        plot (day(1:ld,j), polychlcm2(:,1:2));
    end
    grid on;
    xlabel(strcat...
        (['time, days -- plotted by ' prog_name ' on ' date '.']));
    ylabel('\mug chl/cm^2.d');
    legend('chl', 'chl change','Location', 'Best');
    tpos = 0.7*max(ylim) + 0.3*min(ylim);
    text(0.2, tpos, ['1 = ' num2str(sprop,2) ' d^{-1}']);
    tpos = 0.6*max(ylim) + 0.4*min(ylim);
    tpos = 0.5*max(ylim) + 0.5*min(ylim);
    xlim(timelinezero);
% output second diagram
printname=strcat(prog_name,tfm(1:length(tfm)-4),'F2');
orient tall
ofn=strcat(printname,',' ,pt);
switch pt
    case 'ai'
        print('-dill', ofn);
    case 'pdf'
        print('-dpdf', ofn);
    case 'ps'
        print('-dpsc2', ofn);
end
fprintf(strcat(['\n===== second graph saved as ' ofn '\n']));
fprintf('%s\n', 'Contains estimated fluxes per Litre.');
```

%  
% =====

```
fprintf('\n%s\n', '*****');
fprintf('%s\n', strcat(['End of ' prog_name ' at: ' datestr(now)]));
fprintf('%s\n\n', '*****');
%
```

### • Function MUX

```
function [muX, qN] = MUX (I, eta, porb)
% MUX - growth for micro -plankton or -phytobenthos
% input:
% I : scalar, 24 hr mean irradiance in muE m-2 s-1
% eta : scalar, heterotroph fraction
% porb : scalar, 0 = pelagic, 1 = benthic
% outout
% muX : matrix, growth ugchl.cm-2.d-1
% qN : scalar, chl yield from nitrogen
%
% -----
%
global polychlcm2 chl Nchange NExChange polyN mvol marea muX uSm uIm
...
uSmsee uImsee N fiN
if porb < 0.5,
    % pelagic
    r0a=0.05; % autotroph basal respiration, d-1
    ba=0.5; % autotroph slope of respiration on growth
    r0h=0.07; % heterotroph basal respiration d d-1
    bh=1.5; % heterotroph slope of respiration on growth
    %
    k = 86400; % s d-1
    m3 = 1.25; % planar to scalar irradiance
    astarPH = 0.03; % m2 (mg chl)-1
    phi = 40/1000000; % mg-at C (uE)-1
    Qmaxa = 0.2; % mg-at N (mg-at C)-1
    XqNamax = 6; % mg chl (mg-at N)-1
else
    % benthic
    r0a=0.05; % autotroph basal respiration, d-1
    ba=0.5; % autotroph slope of respiration on growth
    r0h=0.07; % heterotroph basal respiration d d-1
    bh=1.5; % heterotroph slope of respiration on growth
    %
    k = 86400; % s d-1
    m3 = 1.00; % irradiance is effectively planar
    astarPH = 0.03; % m2 (mg chl)-1
    phi = 40/1000000; % mg-at C (uE)-1
    mumax=0.4; % max growth rate (d-1)
    kd=3; % mm-1
    H=1; % mm
    Hmin=0;
    Qmaxa = 0.2; % mg-at N (mg-at C)-1
    XqNamax = 6; % mg chl (mg-at N)-1 or ug chl.(ug-at N)-1
end
%
b=ba*(1+bh*eta)+bh*eta;
r0=r0a*(1-eta)+r0h*eta*(1+ba);
%
alphamax = k * ...
            m3 * astarPH * phi * ...
            Qmaxa * XqNamax * ...
```

```

                                (1-eta) / (1 + b);
Ic = r0 * (1 + b) / alphamax;
% without photoacclimation,
qN = XqNamax * (1-eta);
%
if porb < 0.5,
    % pelagic - no saturation, linear response
    growthrate = alphamax * (I - Ic)
else
    Ik = 100; % irradiance, muE m-2 s-1, at which p = half pmax
    % Growth from light
    %Parameters
    km=86.400; %s.d-1 micro(nano)-1
    quantum=50; %nmol C.uE-1
    X=0.4; % ug chl.(ug at-C)-1 -> ug chl.(umol C)-1?
    aPHm=0.2; %cm2.(ug chl)-1
    m5=0.3; % Kirk
    bbX=0; %cm2.(ug chl)-1
    bbPM=0.001; % cm2.ug-1
    PM=10000; % 1.8835 g.cm-3 calculated from density values (lmm)
    %converted to mg.m-2 its 1.8835*10^6 - ug.cm-2
    aPM=0.0004; % cm2.ug-1 from Devlin et al (2008)
    aNP=0.2; %cm2.ug-1
    r0a=0.05; %d-1 algal respiration from LESV report
    r0h=0.03;%d-1 heterotrophs respiration from LESV report
    bma=0.5; % ratio LESV report
    bmh=1.5; % ratio LESV report
    nb=0.125; %from LESV report
    c3=0.3;
    hthc=0.001;
    Rm=0.5; %sediment albedo
    p=0.5;%porosity

    %Equations
    a=((1-c3)*(aPHm+aNP)*chl)/hthc+aPM*PM
    aPH=(1-c3)*aPHm*chl/hthc
    aPHs=c3*aPHm*chl;
    c1=(aPH.*hthc)./(a*hthc)*(1-Rm)+(1-exp(-aPHs))*Rm
    Lm=0.2; %
    r0=r0a*(1-nb)+r0h*nb*(1-bma);
    bm=bma*(1+bmh*nb)+bmh*nb;
    r=r0+bm*Lm
    PM=PM*(1-p);
    uIm=(km*c1*I*quantum*X*1/10000)-r*chl
    % Growth from nutrients
    Nchange
    th=5;
    thi=0.5; %
    Sins=1;%
    D=0.00000001648; %
    aS=0.3; %
    Um=1.5; %
    ksm=0.0005; %
    c2=(1-exp(-aS*(1-c3)*chl));
    c4=(1-exp(-aS*c3*chl));
    Sexch=D*((N-Sins)/thi)*100;
    uSm=qN.*(c2.*(fiN)+c4.*Sexch)
    % Taking the limiting growth
    muX=min(uSm,uIm);
end

```

## **Appendix III**

---

Additional information for Chapter 7

---

The appendix III is divided in two parts. The first (III-1) is composed by the main diagrams, equations and scripts used in the modelling simulations. The essential information needed for the description of each model stage is given here. The second part (III-2) is composed by script files which were used to obtain time-series of the forcing variables used in MATLAB after stage 2.

### III-1 - First Part

#### III-1.1 - Stage 1

The diagram represents the model developed during stage 1 is presented in Figure III.1. The three state variables are represented by the large boxes.

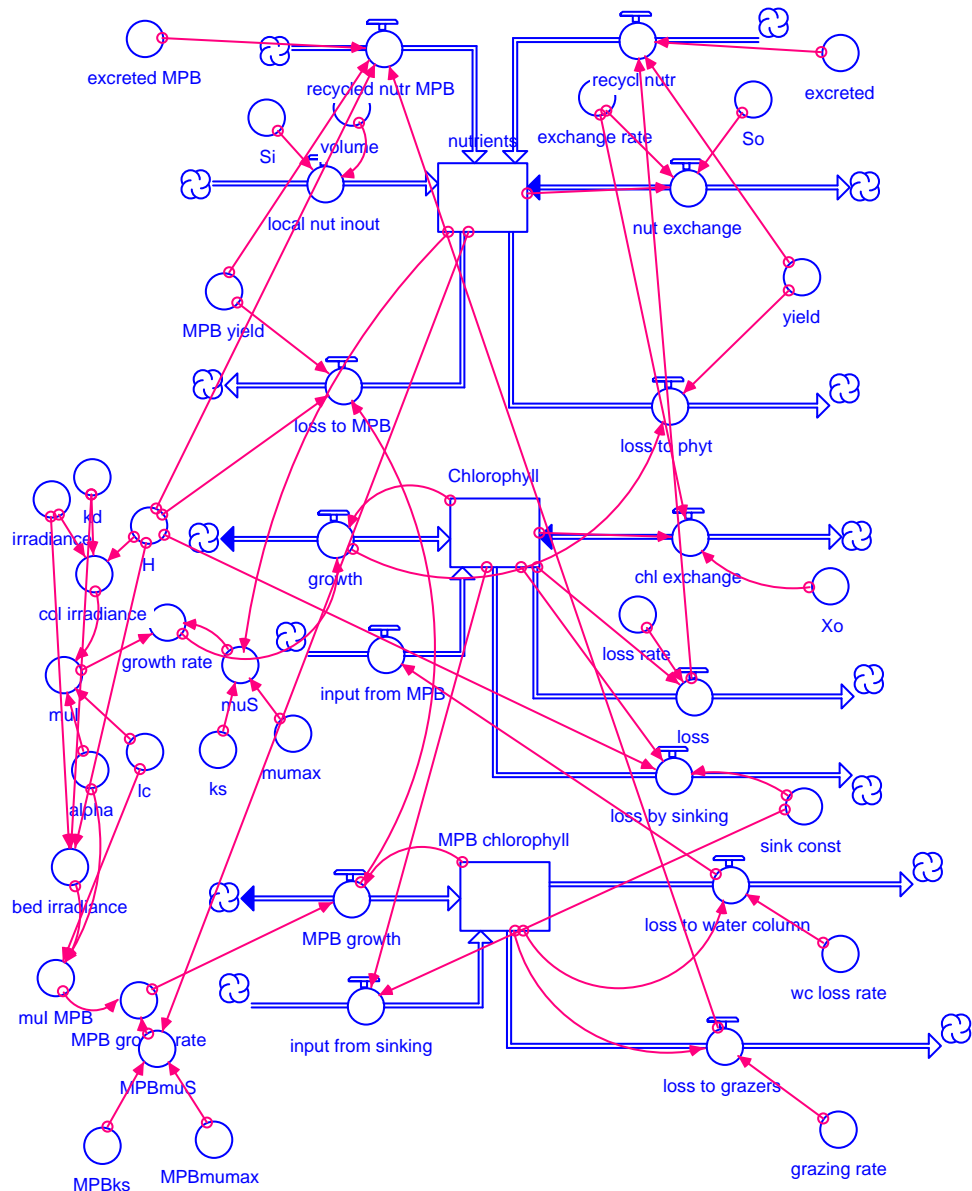


Figure III.1 – STELLA diagram of the stage 1 of the model.



The equations describing the fluxes involved in the definition of each state variable are presented below. State variables are indicated by the big square and fluxes by the circles with arrows. The simple circles indicate functions that are involved in the calculation of fluxes and parameter values.

- Chlorophyll(t) = Chlorophyll(t - dt) + (growth + input\_from\_MPB - chl\_exchange - loss - loss\_by\_sinking) \* dt  
INIT Chlorophyll = 2  
INFLOWS:  
  - growth = (Chlorophyll\*growth\_rate)
  - input\_from\_MPB = (loss\_to\_water\_column)/2
 OUTFLOWS:  
  - chl\_exchange = exchange\_rate\*(Chlorophyll-Xo)
  - loss = Chlorophyll\*loss\_rate
  - loss\_by\_sinking = Chlorophyll\*sink\_const/H
- MPB\_chlorophyll(t) = MPB\_chlorophyll(t - dt) + (MPB\_growth + input\_from\_sinking - loss\_to\_water\_column - loss\_to\_grazers) \* dt  
INIT MPB\_chlorophyll = 270  
INFLOWS:  
  - MPB\_growth = (MPB\_chlorophyll\*MPB\_growth\_rate)
  - input\_from\_sinking = Chlorophyll\*sink\_const
 OUTFLOWS:  
  - loss\_to\_water\_column = MPB\_chlorophyll\*wc\_loss\_rate
  - loss\_to\_grazers = MPB\_chlorophyll\*grazing\_rate
- nutrients(t) = nutrients(t - dt) + (local\_nut\_inout + recycled\_nutr\_MPB + recycl\_nutr - nut\_exchange - loss\_to\_phyt - loss\_to\_MPB) \* dt  
INIT nutrients = 2.1  
INFLOWS:  
  - local\_nut\_inout = Si/volume
  - recycled\_nutr\_MPB = (excreted\_MPB\*(1/MPB\_yield)\*loss\_to\_grazers)/H
  - recycl\_nutr = (excreted\*(1/yield)\*loss)
 OUTFLOWS:  
  - nut\_exchange = exchange\_rate\*(nutrients-So)
  - loss\_to\_phyt = growth/yield
  - loss\_to\_MPB = (MPB\_growth/MPB\_yield)/H
- alpha = 0.006
- bed\_irradiance = 0.4\*irradiance\*EXP(-kd\*H)
- col\_irradiance = 0.4\*irradiance\*(1-EXP(-kd\*H))/(kd\*H)
- exchange\_rate = 0.5
- excreted = 0.5
- excreted\_MPB = 0.5
- grazing\_rate = 0.15
- growth\_rate = IF(mul<muS)THEN(mul)ELSE(muS)
- H = 1.5
- irradiance = 700
- kd = 0.7
- ks = 2
- lc = 10
- loss\_rate = 0.15
- MPBks = 2
- MPBmumax = 1
- MPBmuS = MPBmumax\*((nutrients)/(MPBks+nutrients))
- MPB\_growth\_rate = IF(mul\_MPB<MPBmuS)THEN(mul\_MPB)ELSE(MPBmuS)
- MPB\_yield = 4
- mul = alpha\*(col\_irradiance-lc)
- mul\_MPB = alpha\*(bed\_irradiance-lc)
- mumax = 1
- muS = mumax\*((nutrients)/(ks+nutrients))
- Si = 78000000
- sink\_const = 1
- So = 2.3
- volume = 88000000
- wc\_loss\_rate = 0.15
- Xo = 1.75
- yield = 1.1

### III-1.2 - Stage 2

During Stage 2, the model was transferred to the software MATLAB ®. This software works with scripts (m files). These files contain the description and all the information needed for running the model. The model functions are organized in three script files. The first script is called ana.m and has the solver function with the initial conditions. It is also in this file where the forcing variables time-series are loaded. The final part is to create plots and save outputs. The second script is called cstt.m and is where equations which describe different processes such as growth and loss are described. It also has the differential equations of the state variables. The last script contains only the values of all parameters used in the model. This script is called in the beginning of the cstt script. This allows the use of the values wherever needed.

#### Script ana.m

```

%===== Ana.m Script =====
%Make variables global and set up the time scale
%=====
global irradd cirrad birrad irraddd irradd w wdd wd
tspan=[1:730];
year='2004';
>Loading forcing variables - irradiance
%=====
irradd=load('irradd2004.txt');
%second year worth of data
secondyi=[irradd(:,2) irradd(:,2)];secondyi=secondyi(:);
irraddd=[tspan' secondyi];
%end
>Loading forcing variables - Winds
%=====
wd=load('Finalwinds365.txt');
%second year worth of data
secondyw=[wd(:,2) wd(:,2)];secondyw=secondyw(:);
wdd=[tspan' secondyw];
%
%=====
%Running the main program -> integrating function- ode23
%
% set the options to be passed to the solver
options=odeset('NonNegative',[1 2 3 4]);% set the option tag
% Run the ode solver with the options. try help ode for more help
%
[t,x]=ode23('cstt',tspan,[2.1,2,270,100],options);
%
%Plotting the output
%
subplot(2,1,1);
plot(x(tspan,1:4), 'DisplayName','x(tspan,1:4)', 'YDataSource',
'x(tspan,1:4)'); figure(gcf)
xlabel('time(days)');
ylabel('concentrations');
h=legend('nut','pelchla','bentchla','sednut',4);

```

```

legend1 =
legend({'nut', 'pelchla', 'bentchla', 'sednut'}, 'location', 'best'); hold
on
subplot(2,1,2);
plot (x(tspan,1:2), 'DisplayName', 'x(tspan,1:4)', 'YDataSource',
'x(tspan,1:4)'); figure(gcf)
xlabel('time(days)');
ylabel('concentrations');
h=legend('nut', 'pelchla', 2);
legend1 = legend({'nut', 'pelchla'}, 'location', 'best');
%=====
% write to file (in current working directory)
mChl=x(:,3);
fid=fopen('mChl.xls','w');
fprintf(fid,'%8.2f\n',mChl);
fclose(fid);
%
pChl=x(:,2);
fid=fopen('pChl.xls','w');
fprintf(fid,'%8.2f\n',pChl);
fclose(fid);
%
DAIN=x(:,1);
fid=fopen('DAIN.xls','w');
fprintf(fid,'%8.2f\n',DAIN);
fclose(fid);
%
SedDAIN=x(:,4);
fid=fopen('SedDAIN.xls','w');
fprintf(fid,'%8.2f\n',SedDAIN);
fclose(fid);
% ===== END OF SCRIPT =====

```

### Script cstt.m

```

%===== CSTT script =====
% CSTT model function for Ria Formosa
% contains the differential equations that are solved by the main
script
% by A. Brito, March 2007
% edits by Paul Tett, 16 April 2007
%=====
function xdot=cstt(t,x)
parameters;
fprintf('%8.2f\n',t);
%
global irradd cirrad birrad wd irraddd irradd w wdd
%
irradd=interp1(irraddd(:,1),irraddd(:,2),t,'linear');
w=interp1(wdd(:,1),wdd(:,2),t,'linear');
%
% light and growth
cirrad=0.4*irradd*(1-exp(-kd*H))/(kd*H);
birrad=0.4*irradd*exp(-kd*H);
muI=a*(cirrad-lc);% NB allowed to go negative (=net respiration)
muIm=am*(birrad-lc);% ditto
%
% nutrients and growth
muS = max(0, mum*(x(1)/(ks+x(1)))) );
u=min(muI,muS);
muSm = max(0, mum*(x(4)/(ksm+x(4)))) );
um=min(muIm,muSm);

```

```

%
% Physical
rtide = sin(24*pi*t/365+162)*0.002+0.03;
rwind=(w/164)*Lwind;
WcL=rtide+rwind;
%
% MAIN EQUATIONS FOLLOW =====
% DAIN and chlorophyll in water column are m-3
% chlorophyll in the sediment is m-2 and spread over whole metre
% DAIN in sediment is m-3 in pore water, a fraction p of sediment
% x(n) = state variable; xdot(n) is rate of change of this variable
% conservative terms are given first in each equation
% =====
% x(1) = water column DAIN, mmol/m3
xdot(1) = (E*(So-x(1)) + Si/V + (x(4)-x(1))*d*p*tort/(hs*H) + ...
cnsrvtv
          (exc*L - u)*x(2)/q);% water column biology
% -----
% xd(2)= Pelagic chlorophyll, mg/m3
xdot(2) = E*(Xo-x(2)) + WcL*x(3)/H - (sk/H)*x(2) + ... cnsrvtv
          (u - L)*x(2);% water column biology
% -----
% x(3)= MPB chlorophyll, mg/m2
xdot(3) = sk*x(2) - WcL*x(3) + ... conservative
          (um - mg)*x(3);% benthic biology
% -----
% x(4)=DAIN in sediment pore water, mol/m3
xdot(4) = (((x(1)-x(4))/hs)*(d/hs) + ... conservative
          (PON*decay)/p - x(4)*Nit + ... benthic microbiology
          (excm*g - um)*x(3)/(qm*p));% benthic biology
%
xdot=xdot';
% ===== END OF SCRIPT =====

```

### Script parameters.m

```

% ===== Parameters =====
E=0.5;
So=2.3;
a=0.01;
am=0.005;
ma=0.005;
H=1.5;
kd=0.7;
exc=0.5;
excm=0.5;
g=0.15;
mg=0.15;
ks=2;
lc=10;
L=0.15;
ksm=10;
qm=4;
mu=1;
mum=1;
Si=78000000;
V=88000000;
Lwind=0.1;
Xo=1.75;
q=1.1;
tort=0.7;
PON=100; %mmol/m3

```

```

decay=0.15;
p=0.5; % Its a percentage
hs=0.05; % metres
d=0.001; % m2.d-1
Nit=0.01; % 1% per day
sk=1; % m per day
% ===== END OF SCRIPT =====

```

### III-1.3 - Stage 3

The model functions are still organized in three script files: ana.m, cstt.m and parameters.m. The stage 3 has one main variation from the previous scripts, the inclusion of Dissolved Oxygen. The three files are presented below.

#### Script ana.m

```

%===== Ana.m Script =====
%Make variables global and set up the time scale
%=====
global irradd cirrad birrad irraddd irradd w wdd wd ...
    DOI DOIdd DOo DOodd Tinside
tspan=[1:730];
year='2004';
%Loading forcing variables - irradiance
%=====
irradd=load('irradd2004.txt');
%second year worth of data
secondyi=[irradd(:,2) irradd(:,2)];secondyi=secondyi(:);
irraddd=[tspan' secondyi];
%Loading forcing variables - Winds
%=====
wd=load('Finalwinds365.txt');
%second year worth of data
secondyw=[wd(:,2) wd(:,2)];secondyw=secondyw(:);
wdd=[tspan' secondyw];
%
%=====
%Loading forcing variables - Dissolved Oxygen Inside and Outside
lagoon
%
DOod=load('DOBeach.txt');
%second year worth of data
secondydo=[DOod(:,2) DOod(:,2)];secondydo=secondydo(:);
DOodd=[tspan' secondydo];
%
DOIId=load('DOIInside.txt');
secondydi=[DOIId(:,2) DOIId(:,2)];secondydi=secondydi(:);
DOIdd=[tspan' secondydi];
%
Tins=load('Tinside.txt');
secondyTi=[Tins(:,2) Tins(:,2)];secondyTi=secondyTi(:);
Tinside=[tspan' secondyTi];
%=====
%Running the main program -> integrating function- ode23
%
% set the options to be passed to the solver
%Produce non-negative solutions

```

```

options=odeset('NonNegative',varno0);% set the option tag
% Run the ode solver with the options. try help ode for more help
%
[t,x]=ode23('cstt',tspan,[2.1,2,270,100,100],options);
%
%Plotting the output
%
subplot(3,1,1);
plot(x(tspan,3:4), 'DisplayName','x(tspan,1:4)', 'YDataSource',
'x(tspan,1:4)'); figure(gcf)
xlabel('time(days)');
ylabel('concentrations');
h=legend('nut','pelchla','bentchla','sednut',4);
legend1 =
legend({'nut','pelchla','bentchla','sednut'},'location','best');
title (year);
%
subplot(3,1,2);
plot(x(tspan,1:2), 'DisplayName','x(tspan,1:4)', 'YDataSource',
'x(tspan,1:4)'); figure(gcf)
xlabel('time(days)');
ylabel('concentrations');
h=legend('nut','pelchla','bentchla','sednut',4);
legend1 =
legend({'nut','pelchla','bentchla','sednut'},'location','best');
title (year);
%
subplot(3,1,3);
plot(x(tspan,5:5), 'DisplayName','x(tspan,5:5)', 'YDataSource',
'x(tspan,5:5)'); figure(gcf)
xlabel('time(days)');
ylabel('DO');
title (year);
%=====
% write to file (in current working directory)
mChl=x(:,3);
fid=fopen('mChl.xls','w');
fprintf(fid,'%8.2f\n',mChl);
fclose(fid);
%
pChl=x(:,2);
fid=fopen('pChl.xls','w');
fprintf(fid,'%8.2f\n',pChl);
fclose(fid);
%
DAIN=x(:,1);
fid=fopen('DAIN.xls','w');
fprintf(fid,'%8.2f\n',DAIN);
fclose(fid);
%
SedDAIN=x(:,4);
fid=fopen('SedDAIN.xls','w');
fprintf(fid,'%8.2f\n',SedDAIN);
fclose(fid);
%
DO=x(:,5);
fid=fopen('DO.xls','w');
fprintf(fid,'%8.2f\n',DO);
fclose(fid);
% ===== END OF SCRIPT =====

```

**Script cstt.m**

```

%===== CSTT script =====
% CSTT model function for Ria Formosa
% contains the differential equations that are solved by the main
script
% by A. Brito, May 2008
% edits by Paul Tett, April, June 2007
%=====
function xdot=cstt(t,x)
parameters;
fprintf('%8.2f\n',t);
%
global irradd cirrad birrad wd irraddd irradd w wdd ...
      DOI DOIdd DOo DOodd Tinside
%
% light and growth
irradd=interp1(irraddd(:,1),irraddd(:,2),t,'linear');
cirrad=0.4*irradd*(1-exp(-kd*H))/(kd*H);
birrad=0.4*irradd*exp(-kd*H);
muI=a*(cirrad-lc);% NB allowed to go negative (=net respiration)
muIm=am*(birrad-lc);% ditto
%
% nutrients and growth
Ti=interp1(Tinside(:,1),Tinside(:,2),t,'linear');
muS = max(0, mum*(x(1)/(ks+x(1))) );
u=min(muI,muS);
muSm = max(0, mum*(x(4)/(ksm+x(4))) );
um=min(muIm,muSm);
%
% Physical
w=interp1(wdd(:,1),wdd(:,2),t,'linear');
rtide = sin(24*pi*t/365+162)*0.002+0.03;
rwind=(w/164)*Lwind;
WcL=rtide+rwind;
%
% Dissolved Oxygen
DOo=interp1(DOodd(:,1),DOodd(:,2),t,'linear');
DOI=interp1(DOIDD(:,1),DOIDD(:,2),t,'linear');
Air=dlength*Kw*w;% piston velocity (m d-1)
%
% MAIN EQUATIONS FOLLOW =====
% DAIN and chlorophyll in water column are m-3
% chlorophyll in the sediment is m-2 and spread over whole metre
% DAIN in sediment is m-3 in pore water, a fraction p of sediment
% x(n) = state variable; xdot(n) is rate of change of this variable
% conservative terms are given first in each equation
% =====
% x(1) = water column DAIN, mmol/m3
DConservative=E*(So-x(1)) + Si/V + (x(4)-x(1))*d*p*tort/(hs*H);
DBiology= ((exc*L - u)*x(2)/q);
xdot(1) =DConservative+DBiology;
% -----
% xd(2)= Pelagic chlorophyll, mg/m3
CConservative=E*(Xo-x(2)) + WcL*x(3)/H - (sk/H)*x(2);
CBiology= (u - L)*x(2);
xdot(2) =CConservative+CBiology;
% -----
% x(3)= MPB chlorophyll, mg/m2
MConservative=sk*x(2) - WcL*x(3);
MBiology=(um - mg)*x(3);
xdot(3) = MConservative+MBiology;

```

```

% -----
% x(4)=DAIN in sediment pore water, mol/m3
SConservative=((x(1)-x(4))/hs)*(d*tort/hs);
SMicroB= (PON*decay)/p - x(4)*Nit;
SBiology=(excm*g - um)*x(3)/(hs*qm*p);
xdot(4) = SConservative+SMicroB+SBiology;
% -----
%x(5) is dissolved oxygen, mmol/m3
OConservative=E*(DOo - x(5)) + Air*(DOI - x(5))/H;
OwcBiology=c*u*x(2);
OBBiology=(c*mu*x(3) - R)/H;
xdot(5) = OConservative+OwcBiology+OBBiology;
%
xdot=xdot';
% ===== END OF SCRIPT =====

```

### Script parameters.m

```

% ===== Parameters =====
E=0.5; %Exchange rate (d-1)
So=2.3; % Concentration of water column nutrients outside (mmol.m-3)
a=0.006; % photosynthetic efficiency parameter ((μEm-2s-1)-1.d-1)
am=0.005; % photosynthetic efficiency parameter MPB ((μEm-2s-1)-1.d-1)
H=1.5; % mean depth (m)
kd=0.7; % diffuse attenuation coefficient (m-1)
exc=0.5; % remineralisation rate (d-1)
excm=0.5; % remineralisation rate in sediments (d-1)
g=0.15; % grazing rate (d-1)
mg=0.15; % grazing rate for MPB (d-1)
ks=2; % half-saturation concentration (mmol.m-3)
lc=5; % compensation irradiance (μEm-2s-1)
L=0.15; % loss rate (d-1)
ksm=10; % half-saturation concentration for MPB (mmol.m-3)
qm=4; % yield q (mg chl.mmol-1)
q=1.1; % yield q for MPB (mg chl.m-3)
mu=1; % max growth rate (d-1)
mum=1;
Si=78000000; % input concentration (mmol.m-3)
V=88000000; % volume (m3)
%WcL=0.15;
Lwind=0.1; % Loss rate due to wind action (d-1)
Xo=1.75; % Pelagic chl concentration outside (mg.chl.m-3)
Q10 = 2.0;
mu20 = 2.0;
sk=1; % sinking rate (m.d-1)
hs=0.05;
R=40; % biological oxygen demand per meter square (mmol.m-2.d-1)
dlength=86400; % (s.d-1)
Kw=3E-5; % coefficient (m-1.s)
c=2.69*2.27; % coefficients to transform mg chl into O2
PON=100; %Particulate organic nitrogen (mmol.m-3)
decay=0.1; % Decay rate (d-1)
p=0.5; % Porosity (%) Its a percentage
th=0.05; % thickness (m)
d=0.0001661994; % Diffusion coefficient (m2.d-1)
Nit=0.01; % Denitrification rate (d-1)
Tort=0.7; tortuosity
% ===== END OF SCRIPT =====

```



### III-1.4 - Stage 4

As before, three documents are presented: ana.m, cstt.m and parameters.m. Stage 4 of the dCSTT-MPB model contains several changes from the previous versions, especially regarding the approach to calculate microphytobenthos growth.

#### Script ana.m

```

%===== Ana.m Script =====
%Make variables global and set up the time scale
%=====
global irradd cirrad birrad irraddd irradd w wdd wd kd us c1p c1b c2 c4
WcL ...
    Tinside mum DPhysics DBiology DT DI uDPv uDBv uDTv uDIv uImv uSmv
uSm uIm uml um XmaxI Sflux mumax ...
    umax r rtide rwind muS muI lc ap MLv XmaxS Ti
tspan=[1:730];
year='2004';
>Loading forcing variables - irradiance
%=====
irradd=load('irradd2004.txt');
%second year worth of data
secondyi=[irradd(:,2) irradd(:,2)];secondyi=secondyi(:);
irraddd=[tspan' secondyi];
>Loading forcing variables - Winds
%=====
wd=load('Finalwinds365.txt');
%second year worth of data
secondyw=[wd(:,2) wd(:,2)];secondyw=secondyw(:);
wdd=[tspan' secondyw];
%
%=====
% Making variables available as vectors
uDPv=NaN(730,1);
uDBv=NaN(730,1);
uDTv=NaN(730,1);
uDIv=NaN(730,1);
uImv=NaN(730,1);
uSmv=NaN(730,1);
MLv=NaN(730,1);
%Running the main program -> integrating function- ode23
%
% set the options to be passed to the solver
options=odeset('NonNegative',[1 2 3 4 5]);% set the option tag
% Run the ode solver with the options. try help ode for more help
%
[t,x]=ode23('cstt',tspan,[2,2,270,100],options);
%
%Plotting the output
subplot(3,1,1);
plot(x(tspan,1:2), 'DisplayName','x(tspan,1:4)', 'YDataSource',
'x(tspan,1:4)'); figure(gcf)
h=legend('nut','pelchla',4);
legend1 =
legend({'nut','pelchla','bentchla','sednut'},'location','best');
title(year);
%
subplot(3,1,2);

```

```

plot (x(tspan,3:3), 'DisplayName','x(tspan,1:4)', 'YDataSource',
'x(tspan,1:4)'); figure(gcf)
ylabel('concentrations');
h=legend('bentchla');
legend1 = legend({'bentchla'},'location','best');
%
subplot(3,1,3);
plot (x(tspan,4:4), 'DisplayName','x(tspan,5:5)', 'YDataSource',
'x(tspan,5:5)'); figure(gcf)
legend1 = legend({'sednut'},'location','best');
%=====
% write to file (in current working directory)
mChl=x(:,3);
fid=fopen('mChl.xls','w');
fprintf(fid,'%8.2f\n',mChl);
fclose(fid);
%
pChl=x(:,2);
fid=fopen('pChl.xls','w');
fprintf(fid,'%8.2f\n',pChl);
fclose(fid);
%
DAIN=x(:,1);
fid=fopen('DAIN.xls','w');
fprintf(fid,'%8.2f\n',DAIN);
fclose(fid);
%
SedDAIN=x(:,4);
fid=fopen('SedDAIN.xls','w');
fprintf(fid,'%8.2f\n',SedDAIN);
fclose(fid);
% ===== END OF SCRIPT =====

```

### Script cstt.m

```

%===== CSTT script =====
% CSTT model function for Ria Formosa
% contains the differential equations that are solved by the main
script
% by A. Brito, May 2008
% edits by Paul Tett, 16 April 2007
%=====
function xdot=cstt(t,x)
parameters;
fprintf('%8.2f\n',t);
%
global irradd cirrad birrad wd irraddd irradd w wdd kd us clb clp c2 c4
WcL ...
    Tinside mum DPhysics DBiology DT DI uDBv uDPv uDTv uDIv uSmv
uIm uImv uSm uml um XmaxI Sflux ...
    mumax umax r rtide rwind muI muS lc ap MLv XmaxS Ti
% Physical
decay=0.1;
w=interp1(wdd(:,1),wdd(:,2),t,'linear');
rtide = sin(48*pi*t/365+162)*0.01+0.05;
rwind=(w/164)*Lwind;
WcL=rtide+rwind;
% Grazing pressure
g=0.1;
%
ML=(g+WcL);
% light and growth

```

```

%Optics from Portilla et al 2008
ao=aW+g440+asal*(35-C);
b=bbsPM*psPM;
kd=0.7;
Hm=Vh/Ah;
irrad=interp1(irraddd(:,1),irraddd(:,2),t,'linear');
cirrad=m1*irrad*(1-exp(-kd*Hm))/(kd*Hm);
birrad=m1*irrad*(1-exp(-kd*H));
r0p=r0pa*(1-npb)+r0ph*npb*(1-bpa);
bp=bpa*(1+bph*npb)+bph*npb;
ap=kp*quantump*m3*XqpN*Qmaxa*astarPHp*((1-npb)/(1+bp));
lc=r0p/ap;
muI=ap*(cirrad-lc);% NB allowed to go negative (=net respiration)
% nutrients and growth
%Phytoplankton
Ti=interp1(Tinside(:,1),Tinside(:,2),t,'linear');
mum = mu20*Q10.^((Ti-20)./10);
muS = max(0, mum*(x(1)/(ks+x(1))) );
u=min(muI,muS);
%Microphytobenthos
%Growth due to light flux
PM=pPM*(1-p); %mg.m-3
aPH=(1-c3)*astarPHm*x(3)/hthc;
aPHs=c3*astarPHm*x(3)/hthc;
a=((1-c3)*(astarPHm+astarNP)*x(3))/hthc+astarPM*PM;
clp=(1-exp(-aPHs*hthc))*Rm;
clb=(aPH*hthc)/(a*hthc)*(1-Rm);
Lm=WcL+gm;
r0=r0a*(1-nb)+r0h*nb*(1-bma);
bm=bma*(1+bmh*nb)+bmh*nb;
r=r0+bm*Lm;
%
uIm=(km*(clp*irrad+clb*birrad)*quantum*X)-r*x(3);
%Growth due to nutrient flux
qm=XqN*(1-nb);
c2=(1-exp(-aS*(1-c3)*x(3)));
Sflux=D*p*tort*((x(4)-x(1))/hthc+hbb);
c4=(1-exp(-aS*c3*x(3)));
Swflux=D*(x(1)-sint)/hbb;
Pflux=max(0,Swflux);
%
uSm=qm*(c2*Sflux+c4*Pflux);
%Putting together - Microphytobenthos growth
mumax = mu20*Q10.^((Ti-20)./10);
umax=mumax*x(3);
um=min([uIm,uSm,umax]);
XmaxI=km*(c3*irrad+(1-c3)*birrad)*quantum*X/((Lm*(1+bm)+r0));
XmaxS=qm*(Sflux+Pflux)/ML;
Xmax=max(XmaxI,XmaxS);
%
% MAIN EQUATIONS FOLLOW =====
% DAIN and chlorophyll in water column are m-3
% chlorophyll in the sediment is m-2 and spread over whole metre
% DAIN in sediment is m-3 in pore water, a fraction p of sediment
% x(n) = state variable; xdot(n) is rate of change of this variable
% conservative terms are given first in each equation
% =====
% x(1) = water column DAIN, mmol/m3
DPhysics=E*(So-x(1));
DBiology=exc*Lb*x(2)/q+((exc*Lp - u)*x(2)/q);
DT=((Sflux-(um/qm))/H);
DI=Si/V;
xdot(1)=DPhysics+DBiology+DT+DI;

```

```

% -----
% xd(2)= Pelagic chlorophyll, mg/m3
CConservative=E*(Xo-x(2)) + WcL*c3*x(3)/H - (sk/H)*x(2);
CBiology= u*x(2) - Lp*x(2)-Lb*x(2);
xdot(2) =CConservative+CBiology;
% -----
% x(3)= MPB chlorophyll, mg/m2
MConservative=sk*x(2)*V/Ah - c3*x(3)*WcL;
MBiology=um-x(3)*g;
xdot(3) = MBiology+MConservative;
% -----
% x(4)=DAIN in sediment pore water, mol/m3
SConservative=-Sflux/hs*p;
SMicroB=((PON/(Ah*hs))*decay)/p - x(4)*Nit;%
SBiology=((excm*g*x(3)*Ah/(Ah*hs))/qm*p)+(1-exc)*Lb*x(2)/q*p;
xdot(4) = SMicroB+SBiology+SConservative;
% -----
uImv(floor(t),1)=uIm;
uSmv(floor(t),1)=uSm;
MLv(floor(t),1)=ML;
xdot=xdot';
% ===== END OF SCRIPT =====

```

### Script parameters.m

```

% ===== Parameters =====
E=0.5;
So=2.3;
H=1.5;
exc=0.5;
excm=0.5;
ks=2;
Lp=0.05;
Lb=0.9;
Si=78000000;
V=88000000;
Lwind=0.075;
Xo=1.75;
q=1.1;
Q10 = 2.0;
mu20 = 1.2;
gm=0.15;
%
Vh=140000000; %m3 from Newton and Mudge 2003
Ah=53000000; %m2 from Newton et al 2003
%
%Optics from Portilla et al 2008
m1=0.7; % coefficient for light in the water column.
%waters (2/3 optical depths), larger for shallow waters
r0pa=0.05; %d-1 algal respiration from LESV report
r0ph=0.03;%d-1 heterotrophs respiration from LESV report
bpa=0.5; % ratio LESV report
bph=1.5; % ratio LESV report
npb=0.0625; %from LESV report
kpb=0.0864; % s.d-1 mmol.nmol-1 LESV report
quantump=40; % nnomC uE-1 LESV report
m3=1.3; % ??? guess
XqpN=1.1; % mg chl.mmolN from LESV report
astarPHp=0.02; %m2.mgchl-1 from LESV report
Qmaxa=0.2; %at N: at C from LESV report
%
%Light growth of microphytobenthos

```

```

km=0.086400; %s.d-1 mili(nano)-1
quantum=40; %nmol C.uE-1
X=0.4; % ug chl.(ug at-C)-1 -> ug chl.(umol C)-1?
%
astarPHm=0.02; %m2.(mg chl)-1
m5=0.3; % Kirk ?
bbX=0; %m2.(mg chl)-1
bbPM=0.0001; % m2.mg-1
ppm=2161000000; % mg.m-3 calculated from density values from 2006
%converted to mg.m-2 its 1.8835*10^6
astarPM=0.000003; % m2.mg-1 from Devlin et al (2008) 10 times smaller!
astarNP=0.02; %m2.mg-1
hthc=0.001; %thickness of the top sediment
hbb=0.001; %thickness of the benthic boundary layer 1mm guess?
hs=0.05;% half the 5cm layer collected for quantification - just for
%pore water nutrients.
tort=0.7; %tortuosity
sint=1; %internal concentration of algae 1mmolN.m-3 guess?
Rm=0.5; %sediment albedo
r0a=0.05; %d-1 algal respiration from LESV report
r0h=0.03;%d-1 heterotrophs respiration from LESV report
bma=0.5; % ratio LESV report
bmh=1.5; % ratio LESV report
%
%Nutrient growth of microphytobenthos
XqN=4; % from LESV report
nb=0.125; %from LESV report
c3=0.15;%
aS=0.03; %calculate by me and Paul - 1mg chl=10^8 skeletonema
% cells * 300 um^3 = 0.03 m^2.chl-1
D=0.0001661994; %m2.d-1 from Murray et al 2006, average of values for
%NH4, NO3 and NO2.
PON=5000000000;% mmol organic N
p=0.5; % Its a percentage
th=0.05; % metres
d=0.001; % m2.d-1
Nit=0.01; % 1% per day
sk=1; % m per day
% ===== END OF SCRIPT =====

```

## III-2 - First Part

### III-2.1 - Irradiance

The script is used to obtain the 24-hour mean of PAR at sea-surface in  $\mu\text{E}\cdot\text{m}^{-2}\cdot\text{s}^{-1}$  and it is divided in two different parts. The first works with cloud cover values and was built to bin all the data for each category. Several values for each day were obtained and we wanted the script to work with daily means, so this part allowed that step. The second part used the cloud cover daily means and transformed it into the 24-hour mean of PAR at sea-surface in  $\mu\text{E}\cdot\text{m}^{-2}\cdot\text{s}^{-1}$ . This last part uses an algorithm called Eo\_24.

**Part I – Binning**

```

function [BinnedArray] = ...
    binning(DataForBinning,BinSize,HowManyBins,SmallestIV,LargestIV)
% Binning sorts unordered data into bins according to an index
%variable
%
% minimum syntax:
%   Array(m, 5) = binning(DataForBinning(n,2), BinSize);
%   where m is number of bins used (typically the same as
%HowManyBins),
%   n is number of rows of input data and BinSize is a scalar;
%
% input:
% DataForBinning is an array with 2 columns:
%   column 1 = index variable (e.g. depth, day) vector;
%   column 2 = dependent variable vector;
%   for example, the index value in column 1, row 28 is used to
%       decide the bin for the data value in column 2, row 28.
% BinSize is a mandatory real scalar with a value that should be a
% fraction of the range if the index variable;
% HowManyBins is an optional integer; if supplied it has precedence
% over BinSize except when HowManyBins < 0
% SmallestIV and LargestIV are optional real scalars, setting the
% range of values (of the index variable) selected for inclusion in
%binning.
% If not input, they are computed from the minimum and maximum
% values of the index variable found in DataForBinning.
%
% The range from SmallestIV to LargestIV is divided into the number of
% bins specified by HowManyBins, such that SmallestIV lies in the
% centre of SmallestBin and LargestIV lies in the centre of
%LargestBin.
% Values of the dependent variable are sorted into these bins
% according to the values of the index variable in the same
% rows. In fact, sorted individual values are not stored, but totals
% are accumulated in each bin, allowing calculation of the output
% variables.
%
% output: BinnedArray
%   column 1 = lower bound of index variable for each bin;
%   column 2 = mean value of index variable for each bin;
%   column 3 = mean value of dependent variable in each bin;
%   column 4 = SOS of dependent variable in each bin;
%   column 5 = number of values put in each bin.
%
% PT, 22-27 Dec 06
%
% =====
%
% GLOBALS used only for workspace checking during development
global accumulators fullaccumulators Ndata nonzeroBins
global SmallestBin LargestBin
% -----
%
% FIRST, check and/or calculate all input parameters
if nargin < 2,
    error('too few input arguments'); end
Ndata=length(DataForBinning(:,1)); % (:,1) selects all rows of column
1
if Ndata < 10,
    error('DataforBinning is too small or otherwise wrong');

```

```

end
if nargin < 5, % identify maximum value of the index variable
    LargestIV = max(DataForBinning(:,1));
end
if nargin < 4, % identify minimum value of the index variable
    SmallestIV = min(DataForBinning(:,1));
end
if nargin > 2 && HowManyBins > 1,
    BinSize = (LargestIV-SmallestIV)/(HowManyBins-1);
else
    HowManyBins = ceil((LargestIV-SmallestIV)/BinSize); % integer
end
LargestBin=LargestIV-0.5*BinSize; % lower bound of top bin
SmallestBin=SmallestIV-0.5*BinSize; % lower bound of bottom bin
%
% -----
% NEXT, set up and fill the processing array
% row 1 = index variable, 2 = index variable squared,
% 3 = main variable, 4 = main variable squared, 5 = count
% number of rows set by HowManyBins
accumulators=zeros(HowManyBins+1, 5);
for n=1:Ndata,
    % check to avoid NaN and within range, identify bin
    if isfinite(DataForBinning(n,:)) & ...
        DataForBinning(n,1) >= SmallestIV & ...
        DataForBinning(n,1) <= LargestIV,
        bin=1+floor((DataForBinning(n,1)-SmallestBin)/BinSize);
        % update totals
        accumulators(bin,1)=accumulators(bin,1) + DataForBinning(n,1);
        accumulators(bin,2)=accumulators(bin,2) +
DataForBinning(n,1)^2;
        accumulators(bin,3)=accumulators(bin,3) + DataForBinning(n,2);
        accumulators(bin,4)=accumulators(bin,4) +
DataForBinning(n,2)^2;
        accumulators(bin,5)=accumulators(bin,5) + 1; % counter
    else % do nothing
    end
end
% -----
% FINALLY, calculate the binned data means and variances
% having deleted any empty rows to avoid 'divide by zero' warnings
nonzeroBins=accumulators(:,5)>0;
fullBins=length(accumulators(nonzeroBins, 5));
fullaccumulators=accumulators(nonzeroBins, 1:5);
BinnedArray=zeros(fullBins, 5);
for m=1:fullBins,
    BinnedArray(m,1)=(m-1)*BinSize+SmallestBin; end
BinnedArray(:,2)=fullaccumulators(:,1)./fullaccumulators(:,5);
    % index variable mean
BinnedArray(:,3)=fullaccumulators(:,3)./fullaccumulators(:,5);
    % binned variable mean
correctionterm=(fullaccumulators(:,3).^2)./fullaccumulators(:,5);
BinnedArray(:,4)=fullaccumulators(:,4) - correctionterm;
    % SOS of binned variable,
    % from: sum of x-squared - ((sum of x)squared/n)
BinnedArray(:,5)=fullaccumulators(:,5); % number of values
%
% ===== END OF SCRIPT =====

```

Secondly, the binning script is tested and the files with the daily means are created.

```

% testbinning.m: script to test a simple binning function
% PT, 22-26 Dec 06
%
%
%   clear all;% all variables
%   close all;% figure windows
%
%   prog_name='testbinning';
%
% set current working directory - to where user keeps files
%   cd('/SeShaT/Edinburgh - Napier/Paul');
%
%   fprintf('\n%s\n', '-----');
%   fprintf('%s\n', strcat([prog_name ' started at: ' datestr(now)]));
%   fprintf('%s\n', 'abort with ctrl-C, ctrl-break or <apple>-<.>');
%   fprintf('%s\n\n', strcat(['Current directory is ' pwd]));
%
% GLOBALS used only for workspace checking during development
global accumulators fullaccumulators Ndata nonzeroBins
global SmallestBin LargestBin
% -----
%
% fname='CTDdataR.txt';% example data set - scrambled CTD data
% parameters with example values
maxbins=100;% number of bins
binsize=2;% bin size
smallIV=20;% minimum index variable (depth) that will be selected
largeIV=145;% maximum index value (depth) that will be selected
%
% read in some data and put it in 'exampledata'
%   the data should be ascii text and have two (tab-separated) columns
%   the first being an index variable (such as depth, or year-day
%   the second being the data to be binned, indexed by col. 1
%   rows can be in any order
exampledata=load(fname, '-ascii');
%
% call the binning function - note that several syntaxes are allowed
% sorteddata=binning(exampledata, binsize);% simplest syntax
% sorteddata=binning(exampledata, binsize, maxbins);
% sorteddata=binning(exampledata, binsize, maxbins, smallIV, largeIV);
sorteddata=binning(exampledata, binsize, -1, smallIV, largeIV);
%
% graph the binned data against bin number
numberofbins=length(sorteddata(:,1));
plot(sorteddata(:,2), sorteddata(:,3), 'k-');
hold on
plot(sorteddata(:,2), 100*sqrt(sorteddata(:,4)./sorteddata(:,5)), 'r-');
xlabel('depth or pressure, db');
ylabel('temperature, degree C (and sd temp, * 100)');
title(strcat([num2str(numberofbins) ' bins']));
retrievedbinsize=sorteddata(2,1)-sorteddata(1,1);
minX=min(sorteddata(:,2))-retrievedbinsize;
maxX=max(sorteddata(:,2))+retrievedbinsize;
minY=0.0; % degree C, in this case
maxY=1.1*max(sorteddata(:,3));
axis([minX maxX minY maxY]);
legend('temp', 'sd');
%
% tabulate the binned data

```



```

fprintf('\n%s\n', 'binstart    depth    temp    s.d.    n')
for m=1:numberofbins,
    bs=sorteddata(m,1);% value for start of this bin
    iv=sorteddata(m,2);% mean value of index variable in the bin
    sv=sorteddata(m,3);% mean value of main variable in the bin
    n=sorteddata(m,5);% number of data in the bin
    svsd=sqrt(sorteddata(m,4)/n);% s.d. main variable in the bin
    fprintf('%8.2f %8.2f %8.2f %8.3f %5.0f\n', bs,iv,sv,svsd,n);
end
%
% save the figure
ofn=strcat(prog_name, '.pdf');
print('-dpdf', ofn);
fprintf('\n%s\n', strcat(['figure output as ' ofn]));
%
% ===== THE END =====
    fprintf('\n');
    fprintf(strcat(['\nend of ', prog_name, '\n']));
%
% ===== END OF SCRIPT =====

```

## ***Part II – Eo\_24***

```

% Eo_24
% algorithm to give 24-hr mean solar irradiance at the sea-surface
% draws graphs and also writes an output file of daily values
% The script was built using algorithms from Kirk (1983)
% PT, 23-24 April 2003
% slight mods to output (to give annual mean) on 1 Oct 2003
% originally written in Matlab 5; updated to Matlab 7 on 1 Nov 06
% =====
% angles are in radians unless specified
% =====
clear;clf reset;
% =====
% constant
CONV=2*pi/360.0;% degrees to radians
% =====
% forcing variables -- THESE MAY BE CHANGED BETWEEN LIMITS GIVEN
latitude=36.0;% degrees north - BETWEEN 0 AND 90
global fname
fname=load('1997-Ana.txt.txt');
days=1:365;
%fc=interp1(fname(:,1),fname(:,2),days,'linear'); % Use this comand
for
%the 2004(2) data ! Because it does not have 365 measurements.
fc=fname';% mean fraction of sky covered by cloud - BETWEEN 0.0 AND
1.0
% =====
% parameters
ESC=1367;% W m-2, solar constant
Aa=0.09;% per atmosphere, absorption coefficient for H2O and O3
prog_name='Eo_24';
year='1997';
foutname='irrad1997.xls';
% =====
fprintf('\n%s\n', '-----');
fprintf('%s\n', strcat([prog_name ' started at: ' datestr(now)]));
% =====
% year-day, starting from 0.0 at 00:01 on 1 January
% (February 29th neglected)
J=[0:1:364];

```

```

Jangle=J*(CONV*360/365.25);% corresponding angle (in radians)
% =====
% seasonally-varying solar declination relative to equator)
N=[1 2 3];
aN=[-22.984 -0.34990 -0.13980];
bN=[3.7872 0.03205 0.07187];
a_cos=aN'*ones(size(Jangle)).*cos(N'*Jangle);
b_sin=bN'*ones(size(Jangle)).*sin(N'*Jangle);
declination=0.33281+sum(a_cos)+sum(b_sin);
Rdec=CONV*declination;
% =====
% seasonally-varying maximum solar altitude
Rlat=latitude*CONV;
SHAN2=asin(sin(Rlat)*sin(Rdec)+cos(Rlat)*cos(Rdec));
subplot(2,2,1);
plot(J,SHAN2/CONV);
axis([0 365 0 120]);
xlabel('\fontname{times}\fontsize{12}Julian day');
ylabel('\fontname{times}\fontsize{12}solar hieght at noon (degrees)');
hold on;
site=num2str(latitude);
xfc=mean(fc);
cloud=num2str(xfc);
legend(strcat([site ' \circN; ' cloud ' cloud']));
% =====
% daylight fraction of 24 hours
DAYLIGHT=0.00554*acos(-tan(Rlat)*tan(Rdec))/CONV;
subplot(2,2,2);
plot(J,DAYLIGHT*24.0);
axis([0 365 0 25]);
xlabel('\fontname{times}\fontsize{12}Julian day');
ylabel('\fontname{times}\fontsize{12}hours of daylight');
% =====
% irradiance at noon
OAM=1./(sin(SHAN2)+0.15*(SHAN2+3.8885).^(-1.253));% optical air mass
ROT=1./(0.9*OAM+9.4);% Rayleigh optical thickness
ka=OAM.*ROT.*(0.021.*SHAN2+3.55);% relative optical thickness of
atmosphere
atcorr=0.5.*(exp(-ka)+1-Aa);% relative atmospheric loss at midday
midday=sin(SHAN2).*ESC.*atcorr.*(1-0.62.*fc+0.0019*SHAN2);% W m-2 at
midday
subplot(2,2,3);
plot(J,midday);
axis([0 365 0 1200]);
% =====
% 24hr mean irradiance
xlabel('\fontname{times}\fontsize{12}Julian day');
ylabel('\fontname{times}\fontsize{12}midday W/m2');
title (year);
E0W=(2/pi).*DAYLIGHT.*midday;
%=====
%Conversion of units -> from W.m-2 to uEs-1.m-2
%The conversion factor is taken from Chapter 4 (The Photic Zone) of
the
%Herring et al (1990) book. The chapter was written by Paul. And from
the
%environmental website of Paul in Napier
%Io=1.91.m1.Eo -> Io=PAR photon flux density (uEm-2s-1) immediately
beneath sea surface;
%E0= power density(all wavelengths W.m-2) just above the sea surface
%ml as a typical value of 0.95 for most of the sun angles (loss of 4-
6% by reflection)
E0=E0W*1.8145;

```

```

subplot(2,2,4);
plot(J,E0);
axis([0 365 0 900]);
xlabel('\fontname{times}\fontsize{12}Julian day');
ylabel('\fontname{times}\fontsize{12}24hr mean W/m2');
% =====
% write to file (in current working directory)
y=[E0'];
fid=fopen(foutname,'w');
%fprintf(fid, 'irradiance data for cloud cover at lat. 36 deg.N
(coll=day, col2=24hr W/m2)\n', fc, latitude);
fprintf(fid, '%-8.2f\n',y);
Iyearmean=mean(E0);
%fprintf(fid,'year mean is %8.2f W/m2\n', Iyearmean);
fclose(fid);
fprintf('%s\n', strcat(['Data written to ' foutname ' in ' cd]));
% =====
fprintf('%s\n', strcat(['End of ' prog_name ' at: ' datestr(now)]));
%
% ===== END OF SCRIPT =====

```

### III-2.2 - Wind velocity

The script used to obtain daily means of the wind velocity was adapted, but is mostly the same as presented before to bin the cloud cover values (complete part I).

### III-2.3 - Oxygen Saturation

In this model, it was necessary to work with the oxygen saturation values instead of the oxygen concentration. So, a script was built first to interpolate the values of temperature and salinity obtained in Ria Formosa to a continuous time-series and secondly, to transform it into oxygen saturation concentration according to the functions present in Carpenter (1966).

```

%Script to interpolate the values of Temperature and Salinity
%collected in 2006.
%
%Takes values from the outside and inside of Ria Formosa
%Values from inside are means from Ponte and Ramalhete
%Uses the function interpolation for the values that we have, applying
% the linear method

days=1:365;
load data.mat

global TBeach Tinside SBeach Sinside

TBeach=interp1(tempBeach(1,:),tempBeach(2,:),days,'linear');
Tinside=interp1(tempinside(1,:),tempinside(2,:),days,'linear');
SBeach=interp1(salinityBeach(1,:),salinityBeach(2,:),days,'linear');
Sinside=interp1(salinity(1,:),salinity(2,:),days,'linear');

subplot(4,2,1);

```

```

plot(days,TBeach);
ylabel('TBeach');

subplot(4,2,2)
plot(days,Tinside);
ylabel('Tinside');

subplot(4,2,3);
plot(days,SBeach);
ylabel('SBeach');

subplot(4,2,4);
plot(days,Sinside);
ylabel('Sinside');

y=[Tinside'];
fid=fopen('Tinside.xls','w');
fprintf(fid,'% -8.2f\n',y);
fclose(fid);

%function [DO] = oxysat(T,S);
% oxygen saturation concentration (mu-molar, or mmol/m3)
%
% i.e. concentration of oxygen in sea water of given
% temperature (T, deg C) and salinity (S, psu)
% when in equilibrium with air at standard (sea-surface) pressure
% PT, 26 Feb 05 copied from Validivia_oxygen.xls
% note that matlab 'log' gives natural logarithm (i.e 'ln')
%
% coeff
A1= -173.4292;
A2= 249.6339;
A3= 143.3483;
A4= -21.8492;
B1= -0.033096;
B2= 0.014259;
B3= -0.0017;
%
global DOBeach DO2Beach DOInside DO2Inside
load data.mat % loads data present as several variables in the mat
file.

S1=SBeach;
TCBeach=(273.15+TBeach)/100.0;
DOVBeach=exp(A1+(A2./TCBeach)+(A3.*log(TCBeach))+(A4.*TCBeach)+S1.*(B1
+(B2.*TCBeach)+(B3.*TCBeach.^2)));
DOBeach=DOVBeach*(1000/22.4) % convert from mL/L to mu-molar
DO2Beach=DOVBeach*1.33; %converts ml/L into mg/L.

S2=Sinside;
TCInside=(273.15+Tinside)/100.0;
DOVInside=exp(A1+(A2./TCInside)+(A3.*log(TCInside))+(A4.*TCInside)+S2.
*(B1+(B2.*TCInside)+(B3.*TCInside.^2)));
DOInside=DOVInside*(1000/22.4) %converts from ml/L to mu-molar.
DO2Inside=DOVInside*1.33; %converts ml/L into mg/L.

subplot(4,2,5);
plot(days,DOBeach);
ylabel('DOBeach(mumolar)');

```

```
subplot(4,2,6)
plot(days,DOInside);
ylabel('DOInside(mumolar)');

subplot(4,2,7);
plot(days,DO2Beach);
ylabel('DOBeach(mg/L)');

subplot(4,2,8)
plot(days,DO2Inside);
ylabel('DOInside(mg/L)');

%=====
% write to file (in current working directory)
y=[DOBeach'];
fid=fopen('DOBeach.xls','w');
fprintf(fid,'% -8.2f\n',y);
DOBeachmean=mean(DOBeach);
fclose(fid);
y=[DOInside'];
fid=fopen('DOInside.xls','w');
fprintf(fid,'% -8.2f\n',y);
DOInsidemean=mean(DOInside);
fclose(fid);
%
% ===== END OF SCRIPT =====
```